

AN OVERVIEW OF THE

Colloidal Surfaces For Analysis, Dyeing and Chemical Modification



EDITED BY

The A. Lakshmi, Thomas J. Wilson,
and Andrew Edgar

Cellulose Solvents: For Analysis, Shaping and Chemical Modification

ACS SYMPOSIUM SERIES **1033**

Cellulose Solvents: For Analysis, Shaping and Chemical Modification

Tim F. Liebert, Editor

*Friedrich Schiller University of Jena - Center of Excellence for
Polysaccharide Research*

Thomas J. Heinze, Editor

*Friedrich Schiller University of Jena - Center of Excellence for
Polysaccharide Research*

Kevin J. Edgar, Editor

Virginia Tech - Department of Wood Science and Forest Products

Sponsored by the
ACS Division of Cellulose and Renewable Materials



American Chemical Society, Washington, DC



Library of Congress Cataloging-in-Publication Data

Cellulose solvents : for analysis, shaping, and chemical modification / Tim F. Liebert, editor, Thomas J. Heinze, editor, Kevin J. Edgar, editor.

p. cm. -- (ACS symposium series ; 1033)

"Developed from a symposium ... held at the 235th National Meeting of the American Chemical Society, in New Orleans, Louisiana, April 6-10, 2008"--Pref.

"Sponsored by the ACS Division of Cellulose and Renewable Materials."

Includes bibliographical references and index.

ISBN 978-0-8412-0006-7 (alk. paper)

I. Cellulose--Solubility. 2. Solvents. I. Liebert, Tim. II. Heinze, Thomas, 1958- III. Edgar, Kevin J. IV. American Chemical Society. Cellulose and Renewable Materials Division V. American Chemical Society. Meeting (235th : 2008 : New Orleans, La.) VI. Series.

QD323.C41 2009

661'.802--dc22

2009050036

The paper used in this publication meets the minimum requirements of American National Standard for Information Sciences—Permanence of Paper for Printed Library Materials, ANSI Z39.48n1984.

Copyright © 2010 American Chemical Society

Distributed by Oxford University Press

All Rights Reserved. Reprographic copying beyond that permitted by Sections 107 or 108 of the U.S. Copyright Act is allowed for internal use only, provided that a per-chapter fee of \$40.25 plus \$0.75 per page is paid to the Copyright Clearance Center, Inc., 222 Rosewood Drive, Danvers, MA 01923, USA. Republication or reproduction for sale of pages in this book is permitted only under license from ACS. Direct these and other permission requests to ACS Copyright Office, Publications Division, 1155 16th Street, N.W., Washington, DC 20036.

The citation of trade names and/or names of manufacturers in this publication is not to be construed as an endorsement or as approval by ACS of the commercial products or services referenced herein; nor should the mere reference herein to any drawing, specification, chemical process, or other data be regarded as a license or as a conveyance of any right or permission to the holder, reader, or any other person or corporation, to manufacture, reproduce, use, or sell any patented invention or copyrighted work that may in any way be related thereto. Registered names, trademarks, etc., used in this publication, even without specific indication thereof, are not to be considered unprotected by law.

PRINTED IN THE UNITED STATES OF AMERICA

Foreword

The ACS Symposium Series was first published in 1974 to provide a mechanism for publishing symposia quickly in book form. The purpose of the series is to publish timely, comprehensive books developed from the ACS sponsored symposia based on current scientific research. Occasionally, books are developed from symposia sponsored by other organizations when the topic is of keen interest to the chemistry audience.

Before agreeing to publish a book, the proposed table of contents is reviewed for appropriate and comprehensive coverage and for interest to the audience. Some papers may be excluded to better focus the book; others may be added to provide comprehensiveness. When appropriate, overview or introductory chapters are added. Drafts of chapters are peer-reviewed prior to final acceptance or rejection, and manuscripts are prepared in camera-ready format.

As a rule, only original research papers and original review papers are included in the volumes. Verbatim reproductions of previous published papers are not accepted.

ACS Books Department

Preface

Cellulose, the most abundant terrestrial biomolecule, is produced by plants, sea organisms such as Tunicin from the *Tunicat* class and microorganisms like *Gluconacetobacter xylinus* in huge amounts. It is not only the quantity of the feedstock produced annually making the polymer very attractive as starting material. The polysaccharide also exhibits astonishing properties such as a well-defined, complex, polychiral structure, biocompatibility and biodegradability. Moreover, the molecule contains different reactive functionalities for a selective chemical conversion towards products with adjustable features. Nevertheless, application of cellulose is limited because of the insolubility of the biopolymer in almost all common organic and inorganic liquids. Various more or less exotic solvents were developed to overcome this problem and to make cellulose accessible for tailored modification.

This book was developed from a symposium titled “Cellulose Solvents”, held at the 235th National Meeting of the American Chemical Society, in New Orleans, Louisiana, April 6–10, 2008. The symposium provided a forum for organizing an integrated discussion on the current state of the art. It was organized with the intent to bring together scientists from academia and industry in the expectation that new insight gained would be useful for the development of novel, value added materials from this polymer.

The book highlights different approaches for the dissolution of cellulose and the use of the dissolved polymer for analysis, regeneration, and homogeneous modification. Results on basic investigations concerning the state of dissolution of cellulose in solvents and structural features of the regenerated cellulose are included. Aqueous and non-aqueous solvents, melts, and soluble cellulose intermediates are discussed with the focus on new developments for fiber spinning and the homogeneous chemical conversion of cellulose.

About five years ago this research topic was fueled by the discovery of organic salts with low melting points (ionic liquids) as proper solvents. It has been shown that the properties of such new solvents can be adjusted to the specific tasks and may be permit conversion of cellulose into a broad variety of new, bio-based materials for numerous commercial purposes such as bioplastics, and also into high value products, for example nanomaterials.

The first section of the book “Approaches for the Dissolution of Cellulose”, displays the broad variety of media suitable for the dissolution of cellulose. Such solvents were involved in the first commercial processes for man made fibers, and still new paths for defined regeneration and shaping are being discovered involving dissolution of the polysaccharide. An important development certainly is the application of ionic liquids but alternatively recent advances in the use of molten inorganic salt hydrates, mixtures of organic liquids with salt such as DMSO/tetrabutylammonium fluoride and solvents containing NaOH are discussed.

Although a comprehensive theory for the mechanisms of cellulose solubilization is a matter of ongoing research, impressive advances have been made towards the structural understanding of cellulose-solvent interactions. The new insight into dissolution kinetics and the processes necessary to disrupt the extended hydrogen-bond system of the polysaccharide led to new paths for activation and pretreatment of the polymer. These basic studies combined with considerations on possible side reactions on the cellulose backbone during dissolution are presented in the section “Interaction of Solvents with Cellulose”.

New solvents are exploited to improve the quality of commercial products such as fibers, membranes, sponges and non-woven materials. A major benefit of tailored solvents is the ability to prepare unconventional regenerated cellulose morphologies as well as new blend materials. In the section “Modification of Cellulose using Solvents” the extraction and processing of cellulose and the preparation of cellulose/TiO₂ fibers are discussed. Moreover, recent research on the chemical conversion of cellulose in different solvents leading to nonconventional cellulose is demonstrated. For a specific reaction the influence of the reaction conditions (heterogeneous versus homogeneous) on the accessible structures is evaluated. New solvents also offer the opportunity for direct saccharification of cellulose and to use wood as starting material for cellulose fractionation and derivatization.

There is no doubt about the fact that the use of cellulose solvents will significantly broaden the portfolio of tailored and smart materials based on this unique and widely abundant biopolymer.

The editors are indebted to their respective institutes, the Friedrich Schiller University of Jena, Germany and the Virginia Polytechnic Institute and State University, Blacksburg, VA, for financial and logistic support of this endeavor. We also thank Jessica Rucker, Bob Hauserman and Tim Marney of the American Chemical Society Books Department for their conscientious effort to complete this book.

Tim F. Liebert

Friedrich Schiller University of Jena - Center of Excellence for Polysaccharide Research
Jena, Germany

Thomas J. Heinze

Friedrich Schiller University of Jena - Center of Excellence for Polysaccharide Research
Jena, Germany

Kevin J. Edgar

Virginia Tech - Department of Wood Science and Forest Products
Blacksburg, Virginia

Chapter 1

Cellulose Solvents – Remarkable History, Bright Future

Tim Liebert*

Centre of Excellence for Polysaccharide Research,
Friedrich Schiller University of Jena, Humboldtstrasse 10, D-07743 Jena,
Germany

*Member of the European Polysaccharide Network of Excellence, EPNOE
(www.epnoe.eu). E-mail: tim.liebert@uni-jena.de.

The paper summarizes different approaches for the dissolution of cellulose and the use of these cellulose solutions for analysis, regeneration, and homogeneous modification of the polymer. Aqueous and non-aqueous solvents, melts, and soluble cellulose intermediates are discussed with the focus on new developments for the shaping and the homogeneous conversion of cellulose. It will be shown that these media open up new paths towards nanostructured regenerated cellulose and tailored cellulose derivatives not accessible via heterogeneous reactions. Moreover, the preparation of conventional cellulose products with new structural features obtainable by conversion in cellulose solvents will be illustrated.

The first attempts to dissolve cellulose or cellulose containing material such as cotton or the inner bark of mulberry were described about 150 years ago (1, 2). Since then a huge variety of cellulose solvents have been developed or were discovered by coincidence. Looking at the history of cellulose solvents, it is obvious that this specific area of research had a huge influence on the development of polymer chemistry in general. Thus, the first man-made fiber, Chardonnet silk (3) was obtained with a soluble cellulose derivative and the first man-made plastics, Parkesine (4), and Celluloid (5), were prepared via the same modification reaction. Moreover, the structural features of macromolecules were mainly revealed with cellulose/cellulose solvents. This achievement was honored

with the Nobel Prize for Hermann Staudinger in 1953, presumably the first Nobel Prize for a polymer chemist (6). Today the development of new solvents is fueled by the increasing demand for new techniques suitable for shaping, homogeneous chemical modification, and defined degradation of the most abundant terrestrial organic molecule.

There is still no consensus about the processes necessary to disrupt the hydrogen bond system of cellulose to initiate solvation of the cellulose chains. Some very basic ideas on different possible mechanisms have been published. In 1980 Turbak (7) divided cellulose solvents into four main categories based on the possible interactions of cellulose with solvents:

- Cellulose is acting as a base, the solvent is an acid, e.g. H₂SO₄, trifluoroacetic acid,
- Cellulose is acting as an acid, the solvent is a base, e.g. KOH, Triton,
- Cellulose is a ligand, the solvent is a complexing agent, e.g. Cuam, Cadoxen,
- Cellulose is a reactive compound, it is converted to a soluble transient derivative or intermediate, e.g. xanthate, trifluoroacetate.

Philipp modified this system and categorized cellulose solvents into derivatizing, non-derivatizing, aqueous and non-aqueous solvents (8). Moreover, this classification was combined with the number of components in the solvent system (9). Alternatively, solvents can be grouped into certain modes of interaction with cellulose according to the morphological changes of the polymer determined by microscopy (10).

In this review a historical approach is used to discuss basic families of solvents suitable for the dissolution of cellulose. There were three important discoveries that led to the growth of certain “solvent families”. In 1846 Christian Friedrich Schoenbein described the formation of nitrated cellulose and initiated the functionalization of cellulose to organo-soluble cellulose derivatives, which can be used as soluble intermediates for the modification of the biomacromolecule (11). A decade later Eduard Schweizer showed that aqueous systems such as Cuoxam may dissolve cellulose as well (12). A completely new type of solvent, capable of providing clear solutions of the polymer without chemical modification, was discovered by Charles Graenacher in 1934 (13). He demonstrated that low melting organic salts can be applied as non-aqueous, non-derivatizing cellulose solvents. The discussion on relevant achievements and new tools for the dissolution of cellulose will follow these three lines, i.e.

- Dissolution of cellulose by chemical modification,
- Solvation in aqueous or protic systems,
- Dissolution in non-aqueous, non-derivatizing media.

Besides the description of the pure solvents and their interactions with cellulose, the review is focused on the potential offered by cellulose solvents for the preparation of new materials based on regenerated cellulose and on the homogeneous chemical functionalization of the polymer. Because of the huge amount of published data on homogeneous reactions of cellulose, this approach is illustrated with a few examples; sulphation/sulphonation, carboxymethylation and acylation reactions of cellulose with carboxylic acids after *in situ* activation under homogeneous conditions.



Figure 1. Christian Friedrich Schoenbein who discovered the first process for the dissolution of cellulose

1. Derivatizing Solvents, Intermediates, Transient Derivatives

1.1. Cellulose Nitrate

The first path for the dissolution of cellulose was discovered more or less by coincidence. In 1845 Swiss chemist Christian Friedrich Schoenbein (Figure 1) did experiments with a mixture of $\text{HNO}_3/\text{H}_2\text{SO}_4$ aiming to synthesize explosives (11).

According to the legend of his discovery, he occasionally spilled some of that mixture and cleaned up with his wife's cotton apron, which one day exploded as soon as it was dry. The derivative formed in this process, cellulose nitrate (often misnamed as nitrocellulose), was widely applied as gun cotton and it became the basis for the film industry. It also yielded the first man made plastics when John Wesley Hyatt treated the cellulose derivative with camphor to obtain Celluloid in 1865 (5).

Solutions of this chemically modified cellulose in diethyl ether/ethanol were exploited for the shaping of the polymer by Joseph Swan, who was looking for a better carbon fiber suitable for lamp filaments. He discovered how to de-nitrate the cellulose derivative using ammonium hydrosulphate (14). The first fabrics made from the new artificial silk were shown at the Exhibition of Inventions in 1885. Nevertheless, the Frenchman Count Louis-Marie-Hilaire Bernigaud, Comte de Chardonnet is regarded today as the founder of the regenerated cellulosic fiber industry (3). He perfected cellulosic fibers and textiles in time for the Paris Exhibition in 1889. Although this first man-made fiber process was simple in concept, it proved slow in operation, difficult to scale up safely, and relatively uneconomic compared with later routes (15). Besides nitration with $\text{HNO}_3/\text{H}_2\text{SO}_4$, introduction of nitrite functions, combined with direct dissolution of the polymer, can be achieved with a mixture of *N,N*-dimethylformamide (DMF)/ N_2O_4 (16). Despite its highly toxic nature this homogeneous solution is suitable for subsequent oxidation, acetylation and especially sulphation (17). During preparation of cellulose sulphuric acid half esters (cellulose sulphates, CS) the intermediately formed ni-

trite is attacked by sulphating reagents, e.g. SO_3 , ClSO_3H , SO_2Cl_2 , and $\text{H}_2\text{NSO}_3\text{H}$ (18) (Table 1).

The residual nitrite moieties are cleaved during the work up under protic conditions yielding pure cellulose sulphates.

1.2. Cellulose Xanthate

Historically, the next dissolving method for cellulose which involves partial derivatisation was the viscose process. In 1891 the British chemists Charles Cross, Edward Bevan, and Clayton Beadle, discovered that cotton or wood cellulose, could be dissolved as cellulose xanthate (Figure 2) following treatment with alkali and carbon disulphide (19). The treacle-like yellow solution (initially called "viscous cellulose solution", later simply "viscose") could be coagulated in an ammonium sulphate bath and then converted back to pure cellulose using dilute sulphuric acid. They patented their process in 1892 without mentioning fibers. It was in 1904 that scientists at the Donnersmarck's plant in Germany developed a spinning bath containing a mixture of sulphuric acid and a salt, known as Mueller spinbath (20).

Despite its environmental problems caused by the by-products and the volatile and odiferous CS_2 solvent, the viscose process is still the most important method for the shaping of cellulose. The dissolution process is still a subject of research, mainly focused on optimization or dissolution of different types of celluloses (21). Interestingly, during this dissolution of cellulose a ballooning effect was observed for the first time (Figure 3, (22)).

An interesting alternative for the viscose process was discovered by the Finnish viscose producer Kemira Oy Saeteri (23). Here the intermediate formation of a cellulose carbamate was exploited (Figure 4). This system was based on the original work of Hill and Jacobsen who showed that the reaction between cellulose and urea gave a derivative that was easily dissolved in dilute sodium hydroxide (24, 25).

An industrial route to a stable cellulose carbamate pulp was developed. The carbamate solution could be spun into sulphuric acid or sodium carbonate solutions, to give fibers which when completely regenerated had similar properties to viscose rayon (Figure 5). A variety of methods for the preparation of carbamates were established including activation with ammonia and the use of inert organic solvents (26, 27).

1.3. Hydrolytically Unstable Carboxylic Acid Esters of Cellulose as Intermediates

The unstable intermediates derived from partly inorganic reagents discussed above are well suited to the shaping of cellulose into fibers, membranes and sponges, but problems arise from the use of flammable or toxic reagents and from the formation of toxic or aggressive by-products. In addition, the mixtures applied are too reactive for subsequent functionalization. To exploit the

Table 1. Regioselectivity of the sulphation of cellulose nitrite with different reagents (2 mol/mol AGU) vs. reaction conditions (adapted from (18))

Reaction conditions			Reaction product			
Reagent	Time (h)	Temp. (°C)	DS	Partial DS		
				O-2	O-3	O-6
NOSO ₄ H	4	20	0.35	0.04	0	0.31
NH ₂ SO ₃ H	3	20	0.40	0.10	0	0.30
SO ₂ Cl ₂	2	20	1.00	0.30	0	0.70
SO ₃	3	20	0.92	0.26	0	0.66
SO ₃	1.5	-20	0.55	0.45	0	0.10

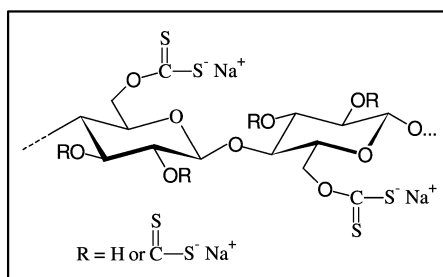


Figure 2. Cellulose xanthate, the intermediate formed during the viscose process

strategy of homogeneous cellulose conversion after intermediate derivatization, hydrolytically unstable carboxylic acid esters of the polymer were investigated. Even **cellulose acetate (CA)** may be regarded as intermediate. CA was first prepared in 1865 by Paul Schuetzenberger (28). The acetylation step itself may give a homogeneous system and the solutions containing co-solvents such as methylene chloride or DMF can be applied for a homogeneous reaction on cellulose. Additionally, it is possible to isolate, purify, and redissolve the carboxylic acid ester and perform the subsequent functionalization on the remaining OH-functions in an inert solvent. Thus, acetylation of cellulose with acetic anhydride in DMF followed by direct sulphation is possible; alternatively, a commercially available CA with DS 2.5 may be sulphated in DMF solution (29). In contrast to sulphation via nitration, the acetyl moieties act as protecting groups and the sulphation with SO₃-Py, SO₃-DMF, or acetylsulphuric acid proceeds exclusively at the unmodified hydroxyl functions, i.e. no transesterification occurs (Figure 6).

If one aims for the synthesis of pure hydrolytically or thermally sensitive products, complete and selective hydrolysis of the acetate functions is hard to achieve. In this case, ester functions have to be introduced that are easily cleavable after subsequent functionalization of the free OH-moieties.

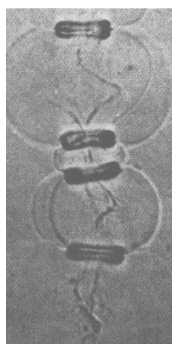


Figure 3. Cellulose fibres swollen with alkali and carbon disulfide

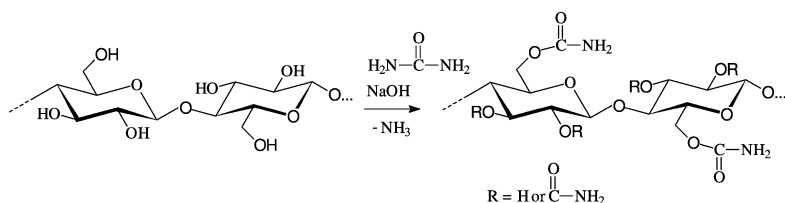


Figure 4. Formation of cellulose carbamate, interesting alternative for the viscose process

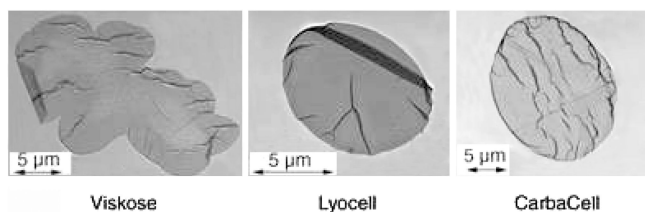


Figure 5. Cross-sections of cellulose fibers obtained by different dissolution and regeneration methods. (from ref. (200) with kind permission from Elsevier)

Cellulose Formates (CF)

The reaction of cellulose with formic acid to prepare cellulose formates (CF) was studied as an alternative way for the production of cellulose fibers (30). Solutions of cellulose (regenerated cellulose, rayon, cellophane) in a surplus of formic acid are obtained without catalyst over periods of 4–15 days, with strong preference for formylation at position C-6 (31, 32). The dissolution is much faster in the presence of sulphuric acid as catalyst. Pure CF soluble in DMF were isolated from the system cellulose/formic acid/phosphoric acid/water (33). Moreover, cellulose formates with DS values up to 2.5, soluble in DMSO, DMF, and pyridine (Py) are obtained by reaction with partially hydrolyzed POCl₃ (as swelling/dehydrating agent) in formic acid (34). CF may also be achieved via a formiminium compound (35). After isolation of the formates, subsequent

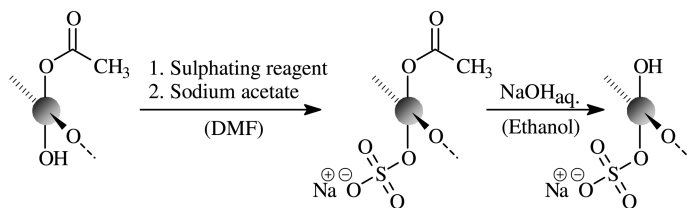


Figure 6. Preparation of cellulose sulphate starting from cellulose acetate, acetyl moieties acting as protective groups. (from ref. (45) with kind permission from Springer)

esterification was carried out in an inert organic solvent. Sulphation may occur in part by replacement of the formyl functions (transesterification) (33). Under inert, water-free reaction conditions transesterifications or cleavage of the formyl moieties can be diminished (36). Thus, an inverse pattern of substitution can be obtained after subsequent removal of the formate ester by simple treatment with water.

Cellulose Trifluoroacetate (CTFA)

Solutions of cellulose in trifluoroacetic acid (TFA) were extensively studied by means of NMR spectroscopy showing that the primary OH-groups are almost completely functionalized during dissolution (37, 38). Kinetics of the dissolution can be influenced by organic liquids with strong electron acceptor behavior (39). In mixtures containing TFA/CH₂Cl₂ trifluoroacetylation occurs only to a limited extent and the polysaccharide is rather slowly degraded (40). Interestingly, the solutions show the formation of mesophases starting from cellulose concentrations as low as 4% (w/w), which can be used to regenerate strong fibers. Attempts were made to exploit solutions of cellulose in TFA directly for the preparation of cellulose esters (C₂-C₁₀) by conversion with the corresponding carboxylic acid anhydrides. It was stated that esters with DS values between 2.9 and 3 were accessible (41). Furthermore, the preparation of mixed esters was achieved (42). Pure CTFA (Figure 7) soluble in DMSO, pyridine, and DMF can be easily prepared by treating cellulose with mixtures of TFA and its anhydride (43) They can be completely saponified with water within 6 min. **Cellulose dichloroacetates (CDCA, Figure 7)** are intermediates with comparable properties. They can be obtained from cellulose by reacting with a mixture of dichloroacetic acid (DCA) and partially hydrolyzed phosphorus oxychloride (PO(OH)_{1.5}Cl_{1.5}), or with a mixture of DCA and dichloroacetic anhydride (44).

These hydrolytically unstable intermediates can be exploited for subsequent functionalization in homogeneous phase giving a variety of organic esters, inorganic esters, carbamates, and ethers with specific distributions of functional groups (45). Reaction of these unstable intermediates with carboxylic acids using *N,N*-carbonyldiimidazole (CDI) as reagent is very efficient. Under aprotic conditions pure products with inverse patterns of functionalization (Figure 8) are obtained, and the primary substituent is simply cleaved off during the aqueous

work up procedure. A remarkable result is the high *O*-3 selectivity of the sulphation of cellulose trifluoroacetate with pyridine/SO₃ (46).

A valuable path for non-statistical etherification of cellulose was studied in detail applying CTFA and CF. The cellulose intermediates dissolved in DMSO can be converted with suspended solid NaOH powder and sodium monochloroacetate into carboxymethyl cellulose (CMC) with a very high DS (34). Using polarizing light microscopy and FTIR spectroscopy it was revealed that addition of solid NaOH induces cleavage of the primary substituents, e.g. trifluoroacetate, and regeneration of cellulose II on the solid particles (Figure 9). Deacylation can be confirmed by the growth of sodium salts of the corresponding acids on the NaOH particles (Figure 10) as needle-like crystals. CMCs synthesized in this “reactive microstructure” contained significantly higher amounts of both 2,3,6-tri-*O*-carboxymethyl- and unsubstituted glucose units in the polymer chain than heterogeneously prepared products which show statistical distribution of all 8 possible monomeric units. This was revealed by HPLC analysis in comparison with statistical calculations (47, 48). Even methyl celluloses with an unconventional content of the different repeating units were obtained using this synthesis strategy. These unconventional cellulose ethers exhibit new properties such as a much higher tendency to cover surfaces (49).

All in all, hydrolytically unstable cellulose esters, especially the CTFA, are promising intermediates because of the simple preparation combined with solubility in a wide variety of common organic solvents, fast cleavage under aqueous conditions, and stability under aprotic conditions. Disadvantages include the expense and corrosivity of the reagents.

1.4. Acetals and Silyl Ethers as Cellulose Intermediates

Methylol Cellulose (DMSO/Paraformaldehyde)

The mixture DMSO/paraformaldehyde is another derivatizing solvent for cellulose. It dissolves cellulose rapidly and almost without degradation even in the case of high cellulose molecular mass. During dissolution the formation of the hemiacetal, i.e., the so-called methylol polysaccharide occurs (Figure 11, (50, 51)). This methylol structure remains intact during subsequent functionalization but can be easily removed by treatment with water. It is noteworthy that, during the dissolution, growth of oligo (oxymethylene) chains may occur. Even cross-linking is possible (Figure 11).

In addition to the methylol functions, the free terminal hydroxyl groups of these chains may also be derivatized in a subsequent step lowering the overall yield of the procedure. DMSO/paraformaldehyde was exploited for the homogeneous synthesis of cellulose esters with trimellitic anhydride, trimethyl acetic anhydride and phthalic anhydride (52). DMF and DMAc may also be used as solvent in combination with paraformaldehyde.

In a mixture *chloral/DMF/Py* cellulose dissolves via reaction of the hydroxyl groups to form soluble chloral hemiacetals (Figure 12), which could be acetylated to products with DS of 2.5 by acetic anhydride or acetyl chloride (53).

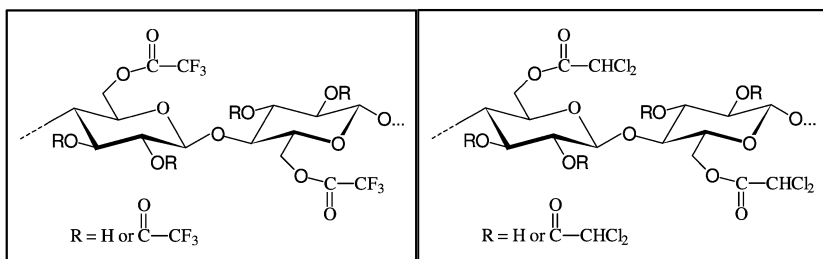


Figure 7. Formulae of cellulose trifluoroacetate and cellulose dichloroacetate accessible by treatment of cellulose with a mixture of acid/acid anhydride

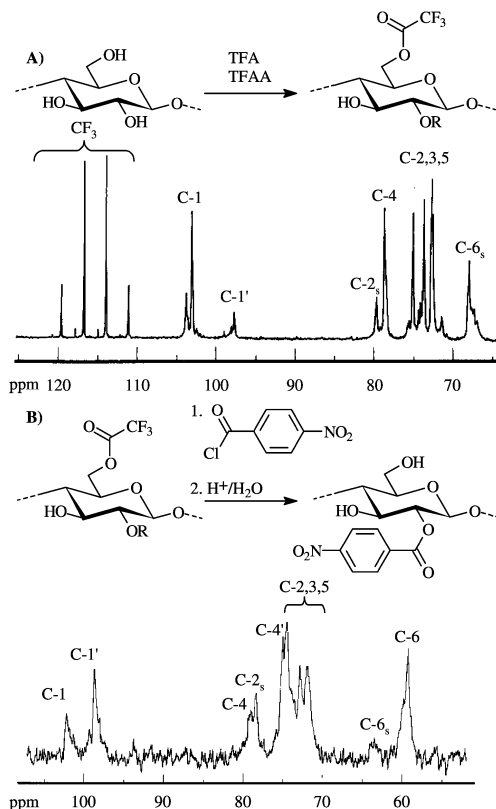


Figure 8. ^{13}C NMR spectra of **A**) cellulose trifluoroacetate (DS 1.50) and **B**) cellulose nitrobenzoate (DS 0.76) obtained via subsequent esterification showing inverse patterns of functionalisation. (from ref. (45) with kind permission from Springer)

Silyl Cellulose (DMF/TMSCl)

Mixtures of trimethylsilyl (TMS) chloride and organic solvents such as DMF are also cellulose-derivatizing solvents. Trimethylsilyl celluloses

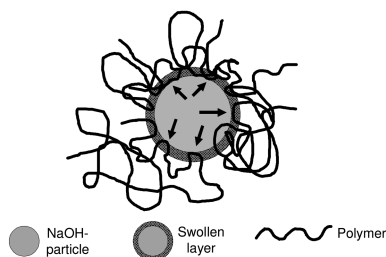


Figure 9. Schematic drawing representing a “reactive microstructure” formed by treatment of a homogeneous solution of cellulose with a solid reagent such as NaOH

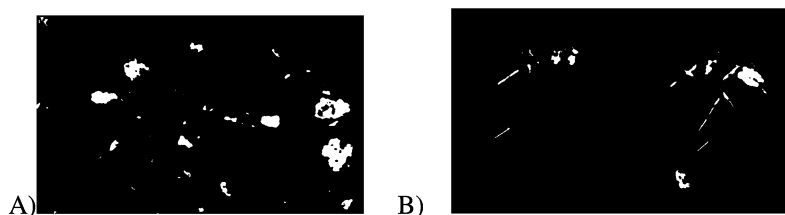


Figure 10. A) NaOH particles in DMSO B) formation of sodium trifluoroacetate crystals (needles) on solid NaOH particles during treatment of cellulose trifluoroacetate dissolved in DMSO with the solid base

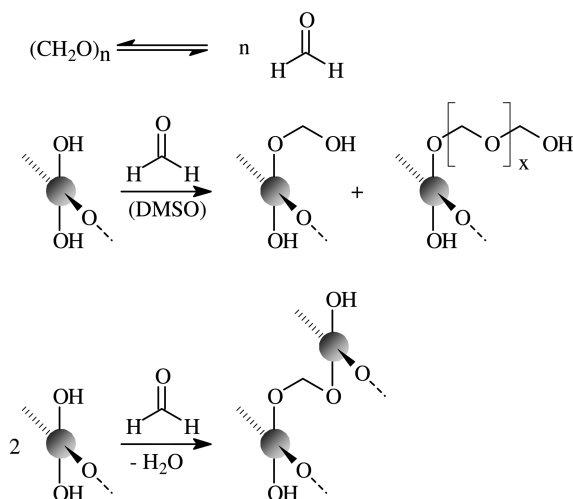


Figure 11. Structure of methylol derivatives formed by dissolution of polysaccharides in DMSO/paraformaldehyde. (from ref. (45) with kind permission from Springer)

(TMSC), the intermediates formed during this dissolution process, were first described by Schuyten (54) and were extensively studied because of their

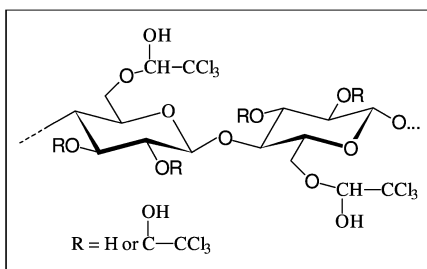


Figure 12. Intermediately formed hemiacetal of chloral and cellulose during the dissolution of the polysaccharide in the mixture chloral/DMF/Py

potential to regenerate cellulose simply by treatment with acids, affording thereby cellulose fibers, particles or films (55). Silylation is also possible with hexamethylenedisilazane (56–58). During the reaction of TMSCl with acid chlorides at elevated temperatures (nitrobenzene at 160 °C) trimethylsilyloxy groups are found to react selectively while the OH-groups are unaffected (58). Thus, depending on reaction conditions it is possible to convert either exposed OH-groups or (by replacement of TMS) the trimethylsilyloxy groups. This is also true for sulphation of TMSCl (59, 60) in which the first step consists of an insertion of SO₃ into the Si-O bond of the silyl ether (Figure 13).

Therefore the DS_{Sulphate} is limited by the DS_{Si} of the starting TMS cellulose and can be adjusted in the range from 0.2 to 2.5 as summarized in Table 2 (61). The sulphation can be carried out in a one-pot reaction as well, i.e., without isolation and redissolution of the TMS cellulose (61).

1.5. Interaction of Carbohydrates with Boric Acid

Boric acid and its derivatives, e.g. its salts or boronic acids are in general suitable for the formation of intermediate derivatives of polysaccharides. They were studied as reagents for cellulose activation (62–67) but are scarcely applied because of unpredictable reactions. Therefore, a basic understanding is indispensable to make them usable as activating or dissolving agents for cellulose. The most reactive site of cellulose towards boronation is the *trans*-1,2-diol system in position 2 and 3. Model studies were carried out with methyl- α -D-glucopyranoside (Me- α -D-glcp) and phenylboronic acid (PBA) using a dehydrating agent or the corresponding anhydride. Me- α / β -glcp initially forms an unstrained, 6-membered ring borate ester through the hydroxyls in position 4 and 6 (Figure 17, **1**, (68, 69)). The product borate (**1**) has only a diol structure at position 2 and 3, making this system a reasonable model for the conversion of oligo- or polyglucans.

Interestingly, mass spectrometry (MS) revealed the formation of a seven membered ring including two boron atoms with the *trans*-1,2-diol moiety in position 2 and 3 (Figure 14, (70–72)) as concluded from significant fragment ions at *m/z* 160 (**I**), 250 (**II**) molecular ion peak at *m/z* 470. Stepwise boronation

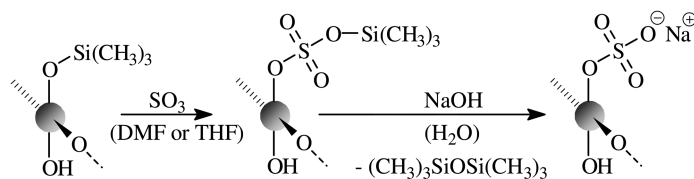


Figure 13. Preparation of cellulose sulphate via trimethylsilyl cellulose. (from ref. (45) with kind permission from Springer)

Table 2. Sulphation of cellulose via TMS cellulose (adapted from (61))

		Reaction conditions			Product
TMS cellulose DS_{Si}	Solvent	Sulphating agent			DS
		Type	Molar ratio		
			AGU	Reagent	
1.55	DMF	SO ₃	1	1.0	0.70
1.55	DMF	SO ₃	1	2.0	1.30
1.55	DMF	ClSO ₃ H	1	2.0	1.00
1.55	DMF	ClSO ₃ H	1	3.0	1.55
2.40	THF	SO ₃	1	3.3	1.84
2.40	THF	SO ₃	1	9.0	2.40

of Me- α -D-glcp with PBA was confirmed by means of ¹H NMR spectroscopy showing the disappearance of the OH-6 and the OH-4 signal in the first step (Figure 15b) and complete conversion of all hydroxyl protons in a second step (Figure 15c). ¹¹B NMR spectroscopy verified the occurrence of a seven-membered ring by comparison with phenylboronate esters of 1,2-ethanediol, 1,3-propanediol and *trans*-cyclohexane-1,2-diol (Figure 16).

'Coordination-induced shifts' for ¹³C NMR spectra were established on the basis of these results, which were used to confirm comparable transformation on oligoglucans. Moreover, it was observed that a simple treatment with water results in complete removal of the intermediately introduced boronates. Thus, conversion of the 1,2 trans diol structures can lead to new activation or even solvent systems for cellulose via intermediate boronation.

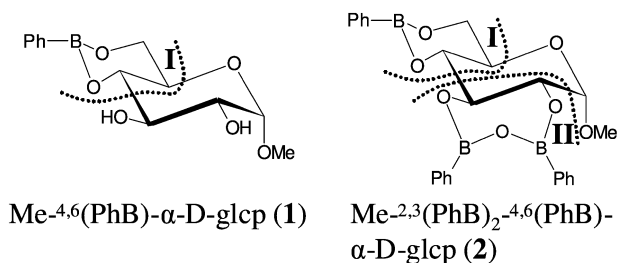


Figure 14. Boronate structures and expected fission processes in MS studies.
(from ref. (72) with kind permission from Elsevier)

2. Aqueous (Protic) Solvents

2.1. Aqueous Complexing Agents

Schweizers Reagent

The family of solvents suitable for the dissolution and regeneration of cellulose to be commercialized as an artificial silk process was based on a discovery made by the Swiss chemist Matthias Eduard Schweizer in 1857. He found that cotton could be dissolved in a solution of copper salts and ammonia and then regenerated in a coagulating bath (73). The fiber process was however invented by a French Chemist, Louis-Henri Despeissis who in 1890 worked on spinning fibers from Schweizer's solution (74). In 1892, German chemist Max Fremery started to use Schweizer's reagent and cotton to make lamp filaments. Together with Austrian engineer Johan Urban he decided to expand into artificial silk and patented a process (75, 76). However, the relatively high costs associated with the need to use cotton cellulose and copper salts prevented it from reaching the large scale of manufacture. Today it is still in use for the preparation of specific cellulose regenerates such as hollow fibers for dialysis.

In addition, it is a very useful tool for the analysis of cellulose and it was among the reagents Hermann Staudinger (Figure 18) exploited to elucidate the macromolecular structure of cellulose for which he won the Nobel Prize in 1953 (6). Today there are numerous alternatives of this basic complexing agent, containing mainly a transition metal and an amine or ammonium component. Among these solvents:

- Cuoxen ($[\text{Cu}(\text{NH}_2(\text{CH}_2)_2\text{NH}_2)_2][\text{OH}]_2$)
- Nioxam ($[\text{Ni}(\text{NH}_3)_6][\text{OH}]_2$)
- Zinkoxen ($[\text{Zn}(\text{NH}_2(\text{CH}_2)_2\text{NH}_2)_3][\text{OH}]_2$)
- Cadoxen ($[\text{Cd}(\text{NH}_2(\text{CH}_2)_2\text{NH}_2)_3][\text{OH}]_2$)
- Nitren ($[\text{Ni}(\text{NH}_2\text{CH}_2\text{CH}_2)_3\text{N}][\text{OH}]_2$)
- Pden ($[\text{Pd}(\text{NH}_2(\text{CH}_2)_2\text{NH}_2)][\text{OH}]_2$)

These metal complexes dissolve cellulose by deprotonating and coordinatively binding the hydroxyl groups in the C2 and C3 position of the AGU as investigated in detail for Pden (Figure 19, (77)). In Pden cellulose is molecularly dispersed to give entirely metallated single strands (78).

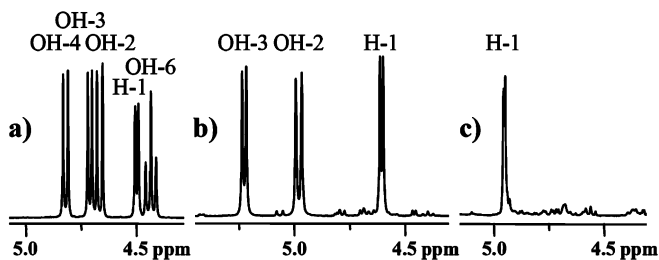


Figure 15. ¹H NMR spectra (hydroxyl and anomeric protons) of (a) Me- α -D-glcp; (b) Me-^{4,6}(PhB)- α -D-glcp (1); (c) Me-^{2,3}(PhB)₂-^{4,6}(PhB)- α -D-glcp (2). (from ref. (72) with kind permission from Elsevier)

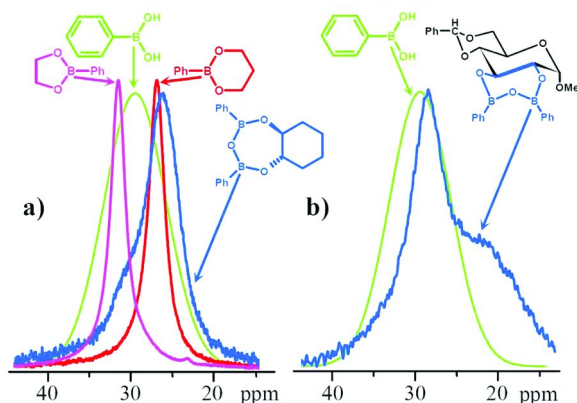


Figure 16. ¹¹B NMR spectra of (a) model compounds; (b) phenylboronate in comparison with PBA. (from ref. (72) with kind permission from Elsevier)

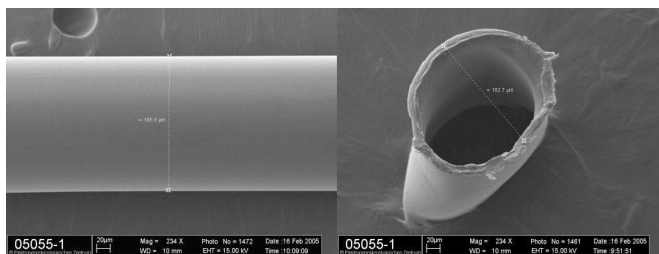


Figure 17. Hollow fiber used for blood dialysis prepared via the Cuoxam process

A detailed comparative light scattering study was published for cellulose in Cuoxam, Nitren, and Cdtren. All three solvents exhibited good solution properties, but only Cdtren was capable of dissolving even cellulose with the highest DP namely cotton linters and bacterial cellulose. A fairly high chain stiffness was found (79). The use of new coordinating solvents such as Pden, Nitren, Zndien and Cdtren thus appears to be the key to manipulating single strands of underivatized



Figure 18. Hermann Staudinger in his institute in Freiburg/Germany. (from ref. (6) with kind permission from Wiley)

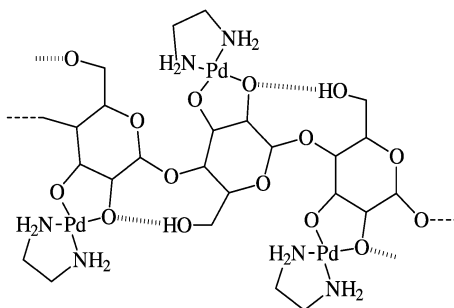


Figure 19. Structure proposed for cellulose dissolved in an aqueous solution of Pden

cellulose. They can be the tool for the synthesis of supramolecular assemblies with pure cellulose.

Carboxymethylation of cellulose with sodium monochloroacetate is possible in Nitren which is the first example for a totally homogeneous carboxymethylation. It yields polymers with the same DS (0-0.7, Table 3), pattern of functionalization and properties as determined for CMC samples obtained in the slurry reaction (80) confirming that a treatment of the cellulose with aqueous NaOH as used in commercial process is a very efficient activation method.

Ferric sodium tartrate complex ($[\text{Fe(III)}(\text{C}_4\text{H}_3\text{O}_6)_3]\text{Na}_6$, known as FeTNa or EWNN) is a solvent belonging to the group of complexing media. It is obtained by mixing FeCl_3 , tartaric acid dihydrate, and NaOH in cold water (81). Jayme and Achwal demonstrated that FeTNa solution dissolves cellulose very efficiently with little degradation of the cellulose molecules (82, 83). FeTNa solutions were applied for analytical purposes such as determination of the molecular weight (84), for the modification of cellulose by regeneration (85) and for surface modification. (86). The fibrillation resistance of Tencel yarns was improved by simply treating with FeTNa solution (see Figure 20).

Table 3. Conditions and Results of the Carboxymethylation of Cellulose in Nitren

<i>Molar ratio</i> ^a	<i>time (h)</i>	<i>DS</i>	<i>solubility in water</i> ^b
1:5:2.5	3	0.11	-
1:10:5	3	0.25	-
1:10:10	3	0.54	+
1:20:10	24	0.44	+
1:40:20	3	0.50	+
1:40:20 ^a	4	0.71	+

^a Anhydroglucose unit/NaOH/sodium monochloroacetate. ^b Key: +, soluble; -, insoluble.

2.2. Aqueous Alkali (Base) Containing Solvents

In contrast to attempts to dissolve cellulose in aqueous acids (87), which are usually combined by severe chain degradation (88), treatment of cellulose with an aqueous solution of bases such as *NaOH*, the mercerization, is one of the most important technical processes for cellulose activation and has been intensively investigated. This activation path is not within the scope of this review, but fundamental understanding of the ternary system cellulose / NaOH / water led to a variety of dissolution procedures.

Thus, the phase diagram established by Sobue et al. (Figure 21, (89)) suggests that there is a dissolution zone of cellulose in aqueous NaOH below 268 K at a NaOH concentration of 7 – 10%.

Dissolution of cellulose in aqueous NaOH can be achieved depending on molecular weight, crystalline form and the degree of crystallinity. Rheology of the cellulose/NaOH/water system was studied in detail (90). It should be mentioned that other aqueous non-alkali bases such as trimethylbenzylammonium (Triton B), dimethyl dibenzylammonium (Triton F) or guanidinium hydroxide are also able to dissolve cellulose or have mercerization-like activity (62).

Isogai has described a procedure for a complete dissolution of microcrystalline cellulose in NaOH (91). Linters cellulose, its mercerized form and cellulose III samples prepared from it had limited solubility values (26-37%) when the same procedure was carried out. Kamide and co-workers at Asahi have been applying the steam explosion treatment to dissolving pulp to make it dissolve directly in sodium hydroxide (92–94). In technical papers, they claimed a solution of 5% of steam-exploded cellulose in 9.1% NaOH at 4°C being spun into 20% H₂SO₄ at 5°C yielding fiber of poor quality.

Although NaOH/H₂O can only dissolve cellulose with low crystallinity and degree of polymerization, it may be exploited for defined shaping of the polymer. Thus, it was shown that irreversible gelation can be used for the preparation of aerogels with a large inner surface. Cylindrical gels were regenerated in water (Figure 22). Regenerated swollen-in-water cellulose samples kept their cylindrical shape with a very slight volume decrease upon drying of less than 10% (95).

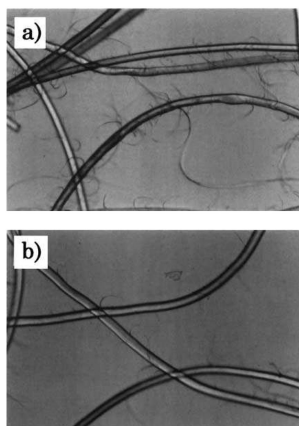


Figure 20. Fibrillation observed by optical microscopy. Photographs show the untreated original (a), and yarns treated with FeTNa solution (b). (from ref. (86) with kind permission from Springer)

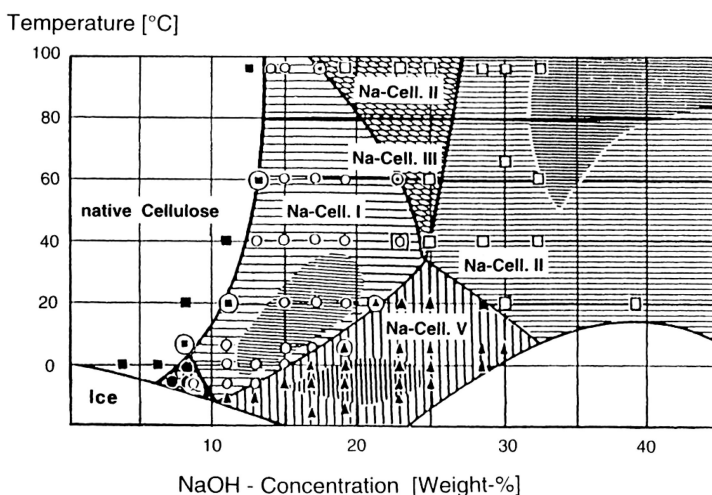


Figure 21. Phases diagram of ternary system cellulose / NaOH / water

NaOH/Poly(ethylene glycol)

A fairly new solvent system for cellulose consists of an aqueous solution of 1.0 wt.% poly(ethylene glycol) (PEG) and 9.0 wt.% of NaOH (96). Formation of a solution was confirmed by optical microscopy, ¹³C NMR and FTIR spectroscopy and intrinsic viscosity measurements. The maximum solubility of cellulose with DP around 800 in the solvent system is 13 wt.%. The solution is stable for 30 days storage at room temperature.

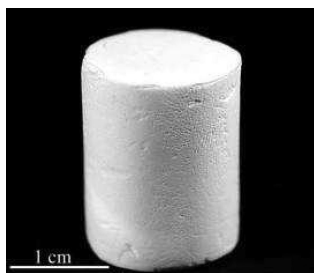


Figure 22. Example of a cylindrical aerocellulose sample obtained from 5% Avicel/NaOH/water gel. (from ref. (95))

NaOH/Urea

Quite a number of publications appeared recently on the dissolution and modification of cellulose in mixtures of an aqueous base with urea and thiourea (97–100). Zhang and co-workers have shown that cellulose can be dissolved in an aqueous solution of NaOH (7 wt %)/urea (12 wt %). Starting from a precooled mixture at -12°C cellulose dissolves within 2 min. The urea hydrates could possibly be self-assembled at the surface of the NaOH hydrogen-bonded cellulose. TEM images and WAXD provided experimental evidence on the formation of a wormlike cellulose inclusion complex being surrounded with urea (101). The solutions are rather unstable and sensitive to temperature, polymer concentration, and storage time (102, 103). Recent alternatives of interest include the systems *LiOH/urea* (104, 105) and *NaOH/thiourea* (106). These solvents were extensively studied towards the regeneration of cellulose by fiber spinning and film casting (107–111). Again cellulose materials with a huge surface were accessible via this path showing different morphologies depending on the work up (Figure 23, (112)).

Moreover, it has been shown that cellulose regeneration can be combined with blending processes. Thus, nanoparticle-containing materials were prepared (113, 114). Besides regeneration of cellulose, the homogeneous chemical modification of cellulose in this medium was intensively investigated. It was demonstrated that these aqueous media are very good solvents for homogeneous etherification reactions of cellulose (115, 116), which is reasonable because the solvent already contains the base necessary to start the reaction.

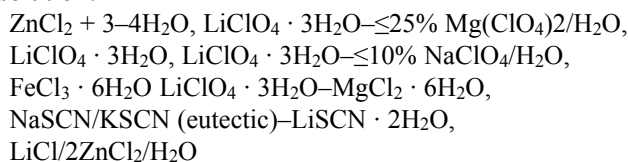
2.3. Aqueous Salt Containing Cellulose Solvents

Treatment of cellulose in aqueous solutions of inorganic salts was among the earliest attempts to solubilize the polysaccharide (117). Swelling and dissolution of cellulose in aqueous zinc chloride was observed (118). Xu and Chen (119) claimed that solutions containing 10–15% cellulose can be spun into alcohol or acetone baths to give fibers with strengths of 1.5 to 2 g/den. Formation of a complex was concluded from ^{13}C NMR measurements on cellobiose (120). Katz and Derksen (121) observed that swelling of cellulose in aqueous calcium and

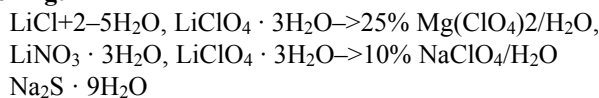
lithium thiocyanate leads to mercerization of cellulose. $\text{Ca}(\text{SCN})_2/\text{H}_2\text{O}$, $\text{LiSCN}/\text{H}_2\text{O}$ were described as effective cellulose solvents in more detail by Warwicker et.al. (122). Lukanoff et al. (123) investigated the the eutectic melt NaSCN/KSCN with different additeves and found that mixtures with $\text{Ca}(\text{SCN})_2 \cdot 3\text{H}_2\text{O}$ or DMSO are able to dissolve cellulose.

In recent years such *inorganic molten salt hydrates* or mixtures with these compounds have attracted attention as new solvents and media for polysaccharide modification. Dissolution of cellulose in $\text{Ca}(\text{SCN})_2 \cdot 3\text{H}_2\text{O}$ occurs in the temperature range from 120 to 140°C within 40 min (124). Coordination of the Ca^{2+} ions at O-6 and O-5 of cellulose backbone is reported. (125). These results were confirmed by ^{13}C and ^1H NMR measurements. A variety of other molten salt hydrates may interact in different ways with cellulose according to their structure and composition:

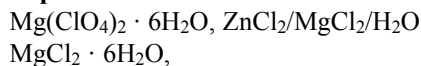
Dissolution:



Swelling:



Decomposition:



Besides the thiocyanate-containing media, molten compounds of the general formula $\text{LiX} \cdot \text{H}_2\text{O}$ ($\text{X}^- = \text{I}^-, \text{NO}_3^-, \text{CH}_3\text{COO}^-, \text{ClO}_4^-$) were found to dissolve polysaccharides including cellulose with DP values as high as 1,500 (126–128). Acetylation studies in such melts (e.g. $\text{NaSCN}/\text{KSCN}/\text{LiSCN} \cdot 2\text{H}_2\text{O}$) at 130°C using a large excess of the acetic anhydride show that the hydrolysis of the reagent is rather fast in this system.

Melts of cellulose in $\text{LiClO}_4 \cdot 3\text{H}_2\text{O}$ were applied for the carboxymethylation of cellulose using solid NaOH particles (129). Gelation occurred during the reaction. Results of the HPLC analysis after chain degradation yielded DS values in the range from 0.34 to 1.18 (Table 4) and a statistical distribution of functional groups. In contrast to other conversions in “reactive microstructure” (47, 48), the solid NaOH partially dehydrates the $\text{LiClO}_4 \cdot 3\text{H}_2\text{O}$ salt and thereby the expected reactive interface on the NaOH surface (Figure 6) is destroyed.

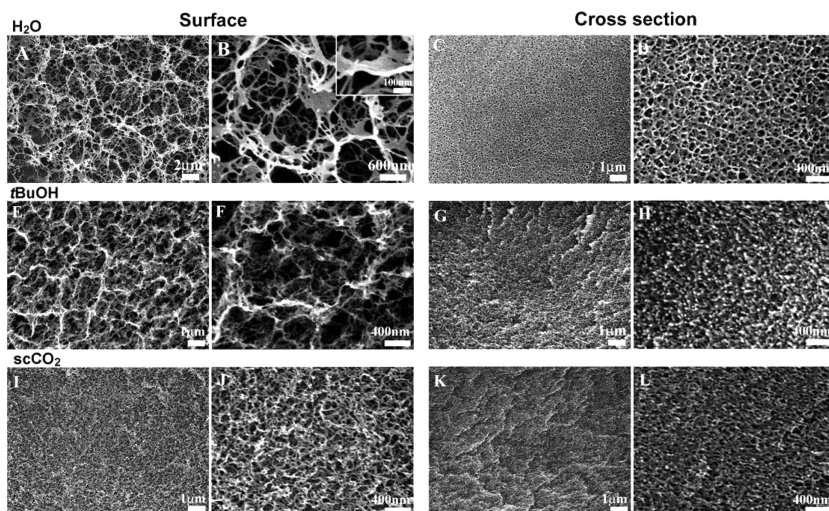


Figure 23. SEM images of aerogels prepared from 4 wt% cellulose in aqueous LiOH/urea solution, regenerated with EtOH, and either freeze-dried from H₂O (A–D) or t-BuOH (E–H), or dried from CO₂ (I–L) as indicated. Low-magnification (A,E,I) and high-magnification (B,F,J) images of the surface. Low-magnification (C, G, K) and high-magnification (D, H, L) images of the cross sections of the aerogels. The inset in part (B) shows the SEM image of a tilted sample. (from ref. (112) with kind permission from Wiley)

Thiocyanate-Containing Solutions

Systems containing thiocyanates and a polar-protic organic liquid turned out to be good cellulose solvents. Thus, dissolution of cellulose was observed in ammonia/ammonium thiocyanate (NH₃/NH₄SCN) (130, 131) and comparable mixtures including hydrazine/thiocyanates (132), hydrazine hydrate/thiocyanates and ethylene diamine/thiocyanates (133, 134). Dissolution is usually achieved by cycling the cellulose/solvent mixture through repeated freezing, thawing and mixing steps. Cuculo et al. (130) revealed that the freeze thaw cycling disrupted the hydrogen bonding between and within cellulose chains and thereby transformed the cellulose crystalline form successively from cellulose I, to cellulose II, to cellulose III, then to amorphous cellulose. Once the cellulose was amorphous, dissolution in the solvent system occurred.

In particular *ethylene diamine (EDA)/KSCN* is a promising system because it is easy to handle and flexible for cellulose processing. EDA/salt can dissolve cellulose without any pretreatment (135). Polarized light microscopy on mixtures containing KSCN, KI, NaSCN and EDA revealed that only potassium thiocyanate was capable of dissolving cellulose (Figure 24).

³⁹K and ¹⁴N NMR experiments conducted with cellobiose at different concentrations in EDA/KSCN led to the conclusion that the interaction of K⁺ ion with cellobiose is stronger than that of the SCN⁻ ion. The solubility and the dissolution rate of cellulose depend on both the solvent composition

Table 4. Conditions and Results of the Carboxymethylation of Cellulose in $\text{LiClO}_4 \cdot 3\text{H}_2\text{O}$ for 4 h at 100°C

No.	Molar ratio ^a	DS	solubility ^b
1a	1:2:4	0.34	-
2b	1:3:6	0.51	-
3c	1:3:10	0.69	+
4d	1:20:10	1.18	+

^a Anhydroglucose unit/NaOH/sodium monochloroacetate. ^b in water. Key: +, soluble; -, insoluble.

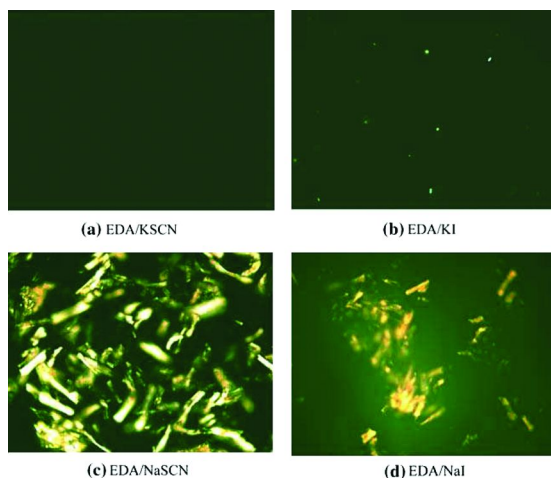


Figure 24. Polarized light microscopy images of 3 wt% of cellulose dissolved in (a) EDA/KSCN; (b) EDA/KI; (c) EDA/NaSCN; and (d) EDA/NaI. (from ref. (136) with kind permission from Springer)

and cellulose molecular weight (136). Cellulose could dissolve faster in the solvent with lower salt concentration but the highest cellulose concentration was obtained in the solvent with 30-35% KSCN. Rheological measurements showed that such cellulose solutions exhibited viscous solution behavior at low KSCN concentration but primarily elastic behavior at high salt concentration (137).

3. Non-Aqueous, Non-Derivatizing Systems

3.1. Molten Organic Salts (Ionic Liquids)

The first report on non-aqueous, non-derivatizing cellulose solvents was published in 1934 by Charles Graenacher. He applied N-alkylpyridinium salts (Figure 25) for the dissolution of cellulose and as media for homogeneous chemical reactions (13).

In 2002, studies were published on the use of comparable salts with melting points below 100°C (known today as ionic liquids (ILs)) as cellulose solvent, in particular for the regeneration of the polysaccharide (138, 139). These publications inaugurated what has become a rich new field of cellulose research. It was shown that the most promising ILs for the modification of cellulose are 1-alkyl-3-methylimidazolium salts (Figure 26).

A huge variety of ILs is known today and the number of low melting organic salts is growing rapidly. Nevertheless, according to the literature (140, 141) and our own experience, ILs with ammonium cations, pyridinium cations, and imidazolium cations are able to dissolve cellulose. Only organic salts with asymmetric cations give melts, which can properly interact with the cellulose backbone. Phosphonium and sulfonium salts studied to date have not proved suitable for cellulose dissolution. Dissolution of cellulose in pyridinium salts is combined with degradation if no protective gas is applied (see Table 5, (142)). If nitrogen is used, degradation can be diminished. Thus, the acetylation of higher molecular mass wood cellulose in the system EPyCl/pyridine was discussed as polymer-analogous reactions (143).

There is no well-accepted theory concerning the interaction between the ILs and the polymer. They are considered as non-derivatizing solvents, i.e. there are no covalent bonds observed by ¹³C NMR studies. It was concluded from ¹³C and ^{35/37}Cl-NMR experiments (144, 145) on BMIMCl solutions that the chloride anion is much more involved in the disruption of the hydrogen bond system than the cation comparable to the interaction cellulose/DMAc/LiCl (see below) (140).

Still, this finding cannot explain the fact that only ILs with nitrogen-containing cations are able to give clear solutions. No measurements are known for ILs with acetate as counter-ion, which dissolve cellulose even better than the chloride (146, 147). Recently, ILs containing formate, methyl phosphate (148–150), diethyl phosphate (151) and dicyanoamide (152) anions were described as cellulose solvents.

Thus, the dissolution mechanism is still a matter of ongoing research. 1-Alkyl-3-methylimidazolium based ILs yield clear solutions after 15 min without activation of the cellulose as demonstrated in Figure 27. Interestingly, the solubility of cellulose in such ILs is directly related to the length of the alkyl chain. But the solubility does not regularly decrease with increasing length of the alkyl chain. An odd-even effect was determined for short alkyl chains (153). Solvents that are liquid at room temperature and show low viscosities are of growing interest for cellulose modification reactions. These solvents can yield reaction media with high cellulose contents, and can facilitate gentle reaction conditions. Among the room temperature ILs (RTILs) suitable for cellulose dissolution are EMIMAc (146, 147) and the formates of allylimidazolium based ILs (148).

AMIMCl has been claimed to be a RTIL (154), but it melts at 55°C when pure. The extraordinarily low viscosities found for AMIM- and 1-allyl-3-ethylimidazolium formates make these potentially valuable ILs. Values of 66 and 67 cPas, respectively, were determined (148).

The advantage of EMIMAc is that it does not have a reactive side group such as the unsaturated function of the AMIM ion. Moreover, EMIMAc is considered to be non-toxic, non-corrosive, and even biodegradable. Surprisingly, EMIMAc

reacts with the reducing end groups of cellodextrins according to the formula depicted in Figure 28, giving a hemiacetal-type structure (155–157).

Cellulose can be regenerated from solutions in IL by precipitation into a variety of nonsolvents including water, alcohols, or acetone (138, 146, 158) allowing adjustment of topographic and morphologic features, especially in case of membranes (155). A huge amount of current work explores this path as an alternative to the traditional cellulose shaping processes and the NMNO method (138, 146, 158, 159). Both membrane preparation and fiber spinning yield high quality products (see Figure 29) making a commercial application reasonable. Even electrospinning was attempted (160) and new blend membranes with entrapped enzymes (161, 162), sensor molecules (163) or with biological activity for example with anticoagulating properties were fabricated (164, 165). ILs may offer the opportunity to dissolve intact wood or lignocellulose materials. This may lead to new methods for blending, fractionation and degradation of such materials (166–168).

Among the early attempts towards the use of organic salt melts for the homogeneous conversion of cellulose were acylation reactions of cellulose in mixtures of *N*-benzylpyridinium chloride or EPyCl with pyridine using carboxylic acid anhydrides or chlorides (13, 143). These systems were exploited for the synthesis of acetates, butyrates, benzoates, phthalates and anthranilic acid esters of cellulose. Detailed investigations of the esterification (142–171) of cellulose with different acid chlorides and anhydrides have shown that, in the case of simple aliphatic esters, complete conversion of the reagent and functionalization of all OH-moieties are possible (see Table 8 (143, 170)). Even the acetylation of high molecular mass cellulose such as bacterial cellulose with a DP of about 6500 was achieved in BMIMCl under homogeneous conditions (172).

Conversion of cellulose with complex carboxylic acids after *in situ* activation was possible in ILs (173). Thus, acylation of cellulose was performed under mild reaction conditions using AMIMCl as solvent and *N,N'*-carbonyldiimidazole (CDI) or 1-ethyl-3-(3'-dimethylaminopropyl)carbodiimide hydrochloride (EDCI) as reagents for the acid activation. This general synthetic route led to rather sophisticated cellulose derivatives such as an ester carrying a pyro-phosphoride moiety (see Figure 30).

Furthermore, esterification with dicarboxylic acid derivatives such succinic anhydride in AMIMCl (174) or in a mixture of BMIMCl/DMSO (175) was successful. The reaction efficiency was drastically increased by application of *N*-bromosuccinimide (NBS) as catalyst (176). Even reaction with unsaturated acid derivatives (e.g. 2-furoyl chloride) was achieved (177).

In case of etherification reactions in homogeneous phase, tritylation was possible with trityl chloride in the presence of pyridine (153). Regioselectively functionalized derivatives were prepared using methoxytritylation reactions (178). The commercially important hydroxyalkylation and carboxyalkylation reactions of cellulose in ILs have scarcely been studied. A patent by Myllymaeki and Aksela (179) claims etherification of this type in a large variety of ILs, but DS values, substitution pattern or properties such as viscosity are not described. A Korean patent (180) claiming hydroxyalkylation in ILs is similarly vague. From our own experience, carboxymethylation under these conditions is possible

but poorly reproducible (170). The conversion of cellulose under alkaline conditions in 1-alkyl-3-methylimidazolium salts is combined with numerous side reactions caused by the proton at position 2. This leads to an unspecific hydrolysis of the etherification reagent. The IL could not be recovered due to the ion exchange. Comparable results were published for carboxyethylation and carboxypropylation of cellulose (181) leading to rather small DS values. An alternative path would be the use of cellulose solvents with an additional alkyl function at position 2, e.g. 1-allyl-2,3-dimethylimidazolium bromide (ADMIMBr) (142) and 1-butyl-2,3-dimethylimidazolium (BDMIMCl) (142, 146) or the reaction in ammonium-type salt melts as reaction medium. Thus, recently triethylmethylammonium formate was found to be a suitable salt melt for the carboxymethylation of cellulose starting under homogeneous conditions (182). For hydroxyalkylation reactions such as hydroxyethylation or hydroxypropylation via ring opening of epoxides, EMIMAc was the solvent of choice because it shows a catalytic effect on the reaction allowing conversion without the addition of a separate base (183). During these conversions partial decomposition of the IL is observed as well. An interesting reaction leading to a cationic ether of cellulose (see Figure 31), is the conversion with choline chloride (184).

The IL employed to dissolve cellulose was a eutectic mixture of choline chloride and urea, with a molar ratio of 1/2.

Silylation of cellulose is very efficient in pure ILs or in mixtures containing a co-solvent, e.g. chloroform, to control the viscosity of the medium (185, 186). The high tendency of these TMSCs towards the formation of supramolecular structures was exploited for the preparation of pure cellulose nanoparticles (Figure 32) by a simple dialysis process.

A conversion with a comparable efficiency is the sulphation of cellulose in ILs (187). The use of co-solvents increases the yield and facilitates gentle reaction conditions, permitting both minimal depolymerization of the cellulose and almost no decomposition of the IL used. Water-soluble cellulose sulphates with low DS and high molecular weight obtained in this way are valuable materials for the formation of polyelectrolyte complexes (PECs) which can be exploited for the immobilisation of enzymes (Figure 33).

Tosylation of cellulose was achieved with AMIMCl as solvent (173). The cellulose tosylates were converted in a subsequent step with bromoundecanol in the presence of an amine to give the corresponding ether.

These examples illustrate the huge potential of the homogeneous conversion of cellulose in ILs for the preparation of tailored derivatives. It has to be noted that the purity of commercial ILs should be controlled before conducting a reaction to guarantee reproducibility. Besides water the most common impurities result from the synthesis process of the ILs. These impurities, e.g. tertiary amines, alkyl halides, methylimidazole, and metal cations may give side products during synthesis in ILs but can also act as catalysts as shown for the silylation (185). In addition ILs are not completely inert under certain reaction conditions as observed for the imidazolium cation during etherification in the presence of a base. But also the anion may interfere during chemical conversions as found for the acetate in EMIMAc (188). Nevertheless, organic salt melts are among the most promising cellulose solvents for the large scale processing of cellulose via dissolution because

they possess structural flexibility and hence they permit properties to be adjusted to a certain task. In most of the processing steps or chemical reactions they are inert and do not cause side reactions and for the majority of the processes recycling of the ILs is reasonable (189).

3.2. Amine Oxides

Again it was C. Graenacher this time together with R. Sallman who applied in 1939 for a patent on the dissolution of cellulose in amine oxides (190). Two examples of oxides that were used are shown in Figure 34.

But it was not until 1969 that Dee Lynn Johnson of Eastman Kodak described the use of cyclic mono(*N*-methylamine-*N*-oxide) compounds (Figure 35) as a solvent for strengthening paper by partially dissolving the cellulose fibres (191).

Other Johnson patents (192) covered the preparation of cellulose solutions using *N*-methylmorpholine-*N*-oxide (NMMO) and speculated about their use as dialysis membranes, food casings (sausage skins), fibers, films, paper coatings, and nonwoven binders. NMMO, which can be prepared by oxidation of *N*-methylmorpholine with hydrogen peroxide, emerged as the best of the amine-oxides and a team at American Enka demonstrated its commercial potential in the late 1970's (193–198). Thus, solutions of up to 23% cellulose were obtained by treating cellulose with NMMO/water mixtures and subsequently removing the water under vacuum (196) to adjust the concentration to the region where dissolution is achieved (see Figure 36, (199)). Moreover, processes for the defined regeneration were developed (193). After overcoming initial difficulties, such as investment costs and recovery of the expensive solvent, the process is now applied in large scale e.g. for the preparation of textile fibers under different brand names: Lyocell (Lenzing), Tencel (Courtaulds), Alceru (TITK Rudolstadt), Newcell (Akzo Nobel).

Fink, et al. have published a good review on new technical opportunities offered by these amine oxide solvents (200). Two problems are still connected with the NMMO process; the instability of the solvent and the tendency of the Lyocell fiber towards fibrillation (201–207). Due to the unique, highly crystalline structure of Lyocell, and weaker lateral links between the crystallites, the fibers undergo localized separation of fibrous elements at the surface (known as fibrillation), mainly under conditions of wet abrasion (204, 208–210). This fibrillation behavior restricts the applications of Lyocell. Suitable approaches to diminish fibrillation include treatments with an alkali, most likely NaOH (211), use of cross-linking agents or reactive dyes such as divinyl sulphone, 4,6-(*p*-beta-sulphatoethylsulphonyl)-anilino-1,3,5-triazin-2(1H)-one and the commercial Cibatex AE4425 (Figure 37, (212, 213)), enzymes and a combination of these methods (214).

The instability of NMMO may cause a safety risk due to its possible spontaneous decomposition; the mechanisms and reasons for decompositions such as ring cleavage are under investigation (215). In addition, side reactions may cause consumption of the expensive solvent and can lead to undesired staining of the cellulose regenerated. A comprehensive review on this problem

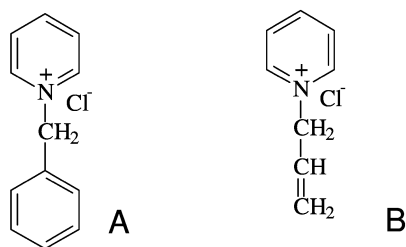


Figure 25. Two examples of *N*-alkylpyridinium salts, namely benzylpyridinium chloride (A) and allylpyridinium chloride (B) used for the dissolution of cellulose by C. Graenacher

was published by Rosenau et al. (216). It was found that in all homolytic reactions of NMMO, cleavage of the N–O bond with formation of an aminium (aminyl) radical is the first step. In contrast, reactions of C-centered tautomers of the radical with dioxygen dominate in the presence of oxygen. Transition metal ions are potent inducers of homolytic reactions of NMMO. Heterolytic reactions in the Lyocell system proceed according to three major pathways: A) reductive deoxygenation of NMMO producing *N*-methylmorpholine, B) *Polonowski* type reactions generating morpholine and formaldehyde, C) autocatalytic processes induced by carbonium–iminium ions leading to quantitative decomposition of NMMO. To stabilize the solvent additives such as propargyl gallate (217) as antioxidant, phosphates (218), bases (219), sterically hindered phenols (220) or mild reductants (221) were suggested.

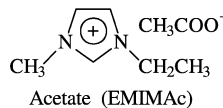
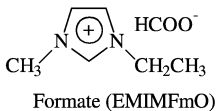
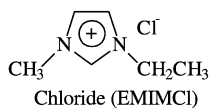
Because of the technical importance of the process there is still a lot of basic research carried out concerning the rheological behavior of the system (222), interaction between cellulose and NMMO (223), the conformation of the cellulose in NMMO (224), more detailed information on the phase diagram (225), and alternative dissolution procedures (226).

Besides fiber spinning, the NMMO system is usable for a large number of tailored cellulose modifications leading to highly porous, ultra-lightweight materials (227), filled cellulose fibers (228–231), flat cellulose films which were prepared on pre-coated substrates (Figure 38, (232)), and electrospun cellulose nanofibers (Figure 39, (233)).

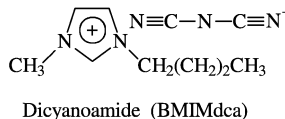
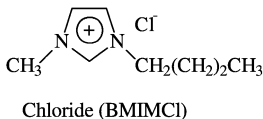
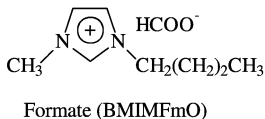
For the majority of chemical modification reactions on cellulose the NMMO system is not stable enough. Still homogeneous acetylation of the polymer dissolved in NMMO was accomplished with vinyl acetate to give a product with DS 0.3. The application of an enzyme (e.g. Proteinase N of *Bacillus subtilis*) as acetylation catalyst seems to be necessary (234). Additionally, carboxymethylation was carried out in the solvent. Both the pure NMMO as well as mixtures with DMSO can be applied. CMC with DS values up to 1.3 were accessible and the concentration of the building units obtained by HPLC after degradation of the polymer showed the typical deviation from statistically expected values. Thus, the reaction proceeds via a “reactive microstructure” even in the presence of the hydrate water of NMMO (129).

Imidazolium salts

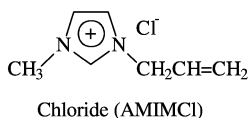
1-Ethyl-3-methylimidazolium salts



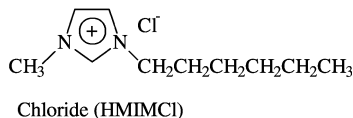
1-Butyl-3-methylimidazolium salt



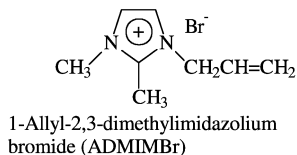
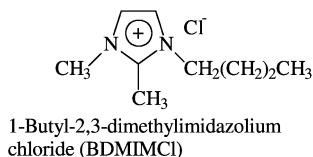
1-Allyl-3-methylimidazolium salt



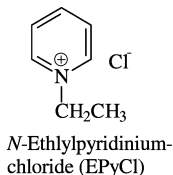
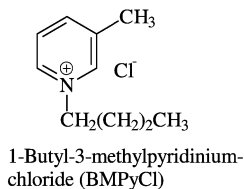
1-Hexyl-3-methylimidazolium salts



Imidazolium salts with substitution at position 2



Pyridinium salts



Ammonium salts

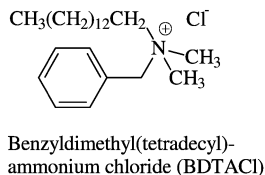


Figure 26. Examples of ILs suitable for the dissolution of cellulose

3.3. Polar, Aprotic, Organic Liquids/Salt

Li Salt Containing Solvents

The specific role of Li cations for the dissolution of cellulose was already mentioned in the chapter on aqueous salt solutions. But it is also possible to prepare non-aqueous solutions of cellulose based on Li salts. Among the first solvents in this regard was certainly *N,N*-dimethylacetamide (**DMAc**)/LiCl discovered in 1979 by Charles McCormick (235). This solvent is still a very important tool for the analysis of cellulose and for the preparation of a wide variety of derivatives

Table 5. Solubility and DP of Cellulose Samples in BMIMCl, BMPyCl, BDTACl

Cellulose		Solvent					
Type	DP	BMIMCl		BMPyCl		BDTACl	
		%	DP ^a	%	DP ^a	%	DP ^a
Avicel	286	18	307	39	172	5	327
Spruce sulfite pulp	593	13	544	37	412	2	527
Cotton linters	1198	10	812	12	368	1	966

^a After regeneration

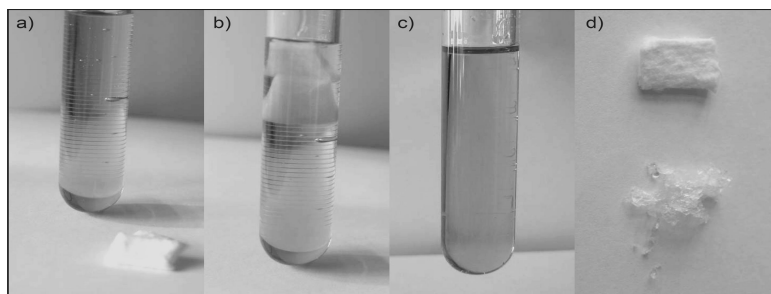


Figure 27. Picture a-c shows dissolution of cellulose (dissolving pulp) in EMIMAc within 15 min. D) shows the starting cellulose and the regenerated material

under lab scale conditions. Its usefulness in analysis is due to the fact that the solvent is colorless and dissolution succeeds without or at least with negligible degradation even in case of high molecular weight cellulose, e.g. cotton linters. Thus, it was possible to investigate the dissolved cellulose by means of ¹³C-NMR spectroscopy (236, 237) electrospray mass spectroscopy (ESI-MS, (238)), size exclusion chromatography (239–241) and light scattering techniques (242). The mechanism of cellulose dissolution in this solvent is still a topic of active research (243). Different solvent-polymer structures have been proposed (Figure 40, (237, 244, 245)).

A number of modified solvent compositions have been investigated. DMAc can be substituted in the solvent mixture with *N*-methyl-2-pyrrolidone (NMP, (246)), *N,N*-dimethylformamide (DMF, (247)), DMSO (248), 1,3-dimethyl-2-imidazolidinone (DMI, also called *N,N'*-dimethylethylene urea, DMEU, (249, 250)), *N,N'*-dimethylpropylene urea (DMPU, (248)), and hexamethylphosphoric triamide (HMPT, (251)). NMP and DMI (Figure 41) were found to dissolve the polysaccharides without major degradation and have a higher thermal stability. In case of the preparation of bromodeoxycellulose it was useful to apply LiBr (251) instead of LiCl.

Regeneration of Cellulose DMAc/LiCl and alternative Li salt containing nonaqueous solvents can be exploited for a tailored shaping of cellulose but

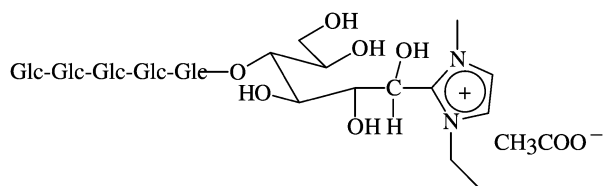


Figure 28. Structure proposed for the conversion of the reducing end group of cellodextrins with EMIMAc. (from ref. (155) with kind permission from Wiley)

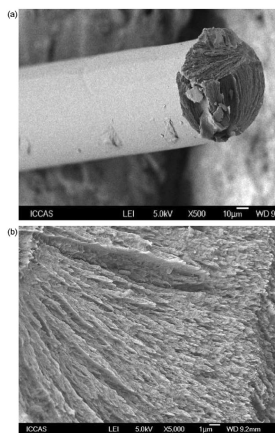


Figure 29. SEM micrographs of fracture surface of regenerated cellulose fiber from AmimCl. (from ref. (159) with kind permission from Elsevier)

incomplete recycling of the expensive solvent system still prevents large scale application.

Nevertheless, sophisticated structures are accessible. Thus, molecularly thin, smooth cellulose films could be deposited on wafer surfaces (Figure 42, (252)). The film structure depends on the cellulose coverage. If it is low, the surface is covered only by a network of cellulose fibrils.

Homogeneous Functionalization DMAc/LiCl provides a fairly inert and thermally stable solvent system for cellulose, which is still an important tool for a homogeneous conversion of the polysaccharide. The esterification of cellulose in DMAc/LiCl using carboxylic acid anhydrides and chlorides was among the first attempts towards chemical modification of the polysaccharide under totally homogeneous conditions (235, 253, 254). It was observed that cellulose in DMAc/LiCl with polymer concentrations higher than 10 % (w/w) forms mesophases. In this case, conversion of cellulose may be combined with unreproducible effects because these anisotropic systems are not fully stable (255). Nevertheless, acetates, propionates, butyrates and mixed acetates/propionates with a stoichiometric control of the acetyl content can be obtained (256, 257). Additionally, preparation of esters with long chains, e.g., n-octanoic to octadecanoic moieties was achieved with the acyl chlorides or with the fatty acid and acetic acid anhydride in the presence of HClO₄(258).

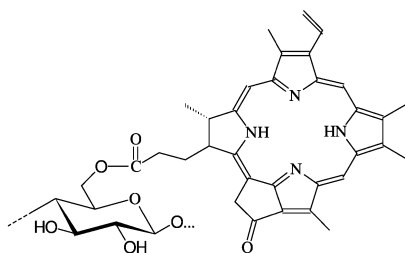


Figure 30. Structure of a cellulose ester carrying a pyro-pheophorbide moiety synthesized in AMIMCl as solvent and N,N' -carbonyldiimidazole as activating agent for the corresponding acid

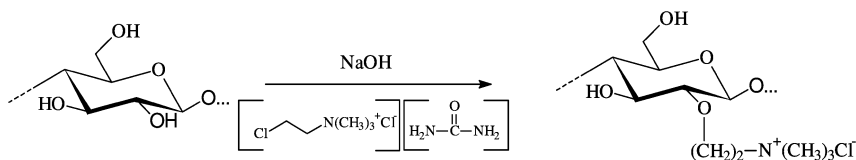


Figure 31. Cationic derivatization of cellulose in choline-urea eutectic mixture

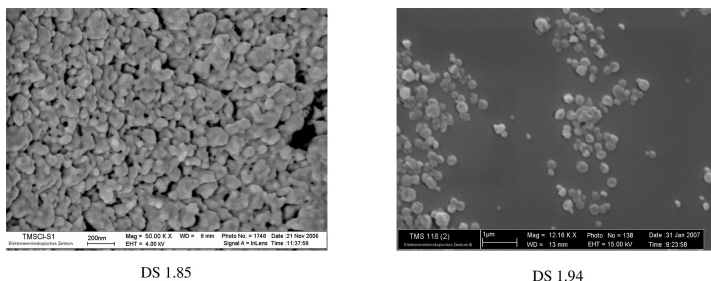


Figure 32. Scanning electron microscope images of particles prepared from trimethylsilyl cellulose with a DS of 1.85 and DS 1.94. (from ref. (185) with kind permission from Wiley)

A broad variety of halogenated, alicyclic, aromatic and unsaturated esters can be synthesized via reaction with acyl chlorides in homogeneous phase including of adamantoyl- (259), 2-furoyl- (260), 2,2-dichloropropyl- (235), and 4-phenyl-benzoyl cellulose (261). Even cellulose methacrylates with DS values of up to 1.3 were accessible, which gel when irradiated by UV due to the cross-linking reaction of lateral double bonds (262). Anhydrides of dicarboxylic acids were applied for the synthesis of water soluble carboxylic acid half esters of cellulose (263). An efficient and sophisticated method is the conversion of cellulose dissolved in DMAc/LiCl with diketene (Figure 43) or with a mixture of diketene/carboxylic acid anhydrides (264). Via this route it is possible to prepare both pure acetoacetates or mixed acetoacetate/carboxylic acid esters of cellulose (especially with acetyl and propionyl moieties). The reaction can as well be carried out in NMP/LiCl.

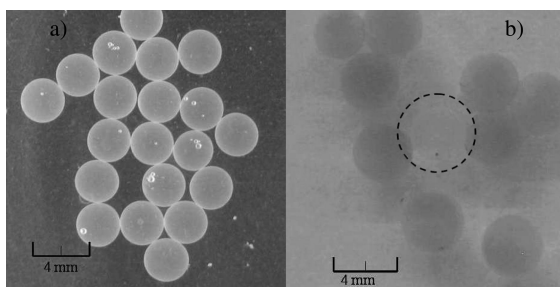


Figure 33. Polyelectrolyte simplex capsules with entrapped glucose oxidase prepared from CS 42: unmodified (a) and stained with Coomassie Brilliant Blue (b), destained capsules without enzyme are marked with a circle. (from ref. (187) with kind permission from Wiley)



Figure 34. Examples of amine-*N*-oxides suitable for cellulose dissolution: A) trimethyl-amine-*N*-oxide, B) Cyclohexyl-*N*-dimethylamine-*N*-oxide

Esterification via *in Situ* Activation

The system DMAc/LiCl was the first non-aqueous system permitting preparation of novel cellulose derivatives using unconventional techniques for polysaccharide modification, i.e. *in situ* activation of the carboxylic acid and one pot synthesis of complex derivatives not accessible with common anhydrides or chlorides. *In-situ* activation of the carboxylic acids is possible with *p*-toluenesulfonic (Tos-Cl). This path was exploited for the homogeneous derivatization of cellulose with waxy acids (ranging from C₁₂, laurylic acid, to C₂₀, eicosanoic acid) leading to derivatives with almost complete functionalization of all OH groups (265). The esters show tailored thermal transition temperatures. Additionally, introduction of fluorine-containing substituents (e.g. 2,2-difluoroethoxy-, 2,2,2-trifluoroethoxy-, and 2,2,3,3,4,4,5,5-octafluoropentoxy functions (266, 267) was achieved, giving products with adjusted hydrophobicity. Other remarkable cellulose derivatives accessible via this path include cellulose anthracene-9-carboxylate (268) and water soluble, non-ionic oxacarbonic acid esters of cellulose (269), e.g. 3,6,9-trioxadecanoic acid ester or 3,6-dioxahexanoic acid ester.

A very powerful condensation agent usable for *in situ* activation and homogeneous conversion of cellulose in DMAc/LiCl is *N,N*-dicyclohexylcarbodiimide (DCC). In combination with 4-pyrrolidinopyridine (PP) it was first exploited by Samaranayake and Glasser for the synthesis of cellulose esters in DMAc/LiCl (270). The highly toxic DCC can be recycled

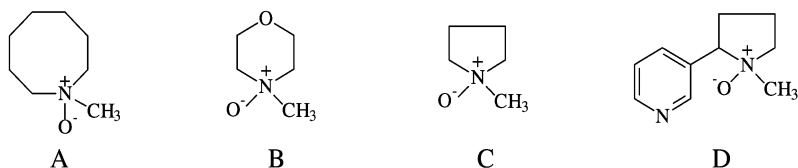


Figure 35. Examples of cyclic mono(*N*-methylamine-*N*-oxides): A) mono-*N*-methylazacyclo heptane-*N*-oxide, B) *N*-methylmorpholine-*N*-oxide, C) *N*-methylpyrrolidine-*N*-oxide, D) nicotine-1-oxide

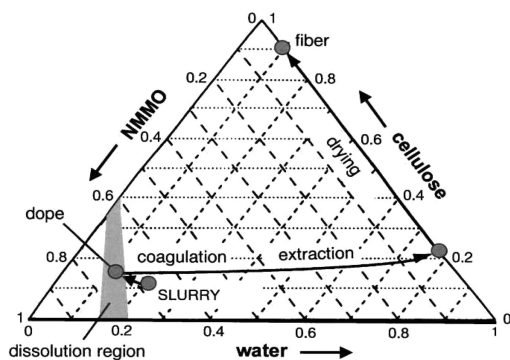


Figure 36. Phases diagram of cellulose / NMMO / water. (from ref. (200) with kind permission from Elsevier)

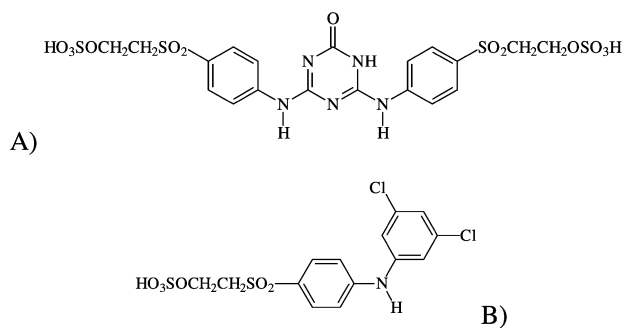


Figure 37. Structure of A) Cibatex AE4425 and B) 4,6-(*p*-beta-sulphatoethylsulphonyl)-anilino-1,3,5-triazin-2(1*H*)-one suitable for the cross-linking of cellulose chains and thereby diminishing fibrillation

from the reaction mixture. Only a modest excess of the reagent is necessary for the preparation of bulky cellulose esters (larger than butyrate) (271–273). Unsaturated esters (e.g. methacrylic-, cinnamic- and vinyl acetic acid ester) and esters of aromatic carboxylic acids including (*p*-*N,N*-dimethylamino)benzoate were synthesized using *N,N*-dimethylaminopyridine (DMAP) as catalyst (274, 275).

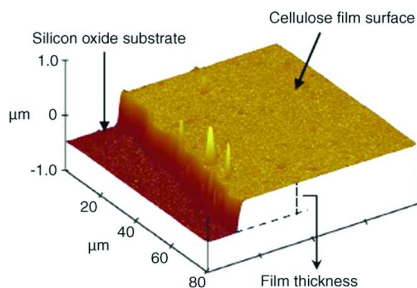


Figure 38. AFM topographical image of cellulose film. Film thickness of 30-50 nm was calculated by measuring the height difference between the top surface of the cellulose film and the silicon oxide substrate surface. (from ref. (232) with kind permission from Elsevier)

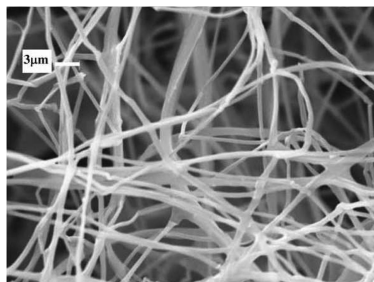


Figure 39. SEM images of electrospun fibers from DP1140 cellulose in NMMO/water. (from ref. (233) with kind permission from Elsevier)

A reagent that allows the introduction of almost any chemical functionality via homogeneous esterification of cellulose in DMAc/LiCl after activation of the acid is *N,N*-carbonyldiimidazole (CDI, Figure 44, (276)). Advantages of this method are: only CO₂ (liberated from the system) and imidazole (can be isolated and reused) are formed, no side reactions occur, very mild conditions (neutral conditions) are applied, negligible degradation is observed, and CDI is a commercial, non-toxic product which can be easily handled.

A selection of cellulose esters synthesized homogeneously in DMAc/LiCl by activation with CDI is shown in Figure 45.

Even highly reactive functions or bulky substituents were introduced without side reactions in a very effective manner. A rather new procedure is the homogeneous cellulose esterification in DMAc/LiCl after *in situ* activation with iminium chlorides (277). The reagent can be simply formed by conversion of DMF with oxalyl chloride and subsequent reaction with the acid under very mild conditions. Esterification is a “one-pot reaction” with cellulose in DMAc/LiCl. The purification is rather easy because most of the by-products are gaseous and are easily liberated from the reaction mixture.

Etherification

Soluble diphenylmethyl ethers of cellulose were prepared by etherification of the macromolecule in DMAc/LiCl (278). A summary of the reagents applied is shown in Figure 46. It was observed that the methoxy substituted reagents are converted much faster with cellulose compared to trityl chloride. They are now frequently used as protective groups. 4,4'-Bis(dimethylamino) diphenylmethyl ether show photoconducting behavior (279).

Synthesis of partially substituted carboxymethyl ethers prepared with solid NaOH as a base and monochloroacetic acid in DMAc/LiCl was the first "conversion in reactive microstructure" reported (280), leading to products with very high DS and unconventional properties (281). By means of HPLC analysis it was revealed that these CMCs contain a significantly higher amount of both tricarboxymethylated and unsubstituted units than predicted by statistical calculations and obtained for CMC synthesized in a slurry of cellulose in isopropanol/water at comparable DS values, therefore it was concluded that the distribution of substituents along the polymer chain was non-statistical. A block-like distribution of CM-functions along the chain was revealed by endoglucanase fragmentation of such CMC samples, followed by analytical and preparative SEC (282). The unconventional substitution pattern yields an unconventional supermolecular structure, i.e. a network-like system as determined by AFM (Figure 47)

These "conversions in reactive microstructure" starting from solutions in DMAc/LiCl are not limited to CMC synthesis but represent a new synthesis strategy for cellulose ethers and sulphonates with unconventional distribution of functional groups (283). Interestingly preparation of tri-*O*-allyl- and tri-*O*-crotyl cellulose in large scale was published by Sachinvala et al. (284) using solutions of cellulose in DMAc/LiCl, allyl- and crotyl chloride and powdered NaOH as base. In addition, the methylation of cellulose in DMI/LiCl yields a tris-*O*-methyl cellulose in a one step procedure (250).

Carbamate

The preparation of carbamates succeeds in high yields, at moderate temperatures and modest reagent concentrations in DMAc/LiCl (247, 253). Thus, homogeneous phase carbanilation with phenylisocyanate produces a completely functionalized derivative which has been widely adopted for the determination of molecular weights in non-aqueous solvents by means of gel permeation chromatography (GPC) (285). Furthermore, cellulose was homogeneously derivatized with pesticides using the isocyanate derivatives of, e.g. 4-amino-(1,1-dimethylethyl)-3-(methylthio)-(1,2,4)-triazine-5(4H)one (metribuzine) to obtain products with a controlled release of the bioactive compound (235).

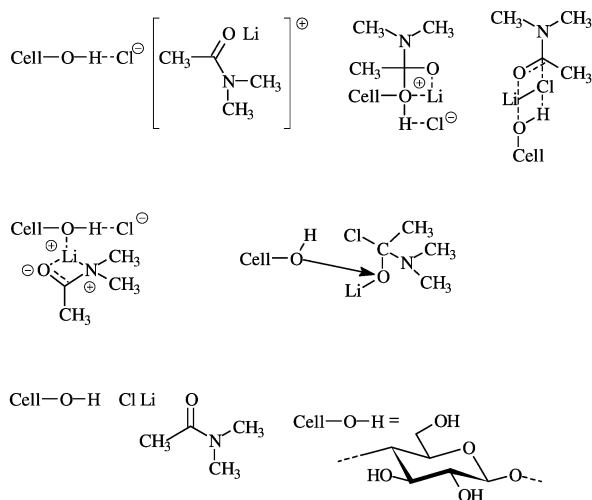


Figure 40. Solvent structures of cellulose in DMAc/LiCl. (from ref. (45) with kind permission from Springer)

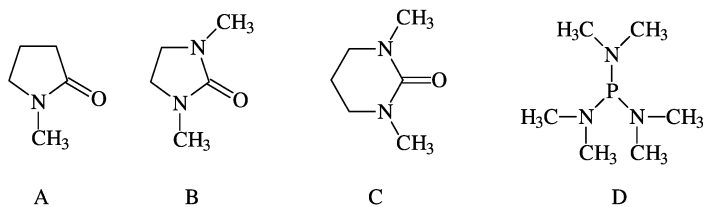


Figure 41. Structures of organic liquids A) *N*-methyl-2-pyrrolidone (NMP), B) 1,3-dimethyl-2-imidazolidinone (DMI or DMEU), C) *N,N'*-dimethylpropylene urea DMPU, D) hexamethylphosphoric triamide able to dissolve cellulose in the presence of LiCl

Silylation

Homogeneous conversion of hexamethyldisilazane with cellulose in DMAc/LiCl gives trimethylsilyl celluloses with broad range of DS values up to complete silylation (DS 2.7-2.9) of the OH groups (286, 287). On the other hand, silyl functions suitable as protective groups can be efficiently introduced via conversion in DMAc/LiCl. Homogeneous hexamethyldisilylation (TMDS) reaction in DMAc/LiCl can be used to synthesize a 2,6-di-*O*-TMDS derivative of cellulose useful for a subsequently regiocontrolled modification of position 3 (288). Alkylation at position 3, followed by treatment with tetrabutylammonium fluoride (TBAF) leads to novel compounds such as 3-*O*-allyl and 3-*O*-methyl cellulose.

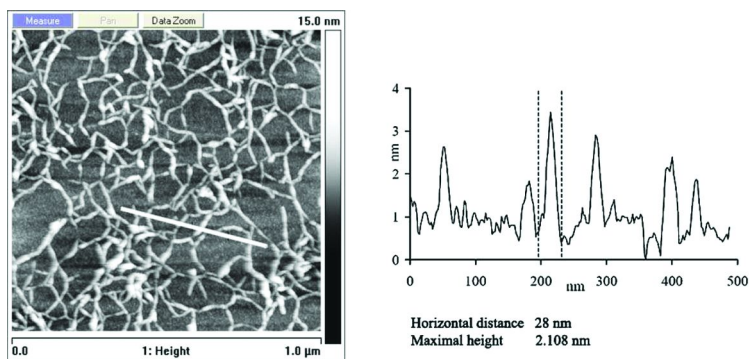


Figure 42. Image of cellulose films spin coated from 0.025 wt% cellulose solution. The section graph shows the dimensions of the cellulose fibrils network. (from ref. (252) with kind permission from Elsevier)

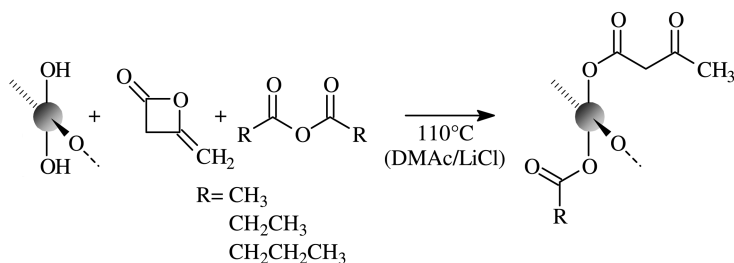


Figure 43. Synthesis of mixed cellulose acetoacetate carboxylic acid esters via conversion with mixture of diketene/carboxylic acid anhydrides. (from ref. (45) with kind permission from Springer)

Introduction of Halogendeoxy Functions

Chlorination of cellulose dissolved in DMAC/LiCl with *N*-chlorosuccinimide/triphenylphosphine is mild and selective. Initially, substitution only of the 6 hydroxyl groups is observed (289). Homogeneous synthesis of bromodeoxycellulose (Cell-Br) was carried out with *N*-bromosuccinimide-triphenylphosphine in three different media (DMF, NMP and DMAC) in combination with LiBr (290). An alternative bromination reagent consists of a mixture of tribromoimidazole, triphenylphosphine and imidazole (291). Homogeneous reactions in DMAC/LiBr yield polymers with DS values of up to 1.6, including bromination with inversion at the C-3 position.

Sulfonates

Homogeneous mesylation (292) as well as tosylation (293) in the solvent system DMAC/LiCl yield uniform and well defined products in contrast to heterogeneous processes. Tosylation has been extensively studied (294).

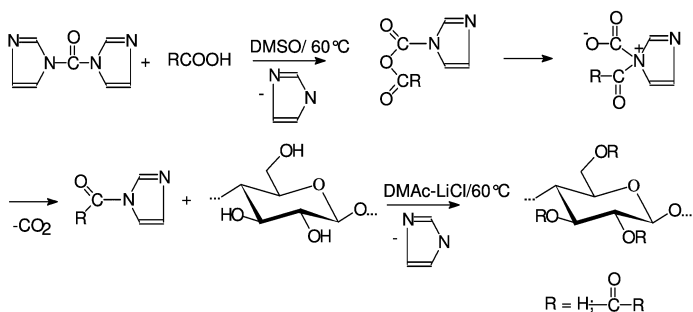


Figure 44. Esterification of cellulose with carboxylic acid in situ activated with CDI

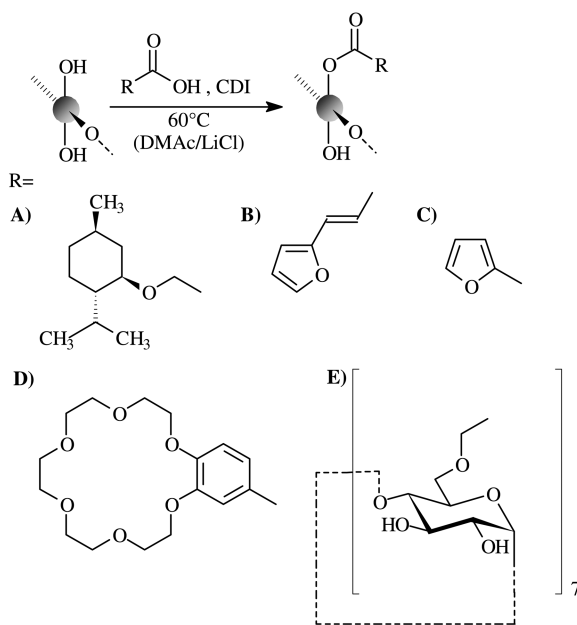


Figure 45. Conversion of cellulose with carboxylic acids applying in situ activation with CDI yielding the esters of **A)** (-)-menthyloxyacetic acid; **B)** 3-(2-furyl)-acrylcarboxylic acid; **C)** furan-2-carboxylic acid; **D)** 4'-carboxybenzo-18-crown-6; **E)** carboxymethyl- β -cyclodextrin. (from ref. (45) with kind permission from Springer)

Cellulose tosylates with DS ranging from 0.4 to 2.3 which are soluble in a variety of organic solvents can be synthesized. Additionally, soluble 5-dimethylamino-1-naphthalenesulfonyl esters of cellulose were prepared in DMAC/LiCl (295). Homogeneously prepared cellulose sulphonates are the basis for a wide variety of cellulose derivatives accessible by nucleophilic substitutions summarized by Belyakova (296) and Hon (297). A fairly new approach with

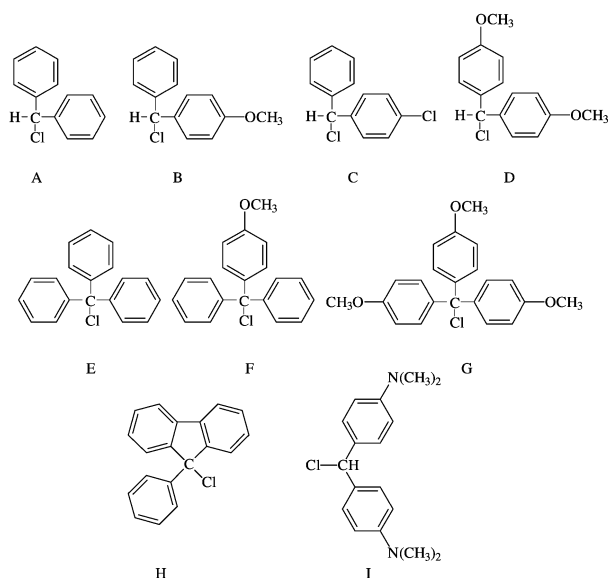


Figure 46. Di- and triphenylether moieties introduced into cellulose with the corresponding chlorides under homogeneous conversion in DMAc/LiCl

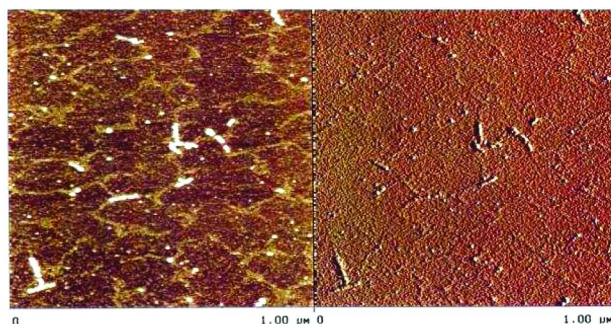


Figure 47. AFM image of CMC with a non-statistical, blocklike structure prepared via cellulose trifluoroacetate. (from ref. (129))

a wide scope is the conversion of tosylate into deoxyazido-moieties and click reactions on these functions (298).

All these examples should illustrate that DMAc/LiCl and related systems containing a Li-salt are the first choice for the efficient and tailored functionalization. Because of the high costs and the complicated recycling of the system it is still limited to lab scale application but for basic research and the preparation of high value products it is the most valuable solvent today.

The novel and powerful solvent **DMSO/TBAF·3H₂O** possesses the advantage that even cellulose with a DP as high as 650 dissolves without any pretreatment within 15 min (299). Highly resolved ¹³C NMR spectra of cellulose can be

obtained showing no hints for the formation of covalent bonds during the dissolution process.

Dewatering of DMSO/TBAF·3H₂O is possible to a certain extent by vacuum distillation but it is well known that TBAF·3H₂O degrades upon water removal, yielding FHF⁻ ions (300), which do not dissolve cellulose in combination with DMSO. Nevertheless, water free TBAF can be obtained by nucleophilic substitution of hexafluorobenzene with cyanide ions (Figure 48 (301)). The mixture with DMSO is a good cellulose solvent as well (302).

The solvent is highly efficient as reaction medium for the homogeneous esterification of polysaccharides by transesterification or by *in situ* activation of complex carboxylic acids. Acylation using acid chlorides and anhydrides is of limited utility in DMSO/TBAF·3H₂O because of side reactions with the TBAF water of hydration. The solvent is a useful medium for the esterification of crude lignocellulosic materials, for example Sisal cellulose, which contains about 14% hemicellulose (303). The DS values of cellulose acetates prepared from Sisal by reaction with acetic anhydride in mixtures of DMSO/TBAF decrease as TBAF concentration increases from 6 to 11% (Table 6) due to the increased extent of hydrolysis of the anhydride and perhaps of the product ester moieties as well. Reactions of cellulose in TBAF/DMSO of reduced water content lead to products comparable to those obtained in anhydrous DMAc/LiCl. In addition, the conversion of cellulose in DMSO/TBAF with more complex carboxylic acids (e.g. furoyl carboxylic acid) via *in situ* activation with CDI was demonstrated (304). It was also successfully applied as reaction medium for the synthesis of allyl cellulose by conversion of the polymer with allyl chloride in the presence of solid NaOH (305).

DMSO/Amine/SO₂

Other non-aqueous, non-derivatizing solvents suitable for homogeneous modification are mixtures with the general composition: polar organic liquid/SO₂/primary, secondary or tertiary aliphatic or secondary alicyclic amine. From the variety of possible mixtures dimethyl sulfoxide (DMSO)/SO₂/diethylamine is most versatile. Investigations concerning the solvent structure, i.e. the specific interaction between the polysaccharide and the components of the mixture showed that it is basically a donor acceptor interaction, i.e. this solvent is a non-derivatizing one ((306) Isogai).

Whereas acylation reactions succeed just to a limited extent, etherification with a great number of different reagents was very efficient. The homogeneous preparation of non-ionic cellulose ethers was extensively investigated by Isogai et al. (307, 308) revealing that a wide variety of completely functionalized cellulose ethers bearing alkyl- and aryl substituents can be synthesized. Usually reaction times of 3-4 h and temperatures of 60-70°C were sufficient for the complete conversion of cellulose dissolved in DMSO/SO₂/DEA with solid NaOH and the corresponding alkyl- and aralkyl halides. Tri-*O*-isopentylcellulose, tri-*O*-arylmethylethers, cellulose ethers containing double bonds and even the tri-*O*- α -naphthylmethyl ether of cellulose can be obtained.

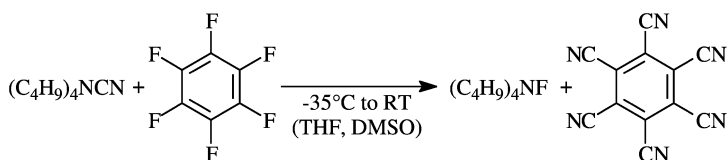


Figure 48. Preparation of anhydrous TBAF

Table 6. Influence of the amount TBAF trihydrate on the efficiency of the acetylation of Sisal cellulose with acetic anhydride in DMSO/TBAF

%TBAF in DMSO	Cellulose acetate	
	DS	Solubility
11	0.30	Insoluble
8	0.96	DMSO, Py
7	1.07	DMSO, Py
6	1.29	DMSO, DMF, Py

4. Conclusion

There is no doubt about the fact that the use of cellulose solvents will significantly broaden the portfolio of tailored and smart materials based on the unique and widely abundant biopolymer. Such solvents were involved in the first commercial processes for man made fibers and plastics, and still new paths for defined regeneration and shaping are being discovered involving dissolution of the polysaccharide. New solvents are exploited to improve the quality of commercial products such as fibers, membranes, sponges and non-woven materials. A major benefit of tailored solvents is the ability to prepare unconventional regenerated cellulose morphologies, e.g. cellulose nanoparticles, aerogels or monomolecular cellulose layers as well as new blend compounds with biological activity involving antibacterial substances, membranes with anticoagulating properties, or nanoparticle containing composites.

In contrast to commercially relevant heterogeneous reactions, homogeneous chemical modification of the cellulose backbone using specific solvents gives the opportunity to apply state of the art organic reagents and techniques to bind almost every chemical functionality on the polymer. Moreover, tailoring of the pattern of substitution is possible starting under homogeneous conditions. On the basis of the AGU it is achieved by regioselective conversion of the cellulose backbone in the dissolved state guaranteeing complete accessibility of the OH-functions. In contrast, modification after defined regeneration from the homogeneous state can give derivatives with a tailored distribution along the polymer chain such as a block-like structure.

The three cellulose solvent families discussed show that the large number of cellulose solvents accessible today may provide approaches for different tasks. Cellulose dissolution via partial derivatization, so called derivatizing solvents, intermediates or transient derivatives were the first choice for fiber spinning, yielding high quality products. Because of toxicity, high reactivity and by-product formation, alternatives for the conventional paths such as the viscose process have been investigated. New derivatizing agents could involve reactive carboxylic acid esters or boronic acid derivatives which may even permit subsequent homogeneous derivatization.

Traditionally the exploitation of aqueous cellulose solvents, i.e., Cuoxam, for the regeneration of cellulose was limited to high value products such as hollow fibers for blood dialysis because of the high costs. Still they are suitable for the analysis of cellulose. Recently a variety of solvents based on aqueous alkali (containing NaOH and urea) were developed which are rather inexpensive and easy to handle. They were shown to be suitable for fiber spinning, membrane and aerogel formation, cellulose blending and homogeneous cellulose modification. The systems are not reasonable for the esterification of the polysaccharide because hydrolysis of the esterification agents is comparably fast. In etherification reactions, especially those involving ring opening, they will certainly be interesting alternatives to common processes. The properties of products accessible by this route are now under investigation, which is the crucial criterion for the evaluation of the commercial potential of such an approach.

Non-aqueous, non-derivatizing solvents offer the largest structural diversity of the solvent families. These solvents are used today for cellulose regeneration under commercial conditions, for example in the Lyocell process, but can also generate defined regenerated morphologies such as monomolecular cellulose layers on support materials. They are still the first choice for the homogeneous functionalization of cellulose. Homogeneous esterification with state of the art synthesis tools is suitable for the introduction of almost every chemical function, at any desired DS level. Polar solvents/salt mixtures are especially useful for lab scale synthesis. ILs could make large scale homogeneous synthesis of cellulose derivatives practical. ILs can be tailored and recycled and may even provide opportunities to combine the processing of wood with the modification of cellulose.

Acknowledgements

The financial support of the “*Fachagentur Nachwachsende Rohstoffe e.V.*” (project 22021905) is gratefully acknowledged. I would like to thank K. Edgar and T. Heinze for their help during preparation of this article.

Abbreviations

AFM Atomic Force Microscopy

AGU	Anhydroglucose units
AMIMCl	1-Allyl-3-methylimidazolium chloride
BMIMCl	1-Butyl-3-methylimidazolium chloride
CA	Cellulose acetate
CF	Cellulose formate
CTFA	Cellulose trifluoroacetate
CDCA	Cellulose dichloroacetates
CDI	<i>N,N</i> -Carbonyldiimidazole
CS	Cellulose sulfate
CM	Carboxymethyl-
CMC	Carboxymethyl cellulose
DCA	Dichloroacetic acid
DMAc	<i>N,N</i> -Dimethylacetamide
DMF	<i>N,N</i> -Dimethylformamide
DMSO	Dimethylsulfoxide
DP	Degree of Polymerisation
DS	Degree of substitution
EMIMAc	1-Ethyl-3-methylimidazolium acetate
EDA	Ethylene diamine
FTIR	Fourier Transform Infrared Spectroscopy
FeTNa	Ferric sodium tartrate complex
GOD	Glucose oxidase
HPLC	High performance liquid chromatography
IL	Ionic liquid
M_N	Number average molecular weight
M_w	Weight average molecular weight
Me- α -D-glcp	Methyl- α -D-glucopyranoside
NMR	Nuclear magnetic resonance
NMNO	<i>N</i> -methylmorpholine- <i>N</i> -oxide
PBA	Phenylboronic acid
PEC	Polyelectrolyte complex
Py	Pyridine
RT	Room temperature
TBAF	Tetrabutylammonium fluoride
TEA	Triethylamine
TMS	Trimethylsilyl-
Trityl	Triphenylmethyl-
Tosyl	<i>p</i> -Toluolsulfonyl-
TFA	Trifluoroacetic acid

References

1. Otto, F. J. *Itzehoer Wochenblatt*; 1846, column 1626.
2. Audemars, G. British Patent 283, 1855.
3. Chardonnet, A. M. French Patent 165,349 (1884).

4. Parkes, A. British Patent 235, 1856.
5. Hyatt, J. W. U.S. Patent 50,359, 1865.
6. Ringsdorf, H. *Angew. Chem.* **2004**, *116*, 1082.
7. Turbak, A. F.; Hammer, R. B.; Davies, R. F.; Hegert, H. L. *Chemtech.* **1980**, *10*, 51.
8. Philipp, B.; Lukanoff, B.; Schleicher, H.; Wagenknecht, W. Z. *Chem.* **1986**, *26*, 50.
9. Heinze, T.; Liebert, T. *Prog. Polym. Sci.* **2001**, *26*, 1689.
10. Cuissinat, C.; Navard, P.; Heinze, T. *Carbohydr. Polym.* **2008**, *72*, 590.
11. Schoenbein, F. *Pogg. Ann.* **1846**, *70*, 220.
12. Schweitzer, E. J. *Prakt. Chem.* **1857**, *72*, 109.
13. Graenacher, C. U.S. Patent 1,943,176, 1934.
14. Swan, J. W. British Patent 5978, 1883.
15. Woodings, C. R. In *Regenerated cellulose fibres*; Woodings, C., Ed.; Consultant, UK Woodhead Textiles Series No. 18, 2001.
16. Schweiger, R. G. German Patent DE 2120964, 1971.
17. Wagenknecht, W.; Nehls, I.; Philipp, B. *Carbohydr. Res.* **1993**, *240*, 245.
18. Schweiger, R. G. *Tappi* **1974**, *57*, 86.
19. Cross, C. F.; Bevan, E. J.; Beadle, C. British Patent 8,700, 1892.
20. Mueller, M. British Patent 10094, 1906.
21. Polyutov, A. A.; Kleiner, Y. Y.; Irklei, V. M.; Gai'braikh, L. S. *Fibre Chem.* **2000**, *32*, 353.
22. Ott, E.; Spurlin, H. M.; Grafflin, M. W. *Cellulose and Cellulose Derivatives, Part I*; Interscience Publisher: New York, 1954.
23. Ekman, K.; Turenen, O. T.; Huttunen, J. I. Finnish Patent 61,033, 1982.
24. Hill, J. W.; Jacobson, R. A. U.S. Patent 2,134,825, 1938.
25. Jacobson, R. A. *J. Am. Chem. Soc.* **1938**, *60*, 1742.
26. Loth, F.; Schaaf, E.; Fink, H-P.; Kunze, J.; Gensrich, H.-J. PCT Patent WO002004046198A1, 2004.
27. Karstens, T.; Stein, A. Production of cellulose carbat. WO001998002464A1.
28. Schuetzenberger, P. *Compt. Rend.* **1865**, *61*, 485.
29. Philipp, B.; Wagenknecht, W.; Nehls, I.; Ludwig, J.; Schnabelrauch, M.; Kim, H. R.; Klemm, D. *Cellul. Chem. Technol.* **1990**, *24*, 667.
30. Rudy, H. *Cellulosechemie* **1931**, *13*, 49.
31. Fujimoto, T.; Takahashi, S.; Tsuji, M.; Miyamoto, M.; Inagaki, H. *J. Polym. Sci., Part C: Polym. Lett.* **1986**, *24*, 495.
32. Takahashi, S.; Fujimoto, T.; Barua, B. M.; Miyamoto, M.; Inagaki, H. *J. Polym. Sci., Part A: Polym., Chem.* **1986**, *24*, 2981.
33. Schnabelrauch, M.; Vogt, S.; Klemm, D.; Nehls, I.; Philipp, B. *Angew. Makromol. Chem.* **1992**, *198*, 155.
34. Liebert, T.; Klemm, D.; Heinze, T. *J. Macromol. Sci., Part A: Pure Appl. Chem.* **1996**, *A33*, 613.
35. Vigo, T. L.; Daighly, B. J.; Welch, C. M. *J. Polym. Sci., Part B: Polym. Phys.* **1972**, *10*, 397.
36. Liebert, T. PhD Thesis, University of Jena, German, 1995.

37. Hasegawa, M.; Isogai, A.; Onabe, F.; Usuda, M. *J. Appl. Polym. Sci.* **1992**, *45*, 1857.
38. Nehls, I.; Wagenknecht, W.; Philipp, B.; Stscherbina, D. *Prog. Polym. Sci.* **1994**, *19*, 29.
39. Cemeris, M.; Musko, N. P.; Cemeris, N. *Khim. Drev.* **1986**, *2*, 29.
40. Hawkinson, D. E.; Kohout, E.; Fornes, R. E.; Gilbert, R. D. *J. Polym. Sci., Part B: Polym. Phys.* **1991**, *29*, 1599.
41. Salin, B. N.; Cemeris, M.; Mironov, D. P.; Zatsepin, A. G. *Khim. Drev.* **1991**, *3*, 65.
42. Salin, B. N.; Cemeris, M.; Mironov, D. P. *Khim. Drev.* **1993**, *5*, 3.
43. Liebert, T.; Schnabelrauch, M.; Klemm, D.; Erler, U. *Cellulose* **1994**, *1*, 249.
44. Liebert, T.; Klemm, D. *Acta Polym.* **1998**, *49*, 124.
45. Heinze, T.; Liebert, T.; Koschella, A. *Esterification of Polysaccharides*; Springer: Heidelberg, Berlin, 2006.
46. Klemm, D.; Heinze, T.; Stein, A.; Liebert, T. *Macromol. Symp.* **1995**, *99*, 129.
47. Liebert, T.; Heinze, T. *Macromol. Symp.* **1998**, *130*, 271.
48. Liebert, T.; Heinze, T. In *Cellulose Derivatives; Modification, Characterization and Nanostructures*, Heinze, Th., Glasser, W. G., Eds.; ACS Symposium Series 688; American Chemical Society: Washington, DC, 1998; p 61.
49. Koetz, J.; Bogen, I.; Heinze, U.; Heinze, T.; Klemm, D.; Lange, S.; Kulicke, W.-M. *Papier* **1998**, *52*, 704.
50. Shigemasa, Y.; Kishimoto, Y.; Sashiwa, H.; Saimoto, H. *Polym. J.* **1990**, *22*, 1101.
51. Masson, J. F.; Manley, R. S. J. *Macromolecules* **1991**, *24*, 5914 and **1991**, *24*, 6670.
52. Saikia, C. N.; Dutta, N. N.; Borah, M. *Thermochim. Acta* **1993**, *219*, 191.
53. Clermont, L. P.; Manery, N. J. *J. Appl. Polym. Sci.* **1974**, *18*, 2773.
54. Schuyten, H. A.; Weaver, J. W.; Reid, J. D.; Juergens, J. F. *J. Am. Chem. Soc.* **1948**, *70*, 1919.
55. Weigel, P.; Gensrich, J.; Wagenknecht, W.; Klemm, D.; Erler, U.; Philipp, B. *Papier* **1996**, *50*, 483.
56. Schempp, W.; Krause, Th.; Seifried, U.; Koura, A. *Papier* **1984**, *38*, 607.
57. Mormann, W.; Demeter, J. *Macromolecules* **1999**, *32*, 1706.
58. Stein, A.; Klemm, D. *Macromol. Chem. Rapid Commun.* **1988**, *9*, 569.
59. Wagenknecht, W.; Nehls, I.; Stein, A.; Klemm, D.; Philipp, B. *Acta Polym.* **1992**, *43*, 266.
60. Klemm, D.; Stein, A.; Erler, U.; Wagenknecht, W.; Nehls, I.; Philipp, B. In *Cellulosics: Materials for Selective Separation and Other Technologies*; Kennedy, J. F., Phillips, G. O., Williams, P. A., Eds.; Ellis Horwood: New York, London, Toronto, Sydney, Tokyo, Singapore, 1993, p 221.
61. Wagenknecht, W.; Nehls, I.; Stein, A.; Klemm, D.; Philipp, B. *Acta Polym.* **1992**, *43*, 266.
62. Klemm, D.; Philipp, B.; Heinze, T.; Heinze, U.; Wagenknecht, W. *Comprehensive Cellulose Chemistry*; Wiley VCH: New York, 1998; Vol. II, p 140.

63. Engelskirchen, K.; Galinke, J. German Patent DE 24,15,154, 1975.
64. Tsas, H. E. German Patent DE 25,35,311, 1976.
65. Majewicz, T. G. U.S. Patent 4,306,061, 1981.
66. Majewicz, T. G.; Ropp, W. S. EP Patent 0,041,364, 1981.
67. Huybrechts, S.; Detemmerman, A.; De Pooter, J.; Blyweertt, R. E. PCT Patent WO 88 07059, 1988.
68. Benner, K.; Kluefers, P.; Labisch, O. *Carbohydr. Res.* **2007**, *342*, 2801.
69. Miyazaki, Y.; Yoshimura, K.; Miura, Y.; Sakashita, H.; Ishimaru, K. *Polyhedron* **2003**, *22*, 909.
70. Ferrier, R. J. *J. Chem. Soc.* **1961**, 2325.
71. Ferrier, R. J. *Adv. Carbohydr. Chem. Biochem.* **1978**, *35*, 31.
72. Meiland, M.; Heinze, T.; Guenther, W.; Liebert, T. *Tetrahedron Lett.* **2009**, *50*, 469.
73. Schweitzer, E. *J. Prakt. Chem.* **1857**, *72*, 109.
74. Despeissis, L. H. French Patent 203,741, 1890.
75. Fremerey, M.; Urban, J. German Patent 111 313, 1899.
76. Fremerey, M.; Urban, J.; Bronnert, E. German Patent 119 098, 1899.
77. Kluefers, P.; Kunte, T. *Angew. Chem., Int. Ed.* **2001**, *40*, 4210.
78. Saalwaechter, K.; Burchard, W.; Kluefers, P.; Kettenbach, G.; Mayer, P.; Klemm, D.; Dugarmaa, S. *Macromolecules* **2000**, *33*, 4094.
79. Ahlrichs, R.; Ballauff, M.; Eichkorn, K.; Hanemann, O.; Kettenbach, G.; Klufers, P. *Chem.-Eur. J.* **1998**, *4*, 835.
80. Heinze, T.; Liebert, T.; Kluefers, P.; Meister, F. *Cellulose* **1999**, *6*, 153.
81. Valtasaari, L. *Paperi Puu* **1957**, *39*, 243.
82. Achwal, W. B.; Sai, B. S. *Angew. Macromol. Chem.* **1970**, *14*, 165.
83. Jayme, G. New Solvent. In *Cellulose and Cellulose Derivatives*; Bikales, N. N., Segal, L., Eds.; Wiley: New York, 1970; Part IV, p 381.
84. Kasaai, M. R. *J. Appl. Polym. Sci.* **2002**, *86*, 2189.
85. El-Wakil, N. A.; Hassan, M. L. *J. Appl. Polym. Sci.* **2008**, *109*, 2862.
86. Kasahara, K.; Sasaki, H.; Donkai, N.; Yoshihara, T.; Takagishi, T. *Cellulose* **2001**, *8*, 23.
87. Northolt, M. G.; Boerstoel, H.; Maatman, H.; Huisman, R.; Veurink, J.; Elzerman, H. *Polymer* **2001**, *42*, 8249.
88. Liebert, T.; Seifert, M.; Heinze, T. *Macromol. Symp.* **2008**, *262*, 140.
89. Sobue, H.; Kiessig, H.; Hess, K. *Z. Phys. Chem.* **1939**, *43*, 309.
90. Roy, C.; Budtova, T.; Navard, P. *Biomacromolecules* **2003**, *4*, 259.
91. Isogai, A.; Atalla, R. H. *Cellulose* **1998**, *5*, 309–319.
92. Yamashiki, T.; Matsui, T.; Saitoh, M.; Okajima, K.; Kamide, K.; Sawada British, T. *Polym. J.* **1990**, *22*, Part 1, 73–83; Part 2, 121–128; Part 3, 201–212.
93. Yamashiki, T.; Kamide, K.; Okajima, K. In *Cellulose Sources and Exploitation*; Kennedy, J. E., Phillips, G. O., Williams, P. A., Eds.; Ellis Horwood: London, 1990; p 197.
94. Yamashiki, T.; Matsui, T.; Kowsaka, K.; Saitoh, M.; Okajima, K.; Kamide, K. *J. Appl. Polym. Sci.* **1992**, *44*, 691.
95. Gavillon, R.; Budtova, T. *Biomacromolecules* **2008**, *9*, 269.
96. Yan, L. F.; Gao, Z. *J. Cellulose* **2008**, *15*, 789.

97. Zhou, J.; Zhang, L. *Polym. J.* **2000**, *32*, 866.
98. Cai, J.; Zhang, L. *Macromol. Biosci.* **2005**, *5*, 539.
99. Cai, J.; Liu, Y.; Zhang, L. *J. Polym. Sci., Part B: Polym. Phys.* **2006**, *44*, 3093.
100. Egal, M.; Budtova, T.; Navard, P. *Cellulose* **2008**, *15*, 361.
101. Cai, J.; Zhang, L.; Liu, S.; Liu, Y.; Xu, X.; Chen, X.; Chu, B.; Guo, X.; Xu, J.; Cheng, H.; Han, C.C.; Kuga, S. *Macromolecules* **2008**, *41*, 9345.
102. Cai, J.; Zhang, L. *Biomacromolecules* **2006**, *7*, 183.
103. Qi, H. S.; Chang, C. Y.; Zhang, L. *Cellulose* **2008**, *15*, 779.
104. Liu, S. L.; Zhang, L. N. *Cellulose* **2009**, *16*, 189.
105. Cai, J.; Zhang, L.; Chang, C.; Cheng, G.; Chen, X.; Chu, B. *ChemPhysChem* **2007**, *8*, 1572.
106. Ruan, D.; Lue, A.; Zhang, L. *Polymer* **2008**, *49*, 1027.
107. Cai, J.; Zhang, L.; Zhou, J.; Li, H.; Chen, H.; Jin, H. *Macromol. Rapid Commun.* **2004**, *25*, 558.
108. Cai, J.; Zhang, L.; Zhou, J.; Qi, H.; Chen, H.; Kondo, T.; Chen, X.; Chu, B. *Adv. Mater.* **2007**, *19*, 821.
109. Cai, J.; Zhang, L.; Wang, L. *Cellulose* **2007**, *14*, 205.
110. Mao, Y.; Zhou, J.; Cai, J.; Zhang, L. *J. Membr. Sci.* **2006**, *279*, 246.
111. Zhang, L.; Mao, Y.; Zhou, J.; Cai, J. *Ind. Eng. Chem. Res.* **2005**, *44*, 522.
112. Cai, J.; Kimura, S.; Wada, M.; Kuga, S.; Zhang, L. *ChemSusChem* **2008**, *1*, 149.
113. Zhou, J.; Li, R.; Liu, S.; Li, Q.; Zhang, L.; Guan, J. *J. Appl. Polym. Sci.* **2009**, *111*, 2477.
114. Qi, H. S.; Chang, C. Y.; Zhang, L. *Green Chem.* **2009**, *11*, 177.
115. Song, Y.; Sun, Y.; Zhang, X.; Zhou, J.; Zhang, L. *Biomacromolecules* **2008**, *9*, 2259.
116. Song, Y.; Zhou, J.; Zhang, L.; Wu, X. *Carbohydr. Polym.* **2008**, *73*, 18.
117. Weimarn, P. P. *Kolloidzeitschrift* **1912**, *11*, 41.
118. Letters, K. *Kolloidzeitschrift* **1932**, *58*, 229.
119. Chen, L. F. U.S. Patent 4,999,149, 1991.
120. Xu, Q.; Chen, L. F. *Textile Techn. Int.* **1996**, *40*, 19.
121. Katz, J. R.; Derksen, J. C. *Rec. Trav. Chim.* **1930**, *50*, 149.
122. Warwicker, J. O.; Jeffries, R.; Colbran, I.; Robinson, R. N. *Shirley Institute Pamphlet*; Manchester, U.K., No. 93, 1966.
123. Lukanoff, B.; Schleicher, H.; Philipp, B. *Cellul. Chem. Technol.* **1983**, *17*, 593.
124. Kuga, S. *J. Colloid Interface Sci.* **1980**, *77*, 413.
125. Hattori, M.; Shimaya, Y.; Saito, M. *Polym. J.* **1998**, *30*, 37, 43, 49.
126. , S.Fischer; , W.Voigt; , K.Fischer *Cellulose* **1999**, *6*, 213.
127. Leipner, H.; Fischer, S.; Brendler, E.; Voigt, W. *Macromol. Chem. Phys.* **2000**, *201*, 2041.
128. Fischer, S.; Leipner, H.; Thuemmler, K.; Brendler, E.; Peters, J. *Cellulose* **2003**, *10*, 227.
129. Liebert, T.; Heinze, T. *Biomacromolecules* **2001**, *2*, 1124.
130. Cuculo, J. A.; Smith, B.; Sangwatanaroj, U.; Stejskal, E. O.; Sankar, S. S. *J. Polym. Sci., Part A: Polym. Chem.* **1994**, *32*, 229, 241.

131. Frey, M. W.; Cuculo, J. A.; Spontak, R. J. *J. Polym. Sci., Part B: Polym. Phys.* **1996**, *34*, 2049.
132. Hattori, K.; Cuculo, J. A.; Hudson, S. M. *J. Polym. Sci., Part A: Polym. Chem.* **2000**, *40*, 601.
133. Hattori, K.; Abe, E.; Yoshida, T.; Cuculo, J. A. *Polym. J.* **2004**, *36*, 123.
134. Frey, M. W.; Chan, H.; Carrancko, K. *J. Polym. Sci., Part B: Polym. Phys.* **2005**, *43*, 2013.
135. Frey, M. W.; Li, L.; Xiao, M.; Gould, T. *Cellulose* **2006**, *13*, 147.
136. Xiao, M.; Frey, M. W. *Cellulose* **2007**, *14*, 225.
137. Xiao, M.; Frey, M. W. *J. Polym. Sci., Part B: Polym. Phys.* **2008**, *46*, 2326.
138. Swatloski, R. P.; Spear, S. K.; Holbrey, J. D.; Rogers, R. D. *J. Am. Chem. Soc.* **2002**, *24*, 4974.
139. Swatloski, R. P.; Rogers, R. D.; Holbrey, J. D. PCT Patent WO 03/029329, 2003.
140. El Seoud, O. A.; Koschella, A.; Fidale, L. C.; Dorn, S.; Heinze, T. *Biomacromolecules* **2007**, *8*, 2629.
141. Zhu, S.; Wu, Y.; Chen, Q.; Yu, Z.; Wang, C.; Jin, S.; Dinga, Y.; Wu, G. *Green Chem.* **2006**, *8*, 325.
142. Barthel, S.; Heinze, T. *Green Chem.* **2006**, *8*, 301.
143. Husemann, E.; Siefert, E. *Makromol. Chem.* **1969**, *128*, 288.
144. Moulthrop, J. S.; Swatloski, R. P.; Moyna, G.; Rogers, R. D. *Chem. Commun.* **2005**, 1557.
145. Remsing, R.C.; Swatloski, R.P.; Rogers, R.D.; Moyna, G. *Chem. Commun.* **2006**, *12*, 1271.
146. Kosan, B.; Michels, C.; Meister, F. *Cellulose* **2008**, *15*, 59.
147. Hermanutz, F.; Gahr, F.; Uerdingen, E.; Meister, F.; Kosan, B. *Macromol. Symp.* **2008**, *262*, 23.
148. Fukaya, Y.; Sugimoto, A.; Ohno, H. *Biomacromolecules* **2006**, *7*, 3295.
149. Fukaya, Y.; Hayashi, K.; Wada, M.; Ohno, H. *Green Chem.* **2008**, *10*, 44.
150. Ohno, H.; Fukaya, Y. *Chem. Lett.* **2009**, *38*, 2.
151. Evlampieva, N. P.; Vitz, J.; Schubert, U. S.; Ryumtsev, E. I. *Russ. J. Appl. Chem.* **2009**, *82*, 666.
152. Liu, Q.; Janssen, M. H. A.; van Rantwijk, F.; Sheldon, R. A. *Green. Chem.* **2005**, *7*, 39.
153. Erdmenger, T.; Haensch, C.; Hoogenboom, R.; Schubert, U. S. *Macromol. Biosci.* **2007**, *7*, 440.
154. Zhang, H.; Wu, J.; Zhang, J.; He, J. *Macromolecules* **2005**, *38*, 8272.
155. Liebert, T. *Macromol. Symp.* **2008**, *262*, 28.
156. Ebner, G.; Schiehser, S.; Potthast, A.; Rosenau, T. *Tetrahedron Lett.* **2008**, *49*, 7322.
157. Handy, S. T.; Okello, M. *J. Org. Chem.* **2005**, *70*, 1915.
158. Michels, C.; Kosan, B. *Lenzinger Ber.* **2005**, *84*, 62.
159. Cao, Y.; Wu, J.; Zhang, J.; Li, H.; Zhang, Y.; He, J. *Chem. Eng. J.* **2009**, *147*, 13.
160. Xu, S.; Zhang, J.; He, A.; Li, J.; Zhang, H.; Han, C. C. *Polymer* **2008**, *49*, 2911.

161. Turner, M. B.; Spear, S. K.; Holbrey, J. D.; Rogers, R. *Biomacromolecules* **2004**, *5*, 1379.
162. Turner, M. B.; Spear, S. K.; Holbrey, J. D.; Daly, D. T.; Rogers, R. D. *Biomacromolecules* **2005**, *6*, 2497.
163. Poplin, J. H.; Swatloski, R. P.; Holbrey, J. D.; Spear, S. K.; Metlen, A.; Graetzel, M.; Nazeeruddin, M. K.; Rogers, R. D. *Chem. Commun.* **2007**, 2025.
164. Murugesan, S.; Mousa, S.; Vijayaraghavan, A.; Ajayan, P. M.; Linhardt, R. J. *J. Biomed. Mater. Res., Part B: Appl. Biomater.* **2006**, *79*, 298.
165. Viswanathan, G.; Murugesan, S.; Pushparaj, V.; Nalamasu, O.; Ajayan, P. M.; Linhardt, R. J. *Biomacromolecules* **2006**, *7*, 415.
166. Sun, N.; Rahman, M.; Qin, Y.; Maxim, M.L.; Rodríguez, H.; Rogers, R. D. *Green Chem.* **2009**, *11*, 646.
167. Tan, S. S. Y.; MacFarlane, D. R.; Upfal, J.; Edye, L. A.; Doherty, W. O. S.; Patti, A. F.; Pringle, J. M.; Scott, J. L. *Green Chem.* **2009**, *11*, 339.
168. Kilpeläinen, I.; Xie, H.; King, A.; Granstrom, M.; Heikkinen, S.; Argyropoulos, D. S. *J. Agric. Food Chem.* **2007**, *55*, 9142.
169. Wu, J.; Zhang, J.; Zhang, H.; He, J.S.; Ren, Q.; Guo, M. *Biomacromolecules* **2004**, *5*, 266.
170. Heinze, T.; Schwikal, K.; Barthel, S. *Macromol. Biosci.* **2005**, *5*, 520.
171. Zhang, J.; Wu, J.; Cao, Y.; Sang, S.; Zhang, J.; He, J. *Cellulose* **2009**, *16*, 299.
172. Schlufter, K.; Schmauder, H.P.; Dorn, S.; Heinze, T. *Macromol. Rapid Commun.* **2006**, *27*, 1670.
173. Granstroem, M.; Kavakka, J.; King, A.; Majoinen, J.; Maekelae, V.; Helaja, J.; Hietala, S.; Virtanen, T.; Maunu, S.-L.; Argyropoulos, D.S.; Kilpeläinen, I. *Cellulose* **2008**, *15*, 481.
174. Liu, C. F.; Sun, R. C.; Zhang, A. P.; Ren, J. L.; Wang, X. A.; Qin, M. H.; Chaod, Z. N.; Luod, W. *Carbohydr. Res.* **2007**, *342*, 919.
175. Liu, C. F.; Sun, R. C.; Zhang, A. P.; Ren, J. L.; Wang, X. A.; Geng, Z. C. *Polym. Degrad. Stab.* **2006**, *91*, 3040.
176. Liu, C. F.; Zhang, A. P.; Li, W.-Y.; Yue, F.-X.; Sun, R. C. *J. Agric. Food Chem.* **2009**, *57*, 1814.
177. Koehler, S.; Heinze, T. *Cellulose* **2007**, *14*, 489.
178. Granstroem, M.; Olszewska, A.; Maekelae, V.; Heikkinen, S.; Kilpeläinen, I. *Tetrahedron Lett.* **2009**, *50*, 1744.
179. Myllymaeki, V.; Aksela, R. PCT Patent WO 2005054298A1, 2005.
180. Park, Y. S.; Park, J. H. Korean Patent KR 2006086069, 2006.
181. Mikkola, J.-P.; Kirilin, A.; Tuuf, J.-C.; Pranovich, A.; Holmbom, B.; Kustov, L. M.; Murzina, D. Y.; Salmia, T. *Green Chem.* **2007**, *9*, 1229.
182. Koehler, S.; Liebert, T.; Heinze, T. *Macromol. Biosci.* **2009**, DOI: 0.1002/mabi.200900156.
183. Koehler, S.; Liebert, T.; Heinze, T.; Vollmer, A.; Mischnick, P.; Moellmann, E.; Becker, W. *Cellulose* **2009**, submitted.
184. Abbott, A. P.; Bell, T. J.; Handa, S.; Stoddart, B. *Green Chem.* **2006**, *9*, 784.
185. Koehler, S.; Liebert, T.; Heinze, T. *J. Polym. Sci., Part A: Polym. Chem.* **2008**, *46*, 4070.

186. Mormann, W.; Wezstein, M. *Macromol. Biosci.* **2009**, *9*, 369.
187. Gericke, M.; Liebert, T.; Heinze, T. *Macromol. Biosci.* **2009**, *9*, 343.
188. Koehler, S.; Liebert, T.; Schoebitz, M.; Schaller, J.; Meister, F.; Guenther, W.; Heinze, T. *Macromol. Rapid Commun.* **2007**, *28*, 2311.
189. Liebert, T.; Heinze, T. *Bioresources* **2008**, *3*, 576.
190. Graenacher, C.; Sallman, R. U.S. Patent 2,179,181, 1939.
191. Johnson, D. L. U.S. Patent 3,447,939, 1969.
192. Johnson, D. L. U.S. Patent 3,508,941, 1970.
193. Franks, N. E.; Varga, J. K. U.S. Patent 4,145,532, 1979.
194. Franks, N. E.; Varga, J. K. U.S. Patent 4,196,282, 1980.
195. McCorsley, C. C. Belgian Patent 868,735, 1978.
196. McCorsley, C. C.; Varga, J. K. U.S. Patent 4,142,913, 1979.
197. McCorsley, C. C. Belgian Patent 875,323, 1979.
198. McCorsley, C. C. Belgian Patent 871,428, 1979.
199. Wachsmann, U.; Diamantoglou, M. *Das Papier* **1997**, *51*, 660.
200. Fink, H. P.; Weigel, P.; Purz, H. J.; Ganster, J. *Prog. Polym. Sci.* **2001**, *26*, 1473.
201. Bredereck, K.; Hermanutz, F. *Rev. Prog. Color.* **2005**, *35*, 59.
202. Fang, K.; Hao, L.; Hu, X.; Shao, H. *Text. Res. J.* **2003**, *73*, 1013.
203. Kasahar, K.; Sasaki, H.; Donkai, N. *Sen'I Seihin Shohi, Kagaku* **2003**, *44*, 480.
204. Karypidis, M.; Wilding, M. A.; Carr, C. M.; Lewis, D. M. *AATCC Rev.* **2001**, *1*, 40.
205. Nicolai, M.; Nechwatel, A.; Mieck, K.-P. *Melliand Textilber.* **1999**, *80*, 848.
206. Mieck, K.-P.; Nicolai, M.; Nechwatel, A. *Melliand Int.* **1997**, *1*, 34.
207. Nicolai, M.; Nechwatel, A.; Mieck, K.-P. *Text. Res. J.* **1996**, *66*, 575.
208. Bredereck, K.; Hermanutz, F. *Rev. Prog. Color* **2005**, *35*, 59.
209. (a) Zhang, W. S.; Okubayashi, S.; Bechtold, T. *Cellulose* **2005**, *12*, 267. (b) Zhang, W.; Okubayashi, S.; Bechtold, T. *Cellulose* **2005**, *12*, 275. (c) Zhang, W.; Okubayashi, S.; Bechtold, T. *Carbohydr. Polym.* **2005**, *59*, 173; (d) Zhang, W.; Okubayashi, S.; Bechtold, T. *Carbohydr. Polym.* **2005**, *61*, 427.
210. Abdullah, I.; Blackburn, R. S.; Russell, S. J.; Taylor, J. *J. Appl. Polym. Sci.* **2006**, *102*, 1391.
211. Goswami, P.; Blackburn, R.; El-Dessouky, H. M.; Taylor, J.; White, P. *Eur. Polym. J.* **2009**, *45*, 455.
212. Bates, I.; Maudru, E.; Phillips, D. A. S.; Renfrew, A. H. M. *Color. Technol.* **2006**, *112*, 270.
213. Bates, I.; Phillips, D. A. S.; Renfrew, A. H. M. *Color. Technol.* **2007**, *123*, 163.
214. Zhang, W.; Okubayashi, S.; Badura, W. *J. Appl. Polym. Sci.* **2006**, *100*, 1176.
215. Konkin, A.; Wendler, F.; Meister, F.; Roth, H.-K.; Aganov, A.O. *Ambacher Spectroch. Acta Part A: Mol. Biomol. Spectr.* **2008**, *69*, 1053.
216. Rosenau, T.; Potthast, A.; Sixta, H.; Kosma, P. *Prog. Polym. Sci.* **2001**, *26*, 1763.
217. Brandner, A.; Zengel, H. G. German Patent DE 3,034,685, 1980.
218. Laity, P. R. PCT Int. Appl. 8,304,415, 1993.

219. Reusche, F. H.; Schoen, P.; Wiesener, W.; Taeger, E.; Schleicher, H.; Lukanoff, B. German Patent 218104, 1985.
220. Michels, C.; Mertel, H. German Patent 229708, 1985.
221. Lukanoff, B.; Schleicher, H. German Patent 158656, 1983.
222. Blachot, J.-F.; Chazeau, L.; Cavaille, J.-Y. *Polymer* **2002**, *43*, 881.
223. Zhao, H.; Kwak, J. H.; Wang, Y.; Franz, J. A.; White, J. M.; Holladay, J. E. *Carbohydr. Polym.* **2007**, *67*, 97.
224. Rosenau, T.; Hofinger, A.; Potthast, A.; Kosma, P. *Polymer* **2003**, *44*, 6153.
225. Biganska, O.; Navard, P. *Polymer* **2003**, *44*, 1035.
226. Doganand, H.; Hilmioglu, N.D. *Carbohydr. Polym.* **2009**, *75*, 90.
227. Liebner, F.; Potthast, A.; Rosenau, T.; Haimer, E.; Wendland, M. *Holzforschung* **2008**, *62*, 129.
228. Vorbach, D.; Taeger, E. *Techn. Text.* **1998**, *41*, 67.
229. Vorbach, D.; Schulze, T.; Taeger, E. *Techn. Text.* **1998**, *41*, 188.
230. Zikeli, S. *Chem. Fibers Int.* **2001**, *51*, 272.
231. Nechwatal, A.; Michels, C.; Kosan, B.; Nicolai, M. *Cellulose* **2004**, *11*, 265.
232. Kim, C.-W.; Kim, D.-S.; Kang, S.-Y.; Marquez, M.; Joo, Y. L. *Polymer* **2006**, *47*, 5097.
233. Yokota, S.; Kitaoka, T.; Wariishi, H. *Appl. Surf. Sci.* **2007**, *253*, 4208.
234. Kloh, E. A.; Koch, W.; Klemm, D.; Dicke, R. German Patent DE 19951734, 2000.
235. McCormick, C. L.; Lichatowich, D. K. *J. Polym. Sci., Part B: Polym. Lett. Ed.* **1979**, *17*, 479.
236. Nehls, I.; Wagenknecht, W.; Philipp, B. *Cellul. Chem. Technol.* **1995**, *29*, 243.
237. El-Kafrawy, A. *J. Appl. Polym. Sci.* **1982**, *27*, 2435.
238. Striegel, A. M.; Timpa, J. D.; Piotrowiak, P.; Cole, R. B. *Int. J. Mass Spectrom. Ion Proc.* **1997**, *162*, 45.
239. Striegel, A. M.; Timpa, J. D. *Carbohydr. Res.* **1995**, *267*, 271.
240. Silva, A. A.; Laver, M. L. *TAPPI J.* **1997**, *80*, 173.
241. Hasegawa, M.; Isogai, A.; Onabe, F. *J. Chromatogr.* **1993**, *635*, 334.
242. Sjoeholm, E.; Gustafsson, K.; Eriksson, B.; Brown, W.; Colmsjoe, A. *Carbohydr. Polym.* **2000**, *41*, 153.
243. El Seoud, O. A.; Regiani, A. M.; Frollini, E. In *Natural Polymers and Agrofibers Composites*; Frollini, E., Leao, A. L., Mattoso, L. H. C., Eds.; USP-IQSC: Sao Carlos, Brazil, 2000; p 73.
244. Philipp, B. *J. Macromol. Sci., Part A: Pure Appl. Chem.* **1993**, *A30*, 703.
245. Spange, S.; Reuter, A.; Vilsmeier, E.; Heinze, T.; Keutel, D.; Linert, W. *J. Polym. Sci., Part A: Polym. Chem.* **1998**, *36*, 1945.
246. El-Kafrawy, A. *Lenzinger Ber.* **1983**, *55*, 44.
247. Morgenstern, B.; Kammer, H. *TRIP* **1996**, *4*, 87.
248. Petrus, L.; Grey, D. G.; BeMiller, J. N. *Carbohydr. Res.* **1995**, *268*, 319.
249. Helinger, H.; Hengstberger, M. *Lenzinger Ber.* **1985**, *59*, 96.
250. Takaragi, A.; Minoda, M.; Miyamoto, T.; Liu, H. Q.; Zhang, L. N. *Cellulose* **1999**, *6*, 93.
251. Turbak, H. F.; Sakthivel, A. *Chem. Tech.* **1990**, *20*, 444.
252. Sczech, R.; Riegler, H. *J. Colloid Interface Sci.* **2006**, *301*, 376.

253. McCormick, C. L.; Dawsey, T. R. *Macromolecules* **1990**, *23*, 3606.
254. McCormick, C. L.; Chen, T. S. In *Macromolecular Solutions, Solvent-Property Relationships in Polymers*; Symor, R. B., Stahl, G. A., Eds.; Pergamon Press: New York, 1982; p 101.
255. Guo, J.-X.; Gray, D. G. In *Cellulosic Polymers, Blends and Composites*; Gilbert, R. D., Ed.; Hanser Publ.: Munich, Vienna, New York, 1994, p 25.
256. Regiani, A. M.; Frollini, E.; Marson, G. A.; Arantes, G. M.; El Seoud, O. A. *J. Polym. Sci., Part A: Polym. Chem.* **1999**, *37*, 1357.
257. Marson, G. A.; El Seoud, O. A. *J. Appl. Polym. Sci.* **1999**, *74*, 1355.
258. Vaca-Garcia, C.; Thiebaud, S.; Borredon, M.W.; Gozzelino, G. *J. Am. Oil Chem. Soc.* **1998**, *75*, 315.
259. Graebner, D.; Liebert, T.; Heinze, T. *Cellulose* **2002**, *9*, 193.
260. Hon, D. N.; Yan, H. J. *J. Appl. Polym. Sci.* **2001**, *81*, 2649.
261. Terbojevich, M.; Cosani, A.; Focher, B.; Gastaldi, G.; Wu, W.; Marsano, E.; Conio, G. *Cellulose* **1999**, *6*, 71.
262. Marsano, E.; De Paz, L.; Tambuscio, E.; Bianchi, E. *Polymer* **1998**, *39*, 4289.
263. Diamantoglou, M.; Kuhne, H. *Papier* **1988**, *42*, 690.
264. Edgar, K. J.; Arnold, K. M.; Blount, W. W.; Lawniczak, J. E.; Lowman, D. W. *Macromolecules* **1995**, *28*, 4122.
265. Sealey, J. E.; Samaranyake, G.; Todd, J. G.; Glasser, W. G. *J. Polym. Sci., Part B: Polym. Phys.* **1996**, *34*, 1613.
266. Sealey, J. E.; Frazier, C. E.; Samaranyake, G.; Glasser, W. G. *J. Polym. Sci., Part B: Polym. Phys.* **2000**, *38*, 486.
267. Glasser, W. G.; Becker, U.; Todd, J. G. *Carbohydr. Polym.* **2000**, *42*, 393.
268. Koschella, A.; Haucke, G.; Heinze, T. *Polym. Bull.* **1997**, *39*, 597.
269. Heinze, T.; Schaller, J. *Macromol. Chem. Phys.* **2000**, *201*, 1214.
270. Samaranyake, G.; Glasser, W. G. *Carbohydr. Polym.* **1993**, *22*, 1.
271. Dave, V.; Glasser, W. G. *J. Appl. Polym. Sci.* **1993**, *48*, 683.
272. Glasser, W. G.; Samaranyake, G.; Dumay, M.; Dave, V. *J. Polym. Sci., Part B: Polym. Phys.* **1995**, *33*, 2045.
273. Edgar, K. J.; Pecorini, T. J.; Glasser, W. G. In *Cellulose Derivatives; Modification, Characterization and Nanostructures*; Heinze, T., Glasser, W. G., Eds.; ACS Symposium Series 688; American Chemical Society: Washington, DC, 1998; p 38.
274. Zhang, Z. B.; McCormick, C. L. *J. Appl. Polym. Sci.* **1997**, *66*, 293.
275. Williamson, S. L.; McCormick, C. L. *J. Macromol. Sci., Part A: Pure Appl. Chem.* **1998**, *A35*, 1915.
276. Liebert, T.; Heinze, T. *Biomacromolecules* **2005**, *6*, 333.
277. Hussain, M. A.; Liebert, T.; Heinze, Th. *Polym. News* **2004**, *29*, 14.
278. Erler, U.; Klemm, D.; Nehls, I. *Makromol. Chem., Rapid Commun.* **1992**, *13*, 195.
279. Heinze, T.; Erler, U.; Heinze, U.; Camacho, J. A.; Grummt, U.-W.; Klemm, D. *Macromol. Chem. Phys.* **1995**, *196*, 1937.
280. Heinze, Th.; Erler, U.; Nehls, I.; Klemm, D. *Angew. Makromol. Chem.* **1994**, *215*, 93.
281. Koetz, J.; Bogen, I.; Heinze, Th.; Heinze, U.; Kulicke, W.-M.; Lange, S. *Colloids Surf., A* **2001**, *183*, 621.

282. Saake, B.; Horner, S.; Kruse, Th.; Puls, J.; Liebert, T.; Heinze, T. *Macromol. Chem. Phys.* **2000**, *201*, 1996.
283. Einfeldt, J.; Heinze, T.; Liebert, T.; Kwasniewski, A. *Carbohydr. Polym.* **2002**, *49*, 357.
284. Sachinvala, N. D.; Winsor, D. L.; Hamed, O. A.; Maskos, K.; Niemczura, W. P.; Tregre, G. J.; Glasser, W. G.; Bertoniere, N. R. *J. Polym. Sci., Part A: Polym. Chem.* **2000**, *38*, 1889.
285. Terbojevich, M.; Cosani, A.; Camilot, M.; Focher, B. *J. Appl. Polym. Sci.* **1995**, *55*, 1663.
286. Schempp, W.; Krause, T.; Seifried, U.; Koura, A. *Papier* **1984**, *38*, 607.
287. Klemm, D.; Schnabelrauch, M.; Stein, A.; Philipp, B.; Wagenknecht, W.; Nehls, I. *Papier* **1990**, *44*, 624.
288. Koschella, A.; Klemm, D. *Macromol. Symp.* **1997**, *120*, 115.
289. Furuhashi, K.-I.; Chang, H.-S.; Aoki, N.; Sakamoto, M. *Carbohydr. Res.* **1992**, *230*, 151.
290. Furuhashi, K.-I.; Koganai, K.; Chang, H.-U.; Aoki, N.; Sakamoto, M. *Carbohydr. Res.* **1992**, *230*, 165.
291. Furuhashi, K.-I.; Aoki, N.; Suzuki, S.; Sakamoto, M.; Saegusa, Y.; Nakamura, S. *Carbohydr. Polym.* **1995**, *26*, 25.
292. Frazier, C. E.; Glasser, W. G. *Polym. Prepr. (Am. Chem. Soc., Div. Polym. Chem.)* **1990**, *31*, 634.
293. McCormick, C. L.; Dawsey, T. R.; Newman, J. K. *Carbohydr. Res.* **1990**, *208*, 183.
294. Rahn, K.; Diamantoglou, M.; Berghmans, H.; Heinze, T. *Angew. Makromol. Chem.* **1996**, *238*, 143.
295. Heinze, Th.; Camacho, J. A.; Haucke, G. *Polym. Bull.* **1996**, *37*, 743.
296. Belyakova, M. K.; Gal'braikh, L. S.; Rogovin, Z. A. *Cellul. Chem. Technol.* **1971**, *5*, 405.
297. Hon, D. N.-S. Chemical Modification of Cellulose. In *Chemical Modification of Lignocellulosic Materials*; Hon, D.N.-S., Ed., Marcel Dekker: New York, Basel, Hong Kong, 1996, p 114.
298. Liebert, T.; Haensch, C.; Heinze, T. *Macromol Rapid Commun.* **2006**, *27*, 208.
299. Heinze, Th.; Dicke, R.; Koschella, A.; Kull, A.; Klohr, E.-A.; Koch, W. *Macromol. Chem. Phys.* **2000**, *201*, 627.
300. Sharma, R. K.; Fry, J. L.; James, L. J. *Org. Chem.* **1983**, *48*, 2112.
301. Sun, H.; DiMagno, S. G. *J. Am. Chem. Soc.* **2005**, *127*, 2050.
302. Koehler, S.; Heinze, T. *Macromol. Biosci.* **2007**, *7*, 307.
303. Ciacco, G. T.; Liebert, T. F.; Frollini, E.; Heinze, T. *J. Cellulose* **2003**, *10*, 125.
304. Hussain, M.A.; Liebert, T.; Heinze, T. *Macromol Rapid Commun.* **2004**, *25*, 916.
305. Heinze, T.; Lincke, T.; Fenn, D.; Koschella, A. *Polym. Bull.* **2008**, *61*, 1.
306. Isogai, A.; Ishizu, A.; Nakano, J. *J. Appl. Polym. Sci.* **1987**, *33*, 1283.
307. Isogai, A.; Ishizu, A.; Nakano, J. *J. Appl. Polym. Sci.* **1984**, *29*, 2097, 3873.
308. Isogai, A.; Ishizu, A.; Nakano, J. *J. Appl. Polym. Sci.* **1986**, *31*, 341.

Chapter 2

Design of Polar Ionic Liquids To Solubilize Cellulose without Heating

Yukinobu Fukaya, Kensaku Hayashi, Seung Seob Kim and
Hiroyuki Ohno*

Department of Biotechnology, Tokyo University of Agriculture & Technology,
2-24-16 Naka-cho, Koganei, Tokyo 184-8588, Japan

*ohnoh@cc.tuat.ac.jp

Polar ionic liquids containing methylphosphonate anions are potential solvents for cellulose. To study the effect of cation structure on the solubility of cellulose, we coupled alkylimidazolium, alkylpiperidinium and alkylammonium cations with the methylphosphonate anion. The physico-chemical properties of the resulting ionic liquids, including thermal properties, hydrogen bonding strength and viscosity have been analyzed in detail. Also their capability to dissolve cellulose has been analyzed. All ionic liquids evaluated in this study were obtained as salts having relatively low melting point (below 55 °C); eight ionic liquids were room temperature ionic liquids. All ionic liquids studied here had relatively strong hydrogen bonding characteristics, especially hydrogen bond basicity. 1-Alkyl-3-methylimidazolium methylphosphonates, except for 1-hydroxyethyl-3-methylimidazolium salt, successfully dissolved 10 wt% of cellulose below 60 °C as a result of their strong hydrogen bond basicity. The lesser solubility of cellulose in 1-hydroxyethyl-3-methylimidazolium salt was attributed to its lower hydrogen bond basicity than the other ILs. Hydrogen bond acidity of ILs was also found to influence the dissolving of cellulose. The temperatures necessary to dissolve 2, 6, and 10 wt% cellulose under mixing for 30 min depended strongly on the hydrogen bond acidity of the ILs. ILs composed of either 1-alkyl-2,3-dimethylimidazolium cation, triethyl-methylammonium cation, or 1-ethyl-1-methylpiperidinium cation exhibited lower hydrogen

bond acidity than 1-alkyl-3-methylimidazolium salts, and were found to be less effective in dissolving cellulose. Among various ILs analyzed, 1,3-dimethylimidazolium methylphosphonate dissolved cellulose best even under mild conditions.

Introduction

It is important to seek materials to replace petroleum and other decreasing natural fuel resources. Cellulose is an attractive starting material for earth-friendly products and is the most abundant biomacromolecule produced on the planet (1). It is now recognized as a cheap raw material for the synthesis of glucose, bioethanol, and other chemicals (2). Nevertheless there are still some obstacles to the use of cellulose. It is a linear polymer, which aggregates to form bundles that are stabilized and stiffened by intra- and inter-molecular hydrogen bonds. The many hydrogen bonds between cellulose chains lead to the formation of highly ordered crystalline regions which are not adequately solvated by water or conventional organic solvents. There have been many attempts to find solvents that dissolve cellulose. In particular, salt / molecular solvent mixed systems have been proposed (3). To improve the solubilization, ionic liquids (ILs) are used (4).

ILs are organic salts designed to melt below 100 °C, preferably at or below room temperature (5). ILs are currently undergoing vigorous investigation as a result of their unique combination of features that includes very low vapor pressure, low flammability, high thermal stability and structural diversity (6). In 2002, Swatloski et al. made the first report that heated alkylimidazolium chloride could dissolve cellulose (7). Cellulose product fabrication (8), derivatization by a homogeneous system (9), and analysis of molecule characteristics (10) have since been undertaken with these chloride salts. Moreover, increasing effort has been directed at biomass processing, i.e., isolation of cellulose from wood samples (11) and hydrolysis of cellulose in chloride salts (12). These results all indicate that polar ILs are versatile solvents for cellulose. Polar ILs should be important in the design of solvents for cellulose. To this end, knowledge of the relation between ion structure and ability to dissolve cellulose is basic to the design of ILs as solvents for biomass.

Recent studies have found that anions, acting as a strong hydrogen bond base, have the capability to be an important component in the design of ILs. For instance, alkylimidazolium acetates were found to dissolve cellulose (13); several acetate-type ILs and even cellulose solutions in these acetate salts are now commercially available. We have also examined an alkylimidazolium carboxylate series as solvents for cellulose (14). We found that alkylimidazolium salts combined with a carboxylate group having a shorter alkyl chain, such as formate, were obtained as low melting, low viscosity polar ILs, which dissolved cellulose under mild conditions (15). We have recently proposed a new class of ILs as solvents for cellulose (16). Alkylimidazolium cations combined with dimethyl phosphate or methyl phosphonate anions exhibit strong hydrogen

bonding basicity and dissolve cellulose. In particular, methylphosphonate ($[(\text{MeO})(\text{H})\text{PO}_2]^-$) salt dissolved cellulose under mild conditions. These results show that choice and design of anion species is important in the preparation of ILs that dissolve cellulose.

A variety of cations have been used for preparation of ILs, such as alkylimidazolium, alkylpyrrolidinium, tetraalkylammonium, and their derivatives (17). Physico-chemical properties of the resulting ILs, such as electrostatic interaction forces, melting temperature, polarity and viscosity, have been found to depend on the cation structure. This should allow us to design better ILs as solvents for cellulose. Indeed, alkyl substituents on the imidazolium cation influence the solubility of cellulose (3). Heinze et al. found using aliphatic ammonium salts and alkylpyridinium that the solubility of cellulose is related to the structure of the cations (18). Zhang et al. have studied the effect of cationic structure on the solubilization of cellulose (19). They proposed a dissolution mechanism of cellulose in ILs in which both cation and anion interact with the hydroxyl groups of cellulose. Although these previous papers observe that the solubility of cellulose depends on the cation structure of ILs, the effects of cation structure on the solubilization of cellulose have scarcely been analyzed. In the present study we prepared a series of ILs with methylphosphonate ($[(\text{MeO})(\text{H})\text{PO}_2]^-$) in order to examine the effect of alkyl chains attached to the *N*-position of the imidazolium ring, as well as the effect of further cation structure, on the ability of the corresponding ILs to dissolve cellulose.

The alkyl side chain and the basic structure of the cation both strongly affect the physico-chemical properties of the IL. We first study the effects of cation structure on the capability of the ILs to dissolve cellulose.

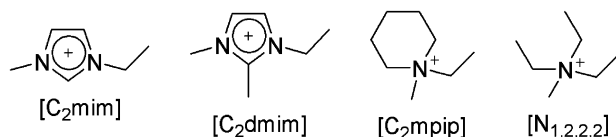
We prepared six ILs based on a series of cations having the ethyl or methyl group, namely 1-ethyl-3-methylimidazolium ($[\text{C}_2\text{mim}]^+$), 1-ethyl-2,3-dimethylimidazolium ($[\text{C}_2\text{dmim}]^+$), triethyl-methylammonium ($[\text{N}_{1,2,2,2}]^+$), 1-ethyl-1-methylpiperidinium ($[\text{C}_2\text{mpip}]^+$), 1-ethyl-1-methylpyrrolidinium ($[\text{C}_2\text{mpyr}]^+$), and 1-methylpyridinium ($[\text{C}_1\text{pyl}]^+$), with $[(\text{MeO})(\text{H})\text{PO}_2]^-$ anion. The $[\text{C}_1\text{pyl}]$ salt gradually turned to a dark brown liquid during the reaction, and signals in $^1\text{H-NMR}$ spectra due to impurities were observed even after the sample had been washed repeatedly with anhydrous diethyl ether. In the case of $[\text{C}_2\text{mpyr}]$ salt, the product decomposed readily to acidic compounds after drying, as a result of decomposition of the cation. We were therefore unable to study these two salts.

Effect of Basic Structure of Cation

Table I sets out melting temperature (T_m), glass transition temperature (T_g) and decomposition temperature (T_{dec}) of our ILs prepared with cations as shown in Chart 1. Among the ILs obtained, both $[\text{C}_2\text{dmim}][(\text{MeO})(\text{H})\text{PO}_2]$ and $[\text{C}_2\text{mpip}][(\text{MeO})(\text{H})\text{PO}_2]$ were solid at room temperature.

Differential scanning calorimetry (DSC) analysis determined that $T_m = 50$ °C for $[\text{C}_2\text{dmim}][(\text{MeO})(\text{H})\text{PO}_2]$ and $T_m = 40$ °C for $[\text{C}_2\text{mpip}][(\text{MeO})(\text{H})\text{PO}_2]$. For the room temperature IL $[\text{C}_2\text{mdeam}][(\text{MeO})(\text{H})\text{PO}_2]$, $T_m = 2$ °C. As reported

Chart 1. Chemical structure of cations.



previously, ILs based on dialkylimidazolium cations are thermally stable, in contrast to alkylammonium salts. Our present results are in good agreement with the literature (20).

The polarity of the ILs prepared here has been estimated via the Kamlet–Taft parameters (α : hydrogen bond acidity, β : hydrogen bond basicity, π^* : dipolarity/polarizability) (16, 18). Table I also lists the Kamlet–Taft parameters of our series of ILs. Since both $[C_2dmim][(MeO)(H)PO_2]$ and $[C_2mpip][(MeO)(H)PO_2]$ were solid at room temperature, the Kamlet–Taft parameters for these two ILs were tentatively determined at around 60 °C. $[C_2mim][(MeO)(H)PO_2]$ had a larger value of α than aliphatic or cyclic ammonium salts. Spectroscopic analysis indicates that the proton on the 2-position of the imidazolium ring contributes to the hydrogen bond acidity (21). Indeed, the α value of $[C_2dmim][(MeO)(H)PO_2]$ was 0.33, much less than that of $[C_2mim][(MeO)(H)PO_2]$. Tetraalkylammonium and dialkylpiperidinium salts also have weaker hydrogen bond acidity owing to the loss of hydrogen bond donor. The weak proton-donating nature of these $[C_2mpip]$ and $[N_{1,2,2,2}]$ cations clearly weakened the hydrogen bonding with the anion species.

Although the value of β depends mainly on the anion species, β depends also on the cation structure. In regard to the value of β , we have reported previously that $[(MeO)(H)PO_2]$ has greater hydrogen bonding capability, especially hydrogen bond basicity, than conventional ILs (22). The series of $[(MeO)(H)PO_2]$ salts prepared here also displayed relatively strong hydrogen bond basicity. Moreover, the β value for $[N_{1,2,2,2}]$ and $[C_2mpip]$ salts was 1.04 and 1.08 respectively, greater than those of a series of alkylimidazolium cation based ILs. Consequently, ILs composed of $[(MeO)(H)PO_2]$ anion and aliphatic or cyclic ammonium cations interact effectively with probe dyes, so that these ILs have higher β value than $[C_2mim][(MeO)(H)PO_2]$.

The dipolarity/polarizability (π^*) was slightly affected by the cation structure. For instance, $[C_2dmim][(MeO)(H)PO_2]$ and $[N_{1,2,2,2}][(MeO)(H)PO_2]$ have slightly higher π^* value than $[C_2mim][(MeO)(H)PO_2]$ and $[C_2mpip][(MeO)(H)PO_2]$. The π^* value of ILs depends on the interaction between ions and the probe dye, *N,N*-diethyl-4-nitroaniline, according to the local electric field (22). Hence, the difference in π^* should reflect the degree of delocalization of positive charge on the cation.

Figure 1 shows the temperature dependence of the viscosity of these ILs. The viscosity of these ILs depends strongly on the cation structure. For example, viscosity of these salts is in the range 25–155 cP at 55 °C, in the following order: $[C_2mim]$ salt (25 cP) < $[N_{1,2,2,2}]$ salt (54 cP) < $[C_2dmim]$ salt (97 cP) < $[C_2mpip]$ salt (155 cP). It is clear that both the ion size and degree of delocalization of the positive

Table I. Physicochemical Properties of ILs

<i>Cations</i>	T_g^a	T_m^a	T_{dec}^b	α	β	π^*
[C ₂ mim] ⁺	-86	— ^c	275	0.52	1.00	1.06
[C ₂ dmim] ⁺	— ^c	50	280	0.33 ^a	1.01 ^a	1.11 ^a
[C ₂ mpip] ⁺	-66	40	260	0.29 ^b	1.08 ^b	1.08 ^b
[N _{1,2,2,2}] ⁺	-81	2	244	0.29	1.04	1.14

^a Temperature (°C) for signal peak, ^b Temperature (°C) at 10 % weight loss, ^c not detected

charge influence the viscosity of the corresponding IL reflecting the interaction force among these ions.

To design ILs as solvents for cellulose, we should choose the anion species carefully. In a study of relaxation times as a function of cellobiose concentration, Moyna et al. found that the anions interact mainly with sugar unit, especially hydroxyl groups (10). Spectroscopic and chromatographic analysis have shown that anions having strong hydrogen bond basicity are necessary to dissolve cellulose (22). However, in this study, solubility of cellulose was found to depend on the cation structure when the same anion was used. Aliphatic and cyclic ammonium salts had greater hydrogen bond basicity than [C₂mim] salts, so that they were expected to dissolve cellulose readily. However, solubilization temperature of cellulose in these ILs was much higher than in [C₂mim][(MeO)(H)PO₂] (Table II). For instance, to dissolve 2 wt% cellulose in [N_{1,2,2,2}][(MeO)(H)PO₂] it was necessary to stir the sample at 100 °C for several hours. Moreover, the [C₂mpip], [C₂dmim] and [N_{1,2,2,2}] salts were unable to dissolve 10 wt % cellulose even after stirring at 100 °C for 30h. As mentioned above, aliphatic and cyclic ammonium salts exhibit weaker hydrogen bond acidity than alkylimidazolium salts. The solubilization temperature of cellulose increased with decreasing hydrogen bond acidity of these ILs. A study of the polarity of cellulose found that it has high hydrogen bonding characteristics; strong hydrogen bonding is also required to adequately dissolve cellulose (23). Consequently, aliphatic and cyclic ammonium salts with weak hydrogen bond acidity are inferior at dissolving cellulose.

In the case of [C₂mim] salt, these cellulose solutions (2–10 wt %) showed no phase separation upon cooling to room temperature or during storage at room temperature for at least several months. They also maintained their homogeneous state even after storage at lower temperature (ca. 5 °C) for several months. These observations imply that these ILs interact well with cellulose molecules. Conversely, a cellulose solution of [N_{1,2,2,2}][(MeO)(H)PO₂] underwent gradual phase separation during cooling of the solution to room temperature. We believe that weak interaction between cellulose molecules with [N_{1,2,2,2}][(MeO)(H)PO₂] owing to this low hydrogen bond acidity is a possible explanation of these results;

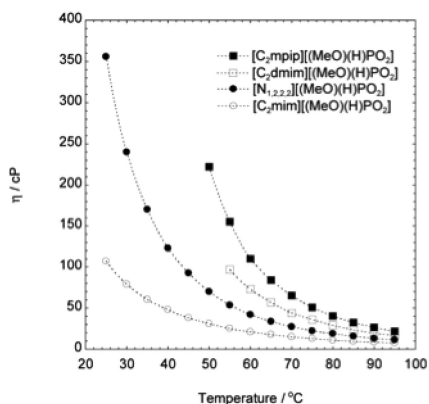


Figure 1. Temperature dependence of viscosity for a series of ILs as seen in Chart 1

detailed investigations of the interaction of the cation with the cellulose chain are under way.

Effects of the Side Chain Attached to the N-Position of the Imidazolium Ring on Solubility of Cellulose

As mentioned, imidazolium based ILs are potential solvents for dissolving cellulose under mild conditions, such as stirring without heating. Several researchers have determined that the structure of the alkyl side chain affects the solubility of cellulose. We next studied the influence of the side chain attached to the N-position of the imidazolium ring. As shown in Chart 2, we prepared seven 1-alkyl-3-methylimidazolium salts having various alkyl side chains.

All imidazolium-based ILs obtained here were liquids at room temperature. According to the DSC measurements shown in Table III, $T_m = 38\text{ }^\circ\text{C}$ for $[\text{C}_1\text{mim}][(\text{MeO})(\text{H})\text{PO}_2]$ and $T_m = 52\text{ }^\circ\text{C}$ for $[\text{C}_2\text{OHmim}][(\text{MeO})(\text{H})\text{PO}_2]$. Nevertheless, both ILs were obtained as room temperature ILs. $[\text{C}_1\text{mim}][(\text{MeO})(\text{H})\text{PO}_2]$ was crystallized by maintaining it at $-20\text{ }^\circ\text{C}$ for several days. In contrast, no crystallization was observed when $[\text{C}_2\text{OHmim}][(\text{MeO})(\text{H})\text{PO}_2]$ was stored at $-20\text{ }^\circ\text{C}$ for a week. These observations imply that $[\text{C}_2\text{OHmim}][(\text{MeO})(\text{H})\text{PO}_2]$ can exist in a relatively stable supercooled state.

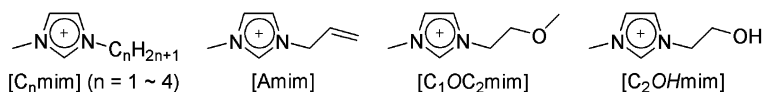
For the other ILs, T_g was in the range -66 to $-86\text{ }^\circ\text{C}$; see Table III. No peaks assigned to freezing or melting were found in the DSC analysis, even when these ILs were cooled slowly and heated at $1\text{ }^\circ\text{C}/\text{min}$. Moreover, crystallization was not observed even when these ILs were stored at $-20\text{ }^\circ\text{C}$ for several months. This observation suggests that these ILs are in stable molten or supercooled states. The asymmetric structure of the anions and cations is expected to lead to poor packing of ions.

Table II. Solubilization temperature of cellulose in methylphosphonate salts under stirring for 30 min

Cations	Solubilization temperature (°C)		
	2 wt%	6 wt%	10 wt%
[C ₂ mim] ⁺	Room temp.	30	40
[C ₂ dmim] ⁺	90	95	>100
[C ₂ mpip] ⁺	85	95	>100
[N _{1,2,2,2}] ⁺	100 ^a	>100	>100

^a stirred for 6h

Chart 2. Chemical structure of cations.



The thermal decomposition temperatures (T_{dec}) of [Rmim][(MeO)(H)PO₂] salts were higher than 270 °C for all salts except [Amim] and [C₂OHmim] salts. In general, allylimidazolium salts have lower T_g or T_m , and also slightly lower T_{dec} , than other 1-alkyl-3-methylimidazolium salts (24).

We next determined the Kamlet–Taft parameters of these alkylimidazolium salts. For these ILs, α lay in the range 0.51 - 0.63. As seen in the first six rows, there is no significant influence of the alkyl side chain on the α value. [C₂OHmim][(MeO)(H)PO₂] has greater hydrogen bond acidity than any other IL evaluated here. We attribute this to the terminal hydroxyl group of [C₂OHmim][(MeO)(H)PO₂]. The π^* value of the ILs was based on the interaction between ions and *N,N*-diethyl-4-nitroaniline, as stated above. Consequently, differences in π^* should be due to the degree of delocalization of the positive charge on the cation. The hydrogen bond basicity of ILs is largely affected by the nature of the anion. Although all ILs evaluated here have the same anion ([(MeO)(H)PO₂]⁻), the β value of [C₂OHmim][(MeO)(H)PO₂] ($\beta = 0.91$) was a little lower than that of 1-alkyl-3-methylimidazolium salts ($\beta = 0.98$ to 1.02). The strong hydrogen bond acidity of [C₂OHmim][(MeO)(H)PO₂] gives rise to a strong interaction between cation and anion, so that there is a weak interaction between [C₂OHmim][(MeO)(H)PO₂] and 4-nitroaniline, lowering the value of β for this IL.

We next evaluated the viscosity of a series of imidazolium-based ILs as shown in Figure 2. For these ILs, the viscosity increased with increasing alkyl chain length. This should be explicable in terms of cation size, van der Waals interaction, and T_g values. Viscosity was lower for [Amim][(MeO)(H)PO₂] than for [C₃mim][(MeO)(H)PO₂], whereas both cations have almost the same alkyl chain length. In general, the imidazolium cation bearing an allyl group had lower viscosity than those with a propyl group, owing to the configurational rotation of the allyl group (27). Moreover, viscosity was slightly

Table III. Physicochemical properties of ILs

<i>Cations</i>	T_g	T_m	T_{dec}	α	β	π^*
[C ₁ mim] ⁺	– <i>c</i>	38	271	0.53	0.99	1.08
[C ₂ mim] ⁺	–86	– <i>c</i>	275	0.52	1.00	1.06
[C ₃ mim] ⁺	–79	– <i>c</i>	277	0.54	1.00	1.02
[C ₄ mim] ⁺	–77	– <i>c</i>	277	0.52	1.02	1.01
[Amim] ⁺	–82	– <i>c</i>	256	0.51	0.99	1.06
[C ₁ OC ₂ mim] ⁺	–72	– <i>c</i>	279	0.51	0.98	1.07
[C ₂ OHmim] ⁺	–67	52	242	0.63	0.91	1.06

a temperature (°C) at signal peak, *b* temperature (°C) at 10 % weight loss, *c* not detected.

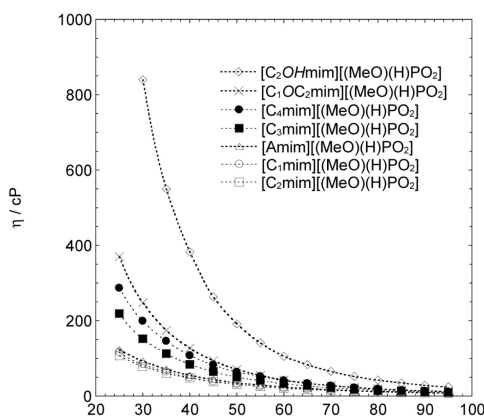


Figure 2. Temperature dependence of viscosity for a series of imidazolium type ILs as seen in Chart 2

higher for [C₁OC₂mim] [(MeO)(H)PO₂] than for [C₄mim] [(MeO)(H)PO₂]; also [C₂OHmim] [(MeO)(H)PO₂] has much higher viscosity than any other 1-alkyl-3-methylimidazolium-based ILs studied here. These findings are attributed to their hydrogen bonding strength.

Since this series of ILs have both strong hydrogen bond basicity and acidity, these ILs were expected to dissolve cellulose. Table IV lists the solubilization temperature of cellulose (2, 6, and 10 wt%) in a series of ILs under stirring for 30 min.

Among a series of methylphosphonate salts evaluated here, the solubilization temperature depends on the cation structure of the ILs used (Table IV). Aliphatic and cyclic ammonium salts with weak hydrogen bond acidity were less effective in dissolving cellulose. Hence, [C₂OHmim] salt, for which α is much higher than any other IL studied here, should be more effective at dissolving cellulose. In fact, [C₂OHmim] salt dissolved cellulose at higher temperature than other 1-alkyl-

Table IV. Solubility of cellulose in a series of methylphosphonate-type ILs

Cations	Solubilization temperature (°C) ^a		
	2 wt%	6 wt%	10 wt%
[C ₁ mim] ⁺	25	30	35
[C ₂ mim] ⁺	25	30	40
[C ₃ mim] ⁺	35	40	45
[C ₄ mim] ⁺	40	45	50
[Amim] ⁺	30	35	40
[C ₁ OC ₂ mim] ⁺	35	40	45
[C ₂ OHmim] ⁺	70	100	>100

^a stirred for 30 min

3-methylimidazolium based ILs. Moreover, this IL did not dissolve 10 wt % cellulose even after mixing at 100 °C for 24 h. [C₂OHmim] salt has lower β ($\beta = 0.91$) than other ILs. Accordingly, cellulose was less soluble in [C₂OHmim] salt.

In this study, we evaluated the ability of ILs as solvents for cellulose by comparing the temperature to give homogeneous solution of cellulose after 30 min mixing at each temperature. Under such conditions, alkyl chain length of the [Rmim] cation was found to affect the solubilization of cellulose. All [Rmim][(MeO)(H)PO₂] successfully dissolved 10 wt% cellulose at temperatures lower than 60 °C, but the solubilization temperature of cellulose increased with increasing alkyl chain length of the imidazolium cation. For instance, to dissolve 2 wt% cellulose, [C₁mim][(MeO)(H)PO₂] and [C₂mim][(MeO)(H)PO₂] do not need heating, but [C₄mim][(MeO)(H)PO₂] salt requires heating to 45 °C. In the case of alkylimidazolium chloride salts, the solubility of cellulose at 100 °C decreased with increasing alkyl chain length (7). Our results are in agreement with the previous study, despite much greater solubility. Rogers *et al.* gave the explanation that the effect of long alkyl chains was directly related to lower Cl anion concentration through the mass-effect (7). However, the solubilization temperature of cellulose in [Amim][(MeO)(H)PO₂], which has almost the same anion concentration as [C₃mim][(MeO)(H)PO₂] in the bulk, was slightly lower than the solubilization temperature in [C₃mim][(MeO)(H)PO₂]. The viscosity of [Amim][(MeO)(H)PO₂] was lower than that of [C₃mim][(MeO)(H)PO₂]; cellulose powder was therefore dispersed more readily in [Amim][(MeO)(H)PO₂] than in [C₃mim][(MeO)(H)PO₂] for a limited mixing time (30 min). Cellulose may therefore dissolve in [Amim][(MeO)(H)PO₂] at a lower temperature than in [C₃mim][(MeO)(H)PO₂]. For the dissolution process within short period of mixing time, the viscosity of ILs is an important factor.

Of course, viscosity is not the only factor influencing the solubility of cellulose. [C₁OC₂mim] salt dissolved cellulose at a lower temperature than [C₄mim], but the viscosity of the former was greater. The *n*-butyl group was less polar than the methoxyethyl side chain. A recent NMR study by Moyna *et al.*

also indicated that the butyl and methyl group of 1-*n*-butyl-3-methylimidazolium chloride had no specific interaction with cellulose (20). Consequently, [C₄mim][(MeO)(H)PO₂] should be less effective in dissolving cellulose, and cellulose was indeed more soluble in [C₁OC₂mim] salt than in [C₄mim] salt.

Conclusion

We have prepared a series of methyl phosphonate ([MeO)(H)PO₂] based ILs with various cations and analyzed their ability to dissolve cellulose. These RTILs had high polarity, especially high hydrogen bonding basicity. The dissolving of cellulose in these ILs depended strongly on their cationic structure. Of these [MeO)(H)PO₂] based ILs, 1-alkyl-3-methylimidazolium salts dissolved cellulose, even at high concentrations, as a result of their high hydrogen bonding acidity. 1,3-Dimethylimidazolium and 1-ethyl-3-methylimidazolium cations were superior to the other cations examined. Conversely, cellulose was less soluble in aliphatic and cyclic ammonium salts with weaker hydrogen bonding acidity. However, 1,3-dialkylimidazolium salts, a hydroxyl group was introduced onto the alkyl chain end, was inferior at dissolving cellulose, these ILs have the greatest hydrogen bonding acidity of the ILs prepared here. The anion species is the major factor that determines the solubility of cellulose, but the present findings indicate that the choice of cation is also important for the design of ILs as solvents for cellulose.

Acknowledgements

This study was supported by a Grant-in-Aid for Scientific Research from the Ministry of Education, Culture, Sports, Science and Technology of Japan (#21225007). This study was also supported by the Nissan Science Foundation (Grant No. 320142).

References

1. Klemm, D.; Heublein, B.; Fink, H-P.; Bohn, A. *Angew. Chem., Int. Ed.* **2005**, *44*, 3358–3393.
2. (a) Himmel, M. E.; Ding, S-Y.; Johnson, D. K.; Andey, W. S.; Nimlos, M. R.; Brady, J. W.; Foust, T. D. *Science*, **2007**, *315*, 804–807. (a) Galbe, M.; Zacchi, G. *Adv. Biochem. Eng. Biotechnol.* **2007**, *108*, 123–130.
3. (a) McCormick, C. L. U.S. Patent 4278790, 1981. (b) Turbak, A. F. U.S. Patent 4302252, 1981. (c) Namikoshi, H. Japan Patent 59-124933, 1984.
4. El Seoud, O. A.; Koschella, A.; Fidale, L. C.; Dorm, S.; Heinze, T. *Biomacromolecules* **2007**, *8*, 2629–2647.
5. (a) Wilkes, J. S.; Zaworotko, M. J. *J. Chem. Soc., Chem. Commun.* **1992**, 965–966. (b) Merrigan, T. L.; Bates, E. D.; Dorman, S. C.; Davis, J. H., Jr.;

- Chem. Commun.*, **2000**, 2051–2052. (c) Wilkes, J. S.; *Green Chem.*, **2002**, *4*, 73. (d) Rogers, R. D.; Seddon, K. R.; *Science*, **2003**, *302*, 792.
6. (a) Welton, T. *Chem. Rev.*, **1999**, *99*, 2071. (b) Wasserscheid, P., Welton, T., Eds. *Ionic Liquids in Synthesis*; Wiley-VCH: Weinheim, Germany, 2003.
 7. Swatloski, R. P.; Spear, S. K.; Holbrey, J. D.; Rogers, R. D. *J. Am. Chem. Soc.* **2002**, *124*, 4974.
 8. (a) Turner, M. B.; Spear, S. K.; Holbrey, J. D.; Rogers, R. D. *Biomacromolecules* **2004**, *5*, 1379. (b) Zhang, H.; Wang, Z.; Zhang, Z.; Wu, J.; Zhang, J.; He, J. *Adv. Mater.* **2007**, *19*, 698.
 9. (a) Wu, J.; Zhang, J.; Zhang, H.; He, J.; Ren, Q.; Guo, Q. *Biomacromolecules* **2004**, *5*, 266. (b) Heinze, T. *Green Chem.* **2006**, *8*, 301. (c) Schluffer, K.; Schmauder, H-P.; Dorn, S.; Heinze, T. *Macromol. Rapid Commun.* **2006**, *27*, 1670.
 10. Remsing, R. C.; Swatloski, R. P.; Rogers, R. D.; Moyna, G. *Chem. Commun.* **2006**, 1271.
 11. (a) Fort, D. A.; Remsing, R. C.; Swatloski, R. P.; Moyna, P.; Moyna, G.; Rogers, R. D. *Green Chem.*, **2007**, *9*, 63. (b) Kilpeläinen, I.; Xie, H.; King, A.; Granstrom, M.; Heikkinen, S.; Argyropoulos, D. S. *J. Agric. Food Chem.* **2007**, *55*, 9142.
 12. (a) Li, C.; Zhao, Z. K. *Adv. Synth. Catal.*, **2007**, *349*, 1847. (b) Li, C.; Wang, Q.; Zhao, Z. K. *Green Chem.* **2008**, *10*, 177.
 13. Hermanutz, F.; Gähr, F.; Uerdingen, E.; Meister, F.; Kosan, B. *Macromol. Symp.* **2008**, *262*, 23.
 14. Ohno, H.; Fukaya, Y. *Chem. Lett.* **2009**, *38*, 2.
 15. Fukaya, Y.; Sugimoto, A.; Ohno, H. *Biomacromolecules* **2006**, *7*, 3295.
 16. Fukaya, Y.; Hayashi, K.; Wada, M.; Ohno, H. *Green Chem.* **2008**, *10*, 44.
 17. (a) McEwen, A. B.; Ngo, H. L.; LeCompte, K.; Goldman, J. L. *J. Electrochem. Soc.* **1999**, *146*, 1687. (b) Vestergaard, B.; Bjerrum, N. J.; Petrushina, I.; Hjuler, H. A.; Berg, W. R.; Egstrup, M. *J. Electrochem. Soc.* **1993**, *140*, 3108. (c) MacFarlane, D. R.; Meakin, P.; Sun, J.; Amini, N.; Forsyth, M. *J. Phys. Chem. B* **1999**, *103*, 4164. (d) Forsyth, S.; Golding, J.; MacFarlane, D. R.; Forsyth, M. *Electrochem. Acta* **2001**, *46*, 1753. (e) Goldman, J.; Hamid, N.; MacFarlane, D. R.; Forsyth, M.; Forsyth, C.; Collins, C.; Huang, J. *Chem. Mater.* **2001**, *13*, 558. (f) Poole, S. K.; Shetty, P. H.; Poole, C. F. *Anal. Chim. Acta* **1999**, *218*, 241. (g) Sun, J.; Forsyth, M.; MacFarlane, D. R. *J. Phys. Chem. B* **1998**, *102*, 8588. (h) Chen, H.; Kwait, D. C.; Gonen, Z. S.; Weslowski, B. T.; Adballah, D. J.; Weiss, R. G. *Chem. Mater.* **2002**, *14*, 4063.
 18. Heinze, T.; Schwikal, K.; Barthel, S. *Macromol. Biosci.* **2005**, *5*, 520.
 19. Zhang, H.; Zhang, W. J.; He, J. *Macromolecules* **2005**, *38*, 8272.
 20. Ngo, H. L.; LeCompte, K.; Hargen, L.; McEwen, A. B. *Thermochim. Acta* **2000**, *357*, 97.
 21. (a) Reichardt, C. *Green Chem.* **2005**, *7*, 339. (b) Muldoon, M. J.; Gordon, C. M.; Dunkin, I. R. *J. Chem. Soc., Perkin Trans. 2* **2001**, 433.
 22. Anderson, J. L.; Ding, J.; Welton, T.; Armstrong, D. W. *J. Am. Chem. Soc.* **2002**, *124*, 14247.
 23. Spange, S.; Fischer, K.; Prause, S.; Heinze, T. *Cellulose* **2003**, *10*, 201.

24. Mizumo, T.; Marwanta, E.; Matsumi, N.; Ohno, H. *Chem. Lett.* **2004**, *33*, 1360.

Chapter 3

Advances in Aqueous Cellulose Solvents

Ang Lue and Lina Zhang*

Department of Chemistry, Wuhan University, 430072

*Correspondence to: L. Zhang (E-mail: lnzhang@public.wh.hb.cn)

Cellulose is an almost inexhaustible source of raw material for the increasing demand for biodegradable products, and its solvent is a key for the research and developments. This chapter summarizes the aqueous cellulose solvents, such as NaOH aqueous, NaOH/urea aqueous, NaOH/thiourea aqueous and LiON/urea aqueous systems with cooling. The dissolution mechanism, solution behaviors, preparation and modifications of the various cellulose materials, as well as their properties and applications were described. The dissolution of cellulose in pre-cooled aqueous solution deals with the formation of new hydrogen-bonded networks between cellulose and solvent molecules, which is at a highly stable state at low temperatures. The aqueous cellulose solvents are simple and low cost, and the preparation method of the cellulose products from the cellulose solution are short production cycle and “green” process. The potential applications of the cellulose fibers, films, hydrogels, microspheres and functional composite materials created from the aqueous cellulose solution were also discussed in this section.

1. Introduction

In the 21st century, the utilization of renewable resources to produce environmental-friendly materials has become an international front which avoids using or producing harmful substances. Cellulose is the most abundant on earth, and it is considered to be an almost inexhaustible source of raw material for the increasing demand for biodegradable and biocompatible products (1–3). However, the full potential of cellulose has not yet been exploited due to a lack

of “green” method and the limited number of common solvents that readily dissolve cellulose (4). Thus, the search for a novel cellulose solvent has long attracted the interests of the scientific and industrial communities. Nowadays, cellophane and rayon fibers prepared through the viscose route are still main cellulose products (5), but it produces serious pollution (use of CS₂). In recent years, the “green” comprehensive utilization of cellulose has attracted much attention from governments and researchers (6). Thus, new and powerful solvents, such as *N*-methylmorpholine-*N*-oxide (NMMO) (7, 8) and ionic liquids (9–12) have been developed for the preparation of the regenerated cellulose films, fibers and other materials. In 2004, D. Klemm won the Anselme Payen Award for his exceptional achievements in the development of new materials based on cellulose (13), and in 2005, R. D. Rogers won the US Presidential Green Chemistry Challenge Awards for his great contributions to cellulose dissolution in ionic liquids (14). Clearly, the regenerated cellulose products prepared from “green” processes have great importance for a sustainable development. By now, many cellulose solvents such as NMMO, LiCl/*N,N*-dimethylacetamide (DMAc), ionic liquids, CarbaCell system, NaOH/H₂O aqueous solution have been developed to avoid the hazardous byproducts, and novel achievements have been got in these systems (6, 15–19). Moreover, some novel solvents including dimethyl sulphoxide (DMSO)/ammonium fluorides, fluoride ionic liquids and DMSO-containing carbanilation mixtures have been presented at the 235th ACS symposium in New Orleans (20–26). Heinze et al have reported that cellulose with a degree of polymerization up to 650 can be dissolved in DMSO containing tetrabutylammonium fluoride trihydrate (TBAF·3H₂O) within 15 min at room temperature (20). It is worth noting that new aqueous cellulose solvents such as NaOH/urea, NaOH/thiourea and LiOH/urea aqueous solutions pre-cooled to -5~-12°C have been developed by Zhang’s group in Wuhan University (27–35). Therefore, it has revealed a new concept and “green” approach for the cellulose dissolution at low temperature.

Commonly, cellulose solvent can be divided into derivative system, such as CS₂/NaOH/H₂O, and non-derivative solvent, such as LiCl/DMAc, ionic liquid, alkali/urea aqueous solution and NaOH/H₂O; or water phase solvent and non-water phase one. It is undoubted that the aqueous cellulose solvents would attract a lot of interests due to the non-toxic system. The present chapter is mainly focused on the aqueous solvents. The preparation pathway, character, dissolution mechanism, and application of the cellulose solutions are summarized, and their advantages and disadvantages are also discussed.

2. NaOH/H₂O System

2.1. Dissolution of Cellulose

Kamide et al (36) have reported that non-crystal cellulose with low molecular weight can be dissolved in NaOH aqueous solution with a 8~10wt% concentration at about 4°C. The applicable cellulose should be the steam-exploded wood pulp

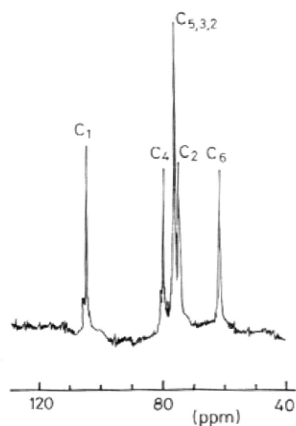


Figure 1. ^{13}C NMR spectrum for BRC-4 dissolved in NaOH- D_2O (1:9, w/w) (36).

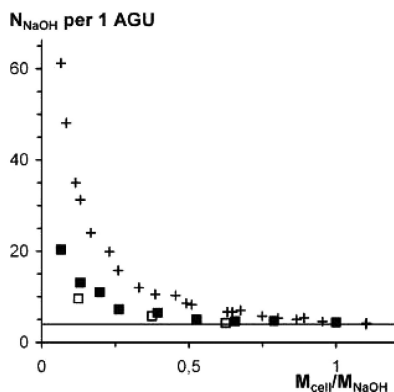


Figure 2. Number of NaOH molecules linked to one anhydroglucose unit (AGU), calculated from melting enthalpy data, as a function of cellulose/NaOH weight ratio in solution. Dark squares: cellulose/7.6NaOH/water; open squares: cellulose/8NaOH/water; and crosses: data from ref (39) for NaOH concentrations of 4.5, 6.2, and 7.9% (41).

with DP lower than 250, rather than the cotton linter pulp with medium molecular weight. Figure 1 shows the ^{13}C NMR spectrum for the cellulose BRC-4 solution in NaOH- D_2O . Except for the C3 and C5 carbon peaks, all others shift to a magnetic field higher than that for solid BRC-4. One C4 carbon peak for the solution is located at 79.9ppm, which is a much higher magnetic field than that (87.9 and about 84ppm) for the original BRC-4 solid. Thus, the C4 carbon peak is very close to the C5 peak at 76.5ppm. This indicates the intramolecular hydrogen bonds of cellulose are completely destroyed. The destruction of the hydrogen bonds leads to the shifting of the C3 peak from 75.1ppm for solid cellulose to 76.4ppm in alkali.

The steam-exploded cellulose can be dissolved in NaOH aqueous solution at low temperature (37), and the microcrystal cellulose has been dissolved in

8~9wt% NaOH aqueous by a freezing-thaw-dilution process (38). A 5wt% or lower concentration cellulose solution can be obtained when NaOH concentration is in the range from 7.9 to 14.9wt% (39). However, the restriction of low molecular cellulose and the easy gelation of the cellulose solution from NaOH/H₂O system suggest that this system is unable for the industrial manufacture. Seger and Fischer have investigated the viscose solution after dilution in 1M NaOH by static light scattering (40) and gave an aggregation number around 10 laterally assembled chains.

2.2. Structure and Interaction of Cellulose Solution

Recently, Navard et al (41) have studied thermodynamic behavior and structure of microcrystalline cellulose/sodium hydroxide aqueous solutions at temperatures below 0°C. Figure 2 shows number of NaOH molecules (N_{NaOH}) linked to one anhydroglucose unit (AGU) calculated from melting enthalpy data. The limit of cellulose dissolution in NaOH/water as being at least four NaOH molecules per one AGU unit as the weight ratio of cellulose/NaOH ($M_{\text{cell}}/M_{\text{NaOH}}$) being one. A combination of NaOH hydrates is able to penetrate into the cellulose structure and to prefer forming some type of network with themselves rather than bind to the cellulose only (as in the mercerization case). The N_{NaOH} per 1 AGU strongly decreases with an increase of $M_{\text{cell}}/M_{\text{NaOH}}$, as a result of the steric hindrance caused by the transition from the dilute to semi-dilute state. The same proportion between NaOH and AGU corresponding to the limit of cellulose dissolution, namely four NaOH per AGU, can be calculated if taking the results of Avicel solubility in NaOH aqueous solutions (39).

Heux et al (42) have investigated the interaction of microcrystalline cellulose from cotton and aqueous sodium hydroxide by ¹³C NMR solid-state spectroscopy. When the concentration of NaOH increased, the initial cellulose spectrum was replaced successively by that of Na-cellulose I followed by that of Na-cellulose II. In Na-cellulose I, each carbon atom occurred as a singlet, thus implying that one glucosyl moiety was the independent magnetic residue in the structure of this allomorph. In addition, the occurrence of the C6 near 62ppm is an indication of a *gt* conformation for the hydroxymethyl group of Na-cellulose I. In Na-cellulose II, the analysis of the resonances of C1 and C6 points toward a structure based on a cellotriosyl moiety as the independent magnetic residue, in agreement with the established X-ray analysis that has shown that for this allomorph, the fiber repeat was also that of a cellotriosyl residue. For Na-cellulose II, the occurrence of the C6 in the 60 ppm region indicates an overall *gg* conformation for the hydroxymethyl groups.

2.3. Cellulose Materials

Budtova et al (43) have fabricated new highly porous pure cellulose aerogel-like material from the aqueous cellulose/NaOH solutions. The solutions have been gelled to obtain shaped three-dimensional objects, then cellulose was

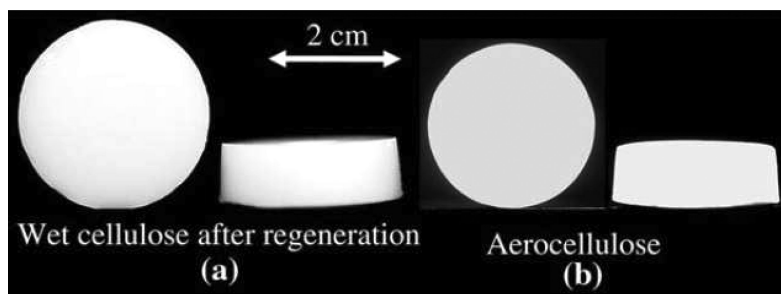


Figure 3. Wet regenerated cellulose from 5% cellulose–NaOH–water solution gelled at 50°C for 20 h, regenerated in 0.1mol/L acetic acid bath at 22°C and washed in water (a) and aerocellulose prepared from it (b) (44).

regenerated and dried in supercritical conditions using CO₂. The porosity of aerocellulose is higher than 95% with pore sizes distribution from a few tens of nanometers to a few tens of micrometers. The internal specific surface area is around 200 to 300m²/g, and density ranges from 0.06 to 0.3g/cm³, depending on the preparation conditions. Figure 3 shows wet regenerated cellulose from 5% cellulose–NaOH–water solution gelled at 50°C for 20h, and aerocellulose prepared from it (44). The regeneration is three times slower when cellulose is in solution, but the increase in bath temperature leads to the increase in diffusion coefficient. Drying of regenerated cellulose in supercritical CO₂ conditions induces sample contraction that is reflected by a denser morphology as compared with freeze-dried samples (44).

Vehviläinen et al (45) have spun novel cellulose fibers (Biocelsol) by traditional wet spinning technique from the alkaline solution prepared by dissolving enzyme treated pulp directly into aqueous sodium zincate (ZnO/NaOH). The spinning dope contains 6wt% of cellulose, 7.8wt% of NaOH and 0.84wt% of ZnO, and the 5% and 15% H₂SO₄ baths containing 10% Na₂SO₄ is used as coagulant. The highest fiber tenacity obtained is 1.8cN/dtex with elongation of 15% and titer of 1.4dtex.

3. NaOH/Urea System

3.1. Mechanism of Cellulose Dissolution at Low Temperature

Zhang et al have revealed that 7wt% NaOH/12wt% urea aqueous solution pre-cooled to -12 °C can dissolve rapidly cellulose having molecular weight below 1.2×10^5 within 2 min even several seconds became of the appearance of the Weissenberg phenomenon (30, 31, 35). This interesting process represents the most rapid dissolution of native cellulose. It is well known that dissolution of normal polymers includes a slow diffusion based on the interchangeability of solvent and polymer, and needs a long time (the heating may accelerate the process).

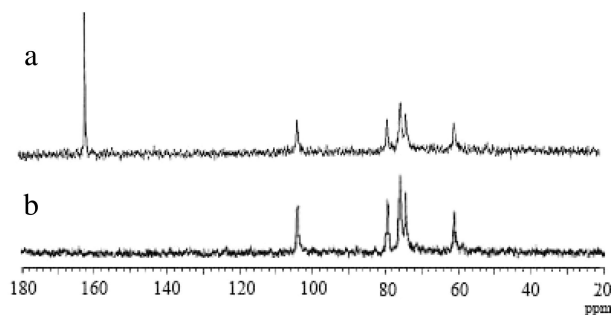


Figure 4. ^{13}C NMR spectra of cellulose solution in 7 wt% NaOH/12 wt% urea/ D_2O (a) and in 9 wt% NaOH/ D_2O (b) at 18°C (35).

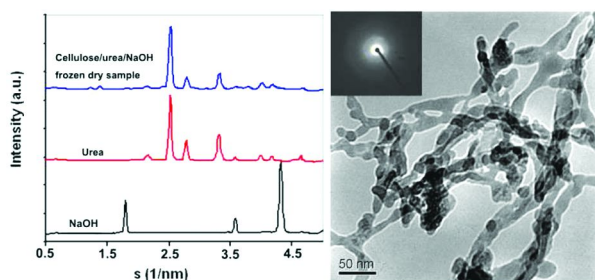


Figure 5. 1D WAXD intensity profiles of NaOH (powder), urea (powder) and cellulose in NaOH/urea solution and then frozen and dried (left) and TEM images of cellulose solution at 5.0×10^{-4} g/ml in 7 wt% NaOH/12 wt% urea aqueous solution pre-cooled to -12°C (right), inset presents the electron diffraction (ED) pattern of the surface (35).

Obviously, the dissolution of cellulose at low temperature differs from the traditional dissolution process. It is worth noting that liquid water forms clusters via a dynamic supramolecular assembly process mainly through hydrogen bonds. It is not hard to imagine that the promotion on a dissolution process by cooling is related to the formation of hydrogen-bonded networks between cellulose and solvent components. The rapid dissolution of cellulose suggests a dynamic self-assembly process driven by hydrogen bonding. The results from ^{13}C NMR, ^{15}N NMR, ^1H NMR, FT-IR, small angle neutron scattering (SANS), transmission electron microscopy (TEM) and wide-angle X-ray diffraction (WAXD) have demonstrated that NaOH “hydrates” can be more easily attracted to cellulose chains through the formation of new hydrogen-bonded networks at low temperatures, while the urea hydrate molecules do not directly associate with cellulose, but can be self-assembled at the surface of the NaOH hydrogen-bonded cellulose to form an inclusion complex (IC), bring cellulose in to the aqueous solution (35). Figure 4 shows ^{13}C NMR spectra of the cellulose sample in 7wt% NaOH/12wt% urea/ D_2O and 7wt% NaOH/ D_2O solutions, respectively. The

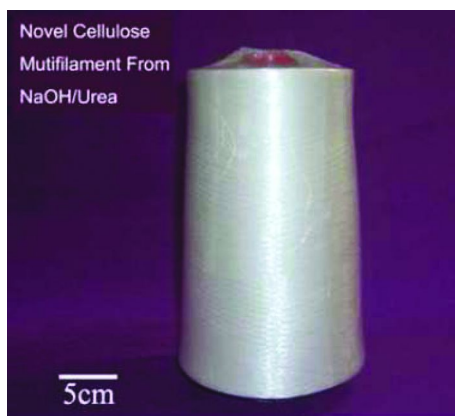


Figure 6. Photo of novel cellulose multifilaments from NaOH/urea aqueous system via pilot-scale machine (55).

chemical shifts of C1 (104.4 ppm), C4 (79.6 ppm), C3,5 (76.2 ppm), C2 (74.5 ppm), and C6 (61.2 ppm) for cellulose in 7wt% NaOH/12wt% urea/D₂O are similar to that in the 9wt% NaOH/D₂O solution (36), indicating that the magnetic environment of cellulose molecules in the alkali/urea system is the same as in the alkali-only system.

The results strongly support that cellulose chains are surrounded directly by NaOH hydrates. The result from SANS profiles of solvents with different components demonstrate that the mixture of NaOH and urea in D₂O forms clusters with smaller sizes based on the smaller slope values at low q , suggesting that the addition of NaOH weakened the association of urea in water. Therefore, the clustering strength of the NaOH/urea is higher than that of urea/D₂O, leading to the complex associated with urea and NaOH hydrates as the predominant species in the system. The hydrogen-bonded network structure is at a highly stable state at low temperatures to create their supramolecular assembly. Furthermore, ¹⁵N NMR and ¹H NMR results strongly support that the urea hydrates are present outside of this sheathlike structure of NaOH hydrogen-bonded with cellulose. A similar conclusion has been deduced on the basis of differential scanning calorimeter (DSC) by Navard et al (46) that the interaction between cellulose and NaOH/water are exactly the same as without urea, and urea is not directly interacting with cellulose or NaOH. Figure 5 shows 1D WAXD intensity profile of NaOH, urea and cellulose solution as well as TEM images of the cellulose dilute solution. The WAXD intensity profiles of the cellulose solution in NaOH/urea are similar to that of urea, and the peaks of NaOH and cellulose disappear in this profile. It demonstrates that the inclusion complex (IC) associated with cellulose and NaOH hydrates are engaged in the urea host, leading to the shield for cellulose and NaOH. From the results of laser light scattering (LLS) and dynamic light scattering (DLS), a apparent average ratio of radius of gyration (R_g) to hydrodynamic radii (R_h) ($\langle R_g/R_h \rangle_{app}$) for cellulose in this solvent has been estimated to be ~ 2.5 , indicating an extended chain or worm-like cellulose chain in the dilute solution.

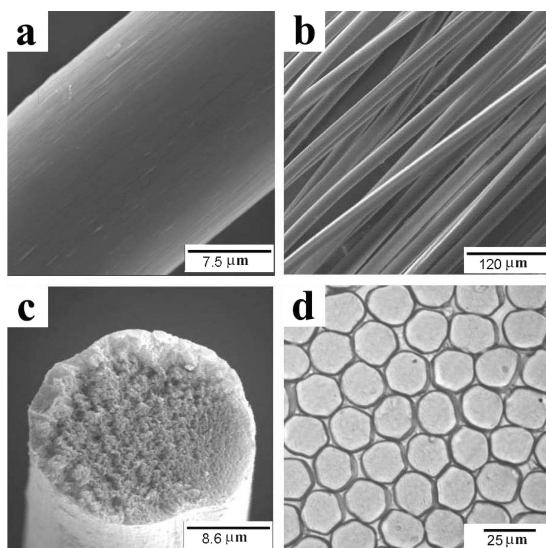


Figure 7. SEM images of the surface (top) and cross section (bottom) of the filaments. A bundle of filaments on the take-up device was observed by using optical microscopy (d) (51).

The TEM image of the cellulose IC displays a worm-like pattern, and their surface is surrounded by urea, which presents a kebab-shape surface, because the electron beam struck the non-metal sample, resulting in the partial melting of urea on the IC surface. The cellulose IC surrounded with urea reduces greatly the self-association of the cellulose molecules, leading to the increased solubility and stability of the cellulose solution. The cellulose solution is relatively unstable and can be very sensitive to temperature, polymer concentration and storage time. Therefore, this cellulose dissolution at low temperature arises as a result of a fast dynamic self-assembly process among solvent small molecules (NaOH, urea and water) and the cellulose macromolecules. According to the dynamic self-assembly definition, if it is controlled to avoid fluctuation or energy exchange, the cellulose solution may be highly stable for a long period of time (47, 48).

3.2. Behaviors of Cellulose Solution

It is difficult to truly disperse cellulose molecules in most “known” solvents at the molecular level. The cellulose chains in solution form aggregates with a radius of gyration, R_g , of about 232nm and an apparent hydrodynamic radius, R_h , of about 172nm (49). It is similar to the value of about 200 nm for the cellulose molecules in NMMO using the same technique (50). The cellulose solution easily aggregates, either a heating or a cooling treatment can induce the gelation processing. The energy of the hydrogen bonds is higher at low temperature, leading to the strong tendency of aggregation of the cellulose molecules. Therefore, the cellulose solution prepared at low temperature forms



Figure 8. Photographs of the cellulose/ Fe_2O_3 nanocomposite fibers of F001 (a), F01 (b), and F05 (c) with different Fe_2O_3 contents, as well as fiberlike Fe_2O_3 nanomaterials calcinated from F05 (d) (54).

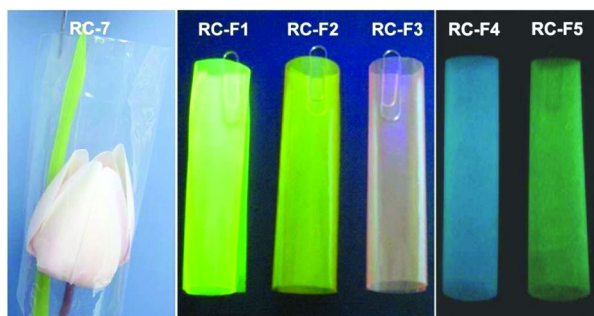


Figure 9. Novel transparent (RC-7), fluorescent (RC-F1, RC-F2 and RC-F3) and long after-glow photoluminescent (RC-F4 and RC-F5) cellulose films (57).

gels by reducing temperature to below 0°C . The cellulose solution can be stored at 0 to 5°C for a long time and still remains in its stable liquid state (31).

Navard et al (46) have studied the binary phase diagram of urea/water, the ternary urea/NaOH/water phase diagram and the influence of the addition of microcrystalline cellulose in urea/NaOH/water solutions by DSC. Urea/water solutions have a simple eutectic behavior with a eutectic compound formed by pure urea and ice (one urea per eight water moles), melting at -12.5°C . When the amount of water is too low to form the two eutectic mixtures, NaOH is attracting water at the expense of urea. A tentative explanation of the role of urea is to bind water, making cellulose-NaOH links more stable.

3.3. Fibers Based on Dissolution of Cellulose in NaOH/Urea System

From the cellulose dope in NaOH/urea system, novel cellulose fibers (47, 51, 52), and the functional fibers with good supermagnetic properties (53, 54) have been fabricated. A 8wt% H_2SO_4 /12wt% Na_2SO_4 aqueous solution has been adopted as the first coagulants, and 4wt% H_2SO_4 aqueous solution as the second coagulant at 10 to 20°C with no evolution of gas during coagulation. This is a “green” process for the fabrication of regenerated cellulose products. Figure 6 shows photo of novel cellulose multi-filaments via pilot-scale machine (55).

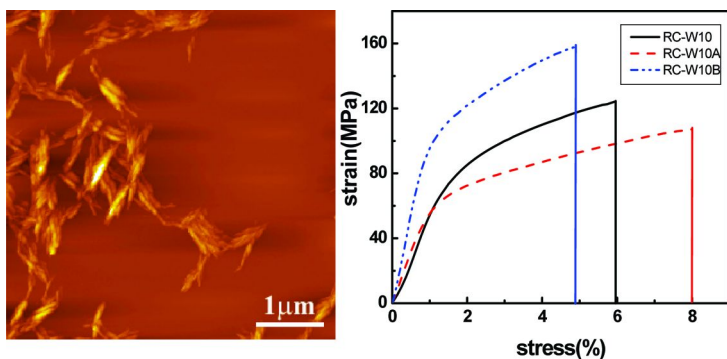


Figure 10. AFM topography image of cellulose whiskers after drying on a mica surface (left) and stress-strain curves of the composite films dried from different process for all-cellulose nanocomposite films (right) (58).

They exhibit smooth surface, compact structure and fine mechanical properties (51, 55). Figure 7 shows scanning electron microscopy (SEM) images of the surface (top) and cross-section (bottom) of the multi-filaments. The fibers possess a circular cross section, which is markedly different from the lobulate shape of the viscose rayon, but similar to cuprammonium rayon (Bemberg) and Lyocell fibers (6). This is as a result of the direct regeneration from the cellulose solution in a quasi-gel state by physical crosslinking (51). Compared to the viscose rayon, the novel fibers exhibit better dye ability, and sulfur content is almost 0 (55).

Further, magnetic nanocomposite fibers have been fabricated by introducing in situ synthesized iron oxide (Fe_2O_3) nanoparticles into the wet cellulose fibers. The cellulose/ Fe_2O_3 nanocomposite fibers (see Figure 8) exhibit a higher mechanical strength than RC fibers, as well as a strong capability to absorb UV rays, superparamagnetic properties, and a relatively high dielectric constant (53). The cellulose/ Fe_2O_3 fibers have been sintered at 600°C to prepare fiberlike Fe_2O_3 macroporous materials (see Figure 8d) by the removal of cellulose matrix. The inorganic nanomaterials display high purity of $\alpha\text{-Fe}_2\text{O}_3$ and possess large specific surface area, weak ferromagnetic properties, and superior electrochemical activity, having a discharge capacity of 2750 mA·h/g (54).

Chu et al (49, 56) have used a simple wet spinning apparatus to regenerate the cellulose fibers from the cellulose solution in NaOH/urea solvent. When coagulated in a $\text{H}_2\text{SO}_4/\text{Na}_2\text{SO}_4$ aqueous solution at 15°C , the regenerated fibers exhibited the highest crystallinity and a crystal orientation comparable to that of commercial rayon fibers. A fibrillar superstructure is observed only at higher flow rates (>20 m/min). The solution flow rate during spinning appears to be one of the most important factors that can simultaneously improve the orientation of both cellulose I-filler phase and cellulose II matrix phase. The low cost and low toxicity of the new solvent in combination with conventional wet-spinning approach show good promise for the development of an economical and environmentally friendly process to produce regenerated cellulose fibers with good properties compatible with existing fibers.

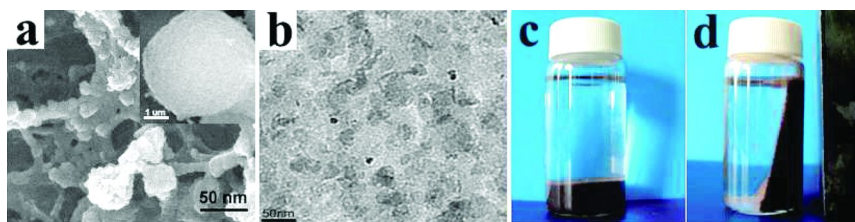


Figure 11. SEM images of the surface of the M30 (a) and the TEM images of the magnetic microspheres of M30 (b), as well as photos of M30 in water (c) and in a magnetic field (d) (59).

3.4. Transparent and Composite Cellulose Films

Transparent regenerated cellulose films with a homogenous structure, excellent optical transmittance (90% at 800 nm), good tensile strength have been prepared in the NaOH/urea system via a “green” process (57). Moreover, the cellulose films embedded with fluorescent dyes and photoluminescent (PL) pigments, respectively, have been fabricated, creating novel PL materials, as shown in Figure 9 (57). The cellulose film and its composite films exhibit good optical transmittance, strong fluorescence and long after-glow emission with biodegradability, leading to the promising applications in the field of information technology, anti-counterfeiting techniques and functional packaging.

All-cellulose composite films have been prepared from native cellulose nanowhiskers and cellulose matrix regenerated from aqueous NaOH/urea solvent system on the basis of their temperature-dependent solubility (58). The composite films are isotropic and transparent to visible light and display good mechanical properties as a result of the reinforcement by the whiskers. Figure 10 shows AFM topography image of cellulose whiskers and stress-strain curves of the composite films dried from different process for the all-cellulose nanocomposite films. The tensile strength and elastic modulus of the nanocomposite films can be tuned to reach 124 MPa and 5 GPa, respectively. Moreover, the tensile strength of the nanocomposite films can reach 157 MPa through a simple drawing process, with the calculated Hermans’ orientation parameter of 0.30.

3.5. Functional Cellulose Materials

Regenerated cellulose microspheres (RCS) have been prepared by using sol-gel transition (SGT) method from cellulose drops in 7wt% NaOH/12wt% urea aqueous solution (59). Moreover, novel magnetic Fe₃O₄/cellulose microspheres (MRCS) can be obtained by in situ synthesis of Fe₃O₄ nanoparticles into the pores of RCS, which are used as the solid template microreactor (59). The magnetic Fe₃O₄ nanoparticles are dispersed uniformly and immobilized in the cellulose matrix, as shown in Figure 11 a and b.

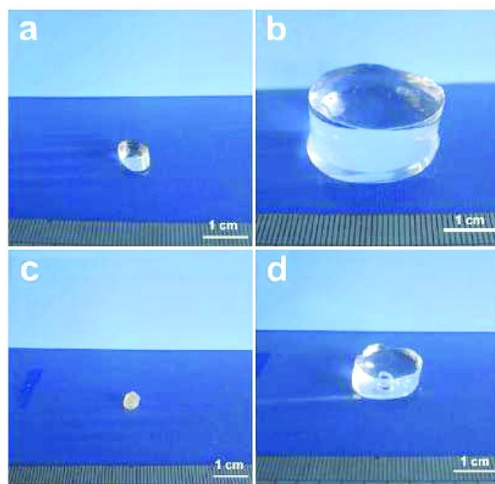


Figure 12. Photographs of GEL91: (a) original hydrogel as prepared in NaOH/urea solution, (b) swollen hydrogel in water, (c) dried gel and (d) hydrogel welling in NaCl solution for a week (60).

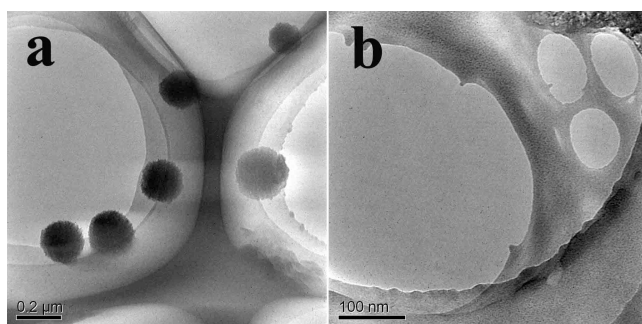


Figure 13. TEM images of cellulose at $4.0 \times 10^{-4} \text{ g mL}^{-1}$ in NaOH/thiourea aqueous solution (a) and cellulose in NaOH aqueous solution (b) (69).

The MRCS microspheres exhibit sensitively magnetic response as shown in Figure 11 (c and d). The Fe_3O_4 nanoparticles in the cellulose microspheres play an important role in both the creation of the magnetic-induced transference and the improvement of the targeting protein delivery and release. It will be important for the applications in the biomaterial fields.

Novel superabsorbent hydrogels have been prepared from carboxymethylcellulose sodium (CMC) and cellulose in the NaOH/urea aqueous system by using epichlorohydrin (ECH) as crosslinker (60), as shown in Figure 12. The CMC contributes to the enhanced size of pore, whereas cellulose as a strong backbone in the hydrogel supports the network for keeping its appearance. Their maximum swelling ratio in water reaches an exciting level of 1000 as the hydrogels still keeping a steady appearance. Moreover, the hydrogels exhibit

smart swelling and shrinking in NaCl or CaCl₂ aqueous solution, as well as the release behavior of bovine serum albumin (BSA). The cellulose-based hydrogels are promising for the applications in the biomaterials area.

3.6. Homogeneously Etherification of Cellulose in NaOH/Urea Aqueous Solution

Based on the unique structure and reactivity of cellulose, chemical modification reactions continue to play a dominant role in the improving of the overall utilization of this biomacromolecules, as mentioned by Heinze et al (61, 62). The solvent system is a stable and more homogeneous system for the synthesis of cellulose ethers, because the etherification of cellulose occurs often under alkali conditions. Various derivatives of cellulose have been created in the NaOH/urea aqueous solution. On the basis of the suitable homogeneous reaction medium of NaOH/urea for the etherification of cellulose, methylcellulose (MC) (64, 65), hydroxyethylcellulose (HEC) (66), hydroxypropyl cellulose (HPC) (64) as well as cyanoethyl cellulose (CEC) (67) have been synthesized in this system under mild conditions without addition of an extra catalyst. The distribution of substitution for water-soluble MC, HEC and HPC samples homogeneous synthesized in NaOH/urea aqueous solutions is summarized in Table 1. The relative reactivity of hydroxyl groups at the C-2 position of cellulose is slightly higher than that at the C-3 and C-6 positions. The low limits for the DS value of water-soluble MC is 0.94, and the low limits for the MS and DS values are 0.57 and 0.49 for water-soluble HEC, and 1.03 and 0.85 for water-soluble HPC. It is difficult to attain cellulose ethers with higher DS value in this system.

Cationic derivatives of cellulose have been homogeneously synthesized by reacting cellulose with 3-chloro-2-hydroxypropyltrimethylammonium chloride (CHPTAC) in NaOH/urea aqueous solutions by Zhou et al (63). This is water-soluble quaternized celluloses (QCs) with DS value of 0.20 to 0.84, which can be controlled by adjusting the molar ratio of CHPTAC to AGU of cellulose and the reaction time. It is noted that QCs can condense DNA efficiently. The cytotoxicity of QCs is relatively low compared with PEI, and the cells had been transfected effectively. Yan et al (68) have synthesized water soluble cationic cellulose by the reaction between microcrystalline cellulose and 2,3-epoxypropyltrimethylammonium chloride in a NaOH/urea aqueous solution. The DS of the cationic cellulose depends on both the ratio of the 2,3-epoxypropyltrimethylammonium chloride to cellulose and the reaction time. The flocculation capacity of the cationic cellulose has been determined with 0.25 wt % kaolin suspension using the standard jar test. Encouraging results have been found and cationic cellulose may be applicable for use as a novel flocculant in wastewater treatment.

Table 1. Distribution of substitution for the water-soluble MC, HEC and HPC samples synthesized in NaOH/urea aqueous solutions

Sample	MS	Total DS	DS			Sources Ref
			C-2	C-3	C-6	
MC-1		0.94	0.47	0.22	0.25	(64, 65)
MC-2		1.09	0.52	0.27	0.27	
MC-3		1.42	0.57	0.40	0.45	
MC-4		1.56	0.67	0.46	0.43	
MC-5		1.69	0.66	0.44	0.59	
HEC-1	0.57	0.49	0.16	0.12	0.21	(66)
HEC-2	0.86	0.72	0.28	0.21	0.23	
HEC-3	1.04	0.84	0.29	0.26	0.29	
HEC-4	1.44	1.14	0.44	0.30	0.40	
HPC-1	0.85	0.83	0.28	0.26	0.29	(64)
HPC-2	1.03	0.85	0.25	0.30	0.30	
HPC-3	1.18	0.93	0.33	0.30	0.30	
HPC-4	1.73	1.18	0.41	0.38	0.39	

4. NaOH/Thiourea System

4.1. Dissolution and Structure of Cellulose in This System

Zhang et al have indicated that NaOH/thiourea/H₂O system has better dissolution ability and needs less energy to dissolve cellulose than NaOH/urea (29, 33, 34, 73, 74). Cellulose can be dissolved rapidly in 9.5 wt% NaOH/4.5 wt% thiourea aqueous solution pre-cooled to -5°C, but cannot be dissolved in the same solvent without prior cooling. The FT-IR results indicates that hydrogen-bonded network structure of a “complex” associated with NaOH, thiourea, and water clusters occurs at low temperature, and it is highly stable at -5°C near its ice point (69). Same as NaOH/urea system, the low temperature creates the full exchange between the hydroxyl groups of cellulose and [OH(H₂O)_n]⁻ ions from NaOH, leading to the cleaving of the chain packing of cellulose, resulting the cellulose dissolution. Furthermore, the cellulose inclusion complex (IC) hosted by thiourea and NaOH, in which cellulose chains associated with NaOH hydrate as guest is engaged, leads to the enhanced solubility (69). The ICs clusters display a sphere shape as shown in Figure 13(a) (69). This is different from that in NaOH/urea system, in which the cellulose ICs exist as worm-like shape (35), as a result of the difference of urea and thiourea in the structure and polar. There is only thin film self-aggregated with cellulose molecules in the NaOH aqueous solution

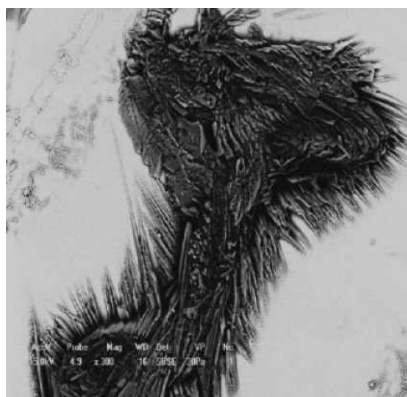


Figure 14. SEM image of microcrystalline cellulose on the surface of newly cleaved mica after treatment with aqueous NaOH/thiourea at room temperature (71).

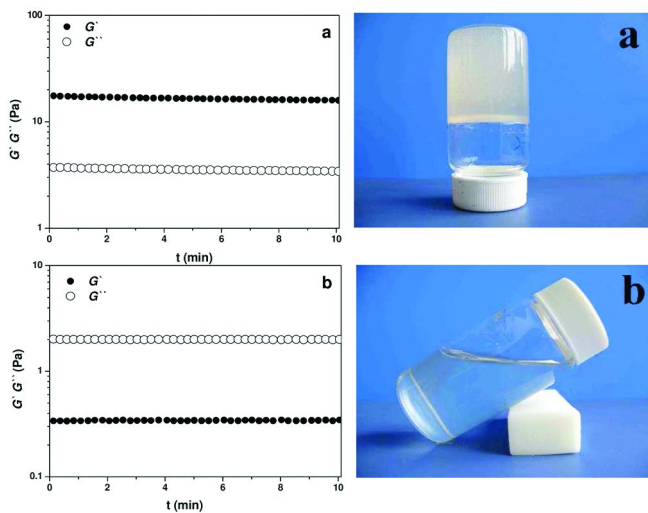


Figure 15. Rheological measurements (left) and photographs (right) of the 3 wt% cellulose solution: (a) gel from the cellulose solution at 30°C for 48h, (b) the cellulose solution obtained from gel (a) by stirring at -57°C (34).

without thiourea or urea (Figure 13b). Obviously, NaOH, urea or thiourea have surrounded the cellulose through formation of new hydrogen-bonded networking to prevent the self-association of the cellulose chains, leading to the improvement of solubility and stability of the cellulose solution.

The results from AFM of the cellulose gels spread on the substrate after being dispersed in the aqueous solution indicates that the average dimension of the cross section for those nanoparticles of the gels is 45.9 ± 8.5 nm (70). The particles packed loosely together to form gel aggregates. One nanoparticle represents a stable network unit, suggesting that the cellulose molecular size become small (less than

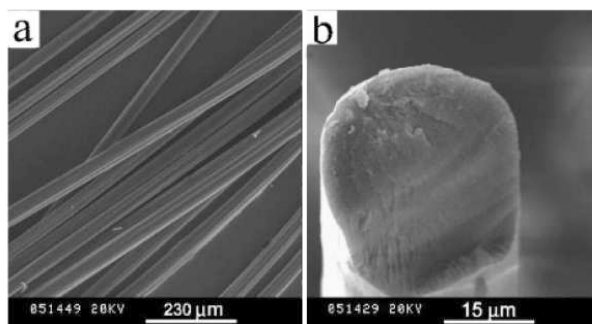


Figure 16. SEM micrographs of the novel multi-filament fibers spun from cellulose solution in a NaOH/thiourea aqueous system pre-cooled to -5°C on an extended laboratory scale (74).

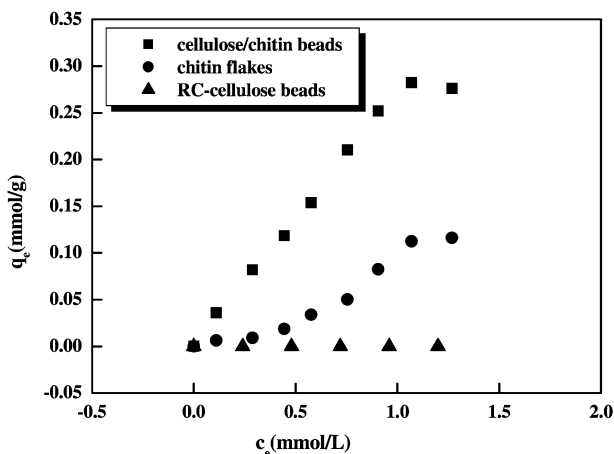


Figure 17. Experimental data on the chitin flakes, cellulose beads and cellulose/chitin beads at $\text{pH}_o=5.0$ and room temperature (75).

47nm) in the system, as a result of the bending of the cellulose chains. The results prove that the intramolecular hydrogen bonds of the cellulose, which sustain the chain stiffness, are destructed, leading to a change from semi-stiff to flexible chains (or random coil) in this system. The results are in good agreement with the spherical ICs of cellulose in NaOH/thiourea system (69).

Yan et al (71) have prepared various kinds of cellulose/cellulose-aggregate films on newly cleaved mica by the deposition of the suspensions of microcrystalline cellulose in water in the presence or in absence of NaOH/thiourea at different temperatures. The topochemistry of the cellulose surfaces have been directly observed by employing SEM-EDX (Figure 14). Both NaOH and thiourea have a homogeneous distribution around the cellulose fibers during the dissolving process, and their synergic interactions play a key role to dissolve the cellulose. The dissolving process is continuous while the ice state formation promotes the dissolving process.

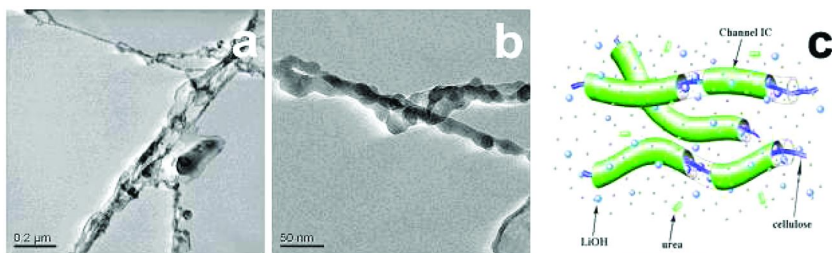


Figure 18. TEM images of cellulose at $4.0 \times 10^{-4} \text{ g mL}^{-1}$ in aqueous 4.6wt% LiOH/15wt% urea (a, b), and schematic inclusion complex model (c) (47).

Gu et al (72) have directly and quickly dissolved untreated cellulose (cotton linter) in NaOH/thiourea/urea aqueous solution. ^{13}C NMR spectra of the cellulose solution indicates that this novel mixture is a direct solvent, and cellulose is dissolved completely. In this process, cellulose I first changes to amorphous cellulose in the solution, and then to cellulose II. Dynamic rheological measurements show that this dissolution method is more effective, leading to a good cellulose solution. This simple technology is promising for substitution of the viscose technology that involves hazardous byproducts.

4.2. Sol-Gel Transition of Cellulose Solution

The cellulose solution in NaOH/thiourea system is most stable at 5°C and the gelation process is partial reversible in the range from $0\text{--}30^\circ\text{C}$ (73). The sol-gel transition of the fresh cellulose solution measured by rheological expanded system (ARES) can be described by Winter-Chambon theory (34). In the temperature range from 10 to 25°C , the loss tangent ($\tan\delta$) at the gel point has been determined according to the Winter and Chambon theory, indicating that the exponents of the scaling laws for the cellulose solution at 10°C before and beyond the gel point are in agreement with the predicted values based on the percolation theory. Figure 15 shows that the gel formed from the cellulose solution at 30°C at long storage time can undergo a transition to a transparent liquid state after stirring at -5°C . At the same time, the loss modulus exceeds the storage modulus, indicating a partially reversible sol-gel transition, as a result of the reconstruction of the hydrogen-bond networks between the solvent and cellulose.

4.3. New Cellulose Materials

Novel cellulose multi-filament fibers have been spun from the cellulose dope in NaOH/thiourea aqueous system on an extended laboratory scale (74). The fibers exhibit cellulose II character and possess a circular cross-section and smooth surface as shown in Figure 16. Although with a lower orientation compared with the commercial viscose rayon, the tensile strength of the novel fibers reaches 1.9-

2.2cN-dtex⁻¹, which is near to the commercial viscose rayon. Moreover, with a drawing progress, the orientation factor increased and mechanical properties are improved.

Biodegradable cellulose/chitin beads have been prepared in NaOH/thiourea system (75). The cellulose/chitin beads can absorb effectively Pb²⁺, Cd²⁺ and Cu²⁺ ions, and the adsorption ability of heavy metals on the beads is higher than that on the pure chitin flakes, as shown in Figure 17. Moreover, these beads can be regenerated up to about 98% by treating with 1mol/L HCl aqueous solution. The mechanisms for the removal of free heavy metal ions by cellulose/chitin beads is based on mainly complexation adsorption model, as well as a affinity of hydroxyl groups of the materials on metals (76).

Microporous membranes have been prepared by blending cellulose and soy protein isolate (SPI) in NaOH/thiourea system (77). The apparent pore size ($2r_e$) measured with SEM, the mean pore size ($2r_f$) obtained by the flow rate method, and the water ultrafiltration rate (UFR) of membranes increase with an increase in SPI content, and are higher than those of the pure cellulose membranes. The microporous membranes also kept high tensile strength in both dry and wet states. In addition, the CS2-n membranes containing a small amount of SPI are suitable for the culture of Vero cells. Therefore, the cellulose membranes can be used as candidates for application in separation technology and biomaterials fields.

5. LiOH/Urea System

5.1. Cellulose Channel Inclusion Complex

Zhang et al have reported that 5wt% LiOH/12wt% urea aqueous solution pre-cooled to -12°C has a more powerful ability to dissolve cellulose, compared to that of NaOH/urea and NaOH/thiourea systems (32). The LiOH hydrates [Li⁺(OH)_m·OH·(OH)_n] combine more easily with cellulose hydroxyl groups to form new hydrogen bonding network at low temperature, resulting in the destroy of the cellulose original hydrogen bonds. LLS has proved that the cellulose molecules exist as a extend chain in LiOH/ urea aqueous solution (32). Moreover, a channel inclusion complex (IC) morphology has been revealed by TEM as shown in Figure 18 (78). Figure 18(c) shows a schematic model to describe the channel cellulose IC hosted by urea hydrate.

When solid cellulose is immersed in the pre-cooled solvent, the hydrogen-bonded network structure between the cellulose macromolecules and small molecules in the solvent is created rapidly, bringing cellulose in the aqueous solution.

5.2. Chain Conformation of Cellulose

The predominant species of the cellulose in LiOH/urea aqueous solution exist as dividual chains in very low concentration. The Mark–Houwink equation for

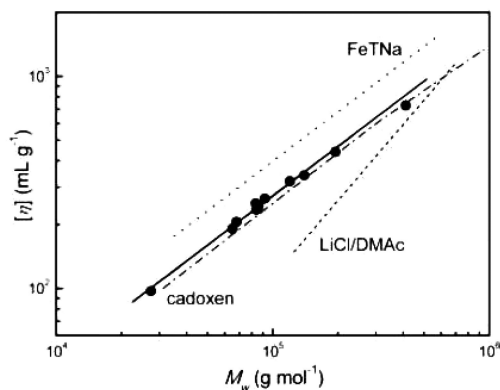


Figure 19. M_w dependence of $[\eta]$ for cellulose in 4.6wt% LiOH/15wt% urea aqueous solution at 25°C (●) and cadoxen (—) at 25°C, 9wt% LiCl/DMAc (---) and FeTNa (- - -) at 30°C (32).

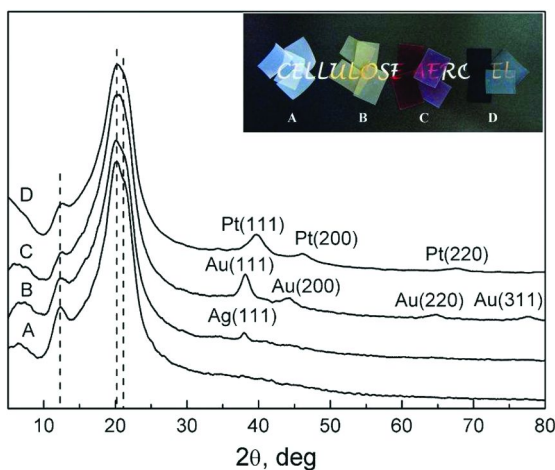


Figure 20. XRD patterns and photographs (inset) of the cellulose (A), silver-(B), gold-(C), and platinum-(D) cellulose aerogels (80).

cellulose in 4.6wt% LiOH/15wt% urea aqueous solution has been established to be $[\eta]=3.72 \times 10^{-2} M_w^{0.77}$ in the M_w region from 2.7×10^4 to 4.12×10^5 , as shown in Figure 19 (32). The persistence length (q), molar mass per unit contour length (M_L), and characteristic ratio (C_∞) of cellulose in the dilute solution are given as 6.1nm, 358nm⁻¹, and 20.8, respectively. The experimental data of the molecular parameters of cellulose agree with the Yamakawa—Fujii theory of the worm-like chain, indicating that the cellulose molecules exist as semi-stiff chains in the LiOH/urea aqueous solution.

5.3. Cellulose Materials Prepared in LiOH/Urea System

Kuga et al have prepared highly porous and strong cellulose aerogels by gelation of cellulose from aqueous LiOH/urea solution, followed by drying with supercritical CO₂ (79). The cellulose hydrogel is composed of interconnected fibrils of about 20 nm wide. By using supercritical CO₂ drying, the network structure in the hydrogel is well preserved in the aerogel. The results demonstrate the ability of this method to give cellulose aerogels of large surface areas (400-500 m²g⁻¹) which may be useful as adsorbents, heat/sound insulators, filters, catalyst supports, or carbon aerogel precursors.

Moreover, the transparent nanoporous cellulose gels obtained from aqueous alkali hydroxide/urea solution have been used as supporting medium for noble metal nanoparticles (80). Silver, gold, and platinum nanoparticles have been synthesized in the gel by hydrothermal reduction by cellulose or by added reductant, as shown in Figure 20. Both methods give nanoparticles embedded with high dispersion in cellulose gels. Supercritical CO₂ drying of the metal-carrying gel can create corresponding aerogels with high transmittance, porosity, surface area, moderate thermal stability, and good mechanical strength. The nanoparticles are dispersed well and stabilized by the cellulose network, apparently prevented from aggregation. The amount and size of metal particles can be controlled through concentration, temperature, and duration of reaction. This facile method would be applicable to other metals for nanoparticle synthesis. The nanostructured materials will be useful as antibacterial, electro-optical, and catalytic applications.

6. Summary

New aqueous cellulose solvents have been developed to dissolve cellulose within 2 min. The rapid dissolution of cellulose at low temperatures is an exciting and surprising phenomenon. The dissolution mechanism of cellulose in pre-cooled aqueous solution deals with the formation of new hydrogen-bonded networks between cellulose and small molecules in the solvent system, which is at a highly stable state at low temperatures. The new solvents and technique for preparation of the advanced cellulose materials and chemical modifications are simple and low cost. The invention of the NaOH/urea solvent system is significant breakthrough for the possible substitution to viscose method, which causes serious pollution because of the use of CS₂. The preparation of the cellulose products from the NaOH/urea are short production cycle and no evaporation of the chemical agents, namely “green” process. The disadvantage of this technique is that the cellulose with a molecular weight lower than 1.2×10^5 can be dissolved in the solvent, and the cellulose concentration is relatively low. However, the cellulose concentration can enhance from 4wt% to 8wt% with a decrease of cellulose molecular weight from 1.0×10^5 to 3.0×10^4 (64).

References

1. Schurz, J. *Prog. Polym. Sci.* **1999**, *24*, 481–483.
2. Eichhorn, S. J.; Young, R. J.; Davies, G. R. *Biomacromolecules* **2005**, *6* (1), 507–513.
3. Klemm, D.; Heublein, B.; Fink, H.-P.; Bohn, A. *Angew. Chem., Int. Ed.* **2005**, *44*, 3358–3393.
4. Zhu, S.; Wu, Y.; Chen, Q.; Yu, Z.; Wang, C.; Jin, S.; Ding, Y.; Wu, G. *Green Chem.* **2006**, *8*, 325–327.
5. Hyden, W. L. *Ind. Eng. Chem.* **1929**, *21*, 405–410.
6. Fink, H.-P.; Weigel, P.; Purz, H. J.; Ganster, J. *Prog. Polym. Sci.* **2001**, *26*, 1473–1524.
7. Graenacher, G.; Sallmann, R. U.S. Patent 2,179,181, 1939.
8. Johnson, D. L. Britain Patent 1,144,048, 1967.
9. Swatloski, R. P.; Spear, S. K.; Holbrey, J. D.; Rogers, R. D. *J. Am. Chem. Soc.* **2002**, *124*, 4974–4975.
10. Turner, M. B.; Spear, S. K.; Holbrey, J. D.; Rogers, R. D. *Biomacromolecules* **2004**, *5*, 1379–1384.
11. Abbott, A. P.; Bell, T. J.; Handaa, S.; Stoddart, B. *Green Chem.* **2006**, *8*, 784–786.
12. Zhang, H.; Wu, J.; Zhang, J.; He, J. *Macromolecules* **2005**, *38*, 8272–8277.
13. News. *Angew. Chem., Int. Ed.* **2005**, *44*, 2320.
14. President Green Chemistry Challenge, United Environmental Protection Agency (EPA744-K-05-001).
15. Ishii, D.; Tatsumi, D.; Matsumoto, T.; Murata, K.; Hayashi, H.; Yoshitani, H. *Macromol. Biosci.* **2006**, *6*, 293–300.
16. Maiti, A.; Pagoria, P. F.; Gash, A. E.; Han, T. Y.; Orme, C. A.; Gee, R. H.; Fried, L. E. *Phys. Chem. Chem. Phys.* **2008**, *10* (33), 5050–5056.
17. Kuang, Q.; Zhao, J.; Niu, Y.; Zhang, J.; Wang, Z. *J. Phys. Chem. B* **2008**, *112*, 10234–10240.
18. Patent EP 1716273 B1, 2005.
19. Fiber formation from liquid crystalline solutions of cellulose CarbaCell in NMMO. Proceedings of the 7th Int. Symp. Alternative Cellulose, Rudolstadt, Germany, 2006.
20. Köhler, S.; Heinze, T. *Macromol. Biosci.* **2007**, *7*, 307–314.
21. Heinze, T.; Dicke, R.; Koschella, A.; Kull, A. H.; Klohr, E.-A.; Koch, W. *Macromol. Chem. Phys.* **2000**, *201*, 627–631.
22. Yanagisawa, M.; Isogai, A. *Biomacromolecules* **2005**, *6* (3), 1258–1265.
23. Dupont, A. L.; Mortha, G. *J. Chromatogr., A* **2004**, *1026* (1-2), 129–141.
24. Lauriol, J. M.; Froment, P.; Pla, F.; Robert, A. *Holzforschung* **1987**, *41*, 109–113.
25. Evans, R.; Wearne, R. H.; Wallis, A. F. A. *J. Appl. Polym. Sci.* **1991**, *42*, 813–820.
26. Henniges, U.; Kloser, E.; Patel, A.; Potthast, A.; Kosma, P.; Fischer, M.; Fischer, K.; Rosenau, T. *Cellulose* **2007**, *14*, 497–511.
27. Zhang, L.; Cai, J.; et al. China Patent ZL 200410012682.4.

28. Zhang, L.; Cai, J.; Zhou, J.; Li, C.; Qi, H.; Mao, Y. PCT: PCT/CN2006/00757.
29. Zhang, L.; Ruan, D.; Zhou, J.; Lue, A.; Li, C. PCT: PCT/CN2006/00756.
30. Cai, J.; Zhang, L. *Macromol. Biosci.* **2005**, *5*, 539–548.
31. Cai, J.; Zhang, L. *Biomacromolecules* **2006**, *7*, 183–189.
32. Cai, J.; Liu, Y.; Zhang, L. *J. Polym. Sci., Part B* **2006**, *44*, 3093–3101.
33. Ruan, D.; Zhang, L.; Zhou, J.; Jin, H.; Chen, H. *Macromol. Biosci.* **2004**, *4*, 1105–1112.
34. Lue, A.; Zhang, L. *J. Phys. Chem. B* **2008**, *112*, 4488–4495.
35. Cai, J.; Zhang, L.; Liu, S.; Liu, Y.; Xu, X.; Chen, X.; Chu, B.; Guo, X.; Xu, J.; Cheng, H.; Han, C. C.; Kuga, S. *Macromolecules* **2008**, *41*, 9345–9351.
36. Kamide, K.; Okajima, K.; Matsui, T.; Kowsaka, K. *Polymer J.* **1984**, *16* (12), 857–866.
37. Cheval, I. U.S. Patent 6,129,867, 2000.
38. Isogai, A.; Atalla, R. H. *Cellulose* **1998**, *5*, 309–319.
39. Kuo, Y-N.; Hong, J. *Polym. Adv. Technol.* **2005**, *16*, 425–428.
40. Fischer, K. *Papier* **1994**, *48*, 769–774.
41. Egal, M.; Budtova, T.; Navard, P. *Biomacromolecules* **2007**, *8*, 2282–2287.
42. Porro, F.; Bédoué, O.; Chanzy, H.; Heux, L. *Biomacromolecules* **2007**, *8*, 2586–2593.
43. Gavillon, R.; Budtova, T. *Biomacromolecules* **2008**, *9*, 269–277.
44. Sescousse, R.; Budtova, T. *Cellulose* **2009**, *16*, 417–426.
45. Vehviläinen, M.; Kamppuri, T.; Rom, M.; Janicki, J.; Ciecchanska, D.; Grönqvist, S.; Siika-Aho, M.; Christoffersson, K. E.; Nousiainen, P. *Cellulose* **2008**, *15*, 671–680.
46. Egal, M.; Budtova, T.; Navard, P. *Cellulose* **2008**, *15*, 361–370.
47. Fialkowski, M.; Bishop, K. J. M.; Klajn, R.; Smoukov, S. K.; Campbell, C. J.; Grzybowski, B. A. *J. Phys. Chem. B* **2006**, *110* (6), 2482–2496.
48. Whitesides, G. M.; Grzybowski, B. *Science* **2002**, *295*, 2418–2421.
49. Chen, X.; Burger, C.; Wan, F.; Zhang, J.; Rong, L.; Hsiao, B. S.; Chu, B.; Cai, J.; Zhang, L. *Biomacromolecules* **2007**, *8*, 1918–1926.
50. Morgenstern, B.; Röder, T. *Papier* **1998**, *52*, 713–735.
51. Cai, J.; Zhang, L.; Zhou, J.; Qi, H.; Chen, H.; Kondo, T.; Chen, X.; Chu, B. *Adv. Mater.* **2007**, *19*, 821–825.
52. Cai, J.; Zhang, L.; Zhou, J.; Li, H.; Chen, H.; Jin, H. *Macromol. Rapid Commun.* **2004**, *25*, 1558–1562.
53. Liu, S.; Zhang, L.; Zhou, J.; Wu, R. *J. Phys. Chem. C* **2008**, *112* (12), 4538–4544.
54. Liu, S.; Zhang, L.; Zhou, J.; Xiang, J.; Sun, J.; Guan, J. *Chem. Mater.* **2008**, *20* (11), 3623–3628.
55. Qi, H.; Cai, J.; Zhang, L.; Nishiyama, Y.; Rattaz, A. *Cellulose* **2008**, *15*, 81–89.
56. Chen, X.; Burger, C.; Fang, D.; Hsiao, B. S.; Chu, B.; Qi, H.; Zhang, L. *J. Biobased Materials and Bioenergy* **2007**, *1*, 266–273.
57. Qi, H.; Chang, C.; Zhang, L. *Green Chemistry* **2009**, *11*, 177–184.
58. Qi, H.; Cai, J.; Zhang, L.; Kuga, S. *Biomacromolecules* **2009**, *10*, 1597–1602.
59. Luo, X.; Liu, S.; Zhou, J.; Zhang, L. *J. Mater. Chem.* **2009**, *19*, 3538–3545.

60. Chang, C.; Duan, B.; Cai, J.; Zhang, L. *Eur. Polym. J.* **2009**, doi: 10.1016/j.eurpolymj.2009.04.033.
61. Heinze, T. *Macromol. Chem. Phys.* **1998**, *199* (11), 2341–2364.
62. Heinze, T.; Liebert, T.; Klüfers, P.; Meister, F. *Cellulose* **1999**, *6* (2), 153–165.
63. Song, Y.; Sun, Y.; Zhang, X.; Zhou, J.; Zhang, L. *Biomacromolecules* **2008**, *9* (8), 2259–2264.
64. Zhou, J.; Zhang, L.; Deng, Q.; Wu, X. *J. Polym. Sci., Polym. Chem.* **2004**, *42*, 5911–5920.
65. Zhou, J.; Xu, Y.; Wang, X.; Qin, Y.; Zhang, L. *Carbohydr. Polym.* **2008**, *74*, 901–906.
66. Zhou, J.; Qin, Y.; Liu, S.; Zhang, L. *Macromol. Biosci.* **2006**, *6*, 84–89.
67. Zhou, J.; Zhang, L. ZL200610124958.7, 2009.
68. Yan, L.; Tao, H.; Bangal, P. R. *Clean* **2009**, *37* (1), 39–44.
69. Lue, A.; Zhang, L.; Ruan, D. *Macromol. Chem. Phys.* **2007**, *208*, 2359–2366.
70. Weng, L.; Zhang, L.; Ruan, D.; Shi, L.; Xu, J. *Langmuir* **2004**, *20*, 2086–2093.
71. Yan, L.; Chen, J.; Bangal, P. R. *Macromol. Biosci.* **2007**, *7*, 1139–1148.
72. Jin, H.; Zha, C.; Gu, L. *Carbohydr. Polym.* **2007**, *342*, 851–858.
73. Ruan, D.; Lue, A.; Zhang, L. *Polymer* **2008**, *49*, 1027–1036.
74. Ruan, D.; Zhang, L.; Lue, A.; Zhou, J.; Chen, H.; Chen, X.; Chu, B.; Kondo, T. *Macromol. Rapid Commun.* **2006**, *27*, 1495–1500.
75. Zhou, D.; Zhang, L.; Zhou, J.; Guo, S. *Water Res.* **2004**, *38*, 2643–2650.
76. Zhou, D.; Zhang, L.; Guo, S. *Water Res.* **2005**, *39*, 3755–3762.
77. Chen, Y.; Zhang, L.; Gu, J.; Liu, J. *J. Membr. Sci.* **2004**, *241*, 393–402.
78. Cai, J.; Zhang, L.; Chang, C.; Cheng, G.; Chen, X.; Chu, B. *ChemPhysChem* **2007**, *8* (10), 1572–1579.
79. Cai, J.; Kimura, S.; Wada, M.; Kuga, S.; Zhang, L. *ChemSusChem* **2008**, *1*, 149–154.
80. Cai, J.; Kimura, S.; Wada, M.; Kuga, S. *Biomacromolecules* **2009**, *10*, 87–94.

Chapter 4

Molten Inorganic Salts as Reaction Medium for Cellulose

S. Fischer* and K. Thümmler

Institute of wood and plant chemistry, Technische Universität Dresden,
Tharandt, Germany

*sfischer@forst.tu-dresden.de

The preparation of cellulose solutions is important for derivatization and blend formation of this natural polymer. Besides solvents like CS_2/NaOH and $\text{NMMNO}\cdot\text{H}_2\text{O}$ unconventional solvent system can be applied for dissolution of cellulose. This group of solvents includes inorganic molten salts and salt hydrates. Inorganic molten salts can be used as efficient solvents for cellulose in a wide range of degree of polymerization. Furthermore molten salts can be applied as reaction medium for the derivatization of cellulose. For both dissolution and derivatization of cellulose the knowledge of the solution state as well as information about chemical interactions with the solvent system is essential. Beside the specific structure of the molten salt hydrate, the cation and the water content of the melt are the most important factors for the dissolving capability of a molten salt hydrate system.

Introduction

The search for new cellulose solvents is still a focus of research. Alternative systems are of special interest for cellulose fiber production and functionalization. Concentrated salt solutions have been known for long time as solvents for cellulose. Intensive investigations have been carried out on swelling and dissolution of cellulose in aqueous zinc chloride.

A review about the swelling ability of inorganic salt solutions was published by Warwicker et al. (1). He stated that a lot of salt systems should be able to swell

or dissolve cellulose. But in later publications only three water/salt-systems were described as effective cellulose solvents in more detail: $\text{Ca}(\text{SCN})_2/\text{H}_2\text{O}$, $\text{LiSCN}/\text{H}_2\text{O}$ und $\text{ZnCl}_2/\text{H}_2\text{O}$.

Lukanoff et al. (2) investigated the dissolving ability of the eutectic melt NaSCN/KSCN and of mixtures of this melt with $\text{Ca}(\text{SCN})_2 \cdot 3\text{H}_2\text{O}$. Only the mixture of NaSCN/KSCN with $\text{Ca}(\text{SCN})_2 \cdot 3\text{H}_2\text{O}$ or dimethyl sulfoxide was able to dissolve cellulose. In addition the authors described molten $\text{LiSCN} \cdot 2.5\text{H}_2\text{O}$ as cellulose solvent.

The solubility of cellulose with different degrees of polymerization (DP) in $\text{Ca}(\text{SCN})_2 \cdot 3\text{H}_2\text{O}$ was discussed by Kuga (3). In the temperature range from 120 °C to 140 °C he observed the solution of the polymer within 40 minutes accompanied by a decrease of DP.

There are several papers discussing the formation of addition compounds between cellulose and the dissolving salts. Xu and Chen (4) worked on the dissolution and fiber formation of cellulose in zinc chloride solutions. The regeneration occurred by precipitation of a zinc-cellulose-complex by alcohol. By treatment with water this complex released cellulose II. The formation of the proposed complex was explained using ^{13}C NMR measurements on cellobiose solutions in zinc chloride.

Systematic investigations regarding the solubility of cellulose in $\text{Ca}(\text{SCN})_2 \cdot 3\text{H}_2\text{O}$ solutions were carried out by Hattori et al. (5, 6). They discussed complex formation between cellulose and $\text{Ca}(\text{SCN})_2$ using IR measurements and reported coordination of the Ca^{2+} ions at O-6 and O-5 of cellulose. These results were also confirmed by ^{13}C and ^1H NMR measurements (7).

Solubility of Cellulose in Molten Salt Hydrates

A multitude of pure molten salt hydrates as well as salt mixtures were investigated with respect to their interaction with cellulose. As a result it turned out to be reasonable to divide the salt hydrates into groups according to their optical visible effect on cellulose. The classification was done as follows: molten salts which a) dissolve, b) swell, c) decompose cellulose, or which d) have no effect on cellulose. Table 1 gives this classification for the molten salt hydrates investigated.

Designation of salt-water-systems:

- e.g. $\text{LiClO}_4 \cdot 3\text{H}_2\text{O}$: the hydrate is solid at room temperature marked by the symbol “•”
- e.g. $\text{ZnCl}_2 + 4\text{H}_2\text{O}$: the hydrate is liquid at room temperature marked by the symbol “+”
- e.g. $\text{ZnCl}_2/\text{MgCl}_2/\text{H}_2\text{O}$: systems of variable compositions marked by the symbol “/”

The melts which were able to dissolve cellulose are very different in composition. They vary in cation and anion and in their water content. This results in the question, which factors determine the dissolving ability of the molten salt hydrates. Until now only one rule for salt-water-systems was published. It

says that salts combining small hard cations with soft polarizable anions have the best dissolving power for cellulose. But the good dissolving ability of lithium perchlorate melts observed by us is inconsistent with this statement, and several other hydrated melts containing lithium with different anions do not show any dissolving ability to cellulose (8).

After a detailed investigation of the melts the following characteristics, that mainly determine the dissolution power towards cellulose were recognized:

- the acidity,
- the water content of the melts,
- and the properties of the coordination sphere of the cations. (9, 10), respectively.

Often these properties influence each other as could be shown by acidity measurements in the system $\text{ZnCl}_2/x\text{H}_2\text{O}$ depending on the amount of water x (11). A change in the water amount correlates with the acidity, which increases with decreasing x . The acidity parameters of the melting systems $\text{ZnCl}_2/\text{H}_2\text{O}$ and $\text{LiClO}_4/\text{H}_2\text{O}$ were investigated using solvatochromic probe molecules. They are comparable to those described for mineral acids. If a hydrated melt should be an effective dissolving agent for cellulose it must have a relative high acidity (12).

The dependence of the dissolving power on the water content in different melt systems could be shown for several systems. Molten $\text{LiClO}_4 \cdot 3\text{H}_2\text{O}$ for instance is an excellent cellulose solvent. An increase of the water amount up to a composition of $\text{LiClO}_4 + 4\text{H}_2\text{O}$ results in a melt which is not able to dissolve the polymer. A significant increase of the swelling grade can be observed by decreasing the water amount of the system $\text{LiCl} + x\text{H}_2\text{O}$ from $x=5$ to $x=2$. The swelling of cellulose in $\text{LiCl} + 2\text{H}_2\text{O}$ is strong enough to cause a transformation of the cellulose modification I into modification II.

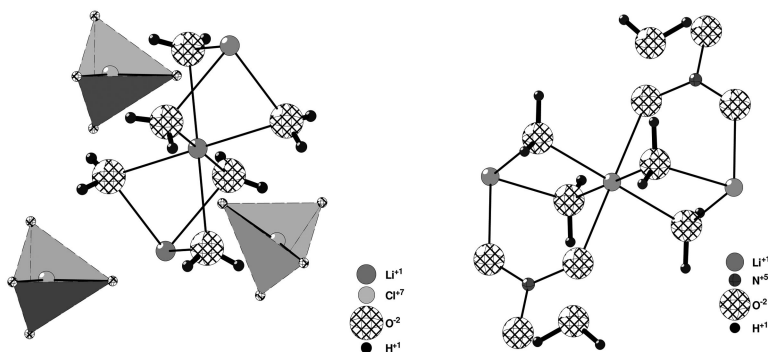
The influence of the structural conditions of the co-ordination sphere of the cations could be explained in Figure 1 by a comparison of the two trihydrates $\text{LiClO}_4 \cdot 3\text{H}_2\text{O}$ (solvent) and $\text{LiNO}_3 \cdot 3\text{H}_2\text{O}$ (no solvent) (8). Although the salts have the same water content, there are differences in their structures. In the case of the perchlorate the water is completely bridged and bound to the cations. The anions do not affect the co-ordination sphere of the lithium ions. The cleavage of the water bridges results in “free” co-ordination sites. The replacement of water molecules by hydroxyl groups of the cellulose is possible, too.

The structure of the nitrate is characterized by water molecules not only bridged between the cations but also at interstitial positions. Because of the bound anions at the cations there is a water deficit at the lithium cations.

The nitrate ions can not be replaced by hydroxyl groups because the water from the interstitial positions will prefer to saturate the co-ordination sphere of the cations.

Table 1. Molten salt hydrates and their interaction to cellulose

<i>group</i>	<i>pure melt</i>	<i>melt mixtures</i>
dissolution	ZnCl ₂ •3•4H ₂ O LiClO ₄ •3H ₂ O FeCl ₃ •6H ₂ O	LiClO ₄ •3H ₂ O - ≤25% Mg(ClO ₄) ₂ /H ₂ O LiClO ₄ •3H ₂ O - ≤10% NaClO ₄ /H ₂ O LiClO ₄ •3H ₂ O - MgCl ₂ •6H ₂ O NaSCN/KSCN (eutectic) – LiSCN•2H ₂ O LiCl/2ZnCl ₂ /H ₂ O
swelling	LiCl•2•5H ₂ O LiNO ₃ •3H ₂ O Na ₂ S•9H ₂ O	LiClO ₄ •3H ₂ O - >25% Mg(ClO ₄) ₂ /H ₂ O LiClO ₄ •3H ₂ O - >10% NaClO ₄ /H ₂ O
decomposition	Mg(ClO ₄) ₂ •6H ₂ O MgCl ₂ •6H ₂ O	ZnCl ₂ /MgCl ₂ /H ₂ O
no effect	NaOOCCH ₃ •3H ₂ O	CaCl ₂ •6H ₂ O

*Figure 1. Crystal structure of LiClO₄•3H₂O (left) and LiNO₃•3H₂O (right)*

Structural Changes of Cellulose Dissolved in Molten Salts Hydrates

The different interactions between cellulose and the solvent are reflected in the properties of cellulose samples regenerated from the molten salts. The regenerated products were characterized by WAXS, ¹³C CP/MAS NMR spectroscopy, surface-area determinations, SEC measurements, solvatochromic and SEM investigations in comparison with the raw material.

Using WAXS the transformation of cellulose I into cellulose II could be observed which indicates a strong swelling or dissolution of the polymer. The crystallinity was investigated using solid state NMR spectroscopy (8, 10).

Raman spectroscopy has been established too as an effective method to discuss the transformation of cellulose regenerated from molten inorganic salts (13).

The transformation of cellulose I into cellulose II is caused by dissolving cellulose I in different molten inorganic salt hydrates. Whereas, the cellulose regenerated from melts of $\text{LiSCN}\cdot 2.5\text{H}_2\text{O}$, $\text{LiClO}_4\cdot 3\text{H}_2\text{O}$ and $\text{LiCl}/2\text{ZnCl}_2+8\text{H}_2\text{O}$ yield by dissolution to a transition into modification II. Beside the X-ray scattering experiments (10) the FT Raman spectra measured after regeneration confirmed the polymorphic changes which are shown in Figure 2. For these regenerated celluloses dissolved by the salt melts mentioned above only the Raman bands characterizing the modification II were detected. There also the intensity maxima which are most typical for following the polymorphic transformation are denoted by crosses.

The molar mass distributions determined according a method of Fischer et al. (14) of cellulose regenerated from different molten hydrates are compared with the raw cellulose in Figure 3.

It is to be seen that the cellulose regenerated from $\text{LiClO}_4\cdot 3\text{H}_2\text{O}$ exhibits no decrease in the molar mass compared with the raw cellulose, the other samples show a slight shortening of the chain length. The decrease of the molar mass observed here was in the range known for the pre-treatment of cellulose with NaOH -water. Therefore it could be proved that dissolving of cellulose in molten salt hydrates is not due to a drastically reduction of the chain length.

Dissolution of cellulose in different melts results in varying morphological properties of the regenerated products. This is indicated by differences in the specific surface-area and the pore size and is clearly recognizable in the SEM pictures. Fiber-like samples similar to the raw cellulose were obtained from the thiocyanate melts, but also lamellar samples (from $\text{LiClO}_4\cdot 3\text{H}_2\text{O}$) and layered structures (from chlorides) were regenerated (10). Examples for the different morphologies obtained are given in Figure 4.

Interaction between Cellulose and the Molten Salt Hydrate

As a very sensitive tool to characterize the state of cellulose in molten salt hydrates NMR spectroscopy can be used. Figure 5 shows the ^{13}C NMR spectra of cellulose dissolved in molten $\text{ZnCl}_2+4\text{H}_2\text{O}$, $\text{LiClO}_4\cdot 3\text{H}_2\text{O}$ and $\text{LiSCN}\cdot 2.5\text{H}_2\text{O}$. The signals of the carbon atoms $\text{C}_1 - \text{C}_6$ are well resolved and the spectrum is very similar to that of cellulose dissolved in conventional solvents like sodium hydroxide solution (15). A derivatization by the solvent can not be observed. Therefore molten salt hydrates can be attributed to the group of non-derivatizing solvent systems.

Due to the different magnetic susceptibilities and melting points of the molten salt hydrates it is difficult to compare the chemical shifts of the carbon nuclei in the different solvents. Nevertheless it can be pointed out that the relative positions of the carbon signals differ for the investigated solvents. Whereas the chemical shifts of the cellulose carbon nuclei are nearly identical in the molten lithium salts, the values for especially C_1 to C_5 are significantly smaller in the $\text{ZnCl}_2+4\text{H}_2\text{O}$ melt. We interpret this as an indication for cellulose – solvent interactions of different strength.

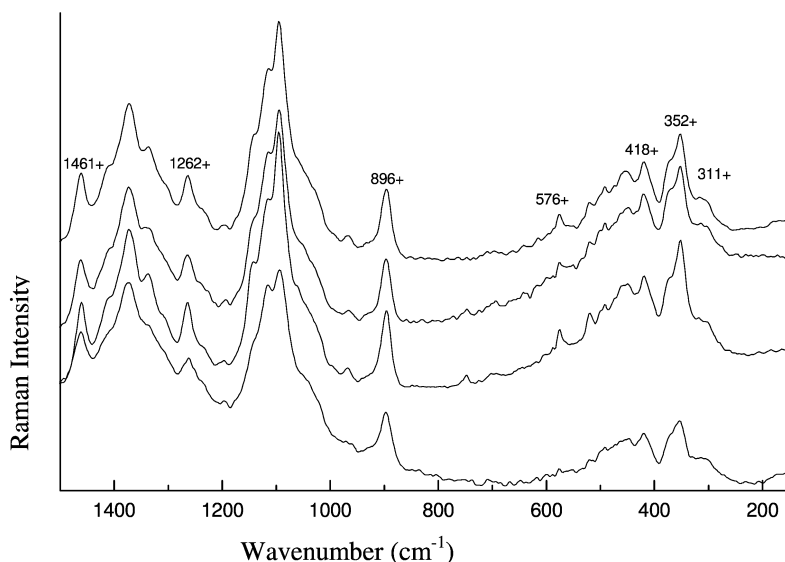


Figure 2. FT Raman spectra of cellulose II regenerated from different molten salts hydrates in the range 1500 - 150 cm^{-1}

Further information about the interaction between cellulose and molten inorganic salts can be acquired by ^7Li NMR investigations (16) and Raman measurements (17).

Röder (18) investigated the structure of cellulose dissolved in molten $\text{LiClO}_4 \cdot 3\text{H}_2\text{O}$ by static laser-light-scattering. The investigation of cellulose solutions in molten $\text{LiClO}_4 \cdot 3\text{H}_2\text{O}$ by static light-scattering measurements at high temperature showed that cellulose molecules form aggregates. The solvent is not able to destroy the intermolecular hydrogen bonds between cellulose chains completely. Single cellulose molecules could not be found. A comparison of the measured form factor function with theoretical models showed that the shape of the particles is between a globular and a homogenous branched structure. The increase of the function in the Kratky plot can be explained with a second component – small particles or arms of fringed micelles. The analysis indicates for cellulose in molten salts comparable structures like for solutions of cellulose in N-methylmorpholine-N-oxide-monohydrate (19).

Reactions of Cellulose in Molten Inorganic Salt Hydrates

Molten inorganic salt hydrates as so-called non-derivatizing solvents were not only established as very efficient solvents for cellulose, they can also be applied as a medium for the chemical functionalization of the polymer. Using molten inorganic salt hydrates as new reaction media etherification (e.g. carboxymethylation) and esterification (e.g. acetylation) of cellulose are possible and will be discussed here.

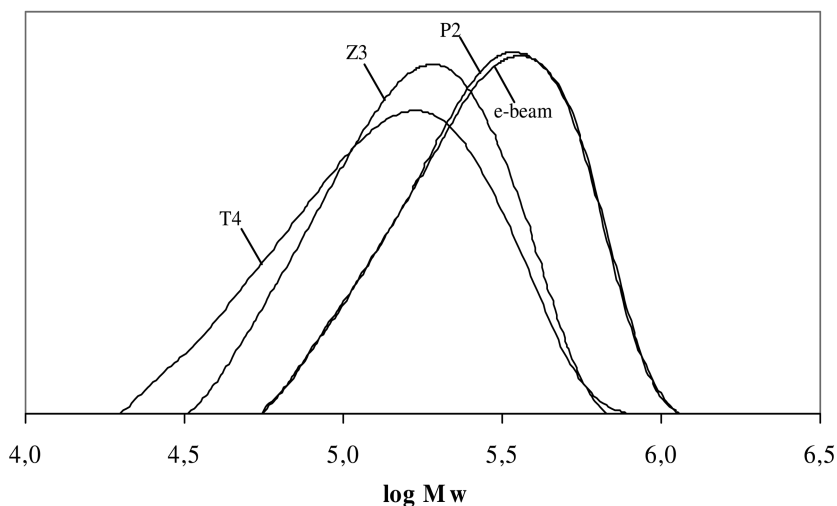


Figure 3. Molar mass distribution of the nitrates of the cellulose samples regenerated from P2: $\text{LiClO}_4 \cdot 3\text{H}_2\text{O}$, Z3: $\text{ZnCl}_2 + 4\text{H}_2\text{O}$, T4: $\text{NaSCN/KSCN/LiSCN/H}_2\text{O}$, C: raw cellulose

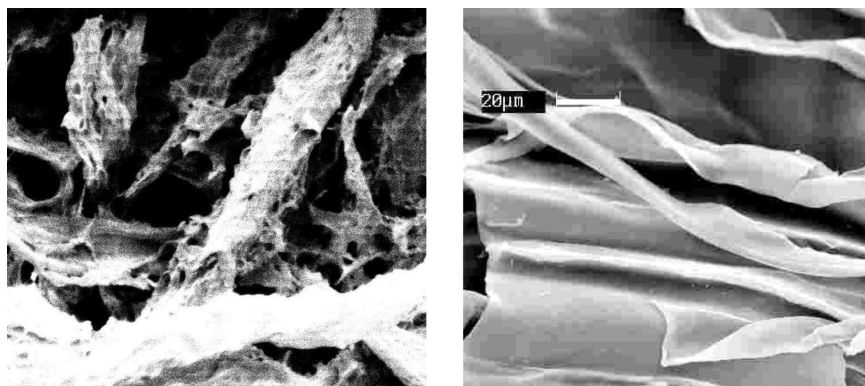


Figure 4. SEM pictures of celluloses regenerated from $\text{NaSCN/KSCN/LiSCN/H}_2\text{O}$ (left) and $\text{LiClO}_4 \cdot 3\text{H}_2\text{O}$ (right)

Carboxymethylation

Because of the fact that the solvent $\text{LiClO}_4 \cdot 3\text{H}_2\text{O}$ was extensively studied (8, 9) preliminary experiments concerning its use as reaction medium were carried out (20). The results were very promising and therefore systematic studies regarding carboxymethylation of cellulose in different inorganic molten salts were started. The method and the preparation procedure were described (21).

The homogeneous carboxymethylation of cellulose in molten $\text{LiClO}_4 \cdot 3\text{H}_2\text{O}$ is possible using sodium monochloracetate in the presence of NaOH.

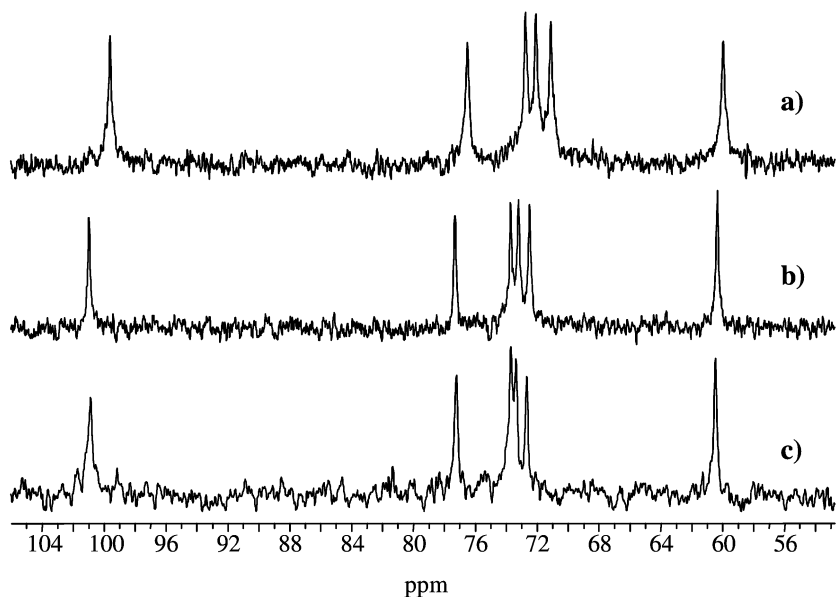


Figure 5. ^{13}C NMR spectra of cellulose dissolved in molten a) $\text{ZnCl}_2\cdot 4\text{H}_2\text{O}$ at 65°C , b) $\text{LiClO}_4\cdot 3\text{H}_2\text{O}$ at 110°C , c) $\text{LiSCN}\cdot 2\text{H}_2\text{O}$ at 130°C

A remarkable finding is that polymers with DS values as high as 2 can be prepared within a short reaction time (4 hours) applying a one-step synthesis. Up to now this was only possible by conversion of cellulose in DMA/LiCl or using the so-called induced phase separation (22, 23) which starts from organo-soluble hydrolytically unstable intermediates. In the case of homogeneous carboxymethylation or reaction in slurry the highest DS reachable in a one step procedure is about 1.3.

Selected samples were characterized by means of ^1H -NMR spectroscopy after chain degradation with a mixture of $\text{D}_2\text{SO}_4/\text{D}_2\text{O}$ (24, 25). A distribution of substituents on the level of the AGU in the order $\text{C-6} > \text{C-2} \approx \text{C-3}$ was discovered and the investigations showed that a complete substitution at position *O*-6 is possible.

Further investigations showed that carboxymethylation is also possible in the system $\text{LiCl}\cdot\text{H}_2\text{O}$ starting from swollen cellulose. The DS of CMC prepared in molten $\text{LiCl}\cdot x\text{H}_2\text{O}$, i.e. in a heterogeneous reaction, is generally lower than the DS of the samples obtained from dissolved cellulose in molten $\text{LiClO}_4\cdot 3\text{H}_2\text{O}$. The DS also depends on the molar ratio AGU:sodium monochloracetate:NaOH and the DS decreases with increasing water content of the molten salt hydrate.

The samples have a similar distribution of carboxymethyl groups like CMCs prepared under homogeneous conditions. The results show a distribution of substituents on the level of the AGU in the order $\text{C-6} > \text{C-3} \approx \text{C-2}$. That means, there is also a difference between carboxymethylation in this swelling medium and conventionally produced CMCs.

Comprehensively it can be said that a etherification like carboxymethylation of cellulose in hydrated melts yields products of a high degree of substitution of up to 1.96 in an one step synthesis within a short reaction time. Consequently, molten $\text{LiClO}_4 \cdot 3\text{H}_2\text{O}$ is an efficient solvent for carboxymethylation of cellulose yielding highly functionalized polymers. Moreover, a specific influence on the distribution of functional groups on the level of the AGU is accessible.

Acetylation

Several molten inorganic salt hydrates were applied as media for the acetylation of cellulose. The formation of cellulose acetate depended on the used molten salt hydrate itself as well as on the water content of the melt (26).

However, the only melt in which the acetylation was successful is the eutectic mixture of NaSCN and KSCN with addition of 10% $\text{LiSCN} \cdot 2\text{H}_2\text{O}$. The most important condition for the success of the reaction was the minimization of the water content of the melt. The acetylation was carried out at a temperature of 130 °C with a high excess of acethanhydride (50–100%). During a short reaction time (0.5–3 h) cellulose acetate with a DS in a range between 1 and 2.5 were obtained. The samples were characterized by IR-spectroscopy. For a detailed characterization X-ray and NMR-measurements were carried out. By these investigations it could be shown that the acetylation in molten thiocyanate leads to the formation of amorphous cellulose acetate (27).

The DS obtained for the cellulose acetates depends on the reaction time and on the molar ratio between AGU and acethanhydride.

For future work we will extend the use of molten salt hydrates to other applications. So it is possible to use the acidic properties of the molten inorganic hydrates for the cleavage of functional groups. For instance cellulose triacetate deacetylation can be carried out in molten $\text{ZnCl}_2 + 4\text{H}_2\text{O}$. After a reaction time of 21h a DS of 1.81 and PDS (C6) of 0.53 were obtained (10). Furthermore molten $\text{ZnCl}_2 + 4\text{H}_2\text{O}$ or $\text{LiClO}_4 \cdot 3\text{H}_2\text{O}$ can be applied as medium for deprotection of triphenylmethyl cellulose. A complete deprotection occurs in the comparatively short reaction time of 3 to 5 hours (28).

Blend Formation

Use of molten salts as medium for the blending of cellulose with synthetic polymers was studied. It was shown that formation of cellulose-polyacrylonitrile-blends is possible by dissolving a mixture of PAN and cellulose in molten thiocyanates simultaneously. $\text{KSCN}/\text{NaSCN}/\text{LiSCN} \cdot 2\text{H}_2\text{O}$ is the first choice for that process because it can dissolve both the naturally and a synthetically polymer completely. Regeneration of the blend from the polymer solution can be simply achieved by cooling the melt to room temperature and treating the polymer/salt mixture with water for a complete removal of the thiocyanates. A homogeneous polymer blend was obtained by this simple procedure.

The thermal properties of the blend were determined. These blends show similar behavior, as described for material made from DMF/N₂O₄ solutions. Examining the structure of the blends by means of NMR spectroscopy did not provide direct information about interactions between the polymers. Nevertheless, the change in the intensity of nitrile signals is a first hint for interactions between the polymer components initiated via this moiety.

In principle, the use of molten salts allows a broad variety of crystallization conditions. It can be distinguished between very quickly crystallizing systems on one hand and systems with extreme tendency towards hypothermia on other hand. The variation of coagulation conditions and the resulting properties of blends are important for tailored preparation of polymer blends and will be the topic of further investigations.

Conclusion

Molten salt hydrates are effective and efficient media for cellulose dissolution. During the investigations regarding the solubility of cellulose in molten salts new solvents were found (LiClO₄·3H₂O). First time factors which determining solution ability of cellulose in molten inorganic salt hydrates was found. This knowledge is a basis for discovering further molten hydrates as solvents for cellulose.

The structural change of cellulose after dissolution depends on the respective hydrated molten salt. Therefore it should be possible to adjust specific cellulose structures by choosing a certain salt melt for cellulose dissolution and regeneration.

For cellulose carboxymethylation and acetylation it was shown exemplary, that molten salt hydrates are efficient solvents for cellulose derivatization yielding highly functionalized polymers.

The results are a basis for further investigations using molten inorganic salts as a reaction medium for cellulose, which will be extended to other polysaccharides.

References

1. Warwicker J. O.; Jeffries R.; Colbran I. ; Robinson R. N. *Shirley Institute Pamphlet. No. 93*, Manchester, 1966.
2. Lukanoff, B.; Schleicher, H.; Philipp, B. *Cell. Chem. Technol.* **1983**, *17*, 593–599.
3. Kuga, S. *J. Colloid Interface Sci.* **1980**, *77*, 413–418.
4. Xu, Q.; Chen, L. F. *Text. Technol. Int.* **1996**, *40*, 19–21.
5. Hattori, M.; Shimaya, Y.; Saito, M. *Polymer J.* **1998a**, *30*, 37–42.
6. Hattori, M.; Shimaya, Y.; Saito, M. *Polymer J.* **1998b**, *30*, 43–48.
7. Hattori, M.; Shimaya, Y.; Saito, M. *Polymer J.* **1998c**, *30*, 49–5.
8. Fischer, S.; Voigt, W.; Fischer, K. *Cellulose* **1999a**, *6*, 213–219.
9. Fischer, S.; Leipner, H.; Brendler, E; Voigt, W.; Fischer, K. *ACS Symposium Series* **1999b**, *737*, 143–150.

10. Leipner, H.; Fischer, S.; Brendler, E.; Voigt, W. *Macromol. Chem. Phys.* **2000**, *201*, 2041–2049.
11. Leipner H. Dissertation A, TU Bergakademie Freiberg, Germany, 2002.
12. Fischer, S.; Voigt, W.; Fischer, K.; Spange, S.; Vilsmeier, E. *Molten Salt Forum* **1998**, *5–6*, 477–480.
13. Schenzel, K.; Fischer, S. *Cellulose* **2001**, *8*, 49–57.
14. Fischer, K.; Schmidt, I.; Hintze, H. *Papier* **1994**, *48*, 769–774.
15. Nehls, I.; Wagenknecht, W.; Philipp, B.; Stscherbina, D. *Prog. Polym. Sci.* **1994**, *78*, 1929–1979.
16. Brendler, E.; Fischer, S.; Leipner, H. *Cellulose* **2002**, *8*, 283–288.
17. Fischer, S.; Leipner, H.; Thümmeler, K.; Brendler, E.; Peters, J. *Cellulose* **2003**, *10*, 227–236.
18. Röder, T. Dissertation A, TU Dresden, Germany, 1998.
19. Röder, T.; Morgenstern, B. *Polymer* **1999**, *40*, 4143–4147.
20. Heinze, Th.; Pfeiffer, K. *Angew. Makromol. Chem.* **1999**, *266*, 37–45.
21. Fischer, S.; Thümmeler, K.; Pfeiffer, K.; Liebert, T.; Heinze, T. *Cellulose* **2002**, *9*, 293–300.
22. Heinze, Th.; Erler, U.; Nehls, I.; Klemm, D. *Angew. Makromol. Chem.* **1994**, *215*, 93–106.
23. Liebert, T.; Heinze, Th. *ACS Symposium Series* **1998**, *688*, 61–72.
24. Gronski, W.; Hellmann, G. *Papier* **1987**, *41*, 668–672.
25. Baar, A.; Kulicke, W-M.; Szablikowski, K.; Kiesewetter, R. *Macromol. Chem. Phys.* **1994**, *195*, 1483–1492.
26. Thümmeler K.; Fischer S.; Peters J.; Liebert T.; Heinze Th. *Cellulose*, **2009**, in press.
27. Fischer S. Habilitationsschrift, TU Bergakademie Freiberg, Germany, 2004.
28. Fischer, S.; Leipner, H.; Liebert, T.; Heinze, Th. *Polym. Bull.* **2001**, *45*, 517–521.

Chapter 5

Dimethyl Sulfoxide and Ammonium Fluorides — Novel Cellulose Solvents

Thomas Heinze* and Sarah Köhler

Centre of Excellence for Polysaccharide Research,
Friedrich Schiller University of Jena, Humboldtstraße 10, D-07743 Jena,
Germany

*E-mail: thomas.heinze@uni-jena.de, Member of the European
Polysaccharide Network of Excellence, EPNOE (www.epnoe.eu)

The present knowledge about new and efficient cellulose solvents dimethyl sulfoxide in combination with ammonium fluorides, in particular tetra-*n*-butylammonium fluoride trihydrate, was reviewed. The paper included our knowledge about the dissolution process and the state of dissolution as well as the homogeneous functionalization of the biopolymer studied up until now. Even anhydrous tetra-*n*-butylammonium fluoride in combination with DMSO dissolved the polysaccharide. Different types of cellulose with degrees of polymerization (DP) up to 1200 were soluble within 1 h at 60°C. It was shown that the non-derivatizing solvent dissolved the polymer with moderate to no depolymerization depending on the dissolution time, temperature and ammonium fluoride used. Various homogeneous reactions of cellulose including acetylation, carbamylation, and acylation with *in-situ* activation of carboxylic acids by *N,N'*-carbonyldiimidazole, as well as typical etherification and grafting reactions were discussed.

The complex supramolecular structures of cellulose formed by inter- and intramolecular hydrogen bonds have hindered the dissolution of the biopolymer in common organic solvents and water. Although various solvents and solvent systems have been developed in the last few decades (1, 2), the efficient dissolution of cellulose has remained a very important topic in polysaccharide

research. For detailed characterization, e.g., the determination of the molecular weight and the molecular weight distribution, required complete dissolution of the polysaccharide. Furthermore, processing of cellulose must be carried out in the solution state because the melting temperature of cellulose is above the degradation temperature. Processing has been of great scientific- and even commercial importance. Moreover, new pathways for the derivatization could be applied with the dissolved biopolymer.

On the one hand, the Viscose- (water; NaOH and CS₂), Cupro- (water, cuprammonium hydroxide) and Lyocell processes (*N*-methylmorpholine-*N*-oxide monohydrate as solvent) were carried out commercially for cellulose regeneration to fibers, films, and sponges, (3). On the other, homogeneous derivatization of cellulose applying these solvents and solvent systems was limited because they contained water and/or the solutions could not be mixed without gelation or even precipitation of the biopolymer. Additionally, side reactions like hydrolysis of the reagents and even of the polymer chain occurred during chemical modification.

Non-aqueous solvents for cellulose have also been developed. *N,N'*-dimethylacetamide (DMA)/LiCl, i.e., a polar aprotic liquid in combination with a salt, was one of the most applied non-derivatizing solvents for laboratory scale purposes (4). Although many investigations have probed the mechanism and state of dissolution, a detailed description of the solvent complex formed has remained elusive (4–8). Nevertheless, a broad variety of homogeneous functionalization reactions were successfully performed. Moreover, DMA/LiCl was used for analytical purposes due to fact that the solvent was colorless and the dissolution succeeded with minimal or no degradation of the cellulose. However, the dissolution of the polymer was time-consuming. The components of the solvent (DMA, LiCl) and the cellulose needed to be water-free and, therefore, had to be dried (9). Moreover, a pre-activation of cellulose was necessary.

Recently, it was found that dimethyl sulfoxide (DMSO) in combination with tetra-*n*-butylammonium fluoride trihydrate (TBAF·3H₂O) efficiently dissolved cellulose (10). In this article, the present knowledge about this novel solvent has been presented. The main focus addressed homogeneous chemistry carried out with DMSO/TBAF as a reaction medium.

The Solvent DMSO/Ammonium Fluorides

Dissolution of microcrystalline cellulose and pulps (DP up to 600) in DMSO/TBAF·3H₂O within 15-30 minutes at room temperature without any pretreatment was reported (10, 11). The dissolution of cellulose with higher DP < 600 gave clear systems after a simple pretreatment (cellulose in DMSO at 60-80°C and stirring) prior to the addition of TBAF·3H₂O. Other ammonium halides (bromide and chloride) in combination with DMSO did not dissolve cellulose; only swelling was observed although other authors described dissolution (12).

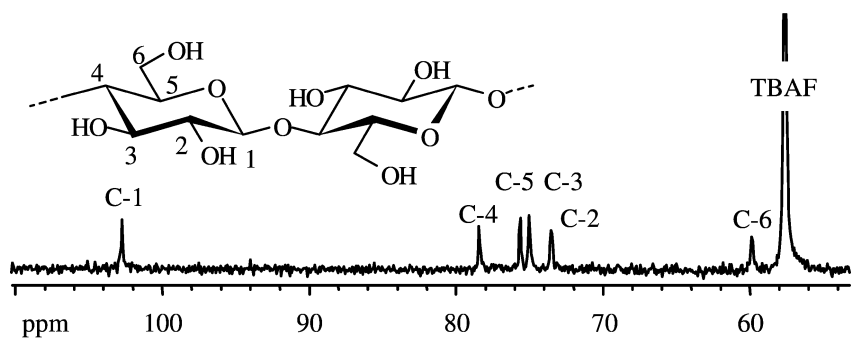


Figure 1. ^{13}C NMR spectrum of cellulose (3%, w/v) dissolved in DMSO/TBAF·3H₂O recorded at 50°C (Number of scans = 9200, Signals below 57 ppm were not shown)

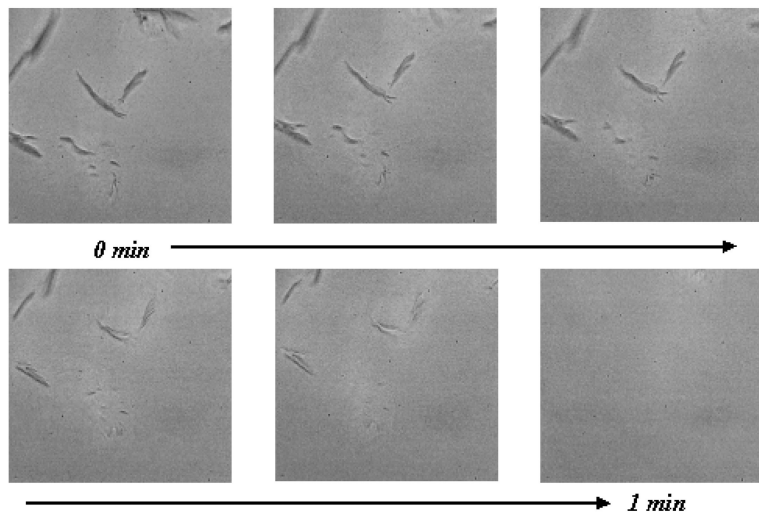


Figure 2. Optical microscopic observation of the dissolution of bleached cotton fibers in water-free DMSO/10 wt.-% TBAF at 35°C.

DMSO/TBAF·3H₂O dissolved cellulose without the formation of covalent bonds, i.e., it was a non-derivatizing solvent. The typical 6 signals of the C atoms of the unmodified anhydroglucose unit (AGU) appeared in the ^{13}C NMR spectrum (Figure 1). Except for peaks of the tetra-*n*-butylammonium moieties (57.7, 22.9, 18.8, and 13.2 ppm), signals appeared as expected at 102.7 (C-1), 78.4 (C-4), 75.6 (C-5), 75.0 (C-3), 73.5 (C-2), and at 59.9 ppm (C-6) the unmodified anhydroglucose unit (AGU). These results were in excellent agreement with those obtained for non-derivatizing cellulose solvents like DMA/LiCl (1).

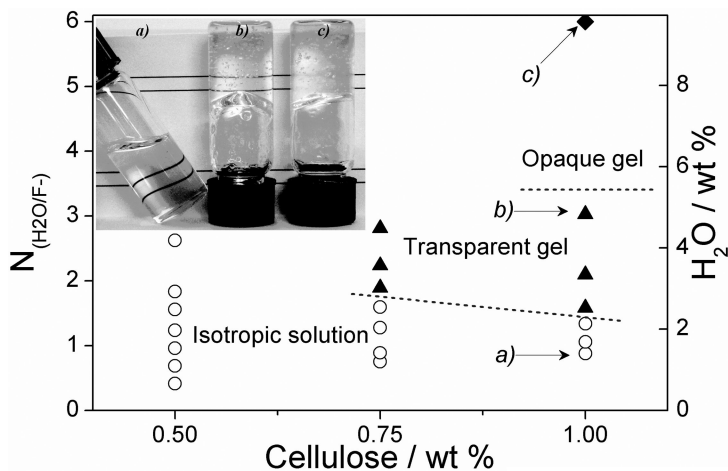


Figure 3. Photo and plot of samples at different cellulose- and water content, ○ Samples at isotropic solutions, ▲ Transparent solutions, ◆ Opaque gels.

Nevertheless, the mechanism of cellulose dissolution in DMSO/TBAF·3H₂O still has not been determined. Water has been recognized to have an important role in this process, just like for DMA/LiCl (9). The fluoride anion interacted more strongly with water than with its voluminous tetra-*n*-butylammonium counter ion or even with DMSO. In the presence of cellulose, interactions of fluoride with both the hydroxyl moiety of the biopolymer and water may have taken place. If the fluoride ion acted as a hydrogen bond acceptor to the OH of cellulose, chain separation and dissolution of the biopolymer may have occurred through the breakage of cellulose-cellulose hydrogen bonds. It was assumed that the presence of a certain amount of water may even have facilitated the dissolution process and minimized chain aggregation (11).

Interestingly, a water free DMSO/TBAF solution prepared according to reference (13) dissolved cellulose quickly even in the presence of the by-product hexacyanobenzene ((14), Figure 2). Up to 4 wt.-% of cellulose (DP up to 1,198) were soluble in the water-free system, which was comparable to the solubility of cellulose in DMSO/TBAF·3H₂O. The mixture of DMSO/TBAF and hexacyanobenzene was stable for about 24 h; then TBAF decomposed in the absence of water and formed difluoride anions (15) without biopolymer dissolution. Thus, the dissolution process of cellulose in DMSO/TBAF was essentially influenced by fluoride anions while water played a minor role, at least up to the TBAF trihydrate. Higher amounts of water were not tolerated; the cellulose precipitated.

Table I. Degree of Polymerization (DP) of the Starting Cellulose and Cellulose after Dissolution and Regeneration (DP_{reg}) from DMSO/TBAF·3H₂O and DMSO/BTMAF·H₂O

<i>DMSO/Salt</i>	<i>Time</i>	<i>Temperature</i>	<i>Cellulose</i>	<i>DP</i>	<i>DP_{reg}</i>
	<i>h</i>	<i>°C</i>			
TBAF·3H ₂ O	0.2	22	Microcrystalline Cellulose	332	330
TBAF·3H ₂ O	1	60	Microcrystalline Cellulose	332	331
TBAF·3H ₂ O	24	60	Microcrystalline Cellulose	332	313
TBAF·3H ₂ O	24	80	Microcrystalline Cellulose	332	236
TBAF·3H ₂ O	1	60	Spruce Sulfite Pulp	600	596
TBAF·3H ₂ O	24	80	Spruce Sulfite Pulp	600	595
TBAF·3H ₂ O	1	60	Cotton Linters	1198	1102
TBAF·3H ₂ O	24	80	Cotton Linters	1198	685
BTMAF·H ₂ O	2.2	80	Microcrystalline Cellulose	290	288

From a practical point of view, typical solvent mixtures contained 6.6 g TBAF·3H₂O (trihydrate is stable and commercially available) in DMSO, thus, the mixture contained 1.71 wt.% water. Through measurement of composition dependence of the ¹⁹F- and ¹H NMR chemical shifts and line widths, greater insight into the dissolution and gelation mechanism for cellulose/DMSO/TBAF and water were obtained (A. Östlund, personal communication). Up to 1 wt.% cellulose and a molar ratio of water to fluoride ions ($N_{(H_2O/F^-)}$) up to 6 could be classified into three categories with respect to their physical appearance: isotropic solutions, transparent solutions, and opaque gels (Figure 3). Note that TBAF was a highly hygroscopic salt and may have contained water in excess of the trihydrate. This water may have influenced solubility and subsequent chemical functionalization of the cellulose.

Other ammonium fluorides, e.g., tetramethylammonium fluoride (TMAF), benzyltrimethylammonium fluoride monohydrate (BTMAF·H₂O), and tetramethylammonium fluoride in combination with DMSO were studied with respect to cellulose dissolution (14). Obviously, the concentration of fluoride ions, determined by the solubility of the salt in DMSO, influenced cellulose dissolution. A certain amount of fluoride anions were required for the conversion of DMSO into a solvent. At room temperature, TBAF·3H₂O exhibited solubility in DMSO of 0.94 mol/L, whereas BTMAF·H₂O only dissolved to concentrations of 0.025 mol/L, and 0.142 mol/L at 90°C. TMAF was almost insoluble in DMSO and thus, TMAF was not appropriate for the preparation of a cellulose solvent. Up to 1 wt.% cellulose was soluble in DMSO/BTMAF·H₂O when the mixture

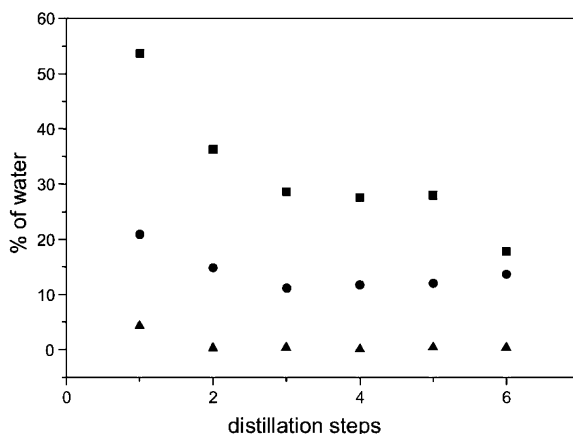


Figure 4. Amount of water (determined by Karl-Fischer method) as a function of distillation steps during the dewatering process for (■) DMSO/TBAF·3H₂O, (●) DMSO/TBAF·3H₂O/Avicel and (▲) DMSO/TBAF·3H₂O/Sisal.

was heated to 85°C for the maintenance of an adequate concentration of fluoride anions, i.e., a minimal amount of 2.2 fluoride anions per AGU. For the case of TBAF·3H₂O, the relationship between the fluoride anions and the AGU depended upon the degree of polymerization (DP) of the cellulose. For instance, dissolution of microcrystalline cellulose (Avicel, DP 332) required a 1/1 (salt/cellulose) ratio while a 3/1 ratio was necessary for spruce sulfite pulp (DP 600) and cotton linters (DP 1,198).

In Table I, the DP (determined by capillary viscometry in Cuen) of both the starting- and the regenerated polymer after dissolution in air were summarized. Obviously, no degradation of microcrystalline cellulose in DMSO/TBAF·3H₂O occurred for dissolution times up to 24 h at 60°C. Depolymerization started after one day at 80°C. Spruce sulfite pulp dissolved in DMSO/TBAF·3H₂O and DMSO/BTMAF·H₂O under various dissolution conditions and showed no difference with DP. Cotton linters cellulose was stable for 1 h at 60°C in TBAF·3H₂O. The prolongation of the treatment to 24 h at 80°C led to degradation of the polysaccharide in both solvents.

Furthermore, DMSO/TBAF·3H₂O completely dissolved ball-milled plant cell-walls and chemical derivatization under homogeneous reaction conditions, including acetylation and methylation was possible (17).

DMSO/TBAF as a Reaction Medium

In order to evaluate the potential of the new solvent DMSO/TBAF·3H₂O for functionalization reactions of dissolved cellulose, etherification and esterification were studied.

Table II. Conditions and Results of various Etherification Reactions in DMSO/TBAF·3H₂O

<i>Cellulose Derivative</i>	<i>No.</i> ^a	<i>TBAF·3H₂O</i> wt.-%	<i>Reagents</i>	<i>Molar Ratio</i>	<i>Time</i> <i>h</i>	<i>Temp.</i> °C	<i>DS</i>
CMC	1a	16.9	SMCA	1/5/10	0.5	70	1.82
CMC	1b	16.9	SMCA	1/5/10	1	70	2.06
CMC	1c	16.9	SMCA	1/5/10	4	70	2.09
CMC	1d	16.9	SMCA	1/10/20	4	70	2.07
CMC	1e	16.9	SMCA	1/10/20	48	70	1.89
BC	2a	4.5	Benzyl Chloride	1/3/3	4	70	0.43
BC	2b	9.0	Benzyl Chloride	1/3/3	4	70	1.22
BC	2c	13.5	Benzyl Chloride	1/3/3	4	70	1.32
AC	3a	18.2	Allyl Chloride	1/38/38	4	50	0.50
AC	3b	18.2	Allyl Chloride	1/38/38	8	50	1.30
AC	3c	18.2	Allyl Chloride	1/38/38	48	50	2.98

^a Starting material for samples **1a-e**: microcrystalline cellulose (DP 330), **2a-c**: cotton linters (DP 400), **3a-c**: spruce sulfite pulp (DP 504)

Etherification Reactions

Carboxymethylation (10, 18, 19), benzylation (20) and allylation (21) of cellulose were investigated (Table II). Carboxymethylation was initiated by the addition of aqueous NaOH to cellulose dissolved in DMSO/TBAF·3H₂O and subsequently sodium monochloroacetate (SMCA) was added (19). The carboxymethyl cellulose (CMC) possessed a statistical distribution of the possible repeating units. This result indicated that the aqueous NaOH activated the polymer chain evenly and no reactivity variation existed between different regions of the polymer dissolved in DMSO/TBAF·3H₂O. These results were comparable to those obtained for a completely heterogeneous reaction (alkali cellulose suspended in organic liquid), a totally homogeneous reaction (cellulose dissolved in Nitren), and a reaction that started homogeneously that used solid NaOH in the presence of water (cellulose dissolved in DMA/LiCl) and led to products with statistical amounts of the different repeating units (23, 24). Moreover, carboxymethylation in so-called reactive microstructures were studied (18, 25).

Table III. Results and Conditions of Esterification Reactions in DMSO/TBAF·3H₂O

Cellulose ^a	Reaction Conditions					Product	
	Molar Ratio ^b	TBAF·3H ₂ O wt.-%	Acylation Agent	Time h	Temp. °C	No.	DS
MC	1/2.3	18.2	Acetic Anhydride	40	70	4a	0.83
MC	1/2.3	18.2	Vinyl Acetate	40	70	4b	1.04
MC	1/2.3	18.2	Vinyl Butyrate	40	70	4c	0.86
MC	1/2.3	18.2	Vinyl Benzoate	40	70	4d	0.95
MC	1/10	18.2	Vinyl Laurate	40	70	4e	2.60
Sisal	1/2.3	10.0	Acetic Anhydride	3	60	5a	0.30
Sisal	1/2.3	7.3	Acetic Anhydride	3	60	5b	0.96
Sisal	1/2.3	6.4	Acetic Anhydride	3	60	5c	1.07
Sisal	1/2.3	5.5	Acetic Anhydride	3	60	5d	1.29

^a MC: microcrystalline cellulose (Avicel, DP 260), Sisal: sisal cellulose (DP 650) ^b Anhydroglucose unit/acylation agent

For those studies, the reaction started homogeneously and solid sodium hydroxide (NaOH) particles dispersed in DMSO were added, resulting in a highly reactive solid reagent/polymer interface; the reactive microstructure. The results presented in Table II show that derivatives with a degree of substitution (DS) higher than 2 were already obtained within 1 h (**1b**) and a maximum DS of 2.09 (**1c**) was achieved. A prolongation of the reaction time and an increase of the amount of reagent did not increase DS. Characterization by ¹H NMR spectroscopy and HPLC after hydrolytic depolymerization that followed literature procedures (23, 24, 26), indicated that CMC with non-statistical repeating units were accessible. In spite of the high amount of water from the use of the trihydrate of TBAF, derivatives with DS < 2 obtained in a single step with controlled structure (non-statistical repeating units). The results agreed with those obtained by the conversion of cellulose with SMCA and solid NaOH in anhydrous DMA/LiCl, i.e., a specific interaction of water with cellulose in DMSO/TBAF·3H₂O existed. Thus, the substituent pattern of CMC within the polymer chain was controlled through utilization of the solvent DMSO/TBAF·3H₂O with aqueous or solid NaOH.

Benzyl cellulose (BC) had some commercial interest in the past due to the solubility in various organic solvents and unique electrical and thermal properties (27). The synthesis of BC was accomplished by the treatment of cellulose dissolved in DMSO/TBAF·3H₂O with NaOH particles suspended in DMSO or aqueous NaOH solution that yielded a highly swollen material for the subsequent addition of benzyl chloride. It was remarkable that the DS of the BCs obtained increased with increased concentration of TBAF·3H₂O (Table II, **2a-2c**). An influence of the salt concentration on the DS also appeared for cellulose acetate synthesized in DMSO/TBAF·3H₂O (see below). Obviously, the amount of TBAF·3H₂O influenced the “accessibility” of the reactive sites on the polymer chains. A salt content of at least 9.0 wt.% was necessary for sufficient cellulose chain separation and accessible hydroxyl groups. A maximum DS of 1.32 was observed in a solvent mixture with 13.5 wt.% TBAF·3H₂O (**2c**). At a salt concentration of 4.5 wt.%, the cellulose dissolved, as evidenced by an optically clear solution. However, the polymer chains were strongly aggregated; a product with a low DS of 0.43 (**2a**) was obtained. It may be assumed that the derivatization occurred preferentially on the outside of the aggregates and led to a non-uniform distribution of substituents on the AGU along the polymer chains, a condition which has also been observed for different products prepared under homogeneous conditions (28).

The etherification of cellulose with allyl chloride was investigated (22). Allyl cellulose (AC), as an organic-soluble cellulose ether, was a promising biopolymer derivative that allowed the design of novel products through subsequent reactions with the double bonds. As described for the benzylation of cellulose, the addition of solid NaOH dispersed in DMSO caused gelation of the reaction mixture, which then reacted with allyl chloride. The results summarized in Table II clearly show that organic-soluble AC with DS of up to 2.89 (**3c**) could be efficiently prepared. The longer the reaction time, the higher the DS of the obtained AC (**3a-3c**). Nevertheless, prolongation of the reaction time (96 h) yielded cross-linking and, hence, rendered the polymers insoluble. Other conditions, e.g., huge amounts of NaOH, may have led to cross-linking, too. As determined by size exclusion chromatography, limited polymer degradation occurred.

Esterification Reactions

Esterification of cellulose has been an important technical process and has remained as one of the most versatile transformations for the design of novel biopolymer based products. The commercial esterification was carried out under heterogeneous conditions, at least at the beginning of the conversion. Typically, cellulose acetate was prepared by the application of a mixture of acetic acid and acetic acid anhydride with a stoichiometric excess of the anhydride. Amorphous regions of cellulose were initially modified followed by the crystallites. Therefore, the cellulose esters present an uneven functionalization pattern at intermediate stages of reaction. As a consequence, structural control of the products was difficult. Therefore, homogeneous reactions (i.e. starting with the dissolved polymer) are considered as synthetic pathways for the control the substitution

Table IV. Results of the Acetylation of Cellulose with Acetic Anhydride in Consideration of the Water Content in DMSO/TBAF·3H₂O (15 h)

Reaction Conditions		Product	
Molar Ratio	Temp.	No.	DS ^a
AGU/Acetic Anhydride	°C		
1/2.3	70	6a	2.07
1/4.3	70	6b	2.30
1/9.3	70	6c	2.60
1/2.3	100	6e	2.24
1/4.3	100	6f	2.42
1/9.3	100	6g	2.77

^a Determined by ¹H NMR spectroscopy after perpropionylation

pattern and, hence, the product properties. The homogeneous functionalization of cellulose with different DP values (330-950) in DMSO/TBAF·3H₂O with acetic anhydride and various carboxylic acid vinyl esters yielded the corresponding pure cellulose esters (Table III, (29)).

TBAF·3H₂O was a hygroscopic salt that may have contained even more water than the trihydrate. The water could have influenced chemical functionalization of cellulose, especially the reactions with reagents that had fast hydrolysis like acetic anhydride. Nevertheless, a cellulose acetate could be prepared (**4a**). The use of vinyl acetate as a reagent yielded a cellulose acetate by transesterification with a fairly high DS (**4b**) due to the fact that vinyl acetate was more stable against hydrolysis. Interestingly, a highly functionalized cellulose laurate with a DS of 2.6 (**4e**) was obtained by treatment of the dissolved cellulose with vinyl laurate. This results indicated that even fatty acid esters of cellulose could be synthesized efficiently by this type of conversion in DMSO/TBAF·3H₂O.

The decrease of the water content of DMSO/TBAF·3H₂O by vacuum distillation and a subsequent acetylation with acetic anhydride led to products of higher DS (see samples **5a-5d** in Tab. III, (22)). Figure 4 shows a plot of the water content in the distillate versus the distillation step. It is obvious from distillation of pure DMSO/TBAF·3H₂O that 55% of the volume consisted of water. Interestingly, by the distillation of DMSO/TBAF·3H₂O/Avicel and DMSO/TBAF·3H₂O/Sisal only contained 22% and 5% water by volume, respectively. Obviously, water was included in the complex structure of the dissolved polymer that was even more pronounced for Sisal cellulose due to the higher molecular weight, the presence of hemicellulose, and aggregation in the dissolved state.

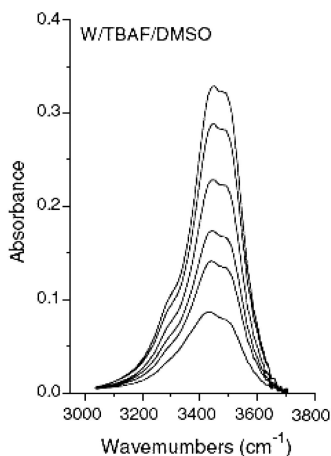


Figure 5. Dependence of peak area on water (*W*) content in 2 wt.% TBAF·3H₂O/DMSO. The concentration of water was 0.1-0.6 mol/l, with increments of 0.1 mol/l.

In order to obtain a solution with little or no aggregation, a sufficient amount of TBAF·3H₂O was necessary (11). Consequently, the hydroxyl groups of the cellulose were more accessible and higher DS values were obtained. However, an increase of the amount of the hygroscopic TBAF·3H₂O led to a strong complexation of the hydroxyl groups by the salt, as already studied for cellulose dissolved in DMA/LiCl, which avoided acetylation. Moreover, the water content in the solvent was higher and thereby, the hydrolysis of acetic anhydride may have occurred faster. The knowledge of the content of water in the solvent was therefore an important parameter for the efficiency of the functionalization, especially for acylation reactions.

The determination of water in DMSO/TBAF·3H₂O was studied by the Karl-Fischer titration method and was problematic because of the presence of hygroscopic salts (9). The quantitative determination was not feasible due to the fact that water was enclosed in the hydrate shell of TBAF·3H₂O. Alternatively, FTIR spectroscopy was successfully applied, using the OH vibration in the range of 3000-3800 cm⁻¹ ((30, 31), Figure 5). After integration of the areas of the peak and subsequent calibration, quantitative analysis of the water in DMSO/TBAF·3H₂O was possible. In considering of the water content at a molar ratio of AGU/acetic anhydride of 1/2.3, a cellulose acetate with a DS of 2.07 (Table IV, 6a) was obtained and represented an almost complete conversion of the reagent. An increase of the molar ratio of reagent to AGU and of the reaction temperature led to highly substituted biopolymer esters with DS up to 2.77 (6g).

The application of water free DMSO/TBAF as a reaction medium in the presence of the by-product tetra-*n*-butylammonium cyanide (obtained by the synthesis of water free TBAF, see above) for acetylation was studied. Cellulose acetate was obtained at a molar AGU/acetic anhydride ratio of 1/3, which was evidenced by the corresponding FTIR spectrum. The characteristic signal of

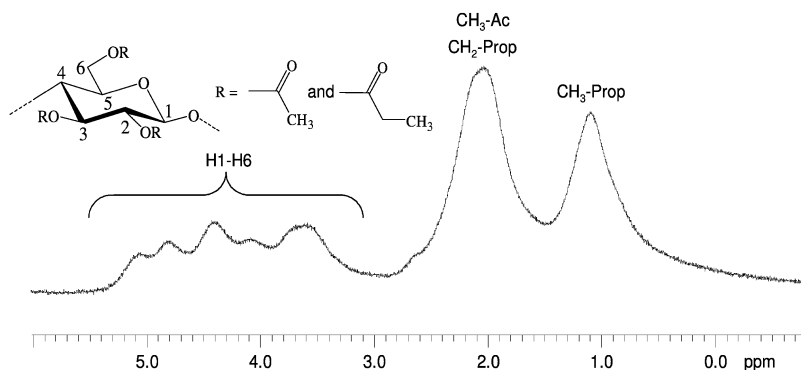


Figure 6. ^1H NMR spectrum of perpropionylated cellulose acetate (Ac means Acetate, Prop means Propionate) synthesized in water free DMSO/TBAF.

Table V. Results of Acylation Reactions with Various Carboxylic Acids from *in-situ* Activation with N,N' -carbonyldiimidazole (CDI)

Reaction Conditions		Product	
Carboxylic Acid	Molar Ratio ^a	No.	DS ^b
Furane-2-Carboxylic Acid	1/3/3	7a	1.91
Acetic Acid ^c	1/3/3	7b	0.51
Stearic Acid	1/2/2	7c	0.47
Stearic Acid	1/3/3	7d	1.35
Adamantane-1-Carboxylic Acid	1/2/2	7e	0.50
Adamantane-1-Carboxylic Acid	1/3/3	7f	0.68
3,5-Bis(benzyloxy)benzoic Acid	1/2/2	7g	0.25

^a Anhydroglucose unit/CDI/carboxylic acid ^b Determined by ^1H NMR spectroscopy after peracetylation (**7c,7d**) and perpropionylation ^c Prepared at 100°C

the ester carbonyl vibration at 1745 cm^{-1} and the broad signal of the hydroxyl vibration at 3439 cm^{-1} were observed and indicated incomplete functionalization of the cellulose. An additional peak at 2219 cm^{-1} is a hint for the existence of nitrogen containing moieties, which was comparable to results of elemental analysis (C: 46.56 %, H: 5.41 %, N: 1.44 %). By electron paramagnetic resonance spectroscopy, it was found that the cellulose acetate included radicals of hexacyanobenzene. This radical occurred during the preparation of water free TBAF in DMSO within 1 h. The separation of the radical from the cellulose derivative by various methods that included repeated extraction with different solvents was not satisfactory. Thus, the characterization and the determination of the DS by means of ^1H NMR spectroscopy were not feasible due to the rather low resolution of the proton signals (Figure 6). Other results showed that the water free DMSO/TBAF synthesized *in-situ* by the reaction of hexafluorobenzene with tetra-*n*-butylammonium cyanide was an efficient cellulose solvent. However, in

Table VI. Conditions and Results for the Homogeneous Reactions of Cellulose in DMSO/TBAF·3H₂O, DMSO/BTMAF·H₂O and DMA/LiCl

Solvent	Reaction Conditions			Product	
	Time h	Temp. °C	Reagent ^a	Molar Ratio ^b	No. DS ^c
DMSO/ TBAF·3H ₂ O	70	40	Vinyl Acetate	1/3	8a 1.25
DMSO/ BTMAF·H ₂ O	70	40	Vinyl Acetate	1/3	8b 0.99
DMA/LiCl	70	40	Vinyl Acetate	1/3	8c 1.21
DMSO/ TBAF·3H ₂ O	3	65	IPB-Isocyanate	1/1	9a 0.25
DMSO/ BTMAF·H ₂ O	3	65	IPB-Isocyanate	1/1	9b 0.25
DMA/LiCl	3	65	IPB-Isocyanate	1/1	9c 0.76
DMSO/ TBAF·3H ₂ O	24	80	FA-Imidazolide	1/5	10a 2.40
DMSO/ BTMAF·H ₂ O	24	80	FA-Imidazolide	1/5	10b 2.10
DMA/LiCl	24	80	FA-Imidazolide	1/5	10c 0.60

^a FA-Imidazolide: 2-furane-carboxylic acid imidazolide, IPB-Isocyanate: 3-isopropenyl- α,α -dimethylbenzyl isocyanate ^b Anhydroglucose unit/reagent ^c Determined by ¹H NMR spectroscopy after perpropionylation (**8**, **10**), calculated from the nitrogen content determined by elemental analysis (**9**)

the context of homogeneous cellulose chemistry required for the synthesis of pure cellulose esters, e.g. cellulose acetate, problems from the by-products have occurred.

DMSO/TBAF·3H₂O was used to study the esterification of cellulose through the application of *in-situ* activation of carboxylic acids with *N,N'*-carbonyldiimidazole (CDI) in DMSO at 80 to 100°C that yielded the corresponding carboxylic acid imidazolide. The only by-products of the activation were imidazole and CO₂, which is liberated from the system. The conversion of cellulose with 2-furane carboxylic acid imidazolide yielded a cellulose ester with a DS of 1.91 (**7a**, Table V) with a considerable reaction efficiency of 63% (32). Moreover, the acetate, stearate, and adamantate of cellulose were prepared by this procedure (33). The aliphatic esters (cellulose acetate and stearate, **7b-d**) possessed rather low DS values of 0.51 and 1.35 compared to products that were obtained by the reaction of cellulose in DMSO/TBAF·3H₂O with carboxylic acid anhydrides; DS values of 1.2 for the acetate and 2.1 for the stearate were realized (28). This study suggested a comparably high reactivity of the aliphatic imidazolides towards hydrolysis was caused by water in the reaction medium. For

cellulose adamantate, preferred reaction at position 2 was observed and cellulose furoate proceeded with complete substitution at the primary hydroxyl group. Depolymerization of the cellulose during the reaction was limited as evaluated by size exclusion chromatography.

Novel bulky esters of cellulose were prepared in DMSO/TBAF·3H₂O by conversion of dendrons based 3,5-bis(benzyloxy)benzoic acid imidazolide that contained carboxylic acid groups (34). The reaction in DMSO/TBAF·3H₂O was more efficient at a rather low molar ratio of cellulose/carboxylic acid/DCI of 1/2/2 (DS 0.25, **7g**) compared to the conversion in DMA/LiCl (DS 0.12). Comparable DS values were obtained with a molar ratio of 1/3/3. It was interesting to note that although the carboxylic acid dendrons were bulky, NMR spectroscopy revealed that the reaction occurred not only with the primary hydroxyl groups but also with the secondary ones.

A comparison of solvent dependent reaction efficiencies for the esterification reaction in DMSO/TBAF·3H₂O, DMSO/BTMAF·H₂O and DMA/LiCl was performed ((31), Table VI). The reaction of cellulose with vinyl acetate in DMSO/BTMAF·H₂O yields a cellulose acetate with a DS of 0.99 (**8b**). Higher DS values of 1.25 and 1.21 were observed (**8a**, **8c**) using DMSO/TBAF·3H₂O and DMA/LiCl as reaction media. The synthesis of cellulose-3-isopropenyl- α,α -dimethylbenzyl carbamate carried out in DMA/LiCl led to a product of a remarkably high DS of 0.76 (**9c**) at a molar ratio of AGU/3-isopropenyl- α,α -dimethylbenzyl isocyanate of 1/1. On the contrary, reactions in solvents containing water gave products of significantly lower DS; in DMSO/TBAF·3H₂O a DS of 0.25 (**9a**) and in DMSO/BTMAF·H₂O a DS of 0.25 (**9b**) resulted and may have been due to hydrolysis the isocyanate moieties. Cellulose furoate was synthesized by the activation of furane-2-carboxylic acid with CDI that led the furane-2-carboxylic acid imidazolide. Different DS values in the three solvents were obtained under comparable reaction conditions. Rather high DS values cellulose furoates were realized in DMSO/TBAF·3H₂O (DS 2.4, **10a**) and DMSO/BTMAF·H₂O (DS 2.1, **10b**), indicative of excellent reaction efficiencies, while a product with a DS of 0.6 (**10c**) was obtained in DMA/LiCl.

The synthesis of novel super absorbent hydrogels was successfully carried out under homogeneous starting conditions using DMSO/TBAF. The cellulose reacted with succinic anhydride in the presence of 4-dimethylaminopyridine. Compared to the reaction in 1-methyl-2-pyrrolidinone/LiCl, in DMSO/TBAF the hydrogel was obtained without any cross-linking agent (35, 36).

Graft polymerizations with ϵ -caprolactone were carried out in DMSO/TBAF a grafting efficiency of 64% while *N*-carboxy- α -amino acid anhydrides possessed an efficiency of 100%. It was assumed that the TBAF increased the nucleophilicity of the hydroxyl groups of cellulose and thereby initiated and sped up the reaction (37).

Conclusions

DMSO in combination with ammonium fluorides, especially tetra-*n*-butylammonium fluoride trihydrate (TBAF·3H₂O) represents a novel cellulose solvent. The cellulose can be dissolved easily and efficiently. The solvent is a suitable medium for homogeneous modification reactions of cellulose. The dissolution of the biopolymer in DMSO/TBAF·3H₂O is essentially influenced by the interaction of fluoride anions with hydroxyl moieties of cellulose. Water of the hygroscopic salt is less important for this process. Anhydrous TBAF in DMSO dissolves cellulose. Other ammonium fluorides (benzyltrimethyl-ammonium fluoride monohydrate) in combination with DMSO dissolve cellulose as well. The crucial issue in this regard is the solubility of the ammonium salt in DMSO; a certain amount of fluoride anions in the solvent is necessary to get cellulose solvent.

The results show that etherification and esterification can be successfully accomplished and even highly functionalized derivatives could be obtained. Nevertheless, functionalization of cellulose with reagents, which are sensitive to hydrolysis, are less effective and the water content in the hygroscopic solvent system should be considered. The water content can be determined simply by FT-IR spectroscopy while a Karl-Fischer titration is not applicable.

References

1. Nehls, I.; Wagenknecht, W.; Philipp, B.; Stscherbina, D. *Prog. Polym. Sci.* **1994**, *19*, 29–78.
2. Heinze, T.; Liebert, T. *Prog. Polym. Sci.* **2001**, *26*, 1689–1762.
3. Klemm, D.; Heinze, T.; Schmauder, H.-P. In *Biopolymers: Biology, Chemistry, Biotechnology, Applications*; Vandamme, E., De Baets, S., Steinbüchel, A., Eds.; Wiley-VCH: Weinheim, 2002; 275–319; Vol. 6: Polysaccharide II.
4. McCormick, C. L.; Callais, P. A.; Hutchinson, B. H., Jr. *Macromolecules* **1985**, *18*, 2394–2401.
5. Nehls, I.; Wagenknecht, W.; Philipp, B. *Cellul. Chem. Technol.* **1995**, *29*, 243–251.
6. El-Kafrawy, A. *J. Appl. Polym. Sci.* **1982**, *27*, 2435–2443.
7. Striegel, A. M. *Carbohydr. Polym.* **1997**, *34*, 267–274.
8. Sjöholm, E.; Gustafsson, K.; Eriksson, B.; Brown, W.; Colmsjö, A. *Carbohydr. Polym.* **2000**, *41*, 153–161.
9. Potthast, A.; Rosenau, T.; Buchner, R.; Röder, T.; Ebner, G.; Bruglachner, H.; Sixta, H.; Kosma, P. *Cellulose* **2002**, *9*, 41–53.
10. Heinze, Th.; Dicke, R.; Koschella, A.; Kull, A. H.; Klohr, E.-A.; Koch, W. *Macromol. Chem. Phys.* **2000**, *201*, 627–631.
11. Ass, B. A. P.; Frollini, E.; Heinze, Th. *Macromol. Biosci.* **2004**, *4*, 1008–1013.
12. Xiao, C. *Fangzhi Xuebao* **1994**, *15*, 120–121.

13. Sun, H.; DiMagno, S. G. *J. Am. Chem. Soc.* **2005**, *127*, 2050–2051.
14. Köhler, S.; Heinze, Th. *Macromol. Biosci.* **2007**, *7*, 307–314.
15. Sharma, R. K.; Fry, J. L. *J. Org. Chem.* **1983**, *48*, 2112–2114.
16. Östlund, A.; Lundberg, D.; Nordstjerne, L.; Holmberg, K.; Nyden, M. Mechanisms of dissolution and gelation of cellulose in TBAF/DMSO solutions – the role of fluoride ions and water. *Biomacromolecules*, in press.
17. Lu, F.; Ralph, J. *Plant J.* **2003**, *35*, 535–544.
18. Liebert, T.; Heinze, Th. *Biomacromolecules* **2001**, *2*, 1124–1132.
19. Ramos, L. A.; Frollini, E.; Heinze, Th. *Carbohydr. Polym.* **2005**, *60*, 259–267.
20. Ramos, L. A.; Frollini, E.; Koschella, A.; Heinze, Th. *Cellulose* **2005**, *12*, 607–619.
21. Rohleder, E. Ph.D. Thesis, Friedrich Schiller University of Jena, Germany, 2009, Rohleder, E.; Heinze, Th.; to be submitted.
22. Heinze, Th.; Lincke, T.; Fenn, D.; Koschella, A. *Polym. Bull.* **2008**, *61*, 1–9.
23. Baar, A.; Kulicke, W.-M.; Szablikowski, K.; Kiesewetter, R. *Macromol. Chem. Phys.* **1994**, *195*, 1483–1492.
24. Spurlin, H. M. *J. Am. Chem. Soc.* **1939**, *61*, 2222–2227.
25. Heinze, Th. *Macromol. Chem. Phys.* **1998**, *199*, 2341–2364.
26. Heinze, Th.; Erler, U.; Nehls, I.; Klemm, D. *Angew. Makromol. Chem.* **1994**, *215*, 93–106.
27. Braun, D.; Meuret, B. *Angew. Makromol. Chem.* **1995**, *224*, 61–71 and references cited therein.
28. Ciacco, G. T.; Liebert, T.; Frollini, E.; Heinze, Th. *Cellulose* **2003**, *10*, 125–132.
29. Heinze, Th.; Liebert, T.; Pfeiffer, K. S.; Hussain, M. A. *Cellulose* **2003**, *10*, 283–296.
30. Fidale, L. C.; Köhler, S.; Pechtl, M. H. G.; Heinze, Th.; El Seoud, O. A. *Cellulose* **2006**, *13*, 581–592.
31. Köhler, S. Diploma Thesis, Friedrich Schiller University of Jena, 2005.
32. Liebert, T.; Heinze, Th. *Biomacromolecules* **2005**, *6*, 333–340.
33. Hussain, M. A.; Liebert, T.; Heinze, Th. *Macromol. Rapid Commun.* **2004**, *25*, 916–920.
34. Heinze, Th.; Pohl, M.; Schaller, J.; Meister, F. *Macromol. Biosci.* **2007**, *7*, 1225–1231.
35. Yoshimura, T.; Uchikoshi, I.; Yoshiura, Y.; Fujioka, R. *Carbohydr. Polym.* **2005**, *61*, 322–326.
36. Yoshimura, T.; Matsuo, K.; Fujioka, R. *J. Appl. Polym. Sci.* **2006**, *99*, 3251–3256.
37. Ikeda, I.; Washino, K.; Maeda, Y. *Sen-I Gakkaishi* **2003**, *59*, 110–114.

Chapter 6

Hydrogen Bond Acceptor Properties of Ionic Liquids and Their Effect on Cellulose Solubility

M. Sellin, B. Ondruschka and A. Stark*

Institute of Technical and Environmental Chemistry,
Friedrich-Schiller University Jena, Germany
*annegret.stark@uni-jena.de

The fact that some ionic liquids can dissolve cellulose is well known, but little systematic data is available regarding the influence of structural aspects of the ionic liquid on the dissolution of cellulose. Using ethanol as model compound, ^1H NMR spectroscopy of a large number of ionic liquids was conducted. The data obtained correlates with the anion-dependent hydrogen bond acceptor properties (determined as β -values by Spange and Lungwitz), and can be used to distinguish between cellulose-dissolving and non-dissolving ionic liquids. From the cellulose solubility in binary ionic liquid mixtures, the modulating effect of both, the non-dissolving anion and the cation has been derived.

The discovery of some ionic liquids (ILs) as cellulose solvents in the year 2002 (1) triggered a lot of research in this field, which has recently been reviewed (2). The solubility of cellulose in organic molten salts is not new and has been described as early as 1934 (3). In general, the choice of non-derivatizing solvents for cellulose available is very limited, which explains the immense interest in the application of ILs in the field of cellulose processing and functionalization.

The number of different ILs capable of dissolving cellulose has been expanded over the last years. Starting with the cation 1-alkyl-3-methylimidazolium ($[\text{C}_n\text{mim}]^+$) combined with nucleophilic anions such as Cl^- , Br^- , and $[\text{SCN}]^-$ (1), anions such as formate (4), acetate (5) and different dialkylphosphates (6), e.g. dimethylphosphate $[\text{CH}_3\text{O.P}(\text{O})_2\text{OCH}_3]^-$ followed (7). Research focusing mainly on chloride and acetate derivatives of $[\text{C}_2\text{mim}]^+$ and $[\text{C}_4\text{mim}]^+$ showed

their potential to dissolve cellulose in high amounts for different applications. However, the cationic structure is not restricted to $[C_n\text{mim}]^+$. The saturated alkyl chain can be replaced by allyl (8) or different phenyl-bearing groups (9). Furthermore, the C2-position of the 1,3-dialkylimidazolium cation can be methylated (10). Additionally, cations with *N*-alkylpyridinium ($[C_n\text{py}]^+$) or tetraalkylammonium ($[C_{\text{nmn}}\text{N}]^+$) structures have been applied (11). For most cationic modifications, the solubility and stability of cellulose were demonstrated using chloride derivatives. The scatter of data available in the literature shows large deviations in capacity and stability, which may be due to variations in the type of cellulose studied (DP, crystallinity), processing conditions and the purity of the ILs used.

Presently, the mechanism of cellulose dissolution is not fully understood. ^{13}C NMR data of the β -1-4-linkage of cellulose and in particular cellulose oligomers in $[C_4\text{mim}]\text{Cl}$ (partially diluted with DMSO) has indicated a disordered structure, similar to that of other non-derivatizing solvents such as DMSO/tetrabutylammonium fluoride (12). Observations from $^{35/37}\text{Cl}$ and ^{13}C NMR T_1 longitudinal relaxation measurements of $[C_4\text{mim}]\text{Cl}$ and $[C_2\text{mim}][\text{CH}_3\text{CO}_2]$ containing cellulose model substances such as cellobiose lead to a picture of very close contact of the anion with the solute, whereas the cation is less effected by the solute (13, 14). Close contact of the anion with OH-groups in saccharides was also found in computer simulations of glucose in $[C_1\text{mim}]\text{Cl}$ (15, 16). The formation of different OH:Cl complexes was found to occur. When the chloride anions are in excess over glucose, three OH-groups interact with three separate chloride anions by hydrogen bonding, while the remaining two OH-groups are involved in interactions with one chloride forming an OH-Cl-HO bridge. The cation forms the outer shell, interacting only to a very small percentage with the saccharide functionalities. The modeling of cellobiose interacting with $[C_4\text{mim}]\text{Cl}$ showed an interaction of one chloride with the C2'-OH (5) (non-reducing ring) and the C6-OH simultaneously, and the position of the cation in the outer shell also bound to the anion (17). These results do not agree with the function of the cation postulated earlier, where interactions between cations and the hydrogen bond acceptor sites in cellulose (18) similar to the cation contact in other cellulose solvents such as $\text{LiCl} / N,N$ -dimethylacetamide, were suggested. The formation of an OH-anion-cation-OH bridge between two cellulose chains can not be excluded. This structure was presumed using viscosity analogies with the non-derivatizing cellulose solvent *N*-methylmorpholine-*N*-oxide (19).

Regardless of the above discussion, it is widely accepted that cellulose dissolution in ILs is mainly governed by the IL anion. For that reason, it was decided to determine the interaction of IL anions with model molecules containing a hydroxyl functionality. It was reasoned that interactions between ILs and ethanol should give insight into the hydrogen bond acceptor (HBA) properties of the anion and the hydrogen bond donor (HBD) properties of the OH-group. The correlation of this study to literature data allows for an interpretation of structural effects on cellulose solubility. Furthermore, an analysis of the data with regard to the influence of the cation type was attempted.

Evidence from ^1H NMR Spectroscopy

A fast and facile method was developed to obtain deeper insight into the effects of a large number of anion and cation types. The ^1H NMR chemical shift of the OH-group in the probe molecule ethanol is well known to be very sensitive to changes in hydrogen bond interactions. If shifted downfield, a strong interaction occurs, reflecting a high apparent HBA ability of the IL.

Because this signal is sensitive to all changes in the surrounding hydrogen bonds it is important to eliminate other influences resulting in the misinterpretation of the chemical shift. Hence, the temperature has to be kept constant and the probe must be virtually free of water or other solvents. Furthermore, since ethanol-ethanol (HBD-HBA) interactions may also affect the overall shift of the signal, it is necessary to conduct the study under constant ethanol concentrations. Since ethanol is capable of taking part as a donor in one hydrogen bond only (20), the picture thus obtained reflects the mean strength of interaction between all hydrogen bond acceptors and ethanol.

Hence, a mixture of ethanol:IL (1:1) was used for all investigations of the interactions between IL constituents and ethanol, and was generally interpreted as the overall HBA property of an IL. The chemical shift of the OH-group (using the CH_3 -group as an internal reference (21)) was obtained as described in the Experimental Section and is called 'OH-shift' from hereon. Ethanol was chosen as a model for several practical reasons. It is well miscible with most ionic ILs, yielding solutions of low viscosity (22, 23). Even for ILs with melting points above room-temperature, well-resolved ^1H NMR spectra are obtained. Interestingly, although this present study has been carried out under equimolar substrate-IL conditions, the variations in interaction fully reflect those obtained in experiments at infinite dilution (γ^∞) using headspace gas chromatography (24).

The resulting 'OH-shifts' are displayed (Table I, Figure 1) for a large number of ILs composed of either the $[\text{C}_2\text{mim}]$ - or $[\text{C}_4\text{mim}]$ -cations. The 'OH-shift' varies over a wide range of ppm and is a very sensitive indicator for changes in HBA properties, hence helpful for the interpretation of differences in IL-solute interactions.

Evidence from Other Investigations

Several other techniques allow for the determination of solvent-solute interactions. For example, the overall polarity, which is a sum parameter of different specific and non-specific interactions, can be probed. The polarity is reflected in constants such as the refractive index, the dielectric constant, the Hildebrand solubility parameter, the permanent dipole moment or the partition coefficient, and can be expressed by comparison to other solvents, *e.g.* in the normalized polarity scale. Furthermore, solubility data, the keto-enol-tautomerism of probe molecules, computer simulations or gas-liquid chromatography with probe molecules eluted from IL-coated columns give indications of solvent-solute interactions (24).

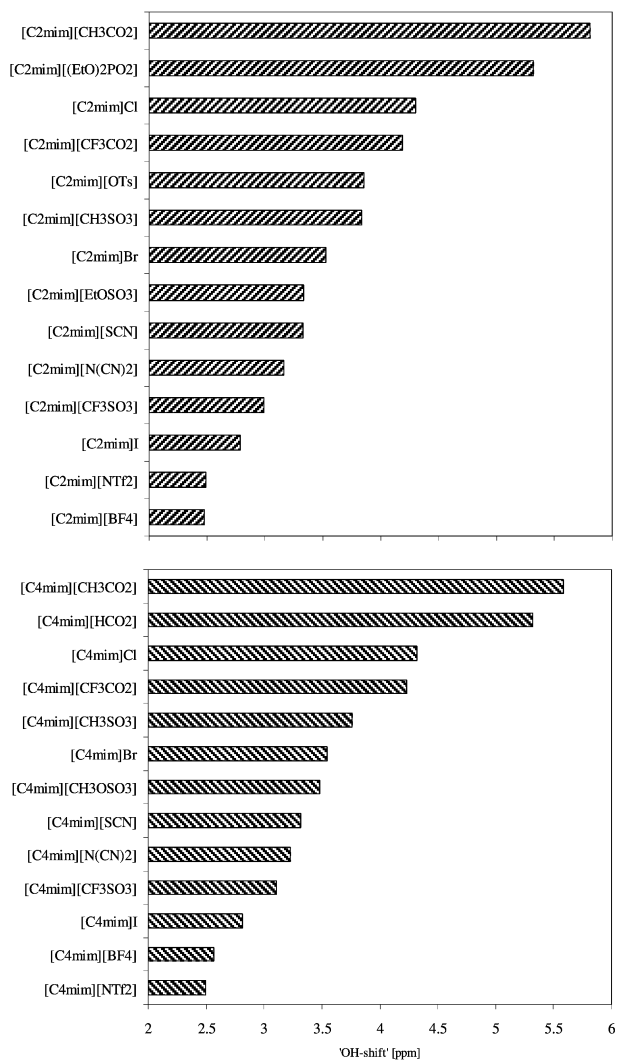


Figure 1. ¹H NMR chemical shift of the ethanol-OH-proton in equimolar ethanol-IL mixtures ('OH-shift') referred to the methyl protons of ethanol. ILs are based on 1-ethyl-3-methylimidazolium ([C₂mim]⁺) and 1-butyl-3-methylimidazolium ([C₄mim]⁺) cations.

From the number of data available for ILs, a large data set obtained from solvatochromic studies with specialized dye molecules reflecting microscopic molecular interactions was singled out for correlation with own data. In particular, the β -value – representing the HBA ability – of ILs has been presented for most anion species with standard IL cations (Table I) (25).

The differences between the $[C_2mim]^+$ and $[C_4mim]^+$ cation series are very small ($R^2 = 0.996$, $N = 11$), as shown for several anions with the ‘OH-shift’ technique of ethanol. Hence, β -values from the solvatochromic study were correlated to the ‘OH-shift’ caused by the anion, irrespective of the cation. In general, a linear correlation was obtained ($R^2 = 0.650-0.800$, $N = 15$) (7, 25), considering that the data has been obtained with differing techniques and probe molecules, and at quite different concentrations. Furthermore, the quality of the IL batches used has shown to exhibit tremendous effects on physico-chemical measurements (26). Future research will have to clarify the nature of these deviations. However, it can be reasoned that for anions with low HBA ability, the β -values reflect this better, since the HBD properties of the IL cation may interfere somewhat to affect the ‘OH-shift’. The solvatochromically obtained β -values, on the other hand, should be insensitive towards this interference. For anions exhibiting a strong HBA ability, on the other hand, the ‘OH-shift’ (e.g. acetate) is reflected by the β -value scale, if the higher literature value is considered.

Anion Effect of ILs on Cellulose Solubility

It is well known from literature data (1, 4–6, 8–11) that good cellulose solubility is obtained for ILs containing the anions Cl^- , $[CH_3CO_2]^-$, $[HCO_2]^-$ and $[(RO)_2PO_2]^-$. The studies on HBA properties presented above agree with the solubilities obtained for ILs bearing these anions. Hence, a strong HBA ability is a prerequisite for cellulose dissolution.

In order to extend the number of cellulose solvents and obtain a detailed understanding about IL interactions with cellulose, a range of ILs was tested with microcrystalline Avicel cellulose at temperatures between 100°C and 130°C. In the first instance, the focus was not on the dissolution capacity for cellulose, but on which IL exhibits any solubility for cellulose at all (Table II). For anions such as $[CF_3CO_2]^-$, $[CH_3SO_3]^-$, etc. (Table II, right column), the solubility was < 1 wt.%, as would be predicted by their (weak) HBA properties. These have been termed ‘non-dissolving ILs’. It appears that cellulose dissolution occurs if the β -value is ≥ 0.85 , or if the ‘OH-shift’ is ≥ 4.3 ppm (Table II, left column).

Our results on the insolubility of cellulose in ILs based on bromide are controversial, in the sense that such ILs have been reported as efficient solvents for cellulose (1, 10), while others find swelling (27) or marginal solubility (28). For none of the bromides investigated, visually transparent cellulose solutions with 1 wt.% Avicel were obtained in this present study, even after stirring for days under vacuum at temperatures up to 130°C. Probably, the HBA strength is not sufficient for the bromide to fully solvate the cellulose chains, but it strongly interferes with

Table I. Different Solvent Parameters of ILs Indicating HBA Interactions of ILs with Constant [C₂mim]⁺ or [C₄mim]⁺ Cation

<i>Anion</i>	<i>'OH-shift' /ppm ([C₂mim]⁺)</i>	<i>'OH-shift' /ppm ([C₄mim]⁺)</i>	<i>β-value (25) ([C₄mim]⁺)</i>
[NTf ₂] ⁻	2.49	2.49	0.42
[BF ₄] ⁻	2.48	2.56	0.55
I ⁻	2.79	2.82	0.75
[CF ₃ SO ₃] ⁻	3.00	3.11	0.57
[N(CN) ₂] ⁻	3.16	3.23	0.64
[SCN] ⁻	3.33	3.32	0.71
[CH ₃ OSO ₃] ⁻		3.48	0.75
[C ₂ H ₅ OSO ₃] ⁻	3.34		
Br ⁻	3.52	3.55	0.87
[NO ₂] ⁻		4.73	0.81
[CH ₃ SO ₃] ⁻	3.84	3.76	0.85
[OTs] ⁻	3.86		
[CF ₃ CO ₂] ⁻	4.14	4.17	0.74
Cl ⁻	4.30	4.32	0.95 (0.87) ^a
[(C ₂ H ₅ O) ₂ PO ₂] ⁻	5.32		1.00 ^b
[HCO ₂] ⁻		5.32	1.00 ^a
[CH ₃ CO ₂] ⁻	5.81	5.59	0.85 (1.09) ^a

^a ref. (7), ^b [C₂mim][[(CH₃O)₂PO₂] ref. (6)

the hydrogen bond network. Therefore, bromide can be considered to be at the border for cellulose dissolution in ILs, which is reflected in the β-values.

In order to get further information about the influence of the different HBA properties of the anion, the solubility of Avicel in binary mixtures of ILs containing anions capable of dissolving cellulose and non-dissolving anions was investigated. The experiments were performed using solutions of 2 wt.% Avicel in mixtures of ILs of varying molar ratios with constant [C₂mim]-cation at 100°C. To the cellulose-dissolving ILs (acetate, diethylphosphate, chloride), non-dissolving ILs were added in increments of 10 mol%. Table III presents the minimum molar ratio of dissolving IL, for which visually clear cellulose solutions (2 wt.%) were obtained.

Table II. Solubility of Small Amounts of Avicel (1 wt.%) in Dry ILs at 100°C to 130°C

<i>Avicel soluble</i>	<i>Avicel solubility < 1 wt.% 'Non-dissolving' ILs</i>
[C ₂ mim]Cl	[C ₂ mim]Br ^a
[C ₄ mim]Cl	[C ₂ mim][CF ₃ CO ₂]
[C ₂ mim][CH ₃ CO ₂]	[C ₂ mim][SCN]
[C ₄ mim][CH ₃ CO ₂]	[C ₂ mim][C ₂ H ₅ OSO ₃]
[C ₂ mim][(C ₂ H ₅ O) ₂ PO ₂]	[C ₄ mim][CH ₃ SO ₃]
[C ₂ mim][HCO ₂]	[C ₂ mim][NTf ₂]
	[C ₂ mim][BF ₄]
[Allylmim]Cl	[C ₂ mim][N(CN) ₂]
[Allyldmim]Cl	[C ₂ mim][SCN]
[Bzmim]Cl	[C ₂ mim][OTs]
[C ₈ mim]Cl	[C ₂ mim]I
	[C ₂ mim][PF ₆]
	[Allylmim]Br ^a
	[Allyldmim]Br ^a
	[Ph-C ₃ mim]Br ^a
	[C ₄ dmim]Br ^a
	[CH ₃ O-C ₂ mim]Br ^a
	[C ₂ dmim]Br ^a

^a no cellulose particles visible but solution is not fully transparent

The differences of solubility in mixtures of [C₂mim]-based ILs can be explained using the HBA scales introduced above: ILs with anions having moderate HBA qualities, such as [C₂mim][CH₃SO₃] or [C₂mim]Br, require lower quantities of cellulose-dissolving IL than ILs composed of anions with low HBA ability, such as [C₂mim][NTf₂] or [C₂mim][BF₄]. Hence, the amount of dissolving IL that has to be added decreases with increasing HBA strength of the non-dissolving anion.

For a particular non-dissolving IL, an increasing potential of the anions Cl⁻ < [(C₂H₅O)₂PO₂]⁻ ~ [CH₃CO₂]⁻ can be stated, also predicted from increases in the 'OH-shift'.

Since it may be argued that these differences of solubility may be due to differences in the molar mass, leading to variations in the number of ions available for interactions with cellulose, the results in Figure 2 present the number of active

Table III. Minimal Molar Ratio (Cellulose-Dissolving : Non-Dissolving IL) Required to Achieve Solubility of 2 wt.% Avicel in Binary Mixtures of ILs

<i>Non-dissolving ILs</i>	<i>Cellulose-Dissolving ILs</i>		
	$\frac{[C_2mim]}{[CH_3CO_2]}$	$\frac{[C_2mim]}{[(C_2H_5O)_2PO_2]}$	$[C_2mim]Cl$
$[C_2mim][NTf_2]$	1.5	2.3	8.0
$[C_2mim][OTs]$	1.0	0.7	1.5
$[C_2mim][PF_6]$	1.0	nd ^a	nd ^a
$[C_2mim][CF_3CO_2]$	0.7	0.4	1.5
$[C_2mim][BF_4]$	0.7	1.0	2.3
$[C_2mim][SCN]$	0.4	0.4	1.5
$[C_2mim][N(CN)_2]$	0.4	0.7	1.5
$[C_2mim][CH_3SO_3]$	0.3	0.3	nd ^a
$[C_2mim]I$	0.3	0.3	nd ^a
$[C_2mim]Br$	0.1	0.1	nd ^a

^a nd: not determined.

$[CH_3CO_2]$ -anions in relation to the cellulose-OH groups, using the composition of ILs and the solubility limits listed in Table III.

Figure 2 shows that the number of $[CH_3CO_2]$ -anions required in each IL mixture to dissolve 2 wt.% cellulose indeed depends on the order of HBA strength of the non-dissolving IL. Although there is neither a linear correlation to the β -values nor the ‘OH-shifts’, a general trend is reflected: a lower ratio of acetate to cellulose-OH is required for non-dissolving ILs with relatively high β -values or ‘OH-shifts’, such as Br⁻ or $[CH_3SO_3]^-$, while a higher ratio is necessary if the non-dissolving IL possesses an anion with low β -values and ‘OH-shifts’, such as $[CF_3SO_3]^-$, $[NTf_2]^-$, $[BF_4]^-$ or $[PF_6]^-$.

The results show coherence between the HBA strength of ILs and the decrease of cellulose-dissolving activity of $[CH_3CO_2]^-$ in such ILs. But how can the HBA strength of a non-dissolving IL be associated to the solubility of cellulose upon adding dissolving IL? Lungwitz and Spange (25) have demonstrated a linear correlation between HBA properties of the anion (β -values of solvatochromic studies) and the HBA-HBD interactions between anion and cation (examined using ¹H NMR shifts of the acidic C2-proton of dialkylimidazolium in $[C_4mim]$ -based ILs diluted in CD₂Cl₂). Hence, it is reasonable to argue that in IL-cellulose solutions, the anion is capable to hydrogen-bond to either a cellulose-OH group or the IL cation, or both. These interactions are strengthened with increasing HBA ability of the anion. When adding non-dissolving $[C_2mim][NTf_2]$ to a $[C_2mim][CH_3CO_2]$ -cellulose solution, the number of potential interactions of $[C_2mim]$ -cations, now associating with $[CH_3CO_2]$ -anions increases, especially since the $[NTf_2]^-$ does not engage in strong interactions with its ‘own’ cation. In this way, the increasing number of $[C_2mim]$ -cations being potential HBD to

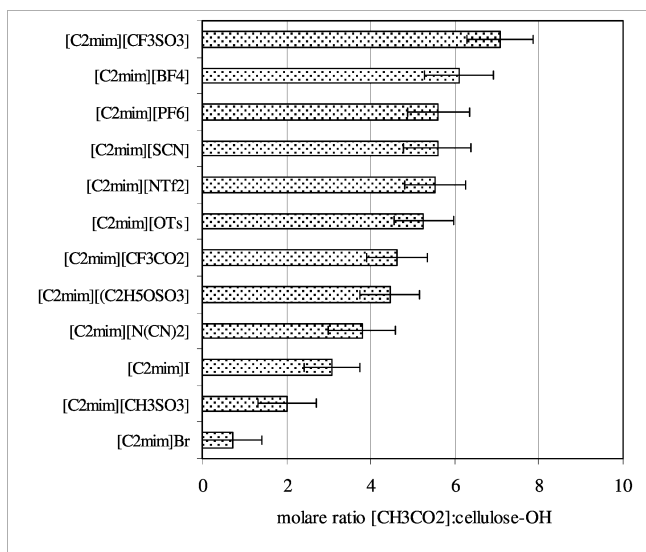


Figure 2. Molar ratio (acetate : cellulose-OH) required to dissolve 2 wt.% Avicel in binary IL mixtures with the compositions stated in Table III.

the [CH₃CO₂]⁻ anion reduces the HBA potential of this anion for interactions with cellulose. This ‘deactivation’ of [CH₃CO₂]⁻ increases with decreasing HBA properties of the second anion in the mixtures.

In our ¹H NMR experiments with equimolar mixtures of ethanol and ILs, there are statistically two potential HBDs (*i.e.* cation and ethanol) present for interaction with every ethanol. A correlation of the ‘OH-shift’ and the chemical shift of the acidic C2-proton of the cation is presented in Figure 3. Both chemical shifts are interpreted as apparent overall hydrogen bond interactions of the anion with the ethanol OH-group and/or the cation donor sites.

As established for the correlation between β-value and C2-H-shift (25), the effect of the anion on the HBD site of the cation increases linearly with the effect on the OH-group of ethanol. Surprisingly, however, differences in interaction mode between mono-nuclear and multi-nuclear anions become apparent, indicating a relatively stronger interaction of the halide anions with the cation. This might be an explanation for the positive effect of the non-dissolving halides (bromide and iodide) on cellulose solubility in the IL mixtures: the halides tend to interact more with the cation, thus making [CH₃CO₂]⁻ relatively better available for interaction with the cellulose OH-groups. This may explain why cellulose is more soluble in mixtures of [CH₃CO₂]⁻ with bromide or iodide than would have been predicted by the ‘OH-shift’ scale.

Similar mechanisms are found with other non-dissolving additives such as water or DMSO. Both compounds can be added in small amounts to ILs without loss of solubility for cellulose, whereas larger quantities will cause insolubility. For [C₄mim]Cl, insolubility of cellulose was reported for water contents greater than 1 wt.% (1). We examined the solubility for cellulose for different amounts of

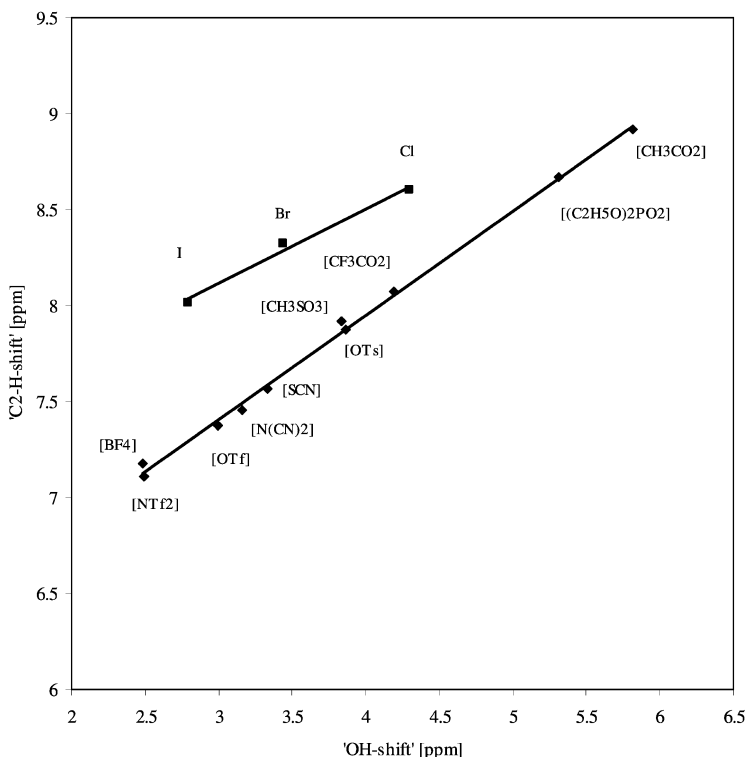


Figure 3. Correlation between ^1H NMR chemical shift of the ethanol OH-proton ('OH-shift') and ^1H NMR chemical shift of the cationic C2-proton ('C2-H-shift') in equimolar ethanol-[C₂mim]-based ionic liquid mixtures.

Avicel in [C₂mim][CH₃CO₂], [C₂dmim][CH₃CO₂] and [C₄mim]Cl as a function of water content in more detail (Table IV).

The critical amount of water leading to insolubility decreases with increasing quantity of cellulose dissolved.

The maximum molar ratio (water : IL) in which Avicel remains soluble is 2.0 and 0.5 for these acetate and chloride ILs, respectively, at small Avicel concentrations (*pseudo*-infinite dilution). In other words, the chloride anion is 'deactivated' for cellulose dissolution once a 2:1 complex with water has formed, whereas the [CH₃CO₂]⁻ is deactivated only at much higher water concentrations (1:2). As predicted from the 'OH-shift' scale, the HBA ability of [CH₃CO₂]⁻ is much stronger than Cl⁻, which may be the reason for its capability to dissolve cellulose even in the presence of excess water. Water-cation interactions are well known in ILs (29), but the cation did not exhibit any positive or negative effect in these experiments (compare [C₂mim][CH₃CO₂] and [C₂dmim][CH₃CO₂]) within the methodical uncertainties. At *pseudo*-infinite dilution, similar is observed when adding non-dissolving DMSO. In this instance, however, much more DMSO has

to be added before cellulose becomes insoluble (20 and 2 molar fractions for [C₂mim][CH₃CO₂] and [C₄mim]Cl, respectively).

In summary, it appears as if the solubility of cellulose can be well described using different measures for HBA strengths of ILs. However, these studies do not give information whether specific anion-cellulose-OH interactions prevail, or if other, more complex interactions should be taken into consideration. For example, the anion [CF₃CO₂]⁻ should possess a reasonably high HBA ability (comparable to that of Br⁻), judging from the ‘OH-shift’ scale, although it does neither dissolve nor swell the cellulose. These aspects are the focus of future research.

Cation Effect of ILs Onto Cellulose Solubility

The hypothesis that the anion may be activated or deactivated for cellulose dissolution has further been followed in a study concerning the effect of the IL cation. The solubility for cellulose was reported to decrease with increasing chain lengths of 1-alkyl-3-methylimidazolium cations (1, 28, 30) and methylation of the C2-position (31). Furthermore, a decreased solubility was found in ILs containing non-aromatic quaternary ammonium cations (11). Increasing viscosity, melting point, molecular mass and steric hinderance were used as arguments for solubility differences, but the question whether the HBA strength of the anion is also tuned by the type of cation can also be raised. β-values for ILs with constant anion and variations in cation type are very rare in the literature. Other examinations can be taken into account using the ‘OH-shift’ scale, ESI-MS (32) and anion nucleophilicity (33) in different ILs.

The results from ¹H NMR measurements of equimolar mixtures of ethanol in ILs (‘OH-shift’) for different cation types are presented in Table V. Although the differences are much smaller than for the anion, it appears as if the variation in chain length of 1-alkyl-3-methylimidazolium cations or replacement of the saturated alkyl chain for an unsaturated (allyl) one does not lead to appreciable differences in the apparent HBA properties of the anion. A small increase of the ‘OH-shift’ was observed for side chains which carry phenyl groups, which is presently difficult to explain. A slight increase of the ‘OH-shift’ is observed for ILs containing *N*-alkylpyridinium or tetraalkylammonium structures. This finding may be due to an increase of HBA interactions of the anion with the OH-group when HBD sites of the cations are weakened or missing.

It has been reported that the solubility of cellulose in ILs is reduced when OH-groups are present in the side chain of 1-alkyl-3-methylimidazolium cations (34). The ‘OH-shift’ of such an IL shows in fact a decrease in the HBA strength of the anion in this case (Table V, [HO-C₂mim]Cl). The additional HBD site in the cation may lead to a further reduction of the anion-ethanol interaction, because the anion now distributes its HBA potential between the different HBD sites. The implementation of additional HBA sites (Table V, [CH₃O-C₂mim]Br) lead neither to an improvement nor to a reduction of the apparent HBA ability of bromide-based ILs.

Table IV. Maximal Molar Ratio (Water : IL) in which Avicel Remains Soluble

<i>wt.% Avicel</i>	$H_2O:$ [C ₂ mim][CH ₃ CO ₂]	$H_2O:$ [C ₂ dmim][CH ₃ CO ₂]	$H_2O:$ [C ₄ mim]Cl
2	1.8-1.9	1.8-1.9	0.4-0.6
4	1.7-1.8		0.4-0.6
6	1.6-1.7		0.3-0.4
8	1.6-1.7		

Table V. ‘OH-shift’ Values of Different ILs Containing Br-, Cl- or [CF₃CO₂]- Anions and Different Cations

<i>Chloride-based ILs</i>	<i>‘OH-shift’/ ppm</i>	<i>Bromide-based ILs</i>	<i>‘OH-shift’/ ppm</i>	<i>[CF₃CO₂]-based ILs</i>	<i>‘OH-shift’/ ppm</i>
[HO-C ₂ mim] ⁺	4.00	[CH ₃ O-C ₂ mim] ⁺	3.50	[C ₄ py] ⁺	4.29
[C ₂ mim] ⁺	4.30	[C ₂ mim] ⁺	3.52	[C8881N] ⁺	4.29
[C ₄ mim] ⁺	4.32	[C ₄ mim] ⁺	3.55	[C ₄ dmim] ⁺	4.19
[Allylmim] ⁺	4.30	[Allylmim] ⁺	3.51	[C ₄ mim] ⁺	4.17
[C ₈ mim] ⁺	4.32	[Allyldmim] ⁺	3.51	[C ₂ mim] ⁺	4.14
[C ₄ dmim] ⁺	4.40	[C ₁₀ mim] ⁺	3.52		
[Ph-C ₁ mim] ⁺	4.53	[Ph-C ₃ mim] ⁺	3.69		

Similar relative changes in anion interactions with varying cations have also been found by Chiappe’s group using the ESI-MS data (32). A qualitative order of anion-cation interaction was obtained for ILs containing bromide, decreasing in the order of [C₂mim]⁺ > [C₄mim]⁺ > [C₁C₁morph]⁺ > [C₄py]⁺ > [C₄C₁pyr]⁺ > [C₄dmim]⁺ > [C₄₄₄₄N]⁺. Anion-cation interactions are reduced if potential HBD sites are weakened. The HBA strength of the anion with a potential HBD solute, such as ethanol, should therefore increase in the reversed order. This reproduces some general trends of the ‘OH-shift’ experiments.

Furthermore, Daguinet and Dyson have measured the activity of the chloride anion in different ILs with the weakly coordinating anion [NTf₂]⁻ (33). Chloride solvation (and thus deactivation in terms of availability for HBA interaction with a solute) increases in the order of [C₅₂₂₂N]⁺ < [C₄C₁pyr]⁺ < [C₄mim]⁺ < [C₄dmim]⁺ < [C₄py]⁺. Although the order does not strictly reflect the one established in the ESI-MS experiments, the highest activity is again found for the ammonium cation.

From a mechanistic point of view, the results presented and their correlation to literature data point to a certain advantage of using non-aromatic quaternary ammonium cations instead of aromatic ones. This advantage, however, is fully

compensated by a resulting higher viscosity, melting point, molecular mass and steric hinderance of such ILs, which make dissolution of cellulose at temperatures below 100 °C difficult, if not impossible. Nevertheless, for other (thermally stable or liquid) solutes, tuning this structural aspect may prove useful in the future. Furthermore, although the results have been discussed in terms of bilateral HBD-HBA interactions, it is likely that concerted, more complex interactions occur, such OH-anion-cation-OH bridging previously proposed in the literature (19).

Conclusions

HBA properties of ILs have been measured using the ^1H NMR chemical shift of ethanol in equimolar ethanol-ILs mixtures. The results for the HBA ability of the anion from this work and from literature determined by alternative methods has been correlated to the solubility of cellulose in ILs, binary IL-mixtures and IL-co-solute mixtures. The general trends in the anion-dependent cellulose solubility can be explained with any of the HBA scales, with little deviations only. The solubility of cellulose in binary IL mixtures depends on the HBA properties of both anions in the IL mixture, where at least one anion has to be chosen from of the group of cellulose-dissolving anions. The HBA property of the second non-dissolving anion governs the ability of the cation to involve the dissolving anion in non-productive hydrogen bonding, thereby reducing its ability to dissolve cellulose. These findings can also be correlated to the HBA scales due to a linear correlation between the HBA effect of the anion on the cation and the HBA effect of the anion on the OH-group of cellulose.

The question of the effect of the cation type on cellulose dissolution can not be fully answered yet. However, it appears that the reduction of HBD sites in the cation improves the HBA property of the anion, which should improve cellulose solubility. Unfortunately, the reduction of HBD sites in the cation is in most cases accompanied by increases of viscosity, melting point and steric hinderance, leading to ILs with unfavourable physico-chemical properties for cellulose dissolution. Hence, cellulose dissolution in ILs presents itself as a trade-off between microscopic and macroscopic properties of the IL's ions.

Experimental Section

All ILs were dried at 80 to 100 °C in vacuum on the day of sample preparation. 1 g of IL was placed in a 1 ml vial and the amount of ethanol was injected with a syringe to obtain the required molar mixture. The vials were shaken with a vortexer until a clear solution was obtained or solid ILs were dissolved in ethanol. The mixture was placed in a standard NMR tube without further solvents. DMSO- d_6 as a locking additive was taken from a fresh bottle and was placed into a 5 mm coaxial insert. NMR tube and coaxial insert were sealed to avoid absorption of water from the atmosphere. ^1H NMR experiments were performed on a Bruker 200 MHz at room temperature.

The ^1H NMR spectra obtained were interpreted as follows: the difference between the chemical shifts of the ethanol- CH_3 group and the ethanol-OH group is called 'OH-shift'. In this way, a *quasi*-internal calibration to the CH_3 -group of ethanol is carried out. Likewise, the chemical shifts of the acidic C2-proton in imidazolium-based cations are presented as differences using the CH_3 -group in the side chain of the cation as reference ('C2-H-shift').

All ILs were prepared according to literature methods (35, 36), except for $[\text{C}_2\text{mim}][\text{CH}_3\text{SO}_3]$ (Iolitec, 99 %), $[\text{C}_2\text{mim}][\text{N}(\text{CN})_2]$ (Fluka, purum > 98.5 %), $[\text{C}_2\text{mim}][\text{CF}_3\text{SO}_3]$ (Iolitec, 99 %), $[\text{C}_2\text{mim}][\text{OTs}]$ (Merck, for synthesis), $[\text{C}_2\text{mim}][\text{SCN}]$ (Merck, for synthesis, 273 ppm halide), $[\text{C}_4\text{mim}][\text{BF}_4]$ (Fluka, purum > 97 %), $[\text{C}_4\text{mim}][\text{CH}_3\text{SO}_3]$ (Solvent Innovation, puriss. 99 %), $[\text{C}_4\text{mim}][\text{N}(\text{CN})_2]$ (Fluka, purum > 97 %), $[\text{C}_4\text{mim}][\text{HCO}_2]$ (BASF), $[\text{C}_4\text{mim}][\text{CF}_3\text{SO}_3]$ (Fluka, purum > 95 %), $[\text{C}_4\text{mim}][\text{SCN}]$ (Fluka/BASF-quality, > 95 %), $[\text{C}_4\text{mim}]\text{Cl}$ (Merck, for synthesis), $[\text{C}_4\text{mim}]\text{I}$ (Iolitec > 98 %), $[\text{Allylmim}]\text{Cl}$ (Iolitec > 98 %), and $[\text{C}_4\text{dmim}]\text{Cl}$ (Merck, for synthesis) which were used as received.

Halide contents were determined to be below the limit of detection (< 200 ppm) (37), except for those where the halide content is specified (commercial source) and $[\text{C}_2\text{mim}][\text{BF}_4]$ (252 ppm halide), and $[\text{C}_4\text{mim}][\text{CH}_3\text{CO}_2]$ (1400 ppm halide)(own synthesis).

Acknowledgements

The authors thank C. Palik for her valuable contribution in the laboratory, and Dr. M. Friedrich, B. Rambach and A. Blayer for NMR measurements. Parts of this work have been financially supported by BASF SE and the German Federal Environmental Foundation (DBU, AZ 24762). The donation of IL samples (BASF SE, Merck KGaA, Sigma-Aldrich Chemie GmbH) is greatly appreciated. For financial support, A.S. is indebted to the Friedrich-Schiller University (HWP) and the DFG for funding within the Priority Programme SPP 1191 Ionic Liquids.

References

1. Swatloski, R. P.; Spear, s. K.; Holbrey, J. D.; Rogers, R. D. *J. Am. Chem. Soc.* **2002**, *124*, 4974–4975.
2. El Seoud, O. A.; Koschella, A.; Fidale, L. C.; Dorn, S.; Heinze, T. *Biomacromolecules* **2007**, *8*, 2629–2647.
3. Graenacher, C. U.S. Patent 1943176, 1934.
4. Fukaya, Y.; Sugimoto, A.; Ohno, H. *Biomacromolecules* **2006**, *7*, 3295–3297.
5. Kohler, S.; Liebert, T.; Schobitz, M.; Schaller, J.; Meister, F.; Gunther, W.; Heinze, T. *Macromol. Rapid Commun.* **2007**, *28*, 2311–2317.
6. Fukaya, Y.; Hayashi, K.; Wada, M.; Ohno, H. *Green Chem.* **2008**, *10*, 44–46.
7. Ohno, H.; Fukaya, Y. *Chem. Lett.* **2009**, *38*, 2–7.

8. Wu, J.; Zhang, J.; Zhang, H.; He, J. S.; Ren, Q.; Guo, M. *Biomacromolecules* **2004**, *5*, 266–268.
9. Kilpelainen, I.; Xie, H.; King, A.; Granstrom, M.; Heikkinen, S.; Argyropoulos, D. S. *J. Agric. Food Chem.* **2007**, *55*, 9142–9148.
10. Barthel, S.; Heinze, T. *Green Chem.* **2006**, *8*, 301–306.
11. Heinze, T.; Schwikal, K.; Barthel, S. *Macromol. Biosci.* **2005**, *5*, 520–525.
12. Moulthrop, J. S.; Swatloski, R. P.; Moyna, G.; Rogers, R. D. *Chem. Commun.* **2005**, 1557–1557.
13. Remsing, R. C.; Swatloski, R. P.; Rogers, R. D.; Moyna, G. *Chem. Commun.* **2006**, 1271–1273.
14. Remsing, R. C.; Hernandez, G.; Swatloski, R. P.; Masefski, W. W.; Rogers, R. D.; Moyna, G. *J. Phys. Chem. B* **2008**, *112*, 11071–11078.
15. Youngs, T. G. A.; Holbrey, J. D.; Deetlefs, M.; Nieuwenhuyzen, M.; Gomes, M. F. C.; Hardacre, C. *ChemPhysChem* **2006**, *7*, 2279–2281.
16. Youngs, T. G. A.; Hardacre, C.; Holbrey, J. D. *J. Phys. Chem. B* **2007**, *111*, 13765–13774.
17. Novoseloy, N. P.; Saschina, E. S.; Petrenko, V. E.; Zarborski, M. *Fibre Chem.* **2007**, *39*, 153–158.
18. Zhang, H.; Wu, J.; Zhang, J.; He, J. S. *Macromolecules* **2005**, *38*, 8272–8277.
19. Michels, C.; Kosan, B. *Lenz. Ber.* **2005**, *84*, 62–70.
20. Torrie, B. H.; Weng, S. X.; Powell, B. M. *Mol. Phys.* **1989**, *67*, 575–581.
21. Hoffmann, M. M.; Conradi, M. S. *J. Phys. Chem. B* **1998**, *102*, 263–271.
22. Arce, A.; Rodil, E.; Soto, A. *J. Sol. Chem.* **2006**, *35*, 63–78.
23. Gomez, E.; Gonzalez, B.; Calvar, N.; Tojo, E.; Dominguez, A. *J. Chem. Eng. Data* **2006**, *51*, 2096–2102.
24. Stark, A. *Top. Curr. Chem.* **2009**, in print, DOI: 10.1007/128_2009_43.
25. Lungwitz, R.; Spange, S. *New J. Chem.* **2008**, *32*, 392–394.
26. Seddon, K. R.; Stark, A.; Torres, M. J. *Pure Appl. Chem.* **2000**, *72*, 2275–2287.
27. Cuissinat, C.; Navard, P.; Heinze, T. *Carbohydr. Polym.* **2008**, *72*, 590–596.
28. Vitz, J.; Erdmenger, T.; Haensch, C.; Schubert, U. S. *Green Chem.* **2009**, *11*, 417–424.
29. Mele, A.; Tran, C. D.; Lacerda, S. H. D. *Angew. Chem., Int. Ed.* **2003**, *42*, 4364–4366.
30. Erdmenger, T.; Haensch, C.; Hoogenboom, R.; Schubert, U. S. *Macromol. Biosci.* **2007**, *7*, 440–445.
31. Kosan, B.; Michels, C.; Meister, F. *Cellulose* **2008**, *15*, 59–66.
32. Bini, R.; Bortolini, O.; Chiappe, C.; Pieraccini, D.; Siciliano, T. *J. Phys. Chem. B* **2007**, *111*, 598–604.
33. Daguinet, C.; Dyson, P. J. *Inorg. Chem.* **2007**, *46*, 403–408.
34. Bentivoglio, G.; Sixta, H.; Schottenberger, H.; Röder, T.; Fasching, M. 45, *Chemiefasertagung, Dornbirn*, 2006.
35. Wilkes, J. S.; Zaworotko, M. J. *Chem. Commun.* **1992**, 965–967.
36. Bonhôte, P.; Dias, A. P.; Papageorgiou, N.; Kalyanasundaram, K.; Grätzel, M. *Inorg. Chem.* **1996**, *35*, 1168–1178.
37. Stark, A.; Behrend, P.; Braun, O.; Muller, A.; Ranke, J.; Ondruschka, B.; Jastorff, B. *Green Chem.* **2008**, *10*, 1152–1161.

Chapter 7

On the Specific Behaviour of Native Cellulose Fibers upon Dissolution

N. Le Moigne and P. Navard*

Mines ParisTech, CEMEF, CNRS UMR 7635, BP 207,
1 rue Claude Daunesse, F-06904 Sophia Antipolis Cedex,
France

*E-mail: patrick.navard@mines-paristech.fr

Member of the European Polysaccharide Network of Excellence (EPNOE),
www.epnoe.eu.

This chapter deals with a description of the mechanisms of swelling and dissolution of native cellulose fibers at the different scale of the fiber structure, i.e. from the walls to the macromolecular chains. New observation by scanning electron microscopy of the cellulose fibers after regeneration upon dissolution suggest that the structural transition between primary wall and S1 wall is very sharp. The distribution of precipitated cellulose around swelling fibers shows that cellulose chains are escaping the fiber at an early stage of the dissolution process.

Introduction

Cellulose is a major source of materials for paper, films and textile industry as well as food, paints, cosmetics or pharmaceuticals industry. The difficulties of cellulose processing have attracted the attention of numerous scientists over the last century and the swelling and dissolution of cellulose fibers have been studied in a wide range of conditions. The most spectacular effect of the swelling and dissolution of natural cellulose fibers is the ballooning phenomenon. The swelling can take place in some selected zones along the fibers. This heterogeneous swelling gives the impression of having “balloons” growing. The ballooning phenomenon has been observed long ago, first by Nägeli in 1864 (*1*), then by

Penner in 1883 (2), Fleming and Thaysen in 1919 and 1921 (3, 4), Marsh et al. in 1941 (5), Hock in 1950 (6) or Rollins and Tripp in 1952 (7, 8) (Numerous other studies are also reported in reference (9)). In 1954, an explanation of this phenomenon was proposed (10). It must be noticed that similar explanations were suggested in all the preceding references. For a wide range of cellulose fibers, the microfibrils of the secondary wall are aligned in a helical manner towards the long axis of the fiber. It was deduced that swelling must be greater transversely than lengthwise (as it is generally observed for fibers where the orientation of the cellulose chains is mainly in the fiber direction). Consequently, the author proposed: “when raw cotton fibers are placed in certain swelling agent, the radial expansion of the cellulose in the secondary wall causes the primary wall to burst. As the expanding swollen cellulose pushes its way through the tears in the primary wall, the latter rolls up in such a way as to form collars, rings or spirals which restrict the uniform expansion of the fiber” and forms balloons. All authors assume that the ballooning phenomenon has structural origins, i.e. linked to morphological variations within the cellulose fibers. Cuissinat and Navard (11, 12) described the main regions implied in the ballooning in details. As shown on Figure 1, three zones have been identified: the membrane, the inside of the balloons and the unswollen sections. However, the exact origin of these three zones was not reported.

Stawitz and Kage (13) reported earlier a heterogeneous swelling and dissolution for carboxymethylcellulose fibers. Fibers were shown to swell by ballooning with a helical structure around the balloons. Then, the breakage of the helical structure and the unswollen sections between the balloons leads to a high homogeneous swelling. Finally, the highly swollen sections are then tear into thin sections and finally into fragments.

Chanzy et al. (14) investigated the swelling and dissolution of various cellulose fibers, both native and regenerated, in *N*-methylmorpholine-*N*-oxide (NMMO) with different amounts of water. Four domains of water concentration were found to be important. When the amount of water was low (NMMO- 16% water), cellulose fibers, such as ramie, cotton and wood were dissolving rapidly by fragmentation without significant swelling. At higher water concentration (e.g., NMMO- 18-20% water), ramie fibers exhibited a heterogeneous swelling: a ballooning phenomenon was observed in localized places. In the case of wood and cotton fibers, the ballooning was well defined and the difference of swelling with ramie fiber was attributed to a difference of organization of the cellulose microfibrils within the various species. After the removal of the swelling agent, they observed that the initial ramie fibers were converted into an unoriented cellulose II crystalline structure. Chanzy et al. called this region “irreversible swelling”. With more water (e.g., NMMO- 20% and more), ramie fibers were sometimes having both cellulose I and II after the removal of the swelling agent but most of the time the cellulose I structure of the cellulose crystals was preserved. When water amounts were above 28%, no visible change was observed which thus corresponds to a region of non-activity. The most important result in this study is that by changing the water amount from 16% to 20 % w/w, an important transition from a dissolution by fragmentation of cellulose to irreversible swelling by ballooning was observed. In addition, pronounced

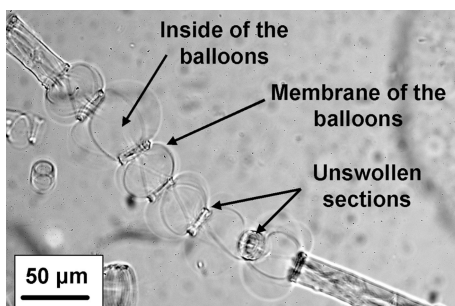


Figure 1. Identification of the three zones of a wood fiber swollen by ballooning in NMMO- 22% water.

differences were found in the crystalline structures of the fibers as a function of the amount of water in the solvent mixture.

Based on the preceding study, Cuissinat and Navard (11, 12) performed observations by optical microscopy of free-floating fibers between two glass plates for a wide range of solvent quality. They identified four main dissolution modes for wood and cotton fibers as a function of the quality of the solvent, in NMMO:

- Mode 1: Fast dissolution by fragmentation in good quality solvent (below 17% water w/w).
- Mode 2: Swelling by ballooning and full dissolution in moderate quality solvent (from 18 to 24 % water w/w).
- Mode 3: Swelling by ballooning and no complete dissolution in bad quality solvent (from 25 to 30 % water w/w).
- Mode 4: Low homogeneous swelling and no dissolution in non solvent (above 35 % water w/w).

These different dissolution mechanisms are summarized in Figure 2. These mechanisms have been also observed with ionic liquids solvent (15) and for a wide range of plant fibers (16) and some cellulose derivatives if the derivatization occurred without dissolution (17). These different studies point out the strong influence of the morphological structure in the dissolution mechanisms. If the original wall structure of the native fiber is preserved, the dissolution mechanisms are similar for wood, cotton, other plant fibers and some cellulose derivatives, the solvent quality driving the type of mechanism that will occur for a given fiber type.

In the studies cited above, the roles of the different levels of the cellulose structure in the swelling and dissolutions mechanisms were not well established. By controlling the quality of the solvent, the dissolution conditions and the fiber sources, it is possible to reveal the characteristic mechanisms of the swelling and dissolution at the different length scales of the cellulose structure from the cell walls to the macromolecular chains. This will be discussed in the next paragraphs.

Dissolution Mechanisms of Native Cellulose Fibers

Dissolution of a Solid Polymer

Common synthetic polymers are dissolving in several steps (18, 19) as illustrated in Figure 3. When the polymer is placed in contact with the solvent (A), the solvent swells the solid phase that goes above the glass transition T_g (T_g decreases with increasing concentration of solvent) (B). The swelling increases up to the point of disentanglement (C). Finally, the polymer chains can move out of the swollen phase to the solvent phase (D) and the solubilization is completed (E). The dissolution indeed occurs from the outside to the inside of the solid polymer. Mechanisms are somewhat similar for amorphous and crystalline zones and the main differences are seen in terms of kinetics.

Dissolution of Native Cellulose Fibers

Influence of the Cell Wall Structure

We demonstrated recently (20) that the mechanism is inversed for native cellulose fibers. In fact, by studying the dissolution of raw cotton fibers, *Gossypium barbadense*, at different growth stages in varying solvent quality, we showed that the primary wall, the secondary S1 wall and S2 wall that are arranged concentrically could behave very differently depending on the solvent strength. When the solvent is very good, i.e. NMMO- 18 % water (w/w) and below, the whole fiber fragmentates and dissolves fast. When placed in a moderate quality solvent (NMMO- 20% water w/w), the cotton fibers are dissolving from the inside to the outside following the sequence illustrated in Figure 4, thus revealing a gradient of dissolution capacity. Same mechanisms have been observed for wood pulp fibers.

- (A) The solvent penetrates inside the fiber
- (B) The S2 wall dissolves by fragmentation
- (C) The S1 wall swells under the pressure of the dissolving S2 wall
- (D) The primary wall breaks to form collars (called unswollen sections in (11, 12, 15–17)) and eventually helices

Influence of the Chemical Environment of the Cellulose Chains

The gradient in dissolution capacity of successively deposited cell wall layers described above has to be related with the specific composite structure of cellulose fibers. The primary wall is composed of many components. Cellulose and hemicelluloses are present as well as pectins and proteins (21) while the secondary S2 wall contains almost only cellulose and hemicelluloses. These components were shown by dynamic FTIR spectroscopy experiments to be strongly linked together (22). As described by Klemm et al. (23), the cellulose microfibrils are also differently arranged and compacted within the structure

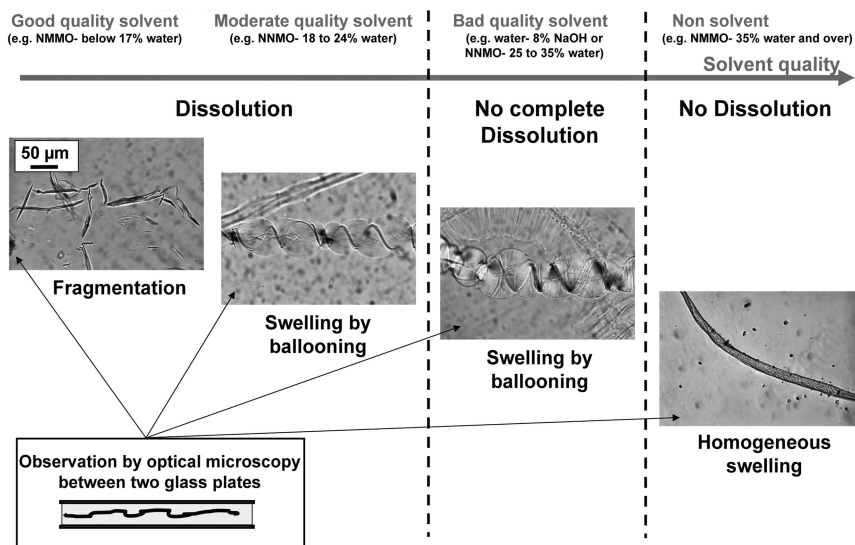


Figure 2. The four different swelling and dissolution mechanisms of wood pulp and cotton fibers as a function of the solvent quality.

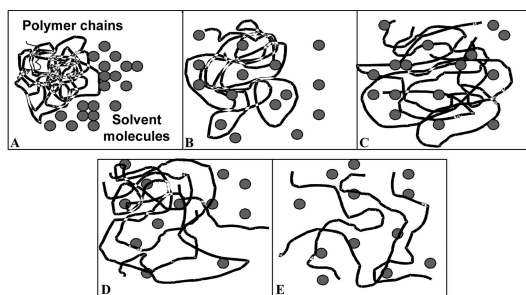


Figure 3. Dissolution steps of a solid synthetic polymer in a solvent.

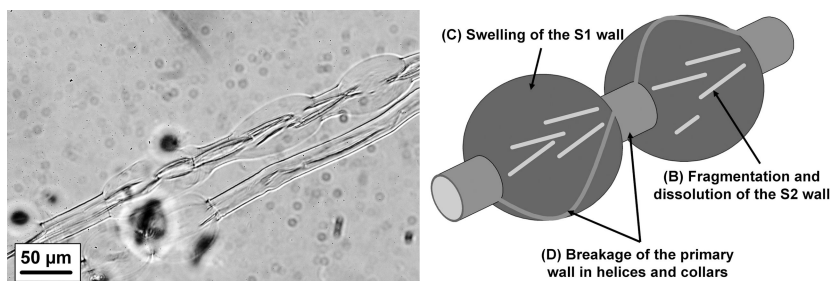


Figure 4. Dissolution of a raw cotton fiber, *Gossypium barbadense*, in NMMO - 20% water w/w (left); Description of the dissolution steps of a cellulose fiber in a moderate quality solvent (right).

depending on the considered wall. The higher amount of non-cellulosic materials and the structural organisation in older wall layers, i.e. the outside walls, may explain their lower dissolution capacity. Independently of solvent systems, this explanation pre-supposes that some of the non-cellulosic components as the hemicelluloses are still bound to cellulose after pulping and could impede the dissolution.

This assumption is supported by recent results (24). We found by a selective separation by centrifugation of insoluble and soluble cellulose fractions in NaOH-water mixtures and further analyses by size exclusion chromatography a large superposition of their molar mass distributions meaning that a fraction of short cellulose chains do not dissolve while a fraction of longer ones do. It indicates that some cellulose chains are less accessible than others and embedded in regions difficult to dissolve. As shown on Figure 5, the carbohydrate composition analysis of the different fractions reveals that soluble fractions contains a lower amount of mannan than the insoluble ones.

Beyond thermodynamic considerations, the dissolution capacity of cellulose chains is thus very dependent of their localization in the cell wall structure and the chemical environment around the cellulose chains, as the hemicelluloses matrix, should be considered as a key parameter for the dissolution efficiency.

Influence of the Chain Mobility

As pointed out by Isogai and Attala (25), “the disruption of long range order present in solid cellulose samples may be viewed as the key” to improve cellulose dissolution. This statement was recently highlighted by dissolution experiments in moderate quality solvent where it was shown that a uniaxial elongational stress is able to prevent full dissolution or decrease the efficiency of a chemical derivatization (24, 26). Even if the solvent has a full access to the cellulose chains, the chains must perform conformational conversions to dissolve that are limited if the whole chains is blocked into a long range fixed H-bond network. The acetylation of Lyocell fibers without tension leads to degree of substitution (DS) values up to 1.3 while, under tension, DS values are in a much lower range of 0.2 to 0.5 (26).

Swollen Morphologies Observed by Scanning Electron Microscopy

In the preceding paragraph, the mechanisms of swelling and dissolution were described in details from the morphological scale by means of optical microscopy to the macromolecular scale by means of molar mass measurements and carbohydrate composition analyses. However, optical microscopic observations do not show a complete visualization of the surface and volume of the swollen morphologies. Since, the more contrasted behaviour are seen when the cellulose

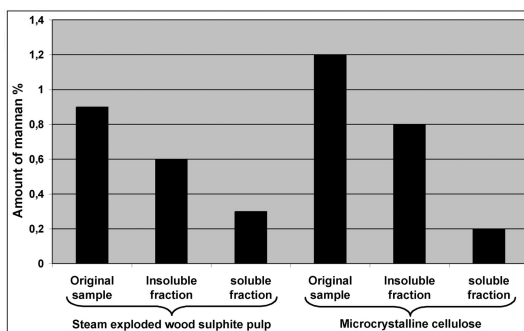


Figure 5. Comparison of the amount of mannan in the insoluble and soluble fractions of a steam exploded softwood (spruce) sulphite pulp and a microcrystalline cellulose after dissolution in NaOH-water mixtures.

fibers are swelling by ballooning, we will investigate in these paragraph the possibility to observe ballooned fibers by scanning electron microscopy.

Experimental Protocol

The swelling experiments were performed on bleached cotton fibers (Mn = 262,900 g/mol ; Mw = 606,300 g/mol determined by gel permeation chromatography). While observed by optical microscopy in transmission mode with a Metallux 3 (Leitz) equipped with a Linkam TMS 91 hot stage, fibers were swollen in NMMO- 22% water (w/w) at 90°C between two glass plates up to the formation of balloons and distilled water was then injected by capillarity to stop the dissolution process.

Swollen fibers were then extracted from the two glass plates and deposited on a sample holder covered with a carbon tape. The sample holder was directly introduced on the stage of the scanning electron microscope (Philips FEI XL30 ESEM with LaB6 gun). Swollen fibers were observed in environmental mode. The environmental mode preserves humidity and prevents drying which could induce modifications of the fibers (pore or cavity closure, plastic deformation). Humidity level must be carefully monitored since too much humidity is obstructing the observation (only water layers are then observed). The best conditions were the following: pressure 5.5 mbar, acceleration voltage 15 keV and relative humidity 30%.

Results and Discussion

In the dried state, some grooves can be seen at the surface of the bleached cotton (Figure 6 left). Upon swelling, the grooves previously observed are deeper (Figure 6 right) and the fiber loses its kidney shape (27, 28) to take a regular cylinder shape that exhibits swelling ratio of 1.5 (defined as the initial diameter over the swollen diameter).

After this first low regular swelling, ballooning occurs beginning by small excrescences scattered along the fibre length to finally give fully developed balloons with swelling ratio up to 5.3 (Figure 7). As can be seen, the longitudinal grooves are present on the cylindrical sections linked to the balloons (see insert in Figure 7), while they are not observable on the surface of the balloons. On the contrary, the surface of the balloons is very smooth (it can be surrounded by some remaining crystals of NMMO) and the outside wall with grooves is not present anymore. As previously described, the ballooning is thought to occur by (i) the breaking of the primary wall, i.e. the outside wall with grooves, and (ii) the swelling of the S1 wall that contains the dissolved S2 wall. It is very clear that the interface between primary wall and S1 layer, which is the surface of the balloon seen on figure 7 is very smooth and regular, without any remaining parts of the primary wall. The transition in terms of structure and composition from the primary wall to the S1 wall is very sharp, as seen with the neat splitting of these two walls. This shows that there should be a very clear change in biosynthesis at the primary wall-S1 transition, with a rather low adhesion between these two layers. The very smooth surface of balloons can be either an image of reality, i.e. a very smooth interface between primary wall and S1, or due to the high swelling. Based on these microscopic observations, the cohesion between the primary wall and the S1 wall can thus be considered as rather weak.

It has to be emphasized that the distilled water injected to stop the dissolution process may have slightly modified the macroscopic morphology of the ballooned fibers due the cellulose I - cellulose II transition. After several minutes, the electron beam leads to a strong degradation of the sample that prevents any further observation.

Diffusion of the Cellulose Chains upon Dissolution

As previously described, the dissolution of cellulose fibers in NMMO- 20% water occurs first by a ballooning stage. We know that during this process, cellulose is dissolved inside the balloon, but nothing is known about the possibility to have already cellulose chains escaping from the balloons. One way to investigate this point is to send a regenerating medium like distilled water during the dissolution and to look if it is possible to see the traces of precipitated cellulose outside the balloon.

Experimental Protocol

We achieved the partial dissolution of bleached cotton fiber ($M_n = 262,900$ g/mol ; $M_w = 606,300$ g/mol determined by gel permeation chromatography) in NMMO- 20% water (w/w) at 90°C between two glass plates. No convection was applied to the system. Several droplets of water were then injected by capillarity during the dissolution after the beginning of the ballooning stage. The additional water dilutes the solvent and precipitates the dissolved cellulose chains that can

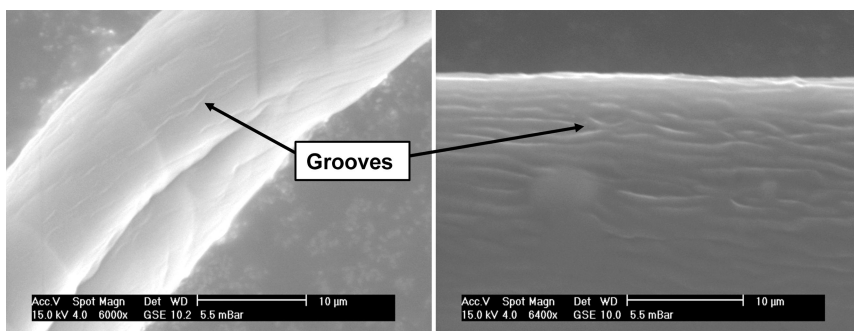


Figure 6. Bleached cotton fiber in the dried state (left) ; Bleached cotton fiber in the swollen state before that the ballooning occurs (right).

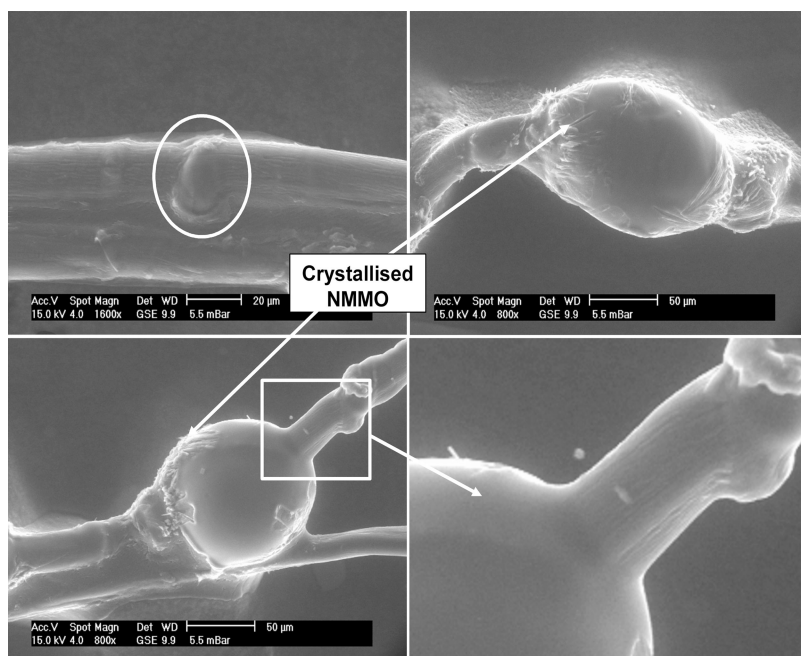


Figure 7. First excrescence along the fiber (top left) ; Fully developed balloons surrounded by some crystals of NMMO (top right and bottom).

then be easily observed. The samples were investigated in transmission mode by optical microscopy with a Metallux 3 (Leitz) equipped with a Linkam TMS 91 hot stage and the data were recorded with a high resolution 3-CCD camera (1360*1024 pixels) JVC KY-F75U.

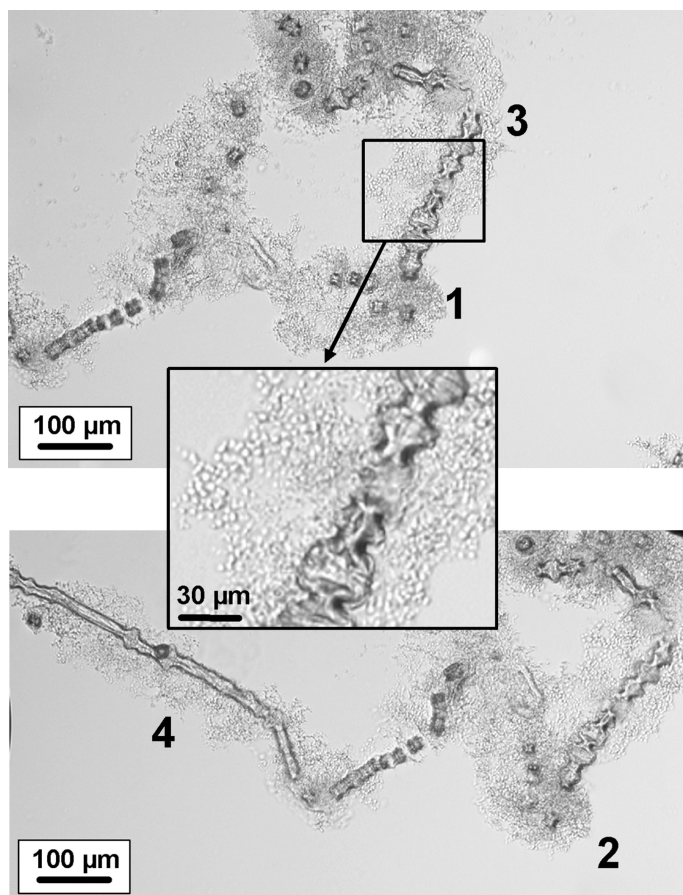


Figure 8. Precipitation of the dissolved cellulose during the dissolution of a bleached cotton fiber in NMMO - 20 % water. Tiny cellulose gel droplets can be observed around the partially dissolved fibers.

Results and Discussion

The precipitation of dissolved cellulose in NMMO-water by the addition of distilled water generates tiny cellulose gel droplets of nearly spherical shape around the dissolving fibers with diameter ranging from 1 to 10 μm (see insert in Figure 8). It is not possible to firmly establish by which mechanism the phase separation occurred, either spinodal decomposition or nucleation and growth. The fact that neighbouring droplets are of the same size, aligned along strings and sometimes attached suggests that the mechanism is a spinodal decomposition. This is supported by several studies made on cellulose objects regenerated from NMMO solutions (29–31) or during regeneration by NMR (32).

The possibility to visualize dissolved cellulose when precipitated enables to analyse its distribution around the dissolving cotton fiber. As expected, the

concentration of precipitated cellulose is higher in fully dissolved regions (zones 1 and 2). However, it is intriguing to observe the presence of smaller concentration of precipitated cellulose around ballooned regions as well as around unswollen regions (zones 3 and 4 respectively). Although dissolution begins by the inside of the fiber with the fragmentation of the S2 wall, these observations show that some dissolved cellulose chains are able to leave the dissolving cellulose fiber during the early stage of swelling and dissolution even before ballooning occurred. Nothing is known about the molar mass distribution of these chains. They may come from the surface of the fiber or most likely from the inside of the fiber meaning that the outside walls, i.e. the primary wall and the S1 wall, are porous enough to enable the diffusion of the dissolved cellulose chains even in the non-swollen state.

Conclusions

Native cellulose fibers exhibit complex dissolution mechanisms that have to be related to their specific structure. Contrary to classical semi-crystalline polymers, which can be considered as binary system with an amorphous and a crystalline phase, native cellulose fibers are composed of several layers varying in terms of structure and composition. Consequently, the behaviours can be rather different depending on the zones of the structure considered. Despite advanced knowledge in the chemical modification and dissolution of cellulose fibers, the swelling and dissolution of cellulose still remain a complex scientific field and a breakthrough should be made by the understanding and the integration of all the biosynthesis processes.

References

1. Nägeli, C. *Sitzber. Bay. Akad. Wiss. München* **1864**, *1*, 282–323; *2*, 114–171.
2. Pennetier, G. *Bull. Soc. Ind. Rouen* **1883**, *11*, 235–237.
3. Flemming, N.; Thaysen, A. C. *Biochem. J.* **1919**, *14*, 25–29.
4. Flemming, N.; Thaysen, A. C. *Biochem. J.* **1921**, *14*, 407–415.
5. Marsh, J. T. *Mercerising*; Chapman & Hall Ltd: London, 1941.
6. Hock, C. W. *Text. Res. J.* **1950**, *20*, 141–151.
7. Tripp, V. W.; Rollins, M. L. *Anal. Chem.* **1952**, *24*, 1721–1728.
8. Rollins, M. L.; Tripp, V. W. *Text. Res. J.* **1954**, *24*, 345–357.
9. Warwicker, J. O.; Jeffries, R.; Colbran, R. L.; Robinson, R. N. *A Review of the Literature on the Effect of Caustic Soda and Other Swelling Agents on the Fine Structure of Cotton*; St Ann's Press: Manchester, 1966; Shirley Institute Pamphlet 93.
10. Hock, C. W. In *Cellulose and cellulose derivatives*, 2nd ed.; Ott, E., Spurlin, H. M., Grafflin, M. W., Eds.; Interscience Publisher: New York, London, 1954; Part 1, pp 347–392.
11. Cuissinat, C.; Navard, P. *Macromol. Symp.* **2006**, *244*, 1–18.

12. Cuissinat, C.; Navard, P. *Macromol. Symp.* **2006**, *244*, 19–30.
13. Stawitz, J.; Kage, M.P. *Das Papier* **1959**, *13*, 567–572.
14. Chanzy, H.; Noe, P.; Paillet, M.; Smith, P. *J. Appl. Polym. Sci.* **1983**, *37*, 239–259.
15. Cuissinat, C.; Navard, P.; Heinze, T. *Carbohydr. Polym.* **2008**, *72*, 590–596.
16. Cuissinat, C.; Navard, P. *Cellulose* **2008**, *15*, 67–74.
17. Cuissinat, C.; Navard, P.; Heinze, T. *Cellulose* **2008**, *15*, 75–80.
18. Miller-Chou, B. A.; Koenig, J. L. *Prog. Polym. Sci.* **2003**, *28*, 1223–1270.
19. Narasimhan, B.; Peppas, N. A. *J. Polym. Sci., Part B: Polym. Phys.* **1998**, *36*, 2607–2614.
20. Le Moigne, N.; Montes, E.; Pannetier, C.; Höfte, H.; Navard, P. *Macromol. Symp.* **2008**, *262*, 65–71.
21. Klemm, D.; Schmauder, H. P.; Heinze, T. In *Biopolymers*; De Baets, S., Vandamme, E. J., Steinbüchel, A., Eds.; Wiley-VCH: Weinheim, 2002; Vol. 6, pp 275–319.
22. Stevanic, J. S.; Salmén, L. *Cellulose* **2008**, *15*, 285–295.
23. Klemm, D.; Philipp, B.; Heinze, T.; Heinze, U.; Wagenknecht, W. *Comprehensive Cellulose Chemistry*; Wiley-VCH: Weinheim, 1998; Vol. 1, pp 9–165.
24. Le Moigne, N. Ph.D. dissertation, Ecole Supérieure Nationale des Mines de Paris, Sophia Antipolis, France, 2008. <http://pastel.paristech.org/4570/>
25. Isogai, A.; Atalla, R. H. *Cellulose* **1998**, *5*, 309–319.
26. Spinu, M.; Heinze, T.; Navard, P.; CEMEF, Mines ParisTech; Kompetenzzentrum Polysaccharidforschung, Friedrich-Schiller-Universität Jena, unpublished work.
27. *Cotton fibers: developmental biology, quality improvement and textile processing*; Basra, A. S., Ed.; Food Products Press/Haworth Press: New York, London, Oxford, 1999.
28. Kassenbeck, P. *Text. Res. J.* **1970**, *40*, 330–334.
29. Biganska, O.; Navard, P. *Cellulose* **2009**, *16*, 179–188.
30. Zhang, Y.; Shao, H.; Wu, C.; Hu, X. *Macromol. Biosci.* **2001**, *1*, 141–148.
31. Mortimer, S. A.; Péguy, A. *J. Appl. Polym. Sci.* **1996**, *60*, 305–316.
32. Laity, P. R.; Glover, P. M.; Hay, J. N. *Polymer* **2002**, *43*, 5827–5837.

Chapter 8

Side Reactions in the System Cellulose/1-Alkyl-3-methyl-imidazolium Ionic Liquid

Michael Schrems¹, Gerald Ebner¹, Falk Liebner¹, Ernst Becker²,
Antje Potthast¹ and Thomas Rosenau^{1,*}

¹University of Natural Resources and Applied Life Sciences Vienna (BOKU),
Department of Chemistry and Christian Doppler Laboratory
“Advanced Cellulose Chemistry and Analytics”, Muthgasse 18,
A-1190 Vienna, Austria

²Blue Globe Energy GmbH, Willy-Brandt-Platz 6, D-68161 Mannheim,
Germany
*thomas.rosenau@boku.ac.at

In solutions of cellulose in 1-alkyl-3-methyl-imidazolium ILs, both the ionic liquid and the cellulose are evidently not inert. Side reactions can be distinguished according to whether they involve the cation or the anion of the ionic liquid or just autodegradation products of the IL. Ionic liquids with 1-alkyl-3-methyl-imidazolium cations react at C-2 with cellulose at its reducing end (and, if present, other aldehyde functionalities along the chain), forming a carbon-carbon bond. The reaction is strongly catalyzed by bases, so that commonly present impurities in ILs, such as their thermal degradation products, promote this reaction. These thermal degradation products are mainly imidazole, *N*-alkylimidazole, *N*-methylimidazole and methylene-bridged dimers. Side reactions of ILs anions are more divers and depend on the respective reaction system. Acetate as the IL anion is generally unsuitable for esterifications by acylating agents (halides, anhydrides), both organic and inorganic ones, for methylations (alkyl halides, dialkyl sulfate), or for silylations (trimethylsilyl halides), since the reagents coreact with the IL anion rather than with the cellulosic hydroxyls. Chloride anions in the IL cannot be used for alkylations (alkyl halides, dialkyl sulfate) or oxidations (NMMO, periodate).

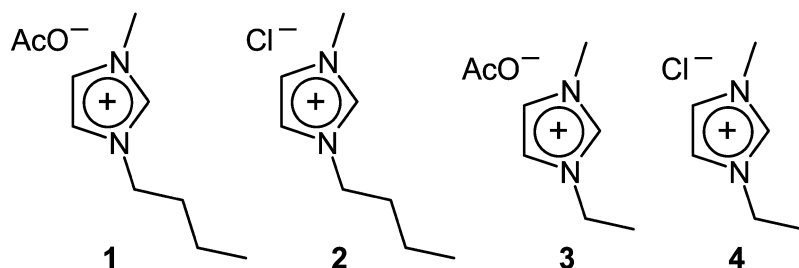
Introduction

Within the past several years, ionic liquids (ILs) have attracted much interest in cellulose chemistry as dissolution (1, 2) and derivatization media (3–6). There is also industrial interest in the use of ILs for production of cellulosic fibers and shaped cellulose in general (7–9). The far-reaching non-reactivity and good solvent properties of ILs seems to render them competitors to the Lyocell technology which is based on *N*-methylmorpholine-*N*-oxide monohydrate (NMMO/H₂O). Although this solvent is also able to dissolve celluloses directly, it needs elevated temperatures, is a rather strong oxidant and tends to be quite unstable. Those disadvantages could, in principle, be overcome by ILs which in addition are able to dissolve larger percentages of cellulose compared to NMMO, but the chemical and technological research towards a large-scale application is still in a juvenile state. Especially 1-butyl-3-methyl-imidazolium (BMIM) and 1-ethyl-3-methyl-imidazolium (EMIM), both as acetate or chloride (1 – 4, Scheme 1), have found wide utilization in cellulose and polysaccharide chemistry.

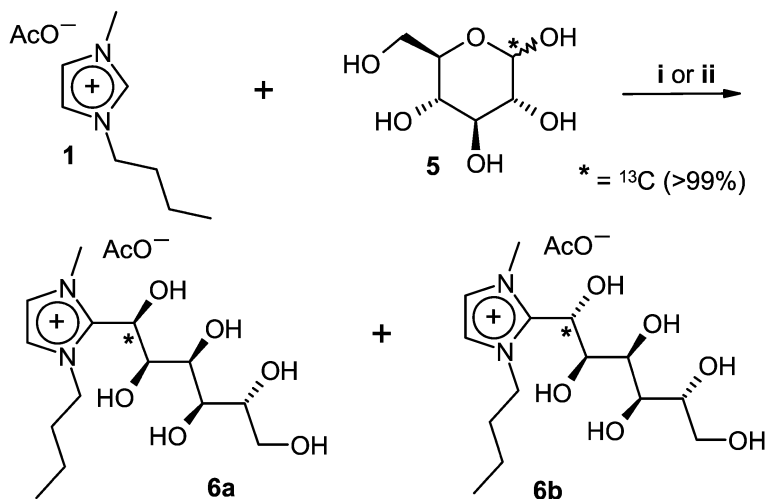
It has been realized that the integrity of the cellulose chain during dissolution and derivatization in ILs is largely dependent on the purity of these solvents and of the absence of IL-derived byproducts. We recently observed that cellulose after dissolution in imidazolium-based ILs and re-precipitation showed less fluorescence with the carbonyl-selective fluorescence label CCOA (10) than the starting cellulose labeled directly. The carbonyl groups (*e.g.* the reducing ends) seemed to be somehow “inactivated” towards labeling, possibly indicating a reaction between the ILs and carbonyl groups of the cellulose. Such carbonyls are present in the form of a hemiacetal at the reducing end of the cellulose chain, and as keto (C-2, C-3) or aldehyde (C-6) groups along the cellulose chain, which are the result of random oxidation during cellulose processing (pulping, bleaching) and aging.

In the literature, the reactivity of C-2 in imidazolium moieties finds ample coverage (11). In particular, there is one report on side reactions of imidazolium-based ionic liquids in base-catalyzed Baylis–Hillman reactions (12), where it was shown that 1-butyl-3-methylimidazolium (BMIM) ionic liquids participate in the reaction with aldehyde groups, being deprotonated at C-2 to give species capable of reacting with electrophiles, such as benzaldehyde. Also the acetylating action of BMIM acetate onto cellulose has been demonstrated recently (13) showing that also the anion part of the IL can be involved in side reactions. In this paper we would like to communicate that 1-alkyl-3-methylimidazolium ILs react with aldose carbohydrate model compounds and with cellulose, demonstrating that neither the heterocyclic cation nor the anion of ILs commonly used in cellulose chemistry (EMIM acetate and chloride, BMIM acetate and chloride) behave in an inert manner (towards cellulose or coreactants), and that thermal degradation products of the ILs promote some of these side reactions.

Scheme 1. Chemical structure of the ionic liquids 1-butyl-3-methyl-imidazolium acetate (BMIM-OAc, **1**), 1-butyl-3-methyl-imidazolium chloride (BMIM-Cl, **2**), 1-ethyl-3-methyl-imidazolium acetate (EMIM-OAc, **3**), and 1-ethyl-3-methyl-imidazolium chloride (EMIM-Cl, **4**).



Scheme 2. Reaction of BMIM-OAc (**1**) with 1-¹³C-D-glucopyranose (**5**) to the diastereomeric addition products **6a** and **6b**.



i: **1** / **2** = 20 / 1 (w/w), r.t., 7 d;
 ii: **1** / **2** = 20 / 1 (w/w), 2-5% auxiliary base
 (TEA, imidazole, 1-methylimidazole)

Results and Discussion

Reactions of the IL Cations

To simulate the reactivity of the reducing end of celluloses we used D-glucose as a very simple, but well fitting model compound. It is present as natural mixture of α - and β -D-glucopyranoside. A glucose with a ¹³C-label at position C-1 (>99%, **5**) allowed following the reaction at the reducing end more

specifically. The intensity gain by roughly the factor 100 in ^{13}C NMR would allow to reliably detect even minor side reactions at this position: if 10% of the glucopyranose in a 10% solution in 1-alkyl-3-methylimidazolium ILs would form a byproduct, its corresponding resonance would still be in the same intensity order as those of the solvent. Figure 1 shows the ^{13}C NMR spectrum of the 1-butyl-3-methylimidazolium acetate (**1**, Fig. 1A), and of 5% 1- ^{13}C -D-glucose (**5**) in this IL immediately after dissolution (Fig. 1B). The resonances at approx. 99 ppm and 93 ppm correspond to the β -D-glucopyranose and α -D-glucopyranose forms, respectively [The small resonances between 60 and 80 ppm belong to the (non-labeled) peaks of the glucose atoms C-2 to C-6, the peaks at 97 and 105 ppm to the (labeled) C-1 of the glucofuranosides in equilibrium concentration (<0.5%)]. After 7 days of storage under inert atmosphere at room temperature, clearly two new signals (at approx. 65 ppm and 67 ppm) had developed (Fig. 1C), which originate from the addition products **6a** and **6b**, formed by electrophilic attack of C-2 of the imidazolium at the anomeric carbon of **5** (Scheme 2) [The assignment of the two shifts to the two diastereomeric products was based on the calculated NMR shifts (Spartan 2004, HF, 6-311G(d,p)) with the resonance of the former C-1 appearing at higher field for **6a**].

The same outcome was observed already after 2h in the presence of catalytic amounts of triethylamine (TEA, additional small resonances at 11.7 ppm and 45.7 ppm) at r.t., see Fig. 1D. In both cases, about 15% of the glucopyranose were converted into the corresponding addition product by reaction with BMIM-OAc (**1**). It was evident that the IL reacted with the glucopyranose both at longer reaction times and upon base catalysis.

The same reaction was confirmed for other aldopyranoses, such as mannose, xylose, cellobiose and cellotriose. The reaction rates, as roughly approximated by ^{13}C NMR using 2- ^{13}C -BMIM-OAc (**14**) (**1***, see also Scheme 3) were very similar in all cases, and also the catalytic effect of bases was always provable. Assuming similar reactions to occur under similar conditions with aldehyde/hemiacetal functions in cellulose, we faced the analytical problem that the amount of IL bound to cellulose (**7**) would be rather small. In the case of an IL cation reacting with glucose, both moieties are present in a 1:1 ratio in the product. At a cellulose DP (degree of polymerization, number of anhydroglucose units) of 500, there is per 500 glucopyranose units just one reducing glucopyranose end available for reaction with the IL, giving a 500:1 ratio (provided that indeed all reducing ends would react). Such a small amount of derivatized reducing ends is impossible to track down by NMR and is also within the error limits of microanalysis (N content). However, when we used isotopically labeled ionic liquid (2- ^{13}C -BMIM-OAc, **1***), the NMR resonance intensity of the co-reacting C-2 in the IL is multiplied by approx. 100, and thus approaches the detectable range. Indeed, a cellulose dissolved in **1*** for 7 d, then precipitated, and finally measured by NMR in DMAc- d_9 /LiCl (2.5%, w/w) shows a weak but clearly discernible resonance at 147.8 ppm, corresponding to C-2 in the imidazolium moieties of the endwise-derivatized cellulose (**8**), see Scheme 3. The same outcome was observed when the cellulose was dissolved in **1*** in the presence of 3% TEA or imidazole, precipitated and re-dissolved for NMR measurement. C-2 in **1** (and **1***) resonates (^{13}C NMR) at 137 ppm. This resonance was absent

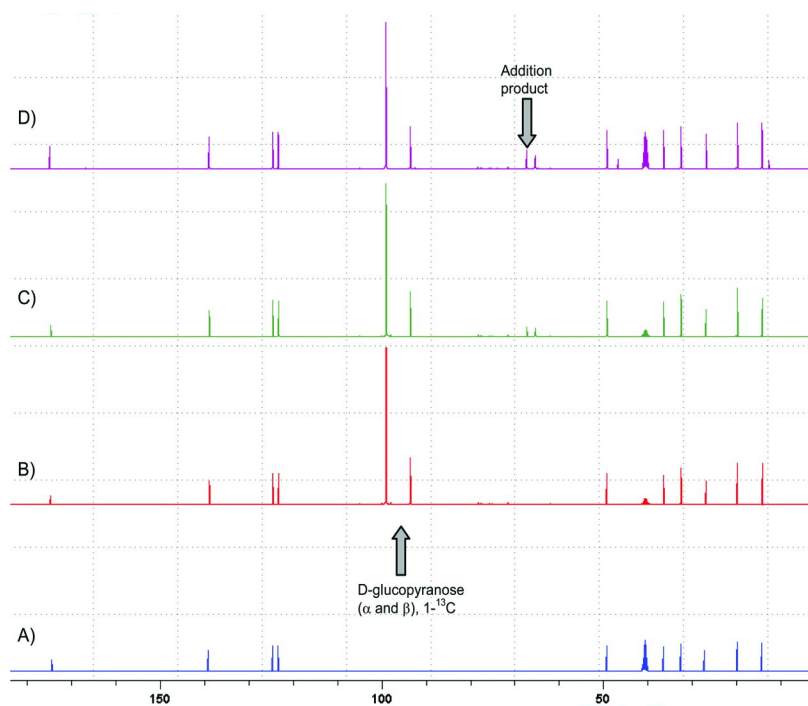
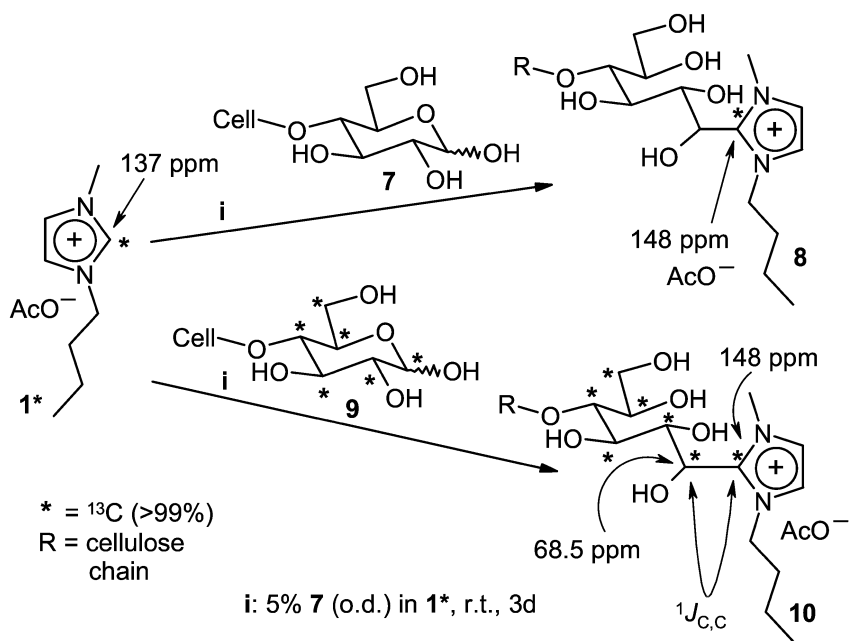


Figure 1. ^{13}C NMR spectra (ppm). A) BMIM-OAc (**1**); B) BMIM-OAc and 5% $1\text{-}^{13}\text{C}$ -D-glucose (**5**, 5%, w/w), spectrum acquired immediately after dissolution; C) composition as in B), measured after 7 d at r.t., D) BMIM-OAc, 5% $1\text{-}^{13}\text{C}$ -D-glucose (**5**, 5%, w/w), and 3% TEA (w/w), spectrum acquired after 2 h.

in **6a/b** and in the precipitated derivatized “BMIM-cellulose” **8**, and just the C-2 resonance at 147.8 ppm was present. In the case of using ^{13}C -perlabeled cellulose (**9**) (**15**) the direct carbon-carbon linkage between the reducing end of cellulose and C-2 of the IL heterocycle in the labeled “BMIM-cellulose” **10** became evident by the direct homonuclear coupling of these two carbons with a $^1J_{\text{C,C}}$ of 38 Hz, which split the IL-C-2 resonance into a doublet (d, 148 ppm, coupling with cellulose-C-1, *i.e.* the reducing end) and the signal of the reducing end of cellulose into a doublet of doublets (dd, 68.5 ppm, coupling with IL-C-2, $^1J_{\text{C,C}} = 38$ Hz, and with C-2 of cellulose, $^1J_{\text{C,C}} = 19$ Hz), see Scheme 3.

Preliminary experiments have shown that addition of strong bases to the addition products between glucose (or other aldoses or cellulose, respectively) and IL apparently caused a reversal of the addition reaction (a retro-aldol type cleavage). This is in line with observations on the reversible addition of 1-butyl-3-methyl-imidazolium IL to benzaldehyde (**9**). This finding, which is current under further scrutiny, implies that cellulose derivatized in 1-alkyl-3-methyl-imidazolium ILs becomes derivatized at the reducing end according to Figure 3, but might lose the IL moiety over time in a reversal of the addition process. Due to the negligible vapor pressure of the ILs, the released IL, although present in minute amounts only, cannot leave the cellulosic material and

Scheme 3. Reaction of ^{13}C -labeled 1-butyl-3-methylimidazolium IL (1^*) with cellulose (**7**) at its reducing end to the “BMIM-cellulose” derivative **8** and with ^{13}C -perlabeled cellulose **9** to “labeled BMIM-cellulose” **10**, both products having ^{13}C NMR-detectable cellulose-IL linkages.

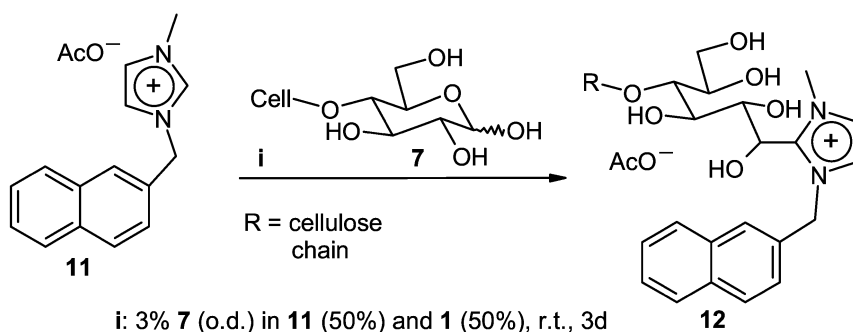


will accumulate there, which should be kept in mind as a possible problem for medical and physiological application scenarios of IL-processed celluloses.

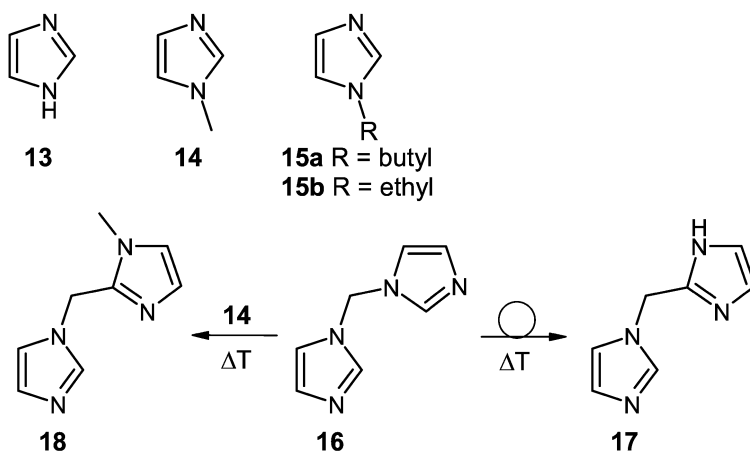
To further prove the derivatization of cellulose by ILs based on 1-alkyl-3-methyl-imidazolium, we used 1-(2-naphthylmethyl)-3-methyl-imidazolium acetate (NapMIM, **11**) instead of BMIM-OAc (**1**). Having otherwise similar reactivity, **11** carries a UV- and fluorescence-active naphthyl moiety, which can be used to report the IL moiety in derivatives. While the reaction product of BMIM with cellulose has no fluorescence, the analogous NapMIM-cellulose derivative (**12**) is strongly fluorescent (Scheme 4). This property can be used to verify by size exclusion chromatography (SEC) (For details of the GPC system used see part b of ref (8)) whether indeed an IL-based moiety is attached to cellulose after dissolution of cellulose in this ionic liquid. In the case of IL being only adsorbed or adherent to cellulose, fluorescence would occur only in the SEC exclusion peak (long retention times), but not along the molecular weight distribution of the cellulose. If, on the contrary, the IL was covalently bound to the cellulose, there would be a discernible fluorescence signal also along the molecular weight distribution, indicating the endwise derivatization of the cellulose chains by the IL.

Indeed, as given in Figure 2, the cellulose was derivatized by NapMIM (**11**) as seen by the distinct fluorescence signal of this compound. The cellulose was dissolved in the IL for 3d, subsequently re-precipitated and re-dissolved for the

Scheme 4. Reaction of (2-naphthylmethyl)methyl-imidazolium IL (NapMIM-OAc, **11**) with cellulose at its reducing end to fluorescent derivative **12**, that is detectable with fluorescence-SEC.



Scheme 5. Thermal degradation products of B(E)MIM ionic liquids upon thermal stress (200°C for 24 h, closed vessel, inert atmosphere).



SEC measurement. Similar results were obtained also after only 8h of dissolution time. Thus, already after such relatively short times in IL solution, the cellulose reacted with the 1-alkyl-3-methyl-imidazolium IL, which caused a derivatization at the reducing end as shown in Schemes 3 and 4. The fact that the fluorescence signal follows the molecular weight distribution (MWD) of the cellulose quite closely in shape moreover demonstrated that this endwise derivatization occurred more or less independent of the chain length: derivatization proceeded in all molecular weight regions equally well, and no region was suppressed or preferred.

Thermal Degradation of ILs

It has been recognized frequently that reactions in ILs – also reactions of cellulose – are dependent with regard to rate, yield, and side processes on the

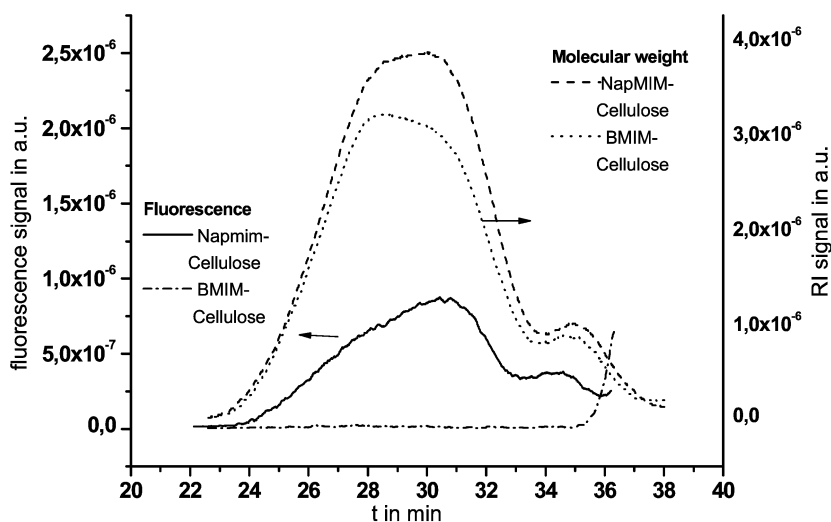


Figure 2. Molecular weight distributions (right y-axis) and fluorescence signals (left y-axis) of BMIM-derivatized (**8**) and NapMIM-derivatized (**12**) cellulose. No fluorescence was detectable in the case of BMIM (dash-dot line), whereas cellulose dissolved in NapMIM gave a clear fluorescence signal over the whole range of the molecular weight (solid line). The shape of the molecular weight distribution did not change significantly upon reaction with either IL (cf. refractive index (RI) signal).

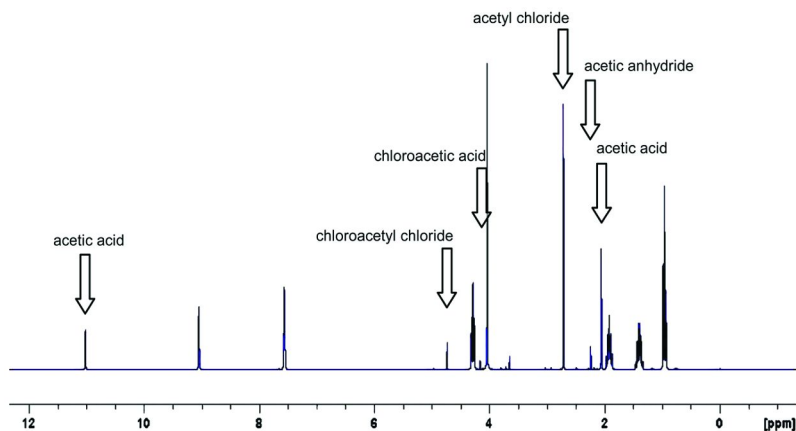


Figure 3. ^1H NMR spectrum (ppm scale) of a mixture of BMIM-OAc (**1**) and sulfonyl chloride (molar ratio 2:1), acquired 15 min after mixing. Besides the evident major peaks of acetyl chloride (**22**) and acetic anhydride (**23**), some minor byproducts (chloroacetic acid, chloroacetyl chloride) are visible.

purity and “freshness” of the ILs. This effect is also related to the recyclability of ILs, with byproducts possibly accumulating and affecting the outcome of the processes. The recyclability is, however, not the subject of this study. We

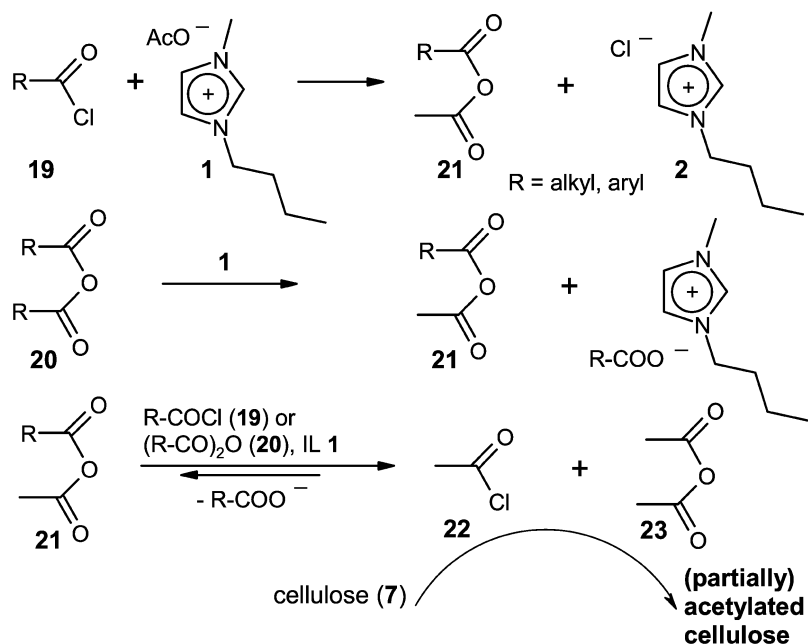
were focusing instead on the thermal stability of the ILs **1** – **4**, starting from the observation that the side reaction with glucose (Scheme 2) and cellulose (Scheme 3) proceeded clearly faster in ILs that were heated for some time, whereas the reaction was much slower in freshly purified (extracted, silica gel filtered) ILs. This indicated the formation of basic compounds – as the above side reaction is catalyzed by bases – which were highly likely derived from the heterocyclic IL cation. Applying extraction in combination with adsorption to acidic alumina (Brockmann grade II), we were able to isolate the degradation products shown in Scheme 5 (16). Thermal degradation produces imidazole (**13**), *N*-methylimidazole (**14**), *N*-alkylimidazole (**15a**, alkyl = butyl, from **1** and **2**; **15b**, alkyl = ethyl, from **3** and **4**). Apart from these compounds, dimeric compounds (**16** – **18**) were found, in which the methyl group was converted into a methylene bridge. Interestingly, the former 1-alkyl group (butyl or ethyl) was not found in any of the dimeric compounds, although the reason for this behavior cannot be conclusively accounted for at the moment. Bis(1-imidazolyl)methane (**16**) was shown to be a precursor of 2-(imidazol-1-ylmethyl)-imidazole (**17**): under thermal treatment ($T > 150^{\circ}\text{C}$) the former is rearranged into the latter. The preliminary elimination product, an *N*-(methylene)imidazolium cation being a Mannich intermediate, performs an electrophilic attack at C-2 of imidazole. Product **17** can be regarded as a Mannich base formed from imidazole and formaldehyde, the C₁-bridging unit being formed from the former *N*-methyl group. Analogously, attack of the *N*-(methylene)imidazolium at C-2 of *N*-methylimidazole (instead of imidazole) produces the degradation product 2-(imidazol-1-ylmethyl)-1-methyl-imidazole (**18**). Carried out in a sealed autoclave, thermal treatment of **1** – **4** at 200°C for 24 h generated 0.08%, 0.02%, 0.05% and 0.006% of net degradation products, indicating the BMIM derivatives to be slightly less stable compared to the EMIM counterparts, and the acetate anions being slightly promotive to degradation as compared to chloride, possibly due to their higher basicity.

It is important that the thermal degradation products (**13** – **18**) carry secondary, tertiary and aromatic amine functionalities and are thus all relatively strong bases, which explains their promoting effect on the above reaction between 1-alkyl-3-methyl-imidazolium and the reducing ends of aldopyranoses/cellulose (Schemes 2 and 3). The degradation products will have accumulated in ILs after long thermal stress, so that those ILs are much more likely to undergo side reactions with cellulose than freshly purified ones. Thus, removal of such degradation impurities (and of bases in general) is an easy preventive measure to minimize such side reactions. All thermal degradation products shown in Scheme 5 have been unambiguously identified by their NMR (¹H, ¹³C) and MS data, also in comparison to authentic samples that were either commercially available (**13** – **15**) or synthesized according to standard protocols (**16** – **18**).

Reactions of the IL Anions

The anions of BMIM/EMIM-type ionic liquids can vary widely. Whereas in earlier days of IL research some complex anions, such as for instance PF₆⁻, AlCl₄⁻ or BF₄⁻, were more common, nowadays mainly acetate and chloride are

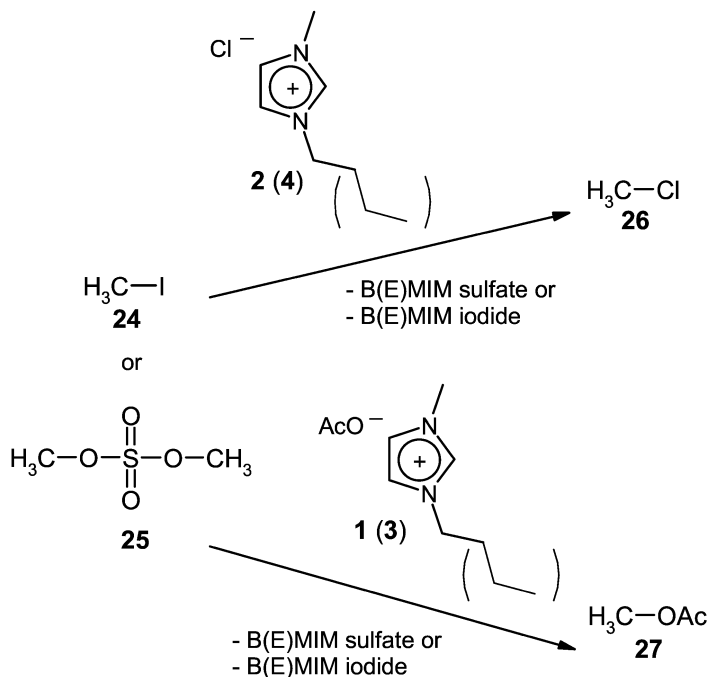
Scheme 6. Side reactions of BMIM-OAc (**1**) in esterifications with carboxylic acid chlorides (**19**) or anhydrides (**20**) causing formation of strongly acetylating agents (**21** – **23**) and eventually cellulose acetylation. The same generation of the strongly acetylating species acetyl chloride (**22**) and acetic anhydride (**23**) from the IL counter-anion acetate occurs as well with inorganic chlorides and anhydrides, see Figure 3 and text.



used, especially in cellulose chemistry and processing. Also the anions in ILs – chloride and acetate in this study – are not inert with regard to cellulose integrity. While the cation (1-alkyl-3-methyl-imidazolium) reacts directly with the solute cellulose, the reactions of the anions do not occur directly with cellulose, but primarily with reagents that are added for cellulose derivatization. This way, intermediates are formed which, in turn, might then cause side reactions with cellulose. In the following, examples for such reactions of IL anions are given. It should be mentioned that – while the reaction of cellulose with the cations was quite unexpected – some of the reactions of the IL anions were more evident and followed quite obviously from general chemistry.

A general case for IL anion side reactions is the attempted esterification of cellulose in BMIM-OAc (**1**) with organic or inorganic acid chlorides (**19**) or anhydrides (**20**), which does not give the expected esters of the carboxylic acid, the first example of this behavior being described in (10). Instead, cellulose acetate or mixed esters are formed. Both reagents **19** and **20** form reactive intermediates with the acetate anion of the IL: the mixed carboxylic acetic anhydride (**21**), acetyl chloride (**22**), and acetic anhydride (**23**), see Figure 3 and Scheme 6. The same reaction occurs with inorganic acid chlorides, e.g. sulfuryl

Scheme 7. Side reactions of EMIM/BMIM acetates and chlorides in methylations of cellulose with methyl iodide (24) or dimethyl sulfate (25) causing consumption of the methylating agent by formation of methyl chloride (26) which is volatile and in addition a much weaker methylating agent, or methyl acetate (27), respectively, which has no methylating activity.



chloride, thionyl chloride, phosphoryl chloride, or anhydrides, *e.g.* phosphorous pentoxide, sulfur trioxide and its complexes (Figure 3).

Also in these cases acetyl chloride (22) and acetic anhydride (23) are generated, which both cause cellulose acetylation as a side reaction. These acetylating compounds, their occurrence being experimentally confirmed by NMR (Figure 3) and GC/MS detection, are formed according to dynamic equilibria, independent of the presence of cellulose in the reaction system. However, in the presence of cellulose, the reactive intermediates are consumed by acetylation of cellulose and are continuously regenerated as long as acid chloride/anhydride as the starting material is present. Simultaneously, acetate as the IL anion is replaced by the corresponding carboxylate/acid anion. As a consequence, BMIM-OAc (1) and EMIM-OAc (3) cannot be used as solvents for esterification of cellulose with organic and inorganic acids, if the corresponding acid chlorides or anhydrides are to be used as the acylating agents. In these cases, acetylation of cellulose will inevitably occur as side reaction or even as the main process. By analogy to the acetate anion, also any other carboxylate as the BMIM counter-anion (as *e.g.* in BMIM benzoate or BMIM propionate) will cause formation of the corresponding cellulose carboxylic acid ester (benzoate or

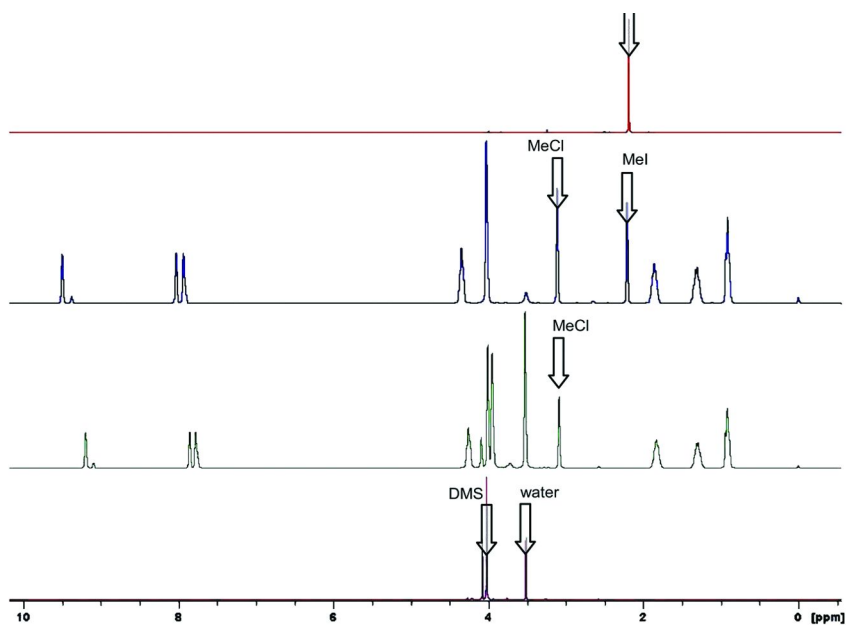


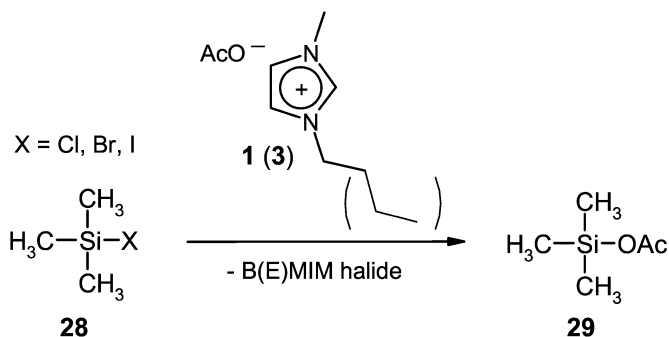
Figure 4. ^1H NMR spectra (ppm scale). Upper trace: methyl iodide (**24**), second upper trace: a mixture of BMIM chloride (**2**) and methyl iodide (**24**), acquired 15 min after mixing, second lower trace: a mixture of BMIM chloride (**2**) and dimethyl sulfate (DMS, **25**) acquired 15 min after mixing, lower trace: dimethyl sulfate (**25**). In the two middle spectra, the formation of methyl chloride (**26**) from the methylating agents is evident.

propionate, respectively) if an esterification of cellulose with organic/inorganic halides or anhydrides in this system is attempted.

Another side reaction of IL anions occurs if methylation of cellulose is carried out in BMIM chloride (**2**) or EMIM chloride (**4**), applying e.g. methyl iodide (**24**) or dimethyl sulfate (**25**) as methylating agents under alkaline conditions (Scheme 7).

In BMIM/EMIM chloride, both methylating agents are converted into methyl chloride (**26**) by nucleophilic substitution involving the chloride anion of the IL, which is replaced by iodide or (methyl)sulfate, respectively (see Scheme 7 and Figure 4). The methyl chloride (**26**) partly leaves the reaction system, as it is a volatile gaseous compound – but even dissolved portions react by 2 to 3 orders of magnitude slower than Me-I under otherwise identical conditions. If BMIM/EMIM acetates (**1**, **3**) are used for methylations, the main reaction is the conversion of the anion into methyl acetate (acetic acid methyl ester, **27**) rather than methylation of the (cellulosic) substrate (Scheme 7). Thus, neither 1-alkyl-3-methylimidazolium chlorides (**2**, **4**) nor 1-alkyl-3-methylimidazolium acetates (**1**, **3**) can be used in methylation reactions of celluloses, since the commonly used methylating agents are either lost or at least “inactivated” by side reactions with the chloride/acetate anion of the IL solvent.

Scheme 8. Side reactions of EMIM/BMIM acetates in trimethylsilylations of cellulose with TMS reagents (**28**, see text), causing formation of trimethylsilyl acetate (**29**), which is volatile and has no trimethylsilylating activity.



The last example for side reactions of IL anions to be given here is the attempted trimethylsilylation in 1-alkyl-3-methylimidazolium acetates (**1**, **3**) by common trimethylsilylating agents $\text{Me}_3\text{Si-X}$ (TMS-X, **28**), such as TMS halides, hexamethyldisilazane, or *N,O*-bis(trimethylsilyl)trifluoroacetamide (BSTFA). Instead of silylating cellulose, the silylating agent converts the acetate anion into trimethylsilyl acetate (**29**), even nearly quantitatively (Scheme 8 and Figure 5). In the corresponding IL chlorides (**2**, **4**), by contrast, the trimethylsilylation proceeds as expected.

Conclusions

The heterocyclic IL cation reacts at C-2 with the reducing ends of cellulose and aldopyranose model compounds. The resulting modification of the cellulose might be rather minor relative to the number of glucopyranose units per cellulose chain, but might be of crucial importance for the processing of cellulose and cellulose derivatives for use in medical and biological applications where even minor impurities might induce adverse effects. Furthermore, this means that the ionic liquid cannot be quantitatively recycled, which might affect process costs negatively. The use of 1-alkyl-3-methylimidazolium ILs in the processing of oxidized cellulose, such as TEMPO-oxidized or periodate-oxidized cellulose, seems to be rather problematic, as the side reactions with the solvents will become predominant in those cases. By applying 2-alkylsubstituted ILs (**17**), the reaction with the reducing end of cellulose can be completely avoided, since the reacting center in the imidazolium cation is blocked by the substituent. The side reaction can at least be suppressed by the absence of bases and short reaction or contact times of less than 2 h, if practicable for the respective reaction system. Such bases can be auxiliary bases, or also common impurities in 1-alkyl-3-methylimidazolium-type ILs (imidazole, *N*-methylimidazole and *N*-alkylimidazole) as formed by thermal stress to the ILs.

With regard to non-inert anions, the use of BMIM acetate cannot be recommended in (organic and inorganic) esterifications of cellulose with acid

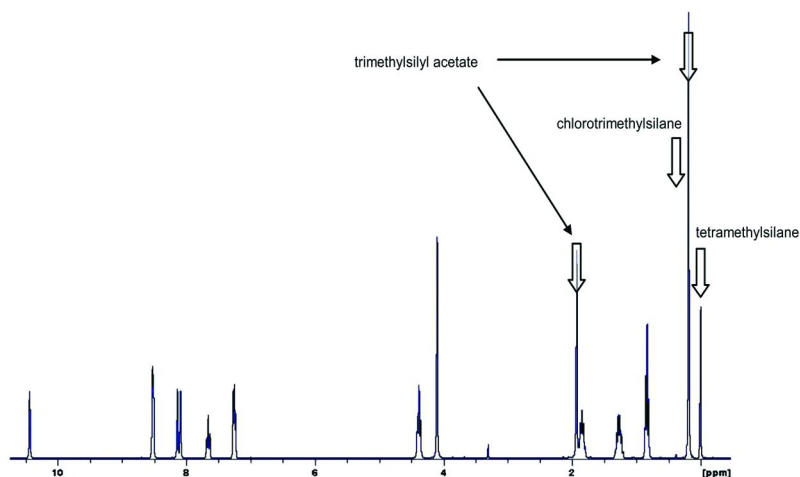


Figure 5. ^1H NMR spectrum (ppm scale) of a mixture of BMIM-OAc (**1**), $\text{Me}_3\text{Si-Cl}$ and pyridine (molar ratio 2:1:1), acquired 15 min after mixing. While the starting material $\text{Me}_3\text{Si-Cl}$ has been almost completely consumed, the product peak of trimethylsilyl acetate (**29**) becomes prominent. The resonances of the acetate moieties in **1** and **29** coincide.

chlorides and anhydrides, as the anion is converted into strongly acetylating species affording (partially) acetylated cellulose rather than the desired organic or inorganic esters. Cellulose methylation in B(E)MIM chloride and B(E)MIM acetate does not proceed, since the anion consumes the commonly used methylating agents methyl iodide and dimethyl sulfate by conversion into methyl chloride and methyl acetate, respectively, which exhibits largely inferior or no methylation behavior. Analogously, B(E)MIM acetate can also not be used for trimethylsilylations, since trimethylsilyl acetate is formed.

In conclusion, it was shown that 1-alkyl-3-methylimidazolium ILs react either with cellulose itself or with derivatization agents in the system. Both the cation and the anion of the IL might be involved in those side reactions, demonstrating unambiguously that ILs are not at all inert solvents for cellulose. These results recommend caution when progressing with the use of ILs in cellulose processing, especially with regard to usage of the cellulosic products in biological and biomedical applications.

Acknowledgements

The financial support by the Austrian Science Fund (Fonds zur Förderung der wissenschaftlichen Forschung (FWF), project P-17426) and by the Christian Doppler Research Society (CD lab “Advanced Cellulose Chemistry and Analytics”) is gratefully acknowledged. The authors would like to thank Dr. Andreas Hofinger, Department of Chemistry at the University of Agricultural

Sciences Vienna, and Dr. Lothar Brecker, Institute of Organic Chemistry at the University of Vienna, for recording the NMR spectra.

References

1. Zhu, S.; Wu, Y.; Chen, Q.; Yu, Z.; Wang, C.; Jin, S.; Dinga, Y.; Wuc, G. Dissolution of cellulose with ionic liquids and its application: A mini-review. *Green Chem.* **2006**, *8*, 325–327.
2. Swatloski, R. P.; Spear, S. K.; John, D.; Holbrey, J. D.; Rogers, R. D. Dissolution of cellulose with ionic liquids. *J. Am. Chem. Soc.* **2002**, *124*, 4974–4975.
3. Wu, J.; Zhang, J.; Zhang, H.; He, J.; Ren, Q.; Guo, M. Homogeneous acetylation of cellulose in a new ionic liquid. *Biomacromol.* **2004**, *5*, 266.
4. Barthel, S.; Heinze, T. Acylation and carbanilation of cellulose in ionic liquids. *Green Chem.* **2006**, *8*, 301.
5. Heinze, T.; Schwikal, K.; Barthel, S. Ionic liquids as reaction medium in cellulose functionalization. *Macromol. Biosci.* **2005**, *5*, 520.
6. Heinze, T.; Pfeifer, A.; Petzold, K. Functionalization pattern of *tert*-butyldimethylsilyl cellulose evaluated by NMR spectroscopy.. *BioResources* **2008**, *3* (1), 79–90.
7. Sun, N.; Swatloski, R. P.; Maxim, M. L.; Rahman, M.; Harland, A. G.; Haque, A.; Spear, S. K.; Daly, D. T.; Rogers, R. D. Magnetite-embedded cellulose fibers prepared from ionic liquid. *J. Mater. Chem.* **2008**, *18*, 283–290.
8. Hermanutz, F.; Meister, F.; Uerdingen, E. New developments in the manufacture of cellulose fibers with ionic liquids. *Chem. Fiber Int.* **2006**, *6*, 342–343.
9. Liebert, T. Innovative concepts for the shaping and modification of cellulose.. *Macromol. Symp.* **2008**, *262*, 28–38.
10. (a) Röhring, J.; Potthast, A.; Rosenau, T.; Lange, T.; Ebner, G.; Sixta, H.; Kosma, P. A novel method for the determination of carbonyl groups in cellulose by fluorescence labeling. 2. Validation and applications. *Biomacromol.* **2002**, *3*, 969–975. (b) Potthast, A.; Röhring, J.; Rosenau, T.; Borgards, A.; Sixta, H.; Kosma, P. A novel method for the determination of carbonyl groups in cellulose by fluorescence labeling. 3. Monitoring oxidative processes. *Biomacromol.* **2003**, *4*, 743–749.
11. (a) Miyashita, A.; Kurachi, A.; Matsuoka, Y.; Tanabe, N.; Suzuki, Y.; Iwamoto, K.; Higashino, T. Synthesis and reactivities of 1,3-dimethyl-2-(α -hydroxybenzyl)imidazolium and 1,3-dimethyl-2-(α -hydroxybenzyl)benzimidazolium iodides. *Heterocycles* **1997**, *44*, 417–426. (b) Miyashita, A.; Matsuda, H.; Higashino, T. Catalytic action of azolium salts. III. Aroylation of *N*-phenylbenzimidoyl chlorides with aromatic aldehydes in the presence of 1,3-dimethylimidazolium iodide. *Chem. Pharm. Bull.* **1992**, *40*, (10), 2627–2631. (c) Davis, J. H., Jr.; Forrester, K. J. Thiazolium-ion based organic ionic liquids (OILs).

- Novel OILs which promote the benzoin condensation. *Tetrahedron Lett.* **1999**, *40*, (9), 1621–1622. (d) Nair, V.; Bindu, S.; Sreekumar, V. *N*-Heterocyclic carbenes: Reagents, not just ligands. *Angew. Chem., Int. Ed.* **2004**, *43*, (39), 5130–5135. (e) Estager, J.; Leveque, J.M.; Turgis, R.; Draye, M. Solventless and swift benzoin condensation catalyzed by 1-alkyl-3-methylimidazolium ionic liquids under microwave irradiation. *J. Mol. Catal. A: Chem.* **2006**, *256*, 261–264. (f) Tommasi, I.; Sorrentino, F. 1,3-Dialkyl-imidazolium-2-carboxylates as versatile *N*-heterocyclic carbene-CO₂ adducts employed in the synthesis of carboxylates and α -alkylidene cyclic carbonates. *Tetrahedron Lett.* **2009**, *50*, 104–107.
12. Aggarwal, V.K.; Emme, I.; Mereu, A. Unexpected side reactions of imidazolium-based ionic liquids in the base-catalyzed Baylis–Hillman reaction. *Chem. Commun.* **2002**, 1612–1613.
 13. Köhler, S.; Liebert, T.; Schöbitz, M.; Schaller, J.; Meister, F.; Günther, W.; Heinze, T. Interactions of Ionic Liquids with Polysaccharides. 1. Unexpected acetylation of cellulose with 1-ethyl-3-methylimidazolium acetate. *Macromol. Rapid Commun.* **2007**, *28*, 2311–2317.
 14. Yoneda, Y.; Ebner, G.; ; ; Takano, T.; Nakatsubo, F. Potthast A. Rosenau T. Synthesis of the perdeuterated cellulose solvents 1-ethyl-3-methylimidazolium acetate (EMIM-OAc-d₁₄) and 1-butyl-3-methylimidazolium acetate (BMIM-OAc-d₁₈) and of 2-¹³C-butyl-3-methylimidazolium acetate.. *J. Labeled Comp. Radiopharm.* **2009**, *52*, 223–226.
 15. Adelwöhrer, C.; Takano, T.; Nakatsubo, F.; Rosenau, T. Chemical synthesis of ¹³C-perlabeled cellulose with >99% isotopic enrichment according to a cationic ring-opening polymerization approach. *Biomacromol.* **2009**, in press.
 16. Liebner, F.; Yoneda, Y.; Potthast, A.; Rosenau, T. Thermal degradation products of 1-alkyl-3-methylimidazolium ionic liquids and their side reactions in ionic liquid/cellulose solutions. *Holzforschung* **2009**, in press.
 17. The protective effect of an alkyl-substitution at C-2 against side reactions of the IL has also be reported for Baylis–Hillman reaction in [bdmim][PF₆] ionic liquid: Hsu, J. C.; Yen, Y. H.; Chu, Y. H. Baylis–Hillman reaction in [bdmim][PF₆] ionic liquid. *Tetrahedron Lett.* **2004**, *45*, 4673–4676.

Chapter 9

Cellulose Solubility: Dissolution and Analysis of "Problematic" Cellulose Pulps in the Solvent System DMAc/LiCl

Ute Henniges, Sonja Schiehser, Thomas Rosenau and Antje Potthast*

University of Natural Resources and Applied Life Sciences (BOKU),
Department of Chemistry and Christian-Doppler Laboratory
"Advanced cellulose chemistry and analytics", Muthgasse 18,
A-1190 Vienna, Austria
*antje.potthast@boku.ac.at

The basics of cellulose dissolution and the factors influencing dissolution of pulps are introduced. The influence of derivatizing systems on cellulose was studied. Carbamation of celluloses by isocyanates in DMSO will cause some degradation of cellulose. Several approaches to improve cellulose solubility in the DMAc/LiCl system are discussed, including several pre-treatments, and recommendations are given for which type of pulp samples the specific pre-treatment is appropriate.

Introduction

Cellulosic pulps used for any further processing such as textile and paper production mainly contain cellulose; however hemicelluloses and some lignin are also present. Modern papers for example are usually made out of wood fiber pulps containing different types of hemicelluloses in significant amounts and, depending on pulping parameters, also more lignin to increase the pulp yield.

In nature, cellulose occurs in different modifications, sometimes rather pure, *e.g.* seed hair from cotton plants, sometimes in intimate contact with hemicelluloses and lignin in wood. Next to wood and annual plants, for example straw, hemp or jute, cellulose is also produced by bacteria and algae in a very pure form. Cellulose is a linear homopolymer consisting of D-anhydroglucopyranose units (AGUs) connected by 1,4- β -glycosidic bonds. The number of AGUs linked

together is described as Degree of Polymerization (DP). The polysaccharide cellulose is always polydisperse, *i.e.* it has a distribution of molecules of different chain lengths. The polydispersity of cellulose explains why statements on molecular weight (MW) are based upon statistical evaluations using different statistical moments to calculate averages (*I*). This characteristic of cellulose – the difference length of its molecules – is either expressed as an average DP determined by viscosity measurements or as molecular weight distribution (MWD) obtained through gel permeation chromatography (GPC). The distinctive polydispersity of the cellulose polymer is only reflected by the shape of the MWD and not by average viscosity.

Single cellulose molecules are stabilized by strong intra- and intermolecular hydrogen bonds. Single bonds of this type are not very strong, but the abundance of bonds and their tendency to enforce higher degrees of order, especially crystalline regions, turn cellulose into a polymer that is not easily dissolved. For any case of chain length determination – DP, molecular weight, and/or MWD – the dissolution of cellulose is required beforehand.

The second next important polysaccharides in pulps, hemicelluloses, are polymers with a lower molecular weight (between DP 50 and 200) than cellulose containing various carbohydrates. They occur in a large variety of structural types, divided into four general groups (2):

- Xyloglycans (xylans), the most abundant hemicellulose type, main variants being glucuronoxylans, (arabino)glucuronoxylans and arabinoxylans.
- Mannans built out of mannose and a second aldopyranose. They are subdivided into galactomannans, glucomannans and galactogluco-mannans that differ in their degree of branching (3).
- Xyloglucans, representing the major constituent of the primary cell wall of all higher plants.
- Mixed-linkage β -glucans, also known as cereal β -glucans.

In hardwoods the major hemicellulose constituent comprises xylans, while mannans predominate in softwood.

While cellulose molecules form regular structures, hemicelluloses help to partly aggregate these arranged cellulose molecules into microfibrils. These microfibrils form macrofibrils in turn, having again hemicelluloses and additionally lignin linking them together. Thus, a close network between hemicelluloses and other wood components is formed, partly stabilized by chemical bonds, partly by hydrogen bonds (*I*). In papermaking, hemicelluloses are appreciated because they add to yield and contribute to fibre-fibre bonds. Additionally, they provide flexibility to the cellulose fibers. This feature was explained by internal stress redistribution and increased swelling ability that hinders hornification of fibers (4, 5). On the other hand, hemicelluloses add to solubility problems due to the variety of interactions they contribute to.

Lignin, the strengthening agent in wood, is characteristic for higher plants. There are three main building units, *p*-coumaryl alcohol, coniferyl alcohol and sinapyl alcohol. Their ratios and occurrence differ; softwood lignin mainly contains coniferyl subunits, hardwood lignin is built by both, coniferyl and sinapyl units, and the lignin of annual plants, such as grasses, is characterized by the predominant presence of *p*-coumaryl building blocks (6). It is generally accepted

today, that lignin is not simply deposited between cell wall polysaccharides, but directly and covalently linked to at least a part of them. These intimate associations are called lignin-polysaccharide (lignin-carbohydrate) complexes (6). Except for ground wood and mechanical pulp where lignin is retained, pulp processing aims at the removal and modification (fragmentation, solubilization) of lignin (6).

These three pulp constituents – cellulose, hemicelluloses, and lignin – are typically easily dissolved in isolated form and also often characterized after they have been separated. However, isolation and clean separation into single components is often the main problem of analysis. This holds especially true for lignin that is very hard to isolate in a native state. Consequently, the interactions of these pulp polymers contribute strongly to dissolution problems in pulp.

When it comes to the analysis of papers or textiles, either historic or modern ones, further problems arise with additives that were included to achieve the desired properties of the end product. Different types of sizing agents, fillers, surface treatments and writing / printing / dyeing media considerably increase the complexity of the material and often negatively affect its dissolution behavior. While historic surface sizing and fillers such as gelatin and small amounts of naturally occurring calcium carbonate are generally easy to handle as the amounts are either very small (fillers like calcium carbonate) or the substance itself is easily removed (gelatin), modern sizing and filling is much more difficult to deal with. Sizing lowers the accessibility of the fibers and some fillers, such as titanium oxide, seem to form cross-links that are hard to overcome.

Fibers for textiles bear problems for dissolution due to their high orientation and the added avivage that modifies the surface and hinders the solution agent to enter the fiber.

Dissolution of Cellulosic Pulps

Generally, there are two big categories of cellulose solvents: non-derivatizing and derivatizing ones. Among the non-derivatizing solvents, copper ethylenediamine (abbreviated cuen, cuene or CED), cadmium oxide in ethylenediamine (cadoxen or cadox), *N*-methylmorpholine-*N*-oxide monohydrate (NMMO), and *N,N*-dimethylacetamide/lithium chloride (DMAc/LiCl) are the most common and important ones. Also ionic liquids, for examples those containing 1-alkyl-3-methylimidazolium cations with a range of anions from small, hydrogen-bond acceptors (Cl⁻, AcO⁻) to large, non-coordinating anions ([PF₆]⁻), have obtained much attention within the past several years (7), and also belong to the group of non-derivatizing solvents for cellulose. The same is true for molten inorganic salt hydrates such as LiClO₄·3H₂O (8). The non-derivatizing solvents may be further subdivided in metal-complex cellulose solvents (cuen and cadoxen), salt-free solvents (NMMO), and salt containing solvents (DMAc/LiCl, LiClO₄·3H₂O).

When regarding cellulose analysis by GPC and light scattering experiments which provides the most comprehensive data on MWD among the analytical

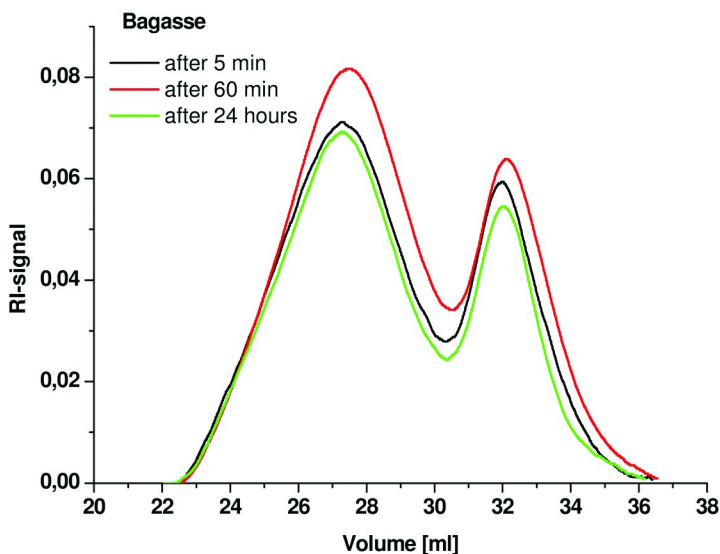


Figure 1. Elution profiles of Bagasse pulp after different time intervals of dissolution. The characteristic distribution was already obtained after only five minutes, when not yet dissolved material was still clearly visible in the reaction vial.

methods, metal-complex cellulose solvents are not appropriate. Additionally, they are aqueous and highly alkaline which causes degradation, especially of oxidized cellulose, during the dissolution process (9). Especially DMAc/LiCl is known to be very suitable for GPC without causing any damage to the cellulose (10–13) as long as degradative pre-treatments (such as heating to more than 80°C) are avoided (14). The precise solution mechanism of the DMAc/LiCl system is still not completely clarified (15).

Derivatizing solvents, i.e. more precisely derivatizing agents that change cellulose in a way that it becomes soluble, the second category of cellulose solvents, interact chemically with cellulose on a molecular level. There are different processes that have gained industrial importance. However, when it comes to cellulose analytics, polymer-analogous derivatization with an isocyanate, mostly either phenyl or ethyl, is chosen (16, 17).

The properties upon swelling and dissolution of cellulose are strongly determined by its network of intra- and intermolecular hydrogen bonds originating from the three hydroxyl groups per AGU (15). Dissolution of cellulose implies a breakdown of the supra molecular structure, because an external reagent disturbs the intermolecular bonding forces and exerts stronger interactions than intermolecular bonds. The most important association to break seems to be the OH(6)---O(3') link (15, 18). Dissolution is strongly connected to accessibility and swelling capacity of a chosen solvent (1). Additionally, it was found that the origin of cellulose plays an important role: while the analyzed bacterial and plant celluloses could be dissolved in DMAc/LiCl, cellulose of animal origin remained insoluble (19). Crystallinity, however, does not seem to have a big influence

on solubility as no obvious correlation between solubility and crystallinity can be detected (20, 21). Enhancing the accessibility by activation procedures, *e.g.* solvent exchange starting with swelling in water followed by ethanol, methanol or acetone (15), is the most promising way to get cellulose dissolved when using the DMAc/LiCl system.

While pure cellulose itself usually does not cause solubility problems with the solvent systems introduced above, the situation is different for pulps. Lignin and hemicelluloses, contained in large amounts in ground wood pulps, but partly also in chemical pulps, have a negative impact on pulp solubility and dissolution is rendered rather difficult. The major obstacle for softwood kraft pulp dissolution was found to be its stiffness caused by lignin leading to low a swellability of the fibers in high kappa number pulps (21). This is certainly also true for pulps containing large amounts of ground wood. On the other hand, isolated lignin is easily soluble in the DMAc/LiCl-system and even fully bleached softwood kraft pulps could not be completely dissolved (21). When analyzing non-dissolved residues of softwood kraft pulp it was found that the content of lignin and mannans is raised before dissolution. This observation was explained by associations and/or bonds that exist between the two components (22). When raw materials for paper production have been pulped, hemicelluloses are known to possess gelling properties that hinder cellulose accessibility. Hemicelluloses partly dissolve upon Kraft cooking conditions and, in a later stage of the cooking process, re-precipitate on the cellulose fibers (23).

Still, residues in the cellulose solution obtained with DMAc/LiCl do not necessarily mean that the MWD is wrong or completely distorted. DMAc/LiCl peeling experiments – the dissolution process was disrupted after very short time intervals – showed that the characteristic distribution of the pulp has already been detected in all dissolved parts, also if considerable amounts of non-dissolved cellulose were still present (figure 1).

Cellulose Degradation in Derivatization Systems

In a detailed study the presence of dimethylsulfonium ions and the derived methyl(methylene)sulfonium ylide in carbanilation mixtures consisting of dimethyl sulfoxide (DMSO), phenyliso-cyanate (Ph-NCO) and cellulose was proved (24). The addition of a specific and readily separable trapping agent and its subsequent extraction into n-hexane provided a mixture of non-reacted trap and a specific product, a cyclopropane derivative that was proof of the formation of the sulfonium ylide species. Blank experiments confirmed the absence of such reactive species (and of cyclopropanated product if trapping agent was added) in pyridine/DMSO carbanilation system, in DMSO alone, and in Ph-NCO alone.

The next step was the demonstration of the direct chemical interaction of sulfoxide and cellulose beyond a general oxidizing effect, assuming that the sulfonium ylide species would form thioether linkages with cellulosic hydroxyls in a side reaction. Unfortunately, such (thio)ether moieties are quite difficult to detect on cellulose due to their very low concentration which is far beyond a

reliable detection by elemental analysis or other analytical techniques, and due to the fact that the DMSO-derived methyl-thiomethyl ethers have no good (UV or fluorescent) reporter group. In order to prove the direct oxidizing and derivatizing action of isocyanate derivatization (phenyl isocyanate, ethyl isocyanate) on cellulose, one methyl group of DMSO was replaced with a 2-naphthyl residue, as in methyl-(2-naphthyl)-sulfoxide (MNSO). Due to its UV-active and fluorescent naphthyl moiety, detection also of minute amounts attached to cellulose in side reactions became viable (24).

The reaction of cellulose with ethyl isocyanate in pyridine or DMSO caused no UV / fluorescence to appear, as also possible side reactions would leave no fluorescence-detectable residues in cellulose. When MNSO was added into the carbanilation mixture to replace 10 mol% (0.1 eq.) of the solvent DMSO, the dissolved cellulose exhibited considerable UV / fluorescence activity upon gel permeation chromatography analysis (GPC). The distinct fluorescence signal followed the molecular weight distribution, indicating a uniform introduction without significant discrimination effects. This proved that the naphthylthiomethyl residues, by analogy to DMSO-derived methylthiomethyl groups, were covalently bound to the cellulose backbone. Simple adsorption would have caused fluorescence activity to appear in the exclusion peak which was not observed (24). Therefore, GPC confirmed that isocyanate derivatization of pulps (tested for cotton linters and a beech sulfite dissolving pulp) in DMSO causes oxidation and introduces thiomethyl ether moieties in quite small amounts. It was roughly calculated that carbanilation in sulfoxide-based solvents will introduce keto groups in the range between 2 ‰ and 2% of the anhydroglucose units (AGU). These oxidized groups (keto or aldehyde) along the cellulose chain constitute spots of pronounced chemical instability. Under basic conditions, according to β -elimination processes, subsequent cleavage will easily occur (9).

Improvement of Cellulose Solubility

Especially the DMAc/LiCl system, a non-derivatizing dissolution medium as mentioned above, is a very good solvent for pure cellulose. It is also very suitable for GPC analysis which allows a full characterization of the molecular weight distribution of the analyzed sample. Nevertheless, when it comes to pulps and papers containing large amounts of lignin and hemicelluloses the dissolution is complicated.

In order to improve cellulose solubility several approaches based on the DMAc/LiCl system have been compiled. They are divided into extended standard approaches, mixed systems and alternative approaches, and will be explained more in detail in the following section.

Table 1. Extended standard approaches to improve pulp solubility. All samples have been disintegrated in a mixer; the solvent was DMAc/LiCl 9 % unless stated differently

No.	Pre-treatment	Solvent exchange	Activation
1a	Extraction with acetone	none	DMAc overnight
2a	Extraction with CH ₂ Cl ₂	none	DMAc overnight
3a	Enzymatic (pectinase) ¹	none	DMAc 3 times for 30 minutes
4a	Enzymatic (mannanase) ¹	none	DMAc 3 times for 30 minutes
5a	None	Ethanol, DMAc	Freeze drying
6a	None	Ethanol, DMAc	Supercritical CO ₂ extraction ² (several modifications)
7a	Reduction with NaBH ₄ (24h)	Ethanol	DMAc overnight
8a	Reduction with TBAB (24h)	Ethanol	DMAc overnight

¹ Sjöholm, E.; Gustafsson, K.; Pettersson, B.; Colmsjö, A., Characterization of the cellulosic residues from lithium chloride/N,N-dimethylacetamide dissolution of softwood kraft pulp. *Carbohydrate Polymers* **1997**, *32* (1), 57–63 ² Supercritical CO₂ extraction experiments were performed by DI Emmerich Haimer, Department of Material Sciences and Process Technology at BOKU Vienna.

Extended Standard Approaches

The standard approach to DMAc/LiCl dissolution of cellulose pulp or paper is usually described by a sequence of mechanical disintegration, activation, solvent exchange, and final dissolution (25). This sequence has been extended using various pre-treatments to improve accessibility of the pulp as described in table 1 before starting the actual dissolution process. One important aspect for the dissolution of cellulose is the accessibility of the cellulose for the dissolving agent. As aqueous disintegration of the sample in a mixer for about one minute is obviously not enough to sufficiently increase accessibility in difficult-to-dissolve samples, several other approaches were tested. They mainly address problems with the dissolution of highly oxidized pulps, real papers that contain sizing agents, and fibers with surface treatment agents.

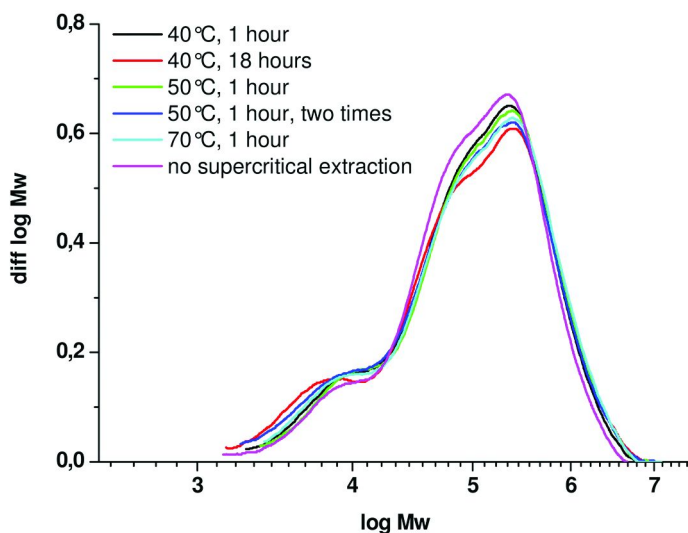


Figure 2. Supercritical CO_2 treatments of bleached beech sulfite pulp at different temperatures and for different time intervals in comparison with the standard dissolution procedure.

The improvement of accessibility in examples no. 1a and 2a (table 1) is based on previous Soxhlet extraction using acetone or dichloromethane to remove parts of the sizing agent or surface treatment that obstructs solvent access to paper fibers. The extraction was completed by additional activation using DMAc overnight. Sizing agents of many papers belong to the alum rosin type. Rosin consists mainly of abietic acid, which is combined with caustic to form salts (rosinates or pinates) that are known as rosin soaps. The pre-treatment with dichloromethane was also successful to remove the avivage on viscose or Lyocell fibers: while non-extracted fibers were not soluble in the DMAc/LiCl-system even after extended solution time and no MWD could be measured at all, the fiber dissolved readily after Soxhlet-extraction in dichloromethane for six hours.

Another idea, an enzymatic pretreatment, was followed in examples no. 3a and 4a. This approach was tested for sulfite kraft pulps with a moderate kappa number. Both enzymes tested, pectinase and mannanase, proved to reduce the amount of non-soluble material. However, the pectinase activity was found to be quite unspecific and led to pulp degradation, while mannanase did not show these negative effects and improved solubility (21).

It might be assumed that in lignin-containing papers the activation of cellulose needs a mechanical impact via freeze drying or supercritical CO_2 extraction to open the cellulose structure and disrupt bonds and aggregates (26). This approach is described in examples 5a and 6a. Both approaches have been used successfully to improve accessibility. Freeze drying was suggested to improve dissolution of cellulose (12, 27), while supercritical CO_2 extraction followed by steam explosion was studied in the context of improving enzymatic activity on pulps (28, 29). However, steam explosion normally causes degradation of cellulose and in some

Table 2. Mixed approaches to improve the solubility of pulp. *: samples have been disintegrated in a mixer before pre-treatment. EIC: ethyl isocyanate

No.	Pre-treatment	Solvent exchange	Activation	Solvent
1b	None	Water (1h)	3x DMAc	DMAc/ LiCl 8% + EIC
2b	None	water (48 h)	3x DMAc	DMAc/ LiCl 8% + EIC
3b	None	Acetone (48 h)	3x DMAc	DMAc/ LiCl 8% + EIC
4b	None	Ethanol (48 h)	3x DMAc	DMAc/ LiCl 8% + EIC
5b	Extraction (Acetone)*	DMAc overnight	DMAc + EIC (5 days)	LiCl 9%
6b	Extraction (CH ₂ Cl ₂)*	DMAc overnight	DMAc + EIC (5 days)	LiCl 9%

cases also strong deactivation of cellulose. Freeze drying is a very interesting activation procedure for powder samples as the normal filtration procedures for solvent exchange cause some loss of sample material while freeze drying does not cause such losses. For samples after supercritical CO₂ extraction followed by a mild variant of steam explosion it was verified that the process does not negatively affect the molecular weight of cellulose (figure 2).

Examples no. 7a and 8a are based on a chemical alteration of the pulp via reduction. Both reagents used, borane *tert*-butylamine complex (TBAB) and even faster sodium borohydride (NaBH₄), reduce carbonyl groups to the corresponding hydroxyl groups and are therefore reported to stabilize pulp in bleaching sequences (30). High contents of carbonyl groups contribute to cross-linking via hemiacetal/hemiketal linkages, their reduction to hydroxyl groups should therefore improve accessibility and readiness of dissolution (31, 32). Nevertheless, upon application of an alkaline substance like NaBH₄ on oxidized pulp samples, β -elimination leading to chain scission can be faster than reduction when a certain threshold amount of carbonyl groups is exceeded (33). Therefore, when solubility is improved some degradation of cellulose is expected to have contributed to this improvement, too. Reduction prior to dissolution gives good results for TEMPO-oxidized pulps with very high carbonyl group contents.

Mixed Systems

When applying mixed systems, the power of DMAc/LiCl in direct dissolution is exploited and supported by an extra derivatization step using isocyanates (table 2). The idea is to partly derivatize OH-groups in the cellulose and thereby reduce

Table 3. Alternative approaches to improve pulp solubility. All samples have been disintegrated in a mixer, no pre-treatment was applied

<i>No.</i>	<i>Solvent exchange</i>	<i>Activation</i>	<i>Solvent</i>
1c	Pyridine	Pyridine + EIC (5 days)	LiCl 9%
2c	DMSO	DMSO + EIC (5 days)	LiCl 9%
3c	Ethanol	DMI (over night)	DMI/ LiCl 9%

the ability to form hydrogen bonds. In the late 80s already a large variety of cellulose derivatives in DMAc/LiCl has been presented, among them cellulose methyl carbamate, cellulose ethyl carbamate, and cellulose phenyl carbamate (34). The combination of derivatizing agent and direct solution was also demonstrated to successfully improve cellulose solubility of softwood kraft pulps (35).

Examples no. 1b to 4b follow the guidelines for improved cellulose solubility established at the STFI (35). The STFI standard method was designed for routine work and requires only relatively short solvent exchange and activation procedures (example 1b). For examples 2b to 4b, this standard approach was slightly modified in terms of prolonged solvent exchange to improve cellulose accessibility.

In examples 5b and 6b several extraction steps were performed prior to solvent exchange to additionally increase penetration of the solvent.

Alternative Approaches

Alternative approaches to cellulose dissolution are based on different solvents instead of DMAc, even though still LiCl was used as the second solvent system component (table 3). Like DMAc, alternative solvents are polar and aprotic. Especially DMSO was found to be one of the most efficient swelling media for cellulose (1). Therefore, it forms a part of several cellulose dissolving agents. DMI has been presented as a solvent system that improves cellulose solubility (36, 37). In some studies, alternative dissolution approaches include a severe heating step with temperatures of 150°C or activation in highly concentrated sodium hydroxide (38). Both of these procedures, heating and strong alkalinity, are likely to induce strong cellulose degradation.

Best results have been achieved when replacing the DMAc/LiCl system by DMI/LiCl, even though no high temperature treatment or strongly alkaline pre-swelling were applied. However, the improvements were not considered significant enough to replace the DMAc/LiCl system by DMI/LiCl.

The most unexpected observation was the strong yellowing that occurred when replacing DMAc by DMSO or pyridine. It was not further investigated in detail what caused the yellowing, but it is highly likely that the discoloration is an effect of oxidation and/or formation of by-products that might negatively influence cellulose integrity and properties.

Conclusion

While many common pulp samples may be dissolved comfortably in the DMAc/LiCl system for molecular characterization in GPC set-ups, some specific cases remain difficult to dissolve. Among these are especially pulps and papers with a high lignin content and/or sizing. Several pre-treatments afford significant improvements for cellulose dissolution:

- Highly oxidized pulps will regain solubility after a reduction treatment
- Surface agents of fibers that hinder dissolution may be removed in an extraction step prior to dissolution
- Softwood kraft pulps gain increased solubility after a joined solution and derivatization procedure or after enzymatic treatments

Some approaches, however, have not proven to be viable for analytical purposes that are based on strictly maintained cellulose integrity during dissolution, such as replacing DMAc by pyridine or DMSO.

References

1. Klemm, D.; Philipp, B.; Heinze, T.; Heinze, U.; Wagenknecht, W. *Comprehensive Cellulose Chemistry. Volume 1: Fundamentals and Analytical Methods*, 1998.
2. Ebringerová, A.; Hromádková, Z.; Heinze, T. Hemicellulose. *Adv. Polym. Sci.* **2005**, *186*, 1–67.
3. Ebringerova, A. Structural Diversity and Application Potential of Hemicelluloses. *Macromol. Symp.* **2006**, *232*, 1–12.
4. Correia, F.; Roy, D. N. Analysis of Hemp Chemical Pulp Monosaccharide Degradation Compared with Aspen and Spruce Chemical Pulps. *J. Nat. Fibers* **2005**, *2* (1), 35–58.
5. Spiegelberg, H. L. The effect of hemicelluloses on the mechanical properties of individual pulp fibres. *Tappi J.* **1966**, *49*, 388–396.
6. Fengel, D.; Wegener, G. *Wood: Chemistry, Ultrastructure, Reactions*; de Gruyter: Berlin, 1989.
7. Swatloski, R.; Spear, S. K.; Holbrey, J. D.; Rogers, R. Dissolution of Cellulose with Ionic Liquids. *J. Am. Chem. Soc.* **2002**, *124*, 4974–4975.
8. Fischer, S.; Thümmler, K.; Pfeiffer, K.; Liebert, T.; Heinze, T. Evaluation of molten inorganic salt hydrates as reaction medium for the derivatization of cellulose. *Cellulose* **2002**, *9*, 293–300.
9. Knill, C. j.; Kennedy, J. F. Degradation of cellulose under alkaline conditions. *Carbohydr. Polym.* **2002**, *51*, 281–300.
10. Butler, G. B.; O'Driscoll, K. F.; Wilkes, G. L. The Lithium Chloride/Dimethylacetamide Solvent for Cellulose: A Literature Review. *J. Macromol. Sci., Rev. Chem. Phys.* **1990**, *30C* (1), 405–440.
11. Jerosch, H.; Lavédrine, B.; Cherton, J.-C. Study of the Stability of Cellulose-Holocellulose Solutions in N,N-dimethylacetamide-lithium chloride by Size Exclusion Chromatography. *J. Chromatogr., A* **2001**, *927*, 31–38.

12. Potthast, A.; Rosenau, T.; Buchner, R.; Röder, T.; Ebner, G.; Bruglachner, H.; Sixta, H.; Kosma, P. The cellulose solvent system N,N-dimethylacetamide/lithium chloride revisited: The effect of water on physicochemical properties and chemical stability. *Cellulose* **2002a**, *9* (1), 41–53.
13. Röder, T.; Morgenstern, B.; Schelosky, N.; Glatter, O. Solutions of cellulose in N,N-Dimethylacetamide/lithium chloride studied by light scattering methods. *Polymer* **2001**, *42*, 6765–6773.
14. Potthast, A.; Rosenau, T.; Sixta, H.; Kosma, P. Degradation of cellulosic materials by heating in DMAc/LiCl. *Tetrahedron Lett.* **2002b**, *43*, 7757–7759.
15. Morgenstern, B.; Kammer, H.-W. Solvation in Cellulose-LiCl-DMAc Solutions. *TRIP* **1996**, *4* (3), 87–92.
16. Berthold, F.; Gustafsson, K.; Berggren, R.; Sjöholm, E.; Lindström, M. Dissolution of softwood kraft pulps by direct derivatization in lithium chloride/N,N-dimethylacetamide. *J. Appl. Polym. Sci.* **2004**, *94* (2), 424–431.
17. Evans, R.; Wallis, A. F. A. Cellulose Molecular Weights Determined by Viscometry. *J. Appl. Polym. Sci.* **1989**, *37*, 2331–2340.
18. Kamitakahara, H.; Koschella, A.; Mikawa, Y.; Nakatsubo, F.; Heinze, T.; Klemm, D. Syntheses and Comparison of 2,6-Di-O-methyl Celluloses from Natural and Synthetic Celluloses. *Macromol. Biosci.* **2008**, *8*, 690–700.
19. Matsumoto, T.; Tatsum, D.; Tamai, N.; Takaki, T. Solution properties of celluloses from different biological origins in LiCl*DMAc. *Cellulose* **2001**, *8*, 275–282.
20. Lennholm, H.; Larsson, T.; Iversen, T. Determination of cellulose I_α and I_β in lignocellulosic materials. *Carbohydr. Res.* **1994**, *261*, 119–131.
21. Sjöholm, E.; Gustafsson, K.; Pettersson, B.; Colmsjö, A. Characterization of the cellulosic residues from lithium chloride/N,N-dimethylacetamide dissolution of softwood kraft pulp. *Carbohydr. Polym.* **1997**, *32* (1), 57–63.
22. Sjöholm, E. *Characterisation of Kraft Pulps by Size-Exclusion Chromatography and Kraft Lignin Samples by Capillary Zone Electrophoresis*; KTH: Stockholm, 1999.
23. Potthast, A. Chemistry of (Acid) Sulfite Pulping. In *Handbook of Pulp*; Sixta, H., Ed.; Wiley-VCH: Weinheim, 2006a; Vol. 1, pp 405–427.
24. Henniges, U.; Kloser, E.; Patel, A.; Potthast, A.; Kosma, P.; Fischer, M.; Fischer, K.; Rosenau, T. Studies on DMSO-containing carbanilation mixtures: chemistry, oxidations and cellulose integrity. *Cellulose* **2007**, *14*, 497–511.
25. Schelosky, N.; Röder, T.; Baldinger, T. Molmassenverteilung cellulosischer Produkte mittels Größenausschlusschromatographie in DMAc/ LiCl. *Das Papier* **1999** (12), 728–739.
26. Sjöholm, E.; Gustafsson, K.; Eriksson, B.; Brown, W.; Colmsjö, A. Aggregation of cellulose in lithium chloride / N,N-dimethylacetamide. *Carbohydr. Polym.* **2000**, *41*, 153–161.
27. Sundholm, F.; Tahvanainen, M. Preparation of cellulose samples for size-exclusion chromatography analyses in studies of paper degradation. *J. Chromatogr., A* **2003**, *1008* (2), 129–134.

28. Kim, K. H.; Hong, J. Supercritical CO₂ pretreatment of lignocellulose enhances enzymatic cellulose hydrolysis. *Bioresour. Technol.* **2001**, *77*, 139–144.
29. Zheng, Y.; Lin, H.-M.; Tsao, G. T. Pretreatment for Cellulose Hydrolysis by Carbon Dioxide Explosion. *Biotechnol. Prog.* **1998**, *14*, 890–896.
30. Chirat, C.; Viardin, M. T.; Lachenad, D. Use of a reducing stage to avoid degradation of softwood kraft pulp after ozone bleaching. *Paperi ja Puu/ Paper and Timber* **1994**, *76* (6–7), 417–422.
31. Bouchard, J.; Méthot, M.; Jordan, B. The effects of ionizing radiation on the cellulose of woodfree paper. *Cellulose* **2006**, *13* (5), 601–610.
32. Potthast, A.; Kostic, M.; Schiehser, S.; Kosma, P.; Rosenau, T. Studies on oxidative modifications of cellulose in the periodate system: Molecular weight distribution and carbonyl group profiles. *Holzforschung* **2007b**, *61* (6), 662–667.
33. Henniges, U. *Cellulose analytics by fluorescence labelling and gel permeation chromatography: Description of degradation processes, evaluation of stabilisation procedures and development of a non-destructive alternative*; University of Natural Resources and Applied Life Sciences: Vienna, 2008.
34. McCormick, C. L.; Callais, P. A. Derivatization of cellulose in lithium chloride and N,N-dimethylacetamide solutions. *Polymer* **1987**, *28*, 2317–2323.
35. Berggren, R.; Berthold, F.; Sjöholm, E.; Lindström, M. Improved methods for evaluating the molar mass distributions of cellulose in kraft pulp. *J. Appl. Polym. Sci.* **2003**, *88* (5), 1170–1179.
36. Takaragi, A.; Minoda, M.; Miyamoto, T.; Liu, H. Q.; Zhang, L. N. Reaction characteristics of cellulose in the LiCl/ 1,3-dimethyl-2-imidazolidinone solvent system. *Cellulose* **1999**, *6*, 93–102.
37. Yanagisawa, M.; Shibata, I.; Isogai, A. SEC–MALLS analysis of cellulose using LiCl/1,3-dimethyl-2-imidazolidinone as an eluent. *Cellulose* **2004**, *11*, 169–176.
38. Rousselle, M.-A. Determining the Molecular Weight Distribution of Cotton Cellulose: A New GPC Solvent. *Text. Res. J.* **2002**, *72* (2), 131–134.

Chapter 10

Comparison of Solution-State Properties of Cellulose Dissolved in NaOH/Water and in Ionic Liquid (EMIMAc)

**T. Budtova^{1,*}, M. Egal^{1,A}, R. Gavillon^{1,B}, M. Gericke^{1,2}, T. Heinze²,
T. Liebert², C. Roy^{1,C}, K. Schluffer^{1,2,3} and P. Navard^{1,*}**

¹Mines ParisTech, Centre de Mise en Forme des Matériaux - CEMEF[†],
UMR CNRS/Ecole des Mines de Paris 7635, BP 207, 06904 Sophia-Antipolis,
France

²Centre of Excellence for Polysaccharide Research[†], Friedrich Schiller
University of Jena, Humboldtstraße 10, D-07743 Jena, Germany

³Research Centre for Medical Technology and Biotechnology GmbH
Geranienweg 7, D-99947 Bad Langensalza, Germany

* tatiana.budtova@mines-paristech.fr, tel: +33(0)4 93 95 74 70,
patrick.navard@mines-paristech.fr, tel: +33(0)4 93 95 74 66, fax: +33 (0)4
93 65 43 04

[†]Member of the European Polysaccharide Network of Excellence (EPNOE),
www.epnoe.eu

^Apresent address: BUTAGAZ, Service BCI, RN 113, 13340 Rognac, France

^Bpresent address: L'Oreal, 188-200, rue Paul Hochart, 94550 Chevilly-Larue,
France

^Cpresent address: Arkema, Centre de Recherche & Développement, 27470
Serquigny, France

The rheological and hydrodynamic properties of cellulose dissolved in (8-9%)NaOH/water and in 1-ethyl-3-methylimidazolium acetate (EMIMAc) were studied and compared. The influence of cellulose type, concentration, solution temperature and presence of additives (in the case of cellulose dissolved in NaOH/water) was investigated. While the dissolution power of NaOH/water decreases with temperature increase and cellulose solutions are gelling, the intrinsic viscosities of cellulose in NaOH/water and in EMIMAc are very close in absolute values and behave in the

same way with temperature. This paradox was assumed to be due to the role of water in NaOH/water hydrates.

Introduction

As it is well known, cellulose cannot be melted. Its dissolution is therefore a very important step before processing fibres, films or other objects like sponges and in order to prepare derivatives. The way how cellulose dissolves, the state of the solutions and their flow properties are thus phenomena and properties to be studied. There is a rather important body of literature on dissolution (see, for example ref. (1)) and ways to increase its efficiency, most of the time called cellulose activation. The main results are that plant cellulose fibres are not easy to dissolve due to the complex structure existing in the various cell walls, with mainly the primary wall causing difficulties (2). Activation methods like steam explosion (3) or enzymatic treatments (4) are known to help dissolution. The state of cellulose dissolution was mainly studied by considering polymer-solvent interactions, measuring for example the behaviour of the reduced viscosity or intrinsic viscosity as a function of molar mass or temperature or by assessing their aggregation state by light scattering (5). The main results are that it is quite difficult to molecularly disperse cellulose, aggregates probably hold together by hydrogen bonds being often present.

The rheology of cellulose dissolved in many different solvents has been studied extensively: for example, in cadoxene (6), in LiCl/*N,N*-dimethylacetamide (7, 8), in NMMO monohydrate (9), in mixtures of ammonia or ethylenediamine and thiocyanate salts (10, 11) or in (7-9%)NaOH/water with or without urea or thiourea added (12, 13). Recently some rheological properties of cellulose dissolved in several imidazolium-based ionic liquids were reported (14-17). Cellulose is behaving as a classical semi flexible polymer with a persistence length of a few tens of nanometers. It means that in most cases, its molecular length is large enough for the solution to have the classical characteristics of flexible polymer solution, i.e. a two-region flow curve with a Newtonian plateau at low shear rates, a shear thinning region at high shear rates, at least when these are experimentally accessible, and classical G' and G'' curves.

The general challenges in cellulose dissolution are to improve the solution quality, to increase the cellulose concentration and to avoid any specific problem like gelation or flow instabilities. All these features can be seen, one way or another, by rheological methods. One way to advance in this field will come through the comparison of the flow of different celluloses in different solvents. This is the aim of this paper where we compare the flow and molecular organization of cellulose dissolved in two solvents: 8-9%NaOH/water and an ionic liquid, 1-ethyl-3-methylimidazolium acetate (EMIMAc). The studies were performed at different temperatures and cellulose concentrations. The goal of this publication is to demonstrate the similarities, peculiarities and differences in solution properties of cellulose/NaOH/water and cellulose/EMIMAc.

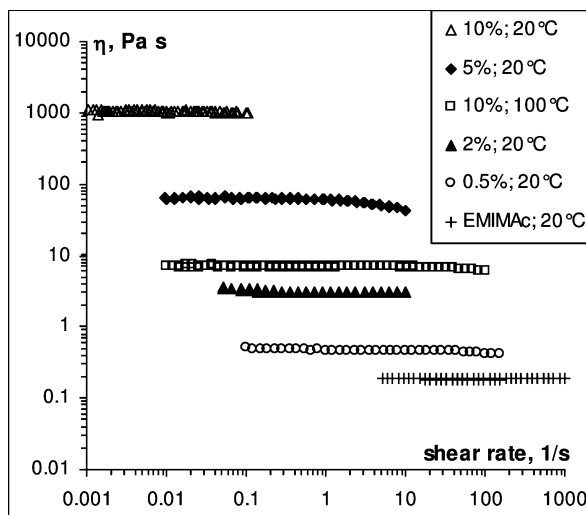


Figure 1. Flow curves of spruce sulfite pulp of various concentrations dissolved in EMIMAc, at 20°C, and of 10% at 100°C.

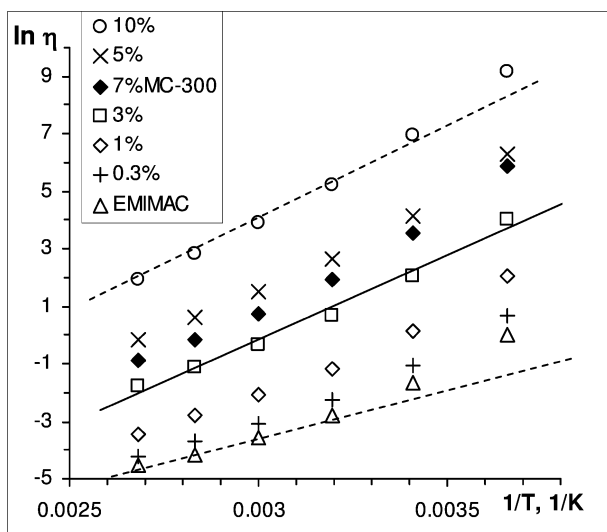


Figure 2. Arrhenius plot for spruce sulfite pulp of various concentrations and for 7%(MC-300), dissolved in EMIMAc. The solid line is an example of a least square linear approximation for 3%(SSP-110)/EMIMAc solution. Dashed lines demonstrate the non-linear character of the data.

Experimental Part

Materials

For the studies of cellulose/NaOH/water solutions, the following cellulose samples were used:

- Avicel microcrystalline celluloses, purchased from FMC Corporation, with a mean degree of polymerization (DP) of 180 and 230, as given by the manufacturer, called “MC-180” and “MC-230” in the following.
- Steam exploded Borregaard cellulose with DP 500, “B-500” in the following, kindly provided by Innovia Films.

NaOH was in pellets of 97% purity, purchased from Aldrich. ZnO was a powder of 98% purity from VWR. Urea was in pellets of 99% purity from Fisher. Distilled water was used for preparing solutions.

For the studies of cellulose/EMIMAc solutions, three cellulose samples were studied:

- Microcrystalline cellulose ($[\eta]_{\text{Cuen}} = 125$, DP = 300), “MC-300” in the following.
- Spruce sulfite pulp ($[\eta]_{\text{Cuen}} = 435$, DP = 1000), “SSP-1000”, both purchased from Fluka.
- Bacterial cellulose ($[\eta]_{\text{Cuen}} = 1343$, DP = 4420), “BC-4420”, was synthesized as follows (18): bacteria of the strain *Gluconacetobacter xylinus* (wild-type strain from the stock collection of the Research Centre for Medical Technology and Biotechnology, Germany) were cultivated in glass vessels containing Schramm-Hestrin medium in static culture at 30°C. After 30 days, the cellulose layers were taken from the culture medium, cut into small pieces, purified, freeze-dried and milled (19).

The degree of polymerization of samples used for the preparation of cellulose/EMIMAc solutions was determined by means of viscometry in cupriethylenediamine hydroxide (Cuen) according to literature (20):

$$\text{DP} = \frac{[\eta]}{0.42} \quad (\text{for DP} < 950)$$

$$\text{DP} = 0.76 \sqrt{\frac{[\eta]}{2.28}} \quad (\text{for DP} > 950)$$

The ionic liquids of type Basionic™, EMIMAc, purity $\geq 90\%$, was used as received from Fluka, lot S47223315081313. The density of EMIMAc was 1.10033 g/cm³ determined with a pycnometer.

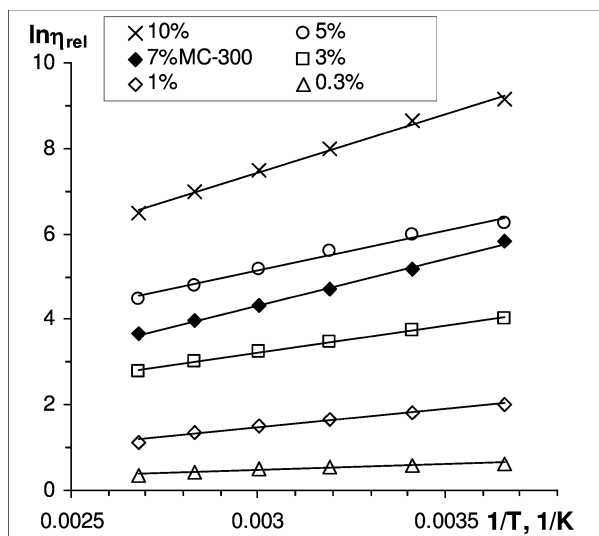


Figure 3. Arrhenius plot for the same data as in Figure 2 but for relative viscosity.

Methods

Dissolution of Cellulose

All celluloses were dried at 100°C in vacuum prior to use. For preparing cellulose/NaOH/water solutions, cellulose was mixed with 8% or 9% sodium hydroxide aqueous solution according to procedure described elsewhere, see for example, ref. (21). In some cases that will be specified, ZnO or urea were added to 8%NaOH/water in the following proportions: 0.7%ZnO/8%NaOH/water and 6%urea/8%NaOH/water (22). Mixing of cellulose/NaOH/water components with or without additives was performed at -6 °C for 2 hours with a stirring rate of 1000 rpm. Ready solutions were stored in refrigerator in sealed vessels to avoid oxygen-induced degradation and to delay gelation.

For preparing cellulose/EMIMAc solutions, solvent and cellulose were mixed in a sealed vessel and the mixtures were stirred at 80°C for at least 48 h to ensure complete dissolution. Cellulose solutions were stored at room temperature and protected against moisture absorption. All concentrations are given in weight per cent. They were recalculated in g/mL for determination of the intrinsic viscosity, taking into account the density of EMIMAc specified above. The density of 8% or 9%NaOH/water was taken to be equal to the one of water.

Rheological Measurements

Rheological measurements of cellulose/EMIMAc and cellulose/8%NaOH/water solutions were performed on a Bohlin Gemini® rheometer equipped

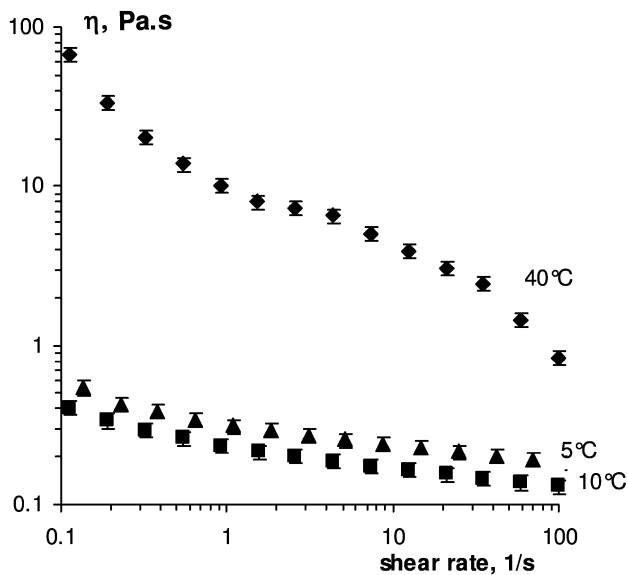


Figure 4. Viscosity-shear rate dependence of 5%(MC-180)/8%NaOH/water at 5°, 10° and 40°C.

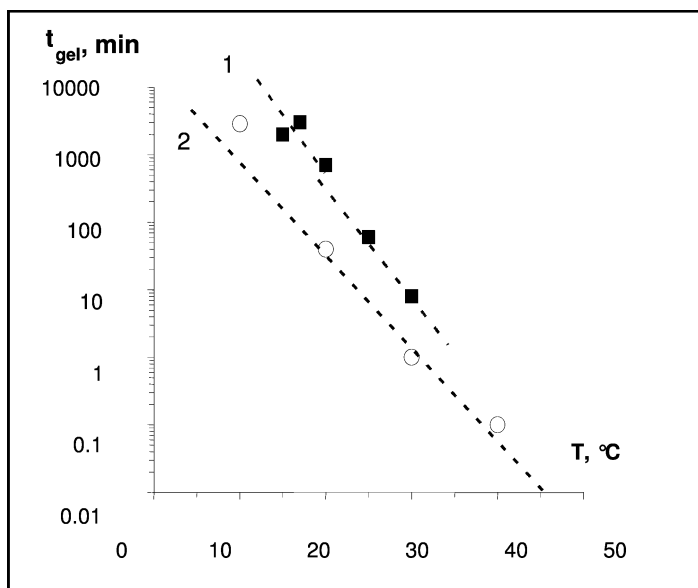


Figure 5. Gelation time vs. solution temperature for 5%(MC-230)/9%NaOH/water (1) and 5%(MC-180)/8%NaOH/water (2). Dashed lines correspond to least square approximations: $t_{gel}(1) = 2 \cdot 10^6 \exp(-0.4T)$ and $t_{gel}(2) = 6 \cdot 10^4 \exp(-0.35T)$

with a plate-plate geometry and a Peltier temperature control system. Special precautions were made in order to protect cellulose/EMIMAc solutions from moisture absorption from the air (17) and cellulose/NaOH/water solutions from water evaporation (23). In both cases, low-viscosity silicon oil ($\eta_{20^\circ\text{C}} \approx 10 \text{ mPa s}$) was placed around the edge of the measuring cell. This method was efficient to allow stable measurements.

Shear steady-state and dynamic properties of (MC-230)/9%NaOH/water solutions were measured using a stress-controlled StressTech rheometer, manufactured by Reologica Instruments, in a Couette cell geometry (two concentric cylinders with a gap of 2 mm), see details in ref. (13).

The viscosity of dilute cellulose/NaOH/water solutions was measured in an Ubbelohde capillary viscometer from Lauda equipped with an automatic dilution burette.

The experimental errors in viscosity measurements obtained with rotational rheometers were lower than 10%. The error in the determination of the intrinsic viscosity was less than 5% when obtained from Ubbelohde viscometer, and about 15% when obtained from steady-state shear data. When not shown on graphs, the error bars are smaller than the symbols.

Results

Flow of Cellulose Solutions and Influence of Temperature

An example of the viscosity (η)-shear rate ($\dot{\gamma}$) dependence of (SSP-1000)/EMIMAc solutions at 20°C of various concentrations and for 10% at 100°C is presented in Figure 1.

Similar results were obtained for solutions of MC-300 and BC-4420. At low shear rates the flow is Newtonian. The beginning of shear thinning can be seen with the increase of shear rates but was hampered by the occurrence of instabilities that were ejecting the fluid out of the gap. Despite a rather large variation of critical instability stress, it seems that the critical stress is around 100 Pa. We did not investigate in details which type of instability was occurring.

The influence of temperature on viscosity of cellulose/EMIMAc solutions is illustrated with Arrhenius plot (Figure 2). It is possible to approximate linearly the experimental data and calculate the activation energies (see example for 3%(SSP-1000)/EMIMAc solution in Figure 2). However, a close look at the data shows that all $\ln(\eta)$ vs. inverse temperature have a concave shape. This specific behaviour seems to be dictated by the solvent (see dashed line for pure EMIMAc, Fig.2), as far as disappears when making the Arrhenius plot for relative viscosity $\eta_{\text{rel}} = \eta/\eta_0$, where η_0 is solvent viscosity (Figure 3).

A more accurate description of the temperature behaviour is provided by the Vogel-Fulcher-Tamman (VFT) equation: $\eta_0 = B\sqrt{T} \cdot \exp(k/T - T_0)$, where k , B and T_0 are adjustable parameters (24). T_0 was determined to be around -100°C to -90°C for cellulose solutions studied. For all cellulose/IL solutions as well as for pure EMIMAc the VFT equation was found to be describe the viscosity-temperature

dependence with a very high accuracy ($R^2 > 0.9999$), allowing prediction of viscosities for any temperature within the given temperature range. This nonlinear $\ln(\eta)$ -inverse temperature dependence has also been reported for several ionic liquids including imidazolium-based ones (25, 26).

Despite the fact that the dependences of $\ln(\eta)$ on $1/T$ of cellulose/EMIMAc solutions are not exactly linear, activation energies were calculated for all solutions studied. The activation energy monotonously increases with concentration increase, from 40 to 70 kJ/g, for cellulose concentrations from 0 to 15%, respectively. These values are of the order of magnitude as those for cellulose of similar concentrations dissolved in other solvents, like in NMMO (9, 21) or in BMIMCl (16, 27, 28). The activation energy of the NaOH solutions is lower, from 20 to 25 kJ/g, and will be shown below.

The flow of cellulose/(8-9%)NaOH/water solutions was studied in details in refs. (13, 22, 23). It was shown that above the overlap concentration C^* , shear thinning is measurable and with temperature increase the solutions are gelling. The illustration of temperature influence is given in Figure 4 for 5%(MC-180)/8%NaOH/water solution. At low temperatures, an increase from 5° to 10°C leads to a viscosity decrease, as usually observed for classical polymer solutions. However, an increase from 10° to 40°C leads to a viscosity jump due to solution gelation. At 40°C a weak gel is formed that is breaking under shear. The shape of the viscosity curve is thus irregular and with a high slope: broken gel pieces are flowing. Being a thermally activated process, gelation is a function of time. The higher temperature is, the quicker gelation occurs (13, 22, 23, 29, 30).

Above $\approx 20^\circ\text{C}$ the gelation time is comparable with the duration of experiment and thus the analysis of viscosity is not possible anymore.

Oscillatory shear dynamic measurements were performed in order to characterise the influence of solution temperature T on gelation kinetics (13, 23). Gelation time t_{gel} was determined in a first approximation as the time when $G'(t) = G''(t)$, where G' and G'' are elastic and viscous moduli that were monitored with time t at a fixed temperature. The results are summarised in Figure 5: gelation time exponentially decreases with temperature increase.

Concluding on the flow behaviour and comparison of cellulose/NaOH/water and cellulose/EMIMAc solutions, results show that the type of cellulose is not greatly changing the flow behaviour, but that there is a large difference in terms of temperature influence. Cellulose/NaOH/water solutions are gelling with temperature increase. The higher temperature, the quicker is the kinetics of gelation. As it will be shown in the following, gelation occurs due to the preferential cellulose-cellulose interactions which are due to the decrease of solvent quality. As for cellulose/EMIMAc solutions, temperature increase leads to a classical viscosity decrease except that $\ln(\eta)$ vs. $1/T$ is non-linear. This is somehow suggesting that EMIMAc is thermodynamically a better solvent for cellulose than (7-9%) NaOH/water, a statement that should be proved.

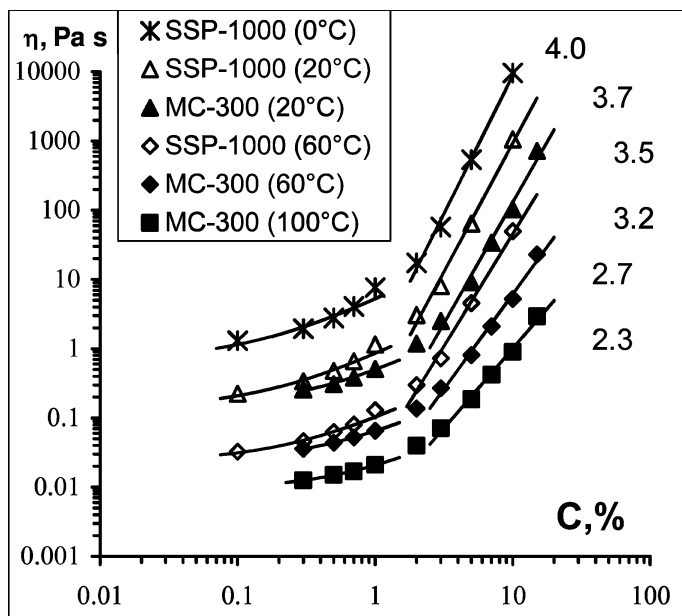


Figure 6. Viscosity-concentration dependence for MC-300 and SSP-1000 dissolved in EMIMAc at various temperatures. Solid lines are power law approximations, the corresponding exponents are shown; lines are linear approximations.

Influence of Cellulose Concentration on Viscosity

An example of the influence of polymer concentration on viscosity of cellulose/EMIMAc solutions is presented in Figure 6 for MC-300 and SSP-1000 samples at selected temperatures. Similar results were obtained for all other studied solutions; they are not shown in order not to overload the graph. The trend of viscosity-concentration dependence is the same as for classical polymer solutions: it is linear in dilute regime, below the overlap concentration (see below), and follows a power law $\eta \sim C^n$ above this overlap concentration. The exponent n was calculated for all cellulose/EMIMAc solutions; it varies from 2.3 - 3 at higher temperatures (60°C-100°C) to 3.5 - 4 at lower temperatures (0°C-40°C), see examples in Figure 6. Comparable values were reported for cellulose/LiCl/DMAc ($n = 3$ for bacterial cellulose and $n = 4$ for cotton linters and dissolving pulp) (7). A slightly higher value of $n = 4.6$ was reported for cellulose/NMMO solutions (9).

For cellulose/NaOH/water solutions, viscosity-concentration dependence can be built only for temperatures that are far enough from gelation. For example, for (MC-230)/9%NaOH/water solution, acceptable temperatures are below 20°C, see Figure 5. The result of viscosity-concentration dependence for this solution is shown in Figure 7. Because the interval of temperatures used is rather narrow,

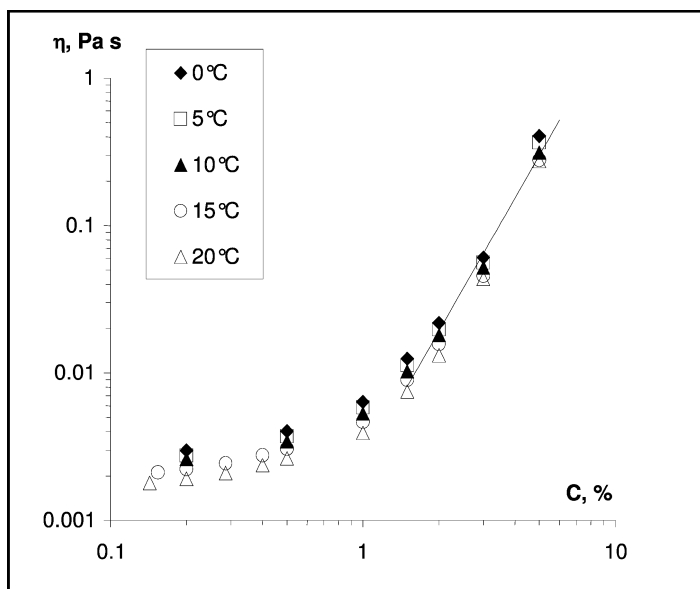


Figure 7. Viscosity-concentration dependence for (MC-230)/9%NaOH/water solutions at temperatures from 0° to 20°C. The line corresponds to the power law dependence with $n = 3$.

from 0° to 20°C, the influence of temperature on the exponent in the power law $\eta \sim C^n$ is not noticeable, and all viscosity-concentration dependences in the semi-dilute region can be approximated with $n \approx 3$. Higher values were obtained for cellulose/NaOH/thiourea/water solutions (components ratio in the solvent was 9.5/4.5/89, cellulose was of DP = 740 obtained with light scattering in 4.6%LiOH/15%urea): $n = 3.5$ -3.7 in the region of cellulose concentrations of 1 - 2.5% at temperatures from 10° to 25°C, respectively, and $n = 5.3$ -5.6 for the region of cellulose concentrations 2.5-4.5% in the same temperature interval (30).

The comparison with (MC-300)/EMIMAc solutions shows that the absolute viscosity values of cellulose/ionic liquid solutions are more than one order of magnitude higher than the ones of cellulose/NaOH/water, which is due to the difference in solvent viscosity. However, the exponent n in $\eta \sim C^n$ is practically the same for both types of solutions at the same temperature.

Intrinsic Viscosities: Influence of Temperature and Additives

The intrinsic viscosities of cellulose in NaOH/water with and without additives like ZnO or urea were determined using dilution measurements in Ubbelohde viscometer. It has been reported in literature that the addition of components like urea (31, 32), thiourea (33, 34) or zinc oxide (35, 36) are helping cellulose dissolution. It was suggested that the highest cellulose dissolution occurs when NaOH/urea/water and NaOH/thiourea/water mass ratios are 7/12/81 and 9.5/4.5/86, respectively (see, for example (32) and (34)). As for the optimal

concentration of ZnO, different proportions have been reported: ZnO/NaOH/water = 5.1/11/83.9 (36), at least 0.1%ZnO dissolved in aqueous NaOH below 10% (36) and around 1%ZnO in 8%NaOH/water (22). The improvement of polymer dissolution should be reflected by the increase of solvent thermodynamic quality and thus of the coil hydrodynamic size, which in turn should lead to the increase of the intrinsic viscosity. The latter was obtained for MC-180 dissolved in aqueous 8%NaOH, 8%NaOH/6%urea and 8%NaOH/0.7%ZnO at various temperatures (Figure 8). All intrinsic viscosity values decrease with temperature increase, with the smallest $[\eta]$ corresponding to cellulose dissolved in 8%NaOH/water.

The addition of urea shows a very small increase in $[\eta]$ values as compared with 8%NaOH/water solvent, being practically within experimental errors. An about 25% intrinsic viscosity increase was obtained with addition of 0.7%ZnO to 8%NaOH/water. These slight improvements of solvent thermodynamic quality are in agreement with the reported facts that it is easier to dissolve cellulose in presence of these additives. These improvements in solubility induced by additives are quickly erased by temperature increase, as can be shown in Figure 8. The influence of temperature on cellulose/NaOH/water solutions can be thus understood as a decrease of solvent thermodynamic quality leading to the preferential polymer-polymer and not polymer-solvent interactions. In dilute solutions this induces the decrease of the size of the macromolecules and in the semi-dilute state, it triggers gelation accompanied by micro-phase separation.

The influence of temperature on the intrinsic viscosity of cellulose of various DP dissolved in EMIMAc is shown in Figure 9. The values of $[\eta]$ for (MC-180)/8%NaOH/water with additives are also added for comparison (filled points). As expected, higher DP values are giving higher values of the intrinsic viscosities. The intrinsic viscosities decrease with temperature increase, and the trend seems to be very similar to the one in 8%NaOH/water.

The absolute values of the intrinsic viscosity of MC-180 dissolved in 8%NaOH/water are very close to those of MC-300 dissolved in EMIMAc, which means that both solvents are of a similar thermodynamic quality. The overlap concentrations for each cellulose sample at a given temperature was determined using $C^* = 1/[\eta]$. As far as the intrinsic viscosity decreases with temperature, C^* increases with temperature: for example, EMIMAc solutions with MC-300 have C^* varying from $C^*_{0^\circ\text{C}} = 0.0077 \text{ g/mL}$ (0.7 %) to $C^*_{100^\circ\text{C}} = 0.0280 \text{ g/mL}$ (2.6 %) and for bacterial cellulose $C^*_{0^\circ\text{C}} = 0.0026 \text{ g/mL}$ (0.24 %) to $C^*_{100^\circ\text{C}} = 0.0055 \text{ g/mL}$ (0.5 %).

As far as the hydrodynamic characteristics of cellulose solutions in EMIMAc and NaOH look so similar, we checked if all data fall on a single master plot. An example for microcrystalline cellulose is given in Figure 10: indeed all data fall on a master plot for polymer concentrations from 0 to 15% and temperatures from 0° to 100°C.

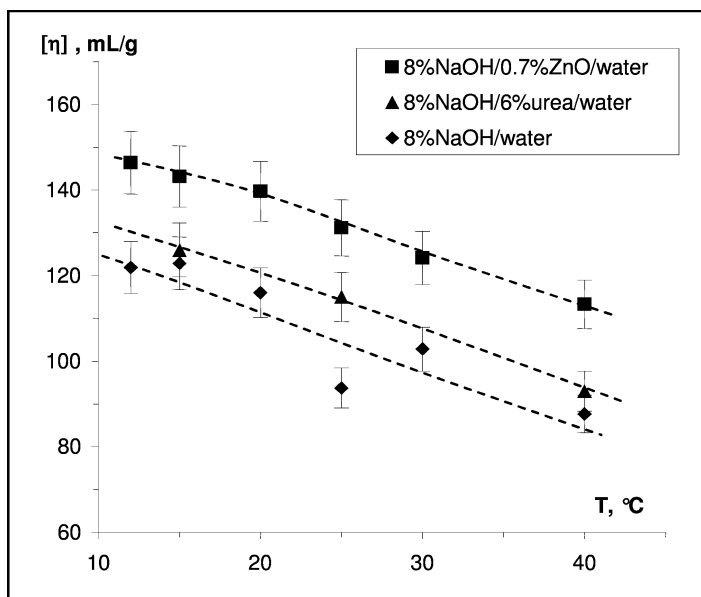


Figure 8. Intrinsic viscosity vs. temperature for MC-180 dissolved in 8%NaOH/water, 8%NaOH/0.7%ZnO/water and 8%NaOH/6%urea/water.

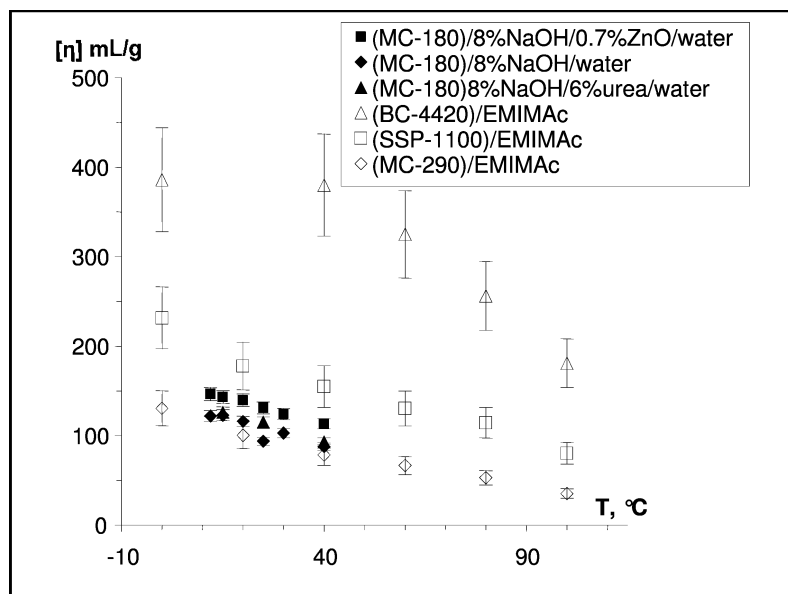


Figure 9. Influence of temperature on cellulose intrinsic viscosity. See details in the text.

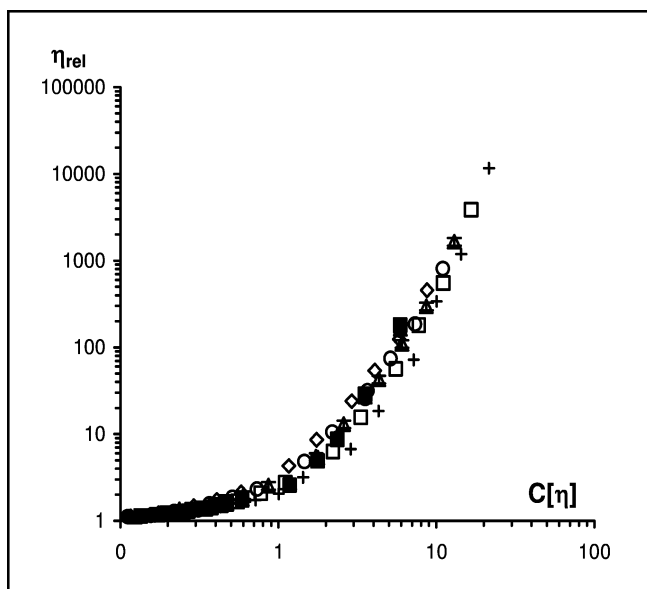


Figure 10. Relative viscosity as a function of $C[\eta]$ at various temperatures for MC-300 dissolved in EMIMAc (open points) and for MC-300 dissolved in 9%NaOH/water (dark points).

A close look on a master plot for cellulose/NaOH/water solutions in dilute region shows that the slope of the best linear fit is not 1, as expected for flexible macromolecules, but 1.23 (Figure 11). As for cellulose/EMIMAc solutions, it was shown that the slope in dilute region is 1.3 (17). The deviation from the slope of 1 has been reported for other polysaccharides, such as dextrane, alginate and carboxymethylamylose (37). All data for microcrystalline celluloses dissolved in NaOH/water and in EMIMAc in dilute region are presented in Figure 12, together with the corresponding best linear fits. The difference between solutions in different solvents is smaller than the experimental errors and thus it can be concluded that in dilute regime, all data also fall on one master plot with the mean value of the slope of the best linear fit being 1.3.

Despite the differences in the behaviour of cellulose dissolved in NaOH/water and in EMIMAc on the macro-structural level (quick gelation in NaOH/water and different solubility limits: 7-9% for cellulose in (7-9%)NaOH/water (38, 39) and at least twice higher in ionic liquids), the hydrodynamic characteristics of cellulose solution in these two solvents are very similar. Indeed, the thermodynamic solvent quality decreases with temperature increase in the same way for both types of solutions, the intrinsic viscosity values of cellulose of a similar DP are very close, and all data fall on a single relative viscosity- $C[\eta]$ master plot. These similarities are, at a first glance, very surprising, because aqueous sodium hydroxide is supposed not to be a very good cellulose solvent (45) and ionic liquids are supposed to be very good ones.

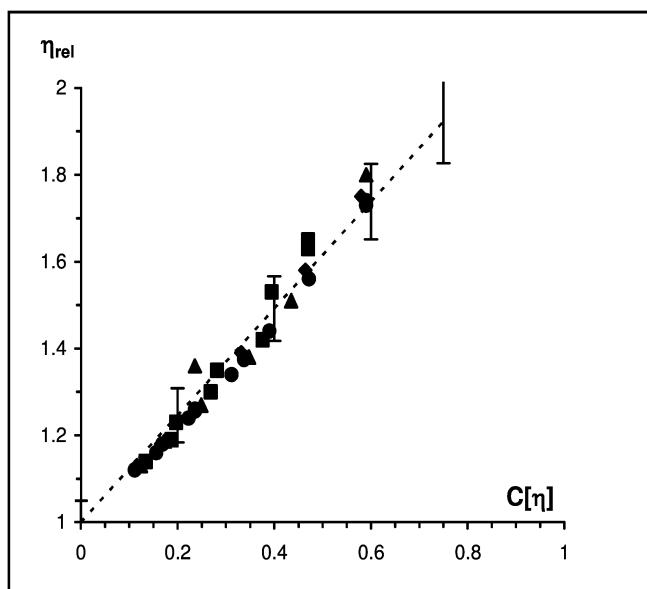


Figure 11. Relative viscosity of (MC-230)/9%NaOH/water as a function of $C[\eta]$ in dilute region. Dashed line corresponds to the linear approximation with the slope of 1.23.

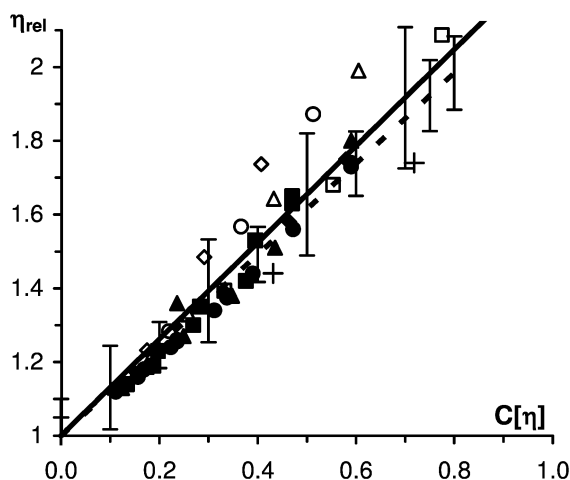


Figure 12. Dilute region: relative viscosity as a function of $C[\eta]$ at various temperatures for MC-300 dissolved in EMIMAc (open points) and for MC-230 dissolved in 9%NaOH/water (dark points). Solid line corresponds to a linear approximation with the slope of 1.31 and dashed line to the slope 1.23.

Table I. Comparison of the rheological and hydrodynamic properties of cellulose/(7-9%)NaOH/water and cellulose/EMIMAc solutions

	<i>Cellulose/ (7-9%)NaOH/water</i>	<i>Cellulose/EMIMAc</i>
Flow properties	Newtonian below C* Shear thinning above C*	Newtonian plateau is measurable at all temperatures and concentrations
Temperature influence (increase)	Induces gelation	Classical decrease of viscosity
Solubility limit	7-9% of cellulose	No exact value reported in literature for this system; $\approx 20\%$ solution of cellulose with DP=570 was used as a spinning dope (14)
Intrinsic	The same values for the same molecular weights	
Viscosity values	The same trend in the decrease of intrinsic viscosity with temperature increase	

As far as temperature-induced gelation of cellulose/NaOH/water solutions is concerned, one way to explain it, keeping in mind the comparison with cellulose/ionic liquids, that the aqueous NaOH solution is, in fact, a mixture of ionic hydrates each being an ion surrounded by a shell of water (40). The size of these hydrates depends on NaOH concentration and temperature (41–43): for example, at concentrations of 7-9% of NaOH in water a metastable hydrate, sodium pentahydrate NaOH·5H₂O (42), is formed when solution is cooled with a low rate. These hydrates make a eutectic mixture with water molecules: (4H₂O, NaOH·5H₂O). Water is linked to cellulose via NaOH; there is also some free water in cellulose/(7-9%)NaOH/water solutions. It was shown that at least four NaOH are needed to dissolve one anhydroglucose unit. More details on the structure of cellulose/NaOH/water solutions and the role of each component can be found in ref. (38). Upon heating, the hydration state of the ions is changing, leading to hydrates that are less able to solvate cellulose, which leads to the decrease of solvent quality and thus to gelation. We may thus say that in the case of NaOH/water, the increase of temperature drastically changes solvent structure and properties, which is not the case of ionic liquids. The lack of detailed knowledge of the exact Na⁺ and OH⁻ hydrate structures when cellulose is present is hampering progress in the understanding of cellulose dissolution in this solvent. The complex structure of NaOH/water solution and the presence of water which is not cellulose solvent could be at the origin of the lower limit of cellulose dissolution as compared with ionic liquids. However, more research is needed to understand these phenomena.

Conclusions

A comparison of the flow and hydrodynamic properties of cellulose dissolved in (8-9%)NaOH/water and in EMIMAc was performed. The results are summarised in Table I. A paradox was obtained: on one hand, cellulose/NaOH/water shows a shear thinning and is gelling while cellulose/EMIMAc solutions even at high concentrations are Newtonian fluids at all temperatures and concentrations studied; on the other hand, the hydrodynamic characteristics of both types of solutions are very similar (values of intrinsic viscosities and their temperature dependence). For both types of solutions, solvent thermodynamic quality decreases in a similar way with temperature increase. The highest cellulose concentration possible to dissolve in NaOH/water is at least twice lower than in EMIMAC. Our hypothesis is that these apparent contradictions, similar hydrodynamic properties vs. different macroscopic behaviour, can be attributed to the fact that the structure and properties of the solvent itself, NaOH/water, change drastically with temperature: from cellulose solvent at -5°C to cellulose non-solvent above 0°C. The presence of free water (not included in NaOH hydrates), which is cellulose non-solvent, is adding the complexity to the peculiar behaviour of cellulose dissolved in (8-9%)NaOH/water.

Acknowledgements

The work was performed within exchange in the frame of the “European Polysaccharide Network of Excellence” (EPNOE), project number NMP3-CT-2005-500375. M. Gericke and T. Liebert thank the “Fachagentur für nachwachsende Rohstoffe e.V.” (project 2202190) for financial support. K. Schluffer is grateful for grants from the European Union, LEONARDO program, for financing her stays in CEMEF. French team is grateful to Spontex (France), Innovia Films (UK) and European Commission (“Aerocell” project No. NMP3-CT2003-505888) for supporting the work on cellulose/NaOH aqueous solutions.

References

1. Le Moigne, N. Ph.D. Thesis, Ecole des Mines de Paris, FR, 2008.
2. Le Moigne, N.; Montes, E.; Pannetier, C.; Hofte, H.; Navard, P. *Macromol. Symp.* **2008**, *262* (1), 65–71.
3. Yamashiki, T.; Matsui, T.; Saitoh, M.; Okajima, K.; Kamide, K. *Br. Polym. J.* **1990**, *22* (2), 121–128.
4. Vehviläinen, M.; Kampuri, T.; Rom, M.; Janicki, J.; Ciechanska, D.; Grönqvist, S.; Siika-Aho, M.; Elg Christoffersson, K.; Nousiainen, P. *Cellulose* **2008**, *15*, 671–680.
5. Aono, H.; Tatsumi, D.; Matsumoto, T. *Biomacromolecules* **2006**, *7*, 1311–1317.

6. Henley, D. *Arkiv Kemi* **1962**, *18*, 327–392.
7. Matsumoto, T.; Tatsumi, D.; Tamai, N.; Takaki, T. *Cellulose* **2001**, *8*, 275–282.
8. McCormick, C. L.; Callais, P. A.; Hutchinson, B. H., Jr. *Macromolecules* **1985**, *18*, 2394–2401.
9. Blachot, J. F.; Brunet, N.; Navard, P.; Cavaillé, J. Y. *Rheol. Acta* **1998**, *37*, 107–114.
10. Frey, M. F.; Li, L.; Xiao, M.; Gould, T. *Cellulose* **2006**, *13*, 147–155.
11. Frey, M. F.; Li, L.; Cuculo, J. A.; Khan, S. A. *J. Polym. Sci., Part B: Polym. Phys.* **1996**, *34*, 2375–2381.
12. Cai, J.; Wang, L. X.; Zhang, L. N. *Cellulose* **2007**, *14*, 205–215.
13. Roy, C.; Budtova, T.; Navard, P. *Biomacromolecules* **2003**, *4*, 259–264.
14. Kosan, B.; Michels, C.; Meister, F. *Cellulose* **2008**, *15*, 59–66.
15. Kuang, Q. L.; Zhao, J. C.; Niu, Y. H.; Zhang, J.; Wang, Z. G. *J. Phys. Chem. B* **2008**, *112*, 10234–10240.
16. Sammons, R. J.; Collier, J. R.; Rials, T. G.; Petrovan, S. *J. Appl. Polym. Sci.* **2008**, *110*, 1175–1181.
17. Gericke, M.; Schlufter, K.; Liebert, T.; Heinze, T.; Budtova, T. *Biomacromolecules* **2009**, in press.
18. Hestrin, S.; Schramm, M. *Biochem. J.* **1954**, *58*, 345–352.
19. Hornung, M.; Ludwig, M.; Gerard, A. M.; Schmauder, H.-P. *Eng. Life Sci.* **2006**, *6*, 537–545.
20. SCAN-CM 15:88.
21. Gavillon, R.; Budtova, T. *Biomacromolecules* **2007**, *8*, 424–432.
22. Egal, M. Ph.D. Thesis, Ecole des Mines de Paris, FR, 2006.
23. Gavillon, R.; Budtova, T. *Biomacromolecules* **2008**, *9*, 269–277.
24. Okoturo, O. O.; VanderNoot, T. J. *J. Electroanal. Chem.* **2004**, *568*, 167–181.
25. Seddon, K. R.; Stark, A.; Torres, M.-J. *ACS Symposium Series*; American Chemical Society: Washington, DC, 2002; Vol. 819, pp 34–49.
26. Froba, A. P.; Kremer, H.; Leipertz, A. *J. Phys. Chem. B* **2008**, *112*, 12420–12430.
27. Liu, L.-Y.; Chen, H.-Z. *J. Cellul. Sci. Technol.* **2006**, *14*, 8–12.
28. Collier, J. R.; Watson, J. L.; Collier, B. J.; Petrovan, S. *J. Appl. Polym. Sci.* **2009**, *111*, 1019–1027.
29. Gavillon, R. Ph.D. Thesis, Ecole des Mines de Paris, FR, 2007.
30. Lue, A.; Zhang, L. *J. Phys. Chem. B* **2008**, *112*, 4488–4495.
31. Zhou, J.; Zhang, L. *Polym. J.* **2000**, *32*, 866–870.
32. Cai, J.; Zhang, L.; Zhou, J.; Li, H.; Chen, H.; Jin, H. *Macromol. Rapid Commun.* **2004**, *25*, 1558.
33. Zhang, L.; Ruan, D.; Gao, S. *J. Polym. Sci., Part B.* **2002**, *40*, 1521–1529.
34. Ruan, D.; Zjang, L.; Zhou, J.; Jin, H.; Chen, H. *Macromol. Biosci.* **2004**, *4*, 1105–1112.
35. Davidson, G. F. *J. Text. Ind.* **1937**, *28*, 27–44.
36. Mikolajczyk, W.; Struszczyk, H.; Urbanowski, A.; Wawro, D.; Starostka, P. WO Patent 02/22924, 2002.

37. Morris, E. R.; Cutler, A. N.; Ross-Murphy, S. B.; Rees, D. A.; Price, J. *Carbohydr. Polym.* **1981**, *1*, 5–21.
38. Egal, M.; Budtova, T.; Navard, P. *Biomacromolecules* **2007**, *8*, 2282–2287.
39. Egal, M.; Budtova, T.; Navard, P. *Cellulose* **2008**, *15*, 361–370.
40. Yamashiki, T.; Kamide, K.; Okajima, K.; Kowsaka, K.; Matsui, T.; Fukase, H. *Polym. J.* **1998**, *20*, 447–457.
41. Pickering, S. U. *J. Chem. Soc.* **1893**, *63*, 890.
42. Cohen-Adad, R.; Tranquard, A.; Peronne, R.; Negri, P.; Rollet, A.-P. *Comptes Rendus de l'Academie des Sciences: Paris, Novembre-December*, 1960; Vol. 251, part 3, pp 2035–2037.
43. Rollet, A.-P.; Cohen-Adad, R. *Rev. Chim. Miner.* **1964**, *1*, 451.
44. Swatloski, R. P.; Spear, S. K.; Holbrey, J. D.; Rogers, R. D. *J. Am. Chem. Soc.* **2002**, *124*, 4974–4975.
45. Cuissinat, C.; Navard, P. *Macromol. Symp.* **2006**, *244* (1), 1–18.

Chapter 11

Aspects of the Interaction of Native and Synthetic Polymers with Direct Dissolving Liquids

**B. Kosan¹, K. Schwikal¹, S. Hesse-Ertelt², A. Nechwatal¹,
F. Hermanutz³ and F. Meister^{1,*}**

¹Thuringian Institute for Textile and Plastic Researchⁱ, Rudolstadt, Germany

²Friedrich-Schiller-University,

Centre of Competence for Polysaccharide Research Jenaⁱ, Germany

³Institute for Textile Chemistry and Chemical Fibres Denkendorf, Germany

*meister@titk.de

ⁱMember of the European Polysaccharide Network of Excellence (EPNOE),
www.epnoe.eu.

Because of the complex super molecular structure of cellulose the moulding into fibres, films and other shapes requires an antecedent chemical modification of the macromolecule or a direct dissolution step using solvents, which don't change its chemical nature. In the system NMMO/H₂O/Cellulose the dissolution could be described on the basis of EDA interactions between cellulose and solvent. Based on the comparison of the different precipitation structures resulted from cellulose dopes in direct dissolving liquids or metal salts/NH₃, cellulose xanthogenate in caustic soda and cellulose acetate in organic solvents different dissolution structures are assumed. Deduced from measurements of its manifest structural viscosity, the detected dissolving enthalpies of cellulose dopes in NMMO/H₂O at different dissolution states and the high tenacity as well as high structural order (crystallinity) in Lyocell fibres and films an insertion of two NMMO monohydrate molecules into the H-bond bridges between OH group at the C6 of the one and at the C3 of the other polymer chain had been postulated leading to a more flexible structure while shaping into fibres.

Because of the good drawability of dopes Lyocell fibres are characterised by outstanding textile mechanic properties but also by an extended fibrillation affinity.

A simple transfer of these conclusions onto dissolution of polymers in ionic liquids (IL) seems not to be possible because of the fragmentary knowledge on IL. From the detected comparable dissolving viscosities and the known properties of cellulose fibres manufactured from solutions in ionic liquids ones had assumed a similar structure of cellulose IL complex as in the kind of the comparable direct dissolving agent (NMMO).

Introduction

The application of polymers as raw material for the manufacturing of man-made fibres, films or other shapes generally requires a thermoplastic deformability of the plastics used. This is because of the fact that most of the common used polymeric materials are shaped via a molten state. Above all this procedure is offering the benefit that a high economic efficiency is reached in case of a sufficient thermal stability.

If polymers are characterised by thermal lability or strong inter-molecular interactions a chemical modification of the polymer or even a shaping via a dissolved state will be preferred.

Cellulose, the most abundant native polymer, is characterised by a complex super molecular structure determined like demonstrated in Figure 1 by an intra and inter molecular hydrogen bridge bonding system.

Intra-molecular bridges alongside the cellulose polymer chain are limiting the free rotation of the AGU's and stiffen the macromolecule. The inter molecular bridges lead to a limitation of the sliding of polymer chains from each other, inhibit a thermoplastic melting before thermal decomposition of cellulose occurs and inhibit its dissolution by common solvents like water, alcohols or dimethylacetamide.

Moulding into fibres or other shapes in a common way will be possible only by a chemical modification of the macromolecule or by dissolution of suitable solvents. The most frequent used commercial process is the treatment of cellulose with carbon disulphide at alkaline conditions. In this well known Rayon process the formed semi-stable cellulose xanthogenate will shaped into rayon fibres and regenerated as cellulose using acidic spinning bathes. A similar but more environmental friendly process, where cellulose is converted by urea is known as carbamate process. Older technologies, which are based on molecular-disperse dissolution by the action of metal complexes, are used today only in minor extent for healthy as well as environmental risks reasons.

More important from the technical point of view is the transformation of cellulose into cellulose acetate, which gives the opportunity to shape it easier into fibres by means of a more or less thermoplastic melt procedure.

..... inter-molecular H bond linkage
 - - - - - intra-molecular H bond linkage

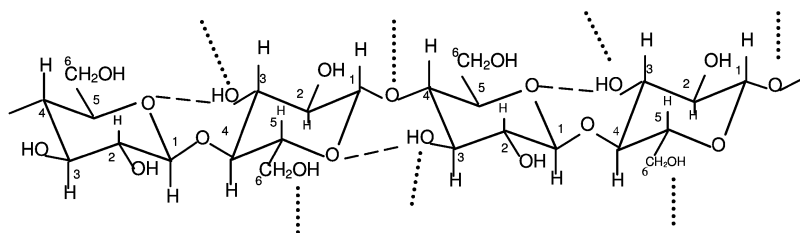


Figure 1. Super molecular structure of the Cellulose macro molecule

A much more environmental friendly alternative offers the application of direct dissolving liquids, which arrange the dissolution of cellulose without any chemical modification. The solvent of choice in this process is N-methylmorpholine oxide (NMMO).

Connected with one mole of water, cellulose is completely dissolved within a short time. The process had been already invented by Graenacher and Sallmann (1) in the thirties of the last century and had been brought into a more technical scale by the works of Johnson (2), Franks (3), Mc Corsley (4) and Chanzy (5).

Opposite to the classical rayon or even acetate fibres the Lyocell fibres represents a whole new fibre type, exhibit significant higher fibre tenacity, a slightly lower fibre elongation and typical fibrillation behaviour.

Figure 2 presents an overview on the state of the technological art in case of cellulose man-made fibres production.

Moreover, ionic liquids like 1-alkyl-3-methylimidazolium chlorides or acetates also exhibit interesting dissolution capabilities. Surprisingly, cellulose dissolution in 1-ethyl-3-methylimidazolium acetate is also mouldable using a classical wet-spinning process (6). Even a simultaneously dissolution and shaping step of cellulose and synthetic polymers like polyacrylonitrile will be succeeded using ionic liquids (7).

Experimental

Materials

The investigations had been carried out using a eucalyptus pre-hydrolysis sulphate pulp (Eu-569) and a cotton linters pulp (CL-454). The most important analytical parameters of the pulps are summarized in Table I. The pulps had been purified before carried out the dissolution steps.

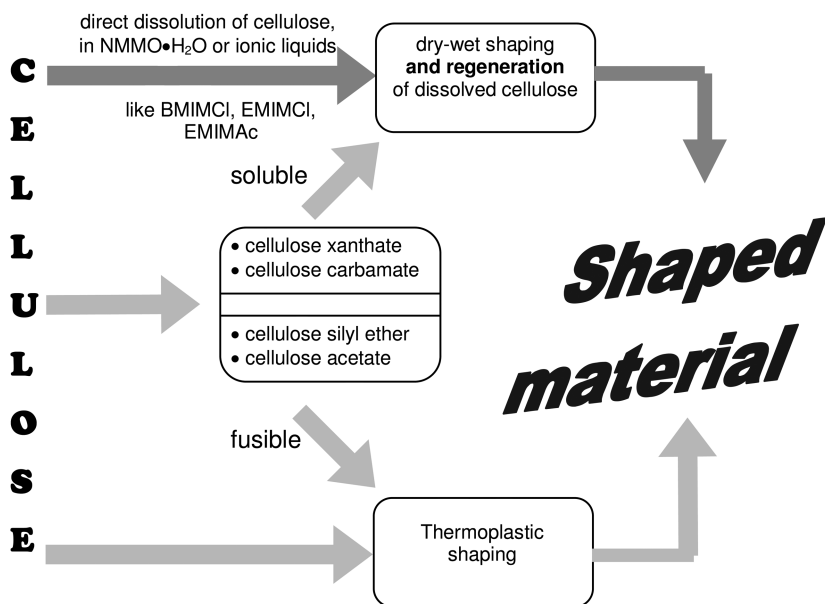


Figure 2. State of the technological art of cellulose forming into staple fibres, filaments, films or non-woven structures

The solvents N-Methylmorpholine-N-oxide monohydrate (NMMO-MH), 1-N-Butyl-3-methylimidazolium chloride (BMIMCl), 1-Ethyl-3-methylimidazolium chloride (EMIMCl), 1-N-Butyl-3-methylimidazolium acetate (BMIMAc) and 1-Ethyl-3-methylimidazolium acetate (EMIMAc) (manufactured by BASF) were in analytical grade and had been used without any pre-treatment or purification.

Preparation of Cellulose Solutions

The preparation of cellulose solutions has been carried out in a special vertical kneader system, linked with a RHEOCORD 9000 (HAAKE). Temperature, torque moment and revolutions per minute (rpm) vs. reaction time were determined on-line.

For the dissolution process the cellulose was disintegrated by means of an ultra-turrax shearing step in water, was separated from excessive water and was transferred in the aqueous ionic liquid in combination with stabilizers. The obtained stable suspension was poured in the vertical kneader system. After this the water was removed at temperatures between 90 and 130 °C, a reduced pressure between 700 and 5 mbar and a shearing rate of 10 to 80 rpm. The dissolving step is visible in a strong increasing of the torque moment. The viscous gel resulting at first was homogenised within an after-dissolution time of 1 hour at a constant torque rate.

Table I. Analytical data of pulps used

<i>Pulp</i>	$[\eta]_{Cuen}$ [ml/g]	DP_{Cuoxam}	α -cel- lulose content [%]	COOH- content [μ mol/g]	CO- content [μ mol/g]	Fe- content [ppm]	Cu- content [ppm]
Eu-569	365	569	96.0	4.2	16.5	2.3	0.7

The resulting cellulose solution was analytically characterised and was used for a further dry-wet shaping process.

The details of the solution preparation in the vertical kneader system as well as the analytical procedures of a dope quality characterisation by means of the particle analysis and a characterisation of the dissolution state by means of rheological measurements were described in former publications (13, 22, 23).

Spinning Trials

A self-constructed piston spinning device, which is consisting of a heatable cylinder, a spin package, an air-conditioned air gap, a spinning bath, a turning round godet and a take-off godet, was used for the shaping trials. The spinning dope is accurately dosed to the spin package by a precise feed rate of the piston. The spin package consists of a filter package, a heatable heat exchanger and the spinneret. The heat exchanger permits beside a homogenisation of the mass temperature also a continuous increasing of the spinning dope temperature from 80 °C up to 120 °C at short dwell periods directly before the entrance into the spinneret. A dope temperature sensor and a dope pressure sensor are positioned at the input of the spinning package.

A further dope temperature sensor is positioned between the heat exchanger and the spinneret. The air gap is arranged between spinneret and coagulation bath and can be handled spatial separated from the compartment air and is continuously movable between 10 and 150 mm through a vertical height adjustment of the spinning bath entrance. It is conditioned by means of a gas flow with definite temperature and moisture. The coagulation bath passes the spinning box, circulates by means of a pump and is adjustable in the height between 10 and 150 mm. The temperature and the flow rate of the spinning bath can vary in a wide range. The capillary bundle and the coagulation bath separate at the exit of the spinning box with a hole in the bottom.

A turning round godet collects the capillary skein and transports it over a traverse to the take-off godet. The finishing is carried out discontinuously after cutting the initial wet fibres into staples of uniform length.

Methods

Pulp Characterisation

The used pulps were characterised concerning the intrinsic viscosities in cuen $[\eta]_{\text{Cuen}}$ according to DIN 54270, part 2.

The average degrees of polymerisation ($\text{DP}_{\text{Cuoxam}}$) were determined in cuoxam. For this purpose the intrinsic viscosities in cuoxam $[\eta]_{\text{Cuoxam}}$ (unit: ml/g) were detected by means of a capillary viscometer and the $\text{DP}_{\text{Cuoxam}}$ was calculated according to the equation (1).

$$\text{DP}_{\text{Cuoxam}} = 2 \cdot [\eta]_{\text{Cuoxam}} \quad (1)$$

The content of α -cellulose were determined as the residue of pulp that is not dissolvable in a 17.5 wt-% NaOH at 20 °C.

The determination of the carboxyl group contents has been carried out by a complexometric titration of zinc ions after removing of the metal ions from the cellulose at first and adding of zinc acetate solution in a second step.

The carbonyl group contents were analysed by measurement of the absorbance at 530 nm after reaction with 2, 3, 5-triphenyltetrazoliumchloride solution.

The contents of metal ions (Fe, Cu) were determined according to DIN EN ISO 11885 (E22).

Fibre Characterisation

The determination of the water retention values of the cellulose fibres has been carried out according to DIN 53814.

The textile fibre parameters were determined according to the following methods:

- fineness according to DIN EN ISO 1973,
- tenacity and elongation according to DIN EN ISO 5079 and
- loop tenacity according to DIN 53843, part 2.

Results and Discussion

In case of a shaping process starting from polymer solution, the knowledge of the interaction between polymer chains and solvent(s) used is of special interest. Moreover, one has taken into account that polymer solutions are characterised by structural, thermodynamic as well as kinetic conditions.



Figure 3. Structures of cellulose regenerates – a cellulose xanthogenate/caustic soda, regenerated from aqueous sulphuric acid - irregular ; b – cellulose acetate/acetone, regenerated from water – irregular/fibrous; c – cellulose/cuoxam, regenerated from water – fibrous; d – cellulose/NMMO / H₂O, regenerated from water – fibrous; e – cellulose/BMIMCl, regenerated from water – fibrous

Cellulose Structure and Dissolvability

Several authors (8, 9) had described the driving force for dissolution of cellulose as electron donor – electron acceptor interaction. The proton of the hydroxyl group of the polymer acts as an electron acceptor, while the O-atoms along the polymer chain and in the ring as well as the hydroxyl oxygen atom are the electron donor sites. An EDA interaction together with the common used, dipolar solvent may occur via the donor and acceptor sites of the solvent molecule.

Another approach had been proposed by Turbak et al., who assumed that cellulose possesses acidic as well as basic sites due to it may react as acid as well as base regarding to the reaction partner.

The interaction model that is using for a description of the dissolution of cellulose in direct dissolving liquids varies from a classical EDA concept. A dissolution progress of cellulose by a layer-by-layer mechanism isn't valid here. Rather a penetration of solvent is necessary before dissolution may occur. For that reason also the molecule size of the solvent plays an important role (24, 25).

Now the question should be entered, how interaction of cellulose macro and solvent molecules may be described in more detail using direct dissolving liquids because of its fundamental importance for the understanding and the most possible quantitative perception of the proceeding processes while direct polymer dissolution. For that reason the structures of regenerated cellulose shapes, the structural changes of solvent and cellulose, the dope characteristics and shaping behaviour should be discussed. (see Figure 3).

Derived from the different fibrous structures of regenerates one may conclude that there are strong differences in dissolution state regarding both to the cellulose and solvent structure. While cellulose acetate and cellulose xanthogenate have been regenerate from a stable or semi-stable cellulose derivative they exhibit more or less a non-fibrous regenerate structure. All the other regenerates had obtained from cellulose had been dissolved without any chemical modification. Concluding from this result, the dissolution of cellulose using NMMO hydrates shouldn't accompanied by any chemical polymer modification.

NMMO is strong hygroscopic and is comfortably manageable in aqueous mixtures. It may form two crystalline and well defined stable hydrates (5).

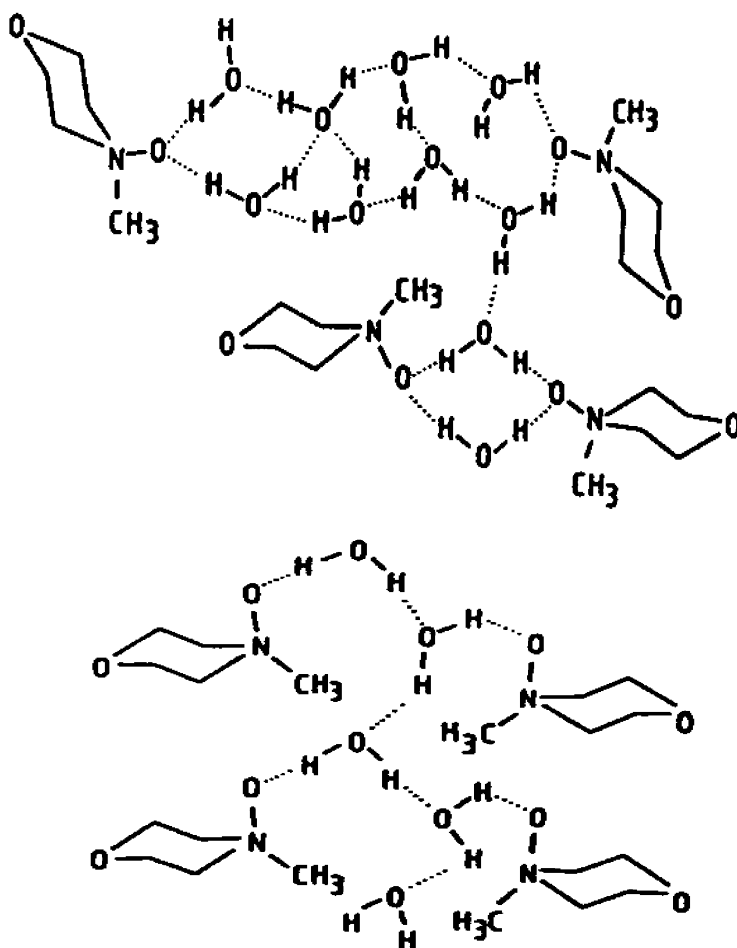


Figure 4. Crystalline structure of NMMO 2.5 hydrate (above) and NMMO monohydrate (down) (see ref. (19))

At water content of about 28% the 2.5 hydrate is formed, which melts at about 39 °C. The monohydrate is stable at a water concentration lower than 13.3. It melts at about 72 °C (see Figure 4).

A decreasing interaction of NMMO and water molecules is indicated conclude from the decrease of melt temperatures at increasing moles of water and the exothermic bonding of water molecules (26). Because of the minor sterical shielding the NMMO oxygen atom exhibits excellent donor activity (23). Finally, NMMO is a basic and polar compound, what is elucidating it ability for hydrogen bonding development.

A high ordered dissolved state is detectable in viscous NMMO melts regarding to WAXS investigations by Weigel (10) whose results could be confirmed by the investigations of Cibik (11).

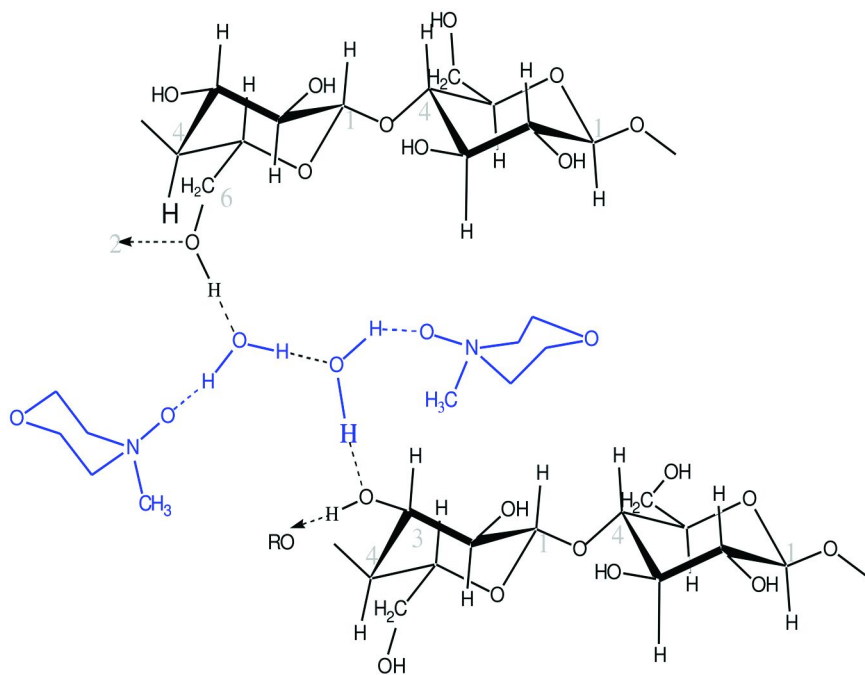


Figure 5. Structure of a cellulose NMMO monohydrate complex according to Michels and Kosan (13)

As a result of the molecular characteristics of NMMO and cellulose at the end of their interaction a cryptoionic complex should be formed, which should give the opportunity for an unhindered diffusion of the solvated macromolecules (27).

Physico-Chemistry Precondition for Cellulose Dissolution

A dissolution state is characterised by an energy minimum or an entropy maximum which have to be reached at the end of a dissolution procedure.

That means, that the overall free dissolving enthalpy should become below zero as a criterion for dissolubility of cellulose in the solvent used. Because the overall free dissolving enthalpy ΔG_s is the sum of enthalpy of “disaggregation” of cellulose crystals ΔG_d , the enthalpy of cellulose/NMMO interaction ΔG_r and theirs mixing enthalpy ΔG_m , all terms should be singly examined.

According to Herlinger et al. (23) the value for ΔG_d is in all cases positive and the value of ΔG_r becomes negatively if a complex between cellulose and NMMO is really formed. In order to get a negative overall free dissolving enthalpy the value of ΔG_m should also become negatively. That would only be the case if the free mixing energy becomes negatively, too, which should be possible if interaction of cellulose and NMMO is strong enough.

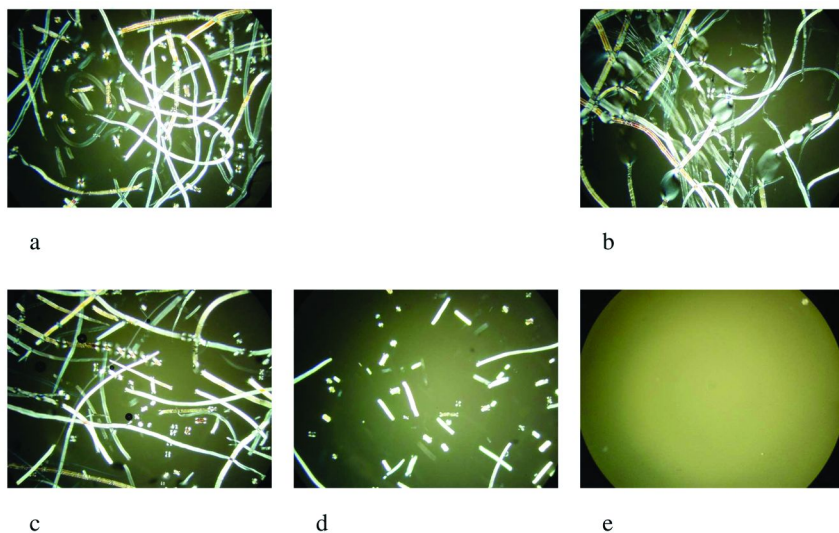


Figure 6. Consecutive dissolution step of a cellulose PAN mixture using BMIMCl: a – nearly completed dissolution of cellulose; b – strong swelling of PAN fibres; c – development of PAN dissolution by a segmental swelling; d – nearly completed dissolution of PAN fibres; e – completed dissolution of cellulose PAN mixture (7)

The investigations of Cibik (11) of the ternary system cellulose/NMMO/H₂O could demonstrate a decreasing of overall free enthalpy if NMMO concentration is higher than 78% and could confirm the existence of two different crystalline NMMO phases from the appearance of two melting peaks in DSC curve.

The NMMO monohydrate phase should be responsible for dissolution of cellulose, because of its free valence for interaction with cellulose hydroxyl group.

As a result of dissolution of cellulose in NMMO monohydrate H-bondings are decomposed (rearranged), spacer molecules will incorporate between macromolecule chains and solvated polymer should be formed.

From a kinetic standpoint of view polymer dissolution as a mixed phase is also be characterised by a dynamic mass as well as phase transfer. That's why the dissolution itself is a very fast step, but won't be performed, before an equilibrium state is achieved. Coming to such an equilibrium state could consume a fairly long time as well known from the reality.

Anyhow, it seems to be imaginably that mass and/or phase transfer may occur, too, by the action of an outside force like shearing or oscillation in a pre-dissolving step without reaching the equilibrium state required for an ideal dissolution. That may lead to a meta-stable mixed phase, which wouldn't decompose into the starting components by itself because of a kinetic inhibition caused by high solution viscosities, to low temperatures and/or pressures. Well known examples are beside others a micro phase segregation, plasticization or gelling.

Table II. Cellulose concentration, molar polymer/solvent ratios and zero shear viscosities of cellulose solutions in BMIMCl compared with NMMO

<i>Solvent</i>	<i>NMMO</i>	<i>BMIMCl</i>	<i>BMIMCl</i>
Cellulose concentration, wt-%	14.4	14.8	11.5
Molar polymer/solvent ratio	1/7.1	1/5.3	1/7.1
Zero shear viscosity (85 °C), Pas	20700	71420	20500

Table III. Cellulose concentration, molar polymer/solvent ratios and zero shear viscosities of cellulose solutions in different IL (pulp Eu-569)

<i>Solvent</i>	<i>BMIMCl</i>	<i>EMIMCl</i>	<i>BMIMAc</i>	<i>EMIMAc</i>	<i>EMIMAc</i>
Cellulose concentration, wt-%	13.6	15.8	13.2	13.5	19.6
molar polymer/solvent ratio	1/5.9	1/5.9	1/5.4	1/6.1	1/3.9
Zero shear viscosity (85 °C), Pas	47540	24900	9690	2283	30560

Indeed, as Berger (23) had pointed-out that cellulose dissolution with a polymer concentration higher than 0.1% isn't a mixed phase any longer, where polymer chains are able for a free diffusion. Moreover, it exhibits non-Newtonian flow behaviour, because of a numerous interlocking and entanglements. Such a view is supported by the indicated aggregates in diluted polymer dissolutions by means of static or dynamic light scattering (12).

Cellulose-Solvent-Interaction in Dissolved State

According to the investigations of Herlinger et al. (21), Michels et al. (13, 14) as well as of Cibik (11) the path of dissolution of cellulose with NMMO could be described as follow. The NMMO monohydrate which is dissolving cellulose within a very short time will be developed from the 2.5 hydrate by water evaporation. Dissolution could be basically recognised as an electron donator – electron acceptor interaction. Because of the low water concentration the coordination vacancies of the NMMO monohydrate will be saturated by the OH group of the cellulose. The formation of cellulose dope corresponds fundamentally to the findings of Cibik, who had determined two separate melting peaks in DSC curves that correspondent to crystalline structure of the both NMMO hydrate (11). Connected to the formation of several stable solvent hydrates are formed, a high ordered state occurs in a first step. The high ordered state won't be significant changed by the addition of polymers like for instance cellulose but slightly disturbed. The improving of the dissolving state of cellulose as detected by the author indicates the significant changing of cellulose I into

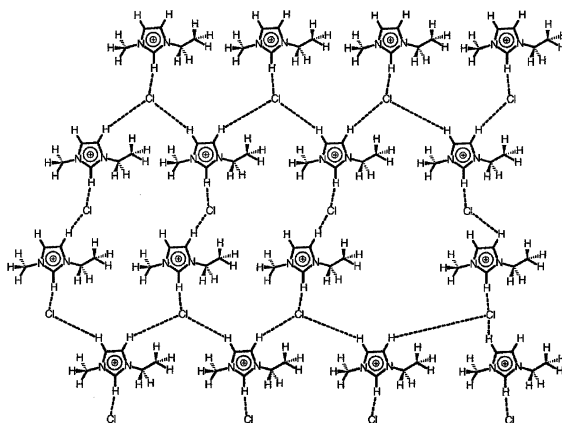


Figure 7. H-bond bridge system of ionic liquids from the group of 1-alkyl-3-methylimidazolium halides (19)

cellulose II modification at a NMMO concentration of $\geq 81\%$. Further the decrease of overall free enthalpy when NMMO content increase to values higher than 75% may be interpreted as increasing interaction between polymer and solvent. All those molecules are used for cellulose dissolution are not any longer available for crystallite growth. For a better understanding of the complex dissolution mechanism Cibik had used the microscopic visualisable changing of cellulose pre-dopes (fibres incidence, fibres length and state of the fibre surfaces) and the wide angle X-ray diffraction, too. By the latter method the content of cellulose II was determined on the basis of regenerated cellulose films. From their results could clarified that cellulose dissolution will progress very fast at NMMO concentrations higher than 82%. At this state NMMO monohydrate is dominating and interacts with cellulose hydroxyl groups. Additional the sterical structure of NMMO monohydrate is much more compatible to cellulose structure. As a result of both facts cellulose is dissolved very fast under those conditions and at temperatures of about 90 °C.

Another interpretation for the decrease of overall melting enthalpy in DSC curves in the case ternary mixture cellulose/NMMO/H₂O had been given by Michels and Kosan (13). They had been stated that there is no free mobility of single dissolved cellulose macromolecules, but an insertion of up to two NMMO monohydrate molecules into the intermolecular H-bond of hydroxyl groups at the C-6 position of one and C-3 position of the other cellulose chain. As a result of such an insertion movability of one cellulose chain against the other will be dramatically changed. Cellulose dopes become deformable while shaping into fibres and films. Moreover the non-Newtonian properties, which could partly caused for the strong intermolecular linkages between different cellulose chains and the tendency to form lyotropic liquid crystal structures seem to be explainable. Even the different fibrous structure of cellulose regenerates had been obtained after cellulose precipitation from NMMO dissolution might be the result of with each other linked macromolecules.

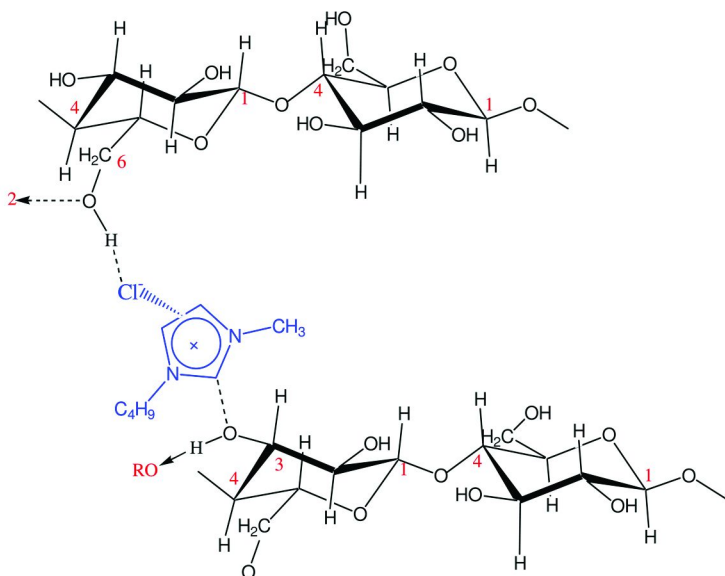


Figure 8. Proposed Structure of a cellulose IL complex according to Michels and Kosan (14)

Figure 5 indicates a proposal for the formed structure in the system NMMO/H₂O/Cellulose developed as a result of cellulose dissolution (13).

Transformation of Experiences in the System Cellulose/NMMO/H₂O onto Dissolution in Ionic Liquids (IL)

If ones now try to use the detected facts of the system NMMO/H₂O/Cellulose for the dissolution of cellulose in ionic liquids it comes apparent that a lot of essential properties of ionic liquids today are investigated insufficient only.

No secured knowledge for stable hydrates of ionic liquids is available so far. Nevertheless the results of Hermanutz and co-workers (6), who had investigated the opportunity for wet-shaping of cellulose dissolved in 1-ethyl-3-methylimidazolium acetate, indicate in some respects a toleration of water or other protic co-solvents inside the dope.

In principle there are some similarities regarding the chemical character of ionic liquids and the properties in the system cellulose/IL, which give reason for the assumption that similar procedures will have to be run for cellulose dissolution as in NMMO/H₂O. The dissolution procedure using IL will also be characterised by a strong swelling and plasticisation of the polymer (15). The following figure describes the forming of a pearl-necklage like swelling structure well known from the dissolution of cellulose in NMMO monohydrate also by the interaction of cellulose with 1-alkyl-3-methylimidazolium.

Surprisingly such a swelling is also observable while the consecutive dissolution of cellulose and polyacrylonitrile (PAN) using 1-butyl-3-methylimidazolium chloride (see Figure 6) (7).

Moreover the known non-Newtonian behaviour of dopes, high zero shear viscosities of cellulose/IL solutions as well as the strong visco-elastic behaviour, which is also found in rheological characterisation might be signs for a lot of similarities between Lyocell dopes in NMMO and cellulose solutions in ionic liquids. Notably analogies exist between cellulose dopes in NMMO and in BMIMCl. Even though the zero shear viscosities of similar concentrated cellulose solutions are significantly higher in BMIMCl using the same pulp (Eu-569), zero shear viscosities are comparable at the same molar polymer - solvent ratio (see Table II).

Significant differences in the solution states seem to exist depending on the changes of the cation and/or anion of the ionic liquid used as solvent for cellulose.

Table III demonstrates some differences in the zero shear viscosities of cellulose in varying ionic liquids solutions.

The zero shear viscosities at comparable molar ratios of dopes containing chloride anion are significantly higher than those of acetate containing dopes. That's why higher cellulose concentrations may be realisable for acetate containing IL.

Nowadays no secured knowledge about the role of water or other impurities is available. For that reason several scientific groups are dealing with the investigation of cellulose/IL solution by means of different analytical approaches (16–18, 20).

An interesting entrance for an explanation of the different characteristics of polymer solutions using NMMO monohydrate and ionic liquids has been given by Dong and co-workers (19). Derived from a calculated structure model of ionic liquids selected from the group of 1-alkyl-3-methylimidazolium halides (see Figure 7) a significant higher stiffness is predicted.

Another fact has been given by Michels (14), who had detected a change of cellulose I into cellulose II modification not until the water content has been decreased significantly below 10%. As a result of their investigations of dissolution behaviour of cellulose pulps in IL they had proposed a similar structure of the cellulose/IL complex as they did in the case of a direct dissolution process using NMMO monohydrate (see Figure 8). For such a structure higher viscosities could be caused by a poorer flexibility of the polymer/IL complex formed, because of missing further spacer molecules between different polymer chains and the more planar structured IL molecule.

References

1. (a) Graenacher C.U.S. Patent 1,946,176, 1934. (b) Graenacher, C.; Sallmann, R.U.S. Patent 2,179,181, 1939.
2. (a) Johnson, D. L.U.S. Patent 3,447,939, 1969. (b) Johnson, D. L. U.S. Patent 3,508,941, 1970.

3. Franks, N. E.; Varga, J. K. U.S. Patent 4,145,532, 1979.
4. McCorsley, C. C. U.S. Patent 4,246,221, 1981.
5. (a) Chanzy, H.; Dubé, M.; Marchessault, R.H. *J. Polym. Letters Ed.* **1979**, *17*, 219. (b) Chanzy, H.; Nawrot, S.; Peguy, A.; Smith, P.; Chevalier, J. *J. Polym. Sci., Polym. Phys. Ed.* **1982**, *20*, 1909. (c) Chanzy, H.; Paillet, M.; Hagede, R. *Polymer* **1990**, *31*, 400.
6. (a) Hermanutz, F.; Massonne, K.; Uerdingen, E. Neue Entwicklung in Lösung und Verarbeitung von Cellulose mit ionischen Lösungsmitteln. 45th International Man-Made Fibre Conference, Dornbirn, Austria, September 20–22, 2006. (b) Hermanutz, F.; Gähr, F.; Uerdingen, E.; Meister, F.; Kosan, B. *Macromol. Symp.* **2008**, *262*, 23
7. Kosan, B.; Nechwatal, A.; Meister, F. Cellulose and Cellulose Multi-component Fibres from Ionic Liquids. 3rd Workshop on Cellulose, Regenerated Cellulose and Cellulose Derivatives, Karlstad, Sweden, November 13–14, 2007.
8. Philipp, B.; Schleicher, H.; Wagenknecht, W. *Cellulose Chem. Technol.* **1978**, *12*, 529.
9. Nakao Sani, O. *To Kogyo* **1971**, *4*, 128.
10. Weigel, P. *Final Report to the BMFT-Project 0310376 A*, Fraunhofer IAP: Golm, 1994
11. Cibik, T. Ph.D. Thesis, TU Berlin, 2003.
12. (a) Morgenstern, B.; Röder, T. *Das Papier* **1998**, *12*, 713. (b) Röder, T.; Möslinger, R.; Mais, U.; Morgenstern, B.; Glatter, O. *Lenzinger Ber.* **2003**, *82*, 118.
13. Michels, C.; Kosan, B. *Lenzinger Ber.* **2005**, *84*, 62.
14. Michels, C.; Kosan, B. *Lenzinger Ber.* **2006**, *86*, 144.
15. Winterton, N. *J. Mater. Chem.* **2006**, *16*, 4281.
16. Moulthrop, J. S.; Swatowski, R. P.; Moyna, G.; Rogers, R. D. *Chem. Commun.* **2005**, 1557.
17. Remsing, R. C.; Swatowski, R. P.; Rogers, R. D.; Moya, G. *Chem. Commun.* **2006**, 1271.
18. Fukaya, Y.; Hayashi, K.; Wada, M.; Ohno, H. *Green Chem.* **2008**, *10*, 44.
19. Dong, K.; Zhang, S. J.; Wang, D. X.; Yao, X. Q. *J. Phys. Chem. A* **2006**, *110*, 9775.
20. Hesse-Ertelt, S.; Schwikal, K.; Kosan, B. *Dissolving and Precipitating Structures of Native Polymers Dissolved in ILs*. Preliminary Report to BMWA Project (VL 07 1902), TITK, 2008.
21. Herlinger, H.; Grynaeus, P.; Hirt, P., et al. *Lenzinger Ber.* **1990**, *69*, 65
22. Kosan, B.; Michels, Ch. *Chemical Fibers Int.* **1999**, *49*, 50–54.
23. Michels, Ch.; Kosan, B. *Chemical Fibers Int.* **2000**, *50*, 561–566.
24. Berger, W.; Keck, M.; Do Van, Sang; Philipp, B. *Z. Phys. Chemie, Leipzig* **1985**, *266*, 436.
25. Schleicher, H.; Philipp, B.; Kabrelian, V. *Das Papier* **1988**, *42*, 653.
26. Taeger, E.; Michels, Ch.; Nechwatal, A. *Das Papier* **1991**, *12*, 784.
27. Berger, W.; Keck, M.; Philipp, B.; Schleicher, H. *Lenzinger Ber.* **1985**, *59*, 88.

Chapter 12

Effect of Enzymatic Treatment on Solubility of Cellulose in 7.6%NaOH-Water and Ionic Liquid

Peter Rosenberg¹, Tatiana Budtova², Monika Rom³ and Pedro Fardim^{*,1}

¹Laboratory of Fibre and Cellulose Technology †, Åbo Akademi University, 20500 Turku, Finland

²Mines ParisTech, Centre de Mise en Forme des Matériaux - CEMEF †, UMR CNRS/Ecole des Mines de Paris 7635, BP 207, 06904 Sophia-Antipolis, France

³Institute of Textile Engineering and Polymer Materials, University of Bielsko-Biala, Willowa 2, 43-309, Bielsko-Biala, Poland

*Corresponding author: pfardim@abo.fi.

†Member of the European Polysaccharide Network of Excellence (EPNOE), www.epnoe.eu.

The effect of enzymatic pretreatment on the properties of cellulose dissolved in aqueous 7.6%NaOH and in an ionic liquid (IL) was investigated and compared with viscose prepared from the same raw material and dissolved in 7.6%NaOH. The enzymatic pretreatment decreased by twice the DP of cellulose as compared with the initial one. This facilitated cellulose dissolution in NaOH. The flow of enzyme-treated pulp dissolved in 7.6%NaOH-water and in IL was studied and compared with cellulose xanthate dissolved in aqueous 4.5%NaOH-water. The solutions of enzyme-treated cellulose in NaOH-water gelled with heating in the same way as non-treated cellulose solutions. The dependence of the intrinsic viscosity as a function of temperature of the enzyme-treated cellulose dissolved in 7.6%NaOH showed the same trend and similar values as for microcrystalline cellulose dissolved in this solvent. The assumed presence of insoluble material in cellulose-NaOH solution was proved by flow cytometry,

which indicated an average particle diameter of the insoluble or swollen entities being around 600 nm. Cellulose beads were prepared from NaOH-water solutions of enzyme-treated pulp and of viscose. SEM images showed that their surface topography was dependent on cellulose treatment. It was shown that the enzyme-treated pulp-NaOH-water system could be used for bead manufacturing.

Introduction

Dissolution of biomass – e.g., cellulose – is generally used as a method of forming the natural polymer into industrial products, such as textile fiber, membranes, beads, sponges, etc. Cellulose is first isolated from the other components present in the plant, often wood. At the moment, this is usually done by chemical pulping. Dissolving grade pulp with high α -cellulose content is often prepared by sulphite cooking, using spruce or beech as raw material.

After pulping, cellulose is purified, possibly treated chemically or by other means, and thereafter dissolved in an appropriate solvent. There are two main types of solvent systems. An example of so-called dissolution via derivatisation is the industrially most commonly used viscose method, where the –OH groups of cellulose are substituted with –OCS₂Na in a xanthogenation stage prior to dissolution in an aqueous NaOH. The major drawback of the viscose method is the environmental and health risks caused by CS₂ (1). The second way is cellulose dissolution in a solvent without any chemical modification, like in N-methylmorpholine-N-oxide monohydrate or (7-9)%NaOH-water. The latter solvent is known to dissolve only low molecular weight cellulose with DP < 400-500. The newest solvents having good capability to dissolve cellulose are so called ionic liquids, which are in fact molten salts that interact through hydrogen bonding between the cellulose polymer and the anion (2). Several ionic liquids have been studied for their ability to dissolve cellulose or other biopolymers such as starch and chitosan or even wood and then form different products, and the results are very promising (3–20). The easiest to handle ILs are liquid at room temperature, such as 1-Ethyl-3-methylimidazolium Acetate (EmimAc): it can dissolve as much as 20% w/w of cellulose. Cellulose can be precipitated from the solvent by adding water or another non-solvent. The drawback of IL systems is a high price and some problems with solvent recovery. Recently, it has been reported that IL's are not inert in respect to cellulose (18).

Another approach to help cellulose dissolution is to perform different pretreatments, such as mechanical, chemical, or enzymatic. The idea is to increase the swelling of the native cellulose by opening up its crystalline structure. Several methods utilizing endoglucanase enzymes have been studied for decades (21–24), and the pretreatment with cellulases seems to increase the solubility of the treated fibers so that they can be dissolved in aqueous (7-9)%NaOH at low temperatures. The so-called Biocelsol method utilizes first mechanical ball mill treatment followed by enzymatic treatment (25, 26). It was noticed that

the solutions prepared in NaOH-water according to the Biocelsol method possess some uncommon properties when cellulose beads were manufactured (27). Even the beads and sponges prepared from this solution had different properties as compared to beads and sponges prepared from other cellulose solutions. The shape of the beads is much more irregular compared to the beads made from viscose. The sponges made from enzyme-treated cellulose are much weaker and harder compared to sponges made from viscose. The textile fibers made from this cellulose solution are much weaker as compared to Rayon or Lyocell fibers (28).

As the enzymatic treatment seems to have potential to increase cellulose solubility in common and low cost aqueous NaOH, it is thus important to investigate and understand the reasons of the different properties of these enzyme-treated pulp solutions as compared with cellulose dissolved in other solvents. In this article, the properties of cellulose solutions were studied by a rheological method that provides information about the state of dissolved polymer and its hydrodynamic characteristics. The shear viscosities of the solutions at various cellulose concentrations and at different temperatures were measured; and the Arrhenius plot was built. We tried to evaluate if cellulose is in a solution or in a suspension state. The sample was also analyzed with flow cytometry for checking the presence of undissolved material and analyzing the particle size. The same enzyme-treated pulp was also dissolved in the ionic liquid, EmimAc, and the rheology of this solution was also studied for comparison. Viscose made from the same dissolving grade pulp was also investigated and compared to the other solutions. The information obtained from the studies gives a better understanding of the challenges in cellulose product manufacturing utilizing enzyme-treated pulp.

Materials and Methods

Materials

The dissolving grade spruce sulphite pulp (“pulp” in the following) was provided by Domsjö Fabriker, Sweden, as air-dried sheets. The mixture of cellulase enzymes used was a culture filtrate from a genetically modified *Trichoderma reesei* strain obtained from VTT, Finland. NaOH was from Merck with pro analysis purity, >99%. EmimAc was from BASF, purity $\geq 90\%$, and used as received. Distilled water was used to prepare aqueous solutions. Ethanol was purchased from Altia, “A” quality, 96.1 vol-%.

Methods

Enzymatic Treatment

The pulp was initially treated by a ball mill(29) and thereafter by a mixture of endoglucanases at 5% pulp consistency for 3 h. The enzyme dosage was 2000

nkatg⁻¹, the pH was adjusted to 5, and the temperature was 50°C. The sample was then washed with NaOH aqueous solution at pH 8-8.5 for the removal of dissolved carbohydrates and residual enzymes. The treated pulp (“enzyme-treated pulp” in the following) was stored in a refrigerator. The R18 content of the enzyme-treated pulp was 93.3%. For storage purposes, the enzyme-treated pulp was immersed in 96% ethanol for solvent exchange, the ethanol was evaporated and the pulp was dried to 95% w/w dryness (according to ISO 638) and preserved in a refrigerator.

DP Determination

The DP of the pulp was determined both before and after the enzymatic treatment. The intrinsic viscosity of the pulp was measured according to ISO 5351-1:1981 (same as SCAN CM 15:88). The pulp was dissolved into 1.00 molL⁻¹ cupriethylenediamine (CED) solution; the capillary viscosimetry measurements were conducted at 25°C. The intrinsic viscosity was calculated using methods described in the literature (30, 31).

Cellulose Dissolution

Enzyme-Treated Pulp

Before preparing solutions, the enzyme-treated pulp was first dried in an oven at 105°C. In order to prepare solutions in 7.6%NaOH-water, the following procedure was used. The dry enzyme-treated pulp was first suspended in warm water and mixed for 2 h prior to dissolving in aqueous NaOH solution. The final cellulose concentration was 4.0% w/w and NaOH concentration was 7.6% w/w. The temperature was adjusted to -7°C for effective dissolving. It was stored in a refrigerator at about +5°C to avoid aging.

Cellulose was mixed with EmimAc at ambient temperature. The mixture was then heated to 90°C and kept under stirring for 24 h followed by cooling down to ambient temperature. The method was performed according to Stegmann et al. 2007 (32).

Viscose

An industrial viscose sample prepared from the same initial sulphite pulp was stored in a freezer at -20°C to avoid ripening, for about six months. The original sample contained 7.2% w/w cellulose of DP 320 given by manufacturer, and 4.5% w/w of NaOH in water. The falling ball viscosity of the initial viscose was 48 s and the degree of ripening 6.1°Ho. The sample contained 27.5% w/w CS₂. Viscose was thawed and the cellulose concentrations were adjusted with aqueous 4.5%NaOH.

All solutions, i.e., enzyme-treated pulp in aqueous 7.6%NaOH and IL, as well as the reference viscose solution in 4.5%NaOH-water, were prepared first

at 4.0 % w/w cellulose concentration. The 4% solutions were then diluted by the corresponding solvent to 3% and 2% cellulose concentrations.

Rheology and Viscometry

The flow of enzyme-treated pulp solution in 7.6%NaOH solvent was studied with Bohlin Gemini[®] rheometer equipped with a cone-plate geometry and a Peltier temperature control system. The other cellulose solutions were studied with Bohlin VOR rheometer utilizing the cone and plate geometry of CP 5/30 at AAU. The viscosities were measured with first increase and then decrease of the shear rates 0.1-230 s⁻¹ with approx. 20 steps in each direction, 8 s waiting time between the steps and 10 s integration times for each step. The measurements were conducted at from 5° to 30°C with a step of 5°C.

A control shear viscosity measurement with each stock solution was repeated daily at the same temperature and shear rate during the storage time to make sure that the storage in the refrigerator did not affect the solutions.

The intrinsic viscosity of the enzyme-treated pulp in aqueous 7.6%NaOH was obtained using a Ubbelohde viscometer, at temperatures of 5-40°C.

Flow Cytometry

The presence of insoluble entities in the solution of the enzyme-treated cellulose in the aqueous 7.6%NaOH was studied using PerkinElmer flow cytometer. The solution was diluted with 7.6% w/w NaOH to a dilute cellulose concentration prior to injecting the sample into the measuring cell. The results were plotted as normalized number of particles vs. particle size.

Beads Preparation and Analysis

Beads were prepared both from enzyme-treated pulp dissolved in 7.6%NaOH-water and cellulose xanthate in 4.5%NaOH-water, in accordance with a spinning disk method described in Rosenberg et al. 2007 (33). The beads were analyzed for their shape, size and surface morphology using JEOL JSM 5500 LV Scanning Electron Microscopy (SEM).

The crystalline structure of the native and regenerated cellulose was analyzed by Wide Angle X-ray Scattering (WAXS) using Seifert URD-6 diffractometer equipped with a scintillation counter. The experiments were carried out in the reflection mode, at room temperature. A Ni-filtered CuK α radiation was applied. Diffraction patterns were registered in the 2 θ range of 4-60°, with a step of 0.1°. The degree of crystallinity was calculated with a modified Hindeleh & Johnson method(34, 35) and the WaxFit computer program (36). By means of the software applied, a linear background was subtracted and the diffraction curves were decoupled into crystalline and amorphous components, by applying generic

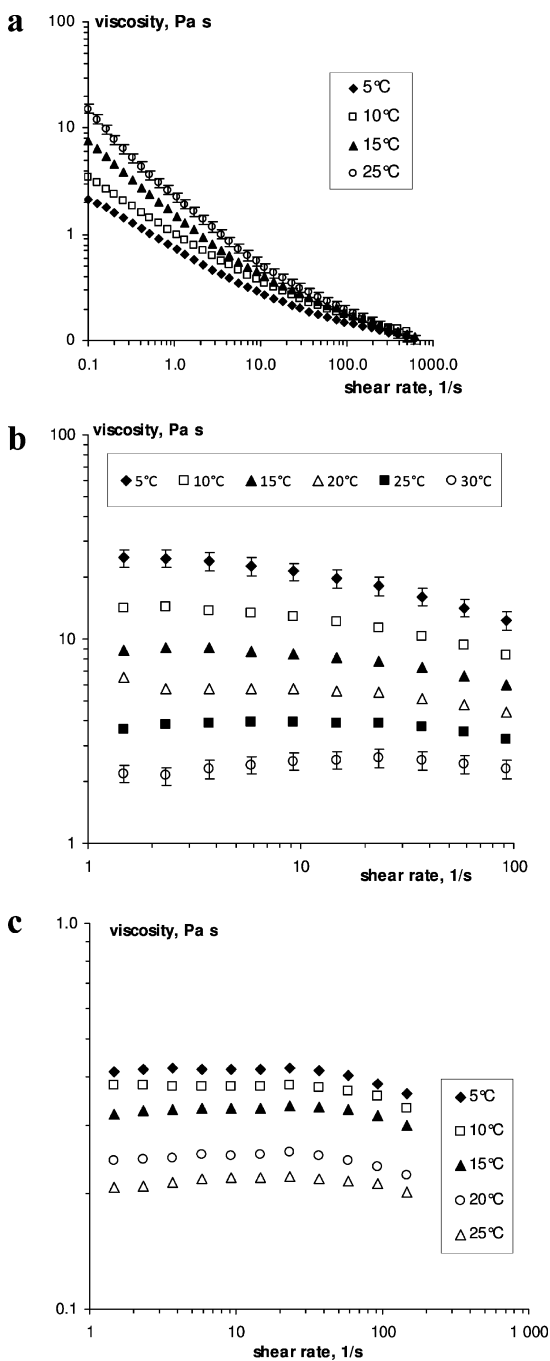


Figure 1. Viscosity vs shear rate at various temperatures for a) 3%enzyme-treated pulp-7.6NaOH-water; b) 3%enzyme-treated pulp-EmimAc and c) 3%viscose-4.5%NaOH-water.

algorithms and a multiobjective optimization procedure. The size of crystallites was estimated with the Scherrer equation (37).

Results and Discussion

The Effect of the Enzymatic Treatment on the DP of Cellulose

The intrinsic viscosity of the original pulp in CED according to ISO 5351-1:1981 was 530 mL g^{-1} , whereas the intrinsic viscosity of the same cellulose after enzymatic pretreatment was 240 mL g^{-1} . This is a clear indication of the drop of cellulose molecular weight. The DP calculated according to SCAN 15:88, $\text{DP} = 1.1 \times [\eta]^{1/0.95}$, was approx. 1800 for the original pulp and 710 for the enzyme-treated one.

The DP decreases to more than half of the original due to the enzymatic treatment. It should be noted that the enzymatic cleavage did not occur only at the ends of the polymer chains, but also in the middle of the chains, since the amount of dissolved sugar – 84 mg g^{-1} – is not very high after treatment. The result obtained suggests that it is the strong decrease of the DP which contributed to the solubility of the enzyme-treated pulp.

Flow of Cellulose Solutions

An example of the flow of 3%enzyme-treated pulp-7.6%NaOH-water solution at various temperatures is given in Figure 1a. The solutions are strongly shear thinning, and viscosity increases with temperature increase. Enzyme-treated pulp solution is not flowing in the same way as previously studied microcrystalline or Borregaard celluloses dissolved in the same solvent (38–40). In refs. (38–40) it was shown that at low temperatures and similar cellulose DP and concentrations, viscosity-shear rate dependences demonstrated very weak shear thinning. The result obtained here means that at the time of the experiment, the enzyme-treated pulp solution overpassed its gel point: it is a weak gel, not a solution which breaks and flows under shear stress.

Another reason of a strong shear thinning could be the presence of undissolved cellulose entities. For example, suspensions of cellulose microcrystals have shown shear thinning(41) and formation of gel-like suspensions (42); their rheological behaviour was similar to enzyme-treated pulp-NaOH-water system.

The results for 3%enzyme-treated pulp-EmimAc and for 3%viscose-7.6%NaOH-water solutions are presented in Figures 1b and c, respectively. At each temperature, a Newtonian plateau can be seen and viscosity decreases with temperature increase, as for classical polymer solution and also as shown for celluloses of various molecular weights dissolved in EmimAc (20). Similar results were obtained for other polymer concentrations. All the solutions studied are not thixotropic. Enzyme-treated pulp in IL had the highest overall viscosity due to the highest solvent viscosity.

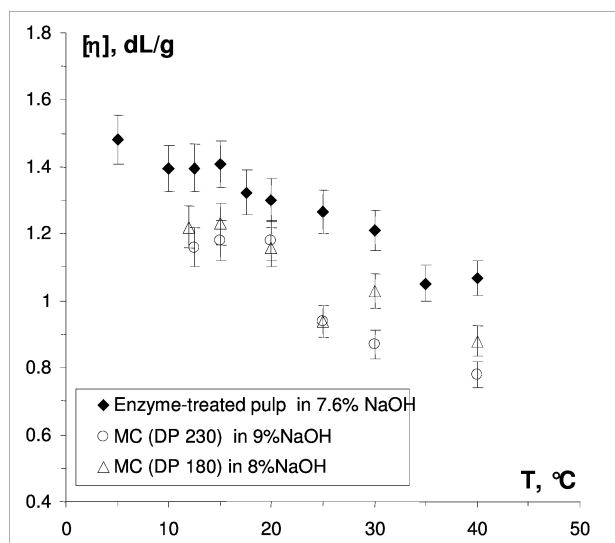


Figure 2. Dependence of enzyme-treated pulp and the intrinsic viscosity of microcrystalline celluloses on temperature. The values for the microcrystalline celluloses are taken from refs. (38) and (44).

Activation Energy

The zero-shear rate viscosity was plotted for cellulose solutions studied as a function of inverse temperature, and the activation energy E_a was calculated using Arrhenius approximation. It was not possible to analyze enzyme-treated pulp-NaOH system in this manner, because it was not a solution but a breaking gel that was flowing. The activation energy in this case makes no sense.

The activation energy of enzyme-treated pulp-EmimAc and of viscose-4.5%NaOH-water solutions did not depend much on polymer concentration within 2-4%, probably because of a narrow concentration interval. The average values obtained were $E_{a \text{ enzyme-treated pulp-EmimAc}} = 63.5 \pm 3 \text{ kJ/mol}$ and $E_{a \text{ viscose-4.5\%NaOH-water}} = 16.5 \pm 3 \text{ kJ/mol}$. The E_a value is much higher for enzyme-treated pulp-EmimAc solution because of a much greater solvent viscosity.

Intrinsic Viscosity of Enzyme-Treated Pulp in 7.6%NaOH

It was interesting to examine the hydrodynamic characteristics of enzyme-treated pulp dissolved in NaOH-water and to compare the results with the ones obtained earlier(38, 43, 44) for the microcrystalline (Avicel) celluloses of DP 180 and 230 dissolved in the same solvent. The intrinsic viscosity of enzyme-treated pulp dissolved in 7.6%NaOH-water was obtained for various temperatures (Figure 2). It should be kept in mind that the DP of microcrystalline cellulose was provided by the manufacturer.

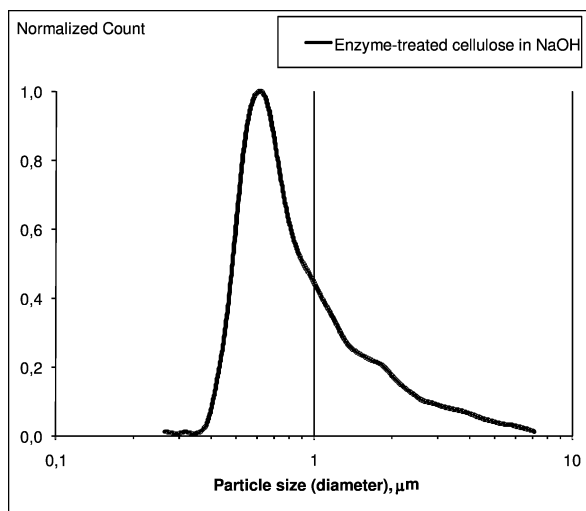


Figure 3. The average particle size of the scattering entities in enzyme-treated pulp-7.6%NaOH-water, from flow cytometry.

In all cases, the presented cellulose intrinsic viscosity decreases with temperature increase, depending on the pre-treatment or molecular weight. This is due to the decrease of solvent thermodynamic quality which leads to preferential cellulose-cellulose interactions that in turn lead to compactization in the dilute state of macromolecules, and gelation in the semi-dilute state. The result obtained shows that the enzymatic treatment does not change the mechanism of cellulose interactions with NaOH hydrates. The values of the intrinsic viscosities of enzyme-treated pulp and microcrystalline celluloses are very close, showing that all cellulose samples presented in Figure 2 are of a similar molecular weight.

Evidence of Undissolved Entities in Enzyme-Treated Pulp-7.6%NaOH-Water

Flow cytometry is based on the light-scattering measurement of fluid containing solid particles. Enzyme-treated pulp dissolved in 7.6%NaOH-water was studied in view of the presence of undissolved cellulose entities. The normalized particle count vs. particle size curve was plotted (Figure 3) and it showed an average particle size of 600 nm, with the particle size varying between 300 and 1700 nm. This is a clear evidence of the presence of insoluble material in enzyme-treated-7.6%NaOH-water solutions, making it suspension-like. As will be shown further with X-ray study, the suspended particles as well as dissolved cellulose are composed of cellulose II. This means that the scattering entities are most likely badly dissolved swollen cellulose, a sort of nano-gel.

Bead Morphology Studied by SEM

The beads prepared from enzyme-treated pulp as well as viscose solutions were analyzed for their shape and surface morphology by SEM. The results showed a difference between the beads (Figure 4), which could not be explained by the parameters of the manufacturing process, these being the same, as well as the cellulose concentration (4%). The reason lies in the difference in the cellulose solution properties, affecting the final properties of the products. While the shape of viscose beads is from spherical to ellipsoidal, the shape of beads from enzyme-treated pulp is absolutely irregular and the size has a much broader distribution. A bead of treated pulp seems to be “composed” of several pieces. The surface of the beads made from enzyme-treated pulp is very irregular and much less smooth as compared to beads made from viscose.

At least two reasons behind the difference in shape and surface of beads from viscose and enzyme-treated pulp can be offered. One corresponds to a macrostructural level and is due to the fact that enzyme-treated pulp-NaOH solutions are weak gels. When these solutions are processed, the gel is broken under flow, and the beads may be made from several pieces and are thus not regular in shape. The second reason is on a more microstructural level, and may be due to the presence of “nano-gels”. These “particles” made of swollen, not well dissolved cellulose may induce irregularities on the surface of the beads.

Crystalline Structure of Cellulose in Beads and Initial Pulp

The type of the crystalline structure of the manufactured cellulose beads was studied to find out if there are any native cellulose crystals left. The presence of native cellulose crystalline structure would indicate that part of the enzyme-treated pulp did not dissolve in the NaOH-water.

The XRD's depicted in Figure 5 show the typical peaks for Cellulose I and Cellulose II. The peaks for the studied cellulose beads made from the regenerated cellulose coming from enzyme-treated pulp-7.6%NaOH-water and viscose-4.5%NaOH-water solutions both show Cellulose II-type crystallinity. This did not exclude the possibility of having partly undissolved cellulose in the solvent, as it was detected by flow cytometry. It merely indicated that the cellulose in these nano-gels, being swollen, was converted into Cellulose II (45, 46).

Conclusions

The effect of cellulose enzymatic treatment on the solution state and hydrodynamic properties in NaOH-water and in EmimAc was investigated. Cellulose beads were prepared from enzyme-treated pulp-7.6%NaOH-water. The results were compared with viscose-4.5%NaOH-water solution.

One important result is that the enzymatic treatment more than twice decreases cellulose molecular weight. This can be one of the reasons for the

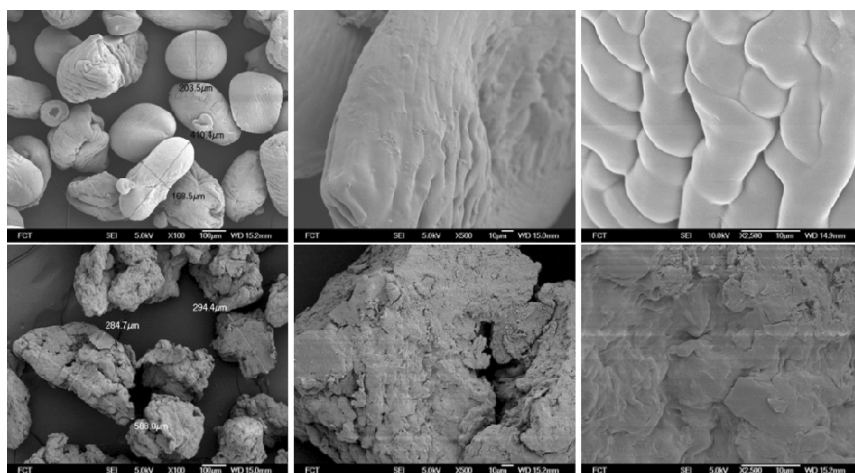


Figure 4. SEM images of beads made from viscose (upper) and from enzyme-treated pulp-7.6%NaOH-water (lower), both having an initial cellulose concentration of 4.0 %. The magnification increases from left to right 100x, 500x, and 2500x.

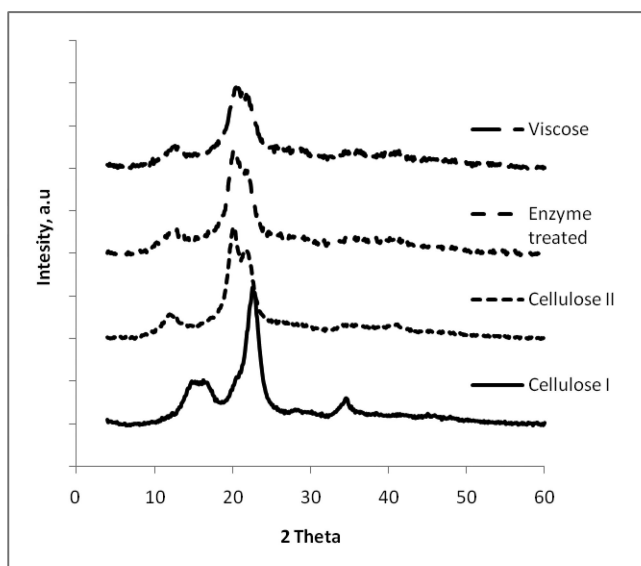


Figure 5. X-ray diffraction spectrum of different crystalline allomorphs of cellulose and beads from enzyme-treated pulp and viscose.

improvement of cellulose solubility. The rheological study of enzyme-treated pulp dissolved in NaOH-water showed that the enzymatic treatment did not modify the behavior of cellulose in this solvent: temperature increase induces gelation. This does not occur for viscose-NaOH-water solutions. The hydrodynamic properties of enzyme-treated pulp in NaOH-water are the same as those of microcrystalline

cellulose: the intrinsic viscosity decreases with temperature increase and the values are very close. Flow cytometry demonstrated the presence of a sort of “particles” suspended in enzyme-treated pulp-NaOH-water system.

The beads prepared from enzyme-treated pulp and viscose, both dissolved in 7.6%NaOH-water, showed different surface morphology. X-ray diffraction demonstrated that cellulose in both types of beads is Cellulose II. The “particles” in enzyme-treated pulp-NaOH-water should thus be a sort of nano-gels made from swollen (not completely dissolved) cellulose.

All this does not make the enzymatic treatment useless, however, since it was possible to form cellulose products from cellulose-NaOH-water. The combination of the enzymatic treatment with the dissolution in NaOH-water still remains a relatively simple, cost-effective, and environmentally friendly method of cellulose processing.

Acknowledgements

This research was partly performed within the Biocelsol project, NMP2-CT-2003-505567; for more information, please see the home page of the project at [http://www.tut.fi/units/ms/teva/enzyme-treated pulp/index.htm](http://www.tut.fi/units/ms/teva/enzyme-treated+pulp/index.htm). The article reflects the views of the authors only: the European Community as well as other project partners are not liable for any use of the information contained therein. The visit of P. Rosenberg to Cemef, France was performed within an exchange within the framework of the “European Polysaccharide Network of Excellence” (EPNOE), project number NMP3-CT-2005-500375. The authors would like to express their thanks to Kristian Steinby and Rasmus Eriksson for technical advice, and to Lari Vähäsalo and Elina Orblin for experiment-related support.

References

1. Dutta, P. K. *Ind. Text. J.* **1996**, *106*, 40.
2. Remsing, R. C.; Swatloski, R. P.; Rogers, R. D.; Moyna, G. *Chem. Commun.* **2006**, *12*, 1271.
3. Heinze, T.; Dicke, R.; Koschella, A.; Kull, A. H.; Klotz, E.-A.; Koch, W. *Macromol. Chem. Phys.* **1999**, *201*, 627.
4. Swatloski, R. P.; Spear, S. K.; Holbrey, J. D.; Rogers, R. D. *J. Am. Chem. Soc.* **2002**, *124*, 4974.
5. Heinze, T.; Schwikal, K.; Barthel, S. *Macromol. Biosci.* **2005**, *5*, 520.
6. Barthel, S.; Heinze, T. *Green Chem.* **2006**, *8*, 301.
7. Turner, M. B.; Spear, S. K.; Holbrey, J. D.; Rogers, R. D. *Biomacromolecules* **2004**, *5*, 1379.
8. Zhu, S.; Wu, Y.; Chen, Q.; Yu, Z.; Wang, C.; Jin, S.; Ding, Y.; Wu, G. *Green Chem.* **2006**, *8*, 325.
9. Kosan, B.; Michels, C.; Meister, F. *Cellulose* **2008**, *15*, 59.

10. Fukaya, Y.; Hayashi, K.; Wada, M.; Ohno, H. *Green Chem.* **2008**, *10*, 44.
11. Xu, Q.; Kennedy, J. F.; Liu, L. *Carbohydrate Polymers* **2008**, *72*, 113.
12. Kosan, B.; Michels, C.; Meister, F.; Bauer, R-U. Method for the Production of Multicomponent Cellulose Fiber, International Patent WO 2007/128268 A2, 2007.
13. Fort, D. A.; Remsing, R. C.; Swatloski, R. P.; Moyna, P.; Moyna, G.; Rogers, R. D. *Green Chem.* **2007**, *9*, 63.
14. Kilpeläinen, I.; Xie, H.; King, A.; Granström, M.; Heikkinen, S.; Argyropoulos, D. S. *J. Agric. Food Chem.* **2007**, *55*, 9142.
15. Bagheri, M.; Rodriguez, H.; Swatloski, R. P.; Spear, S. K.; Daly, D. T.; Rogers, R. D. *Biomolecules* **2008**, *9*, 381.
16. Kadokawa, J-i.; Murakami, M-a.; Kaneko, Y. *Carbohydr. Res.* **2008**, *343*, 769.
17. Egorov, V. M.; Smirnova, S. V.; Formanovsky, A. A.; Pletnev, I. V.; Zolotov, Y. A. *Anal. Bioanal. Chem.* **2007**, *387*, 2263.
18. Köhler, S.; Heinze, T. *Cellulose* **2007**, *14*, 489.
19. Miao, S.; Miao, Z.; Liu, Z.; Han, B.; Zhang, H.; Zhang, J. *Microporous Mesoporous Mat.* **2006**, *95*, 26.
20. Gericke, M.; Schlufte, K.; Liebert, T.; Heinze, T.; Budtova, T. *Biomacromolecules* **2009**, in press.
21. Nagieb, Z. A.; Ghazi, I. M.; Kassim, E. A. *J Appl. Polym. Sci.* **1985**, *30*, 4653.
22. Rahkamo, L.; Siika-Aho, M.; Vehviläinen, M.; Dolk, M.; Viikari, L.; Nousiainen, P.; Buchert, J. *Cellulose* **1996**, *3*, 153.
23. Rahkamo, L.; Viikari, L.; Buchert, J.; Paakkari, T.; Suortti, T. *Cellulose* **1998**, *5*, 79.
24. Rahkamo, L.; Vehviläinen, M.; Dolk, M.; Viikari, L.; Nousiainen, P.; Buchert, J. Proceedings of Niches in the World of Textiles, Tampere, Finland, 1996.
25. Struszczyk, H.; Ciechanska, D.; Wawro, D.; Nousiainen, P.; Matero, M. Direct Soluble Cellulose of Celsol: Properties and Behaviour, In *Cellulose and Cellulose Derivatives*; Kennedy, J., Ed.; Woodhead Publishing: Abington, MA, 1995; p 29.
26. Vehviläinen, M.; Nousiainen, P.; Struszczyk, H. Proceedings of Niches in the World of Textiles, Tampere, Finland, 1996.
27. Rosenberg, P.; Rom, M.; Janicki, J.; Fardim, P. *Cell. Chem. Technol.* **2008**, *42*, 293.
28. Rom, M.; Janicki, J.; Rabiej, S.; Slusarczyk, C.; Vehviläinen, M.; Nousiainen, P.; Ciechanska, D.; Wawro, D. Proceedings of Polymer Fibres Conference, Manchester, UK, 2006.
29. Maier, G.; Zipper, P.; Stubicar, M.; Schurz, J. *Cell. Chem. Technol.* **2005**, *39*, 167.
30. Kasaai, M. R. *J. Appl. Polym. Sci.* **2002**, *86*, 2189.
31. Heywood, R. J.; Emsley, A. M.; Ali, M. *IEE Proc.-Sci. Meas. Technol.* **2000**, *147*, 86.
32. Stegmann, V.; Massonne, K.; Maase, M.; Uerdingen, E.; Lutz, M.; Hermanutz, F.; Gaehr, F. German Patent DE 10 2005 062 608 A1, 2007.

33. Rosenberg, P.; Suominen, I.; Rom, M.; Janicki, J.; Fardim, P. *Cell. Chem. Technol.* **2007**, *41*, 245.
34. Hindeleh, A. M.; Johnson, D. J. *J. Phys. D* **1971**, *4*, 259.
35. Hindeleh, A. M.; Johnson, D. J. *Polymer* **1978**, *19*, 27.
36. Rabiej, M. *Polimery* **2002**, *47*, 423.
37. Scherrer, P. *Nachrichten von der Gesellschaft der Wissenschaften zu Göttingen, Mathematisch-Physikalische Klasse* **1918**, *2*, 98.
38. Roy, C.; Budtova, T.; Navard, P. *Biomacromolecules* **2003**, *4*, 259.
39. Gavillon, R. Ph.D. Thesis, Ecole des Mines de Paris, France, 2007.
40. Budtova et al. in this book
41. Araki, J.; Wada, M.; Kuga, S.; Okano, T. *Colloids Surf., A* **1998**, *142*, 75.
42. Ioelovich, M.; Leykin, A. *Cell. Chem. Technol.* **2006**, *40*, 699.
43. Egal, M.; Budtova, T.; Navard, P. *Biomacromolecules* **2007**, *8*, 2282.
44. Egal, M. Ph.D. Thesis, Ecole des Mines de Paris, France, 2006.
45. Isogai, A.; Atalla, R. H. *Cellulose* **1998**, *5*, 309.
46. Ciolacu, D.; Popa, V. I. *Cell. Chem. Technol.* **2005**, *39*, 179.

Chapter 13

Non-Halide Ionic Liquids for Solvation, Extraction, and Processing of Cellulosic Materials

Michael Hummel^{1,3,5}, Gerhard Laus¹, Alexander Schwärzler¹, Gino Bentivoglio^{1,3}, Egon Rubatscher^{1,3}, Holger Kopacka¹, Klaus Wurst¹, Volker Kahlenberg², Thomas Gelbrich¹, Ulrich J. Griesser¹, Thomas Röder⁴, Hedda K. Weber³, Herwig Schottenberger¹ and Herbert Sixta^{5,*}

¹Faculty of Chemistry and Pharmacy, University of Innsbruck, Innsbruck, Austria

²Institute of Mineralogy and Petrography, University of Innsbruck, Innsbruck, Austria

³Competence Centre of Wood Composites and Wood Chemistry K-Plus, Linz, Austria

⁴Lenzing AG, Department of Pulp Research, Lenzing, Austria

⁵Department of Forest Products Technology, Helsinki University of Technology, Espoo, Finland
*h.sixta@lenzing.com

This article gives a comprehensive overview of the relevant literature with respect to recent developments and potential uses of halide-containing and, preferably, halide-free ionic liquids (ILs) in the field of polysaccharide chemistry and engineering, and then proceeds to forthcoming concepts in industrial processing of (ligno)cellulosic materials. In addition, selected new halide-free ILs are described.

Introduction

The collective term ‘ionic liquids’ (ILs) covers members of different ‘substance classes’ by only two – at the first glance perplexing – chemical and

physical properties, namely their ionic constituents, accompanied by a near room temperature liquidus range.

These general demands can be met by compounds of extremely high structural diversity, thus stimulating their exploration with respect to countless applications in chemistry, materials science and engineering.

Due to their unique solvent properties, suitable ILs have also been recognized and investigated for their potential as innovative process media in the field of carbohydrate research, especially and with escalating interest for industrially relevant renewable polysaccharides, allowing for a wide window of chemical and technical opportunities (1).

Structure optimization of ILs suitable for solubilization, functionalization, reconstitution-reshaping and composite formation of cellulose and related feedstocks was originally focused mainly on halide and pseudohalide-based systems. However, their handling suffers from an adverse corrosion profile and melting points usually above ambient temperature (2). In any case, the search for safer and more convenient alternatives to the established direct solvent *N*-methylmorpholine *N*-oxide (NMMO) has stimulated structure screening, toxicity assessments, and the development of efficient recycling of ILs, respectively (3), although the usually higher shear viscosity remains a significant disadvantage compared to NMMO systems (4).

On the other hand, the manufacture of multi-component fibers is expected to predominantly rely on the implementation of IL-based spinning processes (5).

In general, the multi-ton-accessibility of low-cost ILs which combine a technical advantage with being environmentally benign remains the key precondition to enter the market place as the basis of profitable innovations (6) with 'green engineering liquids' (7).

ILs as Direct Solvents for Cellulosic Biomass

As stated above, halide- and pseudohalide-based ILs were the first identified to exhibit the necessary anion hydrogen bond basicity to effectively break the hydrogen bonds responsible for the strength of the cellulose macrostructure in the order $\text{Br}^- \cong \text{SCN}^- > \text{Cl}^-$. Recently, also dialkylimidazolium fluorides were envisaged supplementarily, but under the aspect of eventual large scale use in biomass processing, the uncertainties of their exact composition and the delicacy of handling liquid hydrogen fluoride were argued to restrict such concepts (8).

As already mentioned, the substitution pattern of the organic cations is of course crucial to the required dissolution power of ILs, as exemplified by 1-allyl-3-methylimidazolium chloride (AMIM Cl), the first functionalized IL introduced as a direct cellulose solvent (9).

In addition to their corrosive behaviour, ILs with the spherical halide anions, tend to have melting points fairly above room temperature (2), which is considered a further disadvantage for industrial applications. Only a very few examples of genuine chloride-based room temperature ILs exist, such as

1-allyl-3-butylimidazolium chloride (ABIM Cl) (10), which has been shown to dissolve cellulosic materials in a technically relevant amount (11).

Even the aforementioned 1-allyl-3-methylimidazolium chloride, with its appraised high cellulose solubility and comparably low viscosity (12), has to be classified, partly depending on its purity, as a metastable subcooled melt at room temperature (10).

Based on systematic theoretical considerations, the solvation ability of ILs as direct solvents for various natural non-carbohydrate polymers, e.g. silk fibroin, wool keratin, and blends of these materials, is mainly attributed to electrostatic interactions (13).

ILs as Matrixes for Derivation, Reconstitution, and Degradation of Cellulosic Materials

Parallel to solvation ability characterizations, ILs as hitherto unconventional solvents have also been introduced for homogeneous modification chemistry, predominantly acylations (14–17) with acetylation being one of the most important commercial derivations of cellulose (18).

ILs have also been used to determine the degree of esterification in cellulose fibers by an ATR-FT-IR-based method (19).

Interestingly, utilization of the teenage RTIL 1-ethyl-3-methylimidazolium acetate (20), the first superior substitute (2) of all halogenide-containing ancestors, gave rise to an unexpected interference. Attempted 2-furoylations, tosylations and tritylations by means of the respective chlorides resulted in the formation of pure cellulose acetate, which was suspected to proceed via intermediate mixed anhydrides (21).

Recently, mono-4-methoxytritylation in AMIM chloride was introduced as a new protection group strategy for cellulose (22).

Due to the high hygroscopicity of many IL-based cellulose solvents, residual or adventive water, which is said to be detrimental for the achievement of high cellulose concentrations, may compete with the polymer to consume the respective acylation reagents, thus affecting the degree of substitution and, additionally, by the liberation of acid, the degree of polymerization (23).

On the other hand, protic IL-water and IL-methanol mixtures, mainly based on EMIM carboxylates or chloride, respectively, have been claimed not to require complete removal of water in recycling steps (24). Moreover, such cellulose solutions are leading to non-fibrillating fibers reconstituted by the respective spinning processes (25).

Upon the addition of pyridine in direct homogeneous acylations of wood-based lignocellulosic materials in ILs, any extended degradation could be avoided. In contrast, base-free addition of isocyanates allowed access to highly carbanilated products (26). Cellulose from corn husk, dissolved in AMIM chloride, was subjected to homogeneous one-step acetylation with acetic anhydride without any catalyst (27).

Water soluble, low-substituted cellulose sulfates (CS), exhibiting heparinoidal and antiviral properties, (14) are favorably accessible by esterification in ILs (BMIM chloride, AMIM chloride, EMIM acetate) and, optionally, in IL-mixtures with aprotic cosolvents (28–30). CS was proven to be suitable for polyelectrolyte complex formation that possess potential for the microencapsulation and immunoisolation of biological matter (29).

Trimethylsilylation of cellulose was accomplished in different imidazolium systems, with the degree of substitution depending on the anion type of the IL (31, 32). Organic co-solvents were used to adjust the solubility of the reactants, and pure cellulose nanoparticles could be obtained by dialysis against water (31).

The intention of benzoylating and lauroylating spruce thermochemical pulp was to establish a new technological platform. The resulting stability-enhanced thermoplastic wood composites can improve the compatibility between the wood-based lignocellulosic materials and polystyrene or polypropylene composite filaments (33, 34).

Cellulose-IL composites have been prepared by in-situ polymerization of a polymerizable IL in cellulose solution (35).

Ultrasound-promoted dissolution of different natural sources of cellulose (microcrystalline, Kraft pulp, cotton linter), allowed dramatic enhancements. Significant differences were observed, depending on the type of cellulose and IL applied, with AMIM chloride yielding the highest solute load. In a subsequent process, carboxyethylation and carboxypropylation experiments have been reported in this study, however, only with halide-containing imidazolium salts (36).

AMIM chloride was also applied for electrospinning experiments of native cellulose. The negligible volatility and the relatively high viscosity of ILs and, in particular, the even higher viscosity of their cellulose solutions is a disadvantage for electrospinning purposes and requires thorough experimental tuning by using DMSO as a cosolvent and optimization of the collection method (37).

Magnetically responsive cellulose fibers (38), films, floes, or beads (39) have been prepared by embedding magnetite particles.

In cellulose-heparin composite fibers, the anti-coagulant activity of the enzyme remained unaffected after the electrospinning process from the ILs EMIM chloride and halogen-free EMIM benzoate (40). Composite films prepared from cellulose, starch and lignin have been prepared in AMIM chloride (41).

A flexible gel material was obtained from 15 % (w/w) solutions of cellulose in 1-butyl-3-methylimidazolium chloride (BMIM Cl) (42) by gradual absorption of water. From BMIM chloride and EMIM acetate, gel forming fibers of carboxymethylcellulose, suitable for use in wound care, could be spun and electrospun, respectively (43).

In polymer gels based on IL-matrixes, the swelling/shrinking behaviour can be observed reversibly in an open environment without the need to consider solvent evaporation, which is a serious drawback of conventional smart gel materials (44).

Dispersed enzymes introduced into cellulosic matrixes can also be formed into membranes. Enzyme-encapsulated films with the active ingredient recoated with a second, hydrophobic IL prior to dispersion in the cellulose/IL solution, can provide an increase in activity relative to that of untreated films by providing a stabilizing

microenvironment, as exemplified for laccase (45), for which, preferably, a surface immobilization approach was reportedly successful as well (46). The feasibility of encapsulation of an antibiotic drug into a porous cellulose-hydroxylapatite matrix reconstituted from BMIM chloride was examined recently (47).

Regeneration of cellulose from ILs was also found to be beneficial for an accelerated enzymatic hydrolysis, which is of relevance for the efficient conversion of lignocellulosic materials into fuel ethanol.

Cellulase showed higher thermostability in the presence of regenerated cellulose, but its deactivation by ILs required their complete removal prior to fermentation (48).

Therefore, enzyme-compatible ILs with alkoxyalkyl-functionalized imidazolium salts, including halide-free, namely acetate- and formate-based task-specific ILs (TSILs) have been designed (49), and patented as well (50).

According to a newly introduced refoldability index, ILs of the protic subclass (PILs) have a pronounced stabilizing action to enzymes (51).

If ILs are hydrated, they maintain – with the exception of cellulose processing – the basic properties of ILs, but a small amount of water is able to facilitate protein solubilities while retaining their activity, which allowed the biocatalytic oxidation of cellulose (52).

The acidic depolymerization of lignocellulose in ILs was accomplished by addition of mineral acids (53), strong organic acids (54), or the use of the intrinsically acidic IL BMIM hydrogen sulfate (55). This objective was also conveniently achieved by the treatment with macroreticulated styrene-divinylbenzene resins grafted with sulfonic acid functional groups (56).

The disintegrative liquefaction of wood has been studied in bisimidazole-based ILs, e.g. 3,3'-Ethane-1,2-diylbis(1-methyl-1H-imidazol-3-ium) tetrachloroaluminate. The liquid/wood ratio and the amount of aluminum chloride, which plays a dual role as a catalyst and a liquefaction reagent, were found to affect the liquefaction rate (57). Furthermore, the conversion of carbohydrates to value-added chemicals, including furans, useful as intermediates or feedstocks, by the utilization of further metal halide-based Lewis acid catalysts in ILs was claimed recently (58).

The acid-catalyzed hydrolysis of cellulose in EMIM chloride was subjected to kinetic modelling, which revealed that the rate of the two competing reactions, polysaccharide hydrolysis and sugar decomposition, vary with acid strength, allowing hydrolysis to be performed with a high selectivity in glucose. With soluble cellulose, xylan, and lignocellulosic biomass, bond scission occurred randomly along the polymer chains, in contrast to end-group hydrolysis observed with aqueous acids (59).

Intentionally, the controlled pyrolytic degradation of cellulose was demonstrated in recoverable dicationic imidazolium ILs to form anhydrosugars (60). Lignocellulosics have been subjected to pyrolysis in BMIM and AMIM chloride, respectively (61).

In contrast to the promising experiences and developments with cellulosic substrates, the characterization of the changes in structure and properties of starch microdispersions in BMIM chloride prompted the investigators to assess only limited applicability as a solvent (62).

General systematic considerations of the dissolving power of BMIM and related salts for polymers led to the following conclusions: they do not represent advantageous solvents for most synthetic polymers, but they do dissolve natural polymers characterized by a large number of H-bridging moieties in the supramolecular framework up to high concentrations. The dissolving power is a function of the anion and the value of the negative charge on its electron-donor sites. ILs containing acetate anions dissolve natural polymers better than their chloride-based counterparts. As also expected, an increase in the length and number of hydrophobic alkyl chains alters the charge distribution in the imidazolium cation and increases the hydrophobicity of the IL. Substitution patterns markedly influence the strength of cation-anion interactions, and higher substitution is accompanied by a decrease in the dissolving power for natural polymers. The aprotic organic solvents DMSO and DMF as diluents of ILs are lowering the dissolving power of imidazolium chlorides and acetates as well, but they affect it differently, with DMF allowing for significantly higher concentrations of cellulose and fibroin in binary mixtures. Cellulose dissolves in binary mixtures of BMIM chloride containing up to 50 wt.% DMF and up to 30% DMSO; for BMIM acetate the limits are 80% and 70% respectively. The observed effects have been attributed to the fact that DMF competes less with the IL for formation of hydrogen bridging with cellulose in comparison to DMSO (63).

Tailoring a new class of ILs as potential solvents for cellulose and related materials under mild conditions crucially depends on the selection of the anionic component (64). New anions acting as strong hydrogen-bonding acceptors were introduced and now begin to replace the chloride salts (the first generation of IL-based polysaccharide solvents).

A series of carboxylate-based ILs are forming low viscosity liquids at room temperature. These ILs were found to be effective in dissolving the same amount of cellulose at lower temperature in comparison to chloride salts. For example, the formate anion forms ILs with low viscosity that dissolve cellulose under mild conditions (65). As mentioned, hydrogen-bonding basicity is necessary to dissolve cellulose in order to weaken the inter- and intramolecular hydrogen bonds of the biopolymer. Solubilization of cellulose was improved with these carboxylates. In order to dissolve 10 wt.% cellulose, BMIM chloride must be heated to 85 °C, whereas BMIM formate dissolves it at 35 °C. Since, according to spectroscopic polarity measurements, the BMIM pivalate salt exhibited higher hydrogen-bond basicity than any other carboxylate salt, it was expected to dissolve cellulose readily, but the solubilization temperature of cellulose in this pivalate was higher than that for other ILs evaluated. Evidently, the alkyl chain of carboxylate anions also significantly effects the dissolving power (64).

In order to obtain an IL with lower viscosity, the new AMIM formate was introduced. It exhibits low viscosity (66 cP at 25 °C) and strong hydrogen-bond basicity, and cellulose could be dissolved in high concentrations under very mild conditions (64). On the other hand, AEIM acetate **10** showed disappointing results (see experimental part).

In spite of their strong hydrogen-bonding basicity and potential to solubilize cellulose, carboxylate salts display relatively poor thermal stability. To overcome these drawbacks, an entirely new class of easily preparable and thermally stable

ILs having sufficient polarity to dissolve cellulose, namely alkyl phosphate and alkyl phosphite type ILs, have been introduced (66). EMIM diethyl phosphate has been shown to be compatible in the acetoacetylation of cellulose via alkylketene dimers (67), and trimethylsilylation with hexamethyldisilazane (32).

Because of their importance as new hydrophilic, halide-free ILs with low price, excellent thermal and hydrolytic stability (68), low toxicity and corrosiveness, EMIM dimethyl phosphate, and related ILs have been studied with respect to vapor pressure characteristics in binary solvent mixtures (69). In addition, the influence of water on the dissolution of cellulose in 1,3-dimethylimidazolium dimethyl phosphate and other ILs was investigated by turbidity measurements in order to distinguish between real dissolution and fine dispersion (70), which should also be considered for the spinning behaviour of cellulose solutions containing protic additives (25). BMIM dimethyl phosphate was also identified as the most suitable IL as solvent for headspace gas chromatographic analysis of residual solvents with very low vapour pressure in pharmaceutical final dosage forms, which commonly rely on excipients containing substantial amounts of carbohydrate derivatives (carboxymethyl-cellulose, guar flour, and corn starch). This unique IL allows the complete dissolution of whole tablets without the necessity of any previous extractive sample preparation and showing by far less matrix interference than BMIM acetate (71, 72). Starting from dimethyl ethyl phosphate and BMIM chloride, one methyl group is selectively replaced, representing an easy access to the room temperature IL BMIM ethyl methyl phosphate **6** with its very aspherically shaped anion (71).

A higher solubilization of cellulose under microwave conditions (14%) versus EMIM acetate (8%) was also reported for (commercial) EMIM diethyl phosphate. The observed coloration of acetate-based ILs was interpreted as an indication of concomitant degradation (73). BMIM acetate was reported to dissolve cellulose to a level of 12 % (73), but the results published for BMIM acetate are contradictory. It was proposed in an earlier paper as an extractant for lignin and it was stated that at the same time “cellulose” dissolves neither at room temperature nor with heating (74). This indicates the importance of specifying all carbohydrate polymers under investigation, and to be aware that comparing results from different origins can only be conclusive – if at all – on a qualitative level. In particular, varying water contents are severely impacting the physical parameters of ILs (70). The resulting solutions or dispersions of polysaccharides, their concentration and molecular weight greatly influence the rheological behaviour, such as viscoelasticity (75). Expectedly, the same applies for the presence of controlled amounts of lignin and hemicellulose (76). For different celluloses in EMIM acetate, the rheological properties have been studied within a large range of concentrations (0-15%), and compared to cellulose dissolved in other solvents (77).

Purity specifications for ILs (78) are of tremendous relevance in the field of cellulose research since side reactions can be induced by residual impurities.

ILs with 1-alkyl-3-methylimidazolium cations are no inert cellulose solvents (79). They react at C-2 with cellulose at its reducing end, forming a carbon-carbon bond. This reaction is strongly catalyzed by bases, such as the commonly present imidazole and methylimidazole (80). This also has to be considered

for high-throughput screening of ILs dissolving (ligno-)cellulose where, after a predrying step of the hygroscopic salts, EMIM acetate, meanwhile patented for the fractionation of lignocellulosic materials (81), was ranked best to dissolve specified brands of cellulose, whereas AMIM chloride proved to be most effective in dissolving (again specified) wood chips (82).

In this context, theoretical approaches like molecular simulations of solubilization dynamics and equilibria (64, 83) and as a further physically well founded computational approach which is independent of experimental data, COSMO-RS (conductor-like screening model for real solvent) provide valuable insights to IL-carbohydrate systems (84). However, for the crucial demands of value-adding industrial processes depending on real-world materials, predominantly empirical practice and experimental science has to pave the way towards customizable extraction and separation methodologies. No question, that even the trivial combination of ‘successful’ cationic and anionic lead structures often results in expedient ILs. It is therefore not surprising that AMIM dimethyl phosphate **8** has been verified to dissolve cellulose (see experimental section).

A current review is distinctly dedicated to the interaction of ILs with cellulose, with particular emphasis on the relationship between dissolving ability and the structure of the anions and cations (85).

ILs as Fractionation Auxiliaries for (Ligno)cellulosic Materials

As generally desired for the characterization of complex mixtures from biogenic sources, the non-destructive fractionation of the various wood or carbohydrate-relevant biomass components still remains a challenge. The development of analytical procedures requires care to preserve the native structure during extraction, as knowledge of the native structure is vital for designing the all-important clean and efficient fractionation process (86). In the case of technical fractionation of renewable bioresources by means of ILs, such a feedback will also benefit state-of-the-art structure optimization of task-specific ILs or mixtures thereof. The same applies for the mechanistic investigation of undesired or intentional degradations. In order to better understand lignin decomposition pathways, unstable intermediates have been identified in ILs (87).

EMIM chloride was reported to be an effective solvent and reagent for the liquefaction of wood components and subsequent depolymerization thereof (88). The first successful or, in other words, the complete dissolution of wood chips and sawdust without prepulping procedures or pressurization (89) was performed in the ‘classic’ halide-based ILs BMIM and AMIM chloride. It was noticed that in addition to the particle size, the water content of wood samples plays a key role in determining its solubility in ILs. Water was found to significantly reduce the solubility in ILs. The selected imidazolium halides allowed the conversion to peracetylated wood derivatives, entirely soluble in chloroform, thus offering a range of new possibilities for structural characterization and quantification of the individual components without the need of their prior isolation (90). Alternatively, transparent amber solutions of wood could be obtained when the

same lignocellulosic samples were dissolved in 1-benzyl-3-methylimidazolium chloride. This realization was based on a designed interaction of the aromatic substituent of the IL-cation with the lignin constituents in the wood (90). A similar rationale was realized by the extraction of lignin from lignocellulose using alkylbenzenesulfonate ILs with arene-aromaticity embedded into the anionic part (91).

In summary, the solubility of lignin is principally influenced by substitution patterns of the cationic components and the nature of the anions as well, as evidenced by comparison of MMIM and BMIM methyl sulfates with its halide counterparts, along with the weakly coordinating anion hexafluorophosphate, resulting in the order $\text{MeSO}_4^- > \text{Cl}^- \cong \text{Br}^- \gg \text{PF}_6^-$ (92).

Recent efforts to entirely dissolve wood have been reported concurrently (82, 88, 93). As mentioned before, EMIM acetate was identified as the superior direct solvent for cellulose, and AMIM chloride to be most effective in dissolving wood (82). On the other hand, complete dissolution and partial delignification of wood in EMIM acetate was described as working better than in BMIM chloride. In addition, it has been shown that variables such as type of wood, initial wood load, and particle size affect dissolution and dissolution rates (93), which obviously makes any direct comparison arguable. Carbohydrate-free lignin and cellulose-rich materials could be obtained by using reconstitution mixtures such as acetone/water 1:1 v/v. An increased degradation of both the IL and cellulose was observed with prolonged heating time (93).

Further Perspectives and Concepts

As outlined above, the application of ILs, halide-containing and, with growing importance, halide-free, has opened new avenues for the efficient utilization of lignocellulosic materials in such areas as fractionation, preparation of cellulose composites and derivatives, analysis (94) and biorefinery concepts, emphasizing other value-added chemicals besides fuel (93).

However, there are still many challenges remaining in putting these potential applications into practical use. In particular, fractionation of lignocellulosic materials is essential for some important applications, such as paper manufacture, and in their conversion into basic chemical feedstocks (94).

Based on the results of IL-research achieved so far, it seems self-evident that the systematic implementation of optimized (95) multi-component IL/IL-based and also IL/VOC-based (volatile organic compounds) extractants is overdue, with the whole plethora of possible permutations remaining to be explored.

Imidazolium-ILs will certainly stand the test of time and continue to dominate the field, but other binary IL/VOC alternatives, such as choline-based/urea eutectics are proven options, e.g. for the cationic functionalization of cellulose (96). Of course, eutectic mixtures have the additional advantage that individual constituents with higher melting points may be included.

Other ILs which dissolve lignocellulosic materials and do not contain imidazolium cations, in particular amidinium salts (chlorides, mesylates,

formates, tosylates, trifluoroacetates, saccharinates, hydrogensulfates, lactates, thiocyanates, trifluoromethanesulfamates, acetates, dimethyl phosphates) derived from alkylated diazabicycloundecene (DBU) have also been demonstrated to be tailorable for technical fractionation purposes (97).

N-allyl-*N*-methylmorpholinium chloride is patented as a cellulose cosolvent (98). Arene sulfonates of trihexyltetradecylphosphonium, quarternary ammonium, and pyrrolidinium-based ILs have also been utilized as extractants of lignin from biomass such as wood chips or bagasse (99). Tetrabutylphosphonium alaninate was reported to dissolve cellulose scarcely in the range of 1% (100).

The more functionalities that are embodied in a molten salt, the more likely a higher melting point and viscosity are to be expected due to collateral modes of molecular interaction. Nonetheless, functionalized protic ILs (PILs) (101), in particular the scarce examples of ILs bearing an additional protonable site (102), have also been considered for cellulose processing (103), see also Figure 6.

Admixture of the free base 1-methylimidazole to ILs (BMIM chloride and acetate) has been claimed to beneficially influence dissolution rate, liquidus range, and viscosity of the respective cellulose solvation systems (104). Incomplete, serendipitous quarternization of methylimidazole by allyl chloride to form an analogous “cocktail” containing 25% of unreacted methylimidazole in AMIM chloride led to similar findings (105), so one can suspect that crude ILs were responsible for the emergence of this patented invention (104). In any case, the aforementioned base-catalyzed degradation of cellulose in imidazolium-IL/imidazole mixtures (80) may be assessed as either desirable or unwanted.

Intriguingly, by systematic alteration of the parent ions or judicious coupling of cation and anion partners, one has the ability to, in principle, fine-tune solvent properties such as viscosity, melting point, density, refractive index, polarity, and water miscibility, creating designer solvents at will. This suggests the possible use of such mixtures in the design and optimization of advanced media for separations or chemical processing (106). The prophetic remarks mentioned above were stated at a time, when the utilisation of IL/IL or IL-cosolvent mixtures, modified by rational design for the selective extraction of lignocellulosic constituents, was still in its infancy. This logical anticipation has been verified by an overwhelming number of sometimes redundant patent applications.

Paul Walden (107) was not the first scientist describing ILs (10, 101), but he was the first who sought and found what he had targeted. Furthermore, the now generally accepted definition of ILs as pure salts with melting points below 100 °C can also be ascribed to this famous physicochemist (108).

Curiously, BMIM chloride, the formerly well-recognized solvent for cellulose (11), can render a last service of amusement before it will eventually be replaced like other imidazolium halides in favour of second and third generation carboxylates and dialkyl phosphates. It can be viewed as leading to a funny dilemma: one polymorph of this substance with a reported melting point of 104.6 °C (109) or 104–105 °C (110), respectively, is by definition not an IL, but another polymorph exhibiting a melting point of 79°C (111) fulfills the ‘IL-criterion.’

Complementary Spectroscopic Tools for the Direct Analysis of ILs and IL-Based Solutions of Lignocellulosic Materials

Beside the established spectroscopic NMR methods (112), advanced NMR techniques, including heteronuclear NMR (86) and isotope labelling of IL constituents (113), have been developed in order to get better insight in solution/interaction phenomena of (ligno)cellulosic materials and their derivatives, in IL solutions. APT NMR spectroscopy (attached proton test) is of special significance (114), since the acidic imidazolium proton at position C-2 may otherwise lead to false interpretations, e.g., the assumption of carbene formation, or immediate exchange with NMR solvents (114).

The imidazolium C-2-protons are also capable of aromatic π -interactions, for example with phenyl rings of the tetraphenylborate anion, in the solid state (confirmed by X-ray structure determinations), and in solution, as evidenced by the shielding in $^1\text{H-NMR}$, and confirmed by NOE NMR experiments (115).

Analytical Concepts To Correlate Solvation Ability and Polarity

Electrospray ionization mass spectrometry (ESI-MS) measurements applied to ILs, allowed for the establishment of cation-anion interaction scales (116). Based on the observation that ILs formed cationic and anionic supramolecular aggregates, a scale of the respective cation-anion interaction strength could be deduced. The qualitative order of intrinsic bond strength to bromide was found to be the following: EMIM > BMIM > *N*-ethyl-*N*-methylmorpholinium > HMIM > OMIM > *N*-butyl-*N*-methylmorpholinium > *N*-butylpyridinium > *N*-butyl-*N*-methylpyrrolidinium > *N*-butyl-4-picolinium > BMMIM > Bu_4N . Similarly, two classes of anions were identified by their interaction energies with BMIM: species tightly coordinated to the cation (including trifluoroacetate, bromide, dicyanamide, and tetrafluoroborate) and weakly coordinating anions (hexafluorophosphate, triflimide). The triflate anion exhibits an intermediate affinity.

In general, the understanding of the solvation principles of ILs, and the relationship between IL structure and solvent polarity is still limited (117). The usual classification criteria used for molecular solvents through various experimental measurements fail to insert ILs into a univocal classification.

In molecular liquids, polarisation is mainly oriental, in contrast to the predominant translational polarisation in ionic solvents (117).

Beside the interpretation of partition methods (118), and dielectric constants (119), the assignment of polarity parameters, extracted from spectroscopic analyses of solvatochromic dyes, are most frequently considered to attribute the polarity of ILs and molten salts. However, this requires some special critical comments. *Polarity* is a general term comprising the overall solvating capacity of a medium. Within molecular solvents the term polarity eludes simple and tidy definition as manifold forces are involved, for example, hydrogen bonding, ionic, dipolar, π - π , n - π , and van der Waals interactions (106). While simple

molecular solvents are frequently limited in the scope (both number and type) of interactions possible with dissolved solutes, ILs, given their structure and diversity, are capable of multiple interactions (106). The scenario becomes even more complicated within ILs as both the cation and anion can have their own distinct interactions; in this sense, a pure IL can be considered a binary mixture (106). While the response from a single probe is essentially an ensemble- or time-average of all possible solute–solvent interactions, the behavior is sometimes dominated by a specific type of interaction (106).

Therefore, any single-parameter approach is unable to dissect *polarity* into its unique individual contributions (106).

Solvatochromic studies of IL/IL binary mixtures underscored the prevalence of hydrogen bond donor and competitive anion coordination effects (106). Investigations of IL/organic mixtures have shown that the polarity of ILs remains largely unaffected by organic cosolvents. In other words, the spectroscopic Kamlet-Taft parameter probes (106) are preferentially solvated by the ILs. However, more specific solvation forces, such as hydrogen bonding, can be influenced indirectly by the strength of the anion–cation interactions, giving counterintuitive results (120).

Photochromism, probed by spiropyrans in a series of dialkylimidazolium carboxylates, was also confirmed to depend strongly on polarity properties and structural details of the ILs (121).

Meanwhile, for highly polar nonhalogen ILs capable of dissolving carbohydrates, e.g. formates (65) and aminocarboxylates (122), specifically the Kamlet-Taft β -parameter (hydrogen bond-accepting ability) has been invoked to specify patent claims (123).

After all, it has to be noted that there is still some deficiency concerning measurements of polarity and preferential solvation phenomena of final solutions of cellulosic materials in ILs (124), although a variety of special fluorophoric reagents (80, 125), solvatochromic dyes (126), e.g. to probe halochromism (127), or acidochromism by indicators grafted onto cellulose (128), or indicators especially suited to determine the acid strength in PILs (129), are accessible by very simple and inexpensive synthetic procedures.

This is of significance, since some solution properties as determined by the solvatochromism of dye molecules depend strongly on the structure of the solvatochromic probes. Therefore, it is advisable to determine such parameters by using several different dyes (65).

The use of more solvatochromic probes to characterize the local environment (cybotactic zone) surrounding the probe would be of special importance for multi-component matrixes (lignocellulosic IL-fractions), since certain probe–solvent or probe–cosolute interactions may be favored causing various probes to perceive differently the components of a solvent–solute mixture. For this reason, the observation of preferential solvation (*i.e.*, selective enrichment of certain solvent species within the immediate environment of the probe relative to the bulk) is not uncommon (106, 127). These local mole fraction excursions caused by solvent sorting within the vicinity of a solute are of key importance in governing the efficiency, selectivity, and outcome of a chemical reaction, extraction, or separation. One must also realize that solvent molecules within

the cybotactic zone are acted upon by the field of the solute itself. In this way, an indicator solute can both report on and influence its own environment. For instance, dielectric enrichment is common in the neighbourhood of a dipolar solute (106).

Paradigm Changes for Binary (Ligno)cellulose Extractants

The solvation power of NMMO relatives for carbohydrates is known to be very sensitive to structural variations since its patent filing date (130), and, of course, attempts were made to gain detailed insight into the strength of R–OH···O–N hydrogen bonds and their implications for the dissolution of cellulose in amine *N*-oxide solvents (131).

Wondrous enough, no investigations of combinations of the only hitherto industrially established direct cellulose solvent NMMO with ILs have been reported so far. However, without disclosing a concrete respective example, NMMO was claimed for being a cooperative aprotic swelling agent for the dissolution of lignocellulosics (132).

We anticipated obtaining unexpected outcomes from such a marriage. Likewise, no attempts to synthesize new ILs by alkylation of NMMO have, to our knowledge, been published. The N–O moiety in ILs was appreciated to have never been claimed in patent applications (133). However, very recently even such embodiments have been claimed (50).

In addition, the weak N–O bond provides access to thermally stable, recoverable, yet intentionally degradable ILs, e.g. by hydrogenolysis (134), or degradation under mild alkaline conditions (135), which is of potential relevance for the decontamination of aqueous effluent streams (136). Furthermore, such concepts bear potential for the desired phlegmatization of solvent systems consisting partially of NMMO (see experimental section).

Results and Discussion

Based on the considerations outlined above, we were tempted to investigate the synthesis of new ILs derived from NMMO.

With regard to the known hazards of pure NMMO compared to the less hazardous NMMO hydrates, dialkyl sulfates obviously represent the alkylation reagents of choice, since they are compatible with aqueous reaction conditions due to their preference of amine and *N*-oxide alkylation in favour of R–OH alkylation ($R_3N > R_3N^+O^- \gg R-OH / H_2O$, Figure 1).

However, the resulting methyl sulfates or, after harsh acidic hydrolysis (137), the finally formed hydrogensulfates, are suffering from the need for tedious methods of ion metathesis to access cellulose-relevant ILs (for example via the commonly known precipitation of calcium or barium sulfates, or by means of ion exchange resins).

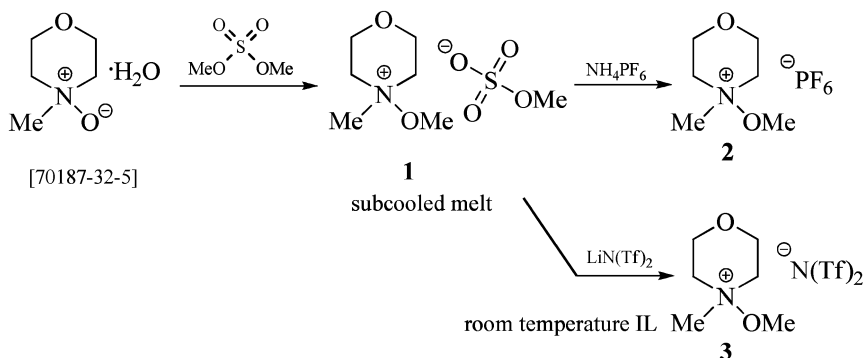


Figure 1. Alkylation of NMMO and subsequent ion metathesis.

The isolation of new quarternary salts by precipitation of the hydrophobic hexafluorophosphates and triflimides (e.g., compounds **2** and **3**), which are likely to be useless for the solubilization of very polar carbohydrate derivatives, is very convenient and justified for supplementary analytical purposes (see also Figure 5).

Dialkyl sulfites represent advantageous substitutes for dialkyl carbonates (8, 138). They (preferably dimethyl sulfite) have been recommended as versatile *N*-quarternization agents (139), since they are more reactive in alkylation and also allow, if required, facile hydrolysis of the primarily formed sulfurous acid monoalkyl esters to sulfur dioxide, which can be subsequently expelled (comparable to carbon dioxide) by the corresponding acid of the anion desired for metathesis.

However, this method is not applicable to NMMO, an oxidant frequently used in organic syntheses (140), and similar amine *N*-oxides, because of the fast preoxidation of dialkyl sulfite to dialkyl sulfate, which finally serves as the effective alkylating species (Figure 2).

Fortunately, this conversion gives the opportunity of in-situ phlegmatization of NMMO and simultaneous introduction of *N,N*-dimethylmorpholinium methyl sulfate, which was previously utilized in a binary IL-water system for determination of the influence of ILs on the activity of chloroperoxidase (141). Thus, a novel customizable binary extractant and reconstitution system is easily available.

The analogous reduction of NMMO with trialkyl phosphites occurs also instantaneously. However, the hereby formed triethyl phosphate showed no subsequent alkylation below 50 °C which would yield the almost thirty year old IL *N*-ethyl-*N*-methylmorpholinium diethyl phosphate (142). It is worth noting, that *N*-ethyl-*N*-methylmorpholinium tribromide, a hydrophobic IL system, is of about the same age (143).

Stability assessments of cellulose solutions in ILs (144), cellulose copolymers synthesized in ILs (145), as well as neat ILs (146, 147), are best conducted by thermoanalytical methods, namely thermogravimetric analysis (TGA), differential scanning calorimetry (DSC) and hot stage microscopy. This applies in particular to hygroscopic or deliquescent ILs, since programmed cycles of water removal

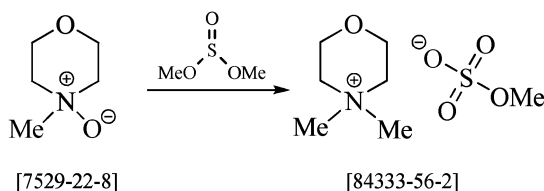


Figure 2. Alkylation of NMMO using dimethyl sulfite.

can be ideally supplemented by the subsequent identification of solid-solid phase transitions prior to melting and decomposition (Fig. 3) (147).

The decomposition is associated with a clear mass loss and occurs in two steps for compounds **1** and **2**. DSC shows that the reaction is strongly exothermic. Compound **3** exhibits the weakest thermolysis. For compound **2**, a trans-formation to a plastic crystalline phase was observed at about 140 °C (see insert in Figure 3b). This was additionally confirmed by X-ray powder diffractometry and hot stage microscopy, which showed a loss of birefringence in this temperature range, indicating the transformation to a cubic phase.

Ironically, crystallography is one of the most powerful tools for the elucidation of intermolecular and interatomic interactions in ILs or low-melting salts (102). Series of related salts of a specific anion (or a cation) have proven to be of particular value for this purpose. By systematically comparing crystal structures that are obtained by varying the respective counterion, it is possible to elucidate the influence of coulombic forces, of steric effects and of heteroatoms with lone pairs as additional hydrogen bond acceptor moieties (HBD basicity) on the overall packing architecture. This approach, supplemented by computational analyses of lattice energies, was used in a study of dialkylimidazolium hexafluorophosphates (148). In conjunction with TG/DSC-studies of the observed phase transitions, it was also employed for *N,N*-di-methylpyrrolidinium, *N,N*-dimethylpiperidinium, and *N,N*-dimethylmorpholinium iodides (149), and quaternary *N*-methylpyrrolidinium chlorides (147).

In the crystal structure of compound **1** (Figure 4), a multitude of short intermolecular CH \cdots O interactions (150), with H \cdots O distances between 2.39 and 2.62 Å and CHO angles between 132° and 160°, arises from the aggregation of cation and anion moieties in the crystal structure. Each cation forms five such contacts to three surrounding methyl sulfate anions (Table I). Moreover, it forms four prominent CH \cdots O interactions with three other cations, each involving an ether oxygen atom (O1, O2).

In the crystal structure of compound **5** (Figure 7), each cation forms nine short CH \cdots O contacts (150) to five surrounding dimethyl phosphate moieties. These interactions are characterized by O \cdots H distances between 2.32 and 2.55 Å and CHO angles between 145° and 164°. They involve alkyl groups (C1, C4, C5, C6) and, significantly, also the allyl residue (C8) of the cation (Table II).

Only two crystal structures of ionic dimethyl phosphates relevant for ILs are currently available for a comparison to compound **5**, namely the ammonium (151) and imidazolium (152) salts.

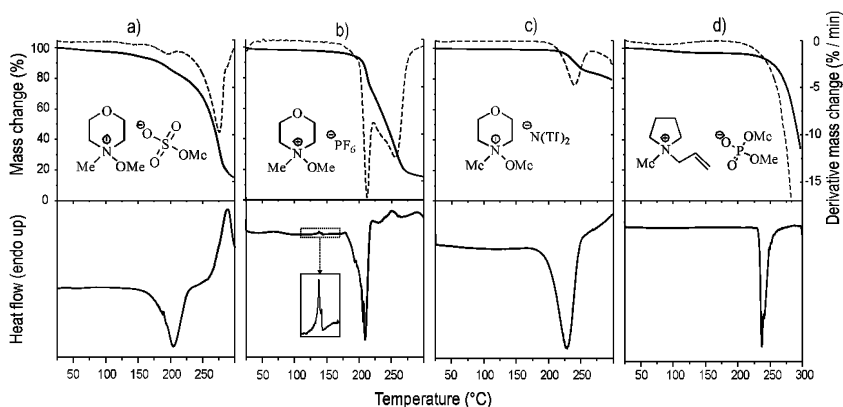


Figure 3. Thermal behaviour and stability of the compounds a) **1**, b) **2**, c) **3**, and d) **5**. The diagrams on top show the TGA curves and the first derivative DTGA curves (dashed lines). The bottom diagrams show the DSC curves (heating rate: 10 K min⁻¹). The insert in the DSC plot b) highlights the transformation to the plastic crystalline state of compound **2**.

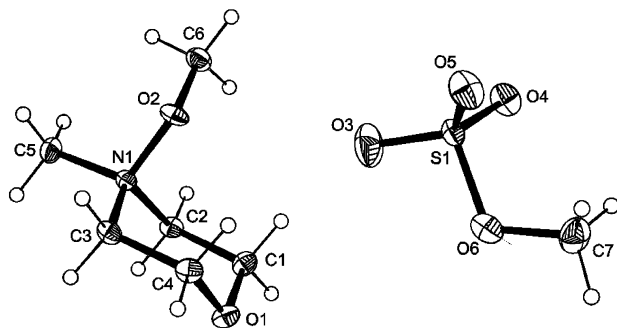


Figure 4. Thermal ellipsoid plot of *N*-methoxy-*N*-methylmorpholinium methyl sulfate **1** at 50% probability level.

In contrast to compound **5**, these cations feature NH groups which can act as hydrogen bond donors. Consequently, classic NH \cdots O bonds between cation and dimethyl phosphate anions dominate the aggregation in these ammonium and imidazole analogues.

Experimental Section

Instrumentation

DSC was performed with a DSC 7 (Perkin-Elmer, Norwalk, Ct., USA). Sample amounts between 2 and 5 mg were used and heated in Al-pans (25 μ l) with perforated lid under a dry nitrogen purge (20 ml min⁻¹). All runs were

Table I. Short CH...O Contacts (Å, deg) in Compound 1

<i>Donor-H...Acceptor</i>	<i>D-H</i>	<i>H...A</i>	<i>D...A</i>	<i>D-H...A</i>	<i>Symmetry code</i>
C1-H1B...O3	0.99	2.50	3.42	154	1-x,1-y,1-z
C2-H2B...O4	0.99	2.47	3.41	160	1-x,1-y,-z
C3-H3A...O2	0.99	2.59	3.33	132	1-x,-y,1-z
C3-H3B...O5	0.99	2.44	3.33	149	1-x,1-y,-z
C5-H5B...O5	0.98	2.45	3.33	149	1-x,1-y,-z
C5-H5C...O4	0.98	2.39	3.30	155	-
C6-H6C...O1	0.98	2.47	3.36	151	-1+x,y,z
C6-H6C...O1	0.98	2.47	3.36	151	-1+x,y,z
C4-H4B...O6	0.98	2.62	3.41	137	2-x,-y,1-z

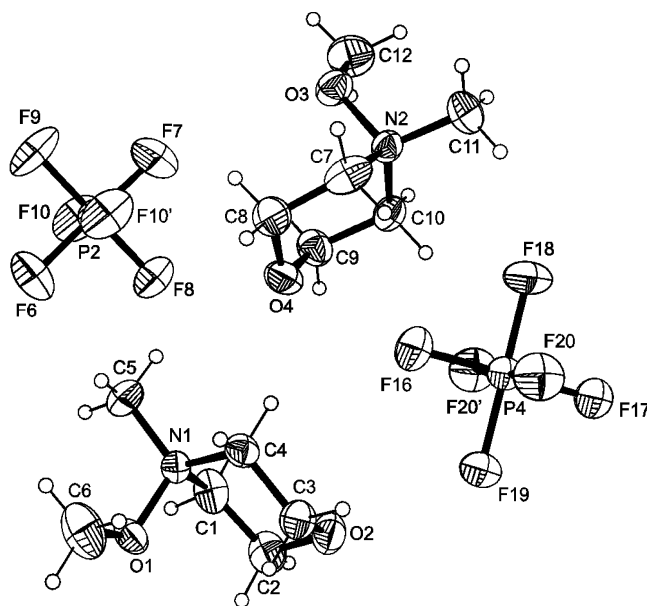


Figure 5. Thermal ellipsoid plot of N-methoxy-N-methylmorpholinium hexafluorophosphate 2 at 50% probability level.

performed at a heating rate of 10 K min⁻¹. The instrument was calibrated for temperature with pure benzophenone (m.p. 48.0°C) and caffeine (m.p. 236.2°C) and the energy calibration was performed with pure indium (purity 99.999%, m.p. 156.6°C, heat of fusion 28.45 J g⁻¹).

TGA was carried out with a TGA7 system (Perkin-Elmer, Norwalk, CT, USA) using 3 to 6 mg of sample in a platinum pan. Dry nitrogen was used as a purge gas (sample purge: 20 mL min⁻¹, balance purge: 40 mL min⁻¹) and the general heating

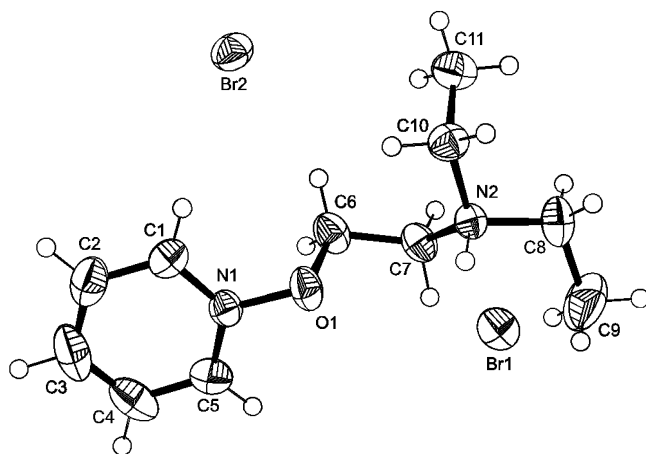


Figure 6. Thermal ellipsoid plot of 1-(2-(*N,N*-diethylamino)ethoxy)pyridinium bromide hydrobromide **4** at 50% probability level, as an example of a protic IL-precursor incorporating the weak *N*–*O* bond.

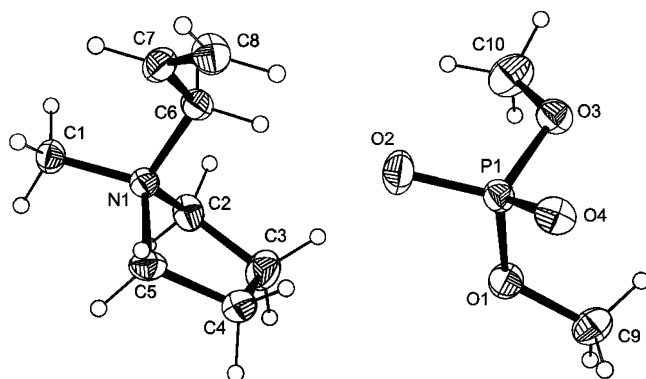


Figure 7. Thermal ellipsoid plot of the novel halide-free, direct cellulose solvent *N*-allyl-*N*-methylpyrrolidinium dimethyl phosphate **5** at 50% probability level.

rate was 10 K min⁻¹. The temperature signal was calibrated with ferromagnetic materials (Alumel and Ni, Curie point standards, Perkin-Elmer).

X-Ray diffraction data were collected on STOE IPDS 2 and Nonius Kappa CCD diffractometers using MoK α radiation.

CCDC 729609–729612 contain the supplementary crystallographic data of this paper (compounds **1**, **2**, **4**, and **5**). These data can be obtained free of charge from The Cambridge Crystallographic Data Centre *via* www.ccdc.cam.ac.uk/data_request/cif.

NMR spectra were recorded using a Bruker AC 300 spectrometer. IR spectra were obtained with a Nicolet 5700 FT spectrometer in ATR mode. All other instrumentation used, has been described in previous communications (133, 134).

Starting Materials

Lithium bis(trifluoromethanesulfonyl)imide was obtained from Solvionic, France. All other chemicals were purchased from Aldrich Chemical Co and used as received.

For preliminary cellulose-dissolving experiments two different types of cellulose were used: FEZ 1167 [Eucalyptus globulus pre-hydrolysis kraft pulp (TCF); purchased from Bahia pulp (Brazil); Mn = 68.800 g/mol; Mw = 200.200 g/mol; intrinsic viscosity ($\eta_{\text{in}}^{\text{en}}$) = 460 ml/g; R18 = 97,4%] and FE 1926 [Eucalyptus globulus kraft pulp (ECF), paper grade; purchased from Ence (Spain); Mn = 61.400 g/mol; Mw = 335.800 g/mol; intrinsic viscosity ($\eta_{\text{in}}^{\text{en}}$) = 817 ml/g; R18 = 91,5%].

N-Methoxy-*N*-methylmorpholinium Methyl Sulfate (1)

Dimethyl sulfate [77-78-1] (2.65 g, 21.0 mmol) was placed in a Schlenk tube under an atmosphere of argon and cooled by means of an ice bath. Anhydrous NMMO [7529-22-8] (2.47 g, 21.0 mmol) was added slowly. Upon complete addition the ice bath was removed and the mixture stirred at r. t. for 14 h to yield 5.10 g of a white viscous liquid (100 % of theory).

Hygroscopic, subcooled melt; occasionally solidifies upon prolonged standing with exclusion of moisture; m.p. of single crystals (Kofler hot stage microscopy under nitrogen; DSC): 58 °C. MS (ESI+): m/z 132.07

^1H NMR (DMSO- d_6): δ 3.39 (3 H, s), 3.50 (3 H, s), 3.81 – 3.86 (11 H, m) ppm. ^{13}C NMR (DMSO- d_6): δ 50.3, 53.5, 55.2, 60.8 (4 C, broad peak) ppm. IR (neat, ATR): 2951, 1462, 1215, 1117, 1057, 991, 867, 743, 609, 576, 552, 496 cm^{-1} . TGA/DSC: see Fig. 3.

Crystal data of **1**: $\text{C}_6\text{H}_{14}\text{NO}_2\text{CH}_3\text{O}_4\text{S}$, $M = 243.28$, triclinic, $P1$, $a = 6.9057(7)$ Å, $b = 8.4882(8)$ Å, $c = 9.5192(7)$ Å, $\alpha = 81.490(7)^\circ$, $\beta = 83.291(8)^\circ$, $\gamma = 87.822(9)^\circ$, $V = 547.94(9)$ Å 3 , $Z = 2$, μ (Mo $K\alpha$) = 0.31 mm^{-1} , $T = 173$ K, $N_{\text{ind}} = 1983$, $N_{\text{gt}} = 1590$, $R_1 [I \geq 2\sigma(I)] = 0.057$, wR_2 (all data) = 0.153.

N-Methoxy-*N*-methylmorpholinium Hexafluorophosphate (2)

A mixture of dimethyl sulfate [77-78-1] (8.06 g, 0.064 mol) and NMMO monohydrate [70187-32-5] (4.36 g, 0.032 mol) was stirred at r. t. for 24 h. NaHCO_3 (2.69 g, 0.032 mol) and 20 ml H_2O were added, and stirring was continued for 3 h at r. t. The product, 4-methoxy-4-methylmorpholinium methyl sulfate, was not isolated, but converted to a hexafluorophosphate. Addition of H_2O (10 ml) yielded a clear solution to which NH_4PF_6 [16941-11-0] (1.31 g, 0.008 mol) was added. The precipitate was ultrasonicated for 1 h, filtered, and dried to yield 0.69 g of the product as a colourless powder (53 % of theory). Single crystals were obtained by slow evaporation of an ACN solution.

Table II. Short CH...O Contacts (Å, deg) in Compound 5

<i>Donor-H...Acceptor</i>	<i>D-H</i>	<i>H...A</i>	<i>D...A</i>	<i>D-H...A</i>	<i>Symmetry code</i>
C1-H1A...O4	0.98	2.43	3.34	153	-x,1/2+y,1/2-z
C1-H1B...O3	0.98	2.59	3.44	146	1-x,1/2+y,1/2-z
C1-H1B...O4	0.98	2.54	3.43	151	1-x,1/2+y,1/2-z
C1-H1C...O4	0.98	2.32	3.27	164	x,1/2-y,1/2+z
C4-H4B...O2	0.99	2.45	3.35	150	-
C5-H5A...O4	0.99	2.58	3.44	145	-x,1/2+y,1/2-z
C6-H6A...O2	0.99	2.49	3.40	154	-
C6-H6B...O4	0.99	2.55	3.41	145	1-x,1/2+y,1/2-z
C8-H8A...O2	0.95	2.38	3.24	151	-
C10-H10B...O1	0.98	2.60	3.52	156	1+x,y,z

M.p. 187-189 °C. ¹H NMR (DMSO-d₆): δ 3.49 (3 H, s), 3.82 (3 H, s), 3.85 (8 H, m) ppm. IR (neat, ATR): 1461, 1296, 1243, 1123, 1087, 1062, 1003, 979, 873, 810, 740, 688, 627, 553, 496, 467 cm⁻¹. TGA/DSC: see Fig. 3.

Crystal data of **2**: C₆H₁₄F₆NO₂P, *M* = 277.15, orthorhombic, *Pnma*, *a* = 12.5019(7) Å, *b* = 13.5717(8) Å, *c* = 26.4160(9) Å, *V* = 4482.1(4) Å³, *Z* = 16, μ (Mo *K*α) = 0.32 mm⁻¹, *T* = 233 K, *N*_{ind} = 2496, *N*_{gt} = 1748, *R*₁ [*I* ≥ 2σ(*I*)] = 0.068, *wR*₂ (all data) = 0.181, see Fig. 5.

***N*-Methoxy-*N*-methylmorpholinium Triflimide (3)**

A mixture of 4-methoxy-4-methylmorpholinium methyl sulfate (5.84 g, 0.024 mol) and lithium bis(trifluoromethanesulfonyl)imide [90076-65-6] (6.88 g, 0.024 mol) in 20 ml H₂O was ultrasonicated for 1 h whereupon a biphasic system formed. The dense phase was isolated via a separatory funnel and the product was dried by means of a vacuum pump to yield 5.9 g of a colourless oil (60 % of theory).

*n*_D²⁰ = 1.4248. ¹H NMR (DMSO-d₆): δ 3.49 (3 H, s), 3.82 (3 H, s), 3.85 (8 H, m) ppm. IR (neat, ATR): 1466, 1347, 1176, 1132, 1051, 1001, 901, 869, 845, 789, 763, 740, 612, 570, 511, 467 cm⁻¹. TGA/DSC: Fig. 3.

1-[2-(Diethylamino)ethoxy]pyridinium Bromide Hydrobromide (4)

A mixture of pyridine *N*-oxide [694-59-7] (3.0 g, 0.032 mol) and 2-(diethylamino)ethyl bromide hydrobromide [1069-72-3] (8.2 g, 0.032 mol) in 30 ml acetonitrile were refluxed for 24 h. The solvent was removed by means of a vacuum pump. Subsequently, the black sticky remainder was washed with diethyl ether for several times, and again dried under vacuum. Afterwards, the crude product was recrystallized from 40 ml acetonitrile. Yield: 31.7 g (93 % of theory).

M.p. 214-216 °C (decomp). ¹H NMR (DMSO-*d*₆): δ 1.27 (6 H, t, *J* = 7.2 Hz), 3.31 (4 H, q, *J* = 7.1 Hz), 3.72 (2 H, t, *J* = 4.0 Hz), 5.11 (2 H, t, *J* = 4.4 Hz), 8.32 (2 H, t, *J* = 7.3 Hz), 8.66 (1 H, t, *J* = 7.8 Hz), 9.67 (2 H, d, *J* = 6.1 Hz) ppm. ¹³C NMR (DMSO-*d*₆): δ 8.99 (2 C), 47.9 (2 C), 49.2, 76.8, 129.8 (2 C), 141.9 (2 C), 146.0 ppm. IR (neat, ATR): 3020, 2966, 2925, 2731, 2658, 2593, 2492, 1471, 1440, 1431, 1396, 1381, 1239, 1174, 1035, 1019, 964, 811, 791, 665, 490 cm⁻¹.

Crystal data of **4**: C₁₁H₂₀Br₂N₂O, *M* = 356.11, triclinic, *P*1, *a* = 7.5599(3) Å, *b* = 7.8231(2) Å, *c* = 12.8945(4) Å, α = 83.003(2)°, β = 83.971(2)°, γ = 88.934(2)°, *V* = 752.73(4) Å³, *Z* = 2, μ (Mo *K*α) = 5.37 mm⁻¹, *T* = 233 K, *N*_{ind} = 3069, *N*_{gt} = 2527, *R*₁ [*I* ≥ 2σ(*I*)] = 0.030, *wR*₂ (all data) = 0.063: see Fig. 6.

1-Allyl-1-methylpyrrolidinium Dimethyl Phosphate (5)

Note: the reaction of quaternary ammonium chlorides with trialkyl phosphates to give alkyl chlorides and dialkyl phosphates has been patented (153), although it has been described earlier (154).

1-Allyl-1-methylpyrrolidinium chloride (147) [1059624-28-0] (26.7 g, 0.165 mol) and trimethyl phosphate [512-56-1] (23.1 g, 0.165 mol) were placed in a round bottomed flask and stirred for 1 hour while the temperature was maintained at 100 °C by means of an oil bath. During this time, vigorous gas evolution was observed. Then, high vacuum (oil pump) was applied for 2 h while keeping the temperature at 100 °C, giving 40.5 g of a slightly yellow liquid (98 % of theory).

Hygroscopic, subcooled melt, occasionally solidifies upon prolonged standing with exclusion of moisture; mp. (Kofler hot stage microscopy under nitrogen): 40-41°C. ¹H NMR (DMSO-*d*₆): δ 2.06 (4 H, m), 3.00 (3 H, s), 3.23 (6 H, d, *J* = 10.3 Hz), 3.49 (4 H, m), 4.07 (2 H, d, *J* = 7.1 Hz), 5.55 (1 H, d, *J* = 10.1 Hz), 5.63 (1 H, d, *J* = 16.1 Hz), 6.06 (1 H, m) ppm. ¹³C NMR (DMSO-*d*₆): δ 21.1 (2C), 47.6, 51.2 (d, *J* = 5.9 Hz, 2C), 62.6 (2C), 64.3, 126.7, 127.2 ppm. IR (neat): 2940, 2832, 1466, 1245, 1181, 1092, 1042, 948, 761, 725, 525 cm⁻¹. TGA/DSC: Fig. 3.

Crystal data of **5**: C₈H₁₆N₂C₂H₆O₄P, *M* = 251.26, monoclinic, *P*₂₁/*c*, *a* = 6.4181(3) Å, *b* = 11.3014(6) Å, *c* = 17.9872(9) Å, β = 95.204(4)°, *V* = 1299.30(12) Å³, *Z* = 4, μ (Mo *K*α) = 0.21 mm⁻¹, *T* = 173 K, *N*_{ind} = 2314, *N*_{gt} = 1868, *R*₁ [*I* ≥ 2σ(*I*)] = 0.041, *wR*₂ (all data) = 0.100.

1-Butyl-3-methylimidazolium Ethyl Methyl Phosphate (6)

1-butyl-1-methylimidazolium chloride [79917-90-1] (20.2 g, 0.116 mol) and ethyldimethyl phosphate [10463-05-5] (155) (17.8 g, 0.116 mol) were placed in a round bottomed flask and stirred for 1 hour while the temperature was maintained at 100 °C. Then, high vacuum (oil pump) was applied overnight while keeping the temperature at 100 °C, giving 31.8 g of a slightly yellow liquid (99 % of theory).

¹H NMR (DMSO-*d*₆): δ 0.87 (3 H, t, *J* = 7.3 Hz), 1.05 (3 H, t, *J* = 7.1 Hz), 1.23 (2 H, m), 1.75 (2 H, m), 3.26 (3 H, d, *J* = 10.3 Hz), 3.61 (2 H, m), 3.86 (3 H, s), 4.18 (2 H, t, *J* = 7.1 Hz), 7.79 (1 H, m), 7.87 (1 H, m), 9.63 (1 H, m) ppm. ¹³C NMR (DMSO-*d*₆): δ 13.3, 16.7 (d, *J* = 6.8 Hz), 18.8, 31.4, 35.6, 48.4, 51.2 (d, *J*

= 5.2 Hz), 59.1 (d, $J = 6.0$ Hz), 122.3, 123.6, 137.2 ppm. IR (neat, ATR): 3046, 2960, 2935, 2874, 2835, 1570, 1465, 1385, 1240, 1175, 1045, 936, 773, 732, 655, 626, 545, 532, 469 cm^{-1} .

1-Allyl-3-butylimidazolium Dimethyl Phosphate (7)

A mixture of 1-allyl-3-butylimidazolium chloride [887276-30-4] (5.99 g, 29.8 mmol) and trimethylphosphate [512-56-1] (4.17 g, 29.8 mmol) was stirred at 100 °C under an atmosphere of argon. After 4 h all volatile compounds were removed by means of a vacuum pump at 80 °C to yield 8.6 g of a slightly brownish viscous liquid (99 % of theory).

$n_D^{20} = 1.4846$. ^1H NMR (DMSO- d_6): δ 0.86 (3 H, t, $J = 7.4$ Hz), 1.22 (2 H, m), 5.98 – 6.1 (1 H, m), 5.98 – 6.1 (1 H, m), 1.76 (2 H, m), 3.27 (6 H, d, $J = 10.3$ Hz), 4.21 (2 H, t, $J = 7.2$ Hz), 4.89 (2 H, d, $J = 5.9$ Hz), 5.28 (2 H, m), 5.98 – 6.11 (1 H, m), 7.85 (1 H, s), 7.96 (1 H, s), 9.77 (1 H, s) ppm. ^{13}C NMR (DMSO- d_6): δ 13.3, 18.8, 31.5, 48.5, 50.7, 51.3 (2 C, d, $J = 5.9$ Hz), 119.9, 122.6, 122.7, 132.1, 136.9 ppm. IR (neat, ATR): 2955, 2938, 2873, 2834, 1563, 1463, 1242, 1174, 1091, 1043, 940, 769, 729, 653, 629, 526, 463 cm^{-1} .

1-Allyl-3-methylimidazolium Dimethyl Phosphate (8)

Note: compound **8** is expressively claimed in a patent application, but was not disclosed as a synthetic example (61).

1-Allylimidazole [31410-01-2] (10.68 g, 98.8 mmol) and trimethyl phosphate [512-56-1] (13.83 g, 98.8 mmol) were placed in a round bottom flask and stirred at 140 °C for 24 hours. Subsequently, high vacuum was applied for 2 h while keeping the reaction mixture at 140 °C affording 23.9 g of a slightly brownish viscous fluid (98 % of theory).

$n_D^{20} = 1.4920$. ^1H NMR (DMSO- d_6): δ 3.28 (6 H, d, $J = 10.4$ Hz), 3.9 (3 H, s), 4.92 (2 H, d, $J = 5.4$ Hz), 5.24 (2 H, m), 6.01 (1 H, m), 7.98 (2 H, broad s), 9.88 (1 H, s) ppm. ^{13}C NMR (DMSO- d_6): δ 35.5, 50.5, 51.4 (2 C, d, $J = 6.3$ Hz), 119.7, 122.5, 123.9, 132.3, 137.7 ppm. IR (neat, ATR): 2941, 2835, 1566, 1454, 1241, 1176, 1090, 1039, 767, 729, 627, 526, 463 cm^{-1} .

1-(2-Hydroxyethyl)-3-methylimidazolium Dimethyl Phosphate (9)

A mixture of 1-(2-hydroxyethyl)imidazole [1615-14-1] (4.92 g, 43.9 mmol) and trimethylphosphate [512-56-1] (6.15 g, 43.9 mmol) was stirred for 3 h in an oil bath kept at 150 °C. Then, the temperature was raised to 170 °C and unreacted reagents were removed by means of a high vacuum oil pump (6 h) to yield 10.9 g of an amber oil (98.5 % of theory).

^1H NMR (DMSO- d_6): δ 3.28 (6 H, d, $J = 10.3$ Hz), 3.67 (2 H, t), 3.86 (3 H, s), 4.23 (2 H, t), 6.39 (1 H, s), 7.73 (1 H, m), 7.79 (1 H, m), 9.39 (1 H, s) ppm. IR

(neat, ATR): 3145, 3075, 2943, 2838, 1570, 1456, 1341, 1231, 1170, 1087, 1035, 874, 776, 733, 653, 623, 527, 463 cm^{-1} .

1-Allyl-3-ethylimidazolium Acetate (10)

A mixture of diethyl sulfite [623-81-4] (21.6 g, 0.153 mol), 1-allylimidazole [31410-01-2] (16.0 g, 0.148 mol), and acetic acid (9.0 ml, 0.157 mol) was stirred under an atmosphere of argon at 100 °C. After 72 h another 1 ml of acetic acid and 10 ml of H_2O were added and the resulting mixture stirred for 24 h at 100 °C to assure complete hydrolysis of excess diethyl sulfite. All remaining volatile compounds were then removed by means of a vacuum pump. After cooling to room temperature, 50 ml of H_2O were added and the resulting aqueous solution extracted with CH_2Cl_2 (10 \times 100 ml) to remove unreacted 1-allylimidazole. The aqueous solution was then dried in vacuum to yield 11.4 g of a slightly brownish viscous liquid (39 % of theory).

$n_{\text{D}}^{20} = 1.5255$. $^1\text{H NMR}$ (DMSO-d_6): δ 1.39 (3 H, t, $J = 7.3$ Hz), 1.81 (3 H, s), 4.21 (2 H, q, $J = 7.3$ Hz), 4.86 (2 H, d, $J = 5.9$ Hz), 5.28 (2 H, m), 5.97 – 6.10 (1 H, m), 7.45 (1 H, s), 7.86 (1 H, s), 9.43 (1 H, s) ppm. IR (neat, ATR): 3093, 2980, 1706, 1645, 1562, 1448, 1423, 1360, 1193, 1163, 1035, 1021, 943, 756, 619, 605, 522, 448 cm^{-1} .

1-(2-Hydroxyethyl)-3-methylimidazolium Acetate (11)

A mixture of glycol sulfite [3741-38-6] (22.9 g, 0.207 mol) and 1-methylimidazole [616-47-7] (8.24 g, 0.100 mol) was stirred under an atmosphere of argon at 90 °C. After 24 h 6 ml of acetic acid and 10 ml of H_2O were added and the resulting mixture stirred for 24 h at 60 °C to assure complete hydrolysis of excess glycol sulfite. All remaining volatile compounds were then removed by means of a vacuum pump to yield 18.6 g of a slightly brownish viscous liquid (100 % of theory).

$n_{\text{D}}^{20} = 1.5175$. $^1\text{H NMR}$ (DMSO-d_6): δ 1.73 (3 H, s), 1.81 (3 H, s), 3.70 (2 H, t, $J = 4.9$ Hz), 3.85 (3 H, s), 4.23 (2 H, t, $J = 4.9$ Hz), 7.69 (1 H, s), 7.74 (1 H, s), 9.22 (1 H, s) ppm. IR (neat, ATR): 3147, 3097, 1736, 1566, 1429, 1385, 1163, 1071, 1023, 865, 736, 650, 621, 605, 521 cm^{-1} .

Preliminary tests of the aforementioned ILs to dissolve cellulose showed good results (<5%) for 1-allyl-3-methylpyrrolidinium dimethyl phosphate (5), 1-butyl-3-methylimidazolium ethyl methyl phosphate (6), 1-allyl-3-methylimidazolium dimethyl phosphate (8), and 1-butyl-3-methylimidazolium dimethyl phosphate [891772-94-4] (68, 153).

N-Methoxy-N-methylmorpholinium methyl sulfate (1), 1-allyl-3-butyliimidazolium dimethyl phosphate (7), and 1-(2-hydroxyethyl)-3-methylimidazolium dimethyl phosphate (9) were able to dissolve cellulose sparingly (< 1%), whereas 1-allyl-3-ethylimidazolium acetate (10) and 1-(2-hydroxyethyl)-3-methylimidazolium acetate (11) did not qualify as solvents for cellulose.

Concluding Remarks

An unparalleled acquisition of essential knowledge was accumulated in the past five years by fundamental IL-research in academic and industrial institutions (2). The outcomes are still snowballing, particularly those dealing with the detailed exploration of ILs for processing onerous polysaccharide sources such as whole wood.

As reviewed above, lots of reports on dissolution of cellulose in ILs and its applications have been published. However, dissolution of wood in ILs is far more demanding due to the complex structure of wood and its three-dimensional lignin network (156).

Everyone who has ever seen giant trunks of log wood disappear in an industrial shredder within seconds will hardly be able to imagine the short term implementation of ILs for large scale processing in wood-reliant and related businesses, especially for the manufacture of bulk commodity fibres. However, niche applications, such as special dyeing procedures (157–159) may probably come to commercial practice earlier.

Several issues and barriers which obstruct the rapid commercialisation of ILs have been summarized recently (136). Most notably, in this context, lack of process engineering studies, absence of scale-up studies, lack of life cycle, and routine-realistic recyclability (146, 160) have to be covered in more detail (136).

Another point of concern is the prevalent industrial apathy due to the high burden of regulatory rules in connection with the introduction of new chemicals (136).

Likewise, toxicological and environmental issues have to be addressed in a profound manner. More than sixty years ago, a series of imidazolium salts, including numerous hitherto neglected “incognito-ILs”, have been screened for their bacteriostatic activity and described as topical antiseptics (161). Meanwhile, ILs have even been recognized to induce new fungal metabolite biosynthetic pathways (162). Therefore, the partial biodegradation of imidazolium salts by alteration or removal of a side chain functionality (163), should not be considered the ultimate goal. Leaving the quarternized cation core unaltered does not justify the assessment of overall reduced toxicity.

Fine-tuning the extraction performance and selectivity for lignin by IL-modified solvent mixtures will certainly represent a significant field of challenging research in the near future.

Both, lignocellulose fractionation technology and effective co-utilization of acetic acid, lignin, and hemicellulose will be vital to the realisation of profitable modern lignocellulose refineries (164). Isolation of large amounts of lignocellulose components through lignocellulose fractionation would stimulate R&D in lignin and hemicellulose applications, as well as promote new markets for lignin and hemicellulose derivative products (164).

Acknowledgements

Financial support and in kind contributions are gratefully acknowledged by M.H., G.B. and E.R. (Wood K1, Competence Centre for Excellent Technologies, Linz, and Lenzing AG, Austria); A.S. (Ratiopharm, Ulm, Germany); T. G. (Liese-Meitner program , grant M1135-N17).

References

1. El Seoud, O. A.; Koschella, A.; Fidale, L. C.; Dorn, S.; Heinze, T. *Biomacromolecules* **2007**, *8*, 2629–2647.
2. Hermanutz, F.; Meister, F.; Uerdingen, E. *Chem. Fibers Int.* **2006**, *6*, 342–344.
3. Hermanutz, F.; Gähr, F.; Uerdingen, E.; Meister, F.; Kosan, B. *Macromol. Symp.* **2008**, *262*, 23–27.
4. Kosan, B.; Michels, C.; Meister, F. *Cellulose* **2007**, *15*, 59–66.
5. Kosan, B.; Nechwatal, A.; Meister, F. *Chem. Fibers Int.* **2008**, *4*, 234–236.
6. Winterton, N. *CHEManager Europe*, April 25, 2008; p 5.
7. Zhao, H. *Chem. Eng. Commun.* **2006**, *193*, 1660–1677.
8. Rijkssen, C.; Rogers, R. D. *J. Org. Chem.* **2008**, *73*, 5582–5584 and references cited therein.
9. Zhu, S.; Wu, Y.; Chen, Q.; Yu, Z.; Wang, C.; Jin, S.; Ding, Y.; Wu, G. *Green Chem.* **2006**, *8*, 325–327.
10. Laus, G.; Bentivoglio, G.; Schottenberger, H.; Kahlenberg, V.; Kopacka, H.; Röder, T.; Sixta, H. *Lenzinger Berichte* **2005**, *84*, 71–85.
11. Bentivoglio, G.; Röder, T.; Fasching, M.; Buchberger, M.; Schottenberger, H.; Sixta, H. *Lenzinger Berichte* **2006**, *86*, 154–161.
12. Zhang, H.; Wu, J.; Zhang, J.; He, J. *Macromolecules* **2005**, *38*, 8272–8277.
13. Novoselov, N. P.; Sashina, E. S.; Kuz'mina, O. G.; Troshenkova, S. V. *Russ. J. Gen. Chem.* **2007**, *77*, 1395–1405 and references cited therein.
14. Heinze, T.; Liebert, T.; Koschella, A. *Esterification of Polysaccharides*; Springer Laboratory, Springer: Berlin, Heidelberg, 2006.
15. Leng, W. *Synthesis of Cellulose Derivatives in Ionic Liquids*; Berichte aus der Chemie: Shaker; 2008.
16. Granström, M.; Kavakka, J.; Majonen, J.; Mäkelä, V.; Helaja, J.; Hietala, S.; Virtanen, T.; Mannu, S.-L.; Argyropoulos, D. S.; Kipeläinen, I. *Cellulose* **2008**, *15*, 481–488.
17. Liu, C.F.; Zhang, A.P.; Li, W.Y.; Yue, F.X.; Sun, R.C. *J. Agric. Food Chem.* **2009**, *57*, 1814–1820.
18. Fischer, S.; Thuemmler, K.; Volkert, B.; Hettrich, K.; Schmidt, I.; Fischer, K. *Macromolecular Symposia* **2008**, *262*, 89–96.
19. Dominguez de Maria, P.; Martinsson, A. *Analyst* **2009**, *134*, 493–496.
20. Wilkes, J. S.; Zaworotko, M. J.; Seiler, F. J. *J. Chem. Soc. Chem. Commun.* **1992**, *13*, 965–967.

21. Köhler, S.; Liebert, T.; Schöbitz, M.; Schaller, J.; Meister, F.; Günther, W.; Heinze, T. *Macromol. Rapid Commun.* **2007**, *28*, 2311–2317.
22. Granström, M.; Olszewska, A.; Mäkelä, V.; Heikkinen, S.; Kilpeläinen, I. *Tetrahedron Lett.* **2009**, *50*, 1744–1747.
23. Heinze, T.; Dorn, S.; Schöbitz, M.; Liebert, T.; Köhler, S.; Meister, F. *Macromol. Symp.* **2008**, *262*, 8–22.
24. Tanoika, H. JP Patent 2008050595 A, 2008.
25. Stegmann, V.; Massonne, K.; Maase, M.; Ürdingen, E.; Lutz, M.; Hermanutz, F.; Gähr, F. WO Patent 2007076979 A1, 2007.
26. Xie, H.; King, A.; Kilpeläinen, I.; Granstrom, M.; Argyropoulos, D. S. *Biomacromolecules* **2007**, *8*, 3740–3748.
27. Cao, Y.; Wu, J.; Meng, T.; Zhang, J.; He, J.; Li, H.; Zhang, Y. *Carbohydr. Polym.* **2007**, *69*, 665–672.
28. Liebert, T.; Heinze, T.; Gerike, M. DE Patent 102007035322 A1, 2009.
29. Gerike, M.; Liebert, T.; Heinze, T. *Macromol. Biosci.* **2009**, *9*, 342–353.
30. Wang, Z.-M.; Li, L.; Xiao, K.-J.; Wu, J.-Y. *Bioresour. Technol.* **2009**, *100*, 1687–1690.
31. Köhler, S.; Liebert, T.; Heinze, T. *J. Polym. Sci., Part A: Polymer Chem.* **2008**, *46*, 4070–4080.
32. Mormann, W.; Wezstein, M. *Macromol. Biosci.* **2009**, *9*, 369–375.
33. Xie, H.; Jarvi, P.; Karesoja, M.; King, A.; Kilpeläinen, I.; Argyropoulos, D. S. *J. Appl. Polym. Sci.* **2009**, *111*, 2468–2476.
34. Xie, H.; Argyropoulos, D. S. U.S. Patent 20080188636 A1, 2008.
35. Murakami, M.a.; Kaneko, Y.; Kadokawa, J.-i. *Carbohydr. Polym.* **2007**, *69*, 378–381.
36. Mikkola, J.-P.; Kirilin, A.; Tuuf, J.-C.; Pranovich, A.; Holmbom, B.; Kustov, L. M.; Murzin, D. Y.; Salmi, T. *Green Chem.* **2007**, *9*, 1229–1237.
37. Xu, S.; Zhang, J.; He, A.; Li, J.; Zhang, H.; Han, C. C. *Polymer* **2008**, *49*, 2911–2917.
38. Sun, N.; Swatloski, R. P.; Maxim, M. L.; Rahman, M.; Harland, A. G.; Haque, A.; Spear, S. K.; Daly, D. T.; Rogers, R. D. *J. Mater. Chem.* **2008**, *18*, 283–290.
39. Swatloski, R. P.; Holbrey, J. D.; Weston, J. L.; Rogers, R. D. *Chim. Oggi* **2006**, *24*, 31–32, 34–35.
40. Viswanathan, G.; Murugesan, S.; Pushparaj, V.; Nalamasu, O.; Ajayan, P. M.; Linhardt, R. J. *Biomacromolecules* **2006**, *7*, 415–418.
41. Wu, R.-L.; Wang, X.-L.; Li, F.; Li, H.-Z.; Wang, Y.-Z. *Bioresour. Technol.* **2009**, *100*, 2569–2574.
42. Kadokawa, J.-i.; Murakami, M.-a.; Kaneko, Y. *Carbohydr. Res.* **2008**, *343*, 769–772.
43. Kershaw, D.; Adams, S. WO Patent 2008062209 A2, 2008.
44. Ueki, T.; Watanabe, M. *Macromolecules* **2008**, *41*, 3739–3749.
45. Turner, M. B.; Spear, S. K.; Holbrey, J. D.; Rogers, R. D. *Biomacromolecules* **2004**, *5*, 1379–1384.
46. Turner, M. B.; Spear, S. K.; Holbrey, J. D.; Daly, D. T.; Rogers, R. D. *Biomacromolecules* **2005**, *6*, 2497–2502.
47. Tsiptsias, C.; Panayiotou, C. *Carbohydr. Polym.* **2008**, *74*, 99–105.

48. Zhao, H.; Jones, C. L.; Baker, G. A.; Xia, S.; Olubajo, O.; Person, V. N. *J. Biotechnol.* **2009**, *139*, 47–54 and references cited therein.
49. Zhao, H.; Baker, G. A.; Song, Z.; Olubajo, O.; Crittle, T.; Peters, D. *Green Chem.* **2008**, *10*, 696–705.
50. Pitner, W.-R.; Eichhorn, J.; Von Hagen, J.; Leland, P. A.; Scott, G. B. I. WO Patent 2009046840 A1, 2009.
51. Byrne, N.; Belieres, J. P.; Angell, A. *Aust. J. Chem.* **2009**, *62*, 328–333.
52. Fujita, K.; Nakamura, N.; Igarashi, K.; Samejima, M.; Ohno, H. *Green Chem.* **2009**, *11*, 351–354.
53. Li, C.; Zhao, Z. K. *Adv. Synth. Catal.* **2007**, *349*, 1847–1850.
54. Holbrey, J.; Fanselow, M.; Seddon, K. R.; Vanoye, L.; Zheng, A. WO Patent 2009030950 A1, 2009.
55. Li, C.; Wang, Q.; Zhao, Z. K. *Green Chem.* **2008**, *10*, 177–182.
56. Rinaldi, R.; Palkovits, R.; Schüth, F. *Angew. Chem. Int. Ed.* **2008**, *47*, 8047–8050.
57. Xie, H.; Shi, T. *Holzforschung* **2006**, *5*, 509–512.
58. Zhao, H.; Hollady, J. E.; Zhang, Z. C. U.S. Patent 20080033187 A1, 2008.
59. Vanoye, L.; Fanselow, M.; Holbrey, J. D.; Atkins, M. P.; Seddon, K. R. *Green Chem.* **2009**, *11*, 390–396.
60. Sheldrake, G. N.; Schleck, D. *Green Chem.* **2007**, *9*, 1044–1045.
61. Argyropoulos, D. U.S. Patent 20080185112 A1, 2008.
62. Stevenson, D. G.; Biswas, A.; Jane, J.-I.; Inglett, G. E. *Carbohydr. Polym.* **2007**, *67*, 21–31.
63. Sashina, E.; Novoselov, N.; Kuz'mina, O.; Troshenkova, S. *Fibre Chem.* **2008**, *40*, 270–277.
64. Ohno, H.; Fukaya, Y. *Chem. Lett.* **2009**, *38*, 2–7 and references cited.
65. Fukaya, Y.; Sugimoto, A.; Ohno, H. *Biomacromolecules* **2006**, *7*, 3295–3297.
66. Fukaya, Y.; Hayashi, K.; Wada, M.; Ohno, H. *Green Chem.* **2008**, *10*, 44–46.
67. Wezstein, M.; Mormann, W. ILs- “New Solvents” for Polysaccharides. Acetoacetylation of Cellulose, IMSAT-8, 8th Conference of Iminium Salts, Bartholomä/Ostalbkreis, Germany, Sept. 11–13, 2007; book of abstracts, pp 114–115.
68. Kuhlmann, E.; Himmler, S.; Giebelhaus, G.; Wasserscheid, P. *Green Chem.* **2007**, *9*, 233–242.
69. Wang, J.-F.; Li, C.-X.; Wang, Z.-H.; Li, Z.-J.; Jiang, Y.-B. *Fluid Phase Equilib.* **2007**, *225*, 186–192.
70. Mazza, M.; Catana, D.-A.; Vaca-Garcia, C.; Cecutti, C. *Cellulose* **2009**, *16*, 207–215.
71. Andre, M.; Bentivoglio, G.; Laus, G.; Nauer, G.; Schottenberger, H. 236th ACS National Meeting, Philadelphia, PA, United States, August 17–21, 2008; ANYL-135.
72. Laus, G.; Andre, M.; Bentivoglio, G.; Schottenberger, H. *J. Chromatogr., A* **2009**, *1216*, 6020–6023.
73. Vitz, J.; Erdmenger, T.; Haensch, C.; Schubert, U. S. *Green Chem.* **2009**, *11*, 417–424.
74. Bogolitsyn, K. G.; Skrebets, T. E.; Makhova, T. A. 2nd International IUPAC Conference on Green Chemistry, Russia, 14–19 September, 2008.

75. Kuang, Q.-L.; Zhao, J.-C.; Niu, Y.-H.; Zhang, J.; Wang, Z.-G. *J. Phys. Chem. B* **2008**, *112*, 10234–10240.
76. Collier, J. R.; Watson, J. L.; Collier, B. J.; Petrovan, S. *J. Appl. Polym. Sci.* **2009**, *111*, 1019–1027.
77. Gericke, M.; Schlufuter, K.; Liebert, T.; Heinze, T.; Budtova, T. *Biomacromolecules* **2009**, *10*, 1188–1194.
78. Stark, A.; Behrend, P.; Braun, O.; Ranke, J.; Ondruschka, B.; Jastorff, B. *Green Chem.* **2008**, *10*, 1152–1161.
79. Schrems, M.; Potthast, A.; Rosenau, T. *Nachwachsende Rohstoffe* **2009**, *51*, 11.
80. Ebner, G.; Schieser, S.; Potthast, A.; Rosenau, T. *Tetrahedron Lett.* **2008**, *49*, 7322–7324.
81. Edye, L. A.; Doherty, W. O. S. WO Patent 2008095252 A1, 2008.
82. Zavrel, M.; Bross, D.; Funke, M.; Büchs, J.; Spiess, A. C. *Bioresour. Technol.* **2009**, *100*, 2580–2587, and references cited therein.
83. Derecskei, B.; Derecskei-Kovacs, A. *Mol. Simulat.* **2006**, *32*, 109–115.
84. Guo, Z.; Lue, B.-M.; Thomasen, K.; Meyer, A. S.; Xu, X. *Green Chem.* **2007**, *9*, 1362–1373 and references cited therein.
85. Pinkert, A.; Marsh, K. N.; Pang, S.; Staiger, M. P. *Chem. Rev.* **2009**, *109*, 6712–6728.
86. King, A. W. T.; Kilpeläinen, I.; Heikkinen, S.; Järvi, P.; Argyropoulos, D. S. *Biomacromolecules* **2009**, *10*, 458–463.
87. Kubo, S.; Hashida, K.; Yamada, T.; Hishiyama, S.; Magara, K.; Kishino, M.; Ohno, H.; Hosoya, S. *J. Wood Chem. Technol.* **2008**, *28*, 84–96.
88. Miyafuji, H.; Miyata, K.; Saka, S.; Ueda, F.; Mori, M. *J. Wood Sci.* **2009**, *55*, 215–219.
89. Myllimäki, V.; Aksela, R. WO Patent 2005017001 A1, 2005.
90. Kilpeläinen, I.; Xie, H.; King, A.; Granstrom, M.; Heikkinen, S.; Argyropoulos, D. S. *J. Agric. Food. Chem.* **2007**, *55*, 9142–9148 and references cited therein.
91. Tan, S. S. Y.; MacFarlane, D. R.; Upfal, J.; Edye, L. A.; Doherty, W. O. S.; Patti, A. F.; Pringle, J. M.; Scott, J. L. *Green Chem.* **2009**, *11*, 339–345.
92. Pu, Y.; Jiang, N.; Ragauskas, A. J. *J. Wood Chem. Technol.* **2007**, *27*, 23–33.
93. Sun, N.; Rahman, M.; Qin, Y.; Maxim, M. L.; Rodríguez, H.; Rogers, R. D. *Green Chem.* **2009**, *11*, 646–655 and references cited therein.
94. Zhu, S. *J. Chem. Technol. Biotechnol.* **2008**, *83*, 777–779 and references cited therein.
95. Palomar, J.; Torrecilla, J. S.; Ferro, V. R.; Rodríguez, F. *Ind. Eng. Chem. Res.* **2009**, *48*, 2257–2265.
96. Abbott, A. P.; Bell, T. J.; Handa, S.; Stoddart, B. *Green Chem.* **2006**, *8*, 784–786.
97. D'Andola, G.; Szarvas, L.; Massonne, K.; Stegmann, V. WO Patent 2008043837 A1, 2008.
98. Zang, H.; Wang, M.; Zhang, Y.; Cheng, B. CN Patent 101215725 A, 2008.
99. MacFarlane, D. R.; Forsyth, S. A. WO Patent 2005017252 A1, 2005.
100. Ohno, H.; Fukumoto, K.; Kagimoto, J.; Inakagi, T. WO Patent 2007023814 A1, 2007.

101. Greaves, T. L.; Drummond, C. J. *Chem. Rev.* **2008**, *108*, 206–237.
102. Bentivoglio, G.; Schwärzler, A.; Wurst, K.; Kahlenberg, V.; Nauer, G.; Bonn, G.; Schottenberger, H.; Laus, G. *J. Chem. Crystallogr.* **2009**, *39*, 662–668.
103. Maase, M.; Stegmann, V. DE Patent 102005017715 A1, 2006.
104. Maase, M.; Stegmann, V. WO Patent 2006108861 A2, 2006.
105. Bentivoglio, G.; Röder, T. private communication, Lenzing, 2006.
106. Fletcher, K. A.; Baker, S. N.; Baker, G. A.; Pandey, S. *New J. Chem.* **2003**, *27*, 1706–1712 and references cited therein.
107. Walden, P. *Geschichte der organischen Chemie seit 1880 / Bd. 2*; Springer: Berlin, 1972.
108. Walden, P. *Bull. Acad. Sci. St. Petersburg.* **1914**, 405–422.
109. Lecocq, V.; Graille, A.; Santini, C. C.; Baudouin, A.; Chauvin, Y.; Basset, J. M.; Arzel, L.; Bouchu, D.; Fenet, B. *New J. Chem.* **2005**, *29*, 700–706.
110. Thomazeau, C.; Olivier-Bourbigou, H.; Magna, L.; Luts, S.; Gilbert, B. *J. Am. Chem. Soc.* **2003**, *125*, 5264–5265.
111. Andre, M.; Loidl, J.; Laus, G.; Schottenberger, H.; Bentivoglio, G.; Wurst, K.; Ongania, K. H. *Anal. Chem.* **2005**, *77*, 702–705 supplemental section.
112. Heinze, T.; Schwikal, K.; Barthel, S. *Macromol. Biosci.* **2005**, *5*, 520–525.
113. Adelwöhrer, C.; Yoneda, Y.; Takano, T.; Nakatsubo, F.; Rosenau, T. *Cellulose* **2009**, *16*, 139–150.
114. Ebner, G.; Hofinger, A.; Brecker, L.; Rosenau, T. *Cellulose* **2008**, *15*, 763–767.
115. Schottenberger, H.; Wurst, K.; Horvath, U. E. I.; Cronje, S.; Lukasser, J.; Polin, J.; McKenzie, J. M.; Raubenheimer, H. G. *Dalton Trans.* **2003**, *22*, 4275–4281.
116. Bini, R.; Bortolini, O.; Chiappe, C.; Pieraccini, D.; Siciliano, T. *J. Phys. Chem. B* **2007**, *111*, 598–604.
117. Chiappe, C.; Malvaldi, M.; Pomelli, C. S.; *Pure Appl. Chem.* **2009**, *81*, 767–776 and references cited therein.
118. Abraham, M. H.; Zissimos, A. M.; Huddleston, J. G.; Willauer, H. D.; Rogers, R. D.; Acree, W. E., Jr. *Ind. Eng. Chem. Res.* **2003**, *42*, 413–418.
119. Izgorodina, E. I.; Forsyth, M.; MacFarlane, D. R. *Phys. Chem. Chem. Phys.* **2009**, *11*, 2452–2458.
120. Mellein, B. R.; Aki, S. N. V. K.; Ladewski, R. L.; Brenneke, J. F. *J. Phys. Chem. B* **2007**, *111*, 131–138.
121. Wu, Y.; Sasaki, T.; Kazushi, K.; Seo, T.; Sakurai, K. *J. Phys. Chem. B* **2008**, *112*, 7530–7536.
122. Ohno, H.; Fukumoto, K. *Acc. Chem. Res.* **2007**, *40*, 1122–1129.
123. Ohno, H.; Fukaya, Y. JP Patent 2006137677, 2006.
124. Fidale, L. C.; Possidonio, S.; El Seoud, O. A. *Macromol. Biosci.* **2009**, DOI 10.1002/mabi.200900034.
125. Laus, G.; Schütz, J.; Schuler, N.; Kahlenberg, V.; Schottenberger, H.; Z. *Kristallogr.- New Cryst. Struct.* **2009**, *224*, 117–118 and references cited.
126. Weingärtner, H. *Angew. Chem., Int. Ed.* **2008**, *47*, 654–670.
127. Laus, G.; Schottenberger, H.; Wurst, K.; Schütz, J.; Ongania, K.-H.; Horvath, U. E. I.; Schwärzler, A. *Org. Biomol. Chem.* **2003**, *1*, 1409–1418.

128. Mohr, G.; Müller, H.; Bussemer, B.; Stark, A.; Carofiglio, T.; Trupp, S.; Heuermann, R.; Henkel, T.; Escudero, D.; González, L. *Anal. Bioanal. Chem.* **2008**, *392*, 1411–1418.
129. D'Anna, F.; La Marca, S.; Noto, R. *J. Org. Chem.* **2009**, *74*, 1952–1956.
130. Johnson, D. L. GB Patent 1,144,048, 1967.
131. Harmon, K. M.; Akin, A. C.; Keefer, P. K.; Snider, B. L. *J. Mol. Struct.* **1992**, *269*, 109–121.
132. Luo, M.; Neogi, A.N.; West, H. U.S. Patent 20090088564 A1, 2009.
133. Laus, G.; Schwaerzler, A.; Schuster, P.; Bentivoglio, G.; Hummel, M.; Wurst, K.; Kahlenberg, V.; Loerting, T.; Schuetz, J.; Peringer, P.; Bonn, G.; Nauer, G.; Schottenberger, H. *Z. Naturforsch., B: Chem. Sci.* **2007**, *62*, 295–308.
134. Laus, G.; Schwaerzler, A.; Bentivoglio, G.; Hummel, M.; Kahlenberg, V.; Wurst, K.; Kristeva, E.; Schuetz, J.; Kopacka, H.; Kreutz, C.; Bonn, G.; Andriyko, Y.; Nauer, G.; Schottenberger, H. *Z. Naturforsch., B: Chem. Sci.* **2008**, *63*, 447–464.
135. Laus, G.; Schwaerzler, A.; Hummel, M.; Wurst, K.; Kahlenberg, V.; Bonn, G.; Schottenberger, H. 236th ACS National Meeting, Philadelphia, PA, United States, August 17-21, 2008; IEC-115.
136. Joglekar, H. G.; Rahman, I.; Kulkarni, B. D. *Chem. Eng. Technol.* **2007**, *30*, 819–828.
137. Wasserscheid, P.; Boesmann, A.; Van Hal, R. WO Patent 2003074494 A1, 2003; U.S. Patent 20040262578 A1, 2004.
138. Mori, S.; Ida, K.; Ue, M. U.S. Patent 4892944, 1990.
139. Szarvas, L.; Massonne, K. WO Patent 2006021302 A1, 2006.
140. Rosenau, T.; Potthast, A.; Kosma, P.; Chen, C.-L.; Gratzl, J. S. *J. Org. Chem.* **1999**, *64*, 2166–2167.
141. Chiappe, C.; Neri, D.; Pieraccini, D. *Tetrahedron Let.* **2006**, *47*, 5089–5093.
142. Finkelstein, M.; Dunkl; F.S.; Ross; S.D. U.S. Patent 4189761, 1980.
143. Shropshire, J.A.; Eustace, Daniel, J. U.S. Patent 4124693, 1978.
144. Dorn, S.; Wendler, F.; Meister, F.; Heinze, T. *Macromol. Mater. Eng.* **2008**, *293*, 907–913 and references cited therein.
145. Yan, C.; Zhang, J.; Lv, Y.; Yu, J.; Wu, J.; Zhang, J.; He, J. *Biomacromolecules* **2009**, DOI: 10.1021/bm900447u.
146. Erdmenger, T.; Vitz, J.; Wiesbrock, F.; Schubert, U. S. *J. Mat. Chem.* **2008**, *18*, 5267–5273.
147. Laus, G.; Bentivoglio, G.; Kahlenberg, V.; Griesser, U. J.; Schottenberger, H.; Nauer, G. *CrystEngComm* **2008**, *10*, 748–752.
148. Reichert, W. M.; Holbrey, J. D.; Swatloski, R. P.; Gutowski, K. E.; Visser, A. E.; Nieuwenhuyzen, M.; Seddon, K. R.; Rogers, R. D. *Cryst. Growth Des.* **2007**, *7*, 1106–1114.
149. Henderson, W. A.; Young, V. G., Jr.; Fylstra, P.; De Long, H. C.; Trulove, P. C. *Cryst. Growth Des.* **2006**, *6*, 1645–1648.
150. Steiner, T. *Cryst. Rev.* **1996**, *6*, 1–51.
151. Giarda, L.; Garbassi, F.; Calcaterra, M. *Acta Crystallogr., Sect. B: Struct. Sci.* **1973**, *29*, 1826–1829.

152. Clark, J. H.; Green, M.; Madden, R.; Reynolds, C. D.; Dauter, Z.; Miller, J. M.; Jones, T. *J. Am. Chem. Soc.* **1984**, *106*, 4056–4057.
153. Ignatyev, N.; Welz-Biermann, U.; Kucheryna, A.; Willner, H. WO Patent 2006 063655, 2006.
154. Gololobov, Y. G.; Oganesyan, A. S.; Petrovskii, P. V. *J. Gen. Chem. USSR (Engl. Transl.)* **1989**, *59*, 1173–1183.
155. In analogy to: Nicolai, F.; Schönburg, C.; v. d. Bruck, G. German Patent DE 1932 564321.
156. Han, S.; Li, J.; Zhu, S.; Chen, R.; Wu, Y.; Zhang, X.; Yu, Z. *BioResources* **2009**, *4*, pp xy (avail. May) and references cited therein.
157. Höffkes, H.; Gross, W.; Oberkobusch, D.; Knübel, G. WO Patent 2007006418 A1, 2007.
158. Knittel, D.; Schollmeyer, E. DE Patent 102006040075 A1, 2008.
159. Earle, M. J.; Seddon, K. R. WO Patent 2009024766 A2, 2009.
160. Massonne, K.; Siemer, M.; Mormann, W.; Leng, W. DE Patent 102007041416 A1; WO Patent 2009027250 A2, 2009.
161. Shepard, E.R.; Shonle, H.A. *J. Am. Chem. Soc.* **1947**, *69*, 2269–2270.
162. Da Costa Silva Peirera, C.M.; N. Rebelo, L.P., Seddon, K.R. E Patent 1995305 A1, 2008.
163. Gmorrissy, S.; Pegot, B. WO Patent 2009024607 A1, 2009.
164. Zhang, Y.-H. P. *J. Ind. Microbiol. Biotechnol.* **2008**, *35*, 367–365.

Chapter 14

Properties of Cellulose/TiO₂ Fibers Processed from Ionic Liquids

Mirela L. Maxim¹, Ning Sun¹, Richard P. Swatloski²,
Mustafizur Rahman¹, Adam G. Harland³, Anwarul Haque³,
Scott K. Spear⁴, Daniel T. Daly⁴ and Robin D. Rogers^{*,1}

¹Department of Chemistry, Center for Green Manufacturing,
The University of Alabama, Tuscaloosa, AL 35487, USA

²Office for Technology Transfer, The University of Alabama, Tuscaloosa,
AL 35487, USA

³Department of Aerospace Engineering and Mechanics,
The University of Alabama, Tuscaloosa, AL 35487, USA

⁴Alabama Institute for Manufacturing Excellence,
The University of Alabama, Tuscaloosa, AL 35487, USA
*rdrogers@bama.ua.edu

Continuous composite fibers of cellulose with dispersed TiO₂ particles were pulled by a dry-jet wet spinning process from 1-ethyl-3-methylimidazolium chloride ([C₂mim]Cl) ionic liquid solutions. The effects of various factors such as cellulose source, degree of polymerization, and concentration, along with the concentration of the additive were evaluated. The surface texture of the fibers depends greatly on the concentration of TiO₂ used, as the particles have the tendency to outcrop the surface. Five weight percent TiO₂ was found to be the optimal concentration that didn't cause significant changes in the mechanical properties of the fibers.

Cellulose has captured the attention of the research community due to the inevitable depletion of petroleum-based resources which has led to the need for more sustainable and environmentally-friendly resources. Cellulose is the most abundant biorenewable material on Earth (*1*), a naturally occurring biopolymer which is used in textile and packaging industries, as well as in body care and

drug delivery products (2). It holds remarkable properties like biocompatibility, hydrophilicity, biodegradability, etc., and it is a very cheap material, but by its nature, it is very difficult to process.

The cellulose recalcitrance to water and conventional organic solvents is a result of the strength of intra- and inter-molecular hydrogen bonding (3). Therefore to successfully process cellulose, either chemical derivatization or physical dissolution in a suitable solvent is required. Currently the most popular process used to obtain cellulose fibers is the Viscose process and it involves the derivatization of cellulose using CS₂ followed by dissolution in sodium hydroxide (4, 5). The process requires a large amount of hazardous chemicals, and even though up to 75% of the CS₂ can be recycled, the additional expenses to make the process meet the required environmental regulations for waste water and air quality are continuously increasing (6).

An alternative technology for fiber manufacturing is the NMMO (N-methylmorpholine-N-oxide) process which involves direct dissolution of cellulose in an organic solvent with a spinning process to produce high-tenacity fibers like Tencel or Lyocell (7). The major drawbacks of the process are poor thermal stability of the solvent (8) and pronounced degradation of both solvent and cellulose due to byproduct formation which require large usage of stabilizers (7) and high expenditure due to safety concerns (6). The tendency of the fibers to fibrillate is another issue which decreases the final performance of the product and therefore limits the use of these fibers in textiles.

Ionic liquids (ILs) represent a new solvent system for cellulose that enables the manufacture of cellulose-based materials in a manner that is highly advantageous from various points of view. ILs, salts with a melting point below 100 °C, offer the advantage of low vapor pressure (9) and cellulose dissolution without pretreatment or chemical derivatization (10–17). Cellulose can be easily regenerated from IL solution using various regeneration solvents, among which the most efficient and cheapest is water. During the regeneration process cellulose can be shaped into different forms such as fibers, membranes, beads, and flocs, etc. Enhanced functionality of the cellulosic materials can be obtained by introduction of additives into the cellulose/IL solution by simple dispersion or direct dissolution (18–26). The cellulose composites can then be reconstituted into different forms and be used as new materials with improved properties.

For example, cellulose as a biopolymer and biocompatible material makes a suitable support for enzyme encapsulation. Preparation of thin membranes with incorporated laccase was possible by precoating the enzyme with a hydrophobic IL which provided the necessary microenvironment for the enzyme to remain active (18). In order to provide more surface active area for enzyme immobilization by loading primary amines on the cellulose surface, cellulose-polyamine composite films and beads were produced from IL solutions (19). Another bioactive cellulose film was produced by codissolution of polyamidoamine (PAMAM) dendrimers along with cellulose in 1-butyl-3-methylimidazolium chloride ([C₄mim]Cl). The films reconstituted with DI water which used 1,3-phenylene diisocyanate as a linker to covalently bond cellulose and dendrimers, showed better performance compared to the composite films for immobilization of laccase on the surface (20).

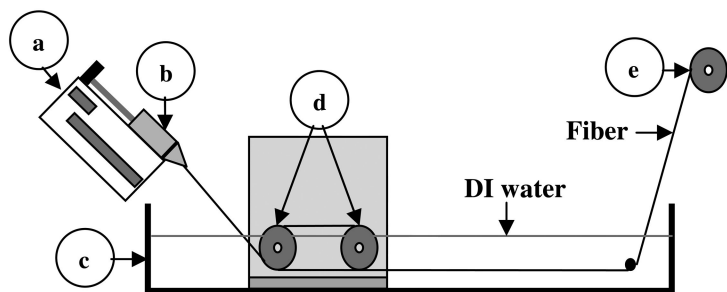


Figure 1. Schematic representation of fiber extrusion apparatus: (a) Extrusion pump; (b) Syringe; (c) Regeneration bath; (d) Godets; (e) Uptake reel

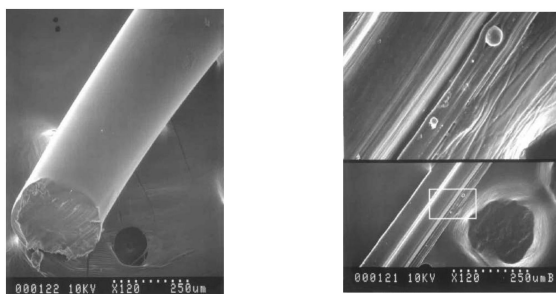


Figure 2. SEM images of plain cellulose fibers extruded from IL solutions: 14 wt% MCC — left; 4 wt% Peach — right.

Organic additives incorporated into cellulose via the IL process can lead to inexpensive sensors. By codissolution of cellulose and 1-(2-pyridylazo)-2-naphthol in $[C_4mim]Cl$ followed by regeneration with water, sensor strips were formed which exhibited a (1:1) response to $Hg(II)$ in aqueous solution (21). Successful NO_x detection was achieved by immobilization of calix[4]arene, a compound known to react with this gas (27), in a cellulose membrane which could then be used for both sensing and storage of nitrosonium ion (NO^+) (22).

The use of inorganic additives in cellulose-based composites has also been facilitated by the IL processing method. Magnetite (Fe_3O_4) has been used to produce magnetically responsive cellulose composites in the form of beads, flocs, and fibers (23, 24). Increased magnetic properties have been shown with the increasing concentration of magnetite in the composite fibers. At the same time, however, tensile strength measurements showed deterioration in the mechanical properties of the fibers with increasing concentration of the additive.

Titanium dioxide (TiO_2) has been widely used as a white pigment for paints and cosmetics, a catalyst in chemical reactions, or a photocatalyst activated by ultraviolet irradiation (28, 29). The antibacterial effect of TiO_2 based on its photocatalytic properties has been studied to create surfaces that would provide protection against infectious diseases, odor, staining, deterioration, and allergies (30). The performance of the TiO_2 particles depends mostly on the polymorph used (rutile or anatase), morphology, and particle size (31).

Several studies have been done to determine the antibacterial effect of TiO_2 as particles, as films (32, 33), or as coatings on cellulose fibers (34). It has been shown that TiO_2 particles of various sizes can be incorporated in cellulosic materials by various methods. Rayon fibers with TiO_2 - SiO_2 complexes have been prepared which show better antibacterial activity due to SiO_2 protection (35). Other methods used for the preparation of TiO_2 /cellulose composites have been reported from NaOH /urea aqueous solution (36) and through a controlled hydrolysis of TiOSO_4 in the presence of cellulose fibers (37).

The study reported here focuses on the preparation of TiO_2 /cellulose composite fibers from cellulose/IL solutions containing suspended titania particles. The fibers are extruded by a dry-jet wet spinning process and regenerated using a water bath. Several properties of the fibers such as surface texture, thermal stability, tensile strength, and elongation at break have been investigated as a function of cellulose source and compared with plain cellulose fibers obtained under similar conditions.

Experimental

Materials

Three types of cellulose with different degrees of polymerization (DP) were used to prepare the fibers. Microcrystalline cellulose (MCC) with an approximate DP of 270 was purchased from Aldrich (Milwaukee, WI); ground Peach (DP = 687) with high hemicellulose content was provided by Weyerhaeuser (Oglethorpe, GA); and ground Pulp (DP = 1056) was provided by International Paper (Natchez, MS) as sheets. The sheets were ground to fine powder using an electric lab mill (Janke & Kunkel Ika Labortechnik, Wilmington, NC). As starting materials, all cellulose types were used as fine white powders.

The IL used for the cellulose dissolution was 1-ethyl-3-methylimidazolium chloride ($[\text{C}_2\text{mim}]\text{Cl}$) from BASF (Ludwigshafen, Germany). It had more than 93% purity, appeared as off-white solid, and was used as received.

Rutile type titanium(IV) oxide (TiO_2) with an average particle size of less than $5\ \mu\text{m}$ was purchased from Aldrich (Milwaukee, WI). The particles were used as received, without preliminary photocatalytic activation.

Blend and Fiber Preparation

The preparation of the spinning dope, the fiber pulling settings and procedures were carried out following a procedure described elsewhere (24). For each sample about 10 g of $[\text{C}_2\text{mim}]\text{Cl}$ was placed in a glass vial and melted in oven at $90\ ^\circ\text{C}$. Cellulose powder was added to the IL and heated in a domestic microwave for up to 1.5 min with 2-3 s pulses and mechanical stirring in between pulses. **[CAUTION: Care must be taken as overheating the cellulose/IL solution can**

cause degradation and burning of the cellulose. Special heat gloves need to be used when handling glass vials with solutions heated in the microwave.]

Cellulose/IL solutions used for the preparation of the plain and composite fibers were obtained having the following cellulose concentrations: 14 wt% for MCC (DP = 270); 7 wt% for ground Peach (DP = 687); 8 wt% for ground Pulp (DP = 1056). For composite fibers the TiO₂ particles were added after complete cellulose dissolution was achieved and mechanically stirred in to obtain homogeneous suspensions with final TiO₂ concentrations of 3.5 wt%, 5.0 wt%, or 7.5 wt% relative to the cellulose mass. The solutions were centrifuged and poured into plastic syringes (BD-10 mL and a tip with inside diameter of ~2 mm). The fibers were prepared by the dry-jet wet spinning set-up schematically represented in Figure 1. The plastic syringe (b) containing the IL-based solution was attached to the extrusion pump (a) which controlled the extrusion rate. To ensure the fluidity of the spinning dope, the syringe was wrapped in a heating jacket that maintained the temperature at 70 °C. The fibers were drawn through an air gap (~5 cm) into the regeneration bath (c) filled with DI water and then led to the godet (d). Finally the fibers were wound on the uptake reel (e). The extrusion conditions of the fibers were as follows: rate of extrusion 0.3 mL min⁻¹, speed of godets 20 rpm at 6.1 V, and speed of the uptake reel 1.44 m s⁻¹ at 3.2 V. After preparation, the fibers were soaked in DI water for 24 h to completely wash out the IL and then air-dried on the spool.

Characterization of Fibers

Scanning Electron Microscopy (SEM)

The surface texture of the plain fibers from various cellulose sources and the composite fibers with different TiO₂ particle concentrations was analyzed by SEM using a Hitachi S-2500 SEM operated at 10 kV accelerating voltage. The samples were mounted on aluminum stubs and then sputter-coated with silver and palladium to make them conductive, thus avoiding charge build-up and degradation.

Thermogravimetric Analysis (TGA)

The thermogravimetric analyses of original cellulose samples, as well as plain and composite fibers, were performed using a TA Instruments TGA 2950 thermogravimetric analyzer. Approximately 10 mg of original cellulose samples were tested at a time. Fibers were cut into small (~0.5 mm) pieces and loaded in the platinum pan. Both fibers and powdered samples were subjected to a 5 °C min⁻¹ temperature ramp starting from room temperature to 600 °C in air.

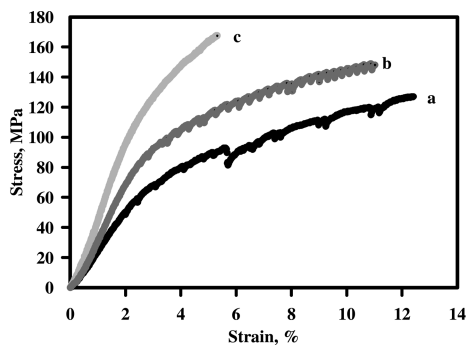


Figure 3. Stress-strain curves for plain cellulose fibers extruded from IL solutions of (a) MCC (black), (b) Peach (dark grey), (c) Pulp (light grey).

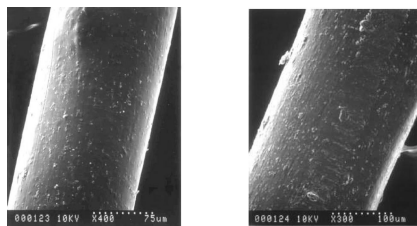


Figure 4. SEM images of composite fibers from MCC (14 wt%) with 3.5 wt% (left) and 7.5 wt% (right) TiO_2 particles.

Tensile Strength

At least five 10 cm long samples were tested in each category after optical screening for a relative uniform cross section of the fiber. The average diameter of each individual fiber was calculated from the measurements at five different sections of the same fiber. The mechanical properties of the fibers were determined using a MTS Q-Test 25 machine attached with a specially designed pneumatic grip suitable for thin and flexible fiber testing. A load cell of 22.4 newton capacity was used for load measurement. The cross head speed was maintained at 1.27 mm min^{-1} and a data acquisition system was used to obtain the data in terms of stress and strain.

Energy Dispersive X-ray Spectroscopy (EDS)

Elemental analysis at the surface of the composite fibers was recorded using a Philips XL30 SEM-EDS instrument at 6.5 kV accelerating voltage. Relative concentrations of C, O, and Ti were determined from different spots of the fibers (at least five spots for each fiber with a 7.5 nm spot size) for statistical analyses.

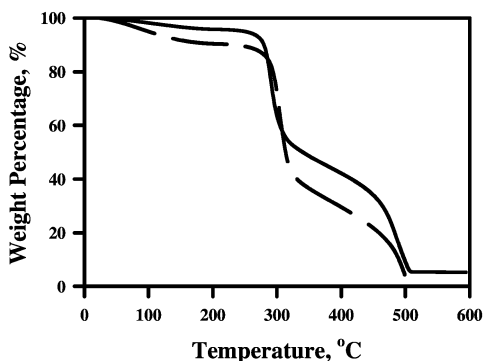


Figure 5. TGA curves for Pulp fibers (8 wt%) with 0% (dashed line) and 5% (solid line) TiO_2 relative to cellulose mass.

Results and Discussion

Characterization of Plain Fibers

Surface Morphology

It has previously been shown for this process (24) that there is a strong dependence between the surface texture of fibers and the concentration of the cellulose used in the solution. Figure 2 shows the SEM images (120 \times magnification) of plain cellulose fibers from MCC (14 wt%; DP = 270) on the left and Peach (4 wt%; DP = 687) on the right. The MCC fibers on the left side have a circular cross section following the exact shape of the syringe tip used for the extrusion. The surface texture is smooth and compact without any cracks. The extrusion of the Peach-sourced fibers (right image) at such a low concentration was favored by the higher DP number of this cellulose source, as well as the presence of hemicellulose which resulted in a higher viscosity cellulose/IL solution. These fibers, however, have a wrinkled surface which was probably caused by the rapid diffusion of IL into water during the regeneration process. Although the extrusion of the fibers at this low concentration was possible, the process was not continuous. To ensure the production of continuous and homogeneous fibers higher concentrations of Peach were ultimately used for both the plain and composite fibers.

Thermal Stability

Thermogravimetric analyses of the original cellulose samples and the fibers regenerated from IL solution showed that the IL processing did not change the thermal stability of the material or produce any chemical modification. Previous studies (24) showed that the onset decomposition temperature for both original and spun materials was around 300 $^{\circ}\text{C}$ and complete degradation temperatures

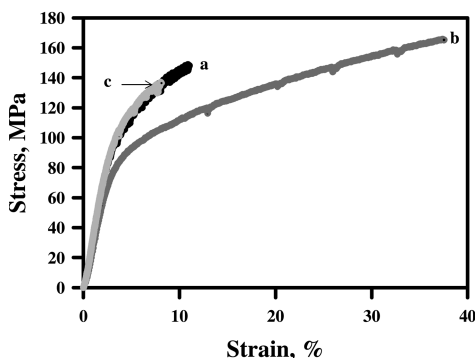


Figure 6. Stress-strain curves for composite cellulose fibers extruded from IL solutions of Peach with concentrations of TiO_2 particles of (a) 0% (black solid line), (b) 3.5% (dark grey line), (c) 5.0% (light grey line).

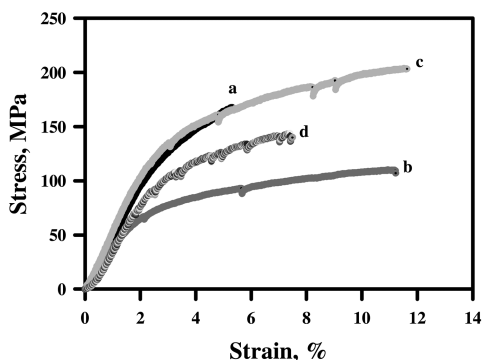


Figure 7. Stress-strain curves for composite cellulose fibers extruded from IL solutions of Pulp with concentrations of TiO_2 particles of (a) 0% (black solid line), (b) 3.5% (dark grey line), (c) 5.0% (light grey line), (d) 7.5% (dotted line).

were between 450 and 500 °C. The samples analyzed from the fibers also seemed to be more thermally stable with a slower two step decomposition curve. This can be attributed to the more compact structure due to the repacking of the molecules after regeneration and the big particle size even after grinding.

The early weight loss for both original cellulose and fibers is due to moisture loss during heating (38). Cellulosic materials are hydrophilic so significant water loss was observed for the fibers that were washed with water during regeneration.

Mechanical Properties

The stress-strain plots for the three types of plain cellulose fibers are shown in Figure 3 and their mechanical properties are compared in Table I. The average data for the ultimate stress and failure strain were calculated for at least five test

Table I. Mechanical Properties of Cellulose Fibers^a

<i>Cellulose Type</i>	<i>TiO₂ (wt%)</i>	<i>Ultimate Stress (MPa)</i>	<i>ΔStress^b (%)</i>	<i>Failure Strain (%)</i>	<i>ΔStrain^b (%)</i>
MCC DP = 270	0	127(11)	0	12(1)	0
	3.5	112(9)	-12	16(4)	33
	5.0	106(15)	-17	5(4)	-58
	7.5	125(5)	-2	10(0)	-17
Peach DP = 687	0	149(8)	0	11(1)	0
	3.5	166(16)	11	38(0)	245
	5.0	137(8)	-8	8(1)	-27
Pulp DP = 1056	0	165(11)	0	5(1)	0
	3.5	110(1)	-33	11(1)	120
	5.0	204(15)	24	12(6)	140
	7.5	137(9)	-17	8(3)	60

^a Numbers in parentheses represent calculated standard deviations for more than 5 samples tested. ^b $\Delta\text{Stress}/\text{strain} = [(\text{stress}/\text{strain of composite fiber}) - (\text{stress}/\text{strain of plain fiber})] / (\text{stress}/\text{strain of plain fiber})$.

samples. The tensile strength results show that there is a strong correlation between the stress and strain values for the fibers and the concentration and DP number of the cellulose source used. Previous work showed that for Peach, hemicellulose facilitated the extrusion of strong fibers even at low concentration (3.8 wt%) over the Pulp fibers with a concentration of 4.3 wt% (24). In this study, we almost doubled the cellulose concentrations (7 wt% for Peach and 8 wt% for Pulp), but the fibers were weaker compared to the ones from low concentration solutions. We believe that this was caused mostly by the higher viscosity of the solution which made the spinning process more difficult using our current extrusion set up. The inability of the equipment to sufficiently stretch the fibers during extrusion led to higher thicknesses and poorer stress-strain properties.

Characterization of Composite Fibers

TiO₂ particles were homogeneously dispersed in cellulose/IL solutions with final concentrations of 3.5, 5, and 7.5 wt% of TiO₂ relative to the cellulose mass. Composite fibers were extruded from these solutions and characterized using the same methods as for the plain fibers.

Table II. Calculated TiO₂ Concentration at the Surface of the Composite Fibers by EDS^a

<i>Fiber type</i>					
<i>Cellulose</i>	<i>TiO₂ (wt%)</i>	<i>C (wt %)</i>	<i>O (wt %)</i>	<i>Ti (wt %)</i>	<i>TiO₂ (wt %) on surface</i>
MCC	3.5	43.9(1)	53.3(1)	2.8(1)	4.7(1)
	5.0	43.2(1)	53.4(1)	3.4(1)	5.6(1)
	7.5	41.7(1)	54.2(1)	4.1(1)	6.8(2)
Peach	3.5	42.8(0)	54.2(1)	3.0(1)	5.0(1)
	5.0	45.0(1)	52.0(2)	3.0(1)	5.0(1)
Pulp	3.5	43.6(1)	53.8(1)	2.6(1)	4.3(1)
	5.0	43.7(3)	53.0(2)	3.3(1)	5.5(1)
	7.5	41.6(2)	53.2(1)	5.2(1)	8.7(2)

^a Numbers in parentheses represent calculated standard deviations for more than five samples tested.

Surface Morphology

With addition of TiO₂ particles to the cellulose/IL solution, white fibers were obtained with a rough surface texture. The SEM images in Figure 4 show the increased density of TiO₂ particles at the surface of the fiber with higher additive concentration used. The dispersion of the particles was fairly homogeneous, but due to surface outcropping by the increased number of particles, the surfaces became rugged and cracks could be seen. It is believed that the increased ruggedness of the fiber surface should enhance the specific properties of the particles due to higher exposure to the activation factors (e.g., UV-light for antimicrobial activity of TiO₂ particles) (35).

Thermal Stability

The thermogravimetric analyses for the composite fibers compared to the plain fibers is presented in Figure 5. The decomposition curves keep the same trend of two step decomposition due to the compact structure of the fibers implying that there was not interference between the TiO₂ particles and the cellulose matrix. The residual weight of the samples studied corresponded to the weight of the additive used in the composite fiber suggesting that almost all the cellulose was decomposed during the heating process.

Mechanical Properties

The stress-strain plots of Peach and Pulp fibers with different concentrations of additive incorporated are shown in Figure 6 and Figure 7, respectively, and the corresponding data are provided in Table I. The general trend for the strength of the composite fibers is typically that with increased concentration of additive, the mechanical properties are degraded. But the data shows that there is an optimal concentration of TiO₂ that can be used to partially preserve the mechanical properties of the fibers. This concentration is 5 wt% TiO₂ and can be explained by a suitable incorporation of the particles in the cellulose matrix that allows the stress transfer at the interface region between the particles and cellulose.

It can also be observed that the elastic modulus of the composite fibers doesn't significantly change compared to the plain fibers. This is most probably due to the low concentrations of the additive used in the fibers. The particle size of additives might also be a critical factor for the mechanical properties. Larger sized particles are homogeneously dispersed in the cellulose/IL solution and don't create the agglomerates that would disturb the adhesion between the particles and the cellulose.

Energy Dispersive X-ray Spectroscopy (EDS)

The results of EDS analyses performed on the surface of the composite fibers are presented in Table II. The purpose of the analyses was to determine the relative concentration of TiO₂ on the surface of the fibers and to predict the photocatalytic activity of the particles when activated by UV-light and their performance against any microbial agent present on the surface. The theoretical concentrations of the TiO₂ particles in case of completely homogeneous dispersion of the particles within the fibers were calculated (data not shown). It was found that the experimentally obtained surface concentrations of TiO₂ were higher than the theoretical values. This implies that although the dispersion of TiO₂ particles in the IL-based solution was homogeneous the extrusion and drying process resulted in production of composite fibers where TiO₂ particles mostly rested on the surface and yet no agglomerations were observed. This is a confirmation of the SEM results which showed the TiO₂ particles outcropping the surface of the fibers. This result indicates that the IL process for fiber preparation helps the formation of composite fibers with an active surface provided by the dispersed additive within the fiber.

Conclusions

The production of cellulose composite fibers from cellulose/IL/TiO₂ suspensions was demonstrated. Increasing concentration of the TiO₂ particles in the spinning dope makes the texture of the fibers surface more rugged, but this could increase the additive particle exposure to UV-light for enhanced

photocatalytic activity. The resultant mechanical properties of the fibers are strongly dependent on the solution viscosity, hence on the cellulose concentration in the IL. The composite fibers with 5% TiO₂ have similar mechanical properties as the plain fibers, which means under these conditions the additive doesn't have a significant effect on resultant stress or strain. EDS measurements confirmed that most of the TiO₂ particles are close to the surface of the fibers providing a large active surface area.

Acknowledgements

The authors thank BASF Corporation for financial support and generous donation of [C₂mim]Cl.

References

1. French, A. D.; Bertoniere, N. R.; Brown, M. R.; Chanzy, H.; Gray, D.; Hattori, K.; Glasser, W. In *Kirk-Othmer Encyclopedia of Chemical Technology*; Kroschwitz, J. I., Ed.; Wiley: New York 2001; Vol. 5, pp 360-394.
2. Kamel, S.; Ali, N.; Jahangir, K.; Shah, S. M.; El-Gendy, A. A. *Express Polym. Let.* **2008**, *2*, 758.
3. Holbrey, J. D.; Chen, J.; Turner, M. B.; Swatloski, R. P.; Spear, S. K.; Rogers, R. D. In *Ionic Liquids in Polymer Systems: Solvents, Additives, and Novel Applications*, Brazel, C. S.; Rogers, R. D., Eds.; ACS Symposium Series 913; American Chemical Society: Washington, DC, 2005, pp 71–87.
4. Wilkes, A. G. In *Regenerated Cellulose Fibers*; Woodings, C.; CRC Press: New York, 2000, pp 37–61.
5. Heinze, T.; Liebert, T. *Prog. Polym. Sci.* **2001**, *26*, 1689.
6. Hermanutz, F.; Meister, F.; Uerdingen, E. *Chem. Fibers Int.* **2006**, *56* (342), 344.
7. Rosenau, T.; Potthast, A.; Sixta, H.; Kosma, P. *Prog. Polym. Sci.* **2001**, *26*, 1763.
8. Buijtenhuijs, F. A.; Abbas, M.; Witteveen, A. J. *Papier* **1986**, *40*, 615–619.
9. *Ionic Liquids in Synthesis*; Wasserscheid, P.; Welton, T.; Wiley-VCH: Weinheim, DE, 2003; p 82.
10. Swatloski, R. P.; Spear, S. K.; Holbrey, J. D.; Rogers, R. D. *J. Am. Chem. Soc.* **2002**, *124*, 4974.
11. Swatloski, R. P.; Holbrey, J. D.; Spear, S. K.; Rogers, R. D. In *Molten Salts XIII: Proceed. Int. Symposium*; Trulove, P. C.; De long, H. C.; Mantz, R. A.; Stafford, G. R.; Matsunaga, M., Eds.; The Electrochemical Society: Pennington, NJ, 2002; p 155.
12. Swatloski, R. P.; Rogers, R. D.; Holbrey, J. D. U.S. Patent 6,824,559 B2, 2004.

13. Wang, W.; Shen, G.; Swatloski, R. P.; Farag, R.; Broughton, R. M., Jr.; Rogers, R. D. Proceedings of the International Nonwovens Technical Conference, Toronto, Canada, September 20–23, 2004; Association of the Nonwoven Fabrics Industry: Cary, NC, 2004.
14. Sun, N.; Swatloski, R. P.; Maxim, M. L.; Broughton, R. M.; Spear, S. K.; Daly, D. T.; Haque, A.; Harland, A. G.; Rogers, R. D. Textile Processing: State of the Art & Future Developments, Proceedings of the 4th International Conference of Textile Research Division, National Research Centre, Cairo, Egypt, April 14–17, 2007; 2007; Vol. 4, p 139.
15. Zhang, H.; Wu, J.; Zhang, J.; He, J. *Macromolecules* **2005**, *38*, 8272.
16. Phillips, D. M.; Drummy, L. F.; Naik, R. R.; De Long, H. C.; Fox, D. M.; Trulove, P. C.; Mantz, R. A. *J. Mater. Chem.* **2005**, *15*, 4206.
17. Xie, H. B.; Li, S. H.; Zhang, S. B. *Green Chem.* **2005**, *7*, 606.
18. Turner, M. B.; Spear, S. K.; Holbrey, J. D.; Rogers, R. D. *Biomacromolecules* **2004**, *5*, 1379.
19. Turner, M. B.; Spear, S. K.; Holbrey, J. D.; Daly, D. T.; Rogers, R. D. *Biomacromolecules* **2005**, *6*, 2497.
20. Bagheri, M.; Rodriguez, H.; Swatloski, R. P.; Spear, S. K.; Daly, D. T.; Rogers, R. D. *Biomacromolecules* **2008**, *9*, 381.
21. Poplin, J. H.; Swatloski, R. P.; Holbrey, J. D.; Spear, S. K.; Metlen, A.; Grätzel, M.; Nazeeruddin, M. K.; Rogers, R. D. *Chem. Commun.* **2007**, 2025.
22. Hines, J. H.; Wanigasekara, E.; Rudkevich, D. M.; Rogers, R. D. *J. Mater. Chem.* **2008**, *18*, 4050.
23. Swatloski, R. P.; Holbrey, J. D.; Weston, J. L.; Rogers, R. D. *Chimica Oggi/Chem. Today* **2006**, *24*, 31.
24. Sun, N.; Swatloski, R. P.; Maxim, M. L.; Rahman, M.; Harland, A. G.; Haque, A.; Spear, S. K.; Daly, T. D.; Rogers, R. D. *J. Mater. Chem.* **2008**, *18*, 283.
25. Viswanathan, G.; Murugesan, S.; Pushparaj, V.; Nalamasu, O.; Ajayan, P. M.; Linhardt, R. J. *Biomacromolecules* **2006**, *7*, 415.
26. Tsiptsias, C.; Panayiotou, C. *Carbohydrate Polym.* **2008**, *74*, 99.
27. Zyryanov, G. V.; Kang, Y.; Rudkevich, D. M. *J. Am. Chem. Soc.* **2003**, *125*, 2997.
28. Wang, R.; Hasimoto, K.; Fujishima, A. *Nature* **1997**, *388*, 431.
29. Mandelbaum, P. A.; Regazzoni, A. E.; Blesa, M. A.; Bilmes, S. A. *J. Phys. Chem. B* **1999**, *103*, 5505.
30. Shin, Y.; Yoo, D. I.; Jang, J. *J. Appl. Polym. Sci.* **2001**, *80*, 2495.
31. Dong, W.; Pang, G.; Shi, Z.; Xu, Y.; Jin, H.; Shi, R. *Mater. Res. Bull.* **2004**, *39*, 433.
32. Maness, P. C.; Smolinski, S.; Blake, D. M.; Huang, Z.; Wolfrum, E. J.; Jacobi, W. A. *Appl. Environ. Microbiol.* **1999**, *65*, 4094.
33. Sunada, K.; Watanabe, T.; Hashimoto, K. *J. Photochem. Photobiol., A* **2003**, *156*, 227.
34. Daoud, W. A.; Xin, J. H.; Zhang, Y. H. *Surface Sci.* **2005**, *599*, 69.
35. Takahashi, T.; Shoji, Y.; Inoue, O.; Miyamoto, Y.; Tokuda, K. *Biocontrol Sci.* **2004**, *9*, 51.

36. Zhou, J.; Liu, S.; Qi, J.; Zhang, L. *J. Appl. Polym. Sci.* **2006**, *101*, 3600.
37. Marques, P. A. A. P.; Trindade, T.; Neto, C. P. *Composites Sci. Technol.* **2006**, *66*, 1038.
38. Scheirs, J.; Camino, G.; Tumiatti, W. *Eur. Polym. J.* **2001**, *37*, 933.

Chapter 15

Novel Cellulose Products Prepared by Homogeneous Functionalization of Cellulose in Ionic Liquids

Susann Dorn¹, Michael Schöbitz^{1,2}, Kerstin Schluffer^{1,3} and Thomas Heinze^{1,*}

¹Centre of Excellence for Polysaccharide Research, Friedrich Schiller University of Jena, Humboldtstraße 10, D-07743 Jena, Germany

²Thuringian Institute for Textile and Plastics Research, Breitscheidstraße 97, D-07407 Rudolstadt, Germany

³Forschungszentrum für Medizintechnik und Biotechnologie GmbH, Geranienweg 7, D-99947 Bad Langensalza, Germany

*thomas.heinze@uni-jena.de, Member of the European Polysaccharide Network of Excellence, EPNOE (www.epnoe.eu).

The paper deals with the application of ionic liquids (ILs) as solvents and as reaction media. IIs, namely 1-butyl-3-methylimidazolium chloride, 1-ethyl-3-methylimidazolium chloride, 1-ethyl-3-methylimidazolium acetate, 1-butyl-2,3-methylimidazolium chloride and 1-allyl-2,3-dimethylimidazoliumbromide, dissolve cellulose and can easily be applied as media for cellulose functionalization. We investigated the homogeneous acylation of cellulose with a degree of polymerization the range from 330 to 6500. Under mild conditions and within short reaction time, at low temperature and low molar ratio, different cellulose esters and dendronized cellulose were obtained.

Introduction

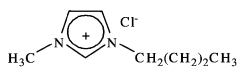
Cellulose is an important raw material of the future. Cellulose is not only the most abundant renewable biopolymer but also a very uniform macromolecule. It consists of β -(1 \rightarrow 4) linked anhydroglucose repeating units, which form a very

compact structure including hydrogen bonding. Cellulose is stereo regular, chiral, biocompatible and reactive. Based on cellulose, a broad variety of chemical products may be prepared. Mostly, chemical modifications of cellulose come along with heterogeneous synthesis pathways. Homogeneous paths open new opportunities for the design of cellulose products with unconventional functional groups and with controlled functionalization pattern (1, 2). By applying a homogeneous synthesis, the degree of substitution (DS) can easily be controlled and more options to introduce novel functional groups with bulky and exotic functions are available (3).

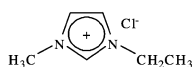
Typical cellulose solvents like *N,N*-dimethylacetamide (DMAc)/LiCl (4) and dimethyl sulfoxide (DMSO)/tetrabutylammonium fluoride (5, 6) are effective homogeneous media for cellulose functionalization in lab scale synthesis. Never the less, some problems appear, especially for industrial application. The system consisting of organic solvent and salt are very difficult to handle because of the combustibility of the organic compound and the recycling is proved to be expensive. In the case of DMSO, some side reactions, like the Swern oxidation may occur and can lead to undesired structures in the products.

Thus, there is an increasing interest in new cellulose solvents that are efficient and recyclable. Ionic liquids (IL) can be an alternative solvent for cellulose, a media for homogeneous cellulose functionalization. ILs are low-melting salts that consist only of cations and anions. ILs are non-flammable, highly thermal stable and have no measurable vapour pressure. So-called designer solvent are more and more in the focus of cellulose chemistry. The first useful IL, ethyl ammonium nitrate, investigated by Walden, generated little interest and until the early 1980s, no detailed information about physical and chemical properties were described. The discovery of tetraalkylammonium ILs, which are air- and moisture stable, leads to an increasing interest for application, especially in spectroscopy, synthesis, and electrochemistry (7). ILs are in the focus of the interest in various fields of research and development (8). At the present, there are several articles concerning the concept of ILs. Next to the synthesis, the properties and different application of ILs, the carbohydrate chemistry in ILs were discussed intensively (9–18). Up to now, the broad variety of structures of ILs was not really estimated in the field of cellulose modification, mainly imidazolium based ILs were studied. Swatowski et al. Found that these ILs, in particular 1-butyl-3-methylimidazolium in combination with several anions, e.g., halides, are able to dissolve cellulose (19, 20). 1-Butyl-3-methylimidazolium chloride (BMIMCl) is announced to be the most efficient solvent for cellulose. Other studies show that 1-allyl-3-methylimidazolium chloride can be used as medium for cellulose acetylation. Cellulose acetates with a high degree of substitution (DS) were obtained (21).

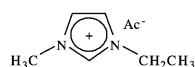
In the course of our studies, we investigated different imidazolium based ILs as reaction medium for cellulose chemistry, on the one hand. Especially the application of IL as reaction medium for the acylation of cellulose will be studied.



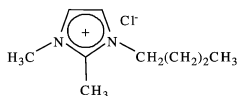
1-Butyl-3-methylimidazolium chloride



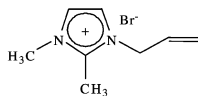
1-Ethyl-3-methylimidazolium chloride



1-Ethyl-3-methylimidazolium acetate



1-Butyl-2,3-dimethylimidazolium chloride



1-Allyl-2,3-dimethylimidazolium bromide

Figure 1. Structures of the ionic liquids used in this studies.

ILs in Cellulose Chemistry

In the context of our investigations, imidazolium based IL with chloride as anion were utilized. Next to BMIMCl, 1-ethyl-3-methylimidazolium chloride (EMIMCl), 1-butyl-2,3-dimethylimidazolium chloride (BDMIMCl), 1-allyl-2,3-dimethylimidazolium bromide (ADMIMBr) and 1-ethyl-3-methylimidazolium acetate (EMIMAc), were applied (Figure 1). The ILs possess a purity of 98%. Because impurities may act as catalyst or inhibitor and/or side reactions may occur.

ILs as Solvent for Cellulose

ILs can dissolve cellulose (19, 20, 22, 23). Depending on the type of cellulose, very high concentrated solution can be achieved. Microcrystalline cellulose (MCC) with a degree of polymerization (DP) of 330 can easily be dissolved in IL as well as high molecular weight bacterial cellulose (BC) with a DP of 6500. The amount of cellulose in the solution depends on the type of IL; BMIMCl is the most efficient solvent for cellulose. EMIMCl and ADMIMBr dissolve less cellulose (22). For dissolving MCC in different ILs of the homologous series of a 1-alkyl-3-methylimidazolium based IL and chloride as anion, unexpected results were found. The solubility of the cellulose depends on the alkyl chain length of the cation. For the methylimidazolium cation, no solubility of the cellulose was found. By applying IL with ethyl, butyl or hexyl as alkyl chain, cellulose can be dissolved without any residue. Longer alkyl chain, like octyl leads to an extensive swelling of the biopolymer. Our studies showed the ILs are non-derivatizing solvents for cellulose (23). The DP values both of the starting material and the regenerated samples were determined by the intrinsic viscosity. No degradation during the dissolution process appears independent of the cellulose type (22). Using the IL as solvent for cellulose, the IL can easily be recycled as hygroscopic liquid. This liquid can be reused without additional purification after 24 h freeze-drying.

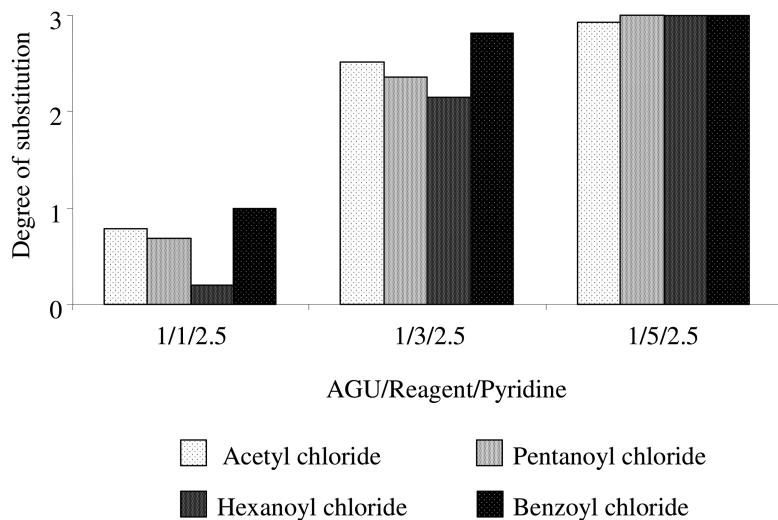


Figure 2. Values of the degree of substitution of cellulose acetate, cellulose pentanoate, cellulose hexanoate and cellulose benzoate, synthesized in 1-butyl-3-methylimidazolium chloride (2 h, 80°C).

IL as Reaction Media

To investigate the reactivity of the cellulose dissolved in IL, the acylation with several reagents was studied (22, 23). The conversion of cellulose in BMIMCl with acid chlorides, like acetyl chloride, pentanoyl chloride, hexanoyl chloride and benzoyl chloride was successfully carried out within 2 h at 80°C. Cellulose esters with a DS in the range from 0.3 to 3.0 were obtained (Figure 2). This reaction requires the addition of 2.5 mol pyridine to the medium. On the one hand pyridine activates the acid chloride to form the reactive acylium ion and, on the other, it neutralizes the liberated HCl. Hexanoyl chloride exposed to be the less reactive reagent used in these studies. Applying a molar ratio of 1/1 (mol anhydroglucose unit (AGU)/mol reagent), a conversion of 30% was achieved. With an increasing molar ratio, the DS obtained increases as well. Thus, a completely substituted cellulose hexanoate was obtained by applying a molar ratio of 1/5. Acetyl chloride and pentanoyl chloride were more reactive than hexanoyl chloride; 1 mol reagent per mol AGU, leads to a cellulose ester with a DS of 0.9 for acetyl chloride and 0.8 for pentanoyl chloride. The DS can be increased up to 3.0 with an input of reagent of 5 mol per mol AGU. In the course of our studies, benzoyl chloride seems to be the most efficient reagent. There was a nearly complete conversion of the reagent, independent of the amount of benzoyl chloride used. Regarding the cellulose esters synthesized, solubility appears in DMSO at a DS > 0.3 and additionally in acetone and chloroform at a DS over 2.0.

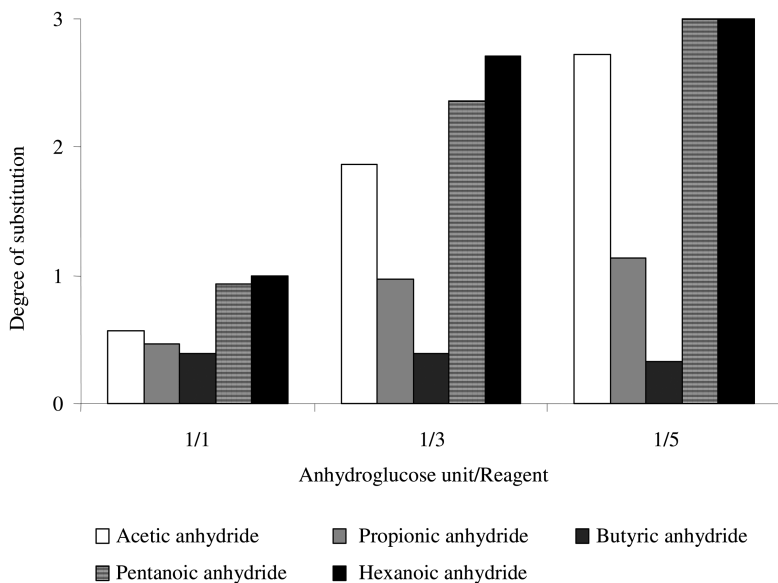


Figure 3. Values of the degree of the substitution of the cellulose derivatives, obtained with different reagent and different molar ratio (mol anhydroglucose unit per mol reagent) in 1-butyl-3-methylimidazolium chloride at 80°C within 2 h.

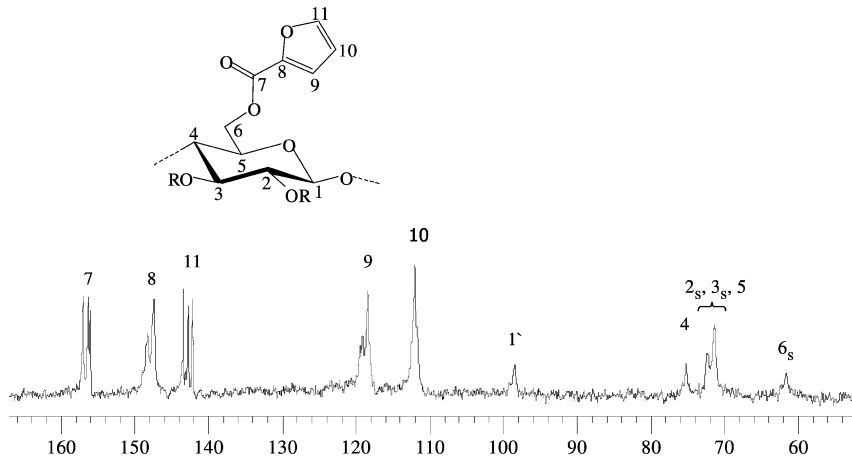


Figure 4. ^{13}C NMR spectrum of a cellulose furoate (DS 3.0) synthesized in 1-butyl-3-methylimidazolium chloride within 3 h at 65°C.

Compared to the results of the acylation with acid anhydrides in BMIMCl (2 h at 80°C), it was found that the acid chlorides were more efficient than the acid anhydrides (acetic anhydride, propionic anhydride, butyric anhydride, pentanoic anhydride and hexanoic anhydride) applied. For the reaction with acetic anhydride the addition of pyridine is not necessary. As shown in Figure

3, propionic anhydride and butyric anhydride lead to low DS ($DS_{\text{propionate}} = 0.9$; $DS_{\text{butyrate}} = 0.4$). The DS values achieved with pentanoic anhydride and hexanoic anhydride are much higher ($DS_{\text{pentanoate}} = 2.4$; $DS_{\text{hexanoate}} = 2.7$) at comparable molar ratio of 1/3 (mol AGU/mol reagent). Except for cellulose butyrate, the DS of the cellulose esters increases with increasing molar ratio. In the case of pentanoic anhydride and hexanoic anhydride, a complete substitution of the cellulose occurred at a molar ratio of 1/5 (AGU/reagent). All products with a DS higher than 0.9 are soluble in DMSO and at DS= 2.3 additional soluble in acetone and chloroform. The DS of the cellulose butyrate (DS= 0.4) could not be enhanced by changing the molar ratio, the reaction temperature or the reaction medium considering the ILs studied. Obviously, there is a relation between the length of the alkyl chain of the acid anhydride and the alkyl chain of the imidazolium based cation of the IL.

Synthesis of cellulose furoate can be realized in BMIMCl as reaction medium. Within 3 h at 65°C, it was possible to prepare soluble cellulose furoates with a DS in the range from 0.5 to 3.0. The DS can be reached independent of the type of cellulose used (MCC, DP 330 or cotton linters, CL, DP 1800). The cellulose furoates are soluble in DMSO and with a DS higher than 2.4, additional soluble in DMA (Table 1). Applying a molar ratio of 1 mol 2-furoyl chloride (FC) per mol AGU, a conversion of 46% of the reagent occurred. The addition of the equimolar amount of pyridine results in a product of a higher DS of 0.62. Pyridine acts in two ways; formation of the reactive acylium ion and as base to bind the HCl liberated. Increasing the amount of FC up to 3 or 5 mol per mol AGU, an increase of the DS up to 3.0 of the cellulose furoates were obtained. The reactivity of the FC depends on the starting biopolymer. Comparing the reaction of MCC and CL with FC, it was found that the CL of comparable high molecular weight is less reactive. At similar molar ratio (1/5, AGU/FC) the cellulose furoate based on CL has the lower DS of 0.67. Cellulose furoate can be synthesized without any impurities in BMIMCl (Figure 4). The ^{13}C NMR spectrum shows the typical peaks of a completely substituted cellulose furoate. The peaks of the AGU can be found in the range from 60 to 100 ppm. In the range from 110 to 150 ppm, the peaks of the carbons of the furoyl moiety and at 159 ppm the carbonyl carbon can be assigned.

Functionalization of Bacterial Cellulose in IL

Next to 1-ethyl-3-methylimidazolium acetate, BMIMCl is able to dissolve MCC, spruce sulphite pulp, cotton linters and even bacterial cellulose (BC) with a very high DP up to 6500. The dissolution process in BMIMCl runs very fast, within 20 min, a clear solution can be achieved (Figure 5). The acetylation of BC with acetic anhydride and the carbanilation with phenyl isocyanate was studied. Within 2 h at 80°C, very high substituted cellulose esters can be obtained. The one pot synthesis occurs under mild conditions without an additional base. With an increasing molar ratio from 1/1 to 1/10 (AGU/reagent) different DS values can be generated (Figure 6). The excess of 3 mol acetic anhydride per mol AGU yields to cellulose acetate with a DS= 2.5. Increasing the molar ratio up to 1/10

Table 1. Degree of substitution and solubility of the cellulose furoates prepared in 1-butyl-3-methylimidazolium chloride within 3 h at 65°C

Cellulose Type ^a	Molar ratio AGU/FC/Py ^b	Cellulose furoate ^c			Solubility ^d		DP ^e
		DS _{overall}	DS _{O-6}	DS _{O-2,3}	DMSO	DMA	
MCC	1/1/0	0.46	0.38	0.08	+	+	-
MCC	1/1/1	0.62	0.47	0.15	+	-	-
MCC	1/3/3	2.43	-	-	+	+	228
MCC	1/5/5	3.00	1.00	2.00	+	+	273
CL	1/3/3	0.67	0.48	0.19	-	-	-

^a MCC: microcrystalline cellulose, CL: cotton linters

^b Anhydroglucose unit/2-furoyl chloride/pyridine.

^c Degree of substitution.

^d DMSO: dimethyl sulfoxide, DMA: dimethyl acetamide.

^e degree of polymerization.

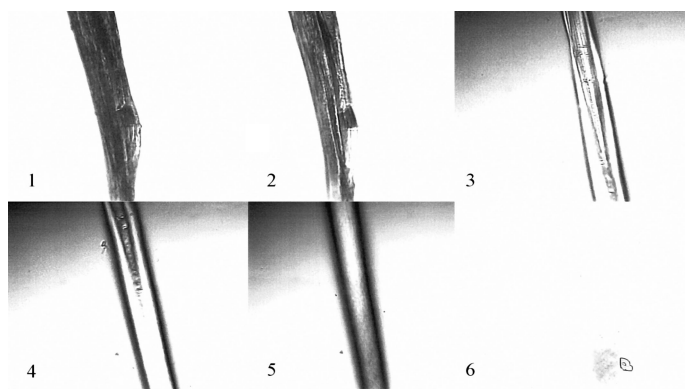


Figure 5. Microscopic images of bacterial cellulose (BC): (1) native BC, (2) after contact with solvent 1-butyl-3-methylimidazolium chloride, (3) after 10 min, (4) after 15 min, and (5) after 20 min dissolution time.

(AGU/reagent), completely substituted products were obtained. The BC acetates possess an unexpected distribution of groups in the order O-6>O-3>O-2 compared to cellulose acetates based on MCC. The cellulose esters are soluble in DMSO at a DS higher 0.7, but they are insoluble in acetone.

The carbanilation could also be successfully carried out. With molar ratio from 1/1 to 1/10 (AGU/ reagent), cellulose carbanilates with a DS in the range from 0.4 to 3.0 can be achieved. Applying 10 mol phenyl isocyanate per mol AGU, a completely substituted cellulose carbanilate was obtained within 4 h at 80°C. At a DS > 0.8 solubility in DMSO and at value higher than 2.2, even solubility in DMSO, THF and DMF appeared. The synthesis of cellulose carbanilates in BMIMCl can be used to prepare samples for studying the molecular weight of polymers by the means of SEC. During the reaction, no degradation of the polymer chain occurs (24).

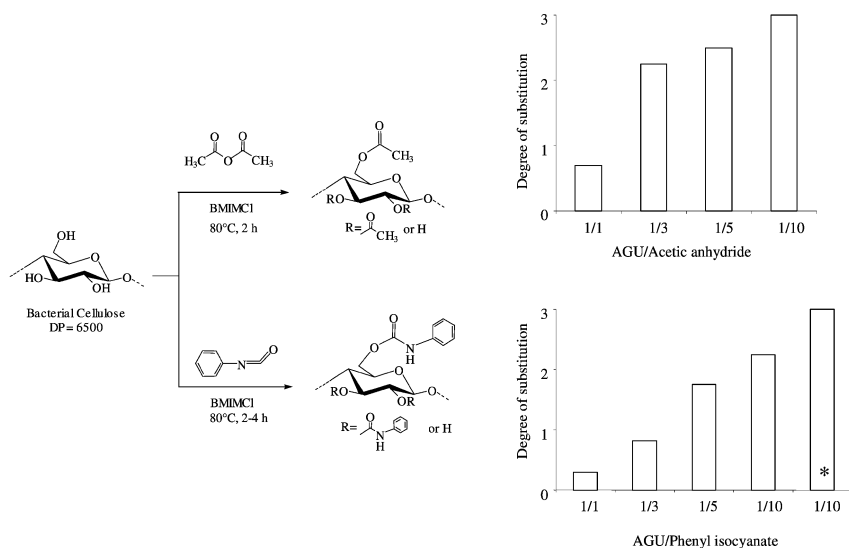


Figure 6. Reaction scheme of the synthesis of cellulose acetate and cellulose carbanilate based on bacterial cellulose in 1-butyl-3-methylimidazolium chloride (BMIMCl) within 2 h (* 4 h) at 80°C and the values of the degree of substitution of the products.

Table 2. DS of dendritic PAMAM-triazolo-cellulose derivatives synthesized homogeneously in EMIMAc by reaction of propargy-polyamidoamin dendrons of 1st, 2nd, and 3rd generation via Copper-Catalysed Huisgen Reaction

Molar ratio ^a	Conditions		Product
	Temperature (°C)	Time (h)	DS ^b
1/2	10	24	0.18
1/2	25	4	0.30
1/1	25	24	0.52
1/2	25	24	0.55
1/2 ^b	25	48	0.60
1/3	25	24	0.48
1/1	25	72	0.28

^a Molar ratio: mol repeating unit 6-azido-6-deoxycellulose (DS=0.75) per mol reagent.

^b Degree of substitution.

Preparation of Special Cellulose Derivatives in IL

Besides esterification reactions, unconventional types of cellulose derivatization were investigated. Namely the preparation of dendronized cellulose applying 1, 3-dipolar cycloaddition. Therefore, 6-azido-6-deoxycellulose (ADC) was dissolved in EMIMAc and the respective dendron was added followed by CuSO₄ and sodium ascorbate as catalysts. The dissolution of ADC occurs within 4 h at 80°C.

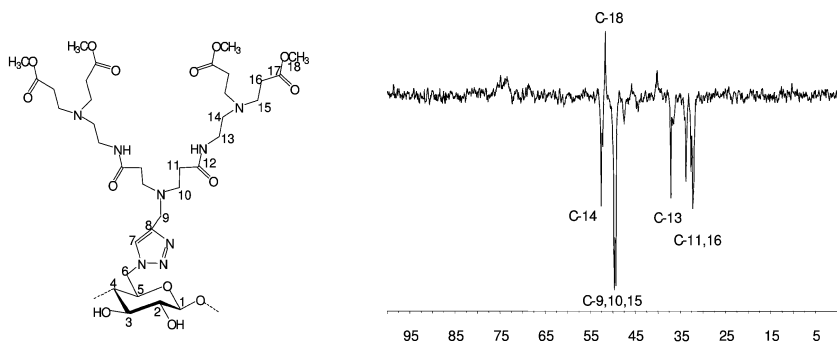


Figure 7. DEPT 135 NMR spectrum of 2nd generation PAMAM-triazolo cellulose, recorded in DMSO- d_6 at 25°C.

The correlation between reaction parameters and DS was investigated for the preparation of first generation of PAMAM-triazolo-cellulose. Using conventional solvents, the Huisgen reaction shows higher efficiency at lower temperature. However, using EMIMAC as a solvent, the DS is higher at ambient temperature. This may be caused by the increased viscosity of ADC solutions in the IL at lower temperature. Optimal conditions are a ratio of ADC and reagent of 1/1 and a reaction time of 24 h. Further increase of both the molar ratio and the reaction time leads to a minor DS increase only. It is well known that the reactivity of the dendrons decreases with increasing bulkiness of the dendron, i.e., with increasing generation. This results from the fact that functional groups along the cellulose backbone may be buried and are not easily accessible as a result of random coil conformation. Moreover, it is possible that the focal points of the dendrons may be buried inside the dendritic branches, which is even more pronounced with increasing generation (25). Therefore, for the attachment of second generation dendrons, the molar ratio was increased to 1/3 and for third generation, due to the high molar mass of the dendron, the reaction time was increased to 72 h (Table 2). Although the increase of time and molar ratio, the DS values for 2nd and 3rd generation PAMAM-triazolo-cellulose derivatives were lower than those of the 1st generation.

All samples obtained were soluble in polar aprotic solvents like DMSO and DMAc. The 3rd generation derivative is also soluble in water. Full structure characterization was carried out by elemental analysis and DEPT 135 NMR analysis (Figure 7). Due to the bulkiness of the dendrons the intensity of the signals of the AGU atoms is significantly reduced in NMR spectra. All signals can be assigned confirming the structure of the products.

Conclusion

ILs dissolve cellulose with a DP in the range from 330 to 6500 without degradation, if the right IL and procedure is provided. Using ILs as reaction media, the purity of the IL must be evaluated. In the course of our studies

various cellulose derivatives were investigated, especially cellulose esters and even unconventional dendronized cellulose sample. Different DS values were achieved by varying the molar ratio of the agent to biopolymer and the reaction time. Depending on the product in question, the reaction begins homogeneously and may end heterogeneously. During the etherification, gels formation and precipitation occurs quite often. BMIMCl can be used as reaction media for the modification of bacterial cellulose. Highly substituted cellulose acetates and cellulose carbanilates can be synthesized with low excess of reagent and without an additional catalyst. IL may be reactive yielding unexpected product. Further studies will be focused on novel products based on cellulose, synthesized homogeneously in Ilon the one hand and, on the other, on the design of IL for particular modification.

References

1. Klemm, D.; Philipp, B.; Heinze, T.; Heinze, U.; Wagenknecht, W. *Comprehensive Cellulose Chemistry*; Wiley-VCH: Weinheim, Germany, 2001.
2. Heinze, T. Chemical Functionalization of Cellulose, In *Polysaccharide: Structural Diversity and Functional Versatility*, 2nd ed.; Dumitriu, S., Ed.; Marcel Dekker: New York, Basel, Hong Kong, 2004; p 551.
3. Heinze, T.; Liebert, T. *Progr. Polym. Sci.* **2001**, *26*, 1689.
4. Williamson, S. L.; McCormick, C. L. *J. Macromol. Sci., Pure Appl. Chem.* **1998**, *A35*, 1915.
5. Heinze, T.; Dicke, R.; Koschella, A.; Kuhl, A. H.; Klohr, E. A.; Koch, W. *Macromol. Chem. Phys.* **2000**, *201*, 627.
6. Hussain, M. A.; Liebert, T.; Heinze, T. *Macromol. Rapid Commun.* **2004**, *25*, 916.
7. Poole, C. F. *J. Chromatogr., A* **2004**, *1037*, 49–82.
8. Dupont, J.; Souza, R. F.; Suarez, P. A. Z. *Chem. Rev.* **2002**, *102*, 3667–3691.
9. Welton, T. *Chem. Rev.* **1999**, *99*, 2071.
10. Olivier-Bourbigou, H.; Magna, L. *J. Mol. Catal. A.* **2002**, *182–183*, 419.
11. Poole, C. F. *J. Chromatogr., A* **2004**, *1037*, 49.
12. Wilkes, J. S. *J. Mol. Catal. A.* **2004**, *214*, 11.
13. Forsyth, S. A.; Pringle, J. M.; MacFarlane, D. R. *Aust. J. Chem.* **2004**, *57*, 113.
14. Chiappe, C.; Pieraccini, D. *J. Phys. Org. Chem.* **2005**, *18*, 275.
15. Murugesan, S.; Lindhardt, R. J. *Current Org. Synth.* **2005**, *2*, 437.
16. Laus, G.; Bentivoglio, G.; Schottenberger, H.; Kahlenberg, V.; Kopacka, H.; Röder, T.; Sixta, H. *Lenzinger Ber.* **2005**, *84*, 71.
17. Wu, G. *Green Chem.* **2006**, *8*, 325.
18. El Seoud, O. A.; Koschella, A.; Dorn, S.; Heinze, Th. *Biomacromolecules* **2007**, *8*, 2645.
19. WO 03/029329, The University of Alabahma, invs: Swatloski, R. P.; Spear S. K.; Holbrey, J. D., *Chem. Abstr.*, **2003**, *138*, 289216.

20. Swatloski, R. P.; Spear, S. K.; Holbrey, J. D.; Rogers, R. D. *J. Am. Chem. Soc.* **2002**, *124*, 4974.
21. Wu, J.; Zhang, J.; Zhang, H.; He, J.; Ren, Q.; Guo, M. *Biomacromolecules* **2004**, *5*, 266.
22. Barthel, S.; Heinze, T. *Green Chem.* **2006**, *8*, 301.
23. Heinze, T.; Schwikal, K.; Barthel, S. *Macromol. Biosci.* **2005**, *5*, 520.
24. Schlufte, K.; Schmauder, H.-P.; Dorn, S.; Heinze, T. *Macromol. Rapid Commun.* **2006**, *27*, 1670.
25. Frauenrath, H. *Prog. Polym. Sci.* **2005**, *30*, 325.

Chapter 16

Dissolution of Cellulose in Ionic Liquids and Its Application for Cellulose Processing and Modification

Liu ChuanFu^{1,*}, Sun RunCang^{1,2}, Zhang AiPing¹ and Li WeiYing¹

¹State Key Laboratory of Pulp & Paper Engineering,
South China University of Technology, Guangzhou, China

²Institute of Biomass Chemistry and Technology,
Beijing Forestry University, Beijing, China

*chfliu@scut.edu.cn

Cellulose is the most abundant renewable bioresource in the world and the most promising feedstock for industry in the future. Ionic liquids as novel and designable solvents have attracted much attention. In this review, the progress of the dissolution of cellulose in ionic liquids is illustrated. As suitable and environmentally friendly media, Ionic liquids also provide a new platform for cellulose processing and modification. The preparation of composite materials, cellulosic derivatives, and biofuels from cellulose in ionic liquids is summarized.

Introduction

Cellulose, the principal structural cell wall component of all territory plants, is the most abundant renewable bioorganic substance on the earth. This polymer consists of a chain of β -(1 \rightarrow 4)-linked glucose residues (1, 2). It is non-toxic, renewable, biodegradable and modifiable, which make it one of the most promising feedstock for industry in the future (3–5). Utilization of cellulose has a long history and there have been well-established technologies for the traditional applications of cellulose in industries including paper, paint, textile, food and pharmaceutical (5, 6). However, due to the stiff molecules and close chain packing via the numerous inter- and intra-molecular hydrogen bonds, it is extremely hard to dissolve cellulose in water and in most common

organic solvents, which constitutes a major obstacle for cellulose application. The efficient dissolution of cellulose is a long-standing goal in cellulose research and development. To date, only a limited number of solvent systems, such as DMAc/LiCl (7), DMF/N₂O₄ (8), NMNO (9), DMSO/TBAF (10), and some molten salt hydrates like LiClO₄·3H₂O (11), have been found efficient for cellulose dissolution. However, these solvent systems currently used for cellulose dissolution suffer drawbacks such as volatility or generation of poisonous gas, difficulty for solvent recovery, or instability in application and processing (12).

The low melting points organic salts known as Ionic liquids (ILs) have attracted increasing attention as novel and designable solvents in recent years (13). ILs are defined as materials that are composed of cations and anions which melt at or below 100°C. These properties make them non-volatile and interesting substitutes for many applications in which the volatile traditional organic solvents causes problems. Today, this is generally accepted that ILs are the promising novel green solvents for most organic and inorganic substances and can be used as green media in many processing and derivatization.

Dissolution of Cellulose in Ionic Liquids

The most common ILs in use are those containing alkylammonium, alkylphosphonium, 1-alkylpyridinium, and 1,3-dialkylimidazolium cations, as seen in Fig. 1 (13). The acidic proton of the imidazolium ring plays an important role in the imidazolium salts, which are the dominant ILs. Anions such as Cl⁻, Br⁻, NO₃⁻, [BF₄]⁻, [PF₆]⁻, CF₃SO₃⁻, and CF₃COO⁻ can be used in combination with the above cations to form low melting temperature ILs (14). The nature of the anion is largely responsible for the chemical properties of ILs.

The dissolution of cellulose in IL, molten *N*-ethylpyridinium chloride in the presence of nitrogen-containing bases, was firstly reported in 1934 (15). However, there had not been the concept of ILs and this finding was thought to be of little practical value at that time. Until recently, the application of ILs in cellulose chemistry has regained attention based on the understanding of ILs. In 2002, Rogers and his co-workers (16) reported ILs including 1-butyl-3-methylimidazolium chloride ([C₄mim]Cl, Fig. 2a) could be used as non-derivatizing solvents for cellulose. They carried out comprehensive studies on cellulose dissolution in ILs and its regeneration to produce advanced cellulose-based materials (17–22). Because of his great contribution, Rogers has become a winner of the 2005 US Presidential Green Chemistry Challenge Awards, indicating the importance of this work in society. Since then, cellulose dissolution of in ILs and its application have attracted the increasing attention. Many kinds of functionalized ILs, especially room-temperature ionic liquid (RTIL), with higher solubility for cellulose were reported. In 2003, Zhang and his co-workers (12, 23) synthesized a novel RTIL, 1-allyl-3-methylimidazolium chloride (AmimCl, Fig. 2b), which has outstanding capability for dissolving cellulose. This RTIL is a nonderivatizing solvent with higher solubility for cellulose than [C₄mim]Cl. Solution containing 5 wt% cellulose in AmimCl

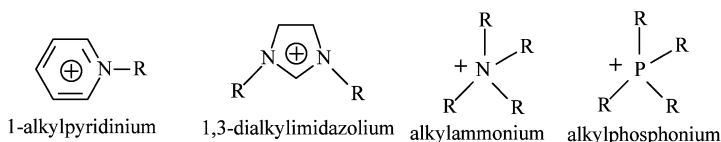


Figure 1. Structure of common cations in ionic liquids

could be formed within only 15 min at 100°C without any pretreatment or activation. In addition, it is more convenient for the application of AmimCl than [C₄mim]Cl because this IL is liquid at room temperature. In 2005, another RTIL, 1-(2-hydroxyethyl)-3-methylimidazolium chloride (HemimCl, Fig. 2c), was reported as the nonderivatizing solvent for cellulose by Luo and his co-workers (24). This IL has relatively high solubility for cellulose. Solutions containing 5% cellulose in HemimCl could be formed at 60°C, and 6.8% at 70°C. However, the relatively low thermal stability of HemimCl limits its application. In 2008, Ohoo and his group (25) reported that a series of RTILs, alkylimidazolium salts containing dimethyl phosphate, methyl methylphosphonate, or methyl phosphonate (26), had the potential to solubilize cellulose under mild conditions. Especially, 1-ethyl-3-methylimidazolium methylphosphonate (Fig. 2d) could enable the preparation of 10 wt% cellulose solution at 45°C within 30 min and 2-4 wt% cellulose solution even at room temperature without any pretreatment and heating. These functionalized ILs exhibit higher solubility for cellulose and more convenience for processing and application.

However, the present reports on cellulose dissolution in ILs mainly focus on the synthesis of functionalized ILs and the effect of dissolution conditions on cellulose solubility. The mechanism of cellulose dissolution in ILs was investigated only in a few publications. It is generally accepted that the high concentration and activity of chloride anion, which is strong hydrogen bond acceptor and highly effective in breaking the extensive hydrogen-bonding network present in cellulose, is responsible for the dissolution of cellulose (16). In addition, the presence of water in ILs significantly decreases the solubility of cellulose through competitively hydrogen-bonding to the cellulose microfibrils which inhibits solubilization. On the other hand, ILs containing “noncoordinating” anions such as [BF₄]⁻ and [PF₆]⁻ are not suitable solvents for cellulose, whereas they can be used as biocides (27, 28) and anti-electrostatic agents for wood (29). However, Navard (30) pointed out that the swelling and dissolution mechanism in ILs were entirely due to the way cellulose fibers are structured, not depending on the type of solvent.

It was accepted that there was no decomposition of cellulose occurred during dissolution in ILs and the regenerated cellulose had almost the same degree of polymerization and polydispersity as the initial one (16, 31). However, the recent studies have indicated that degradation of cellulose during dissolution does occur and the degree of polymerization of regenerated cellulose decreases (32–34). Moreover, the microstructure of cellulose is changed after regeneration from ILs. There are two opinions on the crystalline structure of the regenerated cellulose. Zhai (35) investigated the structural differences between cellulose regenerated from [C₄mim]Cl and untreated cellulose using X-ray diffraction. The data showed

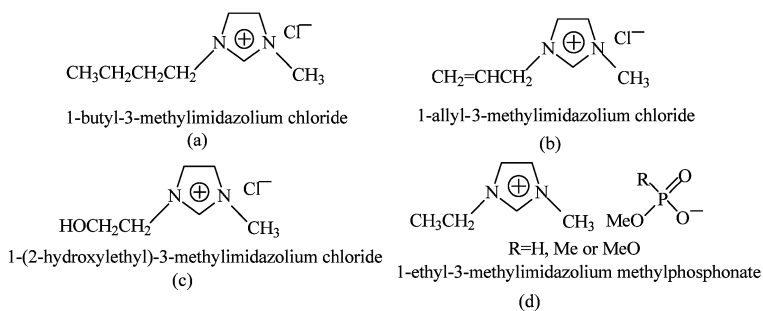


Figure 2. Chemical structure of ionic liquids for cellulose dissolution

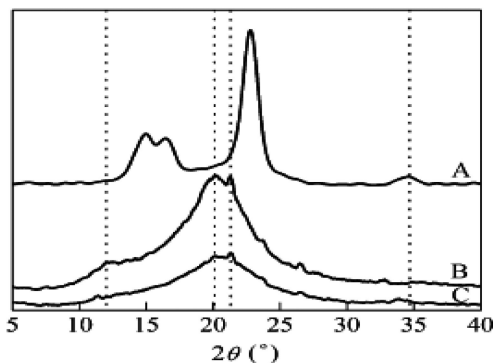


Figure 3. X-ray diffraction patterns for original cellulose (A) and cellulose regenerated from $[C_4mim]Cl$ (B) and $AmimCl$ (C).

that the crystalline form of wood pulp cellulose was transformed completely from cellulose I to cellulose II after regeneration from IL solution, as shown in Fig. 3. The similar results were reported by Zhang (22). Whereas the crystalline structure was found to be completely destroyed during dissolution of cellulose in ILs and the crystalline cellulose I was totally transformed to amorphous cellulose, as seen in Fig. 4, according to our research (36, 37). Similar results were reported in many publications (20, 38–40). However, the mechanism of the transformation of cellulose crystallinity is still not clear.

Preparation of Regenerated Cellulose Materials in Ionic Liquids

The dissolution of cellulose in novel green solvents, ILs, has been providing a new platform for cellulose applications. Cellulose could be precipitated from the IL solution by the addition of anti-solvents such as water, ethanol, acetone, isopropanol, etc. After dissolution and regeneration from ILs, cellulose morphology is significantly changed and a relatively homogeneous macrostructure is obtained. The physicochemical properties of regenerated cellulose are affected by the dissolution and regeneration processes. Different structural forms of

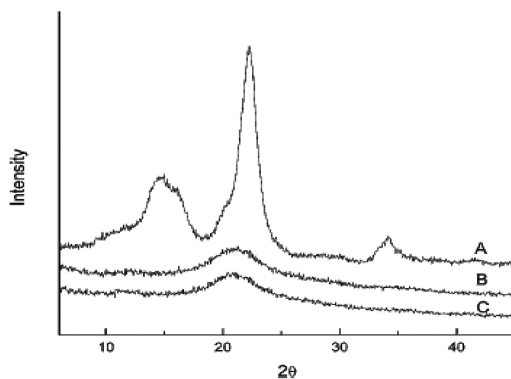


Figure 4. X-ray powder diffraction patterns for untreated Avicel (A) and regenerated Avicel from IL solution with deionized water after incubation at 130°C for 2 h (B) or 30 min (C).

regenerated cellulose such as fibers, films, powders, beads and membranes can be prepared by changing processing conditions, especially regeneration conditions (21). It was reported that cellulose fiber obtained from ILs by dissolution and regeneration in ILs such as $[C_4mim]Cl$, called Ionicell fiber, has good properties similar to those of Lyocell fiber (41). Kosan (42) also successfully prepared cellulose dopes using ILs, which could be shaped by a dry-wet spinning process to manufacture cellulose fibers. Ionicell fiber would be a new kind of environmentally friendly promising fiber following the Lyocell fiber.

Cellulose blended or composite materials can be prepared using ILs. The incorporated functional additives can be dissolved or dispersed in ILs before and after dissolution of the cellulose. With this simple approach, many kinds of cellulose composite materials with different structural forms can be easily obtained. Rogers' group (21) proposed a new method for introducing enzymes into cellulosic matrixes which can be used to produce membranes, films, or beads using a cellulose-in-IL-dissolution and regeneration process. Zhang and his co-workers (43) also developed a method to prepare wool keratin/cellulose blended materials by the dissolution and regeneration of wool keratin fibers in $[C_4mim]Cl$. Pletnev (44) prepared cellulose films containing entrapped analytical reagents suitable for metal-ion detection by joint dissolution of cellulose and the reagents in IL followed by precipitated with water. This method provides a new technology for quantitative determination of transition metal cations. Kadokawa (1, 45) reported a facile method for preparation of composites composed of cellulose and a polystyrene-type polymeric IL using an imidazolium-type polymerizable IL. Cellulose-nanohydroxyapatite composite scaffolds with high and open porosity were successfully prepared by poly(methyl methacrylate) particulate leaching with $[C_4mim]Cl$ as cellulose solvent (46). The preparation of cellulose blended or composite materials using ILs would broaden the conventional cellulose application scope.

Table 1. DS of cellulose succinylated with succinic anhydride in [C₄mim]Cl

Catalyst	Succinylation conditions			Succinylated cellulose	
	Catalyst/SA (%)	Temp. (°C)	Reaction time (min)	Sample No.	DS
	0	100	60	1	0.24
I ₂	8	100	60	2	1.28
DMAP	5	100	60	3	2.34
NBS	5	100	60	4	2.31

Preparation of Cellulose Derivatives Using Ionic Liquids as Reaction Media

Although homogeneous derivation of cellulose has been one focus in cellulose chemistry for a long time, the number of cellulose derivatives commercially available is limited because only heterogeneous synthesis paths are carried out in large-scale processes. Recently, ILs as the nonderivatizing solvents for cellulose have drawn much attention on the potential application of ILs as the novel green homogeneous reaction media for preparation of cellulose derivatives.

Cellulose acetate is one of the most commercially important cellulose derivatives with a wide application in the fields of coating, film, membrane, textile, and cigarette industries (47). Cellulose acetylation with aqueous acetic anhydride or acetyl chloride has been extensively studied because of easily established homogeneous reaction system. Zhang and his co-workers (47–49) reported that the homogeneous acetylation of cellulose with acetic anhydride could be carried out in AmimCl without any catalyst and cellulose acetates with a wide range of degree of substitution (DS) could be obtained under different conditions. Heinze and his co-workers (31, 50, 51) found that it was very easy to synthesize cellulose acetate with high DS in good yield within a short time using different ILs such as [C₄mim]Cl as reaction media and using acetyl chloride or acetic anhydride as acetylation reagent without any catalysts. The reaction of three free hydroxyl groups in cellulose at the C2, C3, and C6 positions all occur during homogeneous modification in ILs, and the order of reactivity is C6-OH > C3-OH > C2-OH (48), similar to that observed in acetylation in DMAc/LiCl system (52). The efficient *O*-acetylation of cellulose was accomplished using a zinc based ionic liquid by Handa (53). Furthermore, ILs can also be used as reaction medium for homogeneous Carbanilation of cellulose with phenyl isocyanate (50, 51), acylation with lauroyl chloride (51) and perpropionylation with propionic anhydride (50). However, it should be noted that it is much difficult to achieve homogeneous modification media for cellulose with solid derivatizing reagents. Carboxymethylation of cellulose in [C₄mim]Cl was proposed by Heinze (31). In addition, carboxymethylated cellulose (CMC) obtained according to this method had relatively low DS and an increase of the

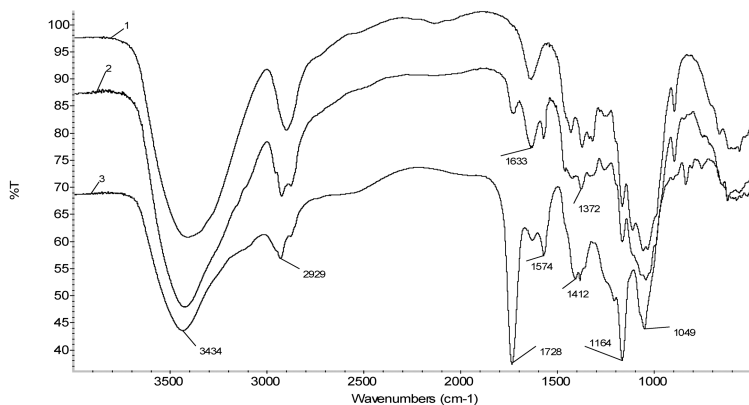


Figure 5. FT-IR spectra of unmodified cellulose (spectrum 1), succinylated cellulose without any catalyst (spectrum 2, sample 1) and with iodine as a catalyst (spectrum 3, sample 2).

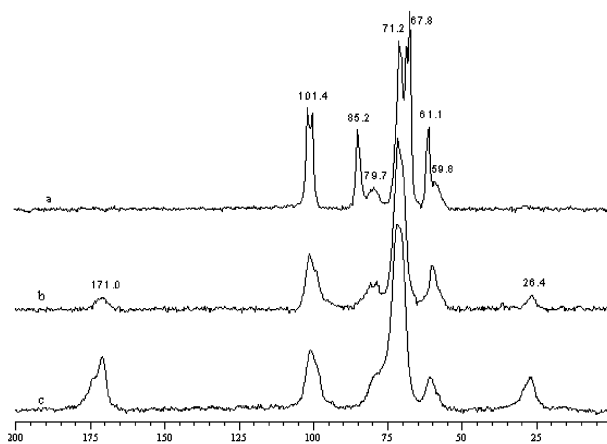


Figure 6. Solid state CP/MAS ^{13}C -NMR spectra of unmodified cellulose (spectrum a), succinylated cellulose without any catalysts (spectrum b, sample 1) and with NBS as a catalyst (spectrum c, sample 3).

dosage of carboxymethylating reagent did not increase the DS. The reason for this unusual result is still unclear. Schubert (54) accomplished homogeneous tritylation of cellulose with trityl chloride in $[\text{C}_4\text{mim}]\text{Cl}$ using pyridine as base. A DS of around 1 was obtained after 3 h reaction time using a six fold excess of trityl chloride, indicating the slow reaction speed.

Cellulose derivatives obtained with solid reagents such as cyclic anhydrides have also been widely used in various applications such as water absorbents for soil in agriculture, natural absorbents for the removal of heavy metal ions in waste water treatment, medicine for drug delivery systems, and thermoplastic materials (55, 56). The esterification of cellulose with cyclic anhydrides does not yield an undesired corresponding carboxylic acid by-product, which is generally

produced with linear chain acylation reactants. These cellulose products also provide a reactive site upon which further modification for other potential utilization such as in pharmaceutical industries is possible. In addition, because carboxylic groups are introduced to cellulose by ester linkages which are more susceptible to hydrolysis and biodegradation than ether linkages, these derivatives are more suitable for the design of biodegradable materials than CMC, the most representative cellulosic derivatives containing carboxylic groups linked by ether linkages (56). In our earlier work, the homogeneous modification of cellulose with solid cyclic anhydrides such as phthalic anhydride (57, 58) and succinic anhydride (32, 34) was investigated without any catalysts. However, phthalation and succinylation is more difficult to occur than acetylation and the obtained cellulose derivatives have relatively low DS. Many kinds of novel catalysts such as *N*-bromosuccinimide (NBS) (59), 4-dimethylaminopyridine (DMAP) (60), and iodine were investigated to improve modification efficiency of cellulose. The results in Table 1 showed that DS of succinylated cellulosic derivatives increased from 0.24 to 1.28 at 100°C for 60 min catalyzed with 8% iodine, to 2.34 with 5% DMAP, and to 2.31 with 5% NBS. FT-IR and CP/MAS ¹³C-NMR spectroscopies further provided evidence of catalyzed succinylation, as shown in Figs 5 and 6. The possible mechanism of succinylation and the actual role of catalysts in ionic liquids are under study. The catalyzed modification of cellulose with other solid modifying reagents using ILs as homogeneous media should be further investigated.

Application of Ionic Liquids in the Preparation of Biofuel from Cellulosic Materials

Besides cellulose composite materials and cellulose derivatives, biofuel such as bioethanol will be another promising application of cellulose in industries in the future. Hydrolysis of cellulose to glucose in aqueous media catalyzed by the cellulase or acid suffers from slow reaction rates in industry due in large part to the highly crystalline structure of cellulose and inaccessibility of cellulase or acid adsorption sites. In order to make the hydrolysis process viable for producing simple sugars for fermentation to produce ethanol fuel and other bio-based products, this highly ordered structure of cellulose has to overcome. Schall (38) made an attempt to disrupt the cellulose structure in [C₄mim]Cl. The results indicated that the initial enzymatic hydrolysis rates were approximately 50-fold higher for regenerated celluloses as compared to untreated cellulose, which was due to the conversion of crystalline cellulose to amorphous cellulose during pretreatment with IL. Kamiya (61) established an enzymatic saccharification of cellulose in an imidazolium type IL with an alkylphosphate anion, which will be very useful in integrated bioprocesses such as bioethanol production from cellulosic materials. A novel method for cellulose hydrolysis catalyzed by mineral acids in [C₄mim]Cl was developed by Zhao (62, 63). This method could facilitate the hydrolysis of cellulose with dramatically accelerated reaction rates at 100°C under atmospheric pressure and without pretreatment.

In short, ionic liquids' the excellent capability of dissolving cellulose make them a promising substitutes to classic solvents for processing cellulose and carrying out reactions in cellulose derivatization chemistry, providing a new platform for cellulose utilization as composite materials, cellulose derivatives, and biofuels. However, many fundamentals have not been totally understood. More comprehensive studies on the fundamentals, such as the mechanism of dissolution and degradation of cellulose macromolecules, transformation of cellulose crystalline structure, the homogeneous chemical modification of cellulose with solid reagents, and the processing of cellulose in ionic liquids, have to be investigated to develop new biopolymers and further prosper the industry.

Acknowledgements

The authors are grateful for the financial support of this research from National Natural Science Foundation of China (Nos. 30871994, 30972325, and 30710103906), Guangdong National Science Foundation (Nos. 07118057 and 8451064101000409), Specialized Research Fund for the Doctoral Program (No. 20070561040) of Higher Education (111 project), and National Basic Research Program of China (No. 2010CB732201).

References

1. Murakami, M. A.; Kaneko, Y.; Kadokawa, J. I. *Carbohydr. Polym.* **2007**, *69*, 378.
2. Sun, J. X.; Xu, F.; Geng, Z. C.; Sun, X. F.; Sun, R. C. *J. Appl. Polym. Sci.* **2005**, *97*, 322.
3. Pandey, A.; Soccol, C. R.; Nigam, P.; Soccol, V. T. *Bioresour. Technol.* **2000**, *74*, 69.
4. Pandey, A.; Soccol, C. R.; Nigam, P.; Soccol, V. T.; Vandenberghe, L. P. S.; Mohan, R. *Bioresour. Technol.* **2000**, *74*, 81.
5. Richardson, S.; Gorton, L. *Anal. Chim. Acta* **2003**, *497*, 27.
6. Focher, B.; Palma, M. T.; Canetti, M.; Torri, G.; Cosentino, C.; Gastaldi, G. *Ind. Crops Prod.* **2001**, *13*, 193.
7. Araki, J.; Kataoka, T.; Katsuyama, N.; Teramoto, A.; Ito, K.; Abe, K. *Polymer* **2006**, *47*, 8241.
8. Philipp, B.; Nehls, I.; Wagenknecht, W. *Carbohydr. Res.* **1987**, *164*, 107.
9. Rosenau, T.; Hofinger, A.; Potthast, A.; Kosma, P. *Polymer* **2003**, *44*, 6153.
10. Ramos, L. A.; Frollini, E.; Heinze, T. *Carbohydr. Polym.* **2005**, *60*, 259.
11. Fischer, S.; Leipner, H.; Thummler, K.; Brendler, E.; Peters, J. *Cellulose* **2003**, *10*, 227.
12. Zhang, H.; Wu, J.; Zhang, J.; He, J. S. *Macromolecules* **2005**, *38*, 8272.
13. Plechkova, N. V.; Seddon, K. R. *Chem. Soc. Rev.* **2008**, *37*, 123.
14. Branco, L. C.; Rosa, J. N.; Ramos, J. J. M.; Afonso, C. A. M. *Chem.-Eur. J.* **2002**, *8*, 3671.

15. Graenacher, C. U.S. Patent 1943176, 1934.
16. Swatloski, R. P.; Spear, S. K.; Holbrey, J. D.; Rogers, R. D. *J. Am. Chem. Soc.* **2002**, *124*, 4974.
17. Swatloski, R. P.; Holbrey, J. D.; Spear, S. K.; Rogers, R. D. *225th National Meeting of the American-Chemical-Society* 2003, 167-IEC.
18. Swatloski, R. P.; Spear, S. K.; Holbrey, J. D.; Rogers, R. D. *225th National Meeting of The American Chemical Society*, 2003; 131-CELL.
19. Swatloski, R. P.; Spear, S. K.; Holbrey, J. D.; Rogers, R. D. *224th National Meeting of The American Chemical Society*, 2002; 076-IEC.
20. Swatloski, R. P.; Rogers, R. D.; Holbrey, J. D. WO Patent, 03/029329, 2003.
21. Turner, M. B.; Spear, S. K.; Holbrey, J. D.; Rogers, R. D. *Biomacromolecules* **2004**, *5*, 1379.
22. Turner, M. B.; Spear, S. K.; Holbrey, J. D.; Daly, D. T.; Rogers, R. D. *Biomacromolecules* **2005**, *6*, 2497.
23. Ren, Q.; Wu, J.; Zhang, J.; He, J. S.; Guo, M. L. *Acta Polym. Sin.* **2003**, 448.
24. Luo, H. M.; Li, Y. Q.; Zhou, C. R. *Polym. Mater. Sci. Eng.* **2005**, *21*, 233.
25. Fukaya, Y.; Hayashi, K.; Wada, M.; Ohno, H. *Green Chem.* **2008**, *10*, 44.
26. Kuhlmann, E.; Himmler, S.; Giebelhaus, H.; Wasserscheid, P. *Green Chem.* **2007**, *9*, 233.
27. Pernak, J.; Zabielska-Matejuk, J.; Kropacz, A.; Foksowicz-Flaczyk, J. *Holzforschung* **2004**, *58*, 286.
28. Przybysz, K.; Drzewinska, E.; Stanislawska, A.; Wysocka-Robak, A.; Cieniecka-Roslonkiewicz, A.; Foksowicz-Flaczyk, J.; Pernak, J. *Ind. Eng. Chem. Res.* **2005**, *44*, 4599.
29. Li, X.; Geng, Y.; Simonsen, J.; Li, K. C. *Holzforschung* **2004**, *58*, 280.
30. Cuissinat, C.; Navard, P.; Heinze, T. *Carbohydr. Polym.* **2008**, *72*, 590.
31. Heinze, T.; Schwikal, K.; Barthel, S. *Macromol. Biosci.* **2005**, *5*, 520.
32. Liu, C. F.; Sun, R. C.; Zhang, A. P.; Ren, J. L.; Wang, X. A.; Qin, M. H.; Chao, Z. N.; Luo, W. *Carbohydr. Res.* **2007**, *342*, 919.
33. El Seoud, O. A.; Koschella, A.; Fidale, L. C.; Dorn, S.; Heinze, T. *Biomacromolecules* **2007**, *8*, 2629.
34. Liu, C. F.; Sun, R. C.; Zhang, A. P.; Ren, J. L.; Geng, Z. C. *Polym. Degrad. Stab.* **2006**, *91*, 3040.
35. Zhai, W.; Chen, H. Z.; Ma, R. Y. *J. Beijing Univ. Chem. Technol.* **2007**, *34*, 138.
36. Liu, C. F.; Zhang, A. P.; Sun, R. C.; Li, W. Y. CN200710032266.4, 2007.
37. Liu, C. F.; Zhang, A. P.; Sun, R. C.; Peng, F.; Li, W. Y. 235th National Meeting of The American Chemical Society, 2008; 097-CELL.
38. Dadi, A. P.; Varanasi, S.; Schall, C. A. *Biotechnol. Bioeng.* **2006**, *95*, 904.
39. Kadokawa, J. I.; Murakami, M. A.; Kaneko, Y. *Carbohydr. Res.* **2008**, *343*, 769.
40. Swatloski, R. P.; Rogers, R. D.; Holbrey, J. D. CN 101007853A, 2007.
41. Zhang, H. H.; Cai, T.; Guo, Q. H.; Shao, H. L.; Hu, X. C. *Syn. Fiber China* **2007**, *11*, 11.
42. Kosan, B.; Michels, C.; Meister, F. *Cellulose* **2008**, *15*, 59.
43. Xie, H. B.; Li, S. H.; Zhang, S. B. *Green Chem.* **2005**, *7*, 606.

44. Egorov, V. M.; Smirnova, S. V.; Formanovsky, A. A.; Pletnev, I. V.; Zolotov, Y. A. *Anal. Bioanal. Chem.* **2007**, *387*, 2263.
45. Kadokawa, J. I.; Murakami, M. A.; Kaneko, Y. *Compos. Sci. Technol.* **2008**, *68*, 493.
46. Tsiopstias, C.; Panayiotou, C. *Carbohydr. Polym.* **2008**, *74*, 99.
47. Cao, Y.; Wu, J.; Meng, T.; Zhang, J.; He, J. S.; Li, H. Q.; Zhang, Y. *Carbohydr. Polym.* **2007**, *69*, 665.
48. Wu, J.; Zhang, J.; Zhang, H.; He, J. S.; Ren, Q.; Guo, M. *Biomacromolecules* **2004**, *5*, 266.
49. Wu, J.; Zhang, H.; Zhang, J.; He, J. S. *Chem. J. Chinese U.* **2006**, *27*, 592.
50. Schlufte, K.; Schmauder, H. P.; Dorn, S.; Heinze, T. *Macromol. Rapid Commun.* **2006**, *27*, 1670.
51. Barthel, S.; Heinze, T. *Green Chem.* **2006**, *8*, 301.
52. El Seoud, O. A.; Marson, G. A.; Giacco, G. T.; Frollini, E. *Macromol. Chem. Phys.* **2000**, *201*, 882.
53. Abbott, A. P.; Bell, T. J.; Handa, S.; Stoddart, B. *Green Chem.* **2005**, *7*, 705.
54. Erdmenger, T.; Haensch, C.; Hoogenboom, R.; Schubert, U. S. *Macromol. Biosci.* **2007**, *7*, 440.
55. Hadano, S.; Onimura, K.; Tsutsumi, H.; Yamasaki, H.; Oishi, T. *J. Appl. Polym. Sci.* **2003**, *90*, 2059.
56. Yoshimura, T.; Matsuo, K.; Fujioka, R. *J. Appl. Polym. Sci.* **2006**, *99*, 3251.
57. Liu, C. F.; Sun, R. C.; Zhang, A. P.; Qin, M. H.; Ren, J. L.; Wang, X. A. *J. Agric. Food Chem.* **2007**, *55*, 2399.
58. Liu, C. F.; Sun, R. C.; Zhang, A. P.; Ren, J. L. *Carbohydr. Polym.* **2007**, *68*, 17.
59. Liu, C. F.; Zhang, A. P.; Li, W. Y.; Yue, F. X.; Sun, R. C. *J. Agric. Food Chem.* **2009**, *57*, 1814.
60. Li, W. Y.; Jin, A. X.; Liu, C. F.; Sun, R. C.; Zhang, A. P.; Kennedy, J. F. *Carbohydr. Polym.* **2009**, *78*, 389.
61. Kamiya, N.; Matsushita, Y.; Hanaki, M.; Nakashima, K.; Narita, M.; Goto, M.; Takahashi, H. *Biotechnol. Lett.* **2008**, *30*, 1037.
62. Li, C. Z.; Wang, Q.; Zhao, Z. K. *Green Chem.* **2008**, *10*, 177.
63. Li, C. Z.; Zhao, Z. K. B. *Adv. Synth. Catal.* **2007**, *349*, 1847.

Chapter 17

Imidazolium Based Ionic Liquids as Solvents for Cellulose Chemistry

Jürgen Vitz^{a,b}, Tina Erdmenger^{b,c} and Ulrich S. Schubert^{*,a,b,c}

^aLaboratory of Organic and Macromolecular Chemistry,
Friedrich-Schiller-University Jena, Humboldtstr. 10, D-07743 Jena,
Germany, Tel.: +49(0) 3641 9482 00, Fax:+49(0) 3641 9482 02,
E-mail: ulrich.schubert@uni-jena.de

^bDutch Polymer Institute (DPI), P.O. Box 902, NL-5600 AX Eindhoven,
The Netherlands

^cLaboratory of Macromolecular Chemistry and Nanoscience, Eindhoven
University of Technology, P. O. Box 513, NL-5600 MB Eindhoven,
The Netherlands

*u.s.schubert@tue.nl, www.schubert-group.com

In recent years, ionic liquids developed to advantageous solvents for the dissolution and homogeneous processing of cellulose. Even if ionic liquids were already known for their capability of efficiently dissolving cellulose for a long time, significant efforts were made in the last years. New candidates were found, but it could be shown, that some ionic liquids are involved in side reactions, too. With the aim for gaining a better insight on the dissolution properties, we screened a wide range of potentially suitable ionic liquids. Remarkable results were obtained, for example an odd-even effect was found for different alkyl side chain lengths, both linear and branched, for the imidazolium based ionic liquids with chloride counterions. Furthermore, 1-ethyl-3-methylimidazolium diethyl phosphate showed promising properties for the dissolution of cellulose, *e.g.* a lower degradation of cellulose than for other ILs, a low melting point, and a low viscosity of the cellulose solution, simplifying the handling.

Introduction

Cellulose ($C_6H_{10}O_5$)_n is a linear β -1,4-glycosidically linked polyglucane and the most abundant form of terrestrial biomass. Cellulose is extracted from wood or cotton and a biodegradable polymer ($1,000 < DP < 15,000$). Cellulose products are produced in great quantities and used for a large number of industrial applications, for example fibers, tissues, or paper including cellophane, rayon, cellulose acetate, carboxymethyl cellulose, and many more (1). In addition, polysaccharides are used in medical areas for tissue engineering, drug delivery systems or specialized hydrogels (2–5).

Besides its broad applicability, cellulose shows one major drawback which is the insolubility in common solvents caused by its fibril structure and the pronounced presence of intra- and intermolecular hydrogen bonds (Figure 1) (1–6).

In industrial processes, cellulose is transferred to the above mentioned products by solubilization and processing followed by subsequent precipitation or solvent evaporation. Another possibility is the heterogeneous derivatization of cellulose (7). A well established process to obtain regenerated, processible cellulose is the xanthogenate route during which cellulose is swollen with aqueous NaOH and subsequently treated with CS₂ leading to a highly viscous sodium-xanthogenate solution. This solution is later treated with acidic solution to reform the cellulose, CS₂ and NaOH. During this process, the cellulose backbone is partially degraded and toxic H₂S is formed as a byproduct (8–10). Other derivatizing solvents like trifluoro acetic acid, formic acid, or *N,N*-dimethyl-formamide/N₂O₄ could also be applied for the functionalization of cellulose with or without isolation of the intermediates (1). Unfortunately, these methods often require extreme conditions, *e.g.* high temperatures and pressures, strong bases or acids thus requiring special equipment.

The easiest way to regenerate cellulose would be its direct dissolution in a solvent and the subsequent precipitation (or the evaporation of the solvent) without the formation of any cellulose derivatives. Newer examples for non-derivatizing solvents with aqueous inorganic complexes are, *e.g.*, cuprammonium hydroxide (Cuoxam, Cuam), cupriethylene diamine (Cuen) and CdO/ethylenediamine (Cadoxen) (11, 12), or non-aqueous solvents together with inorganic salts or gases, *e.g.* DMA/LiCl, DMSO/SO₂, or DMSO/TBAF (1, 13–15). In the last years ionic liquids (ILs) have emerged showing many advantages over other solvent systems for the dissolution of cellulose (16–20). In fact, the ability of salts to dissolve cellulose was known much earlier and already recognized by Graenacher in 1934 (21). This was forgotten or not fully noticed maybe due to the high melting point of the used benzylpyridinium chloride. Almost seven decades later, his ideas were picked-up and it was shown that ionic liquids with lower melting points can also be used as non-derivatizing solvents for cellulose (16, 17). As a result it was assumed that anions, which are strong hydrogen bond acceptors, are most effective. The greatest solubility was achieved by using 1-butyl-3-methylimidazolium chloride which could dissolve up to 25 wt.-% of cellulose under microwave irradiation (17). In particular, 1-butyl-3-methylimidazolium chloride ([BMIM]Cl) and 1-allyl-3-methylimidazolium chloride ([AllylMIM]Cl)(22) are now commonly

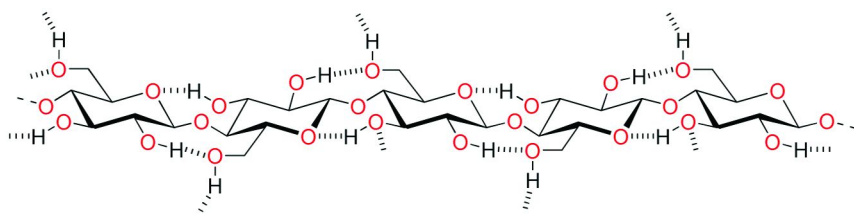


Figure 1. Schematic representation of the structure of cellulose (with hydrogen bonds).

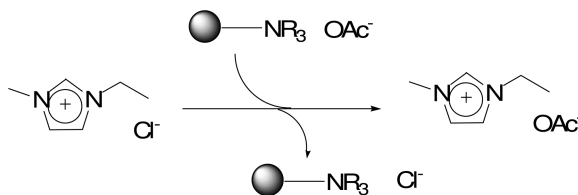


Figure 2. Schematic representation of the anion exchange with “Amberlite IRA-400”.

used; the etherification(23) and esterification (18), the acetylation (24, 25), the carboxy-methylation(18) and tritylation(26) are some examples for possible reactions in these solvents.

These ionic liquids show very promising properties but also disadvantages like high melting points, a high hygroscopicity and sometimes even the degradation of the cellulose backbone (18). In addition, side reactions of the cellulose with the ionic liquids were reported in recent time. In a recent publication, Ebner *et al.* showed that for example the 1-alkyl-3-methyl-imidazolium cations can react at the C-2 position with the reducing end of the cellulose, building a C-C bond. This is catalyzed by bases, such as imidazole and 1-methylimidazole, always present as impurities in imidazolium based ILs. As a conclusion they assumed that this modification of the cellulose backbone is rather minor because of the small number of keto/aldehyde structures compared to the high number of glucopyranose units. Only in case of oxidized cellulose or for certain applications this could become problematic (27).

On the other hand it was shown that 1-ethyl-3-methylimidazolium acetate ([EMIM]Ac) also reacts as a reagent via a mixed anhydride pathway. Thereby, an exchange of the anion of the ionic liquid takes place which also reduces the reusability of the utilized IL (28, 29). Therefore, solutions of cellulose in alkylmethylimidazolium ILs cannot be considered as inert in general.

Thus, we decided to investigate a broader range of ionic liquids for the dissolution of cellulose. In our studies, commercially available as well as tailor-made ionic liquids were used. The aim was to investigate the influence of different side chains and different side chain lengths in combination with various anions on the dissolution properties. A possible degradation of the cellulose during the dissolution process should be minimized by applying thermal heating

Table 1. Water content of different ionic liquids and starting materials/reagents used (41)^a

Entry	IL	Water content (ppm) ^a	Remark ^b
1	[EMIM]Et ₂ PO ₄	5865	i ^c
2	[EMIM]Et ₂ PO ₄	11475	ii ^c
3	[EMIM]Et ₂ PO ₄	6153	iii ^c
4	[EMIM]OAc	6762	iv ^d
5	[EMIM]OAc	8895	iii ^d
6	[BMIM]Cl	2200	v
7	[EMIM](CN) ₂ N	1234	iv ^e
8	[EMIM](CN) ₂ N	426	iii ^e
9	[BMIM]triflate	633	iv ^f
10	[BMIM]BF ₄	141	iv ^f
11	[BMIM]PF ₆	101	iv ^f
12	[BMIM]PF ₆	63	iii ^f
13	1-Methylimidazole	996	iv ^d
14	Triethyl phosphate	178	iv ^d

^a Karl Fischer titration. ^b (i) after preparation; (ii) wet sample, vacuum oven dried; (iii) freeze dried; (iv) as received from supplier. (v) results of Huddleston *et al.*(42) ^c synthesized. ^d Aldrich. ^e Solvent Innovation. ^f Io-li-tec. ^g Acros organics.

or microwave irradiation. Based on these homogeneous reactions, a better control of the degree of functionalization of modified cellulose should be possible, too. The intention was to provide an easier, environmentally friendlier and industrially applicable processing of cellulose. In addition, new modified cellulose products might be accessible in particular in the field of advanced and smart bio-based materials, which are not synthetically available until now.

Results and Discussion

Synthesis of Ionic Liquids

1-Butyl-3-methylimidazolium chloride ([BMIM]Cl)(16, 17) and 1-allyl-3-methylimidazolium chloride ([AllylMIM]Cl)(22, 24, 30) are well known ILs for the dissolution of cellulose. They showed high dissolution properties and a broad compatibility under different types of reactions. For example, [BMIM]Cl, used in our group for the homogeneous tritylation of cellulose (26), can dissolve up to 25 wt.-% of cellulose (as reported by Rogers *et al.*) (17). Other possible reactions in these solvents are the acetylation (24, 25), the esterification and carboxy-methylation (18). However, high melting points, high viscosities and the high hygroscopicity – in general valid for all imidazolium based ionic liquids with a chloride counter anion – makes their handling difficult.

To find other ionic liquids which are able to dissolve cellulose in high amounts, we screened other possible candidates. In this research, the influence of the dissolution properties of the side-chain lengths for the imidazolium based ionic liquids with chloride as counter ions was investigated and a distinct odd-even effect for short side-chain lengths was observed (26). As a consequence of these results, the synthesis of 1-alkyl-3-methylimidazolium based ionic liquids also with branched alkyl side chains as well as with the bromide anion was planned to support the previously described effect. The mentioned ionic liquids could be obtained in microwave reactors after short reaction times in high yields and high purities (31–34). Other ionic liquids with substituted side chains, *e.g.* containing double bonds, halides, a nitrile or a hydroxyl group were synthesized as well.

The bromide or chloride anions could be exchanged to yield different 1-butyl-3-methylimidazolium and 1-ethyl-3-methylimidazolium based ionic liquids. Whereas for some exchange reactions water was found to be the best solvent (35), other exchange reactions must be carried out in dichloromethane or acetonitrile (36–38). The completeness was checked by adding a silver nitrate solution to a solution of the ionic liquid in water (35). An Amberlite IRA-400 exchange resin(39) was used for the preparation of [EMIM]OAc and [BMIM]OAc (Fig. 2). Unfortunately, the exchange resin could not be used for synthesizing ionic liquids with a fluoride anion because the exchange potential increases with increasing atomic number. Therefore, silver fluoride (AgF) was used to synthesize 1-ethyl-3-methylimidazolium fluoride ([EMIM]F) and 1-butyl-3-methylimidazolium fluoride ([BMIM]F).

Dissolution Studies

The newly synthesized ionic liquids as well as commercially available ionic liquids were subsequently used for the dissolution studies of cellulose. A correlation of the water content and the solubility is already known. When using non-dried ionic liquids, the solubility of cellulose is reduced and therefore it is necessary to dry all ionic liquids carefully before use (25). In a recent study, using turbidimetric measurements, it was quantitatively shown that the more water is present less cellulose can be dissolved in [BMIM]Cl. In case of 1,3-dimethylimidazolium dimethylphosphate, cellulose could only be dissolved in an perfectly dried IL (40).

When doing our dissolution experiments, the water content of some ionic liquids was checked before and after drying by Karl Fischer titration (Table 1). From the data obtained it is evident that in particular the vacuum oven (at 40 °C) was not sufficient to dry the ionic liquids; only a freeze dryer was able to remove the water. Interestingly, with the used freeze dryer it was not possible to completely dry [EMIM]Et₂PO₄ and [EMIM]OAc. Once water was absorbed, it was no longer possible to reach the initial values directly obtained for the synthesized [EMIM]Et₂PO₄ (entries 1–3) or the commercial available [EMIM]OAc (entries 4–5). On the other hand, less hygroscopic ionic liquids, *e.g.* [EMIM](CN)₂N (entries 7–8) or [EMIM]PF₆ (entries 11–12), could be dried successfully. For comparison, also [BMIM]triflate and [EMIM]BF₄ were

Table 2. Overview of the results from the dissolution studies for imidazolium based ionic liquids

Entry	Ionic liquid	Solubility (wt.%)	Remarks
1	[DiMIM]I	no sol.	-
2	[DiMIM]Me ₂ PO ₄	10	-
3	[EMIM]F	2	-
4	[EMIM]Cl	10–14	-
5	[EMIM]Br	1–2	colorization
6	[EMIM]EtSO ₄	no sol.	-
7	[EMIM](CN) ₂ N ⁻	no sol.	-
8	[EMIM]TsO ⁻	1	-
9	[EMIM]AcO ⁻	8	colorization
10	[EMIM]Et ₂ PO ₄ ⁻	12–14	-
11	[C ₃ MIM]Cl	1–2	-
12	[C ₃ MIM]Br	no sol.	colorization
13	[BMIM]Cl	20	<i>a</i>
14	[BMIM]Br	2–3	-
15	[BMIM]I	1–2	colorization
16	[BMIM]SCN ⁻	5–7	<i>b</i>
17	[BMIM]BF ₄ ⁻	no sol.	<i>b</i>
18	[BMIM]PF ₆ ⁻	no sol.	<i>b</i>
19	[BMIM]NO ₃ ⁻	no sol.	-
20	[BMIM]NTf ₂ ⁻	no sol.	-
21	[BMIM]F ₃ CSO ₃ ⁻	no sol.	-
22	[BMIM]AcO ⁻	12	colorization
22	[BMIM]Bu ₂ PO ₄ ⁻	no sol.	-
23	[C ₅ MIM]Cl	1	-
24	[C ₅ MIM]Br	1–2	-
25	[C ₆ MIM]Cl	6	-
26	[C ₆ MIM]Br	1–2	-
27	[C ₇ MIM]Cl	5	-
28	[C ₇ MIM]Br	1	colorization
29	[C ₈ MIM]Cl	4	-
30	[C ₈ MIM]Br	1	colorization
31	[C ₉ MIM]Cl	2	-
32	[C ₉ MIM]Br	1	colorization
33	[C ₁₀ MIM]Cl	no sol.	-
34	[C ₁₀ MIM]Br	no sol.	-
35	[AllylMIM]Cl	15	<i>c</i>
36	[AllylMIM]Br	no sol.	-

a 25% under microwave irradiation according to Rogers *et al.*(17) *b* Results of Rogers *et al.*(17) *c* Results of Wu *et al.*(22–24)

measured. As a result, the water content decreases with the anions in the order of OAc⁻ ≈ Et₂PO₄⁻ > (CN)₂N⁻ > triflate > BF₄⁻ > PF₆⁻.

The chemicals, *e.g.* used for synthesizing [EMIM]Et₂PO₄ (entries 13–14), showed a lower water content than the obtained IL (entry 1).

Small 2 mL vials were used for the dissolution studies where first the ionic liquid was filled in. After the vial was placed into a metal holder and heated to about 100 °C, the cellulose was added, too. The dissolution was then checked

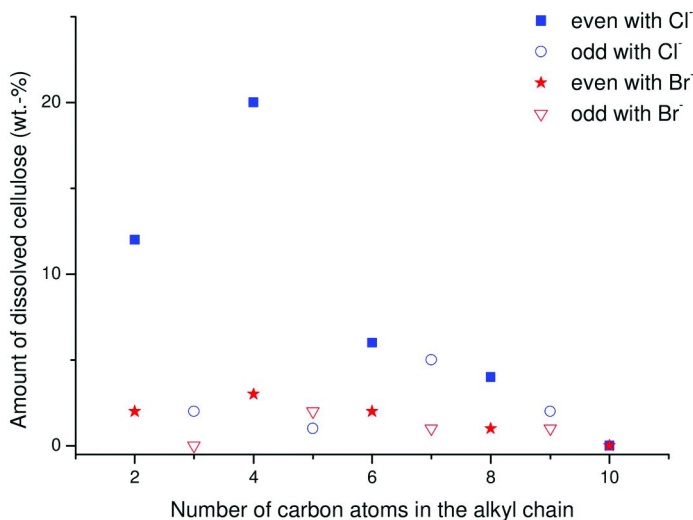


Figure 3. Dependency of the alkyl chain length of 1-alkyl-3-methylimidazolium chloride on the solubility of cellulose at 100 °C (26).

visually. The time required for a complete dissolution was between 15 min and 1 h. The results of the dissolution studies are shown in Table 2 together with literature values.

These screening tests revealed a different behavior of the cellulose in different ionic liquids. Whereas the solutions of cellulose in compatible ionic liquids like [BMIM]Cl and [HMIM]Cl became clear and also stayed in a glassy-like clear state at room temperature (whereby, in particular, the pure chlorides are solids at r.t.), other solutions tend to crystallize back at room temperature, e.g. [EMIM]Cl. If no dissolution could be observed, the cellulose was either only “suspended” in the ionic liquid (e.g. [EMIM]EtSO₄), or rapidly degraded visible by a deep coloration of the solution. This effect was observed very often, in particular when using higher amounts of cellulose.

Influence of the Alkyl Chain Length and Branching

Ionic liquids with chloride as the counter anion, are considered to be most effective (16–18, 22, 43). Up to now, the highest solubility was obtained with 1-butyl-3-methyl-imidazolium chloride ([BMIM]Cl). But in general, only 1-alkyl-3-methyl-imidazolium chlorides with even-numbered alkyl chains (butyl, hexyl and octyl) have been reported (17, 18).

As already mentioned above, we investigated the influence of the alkyl chain length from C₂ to C₁₀ of the 1-alkyl-3-methylimidazolium chlorides on the solubility of cellulose. All experiments were carried out at 100 °C, and the results are presented in Table 2 and Figure 3.

Surprisingly, the solubility of cellulose in 1-alkyl-3-methylimidazolium based ionic liquids does not regularly decrease with increasing length of the alkyl

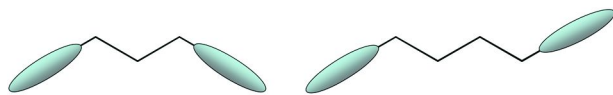


Figure 4. Schematic representation of the orientation of the mesogenic units of odd/even alkyl chains in all trans-conformation. Left: odd n of $(\text{CH}_2)_n$ units (inclined mesogenic units). Right: even n of $(\text{CH}_2)_n$ units (parallel mesogenic units).

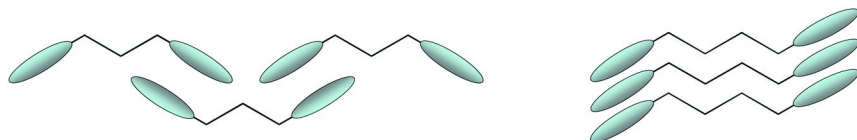


Figure 5. Schematic representation of the packing of odd/even alkyl chains in all trans-conformation. Left: odd n of $(\text{CH}_2)_n$ units. Right: even n of $(\text{CH}_2)_n$ units.

chain. In fact, a strong odd-even effect was observed for the small alkyl chains; pentyl and shorter. Cellulose was more soluble in 1-alkyl-3-methylimidazolium based ionic liquids with even-numbered alkyl chains compared to odd-numbered alkyl chains, below six carbon units. 1-Butyl-3-methylimidazolium chloride ([BMIM]Cl) gave the best performance of the even-numbered alkyl chains, dissolving 20 wt.-% of cellulose. Whereas, 1-heptyl-3-methyl-imidazolium chloride was the most efficient odd-numbered ionic liquid, dissolving 5 wt.-% of cellulose. In general, the first odd-even effect was discovered for the melting temperature of n -alkanes and thereafter it was found that most series containing alkyl chain show odd-even effects for, *e.g.*, transition temperature, volume changes, chiral properties, dielectric properties, and dipole moments (12). The reason for this odd-even effect and the large difference in optimal chain length for the cellulose dissolution is not fully understood at this moment.

A possible explanation might be based on differences in the range of possible conformations for odd and even alkyl chains (12). As described in literature, the mesogenic units of the alkyl chains are oriented differently for odd and even alkyl chains in the all trans-conformation. In case of an even number of CH_2 repeating units, the mesogenic units are oriented parallel to each other, while in case of an odd number of CH_2 repeating units they are oriented inclined to each other, as depicted in Figure 4.

This difference in orientation leads to significantly different packing of the alkyl chains (Figure 5). Alkyl chains with inclined mesogenic groups are packed less efficient (disordered structure with two alternating conformations), leading to a bent alkyl chain (12, 44). In case of parallel mesogenic groups, the packing is more efficient and the molecules closely align in pairs resulting in a linear chain (well-ordered structure).

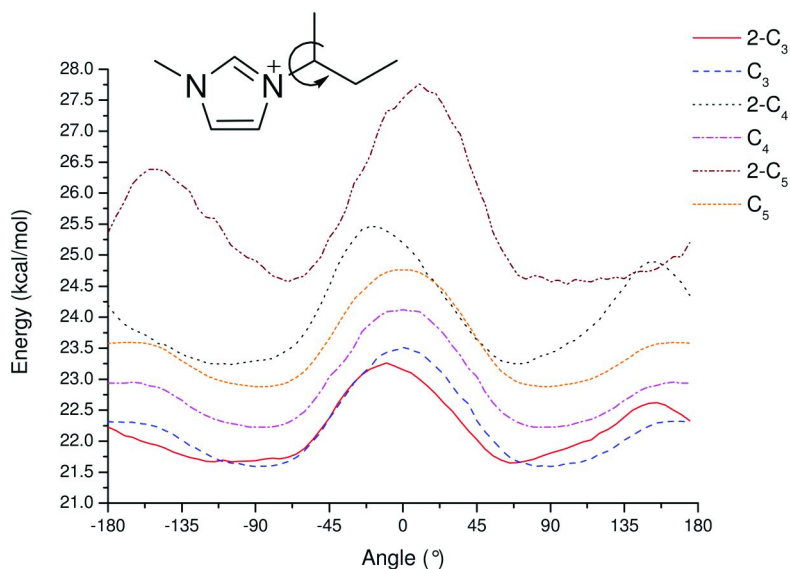


Figure 6. Dihedral angle distribution of the C-N bond (Φ) in the ionic liquids with linear and branched alkyl side chains.

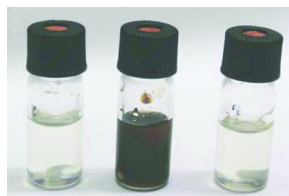


Figure 7. Dissolution of 1 wt.-% cellulose in ionic liquids with branched alkyl side chains: 1-isopropyl-3-methylimidazolium chloride ([2-C₃MIM]Cl) (left), 1-(1-methylpropyl)-3-methylimidazolium chloride ([2-C₄MIM]Cl) (middle) and 1-(1-methylbutyl)-3-methylimidazolium chloride ([2-C₅MIM]Cl) (right).

Therefore, alkyl chains with inclined mesogenic units have a greater propensity to distort from the all trans-configuration with little disruption of the intermolecular packing resulting in a greater range of conformations in comparison to alkyl chains with parallel mesogenic units (12). In general, the range of possible conformations affects melting points, hydrogen bonds, enthalpies and entropies of aliphatic hydrocarbons (44).

In case of ionic liquids, the mesogenic units are the imidazolium ring and the methyl group. The ionic liquids with even alkyl chains showing good cellulose dissolving properties have inclined mesogenic groups (disordered alkyl chain), while the odd alkyl side chains showing no or only bad cellulose dissolving properties have parallel mesogenic groups (ordered alkyl chain).

Table 3. Results for the dissolution studies for imidazolium based ionic liquids with branched side chains

<i>Entry</i>	<i>Branch. IL</i>	<i>Solubility (wt.-%)</i>	<i>Remark</i>
1	[2-C ₃ MIM]Cl	9	-
2	[2-C ₄ MIM]Cl	no sol.	colorization
3	[2-C ₅ MIM]Cl	6	-

Based on this interpretations, we tried to predict the ability of branched ionic liquids to dissolve cellulose. In general, the alkyl chains in the branched ionic liquids are one CH₂ unit shorter than in their linear analogues. Therefore better cellulose solubility is expected for 1-isopropyl-3-methylimidazolium chloride ([2-C₃MIM]Cl) and 1-(1-methylbutyl)-3-methylimidazolium chloride ([2-C₅MIM]Cl), while 1-(1-methylpropyl)-3-methylimidazolium chloride ([2-C₄MIM]Cl) should show no or only bad cellulose solubility. In order to predict if the branched ionic liquids will be able to dissolve more/less cellulose than the ionic liquids with linear alkyl side chains, the conformational energy was calculated for the C-N bond at different angles.

Figure 6 shows in general that the conformational energy increases with longer side chains. Furthermore, in case of [2-C_nMIM]Cl (*n* > 3), the overall conformational energy is much higher than for [2-C₃MIM]Cl or [C_nMIM]Cl (*n* > 1), thus lowering the range of conformation for [2-C_nMIM]Cl (*n* > 3). Therefore, lower cellulose solubility for ionic liquids with branched alkyl side chains compared to linear side chains is expected, as well as for [2-C₅MIM]Cl compared to [2-C₃MIM]Cl.

The dissolution experiments of cellulose in the ionic liquids with branched alkyl side chains ([2-C_nMIM]Cl) (*n* = 3–5) revealed that cellulose was not soluble in [2-C₄MIM]Cl, while [2-C₃MIM]Cl and [2-C₅MIM]Cl in general were able to dissolve cellulose, as it was predicted from the results obtained with the linear analogues. A strong degradation of cellulose in [2-C₄MIM]Cl was observed, since the ionic liquid turned dark brown in relative short time, while the cellulose solution in [2-C₃MIM]Cl and [2-C₅MIM]Cl did not show any change in color (Figure 7).

However, the dissolution of cellulose in the ionic liquid with branched alkyl side chains required longer dissolution times (sometimes more than 1 h) in comparison to the linear analogues. It was found that [2-C₅MIM]Cl was able to dissolve up to 6 wt.-% cellulose, but also a slight degradation was observed, since the color of the solution became a bit brownish (Table 3). In case of [2-C₃MIM]Cl, up to 9 wt.-% of cellulose could be dissolved and no color change was observed. The observed results correspond to the above described expectations.

Since the observed odd-even effect for the chloride containing ionic liquids was remarkable, we also used the synthesized bromides to dissolve cellulose. Thereby, the earlier recognized effect for the chlorides was not observed for the bromides (Table 2). A response to different side chain lengths is not clearly visible maybe due to the overall lower solubility of cellulose in these ionic liquids containing bromide as the counter anion.

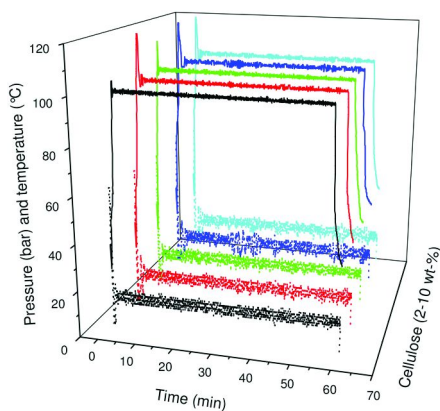


Figure 8. Heating (solid) and power (dot) profiles for the dissolution of cellulose in [EMIM]Cl at different concentrations under microwave irradiation.



Figure 9. Dissolution of cellulose in [EMIM]Cl under microwave irradiation: a) 6 wt-% of cellulose, 100 °C, power between 60 and 140 W, 30 min; b) 2–10 wt-% of cellulose, 140 °C, 80 W, 30 min; c) 2–10 wt-% of cellulose, 160 °C, 80 W, 30 min.

Whereas all the chloride containing ionic liquids with even numbered main alkyl chain show very good dissolving properties, almost all other ionic liquids show less or no dissolution of cellulose. In addition, only the ILs with acetate and phosphate counter anions revealed good dissolving properties for cellulose. For instance, 8 wt.-% of cellulose could be dissolved in 1-ethyl-3-methylimidazolium acetate ([EMIM]OAc) and 12 wt.-% in 1-butyl-3-methylimidazolium acetate ([BMIM]OAc), whereby the solutions became colored, indicating degradation of cellulose. The ability of dissolving cellulose was already described earlier in literature (16, 29, 45). Based on the technology developed by Rogers *et al.* (16) BASF has obtained an exclusive license and offers solutions of cellulose in [EMIM]OAc (5 wt.-%) under the trade name Cellionic (46). Recently, unexpected side reactions were observed under certain conditions in [EMIM]OAc describing that the reaction of cellulose with esterifying- and etherifying agents results in the formation of mixed anhydrides and later to – often exclusively – cellulose acetate (28, 29).

On the other hand, also 1-ethyl-3-methylimidazolium diethyl phosphate ([EMIM]Et₂PO₄) has the ability to dissolve up to 14 wt.-% of cellulose and

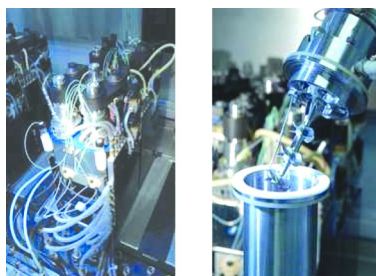


Figure 10. Chemspeed Autoplant A100

1,3-dimethylimidazolium dimethyl phosphate ([DiMIM]Me₂PO₄) up to 10 wt.-%; surprisingly, 1-butyl-3-methylimidazolium dibutyl phosphate ([BMIM]Bu₂PO₄) could not dissolve cellulose at all. In addition, the [EMIM]Et₂PO₄ melts at low temperatures just above room temperature which makes the handling easier.

Dissolution of Cellulose under Microwave Irradiation

Subsequently, a selection of ionic liquids was studied for the dissolution of cellulose under microwave irradiation. First tests were less successful and showed mostly brownish solutions after heating. This suggests a strong degradation of the cellulose under these conditions. However, with the newer microwave reactors it is now possible to set the maximum power introduced into the solvent. Thereby, we found a relationship between the colorization of the cellulose solution and the maximum power introduced. Typical heating and power profiles for the dissolution of cellulose under microwave irradiation show similar temperature and power profiles for different concentrations of cellulose in [EMIM]Cl (Figure 8).

Although a reduced maximum power was chosen, a thermal overshoot could not be avoided when using concentrations above 4 wt.-%. In addition, the maximum power of 60 Watt was reduced automatically after the final temperature was reached. Since the dissolution was performed in the absence of additional solvent and the ionic liquid used showed no significant vapor pressure, the pressure is negligible. For example by dissolving 6 wt.-% of cellulose in [EMIM]Cl, the power could be varied between 60 and 140 Watt without any color change at 100 °C. By using a higher concentration of cellulose (up to 10 wt.-%), a color change was clearly visible at 140 °C and 160 °C (constant temperature/power). In addition between both test series, a more intensive color was visible for the higher temperature (Figure 9).

DP Measurements

These visual results, obtained by the screening experiments using small 2 mL vials or microwave reactors, were also supported by DP measurements

Table 4. Maximum water uptake of different IL's at a relative humidity of 80%

Entry	Ionic liquid	Water uptake (wt.-%)	Solubility of cell. (wt.-%)
1	[C ₂ MIM]OAc	134	8
2	[C ₂ MIM]Cl	106	10–14
3	[C ₂ MIM]Et ₂ PO ₄	97	12–14
4	[BMIM]Cl	88	20
5	[C ₂ MIM](CN) ₂ N	53	-

from dissolved and precipitated cellulose. For our test we used the three ILs [BMIM]Cl, [EMIM]Cl and [EMIM]Et₂PO₄ to dissolve cellulose. As a general procedure 8 wt-% of cellulose was dissolved and the mixture was heated up to 100 °C and left at this temperature for 2 hours. The automated ChemSpeed A100 AutoPlant robot with its internal anchor stirrers was used to ensure an efficient heating, stirring and cooling. According to the described method by Heinze *et al.* (25), the DP values of both the starting cellulose and the regenerated samples were determined by capillary viscometry in Cuen.

Starting with the same Avicel PH-101 sample (DP = 400), the values observed showed that the highest degradation of cellulose appeared in [BMIM]Cl (DP = 310), a slightly lower degradation in [EMIM]Cl (DP = 360). The lowest degradation after 2 hours of heating at 100 °C was found in [EMIM]Et₂PO₄ (DP = 380) (41).

Water Uptake Measurements

Already at the beginning of the dissolution experiments it was observed qualitatively that in general only dried ILs are able to dissolve cellulose. As a result, we were interested to identify the relationship between the water uptake abilities and the ability to dissolve cellulose. These results could be combined with the data obtained by the Karl Fischer titration (Table 1). To perform the water uptake measurements, a “Dynamic Vapor Sorption (DVS)” technique(47) was applied and high values for the absorption of water were observed for [EMIM]Cl, [BMIM]Cl, [EMIM]Et₂PO₄, [EMIM]OAc. Only the ionic liquid [EMIM](CN)₂N showed a lower water absorbance. A sorption isotherm was contracted revealing that the absorption and desorption of water is completely reversible, too. The results are shown in the following Table 4.

The sorption isotherm indicates that for ILs with the same counter ion the water uptake decreases with longer side chains ([EMIM]Cl (106 wt.-%) > [BMIM]Cl (88 wt.-%)). For the same [EMIM] cation the ability to attract water decreases with the anions in the order of OAc⁻ > Cl⁻ > Et₂PO₄⁻ > (CN)₂N⁻. The water uptake for [EMIM]Et₂PO₄ (97 wt.-%) lays in between [EMIM]Cl (106 wt.-%) and [BMIM]Cl (88 wt.-%) and the ability of dissolving cellulose for [EMIM]Et₂PO₄ is slightly higher than for [EMIM]Cl.

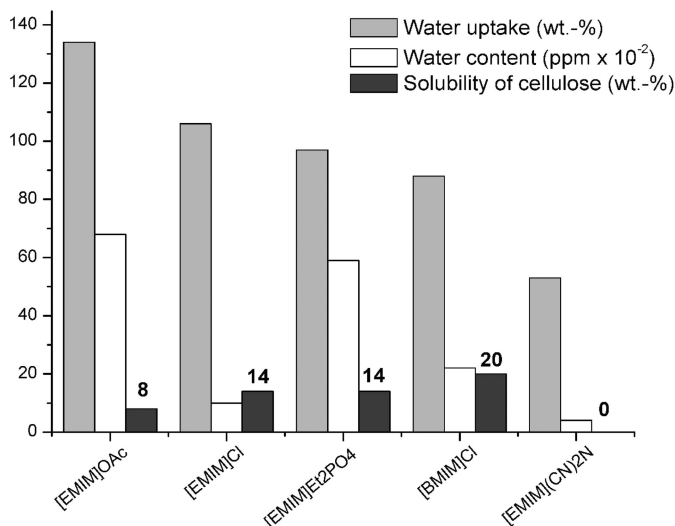


Figure 11. Comparison of the solubility of cellulose in ionic liquids with the water content determined by Karl Fischer titration and water uptake abilities.

When comparing the results for the cellulose dissolution (Table 2) with the water uptake (Table 4), it seems that a lower water uptake for the same cation – [EMIM]⁺ – in the direction OAc⁻ > Cl⁻ > Et₂PO₄⁻ > (CN)₂N⁻ improves the dissolution of cellulose. But at a certain point, the dissolution property of cellulose drops. In the case of [EMIM](CN)₂N, cellulose can not be dissolved at all. On the other hand, [C₃MIM]Cl and [C₅MIM]Cl show a similar water absorbance compared to [EMIM]Cl but they dissolve only very low amounts of cellulose (< 1 wt.-%, Table 2). In comparison with the Karl-Fischer titration (Table 4), the ability to take up water is in line with the water content of the measured ionic liquids. Due to the lack of additional data it is not yet possible to deduce a detailed correlation between the water uptake and the cellulose dissolving ability of the ionic liquids. Additional measurements are necessary to elucidate the relationship more intensively.

Viscosity of IL/Cellulose Solutions

As already mentioned before, ionic liquids sometimes show a degradation of cellulose. In this case, the dynamic viscosity of the cellulose solution in ILs should significantly decrease in time. To show the stability of cellulose in ionic liquid solutions, the ionic liquids [EMIM]OAc and [EMIM]Et₂PO₄ were chosen and the viscosities of the pure ionic liquids, the two 2 wt.-% cellulose solutions and the solutions of cellulose in IL/pyridine were measured on an automated microviscometer based on the rolling/falling ball principle.

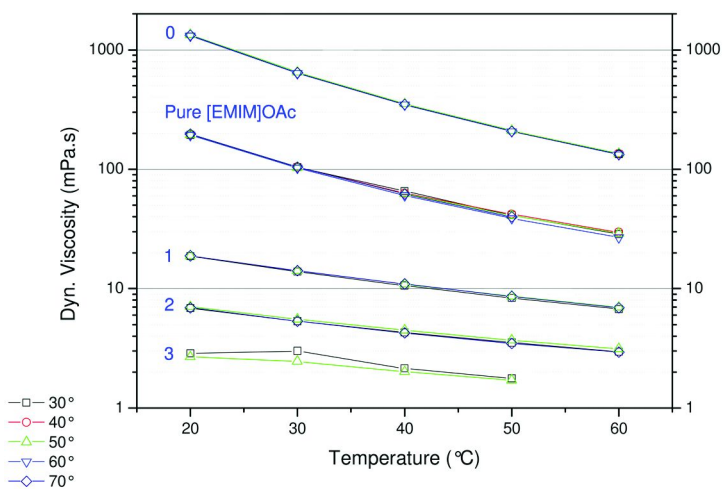


Figure 12. The dependence of dynamic viscosity of pure [EMIM]OAc, [EMIM]OAc/cellulose (0) and three mixed solutions [EMIM]OAc/cellulose/pyridine (1–3) on temperature measured at different angles. Cellulose concentrations in mixed solvents were 2.25 (0), 0.97 (1), 0.64 (2), and $0.48 \cdot 10^{-2}$ g cm^{-3} (3), respectively.

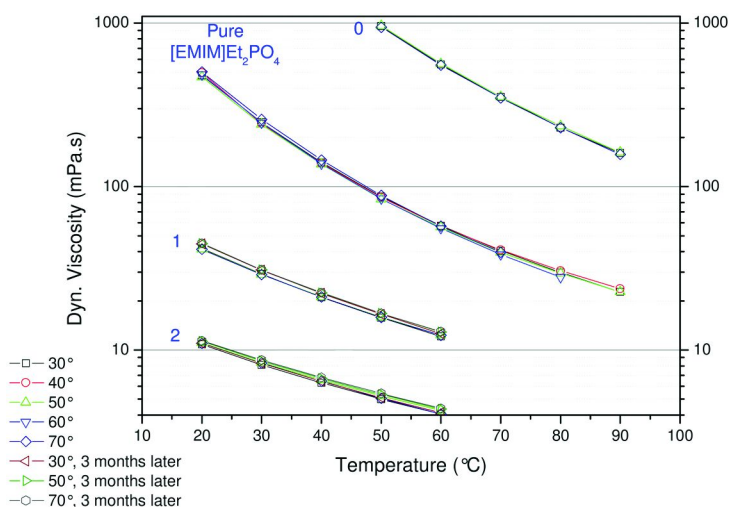


Figure 13. The dynamic viscosity measurements of pure [EMIM]Et₂PO₄, [EMIM]Et₂PO₄/cellulose (0) and [EMIM]Et₂PO₄/cellulose/pyridine solutions (1–2) within an interval of three month. Cellulose concentrations in mixed solvents were 2.36 (0), 1.08 (1), and $0.69 \cdot 10^{-2}$ g cm^{-3} (2), respectively.

The following Figures 12 and 13 show the plots of the dynamic viscosity *versus* the temperature for different measuring angles. As a rule of thumb, the viscosity is reduced to approximately the half of its starting value only by

increasing the temperature by 10 °C. Since water can influence the viscosity of ionic liquids significantly, it is essential that the ionic liquids are severely dried before its use. In addition, the viscosity is independent from the measuring angle, the ionic liquids used behave like a Newtonian liquid (48). On the other hand, the use of ILs as cellulose solvents requires advanced equipment due to their high dynamic viscosity. For example, only adding 2 wt.-% of cellulose to [EMIM]OAc leads to an increase from 200 mPa·s to 1100 mPa·s, in case of [EMIM]Et₂PO₄ from 480 mPa·s to 6900 mPa·s (49).

The viscosity can be significantly decreased by diluting a cellulose/IL solution with an organic solvent; however, a possible precipitation of cellulose must be avoided. The reduction of the dynamic viscosity by adding pyridine is shown in Figures 12 and 13 for three and two different concentrations, respectively. Furthermore, the solutions of [EMIM]Et₂PO₄/cellulose/pyridine were stored and the dynamic viscosity was measured after 3 months again. The viscosities did not change significantly and it can be concluded that the cellulose is stable in these solvent mixtures over a long period at room temperature.

Conclusions

In recent years, ionic liquids became advantageous solvents for the dissolution of cellulose as well as promising reaction media for a number of different reactions to process cellulose. On the other hand, cellulose is a very important source for industrial products and food industry but also for medical applications.

To extend the range of suitable ionic liquids, we screened a number of different ionic liquids. Thereby, the earlier found odd-even effect for the 1-alkyl-3-methylimidazolium chlorides was not observed for the bromides but is also visible for branched analogues. On the whole, only the ILs with chloride, acetate and phosphate counter anions revealed good dissolving properties for cellulose. When using microwave irradiation for the dissolution of cellulose, a correlation of power, temperature, and concentration was found.

Zavrel *et al.* showed that new high-throughput approaches using microtiter plates can be used for the dissolution of cellulose, too, measuring the extinction and scattered light (50). Another option for dissolving and processing cellulose using ultrasound was shown by Mikkola *et al.*. Thereby, the dissolution of cellulose was possible within a few minutes (51). Unfortunately, only [AMIM]Cl and [BMIM]Cl were tested. Both methods are attractive alternatives which could significantly accelerate the search for new IL candidates.

In conclusion, we found that [EMIM]Et₂PO₄ showed very good results for the dissolution of cellulose because almost no color change (and therefore a very low degradation of cellulose) was observed. This was supported by DP measurements from dissolved and precipitated cellulose. In addition, [EMIM]Et₂PO₄ melts at about room temperature which makes the handling easier. In addition, the physico-chemical properties, *e.g.* a good thermal and hydrolytic stability of the dialkylphosphate ionic liquids, show their advantage over well-established ionic liquids. Furthermore, the known biodegradability and, in general, the low-toxicity

of phosphoric acid esters opens an alternative to other halogen-free ionic liquids (28, 49). The stability of cellulose in 1-alkyl-3-methylimidazolium-based IL/pyridine mixtures at different solute concentrations and at different IL/pyridine ratios offers further applications in processing as well as opto-analytical studies.

Acknowledgements

The authors would like to thank the Dutch Polymer Institute (DPI) and the Fonds der Chemischen Industrie for financial support and Solvent Innovation and Merck KGaA for supplying their ionic liquids as a kind gift.

References

1. Heinze, T.; Liebert, T. *Prog. Polym. Sci.* **2001**, *26*, 1689–1762.
2. Moutos, F. T.; Freed, L. E.; Guilak, F. *Nat. Mater.* **2007**, *6*, 162–167.
3. Mooney, D. J.; Silva, E. A. *Nat. Mater.* **2007**, *6*, 327–328.
4. Langer, R. *Science* **1990**, *249*, 1527–1533.
5. Coviello, T.; Matricardi, P.; Marianecchi, C.; Alhaique, F. *J. Control. Release* **2007**, *119*, 5–24.
6. Edgar, K. J.; Buchmann, C. M.; Debenham, J. S.; Rundquist, P. A.; Seiler, B. D.; Shelton, M. C.; Tindall, D. *Prog. Polym. Sci.* **2001**, *26*, 1605–1688.
7. Haftrén, J.; Zou, W.; Córdova, A. *Macromol. Rapid Commun.* **2006**, *27*, 1362–1366.
8. Lyncke, H. GB Patent 190808023, 03.09, 1908.
9. Cross, C. F.; Spruance, D. C. U.S. Patent 763266, 21.06, 1904.
10. Green, P. *J. Chem. Soc., Trans.* **1906**, *89*, 811–813.
11. Vink, H. *Makromol. Chem.* **1963**, *76*, 66–81.
12. Duer, M. J.; Roper, C. *Phys. Chem. Chem. Phys.* **2003**, 3034–3041.
13. Horvath, A. L. *J. Phys. Chem. Ref. Data* **2006**, *35*, 77–92.
14. Heinze, T.; Dicke, R.; Koschella, A.; Klohr, E.-A.; Koch, W.; Kull, A. H. *Macromol. Chem. Phys.* **2000**, *201*, 627–631.
15. Köhler, S.; Heinze, T. *Macromol. Biosci.* **2007**, *7*, 307–314.
16. Swatloski, R. P.; Rogers, R. D.; Holbrey, J. D. WO Patent 03029329, 10.04, 2003.
17. Swatloski, R. P.; Spear, S. K.; Holbrey, J. D.; Rogers, R. D. *J. Am. Chem. Soc.* **2002**, *124*, 4974–4975.
18. Heinze, T.; Schwikal, K.; Barthel, S. *Macromol. Biosci.* **2005**, *5*, 520–525.
19. Ren, Q.; Wu, J.; Zhang, J.; He, J.; Guo, M. *Gaofenzi Xuebao* **2003**, 448–451.
20. Zhu, S.; Wu, Y.; Chen, Q.; Yu, Z.; Wang, C.; Jin, S.; Dinga, Y.; Wu, G. *Green Chem.* **2006**, *8*, 325–327.
21. Graenacher, C. U.S. Patent 1943176, 09.01, 1934.
22. Zhang, H.; Wu, J.; Zhang, J.; He, J. *Macromolecules* **2005**, *38*, 8272–8277.
23. Myllymaeki, V.; Aksela, R. WO Pat. 2005054298, 16.06, 2005.

24. Wu, J.; Zhang, J.; Zhang, H.; He, J.; Ren, Q.; Guo, M. *Biomacromolecules* **2004**, *5*, 266–268.
25. Barthel, S.; Heinze, T. *Green Chem.* **2006**, *8*, 301–306.
26. Erdmenger, T.; Haensch, C.; Hoogenboom, R.; Schubert, U. S. *Macromol. Biosci.* **2007**, *7*, 440–445.
27. Ebner, G.; Schiehser, S.; Potthast, A.; Rosenau, T. *Tetrahedron Lett.* **2008**, *49*, 7322–7324.
28. Köhler, S.; Liebert, T.; Schöbitz, M.; Schaller, J.; Meister, F.; Günther, W.; Heinze, T. *Macromol. Rapid Commun.* **2007**, *28*, 2311–2317.
29. Heinze, T.; Dorn, S.; Schöbitz, M.; Liebert, T.; Köhler, S.; Meister, F. *Macromol. Symp.* **2008**, *262*, 8–22.
30. Granström, M.; Kavakka, J.; King, A.; Majoinen, J.; Mäkelä, V.; Helaja, J.; Hietala, S.; Virtanen, T.; Maunu, S.-L.; Argyropoulos, D. S.; Kilpeläinen, I. *Cellulose* **2008**, *15*, 481–488.
31. Deetlefs, M.; Seddon, K. R. *Green Chem.* **2003**, *5*, 181–186.
32. Varma, R. S.; Namboodiri, V. V. *Chem. Commun.* **2001**, 643–644.
33. Erdmenger, T.; Paulus, R. M.; Hoogenboom, R.; Schubert, U. S. *Aust. J. Chem.* **2008**, *6*, 197–203.
34. Erdmenger, T.; Vitz, J.; Wiesbrock, F.; Schubert, U. S. *J. Mat. Chem.* **2008**, *18*, 5267–5273.
35. Creary, X.; Willis, E. D. *Org. Synth.* **2005**, *82*, 166.
36. Jain, N.; Kumar, A.; Chauhan, S.; Chauhan, S. M. S. *Tetrahedron* **2005**, *61*, 1015.
37. Jain, N.; Kumar, A.; Chauhan, S. M. S. *Tetrahedron Lett.* **2005**, *46*, 2599–2602.
38. Génisson, Y.; Lauth-de Viguierie, N.; André, C.; Baltas, M.; Gorrichon, L. *Tetrahedron Asymm.* **2005**, *16*, 1017–1023.
39. Bass, W. C. U.S. Patent 4252905, 24.02, 1981.
40. Mazza, M.; Catana, D.-A.; Vaca-Garcia, C.; Cecutti, C. *Cellulose* **2009**, *16*, 207–215.
41. Vitz, J.; Erdmenger, T.; Haensch, C.; Schubert, U. S. *Green Chem.* **2009**, *11*, 417–424, Table 1 is reproduced by permission of the Royal Society of Chemistry.
42. Huddleston, J. G.; Visser, A. E.; Reichert, W. M.; Willauer, H. D.; Broker, G. A.; Rogers, R. D. *Green Chem.* **2001**, *3*, 156–164.
43. Abbott, A. P.; Bell, T. J.; Handa, S.; Stoddart, B. *Green Chem.* **2005**, *7*, 705–707.
44. Abe, Y.; Fujiwara, M.; Ohbu, K.; Harata, K. *J. Chem. Soc., Perkin Trans. 2* **2000**, 341–351.
45. Kosan, B.; Michels, C.; Meister, F. *Cellulose* **2008**, *15*, 59–66.
46. BASF. <http://www.basionics.com/en/ionic-liquids/cellionic/>.
47. Thijs, H. M. L.; Becer, C. R.; Guerrero-Sanchez, C.; Fournier, D.; Hoogenboom, R.; Schubert, U. S. *J. Mater. Chem.* **2007**, *17*, 4864–4871.
48. Kuhlmann, E.; Himmler, S.; Giebelhaus, H.; Wasserscheid, P. *Green Chem.* **2007**, *9*, 233–242.
49. Measured on an Anton Paar MCR 301 rheometer.

50. Zavrel, M.; Bross, D.; Funke, M.; Büchs, J.; Spiess, A. C. *Bioresource Technol.* **2009**, *100*, 2580–2587.
51. Mikkola, J.-P.; Kirilin, A.; Tuuf, J.-C.; Pranovich, A.; Holmbom, B.; Kustov, L. M.; Murzin, D. Y.; Salmi, T. *Green Chem.* **2007**, *9*, 1229–1237.

Chapter 18

Structure-Property Relationship of Cellulose Ethers – Influence of the Synthetic Pathway on Cyanoethylation

B. Volkert*, W. Wagenknecht and M. Mai

Fraunhofer Institute for Applied Polymer Research, Geiselbergstraße 69,
14476 Potsdam-Golm, Germany

*E-mail: bert.volkert@iap.fhg.de, www.iap.fraunhofer.de

The insertion of the reactive cyanoethyl groups into cellulose molecules by etherification with acrylonitrile results in products with wide application potential. Highly substituted organo-soluble products on a commercial scale are used in the high-tech sector because of their exceptional properties. Soluble products with a low and medium degree of substitution (DS) are only accessible via homogeneous synthesis. They have been unexplored to a large extent up until now. This paper will give an overview of new examinations of the reaction conditions and the influence of pretreatment and cellulose structure on the DS and DS distribution of cyanoethyl ether and carboxyethyl ether groups respectively. It describes the derivatization under homogeneous conditions into N-methylmorpholine-N-oxide monohydrate (NMMNO*H₂O) and under heterogeneous conditions with native cellulose and after converting native cellulose to amorphous cellulose. The products are characterized by ¹³C-NMR measurements and by rheological examinations.

Introduction

Heterogeneous Cyanoethylation

As a product that is soluble in organic solvents, cyanoethyl cellulose (DS 2.5-2.8) received brief commercial attention in the 1960s as a resin for phosphor in electroluminescent lamps. The desirable properties were a high dielectric constant, i.e., 10-12, and low dissipation factor, i.e., ca 0.02 (1). Bikales has given a general overview of cyanoethylation up to 1965 (2).

Heterogeneous cyanoethylation (DS < 1) only transforms the accessible surface of cellulose. However this leads to a higher susceptibility of cotton fabric to different dyes (3, 4) whereby the swelling and solubility properties remain unchanged. The products of heterogeneous, alkali-catalyzed reaction without pretreatment of the cellulosic material are neither water nor alkali soluble (5). The activation of cellulose with intracrystalline swelling media like aqueous NaI (6), NaOH, urea containing NaOH, liquid ammonia or primary amines leads to an intracrystalline expansion and yields higher reaction rates, NaOH-soluble products and higher DS level (7, 8). Sadovnikova and Kim developed a procedure to synthesize cyanoethyl cellulose (CEC) up to DS 2.8-2.9 and spun fibers of the product by wet or melt spinning processes (9, 10). Organo-soluble cyanoethyl cellulose with a high degree of substitution (DS > 2) is usually produced through activation with aqueous NaOH and acrylonitrile as reagent and reaction medium. The cyanoethyl cellulose that forms is dissolved in the system in accordance with a quasi-homogeneous reaction. DMSO, DMF, acetone, methylene chloride and acrylonitrile are solvents for highly substituted CEC (11). Under heterogeneous reaction conditions, the DS is influenced not only by reaction conditions like medium, temperature, time and concentration of reagent, but also by the morphological structure of the cellulose (12). Even the solubility of products with the same DS differs depending on the reaction conditions (13). Because of the hydrophobic character of the CN-group, the water sorption capacity of CEC decreases with increasing DS (14). Bruson (15) and MacGregor (16) reason that substitution is preferred at C6. Lukanoff observed equal conversion at C6 and C2 + C3 in methodical studies (17).

The highly substituted hydrophobic organo-soluble products exhibit remarkable properties like resistance to microbial degradation or acid hydrolysis (18-21), advanced thermo stability (22-27) and a high dielectric constant (1, 28-31). Various consecutive reactions of CEC are known which reveal a vast field of application. Aminopropyl cellulose can be synthesized by hydration with borane in organic liquids (32-35) and carboxyethyl cellulose is formed by alkaline saponification (7, 18, 36-42). During the heterogeneous treatment of CEC with NaOH under nitrogen, decyanoethylation is observed to be the main reaction under back-formation of acrylonitrile (43, 44). Carbamidoethyl cellulose is formed through reaction of CEC with H₂O₂ (45, 46) and aminoethyl cellulose through Hoffmann degradation of the reaction product (47). The conversion of CEC with hydroxylamine leads to an amidoxime with absorption properties for Ni²⁺, Co²⁺ and Cu²⁺ (48, 49). Even gold and uranyl ions can be extracted from solutions because of the chelating properties of the amidoxime

(50, 51). Grafting CEC with acryl amide yields a product that can be used as a non ion-sensitive absorber with great capacity (52). Grafting with acrylonitrile or 1-vinyl-2-pyrrolidone leads to products that can also be used to extract heavy metal ions, particularly Fe^{2+} and Cu^{2+} (53–55).

Cyanoethyl acetate membranes can be used for desalination or to extract alcohol through reverse osmosis. They are not only more resistant to bacteria, have better toughness and larger flux, but are also very resistant to inorganic acids in comparison to cellulose acetate membranes (56–58).

Homogeneous Cyanoethylation

Etherification after dissolution of cellulose has been described in the derivatizing system DMSO/ paraformaldehyde or in non-derivatizing solvents like lithium chloride/ dimethyl acetamide, N-methyl-2-pyrrolidone, N-ethyl pyridinium chloride, benzyltriethyl ammonium hydroxide, SO_2 / amine/ DMSO or N-methylmorpholine-N-oxide (NMMNO) (59). The non-derivatizing system NMMNO is of great interest because it is used industrially for forming cellulose fibres and films.

After cyanoethylation of cellulose in homogeneous phase complete solubility of CEC in water or aqueous NaOH even in a low DS range was observed. MacGregor describes the conversion of cellulose xanthogenate in viscose with acrylonitrile in the homogeneous phase into alkali or water soluble CEC (16, 60, 61). Compton reports the production of alkali-soluble CEC (DS 0.25) through the pretreatment of regenerated cellulose with NaOH containing urea and the reaction with acrylonitrile in a kneader (62). The author received alkali-soluble products with DS 0.2-0.3 and water-soluble products with DS 0.7-1. Johnson describes, in a patent, the homogeneous conversion of cellulose dissolved in $\text{NMMNO} \cdot \text{H}_2\text{O}$ / DMSO with acrylonitrile in the presence of catalytic amounts of trimethylbenzyl ammonium hydroxide to water-soluble CEC (63). He used a large molar ratio of acrylonitrile/ AGU ≈ 40 and a reaction time of 1 h at 105 °C. Philipp et al. published their own results of homogeneous functionalization of cellulose in several organic solvent systems for example the etherification in $\text{NMMNO} \cdot \text{H}_2\text{O}$ (59). With DS > 0.05, the resulting CEC was soluble in 10 % NaOH; with DS > 0.8, the products were water-soluble. The homogeneous conversion yielded products with DS 0.05-1.

Comparison of the Heterogeneous, Quasi-Homogeneous and Homogeneous Processes

In former publications, it could be shown that an increase in accessibility of cellulose by activation has a great effect on solubility and viscosity behavior of homogeneously synthesized cellulose ether (CMC, HEC, HPC, SEC) (64–66).

Table I. Influence of the reaction conditions on DS and viscosity values of heterogeneously synthesized CEC

Sample	Cellulose [#]	Procedure	Pre-treatment	Medium	mol AN/ mol AGU	T [°C]	t q[h]	DS _{CN} (NMR)	DS _N (EA*)	Solubility resp. viscosity (2 %) [mPa*s at γ̇ 2.55 s ⁻¹]		
										H ₂ O	2 N NaOH	DMSO
CN-T1	T 10	A	none	2% NaOH	4	40	5	-	0.18	swollen	swollen	swollen
CN-T2	T 10	A	none	2% NaOH	4	40	1	0.18	0.17	swollen	swollen	swollen
CN-T3	T 10	A	none	2% NaOH	4	20	1	-	0.18	swollen	swollen	swollen
CN-T4	T 10	A	none	2% NaOH	2	40	5	-	0.1	swollen	swollen	swollen
CN-T5	T 10	A	none	2% NaOH	8	20	1	0.41	0.45	-	dissolved	238
CN-T6	T 10	B	18% NaOH	2% NaOH	4	40	1	0.36	0.41	swollen	swollen	swollen
CN-T7	T 10	C	18% NaOH	10% NaOH	4	20	1	-	0.45	237	dissolved	220
CN-T8	am.Cell.F	A	none	2% NaOH	4	40	1	0.37	0.44	swollen	partially dissolved	swollen
CN-T9	am.Cell.F	A	none	2% NaOH	4	20	1	-	0.54	swollen	viscous solution	partially dissolved
CN-T10	am.Cell.F	B	18% NaOH	2% NaOH	4	40	1	-	0.37	swollen	partially dissolved	swollen
CN-T11	am.Cell.F	C	18% NaOH	10% NaOH	4	40	1	0.46	0.42	89	dissolved	303
CN-T12	am.Cell.F	C	18% NaOH	10% NaOH	4	20	1	0.6	0.55	partially dissolved	dissolved	380

[#] T 10: Temming 10; am.Cell.F: amorphous Cellunier F * EA: elementary analysis

In addition to these results, this paper focuses on the homogeneous synthesis of CEC. The differences between heterogeneous, quasi-homogeneous and homogeneous cyanoethylation procedures will be shown. Also the decisive influence of the reaction conditions on the accessibility and reactivity of cellulose molecules and the effect on the macroscopic properties of the product like solubility in water, NaOH and DMSO and structure viscosity will be pointed out.

Experiment

Materials

For the Heterogeneous Procedure:

Two different cellulose materials were used as starting material (Temming 10 linters from Steinbeis Papier Glückstadt GmbH & Co. KG [DP_{Cuoxam} = 425] and Cellunier-F wood pulp from Rayonier, Inc. which was decrystallized [DP_{Cuoxam} = 450]). Trifluoroacetic acid [TFA], NaOH and acrylonitrile [AN] were purchased from Fluka and used as received.

For the Homogeneous Procedure:

Two different cellulose materials were used as starting material (wood pulp Ultraether F from Rayonier, Inc. [DP_{Cuoxam} = 1625] and cotton-linters Temming 500 from the company Temming [DP_{Cuoxam} = 640]). NMMNO was received as a 50 % aqueous solution from Degussa AG. All cosolvents (dimethyl sulfoxide [DMSO], N-methyl pyrrolidone [NMP], N,N'-dimethylacetamide [DMAc], t-butanol [t-BuOH]), all precipitants and washing media (methanol [MeOH], ethanol [EtOH], isopropanol [i-PrOH], acetone), all bases and catalysts (sodium hydroxide [NaOH], potassium hydroxide [KOH], benzyl trimethylammonium hydroxide [Triton B, 40 % aqueous or methanolic solution], tetraethylammonium hydroxide [TEAH], ethylenediamine [EDA], tri-n-butylamine [TBA], anion exchanger [AIE; Amberlyst A26]), the stabilizer (propyl gallate [PG]) and the cyanoethylation reagent acrylonitrile [AN] were purchased from Fluka in pure grade and used as received.

Measurements

Determination of the Degree of Polymerization (DP) of Cellulose in Cuoxam Solution

For dissolving the cellulose sample, a brown wide-necked bottle of 100-110 ml capacity was used and the weighed sample was dissolved in 100 ml of Cuoxam solution (aqueous solution of [Cu(NH₃)₄](OH)₂ · 3H₂O) at 20 °C. Pieces of metallic

copper were used to minimize the air volume above the solution in the bottle. The mixture was kept for 5 min at 20 °C, vigorously shaken, and then placed again in a water bath at 20 °C. This procedure was repeated until the sample was completely dissolved. The viscosity measurement was performed in a Doering viscometer (67). The viscosity was calculated from the efflux time of this cellulose solution and of the blank Cuoxam solution.

The DP was calculated from the specific viscosity

$$\eta_{\text{spec}} = \frac{\eta - \eta_0}{\eta_0} \quad (1)$$

according to

$$\text{DP} = \frac{2000 * \eta_{\text{spec}}}{c * (1 + 0,29 * \eta_{\text{spec}})} \quad (2)$$

where η = viscosity of the cellulose solution; η_0 = viscosity of the solvent; c = concentration of cellulose [g/l].

The determination was always performed in duplicate.

Solubility

For the determination of the solubility, 0.1 g of air-dried product was suspended in 5 ml H₂O, 2N NaOH or DMSO. The dissolution, gel formation or swelling was evaluated after 48 h of stirring at 20 °C.

Elementary Analysis

The DS_N was calculated from the N content measured through elementary analysis using a Fisons Instruments Elemental Analyzer EA 1110.

Viscosity

The viscosity of a 2 % CEC solution in water, 2N NaOH and DMSO was measured using a rotary viscometer (VT550, Haake) with a conical cylinder (MV-DIN) at 20 °C. The viscosity was measured in dependence of shear rate in the range of $\dot{\gamma} = 0\text{-}10 \text{ s}^{-1}$. The shear viscosity was determined at a shear rate of $\dot{\gamma} = 2.55 \text{ s}^{-1}$.

Table II. Applicable catalysts for the homogeneous cyanoethylation of cellulose depending on the cosolvent in NMMNO*H₂O^a

<i>Catalyst</i>	<i>DMSO</i>	<i>NMP</i>	<i>DMAc</i>	<i>t-BuOH</i>
AIE	-	+	+	n.e.
Triton B	+	+	n.e.	+
NaOH	+	+	+	-
KOH	+	+	+	+(with gel)
NaOAc	-	-	n.e.	n.e.
alkali cellulose	-	-	n.e.	n.e.

^a n.e.: not examined

¹³C-Liquid NMR

The ¹³C-NMR spectra were recorded using a Varian UNITY 400 NMR spectrometer at a frequency of 100.58 MHz. For the determination of the DS and the distribution of substituents in the AGU of derivatized cellulose, the samples were hydrolyzed with trifluoroacetic acid (TFA) according to Fengel et al. (68), dissolved in D₂O and analyzed with the high-resolution liquid ¹³C-NMR. The measurements were carried out using a quantitative method without Nuclear-Overhauser effect (69).

Activation/Reactions

Preparation of Amorphous Cellulose (65)

110 g Cellulose (DP_{Cuoxam} = 450, Cellunier-F) was suspended in 1700 g of 50 % NMMNO solution with 0.01 g PG/g cellulose as stabilizer and swelled for 24 h at 20 °C. Suction filtration of the cellulose resulted in a filter cake with a mass ratio of 1:8 of cellulose to 50 % NMMNO. Both the filter cake and the filtrate were dewatered. The filtrate was concentrated in a rotary evaporator at 90 °C/65 mbar to a concentration of about 80 %. At the same time the residual NMMNO in the filter cake was dewatered at < 85 °C/65 mbar in a 2-L-stirring reactor. After achieving the desired NMMNO concentration, the warm filtrate was added to the cellulose pulp. The small residual amount of water was distilled off at 110 °C/60-65 mbar until the NMMNO monohydrate concentration was achieved and the cellulose was dissolved.

Isopropanol as a precipitant was slowly added to the solution under vigorous stirring in the presence of an ultra turrax until the gel point was obtained (T = 105-110 °C). From this point on, the rate of addition was accelerated until the cellulose was precipitated. The amorphous cellulose was filtered off, washed

several times with *i*-PrOH, and stored as an *i*-PrOH wet sample. The absence of ordered structures was detected by ^{13}C -CP/MAS NMR (65).

Heterogeneous Cyanoethylation

If Cellunier-F was used, it was activated by amorphization with the procedure described above. Temming 10 linters was used as native material.

Procedure A

10 g (dry weight) of cellulose (0.062 mol) were suspended in 200 mL 2 % aqueous NaOH (1.6 mol/mol AGU). The mixture was cooled to 4 °C and 16.5 mL of acrylonitrile (4 mol/mol AGU) were added all at once under moderate stirring. The reaction mixture was heated to 40 °C incrementally (5 °C every 5 minutes). After 1 h the reaction was stopped by adding a solution of 10 % glacial acetic acid in ethanol until the mixture reacted neutrally. The product was filtered off, washed several times with ethanol and oven-dried at 40 °C under reduced pressure.

Procedure B

Cellulose was suspended in 18 % aqueous NaOH with a liquor ratio of 1:20 for 1 h under moderate stirring at room temperature (16 mol/mol AGU). The alkaline cellulose was filtered off and washed with distilled water until it was neutral. Cyanoethylation was carried out according to the general procedure.

Procedure C

Cellulose was suspended in 18 % aqueous NaOH with a liquor ratio of 1:20 for 1 h under moderate stirring at room temperature. Then NaOH was diluted with distilled water until a concentration of 10 % was reached (16 mol/mol AGU). The mixture was cooled to 4 °C and AN (4 mol/mol AGU) was added all at once. The temperature was rapidly adjusted to 20 °C and cyanoethylation was run for 1 h. The reaction was stopped by neutralization with acetic acid and precipitation in ethanol. The product was filtered off, washed several times with ethanol and dried at room temperature.

Quasihomogeneous Cyanoethylation

The process is called quasi-homogeneous if the reaction product dissolves in the system during the cyanoethylation (CN-T12).

Table III. Influence of reaction conditions on the solubility and viscosity of CEC during homogeneous cyanoethylation (solution of 3.2 % cellulose in NMMNO*H₂O)

Sample	DP Cellulose	30 % cosolvent in NMMNO	PG ^a	Base mol/mol AGU	AN mol/mol	T [°C]	t [h]	DS _N	Solubility resp. viscosity (2%) [mPa*s at $\dot{\gamma} = 2.55 \text{ s}^{-1}$]		
									2N		
									H ₂ O	NaOH	DMSO
CN-M1	1625	NMP	-	0.5 AIE/NMP	8	65	0.5	0.84	5750	+	+
CN-M2	1625	NMP	+	0.1 Triton B/NMP	6/NMP	65	96	0.05	-	-	-
CN-M3	1625	NMP	+	0.3 Triton B/NMP	6/NMP	65	3	0.36	swollen	+	+
CN-M4	1625	NMP	+	0.3 Triton B/NMP	6/NMP	65	24	0.30			
CN-M5	1625	NMP	+	0.4 Triton B/NMP	6/NMP	65	3	0.27			
CN-M6	1625	NMP	+	0.4 Triton B/NMP	6/NMP	65	24	0.19			
CN-M7	1625	NMP	+	0.5 Triton B/NMP	6/NMP	65	0.17	0.59	+	+	+
CN-M8	1625	NMP	+	0.5 Triton B/NMP	6/NMP	65	1	0.41			
CN-M9	1625	NMP	+	0.5 Triton B/NMP	6/NMP	65	24	0.23	-	+	-
CN-M10	1625	NMP	+	0.5 Triton B/NMP	6/NMP	75	0.25	0.35			
CN-M11	1625	NMP	+	0.5 Triton B/NMP	6/NMP	75	0.5	0.34	swollen	+	+
CN-M12	1625	NMP	-	0.5 Triton B/NMP	6	65	0.5	0.52	+	+	+
CN-M13	1625	NMP	+	0.5 Triton B*/NMP	6	40	0.25	0.60	+	+	+
CN-M14	1625	NMP	+	0.5 Triton B*/NMP	6	40	0.5	0.41			
CN-M15	1625	NMP	+	0.5 Triton B*/NMP	6	40	1	0.16			
CN-M16	1625	NMP	+	0.5 Triton B*/NMP	6	85	1	0.2			

Continued on next page.

Table III. (Continued). Influence of reaction conditions on the solubility and viscosity of CEC during homogeneous cyanoethylation (solution of 3.2 % cellulose in NMMNO*H₂O)

Sample	DP Cellulose	30 % cosolvent in NMMNO	PG ^a	Base mol/mol AGU	AN mol/mol	T [°C]	t [h]	DS _N	Solubility resp. viscosity (2%) [mPa*s at $\dot{\gamma} = 2.55 \text{ s}^{-1}$] 2N		
									H ₂ O	NaOH	DMSO
CN-M17	1625	NMP	+	0.3 NaOH/50 % NMMNO	6/NMP	65	1.5	0.16	-	+	-
CN-M18	1625	NMP	+	0.1 NaOH/50 % NMMNO	6	65	1.25	0.16	-	+	swollen
CN-M19	1625	NMP	+	0.2 NaOH/50 % NMMNO	6	65	1.25	0.63	5300	+	+
CN-M20	1625	NMP	+	0.2 NaOH/50 % NMMNO	6	65	1.5	0.4			
CN-M21	1625	NMP	-	0.3 NaOH/50 % NMMNO	6	65	1.5	0.58	1430	+	+
CN-M22	1625	NMP	+	0.3 NaOH/50 % NMMNO	6	65	1.25	0.65	+	+	+
CN-M23	1625	NMP	+	0.3 NaOH/50 % NMMNO	6	65	1.5	0.31	-	+	32760
CN-M24	1625	NMP	+	0.3 NaOH/50 % NMMNO	6	65	1.5	0.44	+	+	34700
CN-M25	1625	NMP	+	0.3 NaOH/50 % NMMNO	6	65	2	0.34	swollen	+	43170
CN-M26	1625	NMP	+	0.1 KOH/50 % NMMNO	6	65	1.5	0			

Sample	DP Cellulose	30 % cosolvent in NMMNO	PG ^a	Base mol/mol AGU	AN mol/ mol	T [°C]	t [h]	DS _N	Solubility resp. viscosity (2%) [mPa*s at $\dot{\gamma} = 2.55 \text{ s}^{-1}$] 2N		
									H ₂ O	NaOH	DMSO
CN-M27	1625	NMP	+	0.3 KOH/50 % NMMNO	6	65	1.5	0.45	swollen	+	+
CN-M28	375	NMP	+	0.3 KOH/50 % NMMNO	6	65	1.5	0.38	swollen	+	+
CN-M29 [#]	375	NMP	+	0.3 KOH/50 % NMMNO	6	65	1.5	0.53	gel particles	+	+
CN-M30	1625	DMAc	+	0.3 NaOH/50 % NMMNO	6	65	1.5	0.70	gel	+	31200
CN-M31	1625	DMAc	+	0.2 NaOH/50 % NMMNO/ t-BuOH	6	65	0.33	0.84	6900	+	8060
CN-M32	1625	DMSO	+	0.3 KOH/50 % NMMNO	6	65	1.5	0.58	+	+	+
CN-M33	1625	DMSO	+	0.3 KOH/50 % NMMNO	6	65	1.5	0.65	swollen	+	liquid gel
CN-M34	375	DMSO	+	0.3 KOH/50 % NMMNO	6	65	1.5	0.53	+	+	+
CN-M35 [#]	375	DMSO	+	0.3 KOH/50 % NMMNO	6	65	1.5	0.79	+	+	+
CN-M36	1625	t-BuOH	+	0.3 KOH/50 % NMMNO	6	65	1.5	0.25	-	+	liquid gel

^a PG = propyl gallate * 35 % in MeOH # 4.5 % cellulose solution

Homogeneous Cyanoethylation

Cellulose was dissolved according to the amorphization procedure described above. Instead of precipitation, the solution was diluted with the corresponding co-solvents. Dissolution of cellulose was usually carried out at 105 °C, dilution with DMSO, DMAc or NMP at 105 °C, dilution with t-BuOH at 85 °C. As denoted in Table III small amounts of the soluble basic catalysts (Triton B, NaOH, KOH) were added in diluted form. The solid phase catalyst (AIE) was added as a suspension in organic solvent at a ratio of 1:5. AN was added in pure or diluted form.

Example of the Principal Procedure

A melt solution of 3.5 g cellulose ($DP_{\text{Cuoxam}} = 1625$, Ultraether F) in 112 g of NMMNO*H₂O containing 0.035 g PG was diluted with 60 ml NMP or DMAc or DMSO at 105 °C under stirring and cooled to 90 °C. A solution of 0.26 g NaOH or 0.36 g KOH in 12 g 50 % aqueous NMMNO-solution (0.3 mol NaOH or KOH/mol AGU) was added within 60 min. The mixture was cooled to 65 °C and 8.5 mL AN (6 mol/mol AGU) were added within 5 min for cyanoethylation. After a reaction time of 15 to 90 min at 65 °C the reaction product was precipitated by pouring said solution into the three-fold volume of a mixture of acetone/ethanol (3:1), neutralized with 10 % acetic acid in ethanol, washed with ethanol and dried under reduced pressure.

Results and Discussion

The excellent properties of CEC samples with high DS described in the introduction necessitated a comparison between CEC samples with low DS synthesized via heterogeneous and homogeneous pathways.

The reaction conditions were modified to obtain low DS values and the influence of amorphization, mercerization, catalyst type and reaction temperature was examined. The results show the decisive influence of the cellulose structure and solubility in the system on the DS.

Heterogeneous Procedure

Both pretreated and native cotton linters and amorphous cellulose were used. Generally the reaction was carried out in 2 % NaOH with 4 mol AN/mol AGU. For better accessibility, a mercerizing step with concentrated NaOH (18 %) was inserted. The slurry was either diluted to 10 % before cyanoethylation or washed until it was neutral and then cyanoethylation was carried out in 2 % NaOH. The solubility and viscosity were evaluated in water, NaOH and DMSO.

The influence of various reaction conditions on DS, solubility and viscosity are shown in Table I.

The results presented in Table I show that the DS values of CEC samples made from amorphous cellulose are higher than those made of native linters. Mercerizing of linters in 18 % NaOH before cyanoethylation leads to higher DS than cyanoethylation without pretreatment, while mercerizing of amorphous cellulose does not have any further effect on the DS. A reaction temperature of 20 °C is more favorable than 40 °C. The viscosity is very low after heterogeneous cyanoethylation and the products with low DS are poorly soluble in DMSO, NaOH or water. However, the sample CN-T7 is completely soluble in DMSO, NaOH and water although the DS is lower than for sample CN-T12 which is only partially soluble in water.

Homogeneous Procedure

Fundamentally the solubility of cellulose and the derivative formed in NMMNO*H₂O-systems is important in the homogeneous conversion during the entire reaction time.

The compatibility of the cellulose solution in NMMNO*H₂O with organic cosolvents has been reported elsewhere (65). The melt temperature of the solution can be lowered by adding suitable organic solvents. Therefore derivatization reactions are practicable at temperatures below 85 °C.

Coagulation of cellulose occurred after the addition of 1N aqueous NaOH to a solution of cellulose in NMMNO*H₂O. Therefore some preliminary tests were carried out. Compatibility/coagulating tests were carried out with 3-5 % cellulose solutions in NMMNO*H₂O. For exploratory analysis, various bases dissolved in different solvents were slowly added to the cellulose solution under intensive stirring at 85 °C. The compatibility was evaluated visually. The addition of aqueous solutions of alkali hydroxides and alcoholates causes strong coagulation, but small amounts of NaOH (0.1 mol/mol AGU) dissolved in aqueous NMMNO are compatible. A solution of Triton B in DMSO or aqueous NMMNO is more compatible with the cellulose solution. Amines like TBA or EDA cause no coagulation, but they fail to result in an etherification reaction.

The first experiments with NMMNO*H₂O melt solutions at 85 °C, 8 mol AN/mol AGU and 1 mol Triton B/mol AGU as catalyst did not result in soluble products. Therefore the cellulose solution was diluted with NMP and homogeneous etherification was observed if small amounts of alkali hydroxides dissolved in 50 % NMMNO instead of water, Triton B dissolved in NMP or aqueous NMMNO or a pearl-like anion exchanger (AIE) was used as catalyst. AIE is compatible in combination with the solvents mentioned only after prior dehydration. After adding AIE, the cellulose solution turns colorless and clear.

Table II gives an overview of the applicable cosolvent/catalyst combinations for synthesis of soluble CEC up to a DS_N of 0.8. The gel particles occurring after adding NaOH or KOH disappear during the conversion with AN.

AIE, Triton B, NaOH and KOH are suitable for the production of NaOH-, DMSO or H₂O soluble CEC under specific conditions which will subsequently be described.

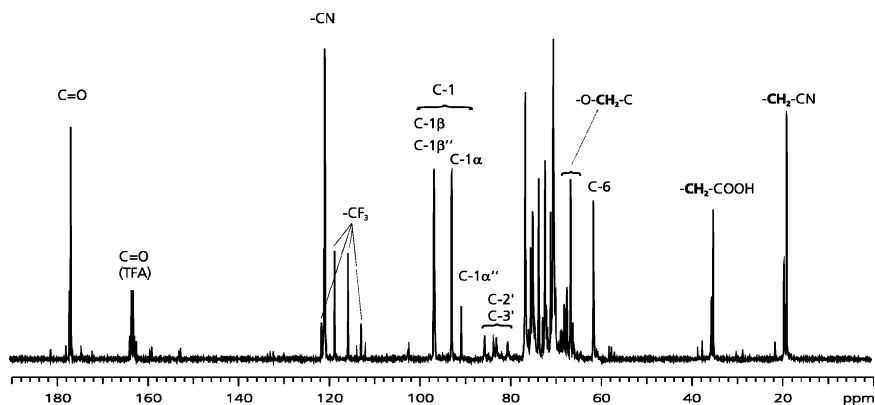


Figure 1. ^{13}C -NMR spectrum of cyanoethyl cellulose (CN-M31) hydrolyzed with trifluoroacetic acid)

Table III presents the various homogeneous reaction conditions and the resulting DS_N , solubility and viscosity after cyanoethylation.

The influence of catalyst type, molar ratio, temperature etc. on the macroscopic properties will be discussed.

The most favorable molar ratio of catalyst per AGU for obtaining soluble products is 0.5 for Triton B and 0.2-0.3 for NaOH and KOH. Even at a low ratio of 0.1 mol NaOH/mol AGU, an alkali-soluble CEC (CN-M18, $\text{DS}_\text{N} = 0.16$) is obtained. Generally it should be noted that the highest DS values occur at short reaction times; the DS_N decreases with increasing reaction time. However, the decrease of DS_N with increasing reaction time could be caused by reversibility of the Michael-Addition or by increasing hydrolysis of CEC to carboxyethyl cellulose. It will be discussed later on whether the decreasing DS is due to decyanoethylation or hydrolysis of CN-groups to carboxyethyl groups (see section ^{13}C -NMR spectroscopic determination).

The favorable temperature for the synthesis of CEC with DS values up to 0.6 within 10-15 min is between 40 and 65 °C. At a temperature of 40 °C the $\text{NMMNO} \cdot \text{H}_2\text{O}/\text{NMP}$ system tends to crystallize. Temperatures higher than 65 °C lead to lower DS_N values at similar reaction times (CN-M11 and -M12).

Comparative examinations with DMSO or NMP as cosolvent and KOH as a base were carried out under variation of cellulose concentration and the DP of the cellulose (CN-M33 to -M35, -M27 to -M29). Compared to NMP, 30 % higher DS values were obtained by using DMSO as cosolvent under similar conditions (CN-M33/-M27, -M34/-M28, -M35/-M29). At a lower DP of the cellulose, the solubility of CEC in water improves at comparable DS and the products are completely soluble in NaOH and DMSO (CN-M33/-M34). DS and solubility in water increase with higher cellulose concentration in the reaction system (3.2 to 4.5 % for linters; CN-M34/-M35, -M28/-M29). A degree of substitution up to 0.8 is obtainable in DMSO (CN-M35).

Table IV. ^{13}C -NMR spectroscopic investigations of DS distribution of heterogeneously synthesized CEC samples

<i>Sample</i>	<i>Catalyst</i>	<i>t</i> [h]	<i>T</i> [°C]	(-CN) 120 ppm	(-COOH) 176 ppm	ΣDS	(-CH ₂ - CN) 19 ppm	(-CH ₂ - COOH) 35 ppm	<i>C-6'</i>	(<i>C-2'+3'</i>) 80-86 ppm	$\text{DS}_{6'}$ / DS_{2+3}	DS_N (EA*)
CN-T1	NaOH/H ₂ O	5	40	0.2	0.05	0.25	0.18	0.05	0.24	-	-	0.18
CN-T2	NaOH/H ₂ O	1	40	0.2	0.04	0.24	0.18	0.06	0.22	0.05	4.4	0.17
CN-T3	NaOH/H ₂ O	1	20	-	-	-	-	-	-	-	-	0.18
CN-T5	NaOH/H ₂ O	1	40	0.46	0.11	0.57	0.41	0.13	0.35	0.05	7	0.45
CN-T6	NaOH/H ₂ O	1	40	0.42	0.07	0.49	0.36	0.1	0.34	0.06	5.7	0.41
CN-T7	NaOH/H ₂ O	1	20	-	-	-	-	-	-	-	-	0.45
CN-T8	NaOH/H ₂ O	1	40	0.43	0.11	0.54	0.37	0.13	0.34	0.08	4.25	0.44
CN-T9	NaOH/H ₂ O	1	20	-	-	-	-	-	-	-	-	0.54
CN-T10	NaOH/H ₂ O	1	40	-	-	-	-	-	-	-	-	0.37
CN-T11	NaOH/H ₂ O	1	40	0.46	0.13	0.59	0.46	0.13	0.48	0.17	2.8	0.42
CN-T12	NaOH/H ₂ O	1	20	0.68	0.17	0.87	0.6	0.06	0.58	0.28	2.1	0.55

* EA: elementary analysis

The comparison of the solubility depending on the DS values shows that CEC samples are soluble in 2N NaOH at $DS > 0.15$, in DMSO at $DS > 0.31$ and in water at $DS > 0.50$. Generally CEC samples with DS values > 0.5 are soluble in DMSO and NaOH as well as in water. The addition of PG as a stabilizer leads to higher shear viscosities at comparable DS (CN-M21 and -M19) due to the fact that PG prevents chain degradation. The viscosity is higher in DMSO than in water for samples with similar DS (CN-M31). High DS values and viscosities are also obtainable with an anionic exchanger as catalyst.

^{13}C -NMR Spectroscopic Determination

The CEC samples were hydrolyzed with TFA and afterwards analyzed in D_2O . A typical spectrum (CN-M31; $DS_N = 0.84$; homogeneously synthesized) is shown in Figure 1 with the corresponding signal assignments. In addition to the signals for the CN-group (20 ppm for the CH_2 group and 120 ppm for the CN group), carboxyethyl groups are clearly detected with the CH_2 peak at 35 ppm and the $\text{C}=\text{O}$ peak at 176 ppm.

All C1 signals ranged between 90 and 97 ppm. The value of the integration of these signals was set at 1. The C6' signal is not identifiable because it is overlaid by other cellulose signals, but it can be calculated by subtracting 1-C6.

The DS at position C2 cannot be determined directly from the integrals of the signals $\text{C1}\alpha''$ and $\text{C1}\beta''$ because the signal of $\text{C1}\beta''$ is overlaid by $\text{C1}\beta$. Moreover, it is not sure that the ratio of the signals of $\text{C1}\alpha$: $\text{C1}\beta$ is equal to the ratio of the signals of $\text{C1}\alpha''$: $\text{C1}\beta''$. That is the reason, why the substitution at C2 was not calculated from the shift of the signal of C1 ($\text{C1}\alpha''$).

The ^{13}C -NMR spectroscopic investigations of heterogeneously synthesized samples show that both CN and COOH moieties are present in the CEC samples (Table IV).

The appearance of the COOH groups can be due to the following reasons. On the one hand, it can result from the reaction of CEC with NaOH during the cyanoethylation. On the other hand it can be formed during hydrolysis with trifluoroacetic acid. This can be proved by comparing the DS values from the elementary analysis or ^{13}C -NMR spectroscopic investigations.

The single values of DS_{CN} and DS_{COOH} , resulting from the signals of -CN and -COOH, are consistent with those, which were determined via the signals of vicinal CH_2 -groups from $-\text{CH}_2\text{-CN}$ and $-\text{CH}_2\text{-COOH}$ respectively.

The DS_N from the elementary analysis correlates with the DS_{CN} . Therefore the most of the COOH groups must be formed during cyanoethylation due to the strong alkaline reaction system (1.6-16 mol NaOH/ mol AGU) that leads to hydrolysis of the CN groups. Remarkably there seems to be no hydrolysis of CN moieties during the TFA treatment. Maybe the amount of existing COOH groups impedes further hydrolysis.

Table V. ^{13}C -NMR spectroscopic investigations of DS distribution of homogeneously synthesized CEC samples

<i>Sample</i>	<i>Catalyst</i>	<i>t</i> [h]	<i>T</i> [°C]	(-CN) 120 ppm	(-COOH) 176 ppm	ΣDS	(-CH ₂ -CN) 19 ppm	(-CH ₂ -COOH) 35 ppm	<i>C</i> -6'	(<i>C</i> -2'+3')	<i>DS</i> ₆ / <i>DS</i> ₂₊₃	<i>DS</i> _N (<i>EA</i>)
CN-M1	0.5 AIE	0.5	65	0.66	0.27	0.93	0.56	0.28	0.49	0.41	1.20	0.84
CN-M2	0.1 Triton B	0.17	65	0.03	0.03	0.06	0.03	0.02	0.05	0.04	1.25	0.05
CN-M3	0.3 Triton B	3	65	0.28	0.15	0.43	0.24	0.13	0.25	0.15	1.67	0.36
CN-M7	0.5 Triton B	0.17	65	0.49	0.20	0.69	0.41	0.18	0.38	0.30	1.27	0.59
CN-M9	0.5 Triton B	24	65	0.30	0.10	0.40	0.24	0.21	0.25	0.19	1.32	0.23
CN-M11	0.5 Triton B	0.5	75	0.29	0.09	0.38	0.24	0.09	0.19	0.16	1.19	0.34
CN-M12	0.5 Triton B	0.5	65	0.40	0.16	0.56	0.33	0.14	0.32	0.29	1.10	0.52
CN-M13	0.5 Triton B	0.25	40	0.51	0.19	0.70	0.40	0.15	0.36	0.27	1.33	0.6
CN-M17	0.3 NaOH	1.5	65	0.11	0.09	0.20	0.08	0.04	0.12	0.09	1.33	0.16
CN-M18	0.1 NaOH	1.25	65	0.10	0.05	0.15	0.08	0.04	0.08	0.03	2.67	0.16
CN-M19	0.2 NaOH	1.25	65	0.21	0.09	0.30	0.17	0.08	0.38	0.24	1.58	0.63
CN-M21	0.3 NaOH	1.5	65	0.44	0.12	0.56	0.39	0.13	0.30	0.26	1.15	0.58
CN-M22	0.3 NaOH	1.25	65	0.42	0.17	0.59	0.42	0.17	0.38	0.19	2.00	0.65
CN-M31	0.2 NaOH	0.33	65	0.74	0.28	1.02	0.61	0.24	0.51	0.33	1.55	0.84

The substituent distribution of CEC samples made from Temming linters under the given reaction conditions shows a considerable preference for substitution at the reactive primary OH group (DS_6/DS_{2+3} in the range of 4.4 to 7). Even longer reaction times do not lead to higher substitution at the secondary OH groups (CN-T1/-T2), although this could be supposed for equilibrium reactions.

This can also be explained with the low accessibility of cellulose in the heterogeneous system. Therefor the cyanoethylation of pretreated (alkaline swollen) Cellunier-F leads to an increased substitution at the secondary OH groups. This can be concluded from the lower ratio DS_6/DS_{2+3} in the range of 2.1 to 4.25. The very low ratio of 2.1 for sample CN-T12 is the result of the quasi-homogeneous character of this specific reaction. The reduced temperature seems to play an important role in this context. The product dissolved in the reaction medium and reacted under nearly homogeneous conditions. This led to a similar distribution ratio as occurred after homogeneous procedure (see below).

In summary it can be stated that the solution state and the morphology of the cellulose significantly influence the DS distribution.

Table V shows the ^{13}C -NMR spectroscopic investigations of homogeneously synthesized CEC samples.

The DS values, resulting from the signals for -CN and -COOH, are consistent with both the single values and the total DS of those which were determined by the signals of vicinal CH_2 groups from $-\text{CH}_2\text{-CN}$ and $-\text{CH}_2\text{-COOH}$ respectively.

The DS_N from the elementary analysis does not correlate with the DS_{CN} from ^{13}C -NMR spectroscopic investigations. However it correlates with the sum of DS_{CN} and DS_{COOH} . In conclusion, the occurrence of COOH groups results from TFE hydrolysis due to the formation of carboxyethyl moieties from cyanoethyl moieties. Thus the decrease of DS_N at longer reaction times and higher temperatures (Table III) can be explained mainly by decyanoethylation due to equilibrium reaction, but minor alkaline hydrolysis during the reaction cannot be excluded.

The comparison of DS distribution of homogeneously synthesized samples shows a comparable functionalization of primary and secondary OH groups in the DS-range of 0.1-1. This provides a DS distribution of $C6 \geq C3 + C2$. This is an unexpected contrast to the homogeneous synthesis of other cellulose ethers. HPC or HEC show a preference for secondary OH groups while the primary OH group seems to be protected (65).

The DS distribution ratio of $C6$ to $C2 + C3$ is influenced by the catalyst. The ratio is within a range of 1.1-1.3 if Triton B is used as catalyst. The ratio values are slightly higher (1.2-2.7) for NaOH-catalyzed reactions. This indicates a higher substitution at the primary OH group of the AGU.

Rheological Characterization

The viscosity of the CEC samples obtained has been analyzed from 2 % solutions of CEC in water and DMSO.

Generally the flow curves of the heterogeneously synthesized samples show low structure viscosity in DMSO (Figure 2). The products from amorphous

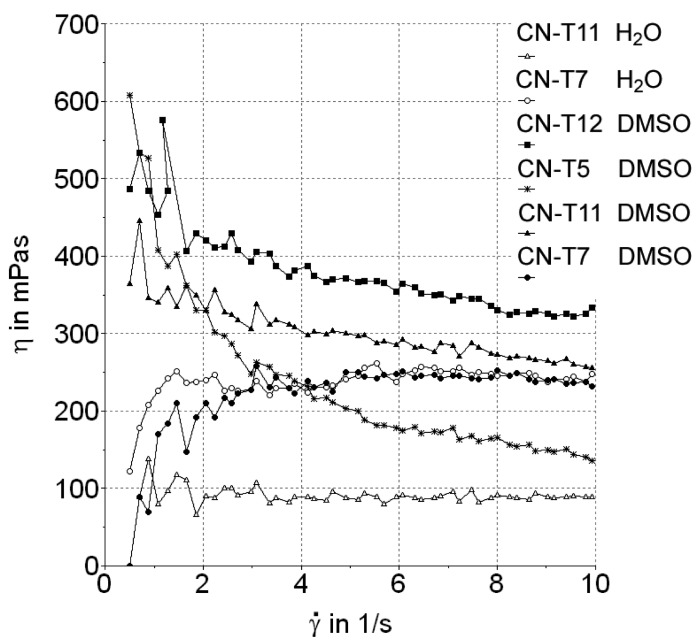


Figure 2. Viscosity of heterogeneously synthesized CEC (2 % solutions)

cellulose (CN-T12 DMSO, CN-T11 DMSO) show higher viscosities than the products from linters (CN-T5 DMSO, CN-T7 DMSO) at comparable DP. CN-T12 shows the highest value due to the quasi-homogeneous reaction conditions and the favorable low temperature.

Due to the poor solubility in water only two samples could be measured. The viscosity for CN-T7 H₂O is higher than for CN-T11 H₂O but both curves do not show any structure viscosity. CN-T7 has the same viscosity in water and in DMSO while CN-T11 shows a remarkable higher value in DMSO than in water.

In contrast to the heterogeneously synthesized samples, the flow curves of the 2 % aqueous CEC solutions from homogeneous synthesis (CN-M19, CN-M31) show a clear structure viscosity with high values ($\eta = 5300\text{-}6900 \text{ mPa}\cdot\text{s}$ at $\dot{\gamma} = 2.55 \text{ s}^{-1}$, Figure 3). Sample CN-M21 has been synthesized in the NMMNO*H₂O system without PG as a stabilizer which causes chain degradation. Therefore the product shows no structure viscosity at low shear rates.

The shear thinning behavior of CEC with low DS is even more distinctive in DMSO (CN-M25 and CN-M23). With $\eta = 32700\text{-}43100 \text{ mPa}\cdot\text{s}$ at $\dot{\gamma} = 2.55 \text{ s}^{-1}$, very high viscosity-values were obtained. This indicates uniformly distributed substituents and an inferior chain degradation during homogeneous cyanoethylation.

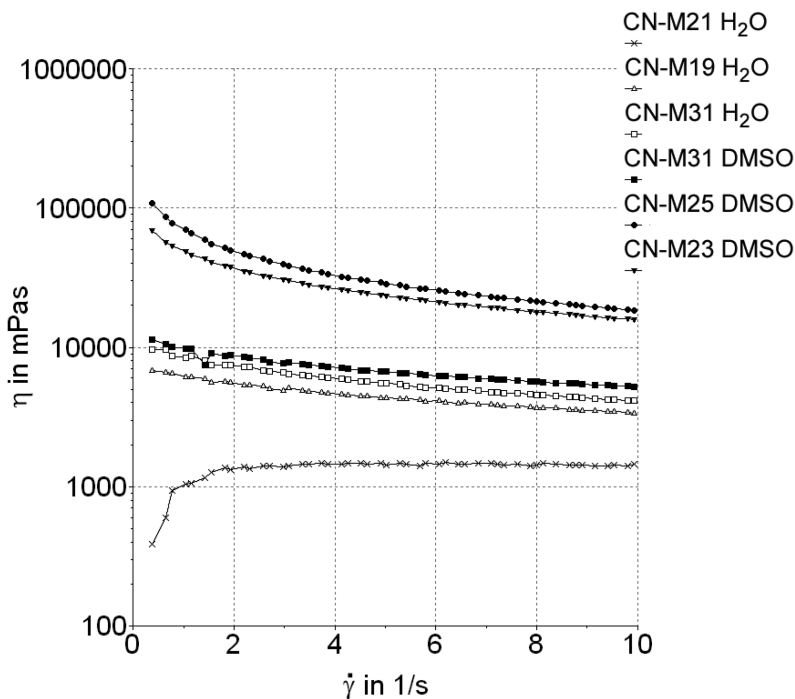


Figure 3. Viscosity of homogeneously synthesized CEC (2 % solution)

Conclusion

The products obtained from heterogeneous reaction are sparingly soluble in water, NaOH and DMSO, compared to homogeneously synthesized samples even at similar DS. Solution state and morphology of cellulose significantly influence the DS distribution of heterogeneous cyanoethylation. The DS distribution of heterogeneously synthesized CEC is $DS_{C6}/DS_{C2+3} \approx 7:1$. In comparison, distribution of quasi-homogeneously synthesized CEC is $DS_{C6}/DS_{C2+3} = 2.1:1$ while distribution of homogeneously synthesized CEC is 1:1.

The homogeneous cyanoethylation occurs if a polar cosolvent like DMSO, NMP or DMAc is added to the cellulose/NMMNO solution. When using NMP as a cosolvent, Triton B, AIE, NaOH and KOH are suitable as catalysts, whereby Triton B and AIE do not affect the homogeneity of the cellulose solution. The most favorable reaction temperature for homogeneous reactions in $NMMNO \cdot H_2O$ is 65 °C. A soluble CEC is formed at this temperature within 15 min. For a high reaction rate, a sufficient concentration of catalyst (0.4-0.5 mol Triton B, 0.3 mol NaOH or KOH/mol AGU) is necessary, since probable viscosity of the cellulose solution impedes migration of the base and AN is dissipated in side reactions.

The highest value obtained for homogeneous conversion in $DS_N = 0.85$. The limit of solubility is in 2N NaOH at $DS \geq 0.15$, in DMSO at $DS \geq 0.35$ and in

water at $DS \geq 0.50$. The DS distribution of homogeneously synthesized CEC is $DS_{C6}/DS_{C2+3} \approx 1:1$. The ratio of C6' to C2' +3' is influenced by the catalyst; the use of NaOH instead of Triton B leads to an increasing substitution at the primary OH group. This is in contrast to HPC or HEC where the primary OH group seems to be protected in the NMMNO*H₂O system.

The very high viscosities of 2 % CEC solutions in water (up to 7000 mPa*s at $\dot{\gamma} = 2.55 \text{ s}^{-1}$) or in DMSO (up to 43000 mPa*s) indicate that only inferior chain degradation takes place during cyanoethylation.

Samples with low DS (0.45-0.85) that are soluble in DMSO as well as in water and NaOH, are only obtainable via homogeneous reaction conditions. After special pretreatment of the cellulose before the heterogeneous reaction, the resulting CEC is soluble in DMSO, water and NaOH within a small DS range around 0.45. With increase of the DS to 0.55, the solubility in water decreases in analogy to the maximum of solubility in 10 % NaOH described in the literature (70).

The influence of catalyst, medium and reaction conditions on the DS distribution has to be examined further.

Application for the homogeneously synthesized products as viscosity regulating additives in aqueous or organic systems is conceivable. Examinations of ion-binding, antifouling, heat resistance or dielectric properties should be performed.

Acknowledgements

We would like to thank Dr. Henrik Wetzel for the elementary analyses and Dr. Jürgen Kunze and Dr. Andreas Ebert for the NMR investigations. The financial support of the Wolff Cellulosics GmbH & Co.KG is gratefully acknowledged.

References

1. Just, E. K.; Majewicz, T. G. *Encyclop. Polymer Sci. Technol.*; Interscience Publishers: New York, 1994; Vol. 3.
2. Bikales, N. M. *Encyclop. Polymer Sci. Technol.*; Interscience Publishers: New York, 1966; Vol. 4, p 533.
3. Hall, A. J. *Textile Mercury Argus* **1955**, 132, 239.
4. El-Hilw, Z. H.; Hebeish, A. J. *Soc. Dyers Colour.* **1999**, 115 (7/8), 218.
5. Lukanoff, B. Dissertation, Akademie der Wissenschaften der DDR, 1967.
6. Bikales, N. M.; Gruber, A. H.; Rapoport, L. *Ind. Eng. Chem.* **1958**, 50, 87.
7. Klenkova, N. J. *Ž. prikl. Chimii (Z. Angew. Chem.)* **1967**, 40 (10), 2191.
8. Lukanoff, B.; Philipp, B.; Schleicher, H. *Cellul. Chem. Technol.* **1979**, 13 (4), 417.
9. Kim, J. N.; Sadovnikova, V. J.; Vostrilova, N. V.; Zaripova, A. M.; Usmanov, Ch. U. *Uzb. Chim. Ž. (Uzb. Chem. Z.)* **1968**, 6, 56.
10. Sadovnikova, V. J.; Kim, J. N. *Chim. Volokna (Chem. Fasern)* **1973**, 3, 72.

11. Gruber, A. H.; Bikales, N. M. *Text. Res. J.* **1956**, 26, 67.
12. Schleicher, H.; Lukanoff, B.; Philipp, B. *Faserforsch. u. Textiltechnik/Z. Polymerforsch.* **1974**, 25, 179.
13. Lukanoff, B.; Schleicher, H.; Philipp, B. *Faserforsch. u. Textiltechnik/Z. Polymerforsch.* **1974**, 25, 339.
14. Dörr, E. *Cellulosechemie* **1932**, 85.
15. Bruson, H. A. *In. Org. Reactions* **1949**, 5, 97.
16. MacGregor, J. H.; Pugh, C. *Proc. 11th Intern. Congr. Pure Appl. Chem.*, 5, 123.
17. Lukanoff, T. *Faserforsch. u. Textiltechnik* **1965**, 16 (11), 540.
18. Friedrich, H. *Melliand Textilberichte* **1961**, 42, 657.
19. Pallaske, M. DE 101 40 224 A1, 2001.
20. Nicholson, M. D.; Merritt, F. M. Cellulose ethers. *Cellul. Chem. Its Appl.*; Horwood: Chichester, 1985; p 363.
21. Kasulke, U.; Dautzenberg, H.; Polter, E.; Philipp, B. *Cellul. Chem. Technol.* **1983**, 17, 423.
22. Plungian, M. *Das Papier* **1962**, 16 (2), L16.
23. Morton, J. L.; Bikales, N. M. *Tappi* **1959**, 42, 855.
24. Poppel, E.; Ciobanu, D. *Zellstoff u. Papier* **1975**, 24 (3), 68.
25. Poppel, E.; Ciobanu, D. *Zellstoff u. Papier* **1975**, 24 (5), 135.
26. Poppel, E.; Ciobanu, D. *Zellstoff u. Papier* **1975**, 24 (11), 323.
27. Sefain, M. Z.; Naoum, M. M.; Fadl, M. H.; El-Wakil, N. A. *Thermochim. Acta* **1994**, 231, 257.
28. Ito, K.; Ono, H.; Mitsubishi *Denki. Lab. Rept.* **1964**, 5, 469.
29. Compton, J. *Text. Res. J.* **1957**, 27, 222.
30. Errico, M. D.; Timney, M. *CA* **1962**, 59, 11736.
31. Goto, K.; Muramoto, M.; Yoshioka, M.; Shiraishi, N. *Mokuzai Gakkaishi* **1991**, 37 (1), 57.
32. Englebretsen, D. R.; Harding, D. R. K. *Int. J. Pept. Res.* **1992**, 40 (6), 487.
33. Kubota, N.; Goto, I.; Nakashima, Y.; Educhi, Y. *Sep. Sci. Technol.* **2003**, 38 (2), 323.
34. Soffev, L. M. USP 3 236 834.
35. Daly, W. H.; Munir, A. *J. Polym. Sci.* **1984**, 22, 975.
36. Sato, T.; Uehara, T.; Adachi-ku, T.; Takenishi, S. EP 0 670 344 A1, 1995.
37. Allen, T. C.; Cuculo, J. A. *J. Polym. Sci., Part D* **1973**, 7, 204.
38. MacGregor, J. H. *J. Soc. Dyers Colour.* **1951**, 67, 66.
39. Sjutkin, V. N.; Bytenskij, V. J.; Slaveckaja, P. A. *Ž. prikl. Chimii (Z. Angew. Chem.)* **1972**, 45 (1), 167.
40. Daul, G. C.; Reinhardt, R. M.; Reid, J. D. *Text. Res. J.* **1955**, 25, 246.
41. Mazzena, L. W., Jr.; Reinhardt, R. M.; Reid, J. D.; Dickson, J. B. *Text. Res. J.* **1956**, 26, 597.
42. Tesoro, G. C.; Sello, S. B. *Text. Res. J.* **1966**, 36, 158.
43. Lukanoff, T.; Philipp, B. *Ž. prikl. Chimii (Z. Angew. Chem.)* **1969**, 42 (1), 170.
44. Lukanoff, T.; Linow, K.-H.; Philipp, B. *Faserforsch. u. Textiltechnik.* **1969**, 20 (8), 383.
45. Senju, R. Japan Kokai 7499177, CA MS 82, 1975; 10, 126 821.

46. Higuchi, M.; Senju, K. *J. Chem. Soc. Japan, Ind. Chem. Sect.* **1971**, 74, 464.
47. Higuchi, M.; Sakata, J.; Senju, R. *J. Chem. Soc. Jpn., Ind. Chem. Sect.* **1970**, 73, 421.
48. Kubota, H.; Shigehisa, Y. *J. Appl. Polym. Sci.* **1995**, 56, 147.
49. O'Donnel, D. W.; Birkinshaw, C.; O'Dwyer, T. F. *Bioresour. Technol.* **2008**, 99, 6709.
50. *Chem. Eng. News* **1962**, 40, 85.
51. Fetscher, C. A. US 3088798, 1963.
52. Yoshinobu, M.; Morita, M.; Sakata, I. *Sen'i Gakkaishi* **1990**, 47 (2), 102.
53. Kamel, S.; Hassan, E. M.; El-Sakhawy, M. *J. Appl. Polym. Sci.* **2006**, 100, 329.
54. Chauhan, G. S.; Singh, B.; Chauhan, S.; Verma, M.; Mahajan, S. *Desalination* **2005**, 181, 217.
55. Chauhan, G. S.; Singh, B.; Kumar, S. *J. Appl. Polym. Sci.* **2005**, 98, 373.
56. Changshen, H.; Xueming, Z. *Desalination* **1985**, 56, 191.
57. Ohya, H.; Jicai, H.; Negishi, Y. *J. Membr. Sci.* **1993**, 85 (1), 1.
58. El-Taraboulsi, M. A.; Mandil, M. A.; Ali, M. H. E.-S. *Carbohydr. Res.* **1970**, 13 (1), 83.
59. Philipp, B.; Lukanoff, B.; Schleicher, H.; Wagenknecht, W. *Zeitschrift für Chemie* **1986**, 26 (2), 50.
60. MacGregor, J. H. GB 588751, 1945.
61. MacGregor, J. H. GB 636020, 1948.
62. Compton, J. *Methods in Carbohydrate Chemistry*. Academic Press: 1963; Vol. 3.
63. US-PS 3 447 939; C 09 D 3/04: 02.09.66, 03.06.69 (Eastman Kodak Company).
64. Wagner, T.; Wagenknecht, W.; Loth, F. *Das Papier* **2002**, 4, T74.
65. Volkert, B.; Wagenknecht, W. *Macromol. Symp.* **2008**, 262, 97.
66. Volkert, B.; Wagenknecht, W.; Fischer, S., Konferenzbeitrag, 229th ACS National Meeting 2005. Abstracts of papers.
67. Doering, H. *Das Papier* **1954**, 8, 383–387.
68. Fengel, D.; Wegener, G.; Heizmann, A.; Przyklenk, M. *Holzforschung* **1977**, 31, 65.
69. Nehls, I.; Wagenknecht, W.; Philipp, B.; Stscherbina, D. *Prog. Polym. Sci.* **1994**, 19, 29–78.
70. Koura, A.; Lukanoff, B.; Philipp, B.; Schleicher, H. *Faserforsch. u. Textiltechnik*. **1977**, 28, 63.

Chapter 19

Opportunities with Wood Dissolved in Ionic Liquids

Haibo Xie^{1,3}, Ilkka Kilpeläinen², Alistair King², Timo Leskinen²,
Paula Järvi² and Dimitris S. Argyropoulos^{*,1,2}

¹Organic Chemistry of Wood Components Laboratory, Department
of Forest Biomaterials, North Carolina State University, Raleigh,
North Carolina 27695-8005

²Laboratory of Organic Chemistry, Department of Chemistry, University
of Helsinki, Finland

³Current Address: National Institute for Cellular Biotechnology Research
Centre, School of Chemical Science, Dublin City University, Ireland

*Tel (919) 515-7708; e-mail: dsargyro@ncsu.edu

Biomass represents an abundant carbon-neutral renewable resource for the production of bioenergy and biomaterials. Shifting society's dependence away from petroleum to renewable biomass resources is generally regarded as an important contributor to building up a sustainable society and effective management of greenhouse gas emissions. An ionic liquids-based processing platform for the efficient transformation of lignocellulosic materials into new materials and value-added chemicals has been developed. We have demonstrated that woody lignocellulosic materials are soluble in certain ionic liquids. The first preparation of homogenous wood solutions not only extends the utilization of lignocellulosic materials from heterogenous to homogenous processing conditions, but also creates a variety of new strategies for converting our abundant lignocellulosic biomass to novel value-added bioproducts. This chapter describes some applications under development, aimed at converting woody lignocellulose into new materials, chemicals and energy using ionic liquids as a processing platform.

1. Introduction

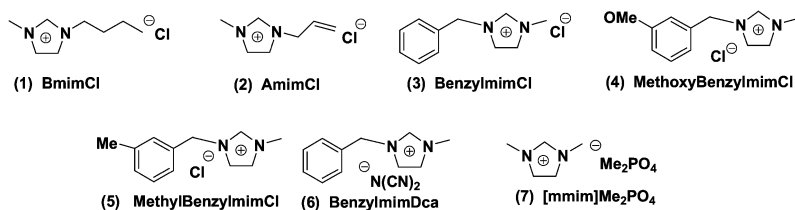
Over the past several decades the contributions of the modern fossil-based energy and chemical industries, while they have enriched our way of life, have placed our environment under immense stress. One of those most noticeable issues is global warming, caused by our over dependence on non-renewable fossil-based resources. From a sustainability point of view, the renewable carbon inherent in biomass is vast, making biomass an attractive alternative as a new carbon source. Shifting society's dependence away from fossil-based energy resources to renewable alternatives, such as biomass, can be regarded as an important contribution towards the establishment of favorable conditions for environmentally sustainable economic solutions (1–3).

It is estimated that by 2025, up to 30% of raw materials for the chemical industry will be produced from renewable sources. To achieve this goal, partially or completely, will require a major re-adjustment of the overall techno-economic approach. This will require entirely new concepts and approaches to be developed if these novel process technologies are to emerge. B. Kamm has provided an overview of these new technologies. As the author points out, the production of value added chemicals from lignocellulosic materials based on environmentally friendlier effective biorefinery platforms will be a step in the right direction (4).

Desirable biorefinery operations will first extract high-value chemicals already present in biomass, and then the biorefinery will focus on processing plant polysaccharides and lignin into feedstocks for bio-derived materials and value-added chemicals (5). This requires the development of innovative process technologies, separation and depolymerization processes, as well as catalytic systems. Supercritical CO₂, near critical water, gas-expanded liquids and ionic liquids (ILs) are well suited to meet these challenges (6–8). These tunable solvents offer distinct green chemistry processing advantages that could be exploited toward the processing of renewable bioresources (9). Among these new technologies, IL-based platforms involve relatively new technology concepts. Research into this field is currently rather extensive as ILs show extremely low vapor pressures, effectively eliminating a major pathway for environmental releases and contamination. Furthermore, some ILs have been shown to possess a strong hydrogen bond-destroying ability, thus imparting good solubility to biopolymers, such as cellulose (10), silk fibroin (11), wool keratin (12), chitin and chitosan (13), etc. Thorough chemical modification of biopolymers can thus be carried out, and after reconstitution, biodegradable composites and advanced materials have been reported (14, 23, 30).

The ultimate goal in our laboratories is to develop new strategies for the transformation of the a variety of lignocellulosic resources into value-added materials and chemicals based on environmentally sustainable and economically viable processing platforms, with ILs' playing a central role in these considerations. A thorough understanding of the way complete wood dissolution occurring in ILs provides a variety of options for the development of novel homogenous processing platforms aiming at the efficient utilization of lignocellulosic resources.

Scheme 1. Structures and Abbreviations of the Examined Ionic Liquids



2. Dissolution of Wood in Ionic liquids

Wood is among the most abundant lignocellulosic resources on the planet. The main components of wood are cellulose (~30% to 50%), lignin (~15% to 30%), hemicellulose (~25% to 30%), and extractives. In general, it is thought that it is practically impossible to dissolve wood in its native form, because the three-dimensional cross-linked lignin network binds the whole wood architecture together. The insolubility of wood in common solvents has severely hampered the development of new processes for its efficient utilization. Therefore, the development of new homogenous processing technologies aiming at wood utilization offer tremendous potential (15–18, 22, 24, 56).

2.1. Solubility-Structure Relationships of Ionic Liquids & Lignocellulosic Materials

In 2007 (18), we reported the details of the dissolution of wood-based lignocellulosic materials and defined the various variables that determine its solubilization efficiency in ILs. A series of imidazolium-based ILs were used in this study, to investigate the relationship between wood solubility and ILs structure (Scheme 1).

Complete wood dissolution [up to 8% (w/w)] can be carried out by simple mixing of dried wood sawdust samples with the ILs (AmimCl or BmimCl) and stirring the mixtures mechanically at 80–120 °C. We found that the solubility of wood-based lignocellulosic material is related to several key factors, such as ILs' structure, size of lignocellulosic materials, water content of both the ILs and lignocellulosic materials, etc. In ILs, both the cation and anion of the salt play a crucial role in the dissolution of wood. During our work we found that AmimCl, and BmimCl showed good ability to dissolve wood. Although the appearance of BmimCl and AmimCl wood solutions were not fully clear, the introduction of a phenyl group into ionic liquids ([Benzylmim]Cl) can result in a completely transparent, amber colored but viscous solution. We conjectured that although ILs have a more complex solvent behavior compared with traditional solvents, such as dispersion, π - π , n- π , hydrogen bonding, dipolar and ionic/charge-charge, In our case, conceivably the active chloride ions in the BmimCl would disrupt the hydrogen bonding interactions present in wood, allowing it to diffuse into the

interior of the wood resulting in a viscous but cloudy solution. However, both BmimCl and AmimCl still can not effectively and fully interact and solvate the aromatic character of lignin imparting a cloudy characteristic to such solutions. Based on the Abraham salvation equation, a cationic moiety with an electro-rich aromatic π -system may create stronger interactions for polymers capable of undergoing π - π and n - π interactions (19), which resulted in a more desirable wood solution in ILs.

The solubility of wood in ILs varies with the particle size of the used lignocellulosic materials. During our work we discovered that the solubilization efficiency of the lignocellulosic materials in ILs was found to be of the order: ball milled wood powder > sawdust \geq TMP fibers \gg Wood chips. The dissolution of fine sawdust (Norway spruce, particle size 0.1–2 mm) in ILs takes place within a few hours, even under ambient conditions. Furthermore, thermomechanical pulp (TMP) samples readily dissolved in BmimCl and/or AmimCl. The water content of a wood sample plays a key role in determining its solubility in ILs. Besides the aforementioned factors, we have determined that the applied temperature and water content play a key role in determining their solubility, usually, the desirable temperature is around 100 °C, but it varies with the lignocellulosic materials, as well as ILs' species. Water was found to significantly reduce the solubility of wood in ILs.

2.2. Rheological Properties of Cellulose and Wood/Ionic Liquids Solutions

In an effort to follow on a more quantitative basis, the process of wood dissolution in ILs, the rheological behavior of cellulose/ionic liquid systems and wood/ILs systems was evaluated. This approach has provided important fundamental information for the development of large-scale bio-materials and biorefinery processes (20, 21). Microcrystalline cellulose (MCC, Molecular weight \sim 60,000 g/mol), was used as a model compound, and it was dissolved in two different ILs (AmimCl) and ([mmim]Me₂PO₄) and the solution's viscosities were measured at different temperatures and concentrations. The effect of concentration on the viscosity is shown for both systems, MCC-AmimCl and MCC-[mmim]Me₂PO₄ in Figure 1. The viscosity behavior of MCC-ILs solutions as a function of shear rate is dependent on the concentration of the solution and temperature. At low concentrations, i.e. 0.5-2.63 m% of MCC in ILs, the solutions behave as Newtonian liquids and the viscosity is not dependent on the shear rate in the temperature range 40-80 °C. However, at 20 °C they are shear thinning. At high concentrations and over the whole temperature range, these solutions are non-Newtonian and shear thinning. The concentration of MCC dissolved in ILs affects the solution properties significantly. When the concentration of MCC is fairly low, 0.5-2.33 m% and 0.5-2.63 m% for MCC-AmimCl and MCC-[mmim]Me₂PO₄, respectively, one may infer that there are no interactions between the polymer coils. However, when the concentration is increased above the critical concentration (M_c), 2.33 m% and 2.63 m% for MCC-AmimCl and MCC-[mmim]Me₂PO₄, respectively, the coils start to interact and form transient entanglements, which manifest to the samples a more viscoelastic behavior.

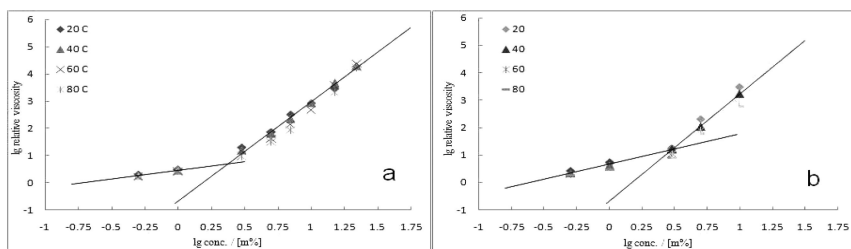


Figure 1. The relative viscosity of (a) MCC-AmimCl- and (b) MCC-[mmim]Me₂PO₄-solutions as function of concentration.

The viscosity of the wood ILs mixtures progressively altered as a function of time is also obtained in the two ILs (Figure 2). As anticipated, the dissolving process of spruce TMP in BmimCl and BenzylmimCl is accompanied by a progressive reduction in the overall viscosity of the mixture. The shapes of these curves can be rationalized on the basis of the resistance to flow of the undissolved wood and the lack of resistance to flow in the case of the dissolved wood. At longer contact times with the solvent the size of the wood fibers become progressively smaller resulting in the decrease viscosity observed. Once complete dissolution has been obtained, the viscosity of the solution remains constant. Furthermore, these measurements allowed for a more detailed description of the actual dissolution kinetics to emerge.

3. Opportunities with Wood Dissolved in Ionic Liquids

3.1. Glucose Production from Pretreated Lignocellulosic Materials with Ionic Liquids

Currently, the production of bioethanol mainly utilizes sugar cane, starch, etc., however, most of them are important food and animal feedstocks, the lignocellulosic materials may be a more ideal source for production biofuels. No commercial wood-based process are available to date possible due to the technological problem and/or economic goals (2). During our work (18, 22), after dissolution of the lignocellulosic material into ILs, it is possible to recover the sample by simply adding a nonsolvent, such as water, into the solution. The X-ray spectra of the regenerated material showed that the X-ray diffraction signals from the crystalline regions of spruce sawdust have disappeared after the dissolution–regeneration process and a fully amorphous material is obtained. Such a transformation is anticipated to allow a greater accessibility for the hydrolytic enzymes to rapidly penetrate and hydrolyze the wood. The pretreated lignocellulosic material in the ILs was then submitted to an enzymatic hydrolysis (18).

Our initial, and completely unoptimized experiments, showed that about 60% of the theoretical amount of glucose was enzymatically released from the wood when predissolved in AmimCl and regenerated by precipitation in water. This

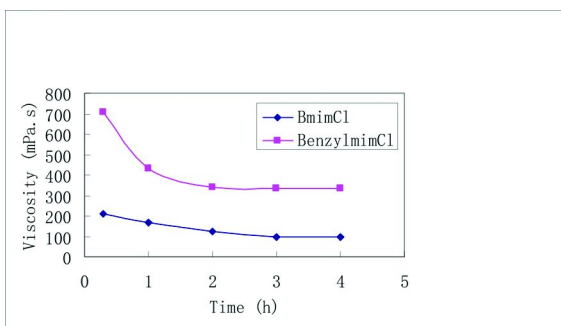


Figure 2. The relationship between the 2% wt spruce TMP in BmimCl, BenzylmimCl and dissolving time at 130 °C

compared to only 12% of glucose units being released from the untreated control wood sample. Similar pretreatments in BmimCl were also found to improve the release of glucose unit but to a significantly lower degree compared to AmimCl. The effective recyclability of ILs within this process provides a promising route for the production of bioethanol directly from lignocellulosic materials, but a number of energy and chemically efficient recycle technologies are still in need of development (18).

3.2. Chemical Modification of Wood in Ionic Liquids

Our research interests in this respect have been focused at how to use wood as a polymeric material by creating completely miscible composites with synthetic commodity plastics. Biodegradable plastics and bio-based composites produced from biorenewable biomass feedstocks are regarded as promising materials that could replace synthetic polymers and reduce global dependence on fossil sources (1). In 2007 (23, 24), Xie et al. reported the effective homogenous chemical modification of wood-based lignocellulosic materials in ILs.

During our efforts to improve the compatibility of lignocellulosic materials with nonpolar thermoplastics, a variety of active chemical reagents were applied to modified lignocellulosic materials in ILs as described in Scheme 2, such as carboxylic acid anhydrides, acid chlorides, and isocyanates, due to their high reactivity toward the hydroxyl groups of lignocellulosic materials. Initially, we investigated the acetylation and benzylation reactions of wood dissolved in ILs using acetyl chloride (AcCl), acetic anhydride (Ac₂O), and benzoyl chloride as acylation reagents. Surprisingly, although acetic anhydride is a desirable acylation reagent for chemical modification of cellulose in ILs, in the absence of pyridine (25), a low Weight Percent Gain (WPG= -30) was obtained for the modification of wood under similar conditions. A significant degradation occurred, possible due to the presence of lignin in the wood compared to pure cellulose. The addition of equivalent amounts of pyridine as an acid acceptor was found to increase the WPG values (WPG=50) significantly under identical conditions, which is close to the theoretically calculated value of 66% (based on 13.3 mmol/g of hydroxyl

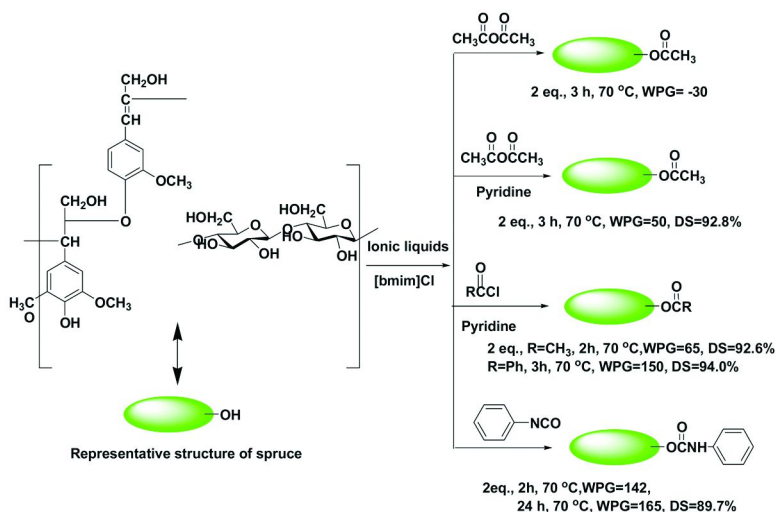
groups present in wood as determined by quantitative ^{31}P NMR) (26, 27, 40–43). As anticipated, acid chlorides, such as acetyl chloride and benzoyl chloride, were found to be more reactive acylation reagents than acetic anhydride, which is evidenced by the higher WPG values of 65%, 150% respectively under similar conditions. An examination of the effect of reaction temperature, time and the required excess of derivatizing reagent was also carried out. On the basis of WPG values obtained, we concluded that increasing the reaction time and temperature did not lead to higher WPG, possible due to partial degradation caused by the presence of the acidic pyridinium acetate formed, while increasing the molar ratio of reagent/substrate beyond 2 did not show any additional significant increase in WPG value. In addition, phenyl isocyanate was commonly used as a “neutral” reagent, for the purpose of wood modification, and a middle WPG value of 142 % was obtained (Theoretical value=187%) under similar reaction conditions. Even after prolonged reaction times (24h), the WPG value only increased to 165%, which is somewhat further from its theoretical value, which demonstrates that the uncatalyzed phenyl isocyanate reaction on lignocellulosic materials is less efficient, as compared to its acylation.

The efficient modification of the lignocellulosic materials in ILs was also evident via the use of infrared spectroscopy, NMR, and quantitative ^{31}P NMR (26, 27, 40–43). For example, a significant decrease in the broad region responsible for the OH stretching vibrations, centered at 3416 cm^{-1} , was apparent in all derivatives, while this decrease was accompanied by a significant increase in the absorption at around $1726\text{--}1752\text{ cm}^{-1}$ characteristic of the carbonyl stretching bands for all derivatives; The appearance of a large acetate $-\text{CH}_3$ signal is apparent in the ^1H NMR spectra of acetylated lignocellulosic material. Similarly, the appearance of strong phenyl proton resonances compared to the anhydroglucose units in the ^1H NMR of benzoylated and carbonylated spruce demonstrates that highly substituted lignocellulosic materials have been obtained; The use of quantitative ^{31}P NMR has been proven to be a useful tool to qualitatively and quantitatively evaluate the various hydroxyl groups present in lignin (26, 27, 40–43). Despite that fact that the wood derivatives, obtained during this work, were only partially soluble in traditional solvents, they were completely soluble in ILs such as AmimCl and BmimCl. Quantitative ^{31}P NMR spectra of spruce and spruce derivatives were therefore obtained using ILs as co-solvents, on which the degree of substitution values (DS) for all wood derivatives were obtained. The DS value of acetylated spruce, benzoylated spruce and carbonylated spruce prepared under optimized conditions were 92.6%, 94.0% and 89.7%, respectively, which demonstrated that highly substituted lignocellulosic materials were obtained (23, 24).

3.3. Highly Compatible Wood Thermoplastic Composites from Lignocellulosic Material Modified in Ionic Liquids

Besides its building and energy applications, wood has been considered to be a pivotal component for the production of bio-composites, also referred to as “wood-thermoplastic composites” or simply “wood-plastic composites” (28). The effective dissolution and modification of wood in ILs are anticipated to result in

Scheme 2. Homogenous functionalization of spruce in *BmimCl*



a significant change in their material properties, such as interfacial compatibility between wood and synthetic polymers, thermal properties and morphological characteristics (29). The thermal properties of the obtained derivatives are of significance as far the eventual utilization of such materials is concerned. We found that the thermal stability of spruce derivatives varies with the structure of the modifying reagent. For example, acetylated (DS=92.6%) and lauroylated spruce (WPG=229%) showed similar thermal stabilities to the original spruce TMP that starts to decompose at around 190 °C. As anticipated, benzoylated spruce (DS=94.0%) showed a higher thermal stability and decomposition temperature (around 220 °C) due to the presence of an aromatic group within the wood structure. However, the carbonylated spruce (DS=89.7%) was found to start decomposing at near 190 °C, and it is seen to be much steeper than either the acetylated or benzoylated spruce. Additional differential scanning calorimetric (DSC) measurements showed that the efficient, homogeneous derivatization of wood in ionic liquids provided an ideal environment for the production of uniformly substituted new materials that showed distinct thermal transitions occurring below their decomposition temperatures (23, 24).

To better understand the effects of the thorough chemical modification of the wood-based lignocellulosic material in ILs and couple the thermal properties of these derivatives to product performance and other characteristics, the morphology of the derivatives was examined using scanning electron microscopy (SEM). These data showed a highly porous and considerably more uniform and isotropic structure throughout. Such morphological properties, when coupled with the chemical and thermal characteristics of the new materials could offer significant benefits as far as increased compatibility and improved processing ability of wood with synthetic polymers are concerned (23, 24). In 2008, Xie, Argyropoulos et al. reported the preparation of WPCs with poly(styrene) and poly(propylene) using completely benzoylated and lauroylated spruce wood.

This work was done on a MiniLab, counter-rotating twin-screw extruder, with the aim to examine the validity of our earlier observations related to the thermal and morphological properties of the prepared wood derivative materials (30).

The analysis of the torque curves, as obtained for the melted wood derivatives with a synthetic polymer, is an excellent method for monitoring the interfacial adhesion and compatibility of the two components. This information was found to be rather useful in probing the effects of the chemical modification of the wood on its melt flow and melt mixing characteristics, with the synthetic polymers examined (30).

A comparison of the final stabilized torque values for the chemically modified and unmodified pairs was also indicative of melt stability and compatibility between the polymers. The stabilized torque value for the benzoylated wood-poly(styrene) pair was about 80 Ncm as opposed to a value of about 60 Ncm, obtained for the TMP/poly(styrene) pair. We conjectured that polymer melts between two miscible polymers are anticipated to give rise to higher torque values, in the mini extruder, as opposed to polymer melts that contain particles or fibers that create voids within the melt structure (30).

Further examination of fractured surfaces of the composites by SEM gave a direct indication about how modification affects the morphology of the composites and interaction between the synthetic polymeric matrix and wood derivatives. A series of comparative SEM pictures for the cross sections of fractured surfaces of benzoylated wood with poly(styrene) composites, and lauroylated spruce with poly(propylene) are obtained (30). We found that pure poly(styrene) and poly(propylene) show a homogeneous fractured surface. With the addition of 10% of unmodified spruce TMP, both of these polymers showed signs of extreme inhomogeneity with large amounts of fiber pullout being apparent. As anticipated, both findings indicate that there is poor adhesion between the two phases, which is possible due to the poor dispersion of the hydrophilic spruce TMP in nonpolar synthetic polymers. We also conjectured that the absorbed water by spruce TMP was evaporated during the blending process leaving cavities within the composites. However, with the addition of modified wood derivatives, and despite some apparent residual fiber-like regions observable within the composite fractions, the interfacial miscibility was obviously increased as evidenced by the excellent and even dispersion of the fibrous structures throughout the fractured surfaces. It is likely that the reduced hydrophilicity and increased Van der Waals interactions between the aromatic or alkyl functionalities both within the wood derivatives and the poly(styrene) and poly(propylene) are responsible for the observed compatibility. The thermal behavior of the as prepared thermoplastic composites were also investigated by DSC, TGA and DTA confirming the miscible blend behavior. The resultant thermoplastic wood composites exhibited good melting characteristics and they were readily extruded into filaments or sheets (30).

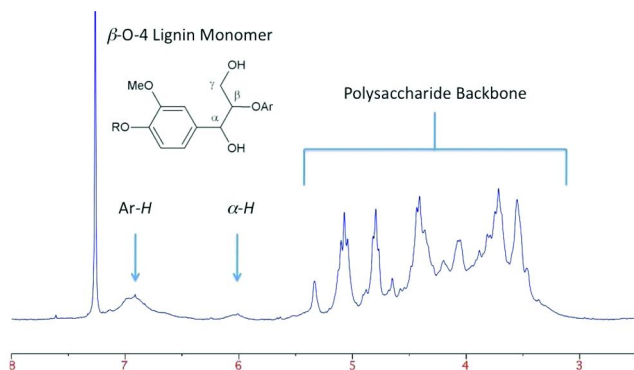


Figure 3. ^1H NMR spectra (CDCl_3) of pulverized Norway spruce wood

3.4. *In-Situ* NMR Analysis of Wood and Its Components based upon Ionic Liquid Pre-Dissolution

In 2003, Lu and Ralph reported the complete dissolution of pulverized wood into a N,N,N,N -tetrabutylammonium fluoride/ d_6 -dimethylsulfoxide (TBAF/ d_6 -DMSO) mixture, followed by a combination of mild chemical modification and ^1H & ^{13}C NMR analysis techniques (31). This has paved the way for the analysis of wood components, such as lignin, without its prior isolation from the wood fiber. More recent accounts have since been published (32, 33), in the form of conference abstracts demonstrating the dissolution and homogeneous solution phase analysis of finely pulverized wood powder in DMSO- d_6 .

The discovery by Swatloski and Rogers et al. (10) that cellulose may be efficiently dissolved into non-derivatizing ILs such as BmimCl has allowed for the dissolution (potential derivatization) and analysis of this biopolymer in solution. As cellulose is generally regarded as the most dissolution resistant purified fraction of wood, using non-destructive solvents, it was later reported by Kilpeläinen, Argyropoulos et al. (18) that imidazolium chloride ILs, such as AmimCl, were able to dissolve pulverized wood. This has further expanded the potential for the analysis of wood biopolymer functionalities based upon pre-dissolution of lignocellulosic materials into non-derivatizing media such as imidazolium-chlorides. Note: although at present, cellulose dissolving ILs (commonly imidazolium acetates (34), chlorides (10), dialkylphosphates (35) and formates (36)) are regarded as non-derivatizing, a recent report by Ebner and Rosenau(37) suggests that imidazolium cations have the potential to react with reducing end groups in cellulose, catalyzed by basic species, in solution. This has however only been confirmed for the imidazolium acetates and considering the abundance of reducing end groups per anhydroglucose unit (AGU), represents only a small and practically unobservable fraction of the molecules, by standard NMR techniques.

3.4.1. ^1H & ^{13}C NMR Analysis

Our work has shown that it is possible to dissolve a lignocellulosic sample into room temperature ILs such as AmimCl or 1,3-dimethylimidazolium dimethylphosphate ([mmim] Me_2PO_4) and run a homogeneous solution phase ^1H or ^{13}C NMR spectrum, in the absence of additional locking solvent. However, the biopolymer to solvent signals are poor (based upon a typical 5 % concentration of substrate) and a reduction in gain (and hence sensitivity) is required with significant losses in the resolution of the peaks. To date, no NMR analyses have been reported of lignocellulosic materials dissolved in pure perdeuterated ionic liquids.

In 2007, Fort and Rogers et al. (38) demonstrated that by the addition of 15% d_6 -DMSO to BmimCl followed by ^{13}C NMR analysis of heat treated samples, it was possible to progressively extract lignocellulose fractions from wood chips. A resonance at 57.2 ppm was thought to be indicative of the presence of 'OMe' functionalities from the lignin monomer units. The proportion of lignin to polysaccharides extracted was estimated by an integration of the 'OMe' to polysaccharide backbone carbon resonances. These were found to remain approximately constant, increasing with time at 80 °C and reaching to ~60% of the total content in 4 different wood species after 24 hr. Furthermore, these authors demonstrated that by the addition of a co-solvent, it was possible to precipitate (fractionate) relatively lignin-free polysaccharide from these solutions. The composition of this polysaccharide was suggested to be cellulose.

Dissolution of pulverized lignocellulose samples into ILs such as [amim]Cl and [mmim] Me_2PO_4 has also allowed for chemical modification of hydroxyl groups, regeneration of the product and subsequent dissolution into a low viscosity and polarity solvent such as CDCl_3 for high resolution NMR analysis of the complete intact sample. This has been demonstrated in the aforementioned publication by Kilpeläinen and Argyropoulos(18) whereby Norway spruce wood sawdust was dissolved in [amim]Cl and the hydroxyl groups acetylated completely using an $\text{Ac}_2\text{O}/\text{Pyr}$ mixture at 80°C over 18 hrs. The product was regenerated by addition of water. Complete functionalisation of all hydroxyls was determined by the absence of an 'OH' stretch in the IR spectra. This acylation reaction has also been reported to be achievable from [mmim] Me_2PO_4 by Olszewska, Argyropoulos et al. (39). The resulting product in CDCl_3 (Figure 3) shows significant proton resonances in the region around 2 ppm corresponding to 'OMe' and 'OAc' functionalities (not shown in Figure 3). In the region from 3-5.5 ppm, the polysaccharide and lignin-aliphatic backbones are clearly intact. Additionally, clearly resolved from this region is a small resonance at 6 ppm, corresponding to α -H resonances from the β -O-4 coniferyl alcohol monomers in softwood lignin. Downfield from this are the Ar-H resonances at 6.25-7.5 ppm from the lignin. Interestingly this acylation reaction is thought to predominantly occur by initial reaction of the acid chloride with the dialkylphosphate anion from the ILs to give the mixed anhydride. It is this species which acts as electrophile in the acetylation of the lignocellulose hydroxyls. Addition of significant quantities of AcCl to [mmim] Me_2PO_4 furnishes [mmim]Cl, which can be observed to crystallize from the reaction mixture. Although this procedure does not

provide satisfactory resolution of different polysaccharide aliphatics from lignin aliphatics, the technique in the future may allow for reasonable lignin content determinations, by integration of Ar-*H* or α -*H* against internal standards. With the formation of alternative acyl esters of lignocellulose, such as benzoylates, it may be possible to integrate 'OME' functionalities against both internal standard and α -*H*, yielding valuable information about the abundance of these functionalities in the pulverized native or processed lignocellulose sample in question.

3.4.2. Quantitative ^{13}P NMR Analysis

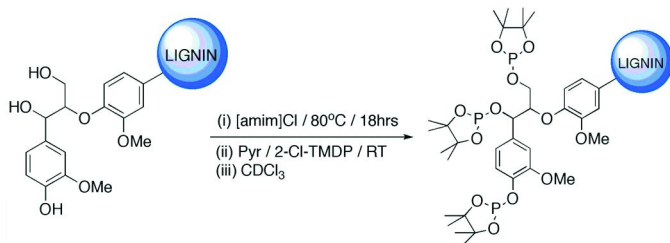
In relation to wood analysis, ^{31}P NMR has traditionally been used for the identification of aliphatic, phenolic (resolved condensed, syringyl, guaiacyl or *p*-hydroxyphenyl) and carbonyl (carboxylic acids) hydroxyls in extracted or enriched lignin preparates, such as milled wood lignin (MWL), cellulolytic enzyme lignin (CEL) and most recently enzymatic mild acidolysis lignin (EMAL) (27, 42, 54).

Typically, the solvent treatment required to pre-dissolve the lignin has been heating overnight in the polar aprotic solvent DMF. Under these conditions, cellulose (MCC) does not dissolve and is neither soluble after the introduction of the reactive species. ILs such as the imidazolium chlorides, such as AmimCl, have now provided a means for the pre-dissolution of MCC, in the pure ILs under mild conditions (80 °C, 2 hrs), followed by complete phosphitylation with 4,4,5,5-tetramethyl-2-chloro-1,3,2 dioxaphospholane (2-Cl-TMDP) and solubilisation in AmimCl/ CDCl_3 mixtures, as demonstrated in publications by King, Argyropoulos et al. (40). EMAL, as a high molecular weight lignin, was also found to be fully reacted and soluble in similar solvent mixtures (Scheme 3).

When this method was applied to Norway spruce sawdust dissolved in high purity, neutral (acid free) AmimCl (41), turbidity was observed both in the 'pre-dissolved' pure ILs mixture and the phosphitylated reaction mixture. This was accompanied by very low values for total observed ^{31}P nuclei, in comparison to an internal standard of known quantity. Actual values were 20% of those expected for MCC (18.52 mmol/g = $1000 \times 3/162$). These observations are an indication of insolubility and somewhat contradictory to the previous reports mentioned earlier concerning wood dissolution and analysis. To resolve this solubility issue, Norway spruce sawdust was pulverized in a planetary mill at 24 hrs intervals to a total milling time of 96 hrs. The ^{31}P labeling and analysis procedure was carried out at each interval and the total observable phosphate esters, in comparison to the internal standard, for each sample plotted as a function of milling time (Figure 4).

The observable phosphate esters for each sample are representative of the total number of available (or reactive) hydroxyls for each sample under these mild dissolution and reaction conditions. This is a measure of the solubility of the wood sample in the ILs, without applying harsh or acidic conditions for dissolution. From Figure 4, it is obvious that significant solubility is only achievable at around 40 hrs milling time. The values seem to maximize at a value of ~ 12.5 mmol/g which is representative of the total number of hydroxyls in Norway spruce wood.

Scheme 3. Typical phosphitylation reaction on a terminal lignin guaiacyl β -O-4 dimer residue.



Analysis of the lignin phenolics from these milled samples shows a similar trend of increasing abundance of phosphate esters with increasing milling time (Figure 4). In this case however, the guaiacyl functionalities, which are the most abundant phenolics in softwood, continue to increase at a faster rate (relative to total quantity in solution), in comparison to the total available hydroxyls values in Figure 4. This is accompanied by a similar rate of increase in carboxylic acids and is indicative of breakage of β -O-4, corroborating previous reports concerning degradation of lignin functionalities with various mechanical treatments (42).

In Figure 5B, the klason content corrected ($100 * \text{mmol/g values} / \text{klason content} = 100\%$ values) guaiacyl hydroxyl abundance values at 50 hrs planetary milling time were found to be the same as those observed for the pure EMAL samples, which had been prepared using 28 days vibratory milling. Extrapolation of the values for the most soluble fractions (72 and 96 hrs) to 0 hrs milling time gives an approximate value (0.65 mmol/g) for the total free guaiacyl phenolic hydroxyls in Norway spruce wood sawdust.

Although no serious assignment about the carbon skeletons of lignin or hemicelluloses can be made, using ³¹P NMR, ILs pre-dissolution and subsequent analysis has afforded a technique that can chart the relative abundance of, most valuably, the common free phenolics that can be observed in lignin from softwoods, hardwoods and grasses, without prior isolation or enrichment of the lignin (43). Continuing development of this technique will afford an excellent tool for analyzing the selectivity of potential bioprocessing methods based upon ILs pre-dissolution, especially in relation to the breakage of common ether bonds found in lignin.

3.5. Pyrolysis of Wood in Ionic Liquids

Fast pyrolysis is regarded as an important approach to produce valuable chemicals from biomass (44, 45). Corresponding problems of this traditional method that involves heterogeneous mass diffusion and transport are low activity and selectivity, cumbersome product separation and the need of high temperatures. Many attempts have been made to improve both the conversion and selectivity of biomass pyrolysis. It is claimed that pre-treatments, solubilization or the presence of additives can lead to increases in the degrees of conversion and the selectivities of the underlying reactions (46).

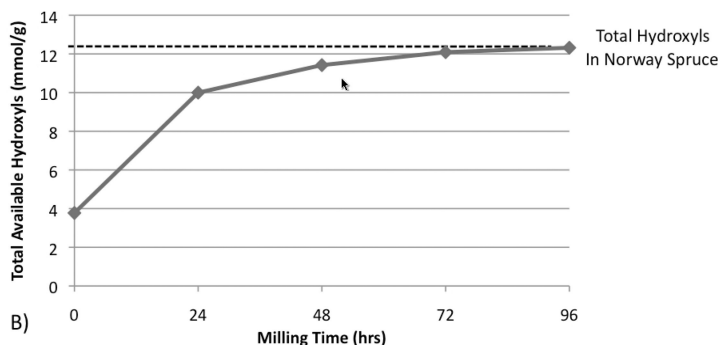


Figure 4. Total available (observable) hydroxyls in Norway spruce at different planetary milling times.

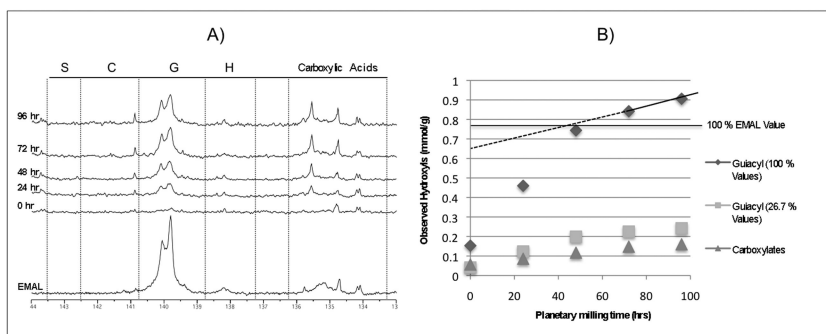


Figure 5. (A) ^{31}P NMR spectra of wood as a function of pulverization. (B) Guaiacyl phenolic hydroxyl and carboxylic acid content in planetary milled Norway spruce for 0 - 96 hrs planetary milling time and EMAL (from 28 days vibratory milling).

ILs are regarded as a good media for high temperature processes due to their negligible vapor pressure and high thermal stabilities (47). Furthermore, the solubilization environment provided by ILs (especially at elevated temperatures) may lead to high conversion and even stereoselectivity on functional group transformation (48). In 2007, Sheldrake et al. (49) reported that dicationic molten salts of ILs can act as good media for the controlled pyrolysis of cellulose to anhydrosugars. In addition, wood liquefaction and hydrolysis by ILs and improved transformation of sugars into valuable chemical intermediates have also been reported (50–52). This further demonstrated that the interaction between ILs and biomass can facilitate the transformation of biomass to valuable chemicals. Levoglucosan (LG) and levoglucosenone (LGO) are two significant molecules that can be produced from the pyrolysis of cellulose. They are highly functionalized compounds due to their carbon-carbon double bonds, the ketone group and the glycosidic linkage. These characteristics make them ideal precursors in organic transformations aimed at compounds of pharmaceutical significance (53). During our study, we used wood, chromated copper arsenate (CCA) treated wood and H_3PO_4 treated wood as our raw materials to investigate

Table 1. Effect of ionic liquids on the pyrolysis/thermolysis of wood samples

Entry	Pyrolysis Methods ^a	Samples	% Tar	% Distillate	% Char	% Total Recovery
1	A	Original wood (Southern pine)	54.5	12.5	27.5	94.5
2	A	CCA-treated wood	52.2	15.2	30.4	94.5
3	A	H ₃ PO ₄ treated	19.1	26.6	49.8	95.5
4	B	Original wood	65.0	22.0	13.0	100.0
5	B	H ₃ PO ₄ treated wood	36.0	24.5	15.0	75.5
6	B	Cellobiose	19.9	36.2	31.0	87.0
7	B	Cellulose	17.6	33.2	19.6	70.3

^a Pyrolysis conditions : A: 350 °C without ionic liquid; B: 180 °C in AmimCl.

the possibility of producing value-added chemical intermediates (LG, LGO) from pyrolysis tar products. Gas chromatography and quantitative ³¹P NMR spectroscopy were the analytical tools that proved to be invaluable for the analysis of these complex degradation mixtures (54–56).

The effective pyrolysis of wood usually requires temperatures in excess of 300 °C. During our work, the fact that the wood was actually dissolved, resulting in a homogeneous solution in ILs, allowed for increased mass and heat transfer during the pyrolysis and facilitated the dehydration reactions of the cellulose and its interaction with the catalytic additives. Consequently, this led to a significant reduction in the required pyrolysis temperatures and an increase in the efficiency of the wood pyrolysis reactions. In actual fact in the presence of ILs, the thermal requirements for the deconstruction of cellulose were so significantly reduced that prompted us in using the term “thermolysis” rather than “pyrolysis” to describe these reactions. As seen in Table 2, the combined yields of tar and distillate were vastly improved when the thermolysis was carried out under the homogeneous conditions provided by the ILs with concomitant reduction in the amounts of the remaining char. For wood alone, these numbers amount to an increase of tar and distillates of about 20% with an accompanying reduction of the char residue. It is also important to note that the homogeneous thermolysis conditions created by the ILs provided for greater amounts of more volatile products as evidenced by the higher percentages of distillate obtained. This can be very important since these distillates can be more readily refined and/or more completely incinerated as fuel or pyrolysis oils. In an effort to better understand the thermolysis of wood in ILs, the presence of H₃PO₄ in treated wood, cellobiose and cellulose was also examined (Table 1, Entries 3 & 5). As anticipated the catalytic effect of acids was apparent in the dehydration chemistry of cellulose and the model carbohydrates examined.

Quantitative ³¹P NMR spectroscopy and gas chromatography (GC-FID) were used as parallel analytical tools for the definition and identification of the chemical

compositions of the pyrolysis fractions. For example, pure LG and LGO resulted in signals of distinct chemical shift values in the ^{31}P NMR spectra centered at 146.6-148.1 and 135.8, respectively.

Typical ^{31}P NMR spectra of tar products obtained during our work are shown in Figure 6. The ^{31}P NMR spectrum (A) of tar product resulting from the heterogeneous pyrolysis of control wood is more complex than those obtained from H_3PO_4 treated wood (B) and the homogeneous thermolysis of original wood (C) in ILs. In addition, there is a large signal due to the presence of LG in spectrum (A) and a dramatically decreased signal for LG is apparent in spectra (B) and (C) accompanied with a new signal of LGO appearing compared to spectrum (A). This is indicative that the dehydration chemistry of cellulose is a lot more facile in the presence of acid catalysts (as anticipated) and in the presence of ILs.

Quantitative analyses of the tar fractions based on ^{31}P NMR and GC-FID confirmed that the yield of levoglucosan (LG) was significantly lower in the ILs thermolysis media (54, 55). In contrast, the yield of LGO was seen to increase when ILs were used as the reaction medium (approximately a 5 fold increase was seen compared to the conventional system; Table 2). For example, the yield of LG in the case of original wood decreased from 3.7% to 0.06%, and the yield of LGO increased from 0.6% to 2.8% when ILs were used (Table 2, Entries 1 & 8). These observations were also confirmed when thermolysis experiments were carried out with microcrystalline cellulose (Table 2, Entries 5 & 6) consisted with published results (50, 54, 55). The yields of LGO from lignocellulosic materials in ILs were seen to be even higher than those of the pyrolysis of pure microcrystalline cellulose (Table 2, Entries 5, 6, 8 & 9). Overall by considering LGO is a marker compound responding to the efficiency of the dehydration operating on cellulose our data indicates that ionic liquids promote this reaction. The lower yield of LG within the final products obtained using IL media indicates that the conversion of LG to LGO was more complete when the ILs were used.

4. Sustainability of the Ionic Liquids Based Biorefinery Platform

Due to their non-volatility, effectively eliminating a major pathway for environmental release and contamination, ionic liquids have been considered as having a low impact on the environment and human health, thus recognized as one of the green solvents for the future. Compared with other conventional solvents-based processing platforms for biopolymers, such as NMNO (57), LiCl/DMAC (58), ethylene diamine/salts (59), etc., ILs based biopolymer processing platforms display many properties, such as high recyclability and a broad applications range due to their relative high chemical and thermal stability. It is envisaged that a biorefinery concept based on ILs may contribute to sustainability by reducing the amount of waste assuming an effective recycling of raw solvents, with the potential for the entire process becoming carbon neutral. Our work on the recycling ability of ILs has shown a number of desirable traits as well as technical challenges to be overcome for diverse applications such as

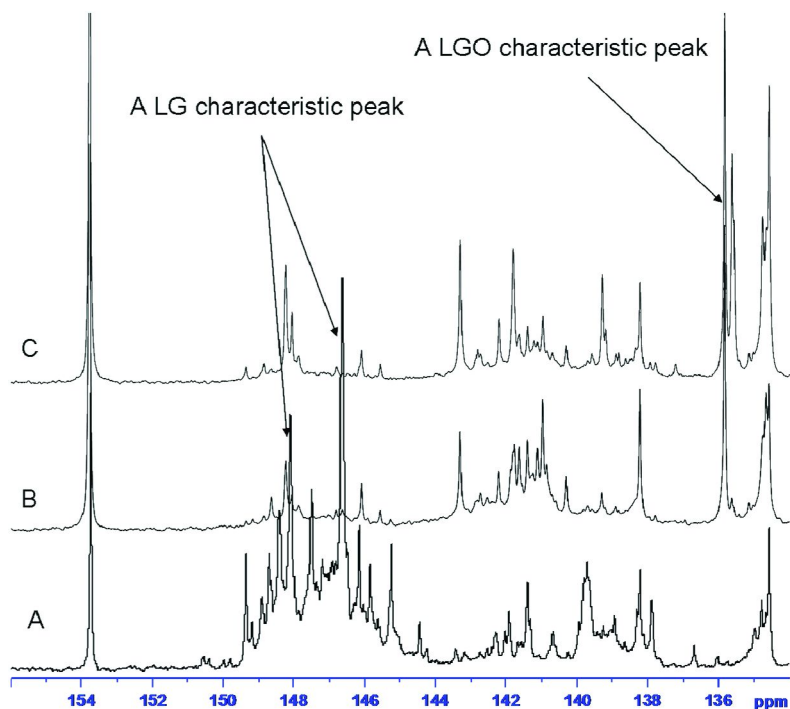


Figure 6. ^{31}P NMR spectra of tar fractions from pyrolysis of (A) Original wood with traditional method (54, 55); (B) H_3PO_4 -treated original wood in an ionic liquids.

Table 2. Analysis of the tar fractions

Entries	Samples	LG (%)	Yield of LGO (%)
1	Original wood	3.7	0.6
2	CCA-treated wood	18.3	0.9
3	H_3PO_4 -treated original wood	19.95	0.6
4	H_3PO_4 -treated CCA wood	20.53	1.3
5	Microcrystalline cellulose	42.5	1.5
6	Microcrystalline cellulose in an ionic liquid	40.5	2.7
7	Cellobiose in an ionic liquid		2.2
8	Original wood in an ionic liquid	0.06	2.8
9	H_3PO_4 -treated original wood in an ionic liquid	0.06	2.9

the wood dissolution process, wood chemical modification and wood thermolysis (18, 22–24, 56).

5. Conclusions & Outlook

The preparation of wood solutions not only extends the utilization of lignocellulosic materials from heterogenous to homogenous conditions but also creates a variety of new strategies for converting our abundant lignocellulosic materials to novel value-added bioproducts. Some potential applications of wood-ILs solution have been explored and include the following:

1. Highly substituted wood-based lignocellulosic derivatives have been obtained with high degrees of reproducibility through homogenous chemical modification in ILs. The resulting wood derivatives show distinct thermal transitions and uniform morphology. Compatible wood composite fibers have been successfully synthesized with polyolefins and polystyrene.
2. After a dissolution-regeneration treatment, wood cellulose can be efficiently digested to glucose.
3. *In-situ* NMR (^1H , ^{13}C & ^{31}P) methods using ILs have been developed for the elucidation of structural information of wood and wood components without the prior isolation of the individual component.
4. The first homogenous thermolysis of wood in ILs has been developed. Under such conditions the cellulose dehydration chemistry was found to be favoured.

Over thousands of years, wood has been used mainly as a raw material for building, fuel, and paper making. These wood processing strategies so far have been limited due to its insoluble characteristics. The dissolution of wood in ILs presents a range of possibilities to utilize wood in an efficient homogenous manner. Significant technological and scientific challenges, however, still remain to be addressed. Amongst others these are: economic syntheses on a large scale; definition of recycling pathways, biodegradation/bioaccumulation studies as well as toxicity and handling considerations.

References

1. Ragauskas, A. J.; Williams, C. K.; Davison, B. H.; Britovsek, G.; Cairney, J.; Eckert, C. A.; Frederick, W. J.; Hallett, J. P.; Leak, D. J.; Liotta, C. L.; Mielenz, J. R.; Murphy, R.; Templer, R.; Tschaplinski, T. *Science* **2006**, *311*, 484.
2. Stocker, M. *Angew. Chem., Int. Ed.* **2008**, *47*, 9200.
3. Bozell, J. J. *Clean: Soil, Air, Water* **2008**, *36*, 641–647.
4. Kamm, B. *Angew. Chem., Int. Ed.* **2007**, *46*, 5056–5058.
5. Morandini, F.; Salamini, F.; Gantet, P. *Curr. Med. Chem.: Immunol. Endocr. Metab. Agents* **2005**, *5*, 103.
6. Nolen, S. A.; Liotta, C. L.; Eckert, C. A.; Glaser, R. *Green Chem.* **2003**, *5*, 663–669.

7. Eckert, C. A.; Liotta, C. L.; Bush, D.; Brown, J. S.; Hallett, J. P. *J. Phys. Chem. B* **2004**, *108*, 18108–18118.
8. Parvulescu, V. I.; Hardacre, C. *Chem. Rev.* **2007**, *107*, 2615–2665.
9. Ritter, S. *Chem. Eng. News* **2004**, *82*, 4–4.
10. Swatloski, R. P.; Spear, S. K.H.; Rogers, R. D. *J. Am. Chem. Soc.* **2002**, *124* (18), 4974–4975.
11. Phillips, D. M.; Drummy, L. F.; Conrady, D. G.; Fox, D. M.; Naik, R. R.; Stone, M. O.; Trulove, P. C.; De Long, H. C.; Mantz, R. A. *J. Am. Chem. Soc.* **2004**, *126*, 14350–14351.
12. Xie, H. B.; Li, S. H.; Zhang, S. B. *Green Chem.* **2005**, *7*, 606–608.
13. Xie, H. B.; Zhang, S. B.; Li, S. H. *Green Chem.* **2006**, *8*, 630–633.
14. El Seoud, O. A.; Koschella, A.; Fidale, L. C.; Dorn, S.; Heinze, T. *Biomacromolecules* **2007**, *8*, 2629–2647.
15. Adler, E. *Wood Sci. Technol.* **1977**, *11*, 169–218.
16. Ämmälähti, E.; Robert, D.; Bardet, M.; Brunow, G.; Kilpeläinen, I. *J. Agric. Food Chem.* **1998**, *46*, 5113–5117.
17. Ralph, J.; Marita, J. M.; Ralph, S. A.; Hatfield, R. D.; Lu, F.; Ede, R. M.; Peng, J.; Quideau, S.; Helm, R. F.; Grabber, J. H.; Kim, H.; Jimenez-Monteon, G.; Zhang, Y.; Jung, H.-J. G.; Landucci, L. L.; MacKay, J. J.; Sederoff, R. R.; Chapple, C.; Boudet, A. M. Solution-state NMR of lignins. In *Advances in Lignocellulosics Characterization*; Argyropoulos, D. S., Ed.; Tappi press: 1999; pp 55–108.
18. Kilpeläinen, I.; Xie, H.; King, A.; Granström, M.; Heikkinen, S.; Argyropoulos, D. S. *J. Agric. Food Chem.* **2007**, *55*, 9142–9148 and reference therein.
19. Anderson, J. L.; Ding, J.; Welton, T.; Armstrong, D. W. *J. Am. Chem. Soc.* **2002**, *124*, 14253–14254.
20. He, C.; Wang, Q. *Polym. Adv. Technol.* **1999**, *10*, 487–492.
21. Järvi, P.; Olszewska, A. M.; King, A. W. T.; Granström, M.; Hietala, S.; Kilpeläinen, I.; Argyropoulos, D. S. Unpublished results.
22. Argyropoulos, D. S. U.S. Patent Application No. 12/026,997, World Patent No. WO2008098032, PCT Int. Appl., Filed Aug. 14, 2008.
23. Xie, H.; King, A.; Kilpeläinen, I.; Granström, M.; Argyropoulos, D. S. *Biomacromolecules* **2007**, *8*, 3740–3748 and reference therein.
24. Argyropoulos, D. S.; Xie, H. U.S. Patent Application No. 12/026,998, World Patent Application No. PCT/US2008/053151, Filed Feb. 6, 2008.
25. Wu, J.; Zhang, J.; Zhang, H.; He, J.; Ren, Q.; Guo, M. *Biomacromolecules* **2004**, *5*, 266–268.
26. Argyropoulos, D. S.; Bolker, H. I.; Heitner, C.; Archipov, Y. *Holzforchung* **1993**, *47*, 50–56.
27. Archipov, Y.; Argyropoulos, D. S.; Bolker, H. I.; Heitner, C. *J. Wood Chem. Technol.* **1991**, *11* (2), 137–157.
28. Rowell, R. M. *Handbook of Wood Chemistry and Wood Composites*; CRC Press: 2005; pp 365–380.
29. Hon, D. N. S.; Chao, W. Y. *J. Appl. Polym. Sci.* **1993**, *50*, 7–11.
30. Xie, H.; Jarvi, P.; Karesoja, M.; King, A.; Kilpeläinen, I.; Argyropoulos, D. S. *J. Appl. Polym. Sci.* **2009**, *111* (5), 2468–2467.

31. Lu, F.; Ralph, J. *Plant J.* **2003**, *35* (4), 535–544.
32. Wang, Z.; Tomoya, Y.; Chang, H. *EWLP Proceedings* **2008**, *04*, 13–15.
33. Rencoret, J.; Marques, G.; Gutiérrez, A.; Nieto, L.; Santos, I.; Jiménez-Barbero, J.; Martínez, Á. T.; del Río, J. I. *European Workshop on Lignocellulosics & Pulp Proceedings EWLP* **2008**, *PII-19*, 340–343.
34. Köhler, S.; Liebert, T.; Schöbitz, M.; Schaller, J.; Meister, F.; Günther, W.; Heinze, T. *Macromol. Rapid Commun.* **2007**, *28*, 2311.
35. Fukaya, Y.; Hayashi, K.; Wada, M.; Ohno, H. *Green Chem.* **2008**, *10*, 44–45, 46.
36. Fukaya, Y.; Sugimoto, A.; Ohno, H. *Biomacromolecules* **2006**, *7*, 3295–3297.
37. Ebner, G.; Schiehsler, S.; Potthast, A.; Rosenau, T. *Tetrahedron Lett.* **2008**, *49*, 7322–7324.
38. Fort, D. A.; Remsing, R. C.; Swatloski, R. P.; Moyna, P.; Moyna, G.; Rogers, R. D. *Green Chem.* **2007**, *9*, 63–69.
39. Olszewska, A. M.; Järvi, P.; King, A. W. T.; Kilpeläinen, I.; Argyropoulos, D. S. *European Workshop on Lignocellulosics & Pulp Proceedings* **2008**, *PI-21*, 222–225.
40. King, A. W. T.; Kilpeläinen, I.; Heikkinen, S.; Järvi, P.; Argyropoulos, D. S. *Biomacromolecules* **2009**, *10*, 458–463.
41. King, A. W. T.; Kilpeläinen, I.; Järvi, P.; Olszewska, A.; Heikkinen, S.; Argyropoulos, D. S. *European Workshop on Lignocellulosics & Pulp Proceedings* **2008**, *09*, 32–35.
42. Guerra, A.; Filpponen, I.; Lucia, L. A.; Saquing, C.; Baumberger, S.; Argyropoulos, D. S. *J. Agric. Food Chem.* **2006**, *54*, 5939–5947.
43. King, A.; W., T.; Zoia, L.; Filpponen, I.; Olszewska, A.; Xie, H.; Kilpeläinen, I.; Argyropoulos, D. S. *J. Agric. Food Chem.* **2009**, *57*, 8236–8243.
44. Mohan, D.; Pittman, C. U.; Steele, P. H. *Energy Fuels* **2006**, *20*, 848–889.
45. Amidon, T. E.; Wood, C. D.; Shupe, A. M.; Wang, Y.; Graves, M.; Liu, S. J. *Journal of Biobased Materials and Bioenergy* **2008**, *2*, 100–120.
46. Dobeles, G.; Rossinskaja, G.; Telysheva, G.; Meier, D.; Faix, O. *J. Anal. Appl. Pyrolysis* **1999**, *49*, 307–317.
47. Ye, C. F.; Liu, W. M.; Chen, Y. X.; Yu, L. G. *Chem. Commun.* **2001**, 2244–2245.
48. Zhao, H. B.; Holladay, J. E.; Brown, H.; Zhang, Z. C. *Science* **2007**, *316*, 1597–1600.
49. Sheldrake, G. N.; Schleck, D. *Green Chem.* **2007**, *9*, 1044–1046.
50. Xie, H. L.; Shi, T. J. *Holzforchung* **2006**, *60*, 509–512.
51. Li, C. Z.; Wang, Q.; Zhao, Z. K. *Green Chem.* **2008**, *10*, 177–182.
52. Li, C. Z.; Zhao, Z. K. B. *Adv. Synth. Catal.* **2007**, *349*, 1847–1850.
53. Witczak, Z. J. In *Levogluconone and Levoglucosans: Chemistry and Applications*; Witczak, Z. J., Ed.; ATL press: Mount Prospect, 1994. Witczak, Z. J. In *Materials, Chemicals and Energy from Forest Biomass*; ACS Symposium Series No. 954; Argyropoulos, D. S., Ed.; The American Chemical Society: Washington, DC, 2006; ISBN: 978-0-8412-3981-4, February 2007.

54. Fu, Q.; Argyropoulos, D. S.; Tilotta, D. C.; Lucia, L. A. *Ind. Eng. Chem. Res.* **2007**, *46*, 5258–5264.
55. Fu, Q.; Argyropoulos, D. S.; Tilotta, D.; Lucian, L. A. Understanding the Pyrolysis of CCA-Treated Wood, Part II, Effect of Phosphoric Acid. *J. Anal. Appl. Pyrolysis* **2008**, *82*, 140–144.
56. Argyropoulos, D. S. U.S. Patent Application No. 12/026,993, World Patent Application No. 12026993, Filed Feb 6, 2008.
57. Augustine, A. V.; Hudson, S. M.; Cuculo, J. A. In *Cellulose Sources and Exploitation*; Kennedy, J. F., Philipps, G. O., Williams, P. A., Eds.; E. Horwood: New York, 1990; p 59.
58. Dupont, A. L. *Polymer* **2003**, *44*, 4117–4126.
59. Frey, M. W.; Li, L.; Xiao, M.; Gould, T. *Cellulose* **2006**, *13*, 147–155.

Chapter 20

Advances in Cellulose Solvent- and Organic Solvent-Based Lignocellulose Fractionation (COSLIF)

Y.-H. Percival Zhang^{1,2,3,*}, Zhiguang Zhu¹, Joe Rollin¹ and Noppadon Sathitsuksanoh^{1,2}

¹Biological Systems Engineering Department, Virginia Polytechnic Institute and State University (Virginia Tech), 210-A Seitz Hall, Blacksburg, Virginia 24061, USA

²Institute for Critical Technology and Applied Science (ICTAS), Virginia Polytechnic Institute and State University, Blacksburg, Virginia 24061, USA

³DOE BioEnergy Science Center (BESC), Oak Ridge, Tennessee 37831, USA

*yhzhang@vtech.va.edu

Cost-effective release of soluble fermentable sugars from lignocellulose, the most abundant form of renewable biomass, is among the most costly steps for emerging biorefineries. Lignocellulosic biomass is a complicated natural composite, primarily consisting of three biopolymers: cellulose, hemicellulose, and lignin. Distinct from high temperature/pressure required for most lignocellulose pretreatments (e.g., dilute acid, ammonia fiber expansion, ammonia recycle percolation, and so on), cellulose solvent- and organic solvent-based lignocellulose fractionation (COSLIF) has been developed to fractionate lignocellulose components (cellulose, hemicellulose, acetic acid, and lignin) at modest reaction conditions (Zhang Y.-H.P., et al. *Biotechnol. Bioeng.* **2007**, *97*, 214–223). Separation of the three polymers can be implemented based on their different solubility in a cellulose solvent (concentrated phosphoric acid), an organic solvent (e.g., acetone or ethanol) and water; recycling of phosphoric acid and the organic solvent can be conducted based on the solvents' different volatilities. Very high glucan digestibilities (e.g., ~96-97% in hour 24) were obtained for several types

of biomass, such as corn stover, switchgrass, hemp hurds and hybrid poplar, at a cellulase loading of 15 filter paper units per gram of glucan. At a low enzyme loading (5 filter paper units per gram of glucan), the digestibility remained as high as 93% at hour 24 for the COSLIF-pretreated corn stover but only reached ~60% for the dilute acid (DA)-pretreated biomass. As compared to the DA-pretreated biomass, higher glucan digestibility and faster enzymatic hydrolysis rates for the COSLIF-pretreated corn stover were in good agreement with (i) more efficient biomass structure destruction and (ii) larger cellulose accessibility to cellulase.

Introduction

Cellulose, the most abundant renewable bioresource (ca. 1×10^{11} tons/year), is mainly produced by terrestrial plants (1–4). Technologies for effectively converting low-cost agricultural and forestry residues (lignocellulosic biomass) to biofuels and biobased products offer many benefits to society, including improved energy security, decreased trade deficits, healthier rural economies, improved environmental quality, nearly zero net greenhouse gas emissions, technology exports, and sustainable utilization of renewable resources (4–9). Effectively overcoming lignocellulose recalcitrance to release soluble sugars is still the largest technical and economic challenge for the emerging biofuels and biobased chemical industries (4, 10, 11).

The conversion of biomass to simple sugars usually involves two sequential steps – lignocellulose pretreatment and enzymatic cellulose hydrolysis (Fig. 1). Two different strategies have been proposed and investigated. The substrate strategy is focused on lignocellulose pretreatment (identification of the best pretreatment methods and optimization of reaction conditions), resulting in increased reactivity of pretreated lignocellulosic feedstock so that commercial available low-cost *Trichoderma* cellulase can work efficiently. The enzyme strategy is focused on improving cellulase performance so that biomass pretreatment could be minimized or avoided. Cellulase development could include (i) construction of artificial cellulosomes that are believed to have much higher specific hydrolysis activity than non-complexed *Trichoderma* cellulase (12–15) or recombinant cellulolytic microorganisms, and (ii) the introduction of recombinant cellulase-expressing bioenergy plants, providing a more reactive structure for enzymatic hydrolysis (16). Biomass recalcitrance can also be reduced by using genetic engineering tools to modify the composition of energy crop plants (17).

Fractionation and co-utilization of all the major components of the lignocellulose feedstock is more and more accepted to be vital for biorefineries because of the tight margins associated with fuel production from cellulose and hemicellulose and feedstock prices (4, 18). Mature industries, such as crude oil refineries and corn-ethanol biorefineries, produce a variety of products from

their multi-component feedstocks. Although corn wet milling-based biorefineries require higher initial capital investment and higher processing costs than dry milling systems, the former is the dominant process for large plants (19, 20) because of higher revenues generated by co-products such as gluten feed, gluten meal, and corn oil (21). These value-added products account for approximately a third to a half of the wet milling total revenue (22), whereas less effective fractionation in the dry milling process results in co-product revenues accounting for only 20% of the total revenue (20).

Given that typical biomass contains 40% glucan, 20% hemicellulose, 20% lignin and 4% acetate (from hemicellulose), biomass-based biorefineries could produce up to 100 gallons of cellulosic ethanol per ton of dry biomass after some process improvements (high sugar liberation yields and high sugar-to-ethanol yields). The delivered biomass costs, including growth, harvesting, collection and delivery, could range from \$60 to \$120 per dry ton. If the selling price of cellulosic ethanol is around \$2.5 per gallon, and no other co-products are produced, the margin between the main product revenue and feedstock costs would be between \$130-190 per ton of biomass. It would be challenging for this narrow margin to cover all the required expenditures, such as cellulase costs (\$0.2-1.0 per gallon of ethanol = \$20-100/ton biomass), distillation (\$0.2-0.4 per gallon of ethanol = \$20-40 per gallon of biomass), pretreatment, waste treatment, labor, tax, and capital depreciation (\$0.4-1.0 per gallon of ethanol = \$40-100 ton of biomass). With the co-utilization of lignocellulose components such as hemicellulose, acetic acid and lignin, a more robust and economically feasible biorefinery is possible. Effective isolation of high-value hemicellulose could provide an especially profitable opportunity. Already, plants producing xylitol as a major product from corn cob hemicellulose have good profits in China. Similarly, isolation of acetic acid prior to ethanol fermentation could further increase revenues (~\$40 per ton of biomass or \$0.40 credit per gallon of ethanol) and would decrease inhibition of ethanol fermentation. Isolation of a large amount of high-quality lignin would generate numerous opportunities for high-end applications, such as carbon fiber polymers (4).

This chapter provides a description and research update for a technology called cellulose solvent- and organic solvent-based lignocellulose fractionation (COSLIF), which can separate lignocellulose components from lignocellulosic biomass.

Cellulose Solvent- and Organic Solvent-Based Lignocellulose Fractionation (COSLIF)

COSLIF Mechanism

A new technology called cellulose solvent- and organic solvent-based lignocellulose fractionation (COSLIF) has been shown to separate lignocellulose components under modest reaction conditions (e.g., 50°C and atmospheric pressure) by using a cellulose solvent, an organic solvent, and water (18). The key

ideas of COSLIF are (1) removal of partial lignin and hemicellulose (eliminating the major obstacles to cellulose hydrolysis and allowing cellulase to access the substrate more efficiently) (4, 23, 24), (2) de-crystallization of cellulose fibers by a cellulose solvent (providing better cellulose accessibility to cellulase) (25, 26), and (3) modest reaction conditions (causing a decrease in sugar degradation, less inhibitor formation, lower utility consumption, and less capital investment) (24, 27, 28).

After searching for a number of cellulose solvents suitable for biomass dissolution and considering their recycling, we find out that concentrated phosphoric acid is a good cellulose solvent for biorefineries. Concentrated phosphoric acid is a modest acid. When its concentration is more than a critical value, it can completely dissolve cellulose under mild conditions (26). Different from a strong acid sulfuric acid, formation of esters between phosphoric acid and cellulose is very weak. When acid concentration is decreased by water dilution, derivation effect becomes negligible.

Figure 2 shows the overall processes of the COSLIF technology, using concentrated phosphoric acid as the cellulose solvent and acetone as the organic solvent, including a solvent recycling scheme. The mechanisms for each unit operation are:

- (1) in the digestion tank, concentrated H_3PO_4 (> 83%) is mixed with grounded lignocellulose at 50°C for ~30-60 minutes depending on biomass type. The cellulose solvent can
 - i) break up all linkages among lignin, hemicellulose, and cellulose;
 - ii) dissolve cellulose fibrils and hemicellulose, which breaks up orderly hydrogen bonds among sugar chains;
 - iii) weakly hydrolyze cellulose and hemicellulose to modestly reduce their degree of polymerization (DP); and
 - iv) provide acidic conditions, which cause removal of acetyl groups from hemicellulose.
- (2) in the precipitation tank, an organic solvent (e.g., acetone or ethanol) is added to precipitate the dissolved cellulose and hemicellulose and to dissolve partial lignin in the organic solvent;
- (3) in washer-1 (solid/liquid separator), organic solvent washes out ~99.5% of phosphoric acid from the precipitated solids and removes more lignin (by leaching);
- (4) in washer-2 (solid/liquid separator), water is used to wash the organic solvent from the solids and to remove water-soluble short-DP hemicellulose fragments from the solid cellulose;
- (5) in the hydrolysis reactors, nearly pure amorphous cellulose is hydrolyzed quickly at 50°C with the *Trichoderma* cellulase;
- (6) in the distiller, the black liquor containing phosphoric acid, acetone, acetone-soluble lignin, and acetic acid can be separated. Highly volatile acetone and modestly volatile acetic acid are separated by fractionation distillation; after removal of the organic solvent, the precipitated lignin can be separated from the concentrated phosphoric acid at the bottom of the column by a solid/liquid separator; and

- (7) in the flash tank, the light liquor containing acetone, a small amount of phosphoric acid and water-soluble hemicellulose can be separated. Acetone can be recovered by flashing. Addition of CaCO_3 can neutralize trace phosphoric acid and form a precipitate of $\text{Ca}_3(\text{PO}_4)_2$; the precipitated $\text{Ca}_3(\text{PO}_4)_2$ can be regenerated to concentrated phosphoric acid by adding concentrated sulfuric acid. Water-soluble hemicellulose remains in the liquid phase.

In all, this technology can fractionate lignocellulose into amorphous cellulose (mainly glucose after hydrolysis), lignin, hemicellulose, and acetic acid at modest reaction conditions (50°C , atmospheric pressure) with simple recycling of the organic solvent and phosphoric acid. This new technology isolates lignocellulose components based on their solubility in different solvents, while using low-cost separation operations, e.g., solid/liquid separation. Cellulose is insoluble in water but soluble in concentrated phosphoric acid. Short-DP hemicellulose fragments are isolated from cellulose because of their high solubility in acetone/water mixtures. A fraction of lignin is soluble in the organic solvent but insoluble in the aqueous phase, so it can be separated from the other lignocellulose components when the organic solvent is removed.

Cellulose Solvent Criteria

A number of cellulose solvents have been used to address biomass recalcitrance, but most of them cannot be applied to the production of low-cost commodities, due to cost issues. Ideal cellulose solvents for biocommodity biorefineries must meet the following criteria:

- (1) able to dissolve cellulose at low temperatures (reduces utility consumption);
- (2) able to dissolve wet cellulose (avoids biomass drying);
- (3) low cost (high recycle ratio or low solvent costs);
- (4) nonvolatile (prevents solvent loss through evaporation);
- (5) thermostable (allowing nearly infinite recycling);
- (6) chemostable (compatible with other reagents);
- (7) nontoxic to enzymatic hydrolysis and microbial fermentation;
- (8) high capacity to dissolve cellulose (> 10 wt. % cellulose/volume);
- (9) fast diffusion rate in solid lignocellulosic biomass (resulting in a shorter reaction time), and
- (10) relatively low viscosity.

The first attempt to overcome lignocellulose recalcitrance by using cellulose solvents was conducted by Professors Mike Ladisch and George Tsao in 1978 (29). After searching for a number of cellulose solvents, they found that Cadoxen, an alkali solution of CdO in aqueous ethylenediamine, could dissolve biomass. The resulting regenerated amorphous cellulose could be hydrolyzed quickly by cellulase (29), but the glucan digestibility was modest. Because Cadoxen is corrosive and toxic, any traces of the solvent in the treated biomass may inhibit subsequent hydrolysis and fermentation steps. With the invention of ionic liquids (IL) that dissolve cellulose (30), several attempts have been made to pretreat biomass by using different IL cellulose solvents (31–33). Enzymatic glucan

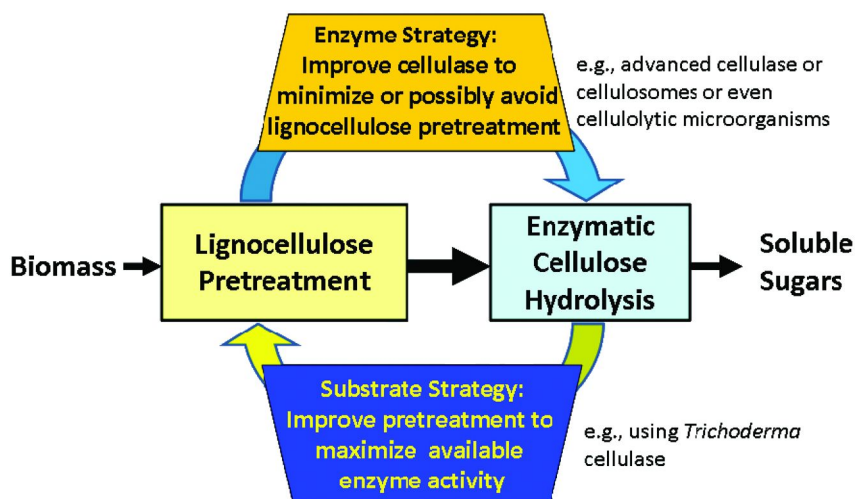


Figure 1. Biomass saccharification paradigms.

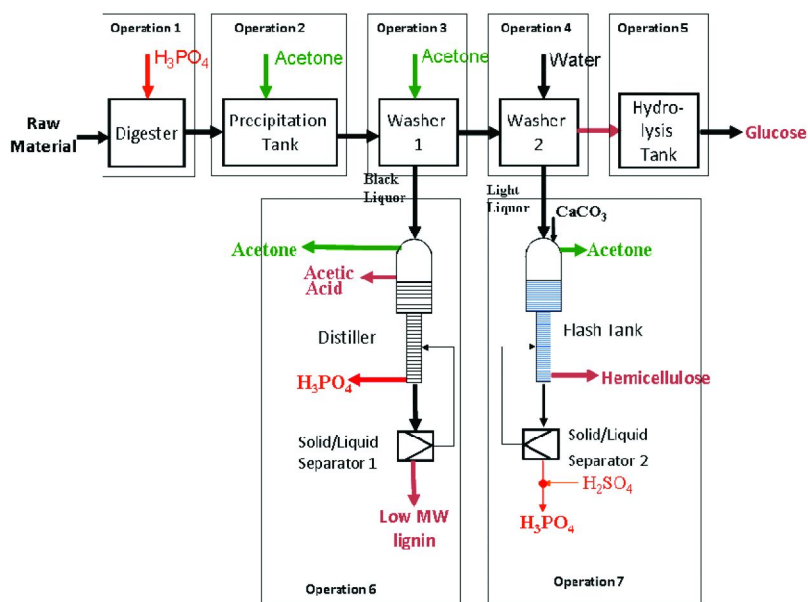


Figure 2. Flowchart of the COSLIF technology with recycling of the cellulose solvent and organic solvent.

digestibility of ionic-liquid pretreated biomass ranges widely (31, 32), suggesting that more research is needed to understand the solvent's mechanisms and develop a cost-effective method to recycle the cellulose solvent. In addition, removing hemicellulose and lignin fractions after biomass dissolution remains a significant challenge.

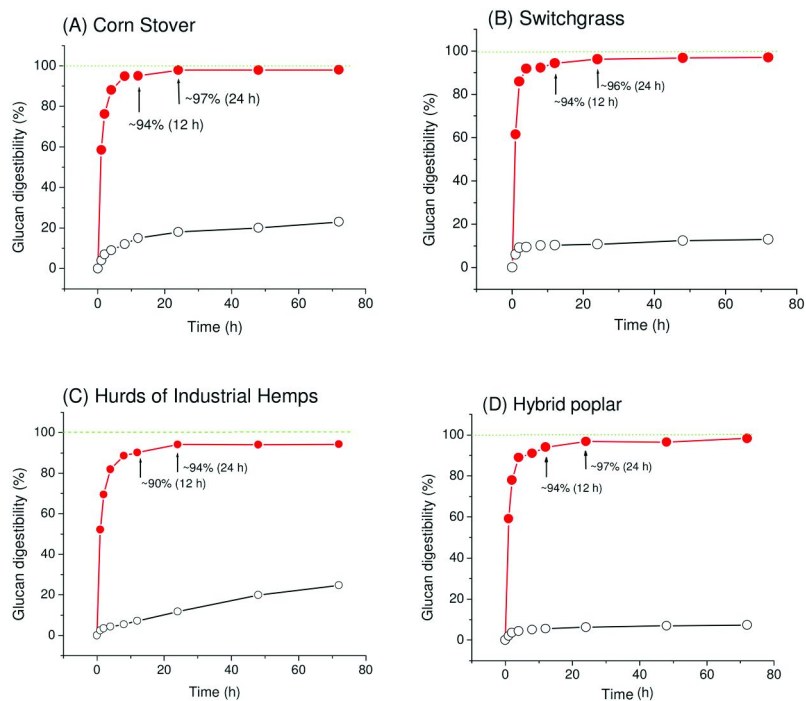


Figure 3. The enzymatic hydrolysis profiles for four examples of COSLIF-pretreated biomass: (A) corn stover, (B) switchgrass, (C) industrial hemp hurds, and (D) hybrid poplar. The hydrolysis conditions were 1% glucan, 15 FPU of cellulase, and 30 units of β -glucosidase per gram of glucan at 50°C.

Important Roles of the Organic Solvent

Addition of the organic solvent has four goals: 1) to precipitate dissolved cellulose and hemicellulose in amorphous forms, resulting in an easy separation of solid saccharides from liquid cellulose solvent; 2) to dissolve partial lignin in the organic solvent and, after separation of this organic solvent mixture from the biomass, recover solid lignin (due to the insolubility of organic phase-dissolved lignin in acidic aqueous solutions); 3) to recycle concentrated phosphoric acid by avoiding dilution and conducting easy acid re-concentration; and 4) to fractionate oligo-hemicellulose sugars from cellulose due to the solubility of the former, and insolubility of the latter, in the organic solvent/water mixture (34).

Enzymatic Hydrolysis, Supramolecular Structures, and Substrate Accessibility

Enzymatic Hydrolysis

Following COSLIF fractionation, nearly pure amorphous cellulose has been obtained for both herbaceous and hardwood lignocellulose, including corn stover, switchgrass, industrial hemp hurds, and hybrid poplar. However, only phosphoric acid beyond the critical concentration (~83%) can efficiently destroy biomass structure; the reaction time ranges from 45 to 60 min, depending on biomass type. Four different well-pretreated biomass types have similar hydrolysis performance at an enzyme loading of 15 filter paper units of cellulase and 30 units of β -glucosidase per gram of glucan. The glucan digestibilities were ~90% at hour 12 and ~94-97% at hour 24 (Fig. 3A-D). These very high sugar digestibilities after enzymatic hydrolysis are attributed to negligible sugar degradation during fractionation and very high enzymatic cellulose digestibility (~97% in 24 hours) during the hydrolysis step. To put this effectiveness in perspective, COSLIF pretreatment can produce more than a 20% increase in sugar yields compared to steam explosion.

Dilute acid (DA) pretreatment has been widely studied (35, 36, 38). This process is usually conducted at high temperatures and high pressures catalyzed by a dilute acid (often sulfuric acid). Dilute acid at high temperatures removes acid-labile hemicellulose. This results in a disruption of the linkages among cellulose, hemicellulose, and lignin (38-42). COSLIF can remove more lignin but retain more hemicellulose than DA (43). The higher sugar retention by COSLIF is attractive because this allows a higher release of fermentable sugars during the enzymatic hydrolysis step. Figure 4 presents the different hydrolysis profiles for the same corn stover pretreated by COSLIF and dilute acid. The glucan digestibility of the COSLIF-pretreated corn stover reached more than 90% at hour 12 and 97% at hour 24. In contrast, the DA-pretreated corn stover had much slower hydrolysis rates, and its final digestibility was 84% at hour 72 (Fig. 4A). At a low enzyme loading (5 filter paper units per gram of glucan), the digestibility remained as high as 93% at hour 24 for the COSLIF-pretreated corn stover but only reached ~60% for the dilute acid (DA)-pretreated biomass (Fig. 4B).

Figure 5 presents the mass balance of switchgrass pretreated by the COSLIF technology and enzymatic cellulose hydrolysis at a low enzyme loading (5 FPU of cellulase and 10 units of β -glucosidase per gram of glucan). Studies of mass balances of pretreatment and enzymatic hydrolysis are highly recommended for evaluating lignocellulose pretreatments (11). The overall glucose and xylose yields of the COSLIF-pretreated switchgrass were 85% and 63%, respectively. With technological improvements (e.g., a supplementary hemicellulase in the enzymatic hydrolysis step, optimization of reaction conditions, pre-extraction of water soluble sugars before pretreatment, and adjustment of washing conditions such as solvent temperatures and flow rates), higher xylose recovery yields are anticipated without sacrificing glucose yields.

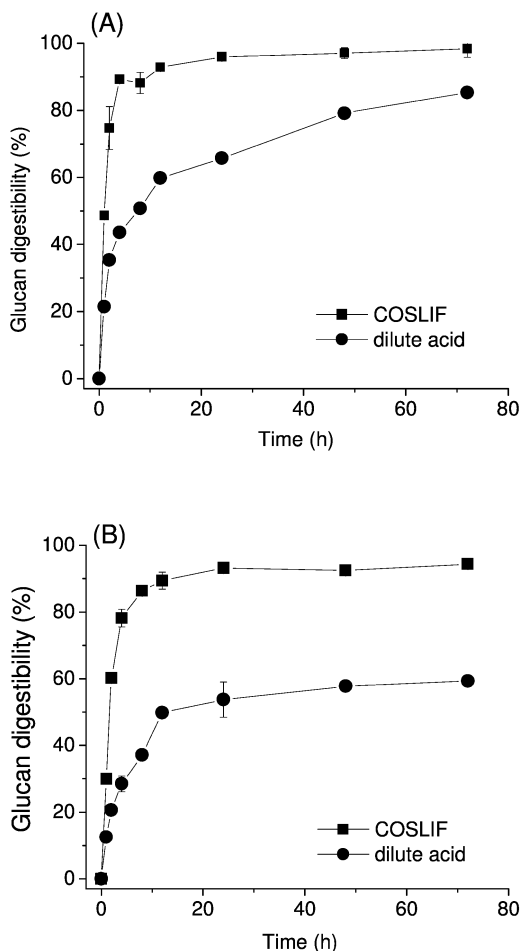


Figure 4. Comparative hydrolysis of corn stover pretreated by COSLIF and dilute acid pretreatments at different enzyme loadings. (A) 15 FPU of cellulase and 30 units of β -glucosidase per gram of glucan, and (B) 5 FPU of cellulase and 10 units of β -glucosidase per gram of glucan.

Supramolecular Structures

The supramolecular structural changes for industrial hemp hurds before and after various pretreatments can be observed by using a scanning electron microscope (SEM) (Fig. 6). The plant cell vascular bundles and fibril structure of intact biomass are easily identified under SEM (Fig. 4A, B). Modest pretreatment conditions (e.g., 84.0% H_3PO_4 , 50°C and 30 minutes) open larger holes on the surface of plant cell walls by removing the most easily-digested fraction (possibly, hemicellulose and some lignin), but the supramolecular fibril structure is only partly destroyed (C, D). A well-treated lignocellulose sample (84.0% H_3PO_4 ,

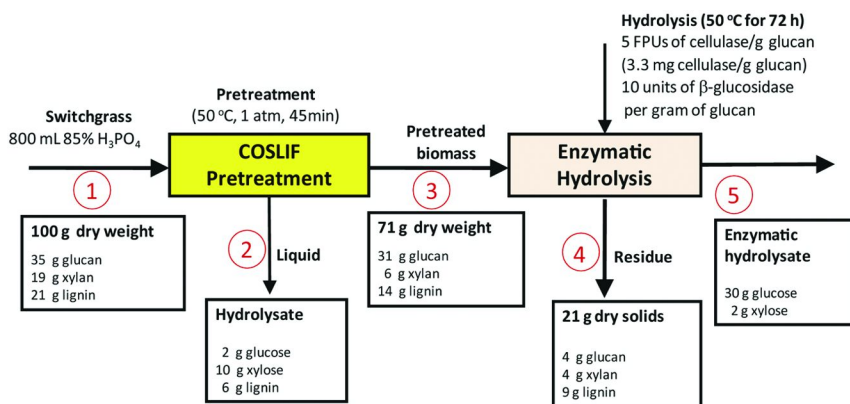


Figure 5. Mass balance of switchgrass pretreated by COSLIF and hydrolyzed enzymatically at an enzyme loading of 5 FPU of cellulase and 10 units of β-glucosidase per gram of glucan.

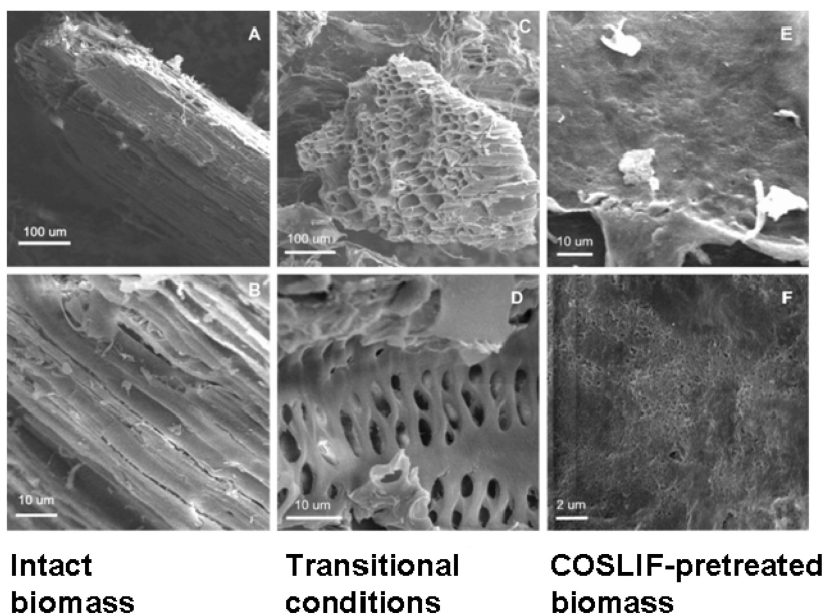


Figure 6. SEM images for COSLIF-pretreated biomass (A, intact, B, modestly-pretreated, and C, well-pretreated)

50°C and 60 minutes) shows all fibrous structures of the lignocellulose completely disrupted (E, F). These images show much more complete structure degradation than similar images taken after treatments such as hot water or ammonia recycle percolation (44, 45).

Substrate Accessibility

Cellulose accessibility to cellulase (CAC, m²/g cellulose) is calculated based on the maximum cellulase adsorption capacity, as described previously (3, 25, 46).

$$CAC = \alpha * A_{\max} * N_A * A_{G2} \quad (1)$$

where $\alpha = 21.2$, for the number of cellobiose lattices occupied by a non-hydrolytic protein called TGC (this acronym describes the protein's three components: thioredoxin, a green fluorescent protein and a cellulose-binding model) (46), A_{\max} = the maximum cellulase adsorption capacity (mole cellulase/g cellulose), N_A = Avogadro's constant (6.023×10^{23} molecules/mol), and A_{G2} = the area of the 110 face of the cellobiose lattice ($0.53 \times 1.04 \text{ nm} = 5.512 \times 10^{-19} \text{ m}^2$) (3).

The total (biomass) substrate accessibility to cellulase (TSAC), including CAC and non-cellulose accessibility to cellulase (NCAC), represents the cellulase adsorption capacity for the entire pretreated biomass sample. For pure cellulosic samples, TSAC equals CAC, since NCAC equals zero. Here a scheme is described for quantitatively determining CAC and NCAC for pretreated lignocellulosic substrates (Fig. 7), based on the facts that (i) BSA can irreversibly bind with the lignin fraction of lignocellulosic biomass (47, 48) and (ii) BSA cannot bind with cellulose. First, TSAC (m²/g biomass) can be estimated from direct adsorption of the TGC protein,

$$TSAC = \alpha * A_{\max, \text{TGC}} * N_A * A_{G2} \quad (2)$$

where $A_{\max, \text{TGC}}$ = the maximum TGC adsorption capacity of the biomass ($\mu\text{mole TGC/g biomass}$).

Secondly, CAC (m²/g biomass) can be measured based on the maximum TGC adsorption capacity after competing adsorption sites are blocked by introducing a large amount of BSA (e.g., 5 g/L) that can non-specifically bind on the surface of the lignin (47). This maximum TGC adsorption capacity of the BSA-blocked biomass is a close approximation to the cellulose accessibility to cellulase (CAC).

$$CAC = \alpha * A_{\max, \text{BSA/TGC}} * N_A * A_{G2} \quad (3)$$

where $A_{\max, \text{BSA/TGC}}$ = a maximum TGC adsorption capacity of biomass after BSA blocking ($\mu\text{mole TGC/g biomass}$).

Therefore, NCAC (m²/g biomass) can be calculated as

$$NCAC = TSAC - CAC \quad (4)$$

The adsorption results suggest that the values of $A_{\max, \text{TGC}}$ and $A_{\max, \text{BSA/TGC}}$ are 2.05 ± 0.15 and $1.64 \pm 0.13 \mu\text{mol/g}$ for COSLIF-pretreated biomass and 1.09 ± 0.08 and $0.84 \pm 0.05 \mu\text{mol/g}$ for DA-pretreated biomass, respectively (43). For the COSLIF-pretreated sample, the TSAC was found to be $14.44 \pm 1.09 \text{ m}^2/\text{g}$

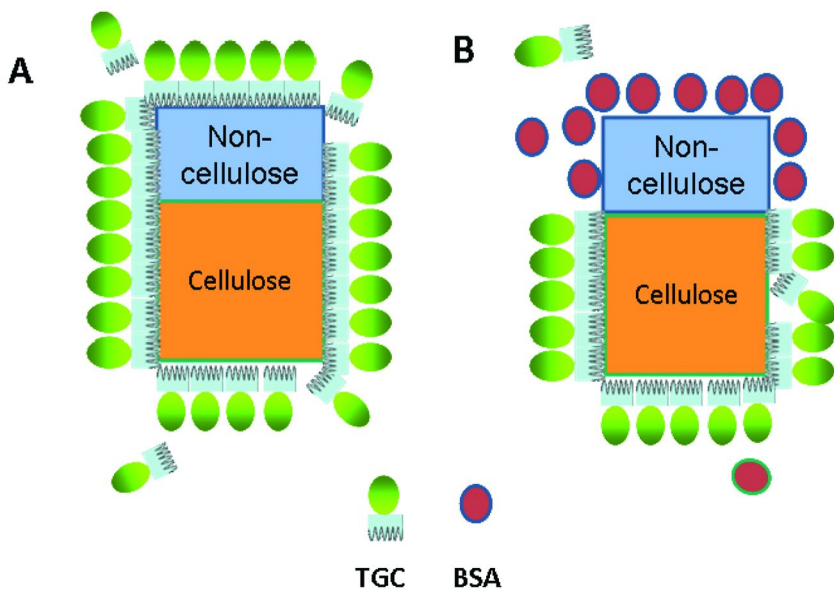


Figure 7. Scheme for quantitative determination of TSAC and CAC for the pretreated biomass. (A) Direct TGC adsorption for determining TSAC, including the cellulose and non-cellulose (lignin) fractions, and (B) Second TGC adsorption for determining CAC after BSA blocking of the lignin fraction.

biomass, where CAC and NCAC are 11.57 ± 0.90 and 2.88 ± 0.20 m²/g biomass, respectively. The much faster hydrolysis rates and higher glucan digestibility observed with the COSLIF-pretreated corn stover were attributed to a much higher CAC (11.57 m²/g biomass) than that of the DA-pretreated corn stover (5.89 m²/g biomass).

Perspectives

Lignocellulose fractionation based on the different solubilities of lignocellulose components in different solvents is a relatively new concept, and the COSLIF technology is in its early stage (18, 24). COSLIF has several advantages, including high glucan digestibility, fast hydrolysis rate, low cellulase use, effectiveness that is nearly feedstock-independent, higher revenues from co-products (acetic acid, lignin, and hemicellulose), and minimal formation of inhibitors. However, this technology also has several challenges, such as the high ratios of cellulose solvent and organic solvent to biomass, which may result in high processing costs for efficient recycling of both solvents or high capital investment. Therefore, further studies of the COSLIF technology will be focused on:

- (1) decreasing cellulose solvent use per unit biomass by finding better cellulose solvents,

- (2) decreasing organic solvent use per unit biomass by using better organic solvents and more efficient washing methods,
- (3) efficiently recycling both solvents through flashing, distillation or fractionation distillation,
- (4) identifying suitable solid/liquid unit operations,
- (5) efficiently regenerating the cellulose solvent,
- (6) characterizing the properties of isolated lignin,
- (7) developing new applications for relatively pure lignin,
- (8) studying the feasibility of cellulase recycling,
- (9) conducting economic analysis based on an ASPEN-Plus model, and
- (10) validating technology feasibility with a pilot plant.

Substantial progress will be made in these areas, and the principles of lignocellulose fractionation would have important applications in lignocellulose-based biorefineries. In the short term, cellulosic ethanol production based on cellulose-rich wastes from existing industries, such as corn fiber from corn ethanol biorefineries, wheat hull from flour processing facilities, and sawdust from lumber manufacturers, is attractive, since integrated biorefineries such as these could not only solve solid waste disposal problems but also produce value-added products such as biofuels. Smaller biorefineries that utilize cellulosic waste from on-site manufacturers could be profitable due to the large saving in feedstock costs (~\$30-90/ton of biomass, i.e. \$0.35-1.00 per gallon of cellulosic ethanol). The application of this nearly feedstock-independent technology on biomass residues from local manufacturers could provide great opportunities to build profitable small-scale biorefineries (i.e. 100 tons of biomass per day) that can produce ~2.8 million gallons of cellulosic ethanol per year, plus acetic acid as a value-added co-product. In the long term, full utilization of all the components of lignocellulosic biomass will be extremely important for the bioeconomy.

Acknowledgements

This work was supported from the DoD (W911SR-08-P-0021), USDA-sponsored Bioprocessing and Biodesign Center, DOE BioEnergy Science Center, USDA, Air Force Office of Scientific Research (FA9550-08-1-0145), DuPont Young Professor Award, and ICTAS.

References

1. Jarvis, M. *Science* **2003**, *426*, 611–612.
2. Zhang, Y.-H. P.; Himmel, M.; Mielenz, J. R. *Biotechnol. Adv.* **2006**, *24* (5), 452–481.
3. Zhang, Y.-H. P.; Lynd, L. R. *Biotechnol. Bioeng.* **2004**, *88*, 797–824.
4. Zhang, Y.-H. P. *J. Ind. Microbiol. Biotechnol.* **2008**, *35* (5), 367–375.
5. Lynd, L. R.; Wyman, C. E.; Gerngross, T. U. *Biotechnol. Prog.* **1999**, *15*, 777–793.

6. Demain, A. L.; Newcomb, M.; Wu, J. H. D. *Microbiol. Mol. Biol. Rev.* **2005**, *69*, 124–154.
7. Lynd, L. R.; Cushman, J. H.; Nichols, R. J.; Wyman, C. E. *Science* **1991**, *251*, 1318–1323.
8. Lynd, L. R.; Weimer, P. J.; van Zyl, W. H.; Pretorius, I. S. *Microbiol. Mol. Biol. Rev.* **2002**, *66*, 506–577.
9. Zhang, Y.-H. P. *Energy Environ. Sci.* **2009**, *2* (2), 272–282.
10. Lynd, L. R.; Laser, M. S.; Bransby, D.; Dale, B. E.; Davison, B.; Hamilton, R.; Himmel, M.; Keller, M.; McMillan, J. D.; Sheehan, J.; Wyman, C. E. *Nat. Biotechnol.* **2008**, *26* (2), 169–172.
11. Zhang, Y.-H. P.; Berson, E.; Sarkanen, S.; Dale, B. E. *Appl. Biochem. Biotechnol.* **2009**, *153*, 80–83.
12. Zhang, Y.-H. P.; Lynd, L. R. New generation biomass conversion: Consolidated bioprocessing. In *Biomass Recalcitrance: Deconstructing the Plant Cell Wall for Bioenergy*; Himmel, M. E., Ed.; Blackwell Publishing: 2008; pp 480–494.
13. Bayer, E. A.; Lamed, R.; Himmel, M. E. *Curr. Opin. Biotechnol.* **2007**, *18* (3), 237–245.
14. Flint, H. J.; Bayer, E. A.; Rincon, M. T.; Lamed, R.; White, B. A. *Nat. Rev. Microbiol.* **2008**, *6*, 121–131.
15. Ding, S.-Y.; Xu, Q.; Crowley, M.; Zeng, Y.; Nimlos, M.; Lamed, R.; Bayer, E. A.; Himmel, M. E. *Curr. Opin. Biotechnol.* **2008**, *19* (3), 218–227.
16. Taylor, L. E. I.; Dai, Z.; Decker, S. R.; Brunecky, R.; Adney, W. S.; Ding, S.-Y.; Himmel, M. E. *Trends Biotechnol.* **2008**, *26*, 413–424.
17. Chen, F.; Dixon, R. A. *Nat. Biotechnol.* **2007**, *25* (7), 759–761.
18. Zhang, Y.-H. P.; Ding, S.-Y.; Mielenz, J. R.; Elander, R.; Laser, M.; Himmel, M.; McMillan, J. D.; Lynd, L. R. *Biotechnol. Bioeng.* **2007**, *97* (2), 214–223.
19. Singh, V.; Johnston, D. *Adv. Food Nutr. Res.* **2004**, *48*, 151–171.
20. McAloon, A.; Taylor, F.; Yee, W.; Ibsen, K.; Wooley, R. *Determining the cost of producing ethanol from corn starch and lignocellulosic feedstocks*; NREL/TP-580-28893; National Renewable Energy Laboratory: Colorado, Oct. 2000, 2000.
21. Kamm, B.; Kamm, M. *Appl. Microbiol. Biotechnol.* **2004**, *64*, 137–145.
22. Wheals, A. E.; Basso, L. C.; Alves, D. M. G.; Amorim, H. V. *Trends Biotechnol.* **1999**, *17*, 482–487.
23. Wyman, C. E. *Trends Biotechnol.* **2007**, *25* (4), 153–157.
24. Moxley, G. M.; Zhu, Z.; Zhang, Y.-H. P. *J. Agric. Food Chem.* **2008**, *56* (17), 7885–7890.
25. Zhang, Y.-H. P.; Lynd, L. R. *Biotechnol. Bioeng.* **2006**, *94*, 888–898.
26. Zhang, Y.-H. P.; Cui, J.-B.; Lynd, L. R.; Kuang, L. R. *Biomacromolecules* **2006**, *7* (2), 644–648.
27. McMillan, J. D. *ACS Symp. Ser.* **1994**, *566*, 292–324.
28. Sathitsuksanoh, N.; Zhu, Z.; Templeton, N.; Rollin, J.; Harvey, S.; Zhang, Y.-H. P. *Ind. Eng. Chem. Res.* **2009**, *48*, 6441–6447.
29. Ladisch, M. R.; Ladisch, C. M.; Tsao, G. T. *Science* **1978**, *201*, 743–745.

30. Swatloski, R. P.; Spear, S. K.; Holbrey, J. D.; Rogers, R. D. *J. Am. Chem. Soc.* **2002**, *124*, 4974–4975.
31. Kilpeläinen, I.; Xie, H.; King, A.; Granstrom, M.; Heikkinen, S.; Argyropoulos, D. *J. Agric. Food Chem.* **2007**, *55*, 9142–9148.
32. Zhu, S. *J. Chem. Technol. Biotechnol.* **2008**, *83* (6), 777–779.
33. Dadi, A. P.; Varanasi, S.; Schall, C. A. *Biotechnol. Bioeng.* **2006**, *95* (5), 904–910.
34. Zhang, Y.-H. P.; Lynd, L. R. *Anal. Biochem.* **2003**, *322*, 225–232.
35. Bernardez, T. D.; Lyford, K.; Hogsett, D. A.; Lynd, L. R. *Biotechnol. Bioeng.* **1993**, *43*, 899–907.
36. Grethlein, H. E. *Bio/Technol.* **1985**, *3*, 155–160.
37. Ooshima, H.; Burns, D. S.; Converse, A. O. *Biotechnol. Bioeng.* **1990**, *36*, 446–452.
38. Schell, D. J.; Farmer, J.; Newman, M.; McMillan, J. D. *Appl. Biochem. Biotechnol.* **2003**, *105/108*, 69–85.
39. Converse, A. O., Substrate factors limiting enzymatic hydrolysis. In *Bioconversion of forest and agricultural plant residues*; Saddler, J. N., Ed.; CAB International: 1993; pp 93–106.
40. Kumar, R.; Wyman, C. E. *Enzyme Microb. Technol.* **2008**, *42* (5), 426–433.
41. Lloyd, T. A.; Wyman, C. E. *Bioresour. Technol.* **2005**, *96*, 1967–1977.
42. Moxley, G.; Zhang, Y.-H. P. *Energy Fuels* **2007**, *21*, 3684–3688.
43. Zhu, Z.; Sathitsuksanoh, N.; Vinzant, T.; Schell, D. J.; McMillan, J. D.; Zhang, Y.-H. P. *Biotechnol. Bioeng.* **2009**, *103*, 715–724.
44. Kim, T. H.; Lee, Y. Y. *Bioresour. Technol.* **2005**, *96*, 2007–2013.
45. Zeng, M.; Mosier, N. S.; Huang, C.-P.; Sherman, D. M.; Ladisch, M. R. *Biotechnol. Bioeng.* **2007**, *97* (2), 265–278.
46. Hong, J.; Ye, X.; Zhang, Y. H. P. *Langmuir* **2007**, *23* (25), 12535–12540.
47. Berlin, A.; Gilkes, N.; Kurabi, A.; Bura, R.; Tu, M.; Kilburn, D.; Saddler, J. *Appl. Biochem. Biotechnol.* **2005**, *121/124*, 163–170.
48. Yang, B.; Wyman, C. E. *Biotechnol. Bioeng.* **2006**, *94*, 611–617.

Subject Index

A

- Accessibility, cellulose, to cellulase (CAC), 375–376
- Acetals, cellulose intermediates, 10–13
- Acetic anhydride
acylation of cellulose with, 112*t*
cellulose esterification in DMSO/ammonium fluorides, 110*t*
- Acetylation, cellulose in molten salt hydrates, 99
- Acid-catalyzed hydrolysis, cellulbiose in ionic liquid, 233
- Acidic depolymerization, lignocellulose in ionic liquids (ILs), 233
- Activation energy, cellulose solutions, 220
- Acylation
cellulose in DMSO/ammonium fluorides, 110*t*, 114*t*
cellulose with acid anhydrides in BMIMCl, 279–280
ionic liquids as matrixes for, 231–232
- Aerogels
cellulose, in LiOH/urea system, 86
morphology of, in LiOH/urea, 20, 22*f*
XRD patterns and photographs of, 85*f*
- Alkali containing solvents, dissolving cellulose, 18–20
- 1-Alkyl-3-methyl-imidazolium ionic liquids (ILs)
dissolution capabilities, 199
hydrogen-bond bridge system of ILs, 208*f*
reacting with cellulose, 235–236
- See also* Cellulose in 1-alkyl-3-methyl-imidazolium ILs
- Alkylammonium cations, ionic liquids, 288, 289*f*
- Alkylations
experimental, 244–251
N-methylmorpholine-*N*-oxide (NMMO), and ion metathesis, 241, 242*f*
NMMO using dimethyl sulfite, 242, 243*f*
See also N-methylmorpholine-*N*-oxide (NMMO) derivatives
- Alkyl chain length, cellulose dissolution, 305–307
- Alkylphosphonium cations, ionic liquids, 288, 289*f*
- 1-Alkylpyridinium cations, ionic liquids, 288, 289*f*
- 1-Allyl-1-methylpyrrolidinium dimethyl phosphate
synthesis, 249
thermal ellipsoid plot, 246*f*
- 1-Allyl-3-butyylimidazolium dimethyl phosphate, synthesis, 250
- 1-Allyl-3-ethylimidazolium acetate, synthesis, 251
- 1-Allyl-3-methylimidazolium chloride (AMIMCl)
acylation of cellulose, 25
alkylation with trimethyl phosphate, 250
Avicel solubility in dry, 127*t*
cellulose dissolution, 28*f*
properties, 24
structure, 29*f*
- Allylation, cellulose in DMSO/ammonium fluorides, 109*t*, 111
- N*-Allyl-*N*-methylmorpholinium chloride, cellulose cosolvent, 238
- Amine oxides

- cellulose dissolution, 27–28, 33*f*
- N*-methylmorpholine-*N*-oxide (NMMO), 27–28, 68
- structures, 34*f*
- Ammonium cations, ionic liquids for cellulose dissolution, 24
- Ammonium fluorides. *See* Dimethyl sulfoxide/ammonium fluorides (DMSO/TBAF)
- Ammonium salts, cellulose dissolution, 29*f*
- Anions, cellulose solubility in ionic liquids (ILs), 125–131
- Antibacterial effect, titanium dioxide on cellulose fibers, 264
- Aqueous cellulose solvents
 - LiOH/urea system, 20, 84–86
 - NaOH/H₂O system, 18, 19*f*, 68–71
 - NaOH/thiourea system, 20, 80–84
 - NaOH/urea system, 20, 71–79, 80*t*
 - See also* Protic solvents
- Avicel cellulose
 - anion effect on solubility in ionic liquids (ILs), 125–131
 - cation effect on solubility in ILs, 131–133
 - dry ionic liquids (ILs), 127*t*
 - intrinsic viscosity of enzyme-treated, 220–221
 - maximal molar ratio (water:IL), 132*t*
 - minimal molar ratio for solubility in binary ILs, 128*t*
 - molar ratio (acetate:cellulose-OH) for, in binary ILs, 129*f*
 - preparation of regenerated, 290–291
- B**
- Bacterial cellulose
 - functionalization in ionic liquids (ILs), 280–281, 282*f*
 - microscopic images, 281*f*
- Bagasse pulp, elution profiles of, during dissolution, 168*f*
- Ballooning effect
 - following, by scanning electron microscopy, 144, 145*f*
 - swollen cellulose fibers, 6, 8*f*
 - zones of swollen wood fiber, 139*f*
- Ballooning phenomenon, cellulose swelling, 137–138
- Benzylation, cellulose in DMSO/ammonium fluorides, 109*t*, 111
- Biocelsol method
 - cellulose dissolution, 214–215
 - See also* Enzymatic treatment
- Biodegradable cellulose/chitin beads, NaOH/thiourea, 84
- Biofuel, preparation from cellulose, 294–295
- Biomass
 - conversion to simple sugars, 366
 - dissolution, 214
 - enzymatic hydrolysis profiles, 371*f*
 - fractionation and co-utilization lignocellulose feedstock components, 366–367
 - ionic liquids as direct solvents for cellulose, 230–231
 - saccharification paradigms, 366*f*, 370*f*
 - typical composition, 367
 - See also* Cellulose solvent- and organic solvent-based lignocellulose fractionation (COSLIF); Wood in ionic liquids (ILs)
- Biopolymer, cellulose, 67–68, 198, 261–262
- Biorefinery operations, 344
- Blend formation, cellulose with polymers in molten salt hydrates, 99–100
- Boric acid
 - ¹¹B NMR spectra of model compounds, 16*f*

- ¹¹B NMR spectra of
phenylboronate, 16*f*
boronate structures and expected
fission, 15*f*
interaction of carbohydrates
with, 13–14
NMR spectroscopy of
phenylboronate esters, 14,
16*f*
- Branched ionic liquids, dissolution,
308–310
- Bromination, cellulose, 38
- Bromodeoxycellulose, synthesis,
38
- 1-Butyl-3-methylimidazolium
[BMIM] ionic liquids
acylation with acid anhydrides
in BMIMCl, 279–280
BMIM chloride as cellulose
solvent, 238
BMIM ethyl methyl phosphate,
249–250
cellulose furoate synthesis, 279*f*,
280
chemical structures, 151
derivatization of cellulose by,
154–155
dissolving power of, 234
functionalization of bacterial
cellulose in BMIMCl, 280–
281, 282*f*
¹H NMR spectrum of mixture of
BMIM-OAc and sulfuryl
chloride after mixing, 156*f*
homogeneous functionalization
of spruce in BMIMCl, 348,
350
properties of cellulose solutions
in, 207*t*
reaction of BMIM-acetate with
1-¹³C-D-glycopyranose, 151
reaction with cellulose, 152–
153, 154
reactivity of C-2, 150
side reactions of, acetates in
trimethylsilylations of
cellulose, 161, 162*f*
side reactions of, in
methylations, 159–160
side reactions of BMIM-OAc in
esterifications, 158–159
thermal degradation, 155–157
See also Cellulose in 1-alkyl-3-
methyl-imidazolium ILs
- 1-Butyl-3-methylimidazolium
cations
¹H NMR of ethanol-OH-proton
of mixtures with ethanol,
123, 124*f*
solvent parameters of ILs and
hydrogen bonding acceptor
interactions, 126*t*
- C**
- Cadoxen, complexing agent, 4, 15
- ε-Caprolactone graft
polymerization,
DMSO/ammonium fluorides,
116
- Carbamates, cellulose, 36
- Carbanilation mixtures, cellulose
degradation, 169, 170
- Carbohydrates, interaction with
boric acid, 13–14
- Carbon-13 nuclear magnetic
resonance
analysis of wood in ionic
liquids, 353–354
cyanoethyl cellulose (CEC),
334, 335*t*, 336
cyanoethyl cellulose (CEC)
hydrolyzed with
trifluoroacetic acid, 332*f*
investigating degree of
substitution (DS) of
heterogeneous CEC, 333*t*
See also Cyanoethylation
- N,N*-Carbonyldiimidazole (DCI) in
DMSO, esterification of
cellulose, 115–116
- Carboxyalkylation, cellulose in
ionic liquids, 25–26

- Carboxylate-based ionic liquids,
low viscosity liquids, 234
- Carboxylate salts, cellulose
solubility, 234–235
- Carboxylic acid esters,
hydrolytically unstable, of
cellulose, 6–10
- Carboxylic acids, acylation of
cellulose in DMSO/ammonium
fluorides, 114*t*
- Carboxymethylation
cellulose, 17, 18*t*
cellulose in DMSO/ammonium
fluorides, 109*t*
cellulose in molten salt hydrates,
97–99
- Cations
basic structure of, in ionic
liquids, 57–60
cellulose solubility in ionic
liquids (ILs), 131–133
ionic liquid preparation, 57
- Cellubiose, acid-catalyzed
hydrolysis, 233
- Cellulase, cellulose accessibility to,
375–376
- Celluloid, man-made plastic, 3, 5
- Cellulose
D-anhydroglucopyranose units
(AGUs), 165–166
anion effect of ionic liquids
(ILs) on, solubility, 125–131
applications, 137, 300
atomic force microscopy (AFM)
image of cellulose film, 28,
35*f*
ballooning phenomenon, 137–
138
behaviors of solution, 74–75
biomacromolecule, 56, 67–68
carboxymethylation, 17, 18*t*
cation effect of ILs on,
solubility, 131–133
cellulose furoate synthesis, 279*f*,
280
chain conformation of, in
LiOH/urea, 84–85
crystalline structure of, in beads
and initial pulp, 222, 223*f*
degree of polymerization (DP)
measurement, 310–311
degree of substitution (DS) of
cellulose acetate, cellulose
pentanoate, cellulose
hexanoate and cellulose
benzoate, 278*f*
derivatization by ionic liquids,
154–155
description, 300
designing ionic liquids as
solvents, 59–60
diffusion of chains upon
dissolution, 144–147
dissolution and structure in
NaOH/thiourea, 80–83
esterification, 33–35, 39*f*
etherification, 36, 40*f*, 79, 80*t*
functional cellulose materials,
77–79
halogendeoxy functions, 38
heating and power profiles for
dissolution, 309*f*
hemicelluloses, 166
homogeneous conversion in
ionic liquids, 26–27
ILs as solvent, 277
importance of dissolution, 180
improving solubility, 170–174
interaction with molten salt
hydrate and, 95–96
ionic liquids for dissolution, 29*f*
mechanism of dissolution in ILs,
122
membrane formation, 232–233
microwave irradiation for
dissolution, 235, 310
modifications, 165–166
physico-chemistry precondition
for dissolution, 205–207
polarized light microscopy of, in
thiocyanate-containing
solutions, 22, 23*f*
properties, 287–288
proposed structure in Pden, 17*f*
pulp constituent, 167

- regeneration, 300–301
regeneration in ionic liquids, 25
renewable resource, 67–68, 198,
261–262, 275–276, 287
rheology of, in different
solvents, 180
SEM images of electrospun
fibers from, in NMMO/water,
28, 35*f*
silylation in ionic liquids, 26
solubility in
methylphosphonate-type
ionic liquids, 63*t*
solubility of Avicel in dry ILs,
127*t*
solubilization temperature in
methylphosphonate salts, 61*t*
solubilization under microwave
vs. EMIM acetate, 235
structure with hydrogen bonds,
301*f*
substrate accessibility, 375–376
succinylated, 292*t*, 293*f*, 294
sulphation, 14*t*
super molecular structure, 199*f*
tosylation in ionic liquids, 26
water uptake measurement,
311–312
X-ray diffraction patterns of
original and regenerated, 289,
290*f*
See also Wood in ionic liquids
(ILs)
- Cellulose accessibility to cellulase
(CAC), 375–376
Cellulose acetate
intermediate, 7, 9*f*
scheme for synthesis of, 280–
281, 282*f*
synthesis, 278, 292
Cellulose aerogels, LiOH/urea
system, 86
Cellulose benzoate, synthesis, 278
Cellulose blends, preparation, 291
Cellulose carbamate, intermediate,
6, 8*f*
Cellulose carbanilate, synthesis of,
281, 282*f*
Cellulose channel inclusion
complex, LiOH/urea system, 84
Cellulose chemistry, ionic liquids
(ILs), 277, 300–302
Cellulose composite materials,
preparation, 291
Cellulose degradation,
derivatization systems, 169–170
Cellulose dichloroacetates,
intermediates, 9, 11*f*
Cellulose dissolved in NaOH/water
and ionic liquid
additives ZnO or urea, 188–189
Arrhenius plot for spruce sulfite
pulp in ionic liquid, 181*f*,
183*f*
cellulose concentration and
viscosity, 187–188
cellulose/EMIMAc solutions,
182
cellulose/NaOH/water solutions,
182
comparing rheological and
hydrodynamic properties,
193*t*
dissolution methods, 183
experimental, 182–185
flow of cellulose solutions, 185–
186
gelation time vs. temperature for
cellulose/NaOH/water, 184*f*
intrinsic viscosities, 188–193
intrinsic viscosity vs.
temperature for cellulose in
NaOH/ZnO/water and
NaOH/urea/water, 189, 190*f*
relative viscosity vs. $C[\eta]$ by
temperature, 191–192
rheological measurements, 183,
185
temperature and intrinsic
viscosity, 189, 190*f*
temperature-induced gelation of
cellulose/NaOH/water, 193
temperature influence, 185–186
viscosity-concentration
dependence for cellulose in
EMIMAc, 187*f*

- viscosity-shear rate dependence
of cellulose/NaOH/water,
184*f*
- Cellulose fibers
- ballooning effect, 6, 8*f*
 - cell wall structure, 140
 - chain mobility, 142
 - characterization, 267–269
 - chemical environment of
cellulose chains, 140, 142
 - dissolution mechanisms, 140–
142
 - dissolution of cellulose in
NaOH/urea, 75–76
 - magnetic nanocomposite fibers,
76
 - mechanical properties, 268–269
 - multi-filaments from
NaOH/urea, 73*f*
 - NaOH/thiourea system, 82*f*, 83–
84
 - N*-methylmorpholine-*N*-oxide
(NMMO) process, 262
 - novel multi-filament, in
NaOH/thiourea, 83–84
 - photographs of cellulose/Fe₂O₃
nanocomposite fibers, 75*f*
 - regeneration from NaOH/urea
solvent, 76
 - scanning electron microscopy
(SEM) images, 74*f*, 263*f*
 - stress-strain curves for plain,
266*f*
 - surface morphology, 267
 - swelling and dissolution
mechanisms, 141*f*
 - thermal stability, 267–268
 - See also* Cellulose/TiO₂ fibers
- Cellulose films
- transparent, fluorescent and
photoluminescent, 75*f*
 - transparent and composite, 77
- Cellulose formats, intermediates,
8–9
- Cellulose furoate
- degree of substitution and
solubility, 281*t*
 - synthesis, 279*f*, 280
- Cellulose gels, transparent
nanoporous, in LiOH/urea, 86
- Cellulose hexanoate, synthesis, 278
- Cellulose in 1-alkyl-3-methyl-
imidazolium ILs
- 1-butyl-3-methyl-imidazolium
acetate (BMIM-OAc)
reacting with 1-¹³C-D-
glucopyranose, 151
 - chemical structures of ionic
liquids (ILs), 151
 - ¹³C-labeled 1-butyl-3-
methylimidazolium IL
reacting with cellulose, 154
 - ¹³C NMR spectra of BMIM-
OAc and 1-¹³C-D-glucose
solutions after dissolution,
153*f*
 - derivatization of cellulose, 154–
155
 - dissolution and re-precipitation,
150
 - ¹H NMR spectra for
methylations, 160*f*
 - ¹H NMR spectrum of mixture of
BMIM-OAc and sulfuryl
chloride, 156*f*
 - molecular weight distributions
and fluorescence signals of
BMIM- and NapMIM-
derivatized cellulose, 156*f*
 - reaction of (2-
naphthalylmethyl)methyl-
imidazolium IL with
cellulose, 155
 - reactions of IL anions, 157–161
 - reactions of IL cations, 151–155
 - reactivity of C-2 in imidazolium
moieties, 150
 - side reactions of BMIM-OAc in
esterifications, 158
 - side reactions of EMIM/BMIM
acetates and chlorides in
methylations of cellulose,
159–160
 - side reactions of EMIM/BMIM
acetates in

- trimethylsilylations of
cellulose, 161, 162*f*
- thermal degradation of BMIM
and EMIM ILs, 155
- thermal degradation of ILs, 155–
157
- Cellulose intermediates
acetals and silyl ethers as, 10–13
- cellulose acetate, 7, 9*f*
- cellulose dichloroacetates, 9, 11*f*
- cellulose formates, 8–9
- cellulose trifluoroacetate, 9–10,
11*f*
- hydrolytically unstable
carboxylic acid esters of
cellulose, 6–10
- methylol cellulose, 10, 12*f*, 13*f*
- silyl cellulose, 11–13
- Cellulose man-made fibers
cellulose/NMMO/H₂O system
for dissolution in ILs, 209–
210
- cellulose-solvent-interaction in
dissolved state, 207–209
- consecutive dissolution step of
cellulose PAN mixture, 206*f*
- experimental, 199–201
- fiber characterization, 202
- methods, 202
- physico-chemistry precondition
of cellulose dissolution, 205–
207
- preparation of cellulose
solutions, 200–201
- pulp characterization methods,
202
- spinning trials, 201
- structure and dissolvability,
203–205
- structure of cellulose NMMO
monohydrate complex, 205*f*
- technological art of formation,
200*f*
- Cellulose multi-filaments,
NaOH/urea system, 73*f*
- Cellulose nitrate
dissolution of cellulose, 5–6
- regioselectivity of sulphation of,
7*t*
- Cellulose nitrobenzoate, ¹³C NMR
spectrum, 11*f*
- Cellulose pentanoate, synthesis,
278
- Cellulose pulps. *See N,N*-
Dimethylacetamide
(DMAc)/LiCl
- Cellulose solvent- and organic
solvent-based lignocellulose
fractionation (COSLIF)
biomass saccharification
paradigms, 366*f*, 370*f*
- cellulose solvent criteria, 369–
370
- enzymatic hydrolysis, 372, 373*f*
- enzymatic hydrolysis profiles
for COSLIF-pretreated
biomass, 371*f*
- flowchart, 370*f*
- future studies, 376–377
- mechanism, 367–369
- roles of organic solvent, 371
- SEM images for COSLIF-
pretreated biomass, 374*f*
- substrate accessibility, 375–376
- supramolecular structures, 373–
374
- technology, 368, 370*f*
- Cellulose solvents
acetals and silyl ethers as
intermediates, 10–13
- categories, 4
- cellulose dichloroacetates, 9, 11*f*
- cellulose fibers swollen with
alkali and carbon disulfide, 8*f*
- cellulose formates, 8–9
- cellulose nitrate, 5–6
- cellulose nitrobenzoate, 11*f*
- cellulose trifluoroacetate
(CTFA), 9–10, 11*f*
- cellulose xanthate, 6, 7*f*
- cross-sections of cellulose
fibers, 8*f*
- formation of cellulose
carbamate, 8*f*

- hemiacetal of chloral and cellulose, 13*f*
- hydrolytically unstable
 - carboxylic acid esters of cellulose, 6–10
- interaction of carbohydrates
 - with boric acid, 13–14
- methylol cellulose, 10, 12*f*, 13*f*
- regioselectivity of sulphation of cellulose nitrite, 7*t*
- silyl cellulose, 11–13
- See also* Aqueous cellulose solvents
- Cellulose/TiO₂ fibers
 - blend and fiber preparation, 264–265
 - calculated TiO₂ concentration at surface, 270*t*
 - characterization, 269–271
 - characterization methods, 265–266
 - energy dispersive X-ray spectroscopy (EDS), 266, 271
 - experimental, 264–266
 - extrusion apparatus, 263*f*
 - mechanical properties, 269*t*, 271
 - scanning electron microscopy (SEM), 265, 266*f*
 - stress-strain curves for composite, 268*f*
 - surface morphology, 270
 - tensile strength, 266
 - thermal stability, 270
 - thermogravimetric analysis (TGA), 265, 267*f*
 - See also* Cellulose fibers
- Cellulose trifluoroacetate (CTFA)
 - ¹³C NMR spectrum, 11*f*
 - formula, 11*f*
 - intermediates, 8–10
- Cellulose whiskers, atomic force microscopy (AFM) image of, 76*f*
- Cellulose xanthate, dissolving cellulose, 6, 7*f*
- Cellulosic materials, biofuel preparation, 294–295
- Cell wall structure, cellulose fibers, 140
- Chain conformation, cellulose in LiOH/urea system, 84–85
- Chain mobility, cellulose fibers, 142
- Chardonnet silk, man-made fiber, 3, 5
- Chemical environment, cellulose fibers, 140, 142
- Chemical modification, wood in ionic liquids, 348–349
- Chlorination, cellulose, 38
- Complexing agents, Schweizers reagent, 15–17
- Composite fibers. *See* Cellulose/TiO₂ fibers
- Composites, wood in ionic liquids, 349–351
- Concentration, cellulose, and viscosity, 187–188
- Conductor-like screening model for real solvents (COSMO-RS), 236
- COSLIF. *See* Cellulose solvent- and organic solvent-based lignocellulose fractionation (COSLIF)
- COSMO-RS (conductor-like screening model for real solvents), 236
- Cotton linters, degree of polymerization after dissolution and regeneration, 107*t*
- Crystalline structure, cellulose in beads and initial pulp, 222, 223*f*
- Crystallinity, dissolution of cellulose, 168–169
- Crystallography
 - interactions in ionic liquids, 243, 245*t*, 248*t*
 - thermal ellipsoid plots, 244*f*, 245*f*, 246*f*
- Cuoxam
 - dissolving cellulose, 4
 - hollow fiber for blood dialysis by, process, 16*f*
- Cuoxen, complexing agent, 15

- Cupro process, dissolving cellulose, 104
- Cyanoethylation
 activation reactions, 325–326, 330
 catalysts for homogeneous, of cellulose, 325*t*
¹³C NMR investigations of degree of substitution (DS) distribution of heterogeneous cyanoethyl cellulose (CEC), 333*t*
¹³C NMR investigations of DS distribution of homogeneous CEC, 335*t*
¹³C NMR spectroscopic determination, 334, 335*t*, 336
¹³C NMR spectrum of CEC hydrolyzed with trifluoroacetic acid, 332*f*
 comparing heterogeneous, quasi-homogeneous and homogeneous, 321, 323
 degree of polymerization (DP) of cellulose in Cuoxam solution, 323–324
 DS and viscosity of heterogeneous CEC, 322*t*
 elementary analysis, 324
 experimental, 323–326, 330
 heterogeneous, 320–321, 326
 heterogeneous procedure, 323, 330–331
 homogeneous, 321, 330
 homogeneous procedure, 323, 331–332, 334
 preparation of amorphous cellulose, 325–326
 quasi-homogeneous, 326
 rheological characterization, 336–337
 solubility and viscosity of CEC during homogeneous, 327*t*, 328*t*, 329*t*
 solubility determination, 324
 viscosity measurement, 324
 viscosity of heterogeneous CEC, 337*f*
 viscosity of homogeneous CEC, 338*f*
- Cyclohexyl-*N*-dimethylamine-*N*-oxide, cellulose dissolution, 27, 33*f*
- D**
- Decomposition
 aqueous salt containing cellulose solvents, 21
 cellulose in molten inorganic salts, 92, 94*t*
- Degradation
 cellulose, 233–236
 cellulose, in derivatization systems, 169–170
See also Decomposition
- Degree of polymerization (DP)
 determination for cellulose, 216, 219
 equation, 182
 measurement for cellulose, 310–311
 polysaccharide cellulose, 166
- Degree of substitution (DS), cyanoethyl cellulose (CEC), 322*t*, 333*t*
- Depolymerization, lignocellulose in ionic liquids (ILs), 233
- Derivatization
 cellulose dissolution, 43
 ionic liquids as matrixes for, 231–232
- Derivatizing solvents, dissolution of cellulose, 168
- Design, ionic liquid solvents for cellulose, 59–60
- Despeissis, Louis-Henri, fiber process, 15
- 1,3-Dialkylimidazolium cations, ionic liquids, 288, 289*f*
- Dialkyl sulfites, alkylation of *N*-methylmorpholine *N*-oxide (NMMO), 242, 243*f*
- Dialysis, hollow fibers for, 15, 16*f*

- Differential scanning calorimetry (DSC), ionic liquids, 57–58
- Diffusion
- cellulose chains upon dissolution, 144–147
 - experimental protocol, 144–145
 - precipitation of dissolved cellulose in NMMO-water, 146–147
- N,N*-Dimethylacetamide (DMAc)/LiCl
- cellulose degradation in derivatization systems, 169–170
 - cellulose dissolution, 29–32
 - cellulosic pulps, 165
 - dissolution of cellulosic pulps, 167–169
 - extended standard approaches, 171–173
 - improvement of cellulose solubility, 170–174
 - mixed systems, 173–174
 - replacing DMAc with dimethyl sulfoxide (DMSO), 174
- Dimethyl sulfoxide (DMSO)
- cellulose dissolution with DMSO/LiCl, 174
 - cellulose with ethyl isocyanate, 170
- Dimethyl sulfoxide/amine/SO₂, cellulose dissolution, 41
- Dimethyl sulfoxide/ammonium fluorides (DMSO/TBAF)
- acetylation of cellulose with acetic anhydride, 112*t*
 - acylation reactions with various carboxylic acids, 114*t*
 - application of water free DMSO/TBAF, 113–115
 - cellulose dissolution, 40–41, 42*t*
 - cellulose esterification with DMSO/TBAF trihydrate, 115–116
 - ¹³C NMR spectrum of cellulose in, 105*f*
 - combination of DMSO with tetra-*N*-butylammonium fluoride trihydrate (TBAF·3H₂O), 104
 - conditions and results for esterification, 110*t*
 - conditions and results for etherification, 109*t*
 - degree of polymerization (DP) of cellulose before and after dissolution and regeneration, 107*t*
 - dissolution of microcrystalline cellulose and pulps in, 104–108
 - esterification reactions, 111–116
 - etherification reactions, 109–111
 - graft polymerizations, 116
 - ¹H NMR spectrum of perpropionylated cellulose acetate, 114*f*
 - homogeneous reactions of cellulose in, 115*t*
 - optical microscopy of cotton fiber dissolution, 105*f*
 - photo and plot of samples with varying cellulose and water content, 106*f*
 - solvent dependent reaction efficiencies, 116
 - use as reaction medium, 108–116
 - water content determination, 113
 - water vs. distillation during dewatering process, 108*f*
- Dipolarity, ionic liquids, 58, 61
- Dissolution
- alkyl chain length and branching of ionic liquids (ILs), 305–310
 - aqueous salt containing cellulose solvents, 21
 - biomass, 214
 - cellulose, by microwave irradiation, 235, 310
 - cellulose in ILs, 56–57, 121–122, 262, 276, 288–290, 301–302

cellulose in molten inorganic salts, 92, 94*t*
cellulose/NMMO/H₂O, in ILs, 209–210
cellulose-solvent-interaction in dissolved state, 207–209
diffusion of cellulose chains upon, 144–147
enzyme-treated pulp, 216, 222–224
experimental protocol, 144–145
heating and power profiles for, of cellulose, 309*f*
importance of cellulose, 180
mechanisms of native cellulose fibers, 140–142
mechanisms of wood pulp and cotton fibers, 141*f*
native cellulose fibers, 140
physico-chemistry precondition for cellulose, 205–207
precipitation of dissolved cellulose during, of bleached cotton fiber, 146*f*
raw cotton fiber, 141*f*
solid polymer, 140
studies using ILs, 303–310
water uptake measurements, 311–312
wood in ionic liquids, 345–347
See also Ionic liquids (ILs)

E

Electrospinning, ionic liquids for, cellulose, 232
Electrospray ionization mass spectrometry (ESI–MS), cation-anion interaction, 239
Energy dispersive X-ray spectroscopy (EDS), cellulose/TiO₂ fibers, 266, 271
Enzymatic hydrolysis, pretreated biomass, 372, 373*f*
Enzymatic treatment
activation energy, 220

average particle size of scattering in pulp with, 221*f*
bead morphology by scanning electron microscopy (SEM), 222, 223*f*
beads preparation and analysis, 217, 219
Biocelsol method, 214–215
cellulose dissolution, 215, 216–217
crystalline structure of cellulose in beads and initial pulp, 222, 223*f*
DP determination of pulp, 216
DP of cellulose by, 219
evidence of undissolved entities in pulp with, 221
experimental, 215–217, 219
flow cytometry, 217
flow of cellulose solutions, 219
hydrodynamic properties of enzyme-treated pulp, 223–224
intrinsic viscosity of pulp with, 220–221
methods, 215–216
molecular weight changes, 222–223
rheology measurement, 217
viscosimetry measurement, 217
viscosity vs. shear rate at various temperatures, 218*f*
Esterification
cellulose, using cyclic anhydrides, 293–294
cellulose in DMSO/ammonium fluorides, 110*t*, 111–116
cellulose with in situ activation, 33–35, 39*f*
ionic liquids as matrixes for, 231–232
side reactions of 1-butyl-3-methyl-imidazolium acetate (BMIM-OAc) in, 158–159
solvent dependent reaction efficiencies, 116
special cellulose derivatives in ionic liquids (ILs), 282–283

- Ethanol, pulp solubility with, and DMI/LiCl, 174*t*
- Etherification
 cellulose, 36, 40*f*
 cellulose in DMSO/ammonium fluorides, 109–111
 cellulose in ionic liquids, 25–26
 cellulose in NaOH/urea system, 79, 80*t*
- 1-Ethyl-3-methylimidazolium (EMIM) ionic liquids
 cellulose dissolved in EMIM acetate (EMIMAc), 180
 EMIM dimethyl phosphate, 235
 side reactions of, acetates in trimethylsilylations of cellulose, 161, 162*f*
 side reactions of, in methylations, 159–160
 spruce sulfite pulp in EMIMAc, 181*f*
 thermal degradation, 155–157
- 1-Ethyl-3-methylimidazolium cations
¹H NMR of ethanol-OH-proton of mixtures with ethanol, 123, 124*f*
 minimal molar ratio for Avicel solubility in binary ILs based on, 128*t*
 molar ratio for Avicel solubility in binary ILs based on, 129*f*
 solvent parameters of ILs and hydrogen bonding acceptor interactions, 126*t*
- 1-Ethyl-3-methylimidazolium acetate (EMIMAc)
 advantage, 24–25
 Avicel solubility in dry, 127*t*
 cellulose dissolution, 214, 216, 222, 237
 cellulose solubilization by microwave vs., 235
 flow of cellulose solutions, 185–186
 reacting as reagent, 301
 relative viscosity vs. C[η] at various temperatures, 191, 192*f*
 rheological and hydrodynamic properties of cellulose in, 193*t*
 structure, 29*f*
 temperature influence on cellulose solutions, 185–186
 viscosity-concentration dependence of cellulose in, 187*f*
- 1-Ethyl-3-methylimidazolium chloride (EMIMCl)
 Avicel solubility in dry, 127*t*
 liquefaction and depolymerization of wood, 236–237
 structure, 29*f*
- Ethylene diamine (EDA)/KSCN, cellulose processing, 22–23
- F**
- Ferric sodium tartrate complex
 complexing media, 17
 fibrillation, 17, 19*f*
- Fiber process
 Despeissis, 15
 spinning trials, 201
See also Cellulose man-made fibers
- Fibers. *See* Cellulose fibers; Cellulose/TiO₂ fibers
- Fibrillation, yarns with FeTNa solution, 17, 19*f*
- Flow properties
 cellulose/NaOH/water and cellulose/ionic liquid, 193*t*
 flow cytometry, 217, 219, 221*f*
 temperature influence, 185–186
- Fluorescent, cellulose films, 75*f*
- Fractionation
 ILs as, auxiliaries for lignocellulosic materials, 236–237

lignocellulosic materials, 235–236
See also Cellulose solvent- and organic solvent-based lignocellulose fractionation (COSLIF)
Fremery, Max, lamp filaments, 15

G

Gelation, cellulose/NaOH/water, 184*f*, 186
Gels, transparent nanoporous cellulose, in LiOH/urea, 86
Glucose production, from pretreated lignocellulosics, 347–348
Gossypium barbadense, dissolution in N-methylmorpholine-*N*-oxide (NMMO), 140, 141*f*
Graft polymerization, ϵ -caprolactone in DMSO/ammonium fluorides, 116

H

Hemicelluloses
pulp constituent, 167
structural types, 166
wood pulp dissolution, 169
Heterogeneous cyanoethylation.
See Cyanoethylation
Hollow fibers, dialysis, 15, 16*f*
Homogeneous functionalization
alternative solvents ionic liquids (ILs), 276
cellulose in Li salt containing solvent, 31–32
cyanoethylation, 321, 323, 330, 331–332, 334
degree of substitution (DS) of dendritic PAMAM-triazolo-cellulose derivatives, 282*t*
functionalization of bacterial cellulose in IL, 280–281, 282*f*
ILs as reaction media, 278–280

ILs as solvent for cellulose, 277
ILs in cellulose chemistry, 277
imidazolium based ILs as reaction medium, 276, 277*f*
preparation of special cellulose derivatives in IL, 282–283
scheme for synthesis of cellulose acetate and cellulose carbanilate, 282*f*
wood in ionic liquids, 348, 350
See also Cyanoethylation
Homogeneous reactions, cellulose in DMSO/ammonium fluorides, 115*t*
Hydrodynamic properties, cellulose/NaOH/water and cellulose/ionic liquid, 193*t*
Hydrogel, photographs of, in NaOH/urea, 78*f*
Hydrogen bonding
bridge system of ionic liquids, 208*f*
cellulose dissolution in self-assembly process, 72–73
cellulose structure with, 301*f*
intra- and intermolecular, 168, 199*f*
solvent parameters in ILs indicating hydrogen bonding acceptor interactions, 126*t*
Hydrolysis, cellulbiose in ionic liquid, 233
Hydroxyalkylation, cellulose in ionic liquids, 25–26
1-(2-Hydroxyethyl)-3-methylimidazolium acetate, synthesis, 251
1-(2-Hydroxyethyl)-3-methylimidazolium dimethyl phosphate, synthesis, 250–251

I

Imidazolium based ionic liquids (ILs)
cellulose chemistry, 276, 277*f*
cellulose dissolution studies, 303–305

- influence of alkyl chain length and branching, 305–310
See also Ionic liquids (ILs)
- Imidazolium cations, ionic liquids for cellulose dissolution, 24
- Imidazolium salts
 cellulose dissolution, 29*f*
 side chain on *N*-position of imidazolium ring on
 solubility of cellulose, 60–64
- Inorganic molten salt hydrates,
 polysaccharide modification, 21
- In situ activation, esterification of cellulose, 33–35, 39*f*
- Inter-molecular bonding, hydrogen bond, 168, 199*f*
- Intra-molecular bonding, hydrogen bond, 168, 199*f*
- Ionicell fiber, 291
- Ionic liquids (ILs)
 abbreviations, 345
 alkylations of, 241–242, 247–251
 alkyl chain length and branching, 305–310
 anion effect of, on cellulose solubility, 125–131
 Avicel solubility in, 125–130
 basic structure of cation, 57–60
 biofuel preparation from cellulosics, 294–295
 cation effect of, on cellulose solubility, 131–133
 cellulose dissolution, 56–57, 121–122, 262, 276, 288–290, 301–302
 cellulose dissolution studies, 303–305
 cellulose/NMMO/H₂O system for dissolution in ILs, 209–210
 chemical structure of cations, 58, 61
 common cations, 288, 289*f*
 concepts, 237–238
 correlation between ¹H NMR of ethanol OH-proton and C2-proton in mixtures, 130*f*
 direct solvents for cellulosic biomass, 230–231
 disadvantages, 301
 fine-tuning solvent properties, 238
 fractionation auxiliaries for lignocellulosic materials, 236–237
¹H NMR of ethanol-OH-proton in ethanol-IL mixtures, 123, 124*f*
 homogeneous conversion of cellulose, 26–27
 hydrogen bond acceptor and donor properties, 122
 hydrogen-bond bridge system, 208*f*
 hydrogen bonding, 56–57
 matrixes for derivation, reconstitution and degradation of cellulose, 231–236
 maximal molar ratio (water:IL) for Avicel solubility, 132*t*
 mechanism of cellulose dissolution in, 122
 minimal ratio (cellulose-dissolving:non-dissolving IL) for solubility, 128*t*
 molar ratio (acetate:cellulose-OH) for Avicel in binary IL mixtures, 129*f*
 molten organic salts, 23–27
N-allyl-*N*-methylmorpholinium chloride, 238
 OH-shift values of Br⁻, Cl⁻ or [CF₃CO₂]⁻ anions with different cations, 132*t*
 parameters indicating hydrogen bond acceptor (HBA) interactions, 126*t*
 perspectives, 237–238
 physicochemical properties, 59*t*, 62*t*
 picture showing dissolution of cellulose in, 30*f*
 preparation of regenerated cellulose in, 290–291

- properties, 56
 - properties of cellulose solutions
 - in, 207*t*
 - proposed structure of cellulose
 - IL complex, 209*f*
 - reaction media, 278–280
 - side chain on *N*-position of imidazolium ring on
 - solubility of cellulose, 60–64
 - silylation of cellulose, 26
 - solubility and DP of cellulose
 - samples in, 30*t*
 - solubility of Avicel in dry ILs, 127*t*
 - solvent-solute interactions, 123, 125
 - structures, 345
 - suitable for cellulose
 - dissolution, 29*f*
 - sustainability, 358, 360
 - synthesis, 302–303
 - temperature dependence of
 - viscosity, 58–59, 60*f*, 62*f*
 - term, 229–230
 - tosylation of cellulose, 26
 - water content, 302*t*
 - See also* Cellulose in 1-alkyl-3-methyl-imidazolium ILs; *N*-methylmorpholine-*N*-oxide (NMMO) derivatives; Wood in ionic liquids (ILs)
 - Isocyanate derivatization, pulps, 170
- K**
- Kamlet–Taft parameters
 - alkylimidazolium salts, 61
 - ionic liquids, 58
- L**
- LiCl. *See* *N,N*-Dimethylacetamide (DMAc)/LiCl
 - Lignin
 - cell wall polysaccharides, 166–167
 - pulp constituent, 167
 - softwood kraft pulp dissolution, 169
 - Lignocellulose
 - depolymerization in ionic liquids, 233
 - fractionation, 366–367, 376–377
 - ionic liquids as fractionation auxiliaries, 236–237
 - paradigm changes for binary, extractants, 241
 - spectroscopic tools for solutions, 239
 - See also* Cellulose solvent- and organic solvent-based lignocellulose fractionation (COSLIF)
 - LiOH/urea system
 - cellulose channel inclusion complex, 83*f*, 84
 - cellulose materials in, 86
 - chain conformation of cellulose, 84–85
 - SEM images of aerogels in, 20, 22*f*
 - Li salt containing solvents, cellulose dissolution, 29–32
 - Lyocell fiber, 262, 291
 - Lyocell process
 - dissolving cellulose, 104
 - N*-methylmorpholine-*N*-oxide monohydrate, 150

M

- Man-made fiber, Chardonnet silk, 3, 5
- Man-made materials, manufacturing, 198
- Man-made plastics
 - Celluloid, 3, 5
 - modification reaction, 3
 - See also* Cellulose man-made fibers
- Mannans, hemicellulose, 166

- Mechanisms
carbohydrate composition of soluble and insoluble fractions, 142, 143*f*
cellulose dissolution in ionic liquids (ILs), 122
cellulose dissolution in NaOH/urea at low temperature, 71–74
cellulose solvent- and organic solvent-based lignocellulose fractionation (COSLIF), 367–369
dissolution of native cellulose fibers, 140–142
hydrogen bonding acceptor strength of ILs and cellulose dissolving, 128–130
- Membrane formation, cellulosic matrixes, 232–233
- Mercerization, cellulose with bases, 18
- Mesylation, cellulose, 38
- Methylations, side reactions of 1-ethyl-3-methyl-imidazolium and 1-butyl-3-methyl-imidazolium acetates and chlorides in, 159–160
- Methylol cellulose, intermediates, 10, 12*f*, 13*f*
- Methylphosphonate salts
solubility of cellulose in series of, 62, 63*t*
solubilization temperature of cellulose in, 61*t*
- Microcrystalline cellulose
degree of polymerization after dissolution and regeneration, 107*t*
esterification in DMSO/ammonium fluorides, 110*t*, 112
NaOH/thiourea system, 81*f*, 82
- Microwave irradiation, cellulose dissolution by, 235, 309*f*, 310
- Mixed-linkage β -glucans, hemicellulose, 166
- Molding, cellulose into shapes, 198
- Molten inorganic salts
acetylation reaction, 99
blend formation, 99–100
carboxymethylation reaction, 97–99
classification of molten salt hydrates, 92
 ^{13}C NMR spectra of cellulose dissolved in, 98*f*
crystal structure of $\text{LiClO}_4 \cdot 3\text{H}_2\text{O}$ and $\text{LiNO}_3 \cdot 3\text{H}_2\text{O}$, 94*f*
decomposition, 94*t*
dissolution, 94*t*
dissolution power, 93
FT Raman spectra of regenerated cellulose from, 96*f*
interaction between cellulose and, 95–96
medium for blending cellulose with polymers, 99–100
molar mass distribution of nitrates of regenerated cellulose, 97*f*
molten salt hydrates and interaction to cellulose, 94*t*
reactions of cellulose in, 96–100
SEM pictures of regenerated celluloses from, 97*f*
solubility of cellulose, 92–93
structural changes of cellulose dissolved in, 94–95
swelling, 94*t*
swelling ability of cellulose in, 91–92
- Molten organic salts, ionic liquids, 23–27, 29*f*
- Morphology
aerogels in LiOH/urea, 20, 22*f*
atomic force microscopy (AFM) image of cellulose film, 28, 35*f*
bead, by scanning electron microscopy (SEM), 222, 223*f*
SEM for observing swelling, 142–144

SEM images of electrospun fibers from cellulose in NMMO/water, 28, 35*f*
SEM of particles from trimethylsilyl cellulose, 32*f*
SEM pictures of regenerated cellulose from molten salt hydrates, 95, 97*f*
surface, of cellulose fibers, 265, 266*f*, 267, 270

N

N-allyl-*N*-methylmorpholinium chloride, cellulose cosolvent, 238

NaOH/H₂O system

aerocellulose, 71*f*
cellulose materials, 70–71
comparing steam exploded softwood sulphite pulp and microcrystalline cellulose in, 143*f*

dissolution of cellulose, 68–70
enzymatic pretreatment of cellulose in, 214–215

protic solvents, 18, 19*f*
rheological and hydrodynamic properties of cellulose in, 193*t*

steam-exploded cellulose in, 69–70

structure and interaction of cellulose solution, 70
wet regenerated cellulose, 71*f*
See also Enzymatic treatment

NaOH/thiourea system

dissolution and structure of cellulose, 80–83
microcrystalline cellulose, 81*f*, 82
multi-filament fibers, 82*f*, 83–84
new cellulose materials, 83–84
rheological measurements and photographs, 81*f*, 83
sol-gel transition of cellulose solution, 83

NaOH/urea system

behaviors of cellulose solution, 74–75

cellulose dissolution at low temperature, 71–74

¹³C NMR spectra of cellulose in, 72*f*

fibers based on dissolution of cellulose in, 75–76

functional cellulose materials, 77–79

homogeneous etherification of cellulose in, 79, 80*t*

photo of novel cellulose multi-filaments from, 63*f*

regenerated cellulose microspheres (RCS), 77

SEM images of surface and cross section of filaments, 74*f*
transparent and composite cellulose films, 77

WAXD intensity profiles of cellulose in, 72*f*

NaOH/water system

addition of ZnO and urea to cellulose/NaOH/water, 189, 190*f*

gelation time vs. solution temperature for cellulose in, 184*f*, 186

relative viscosity vs. C[η] at various temperatures, 191, 192*f*

viscosity-shear rate dependence of cellulose in, 184*f*, 186

2-Naphthylmethyl)methylimidazolium ionic liquid, reaction with cellulose, 154–155

Nioxam, complexing agent, 15

Nitren

carboxymethylation of cellulose, 17, 18*t*

complexing agent, 15

N-methylmorpholine-*N*-oxide (NMMO)

alkylation of, and ion metathesis, 241, 242*f*

- alkylation using dimethyl sulfite, 242, 243*f*
- cellulose dissolution, 27–28, 68, 199
- cellulose/NMMO/H₂O system for dissolution in ILs, 209–210
- cellulose structure and dissolvability, 203–205
- crystalline structure of NMMO 2.5 and monohydrates, 204*f*
- dissolution of raw cotton fiber in, 141*f*
- fiber manufacturing, 262
- Lyocell technology, 150
- phase diagram of cellulose/NMMO/water, 27, 34*f*
- structure of cellulose NMMO monohydrate complex, 205*f*
- swelling and dissolution of cellulose fibers, 138–139
- See also* Cyanoethylation
- N*-methylmorpholine-*N*-oxide (NMMO) derivatives
- advantages of dialkyl sulfites, 242
- alkylation, 241, 242*f*
- crystallography for interactions in ILs, 243, 244*f*
- decomposition, 243
- 1-[2-(diethylamino)ethoxy]pyridinium bromide hydrobromide (4), 248–249
- experimental, 244–251
- instrumentation, 244–246
- intermolecular CH⁺⋯O interactions in compound (1), 245*t*
- N*-methoxy-*N*-methylmorpholinium hexafluorophosphate (2), 247–248
- N*-methoxy-*N*-methylmorpholinium methyl sulfate (1), 247
- N*-methoxy-*N*-methylmorpholinium triflimide (3), 248
- short CH⁺⋯O contacts in compound (5), 248*t*
- stability assessments of cellulose solutions, 242–243
- starting materials, 247
- thermal behavior and stability of, 242–243, 244*f*
- thermal ellipsoid plot of compound (1), 244*f*
- thermal ellipsoid plot of compound (2), 245*f*
- thermal ellipsoid plot of compound (4), 246*f*
- thermal ellipsoid plot of *N*-allyl-*N*-methylpyrrolidinium dimethyl phosphate (5), 246*f*
- Nobel Prize, Hermann Staudinger, 4, 15
- Non-aqueous systems
- amine oxides, 27–28
- carbamate, 36
- DMSO/amine/SO₂, 41
- DMSO/TBAF, 40–41, 42*f*
- esterification via in situ activation, 33–35, 39*f*
- etherification, 36
- introduction of halogendeoxy functions, 38
- ionic liquids, 23–27
- Li salt containing solvents, 29–32
- molten organic salts, 23–27
- polar, aprotic, organic liquids/salt, 29–41
- silylation, 37
- sulfonates, 38–41
- Non-derivatizing solvents
- N,N*-dimethylacetamide/LiCl system, 170–174
- dissolution of cellulose, 167
- Nuclear magnetic resonance (NMR), analysis of wood in ionic liquids, 352–355

O

Organic solvent-based fractionation. *See* Cellulose solvent- and organic solvent-based lignocellulose fractionation (COSLIF)

P

Parkesine, man-made plastic, 3

Pden

complexing agent, 15
proposed cellulose structure in, 17*f*

Phase diagrams

cellulose/*N*-methylmorpholine-*N*-oxide/water, 27, 34*f*
ternary cellulose/NaOH/water, 18, 19*f*

Phosphorus-31 nuclear magnetic resonance

analysis of wood in ionic liquids, 354–355, 356*f*
tar fractions from pyrolysis, 358, 359*f*

Photochromism, ionic liquids (ILs), 240

Photoluminescent, cellulose films, 75*f*

Physico-chemistry, cellulose dissolution, 205–207

Polar ionic liquids. *See* Ionic liquids (ILs)

Polarity

correlating solvation ability and, 239–241
ionic liquids, 58
term, 239

Polarizability, ionic liquids, 58, 61

Polarized light microscopy, cellulose in thiocyanate-containing solvents, 22, 23*f*

Polyamidoamine (PAMAM)

dendrimers
codissolution with cellulose, 262

degree of substitution of dendritic PAMAM-triazolo-cellulose derivatives, 282*t*, 283

Polymers

blending cellulose with, in molten salt hydrates, 99–100
dissolution of solid, 140
dissolution steps, 141*f*

Polysaccharide, degree of polymerization (DP), 166

Polysaccharide modification, inorganic molten salt hydrates, 21

Precipitation, dissolved cellulose in NMMO-water, 146–147

Problematic cellulose pulps. *See* *N,N*-Dimethylacetamide (DMAc)/LiCl

Protic solvents

aqueous alkali solvents, 18–20
aqueous complexing agents, 15–17

aqueous salt containing cellulose solvents, 20–23

carboxylation of cellulose in LiClO₄, 23*t*

LiOH/urea, 20, 84–86

molten salt hydrates, 21

NaOH (sodium hydroxide)/H₂O, 18, 19*f*, 68–71

NaOH/poly(ethylene glycol), 19

NaOH/thiourea, 20, 80–84

NaOH/urea, 20, 71–79, 80*t*

Schweizers reagent, 15–17

thiocyanate-containing solutions, 22–23

See also Aqueous cellulose solvents

Proton nuclear magnetic resonance, analysis of wood in ionic liquids, 353–354

Pulps

alternative approaches to improving solubility, 174*t*
cellulosic, 165
constituents, 167

- dissolution of cellulosic, 167–169
dissolution via derivatization, 214
elution profiles of Bagasse, during dissolution, 168*f*
extended standard approaches to improving solubility, 171–173
mixed approaches to improving solubility, 173–174
See also Enzymatic treatment
- Pyridine
cellulose with ethyl isocyanate, 170
pulp solubility with, and LiCl, 174*t*
- Pyridinium cations, ionic liquids for cellulose dissolution, 24
- Pyridinium salts, cellulose dissolution, 28*f*, 29*f*
- Pyrolysis
³¹P NMR analysis of tar fractions, 358, 359*f*
wood in ionic liquids, 355–358
- Q**
- Quasi-homogeneous. *See* Cyanoethylation
- R**
- Reaction media, ionic liquids (ILs), 278–280, 292–294
- Regeneration
cellulose, to fibers, films and sponges, 104
cellulose fibers from solution in NaOH/urea, 76
cellulose in ionic liquids, 25, 233, 300–301
cellulose in Li salt containing solvent, 30–31
cellulose microspheres, 77
- degree of polymerization of cellulose before and after, 107*t*
preparation of regenerated cellulose in ionic materials, 290–291
structural changes of cellulose in molten salt hydrates, 95, 96*f*
wet cellulose from NaOH/water, 71*f*
X-ray diffraction of original and regenerated cellulose, 289, 290*f*
- Renewable resource, cellulose, 67–68, 198, 261–262, 275–276, 287
- Rheological properties
cellulose/NaOH/water and cellulose/ionic liquid, 193*t*
cyanoethyl cellulose (CEC), 336–337, 338*f*
enzyme-treated pulp solutions, 217, 218*f*
measurement for cellulose solutions, 183, 185
wood in ionic liquids, 346–347
- S**
- Scanning electron microscopy (SEM)
ballooning process, 144, 145*f*
biomass before and after pretreatment, 373–374
cellulose bead morphology, 222, 223*f*
dried and swollen bleached cotton fiber, 144, 145*f*
experimental protocol, 143
precipitation of dissolved cellulose during dissolution, 146*f*
swollen morphologies by, 142–144
- Schoenbein, C. F., cellulose dissolution discovery, 5*f*
- Schweizers reagent, complexing agent, 15–17

- Self-assembly process, cellulose dissolution by hydrogen bonding, 72–73
- Side reactions
reactivity of C-2 in imidazolium moieties, 150
See also Cellulose in 1-alkyl-3-methyl-imidazolium ILs
- Silylation
cellulose, 37
cellulose in ionic liquids, 26
- Silyl cellulose, intermediates, 11–13
- Silyl ethers, cellulose intermediates, 10–13
- Sisal cellulose, esterification in DMSO/ammonium fluorides, 110*t*, 112
- Sodium hydroxide (NaOH)
dissolving cellulose, 18–20
See also Enzymatic treatment; NaOH/H₂O system
- Softwood kraft pulp, dissolution obstacle, 169
- Sol-gel transition, cellulose solution in NaOH/thiourea, 83
- Solubility
anion effect of ionic liquids (ILs) on cellulose, 125–131
Avicel in dry ILs, 127*t*
cation effect of ILs on cellulose, 131–133
cellulose in methylphosphonate-type ionic liquids, 62, 63*t*
cellulose in molten salt hydrates, 92–93
cellulose/NaOH/water and cellulose/ionic liquid, 193*t*
cyanoethyl cellulose (CEC), 324, 327*t*, 328*t*, 329*t*
improving cellulose, 170–174
side chain on *N*-position of imidazolium ring on, of cellulose, 60–64
See also *N,N*-Dimethylacetamide (DMAc)/LiCl; Enzymatic treatment; Ionic liquids (ILs)
- Solubilization temperature, cellulose in methylphosphonate salts, 61*t*
- Solvation, correlating, and polarity, 239–241
- Solvatochromic studies
ionic liquid (IL)/IL binary mixtures, 240
multi-component matrixes, 240–241
- Solvent-based fractionation. *See* Cellulose solvent- and organic solvent-based lignocellulose fractionation (COSLIF)
- Solvent families, discoveries, 4, 43
- Solvents
designing ionic liquids (ILs) as, for cellulose, 59–60
dissolution of cellulose, 4, 43
ILs as, for cellulosic biomass, 230–231
See also Aqueous cellulose solvents; Dimethyl sulfoxide/ammonium fluorides (DMSO/TBAF)
- Spectroscopic tools, solutions of lignocellulosic materials, 239
- Spinning trials
cellulose fibers, 201
ionic liquids for, cellulose, 231, 232
- Spruce sulfite pulp
Arrhenius plot of, in ionic liquid, 181*f*
degree of polymerization after dissolution and regeneration, 107*t*
flow curves of, in ionic liquid, 181*f*
- Staudinger, Hermann
Nobel Prize, 4
photograph, 17*f*
Schweizers reagent, 15
- Steam-exploded cellulose, NaOH aqueous solution, 69–70
- Structural changes, cellulose in molten salts hydrates, 94–95

Succinylated cellulose, preparation, 292*t*, 293*f*, 294
Sulfonates, cellulose, 38–41
Supramolecular structures, biomass before and after pretreatment, 373–374
Surface morphology, cellulose fibers, 265, 266*f*, 267, 270
Sustainability, ionic liquids based biorefinery platform, 358, 360
Swelling
aqueous salt containing cellulose solvents, 21
ballooning effect, 137–138
cellulose in molten inorganic salts, 91–92, 94*t*
mechanisms of wood pulp and cotton fibers, 141*f*
morphologies by scanning electron microscopy (SEM), 142–144
zones of swollen wood fiber, 139*f*

T

Temperature dependence of viscosity
cellulose/NaOH/water solutions, 188*f*
intrinsic viscosities, 188–193
ionic liquids, 58–59, 60*f*, 62*f*, 63
relative viscosity of cellulose in ionic liquid and in NaOH/water, 189, 191*f*
Tencel fiber, 262
Tensile strength, cellulose fibers, 266, 268*f*
Thermal degradation, 1-alkyl-3-methylimidazolium ionic liquids, 155–157
Thermal stability
carboxylate salts, 234–235
cellulose fibers, 267–268
composite cellulose fibers, 270

Thermogravimetric analysis (TGA), cellulose fibers, 265, 267*f*
Thermoplastic composites, wood in ionic liquids, 349–351
Thiocyanate-containing media, dissolving polysaccharides, 21, 22–23
Titanium dioxide (TiO₂) particles
antibacterial effect, 264
dispersion in cellulose, 269
uses, 263
See also Cellulose/TiO₂ fibers
Tosylation, cellulose, 26, 38–40
Transparent, cellulose films, 75*f*, 77
Trimethyl-amine-*N*-oxide, cellulose dissolution, 27, 33*f*
Trimethylsilylations
ionic liquids as matrixes for, 232
side reactions of EMIM/BMIM acetates in, of cellulose, 161, 162*f*

U

Urban, Johan, artificial silk, 15
Urea, addition to cellulose/NaOH/water, 189, 190*f*

V

Viscose process
dissolving cellulose, 6, 104
enzyme-treated cellulose, 216–217
Viscosity
activation energy, 220
carboxylate-based ionic liquids and cellulose, 234
cellulose concentration, 187–188
cyanoethyl cellulose (CEC), 322*t*, 324, 327*t*, 328*t*, 329*t*, 336–337, 338*f*

enzyme-treated pulp solutions,
217, 218*f*
IL/cellulose solutions, 312–314
imidazolium-based ionic liquids,
61–62
ionic liquids, 58–59, 60*f*, 62*f*
Viscosity-shear rate,
cellulose/NaOH/water, 184*f*,
186

W

Water content

determination, 113, 312*f*
dewatering process for
DMSO/ammonium fluorides,
108*f*
ionic liquids (ILs), 302*t*
uptake measurements, 311–312
vacuum distillation, 112

Wood in ionic liquids (ILs)

analysis of tar fractions, 359*t*
chemical modification, 348–349
dissolution, 345–347
glucose production, 347–348
¹H and ¹³C NMR analysis, 353–
354
¹H NMR spectra of pulverized
Norway spruce wood, 352*f*
homogeneous functionalization
of spruce in IL, 350
in-situ NMR analysis, 352–355
opportunities, 347–358
phosphitylation reaction, 355

³¹P NMR spectra of tar fractions
from pyrolysis, 359*f*
³¹P NMR spectra of wood as
function of pulverization,
355, 356*f*
potential applications, 360
pyrolysis, 355–358
pyrolysis/thermolysis by IL,
357*t*
quantitative ³¹P NMR analysis,
354–355
rheological properties, 346–347
solubility-structure
relationships, 345–346
sustainability of ILs based
biorefinery platform, 358,
360
thermoplastic composites, 349–
351
total available hydroxyls in
Norway spruce, 355, 356*f*

X

Xyloglucans, hemicellulose, 166
Xyloglycans, hemicellulose, 166

Z

Zinkoxen, complexing agent, 15
ZnO, addition to
cellulose/NaOH/water, 189,
190*f*